Design and synthesis of small molecule probes for metabolic processes

Andrew G. Cairns

Supervisor: Dr Richard Hartley

Thesis submitted in part fulfilment of the requirements for the degree of Doctor of Philosophy in chemistry

School of Chemistry
University of Glasgow
September 2013

Abstract

Synthesis of a photoactivated uncoupler **I** was completed and subsequently used by collaborators to demonstrate mitochondria uptake.

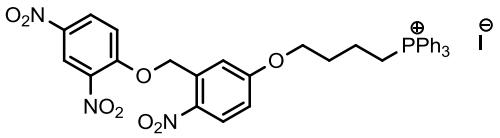

I

The synthesis of a ratiometric, targetable calcium sensor was completed up to intermediate **II** (9 steps), alongside a thiohydantoin heterocycle **III** synthesised in 5 steps. A co-worker has subsequently completed the probe synthesis based on this route, with the resulting probe showing good binding and optical responses in testing.

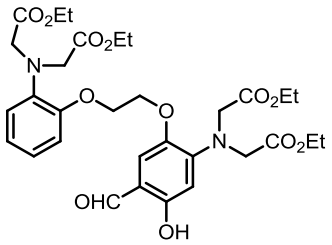

II

9 steps

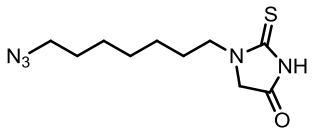

III

5 steps

Numerous routes to 5,6-disubstituted phenanthridinium salts were investigated towards the synthesis of a mitochondrially targeted superoxide probe and hydroxylated standards. In the course of this work a novel cyclisation was developed based on intramolecular S_NAr giving access to 9-benzyloxyphenanthridinium salt **V**.

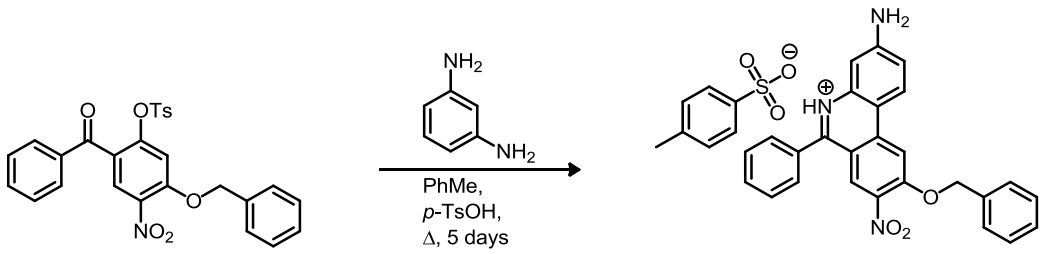

IV **V** 28%

Rapid and high-yielding access to 5,6-disubstituted phenanthridinium salts **IX** was then achieved through forming benzophenones **VIII** via Suzuki coupling and converting these to imines with the alkylamine. The nitrogen atom of the imine then undergoes cyclisation onto the aryl fluoride in an intramolecular S_NAr upon heating. This transformation was shown to have good steric and electronic tolerance in the synthesis of 13 phenanthridinium analogues with 6 structural diversification points. Subsequent DFT calculations by a colleague showed this reaction proceeds in a concerted fashion and as such represents a considerable mechanistic novelty.

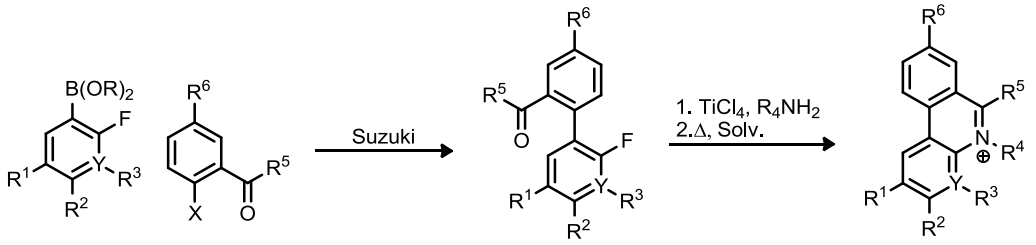

VI **VII** **VIII** **IX** 13 examples, 68%-100%

Efforts towards a new probe for mitochondrial superoxide led to the synthesis of 3-*tert*butyl-dihydrophenanthridine **X**, which does not intercalate into DNA upon oxidation. This concept was refined and lead to the development of neopentyl ethidium **XI** and the targeted analogue MitoBNH **XII** and its deuterated analogue **XIII**.

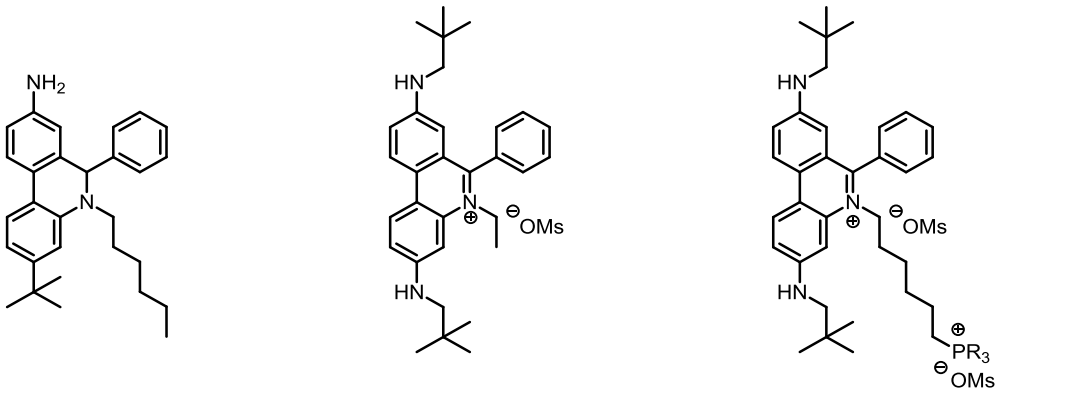

X **XI** **XII** R = Ph
XIII R = $(C_6D_5)_3$

Declaration

This thesis represents the original work of Andrew Gerard Cairns unless explicity stated otherwise in the text. No part of this thesis has previously been submitted for a degree at the University of Glasgow or any other university. The research was carried out at the University of Glasgow (UK) in the Loudon laboratory under the supervision of Dr Richard C. Hartley durng the period October 2009 to December 2012.

Acknowledgements

During the course of my PhD studies I have had the opportunity to work with, learn from, and exasperate many fantastic people. I would like to thank a few of those here, starting with my supervisor, Dr Richard Hartley, who has read bits of this document so many times I am not sure which of us is most pleased to see the back of it. I would like to thank him for the opportunity to undertake research in his group, but also for taking the time to guide my work and teach me so much. I should also thank him for tremendous patience and composure on the many occasions I am sure he was (metaphorically) tearing his hair out.

In a similar vein I would like to thank the venerable and learned Stuart, who was an invaluable source of advice, gently discouraging many of my worst ideas, and was always entertaining and easy to work with in addition - and who is definitely not grumpy, regardless of what Carlos says. Also, Stephen for useful advice but particularly for his entertaining company, and not so much for his singing, and Adam, for many extremely pedantic (and very entertaining) arguments on many an esoteric topic.

Thanks also to Rachel, who doesn't visit often enough but is always engaging, Justyna, who I know doesn't really drink that much vodka but tolerates my nonsense regardless, and Kishore. I would also like to mention the more recent additions in Asma, Masha, Carlos and Helmi, who make me feel a great deal older than I am but also always make me smile.

I should also thank our fellow inhabitants of the Loudon lab, the Sutherland group. In particular Lynne and Adele for listening to a great deal of whining about nearly every topic, Ewen for enduring a great deal of chemistry chat, and Grafto for never snapping and burying me in his garden. Also Filip, Fiona, Mark, Alastair, Lindsay and Lorna for their less recent but no less enjoyable company.

Outside the Loudon lab far too many names come to mind to list here, so in general thanks to all the many students and staff who have made my time here so pleasant. With regard to my work I would like to thank the technical staff who miraculously keep the place running and accommodated so many seemingly random requests, and in particular Stuart Mackay for allowing my lack of planning to constitute his emergency in the printing of this thesis.

I should reserve the final thanks for my family, and in particular my parents for their emotional support throughout my PhD and financial support during my writing up period - you will be delighted to hear I am never, *ever* doing anything like this again.

Abbreviations

(aq)	aqueous solution
(l)	liquid
(vac)	in vacuum
°C	degrees Celsius
µL	microlitre
Å	angstrom
Ac	acetyl
Acetyl CoA	Acetyl coenzyme A
ADP	adenosine diphosphate
AMP	adenosine monophosphate
APCI	atmospheric pressure chemical ionisation
ATP	adenosine triphosphate
APTRA	*o*-aminophenol-*N*,*N*,*O*-triacetic acid
BAPTA	1,2-bis(o-aminophenoxy)ethane-*N*,*N*,*N*',*N*'-tetraacetic acid
BHT	butylated hydroxytoluene
Bn	benzyl
Boc	tert-butyloxycarbonyl
br	Broad (NMR signal)
Bu	butyl
cAMP	cyclic adenosine monophosphate
CCCP	Carbonyl cyanide *m*-chlorophenylhydrazone
cGMP	cyclic guanosine monophosphate
CICR	calcium induced calcium release
COSY	correlation spectroscopy
CRET	chemiluminescence resonance energy transfer
DCM	dichloromethane
DEPT	distortionless enhancement by polarisation transfer
DFT	density functional theory
DHP	dihydropyran
DIBALH	diisobutylaluminium hydride
DIPEA	*N*,*N*-diisopropylethylamine
DME	dimethylether
DMF	dimethylformamide
DMNPE	1-(4,5-dimethoxy-2-nitrophenyl)ethyl
DMSO	dimethylsulfoxide
DNA	deoxyribonucleic acid
DNP	2,4-dinitrophenol
dppf	1,1'-bis(diphenylphosphino)ferrocene
EDCI	1-Ethyl-3-(3-dimethylaminopropyl)carbodiimide
EI	electron impact
Eq	equatorial
eq	equivalent

ESI	electrospray ionisation
Et	ethyl
ETFQOR	electron transferring flavoprotein ubiquinone oxidoreductase
EWG	electron withdrawing group
FAB	fast atom bombardment
$FADH_2$	flavin adenine dinucleotide
FCCP	carbonylcyanide-*p*-trifluoromethoxyphenylhydrazone
FRET	fluorescence resonance energy transfer
FRTA	free radical theory of ageing
g	grams
GPDH	glycerol 3-phosphate dehydrogenase
HMBC	heteronuclear multiple-bond correlation spectroscopy
HOMO	highest occupied molecular orbital
HPLC	high performance liquid chromatography
HRMS	high resolution mass spectroscopy
HSQC	heteronuclear single-quantum correlation spectroscopy
IF	complex I NADH binding site
$InsP_3$	inositol triphosphate
IP_3R	inositol trisphosphate receptor
IPA	isopropyl alcohol
^{i}Pr	isopropyl
IQ	complex I ubiquinone binding site
IRA	anionic ion exchange resin
J	joule
K	Kelvin
L	litre
LC-MS	liquid chromatography-mass specrometry
LiHMDS	lithium hexamethyldisilazide
M	Mole(s) per litre
Me	methyl
MeCN	acetonitrile
mg	milligram(s)
MHz	megahertz
mL	millilitre(s)
mmol	millimole(s)
Mol	mole(s)
MP	melting point
MRC	mitochondrial research centre
Ms	mesyl
MS	mass spectrometry
mtDNA	mitochondrial deoxyribonucleic acid
NADH	Nictoinamide adenine dinucleotide
NHC	*N*-heterocyclic carbene
NMDA	*N*-methyl-D-aspartate receptor

NMR	nuclear magnetic resonance
NOESY	nuclear Overhauser effect spectroscopy
NSI	nanospray ionisation
Nu	nucleophile
o-	*ortho*
OGDH	2-oxo-glutarate dehydrogenase
p-	*para*
Pd/C	palladium on carbon
PDH	pyruvate dehydrogenase
PEPPSI	pyridine-enhanced precatalyst preparation stabilization and initiation
PET	photoinduced electron transfer
PG	protecting group
Ph	phenyl
PMCA	Plasma membrane Ca2+ ATPase
Pt/C	platinum on carbon
RET	reverse electron transfer
Rf	retention factor
RNA	ribonucleic acid
ROS	reactive oxygen species
RT	room temperature
RyR	Ryanodine receptor
SERCA	sarco/endoplasmic reticulum Ca2+-ATPase
SET	single electron transfer
SM	starting material
S_N1	monomolecular nucleophilic substitution
S_N2	bimolecular nucleophilic substitution
S_NAr	nucleophilic aromatic substitution
SOD	superoxide dismutase
T	temperature
^{t}Bu	tertiary butyl
TEMPO	(2,2,6,6-tetramethylpiperidin-1-yl)oxidanyl
Tf	triflyl
TFA	trifluoroacetic acid
THF	tetrahydrofuran
TLC	thin layer chromatoagraphy
TMRE	tetramethyl rhodamine ester
TMS	trimethylsilyl
TMSCl	trimethylsilyl chloride
TPP	triphenylphosphonium
TS	transition state
UCP	uncoupling protein
UV	ultraviolet (wavelength)

Table of Contents

Chapter 1: Metabolism and the mitochondria

1.1 Introduction to metabolism

The etymology of the word 'metabolism' seems initially ironic; coming from the Greek 'metabole', meaning 'to change', the term encompasses the chemical reactions which sustain living organisms, allowing our cells and bodies to function consistently. In reality, however, the story of life is one of continuous chemical change; the order which characterises our construction is actively maintained through a constant balance of competing and intertwined processes. Ultimately we rely on the transformation of raw materials (food, air) to replenish our supply of chemical building blocks, and provide the energy to utilise these.[1] Life fundamentally relies upon increasing entropy[2,3] and avoiding equilibrium,[4,5,6] and metabolism is the continuous process which makes this possible.[7,8,9,10,11]

The complexity, interconnectedness and dynamism of cellular chemistry makes interrogating and understanding metabolic systems tremendously challenging. Some simplifying classifications can be used, however. Metabolic processes can be broken into subdivisions (**Figure 1**). 'Catabolism' refers to the conversion of organic molecules into lower energy products and capturing the energy liberated. 'Anabolism' refers to processes which use this energy to construct complex molecules from simpler building blocks, such as in protein construction in the endoplasmic reticulum. Collections of enzymes and other active biomolecules can also be assigned to 'pathways', referring to their consecutive application to an initial substrate.

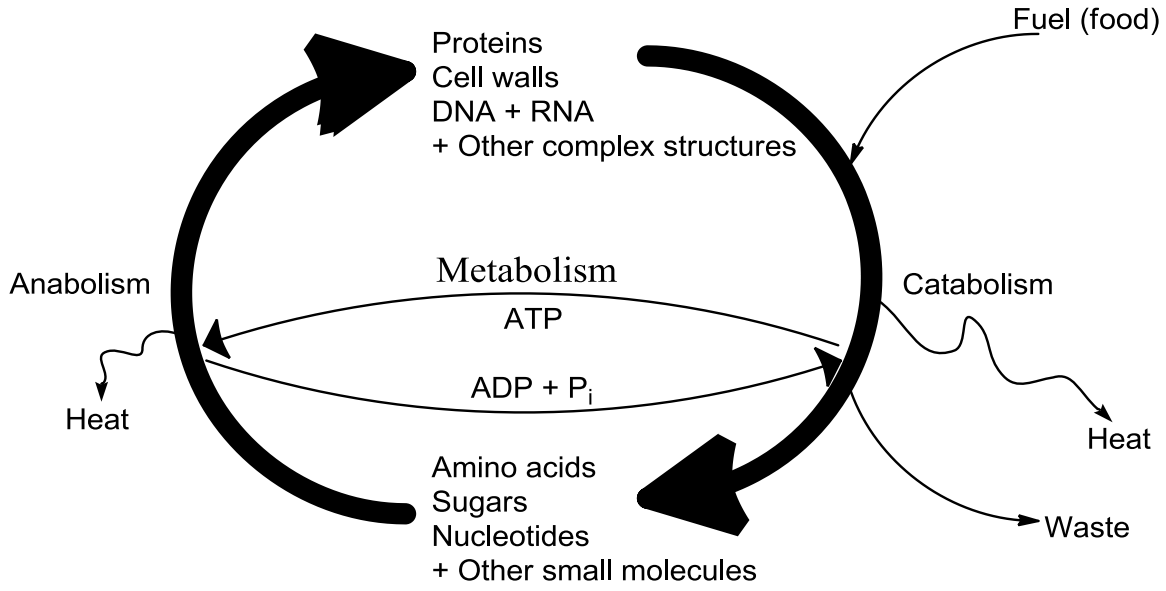

Figure 1 - The linking of catabolic and anabolic processes.

In order for the process of metabolism to work, an effective means of releasing and capturing energy and transporting it between these types of pathway must exist. In humans and other large organisms relatively diverse, complex chemical fuels such as proteins and lipids are broken down

into their subunits, supplying amino acids, fatty acids, mononucleotides and sugars.[12] These are then transported to cells, where further metabolism occurs.

1.2 The cellular organelles

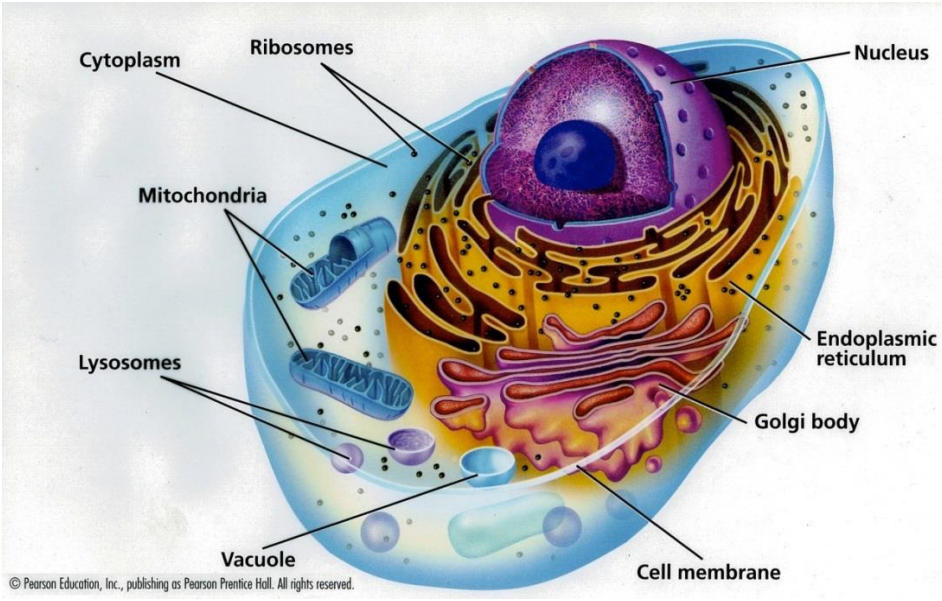

Figure 2 - Simplified schematic of a cell.[13]

Each cell contains a large number of specialised compartments (**Figure 2**), or organelles, which segregate metabolic pathways and chemical environments. Anabolic processes such as the synthesis of DNA (Nucleus) and proteins (Ribosomes) occur at a variety of specific sites, allowing regulation of their chemical environment. The major catabolic processes occur within the mitochondria (**Figure 3**).

1.3 Mitochondria

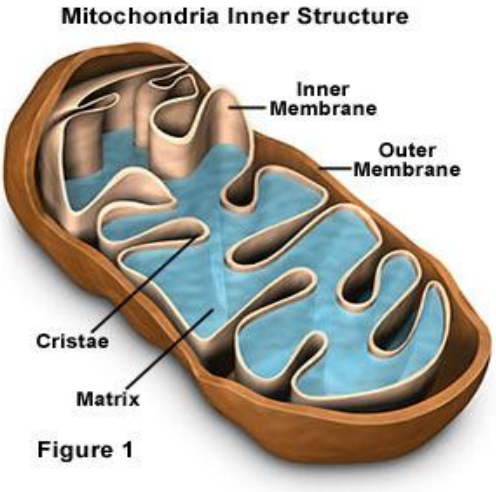

Figure 3 - Basic mitochondrial anatomy, with the electron transport chain located in the inner membrane walls.[14]

Mitochondria are unusual organelles, and probably evolved from prokaryotic symbionts.[15] They have their own DNA and RNA, along with the machinery required to produce some of their own proteins. On average typical animal cells have 1000 mitochondria, with up to 2000 found in some cells. They resemble bacteria in size and shape, and can be very mobile.[16] The outer membrane contains a protein called porin, and is consequently permeable to molecules up to about 5000 daltons in mass.[17] The inner membrane by contrast is impermeable except where specific transport proteins are involved. This membrane has a highly convoluted structure made up of cristae, providing a large surface area. The surface area can vary between cells; a cardiac muscle cell mitochondrion has triple the cristae of an equivalent mitochondrion in a liver cell.[16] Within the inner membrane is the matrix, a dense gel composed of up to 50% protein.[18]

It is within the mitochondrial matrix that many of the major metabolic cycles found in animals occur, including the catabolism by which energy is acquired to sustain the chemical and physical processes carried out within eukaryotic cells. There are many complexities, variations and interlinked processes,[19] but the key processes are remarkably conserved between organisms,[20] and can be simplified as described below (**Figure 4**). Carbohydrates and sugars are ultimately broken down to glucose and then further to pyruvate via glycolysis[21] in the cytosol, producing adenosine triphosphate (ATP). ATP acts as an energy 'currency'[22] within the body by releasing energy via controlled degradation to either adenosine diphosphate (ADP) or adenosine monophosphate (AMP). Glycolysis also produces nicotinamide adenine dinucleotide (NADH), a redox active molecule which can transport high energy electrons. Within the mitochondria more ATP and NADH result from the oxidation of pyruvate to CO_2, first through the pyruvate dehydrogenase complex to Acetyl CoA, then the Krebs cycle, with the electrons liberated being 'stored' in NADH and $FADH_2$ (flavin adenine dinucleotide).

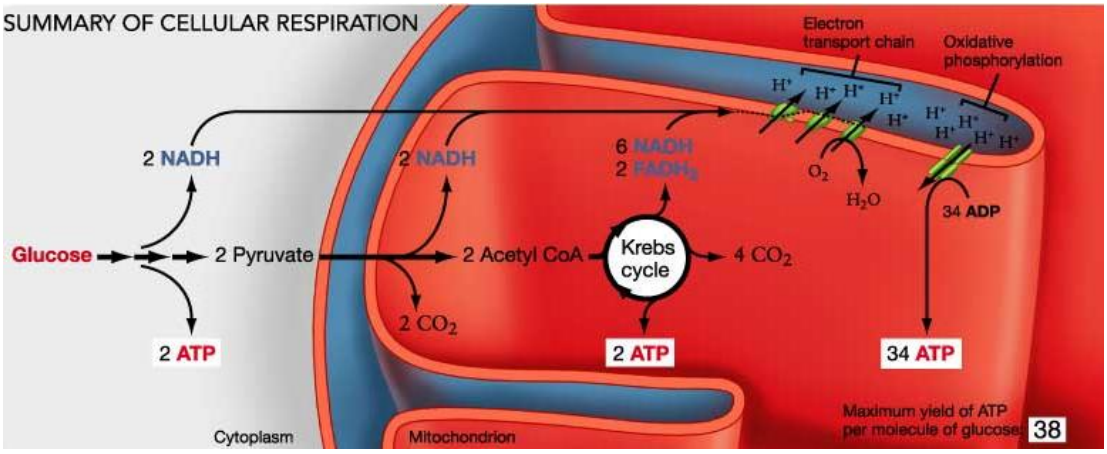

Figure 4 - The link between glucose and ATP.[23]

1.4 The electron transport chain

The electron transport chain is the series of complexes in which enzymes allow electron transfer from NADH and $FADH_2$ to carriers of successively lower energy, ending in reduction of cytochrome c. This complex is then re-oxidised by molecular oxygen to generate water.[18] The energy liberated in these transfers is used to expel protons from the mitochondrial matrix, generating an increasing charge gradient (chemiosmotic potential) across the membrane until the energy required to expel protons against this gradient exceeds that produced by the reduction of oxygen with NADH (**Figure 5**).[24]

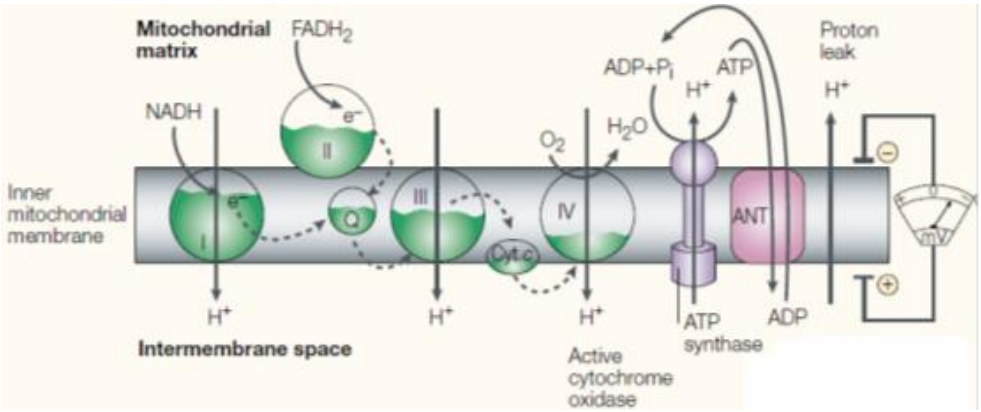

Figure 5 - The electron transfer chain, with the green 'water level' showing the relative electron free energy.[25] Adapted by permission from Macmillan Publishers Ltd: *Nature reviews. Molecular cell biology* Moncada, S.; Erusalimsky, J. D. *3*, 214–20. Copyright 2002.

The complexes of the electron transport chain are all embedded within the impermeable inner mitochondrial membrane, and allow electrons to move via a mixture of redox active mobile electron carriers such as ubiquinone and cytochrome c and quantum tunnelling between metal centres.[26] The physical barrier is vital, preventing the proton concentration equilibrating across the membrane and so allowing different environments to be established in the intermembrane space and the mitochondrial matrix. The charge and concentration difference across the membrane acts as potential energy store. This proton motive force is comprised of a membrane potential of 160 mV a pH difference of approximately half a unit.[27] This electrochemical gradient couples the catabolic electron transport chain to the anabolic process of regenerating ATP from ADP and AMP when it is used to drive ATP synthase in a process termed 'oxidative phosphorylation'.

1.5 Oxidative phosphorylation

Oxidative phosphorylation is catalysed by ATP synthase. This complex is highly conserved and very similar in form and function in all organisms in which oxidative phosphorylation occurs.[28] The membrane bound F_0 portion is associated with proton translocation, and the kinetic energy generated causes rotation of the F_1 subunit in a clockwise manner, catalysing ATP synthesis (**Figure 6**, a).[29] It is estimated that each molecule of ATP synthesised correlates to the translocation of 3-4 protons.[30] The reversible action of ATP synthase allows it to pump protons back out of the mitochondria (**Fig. 6**, b) when the membrane potential has been disrupted.

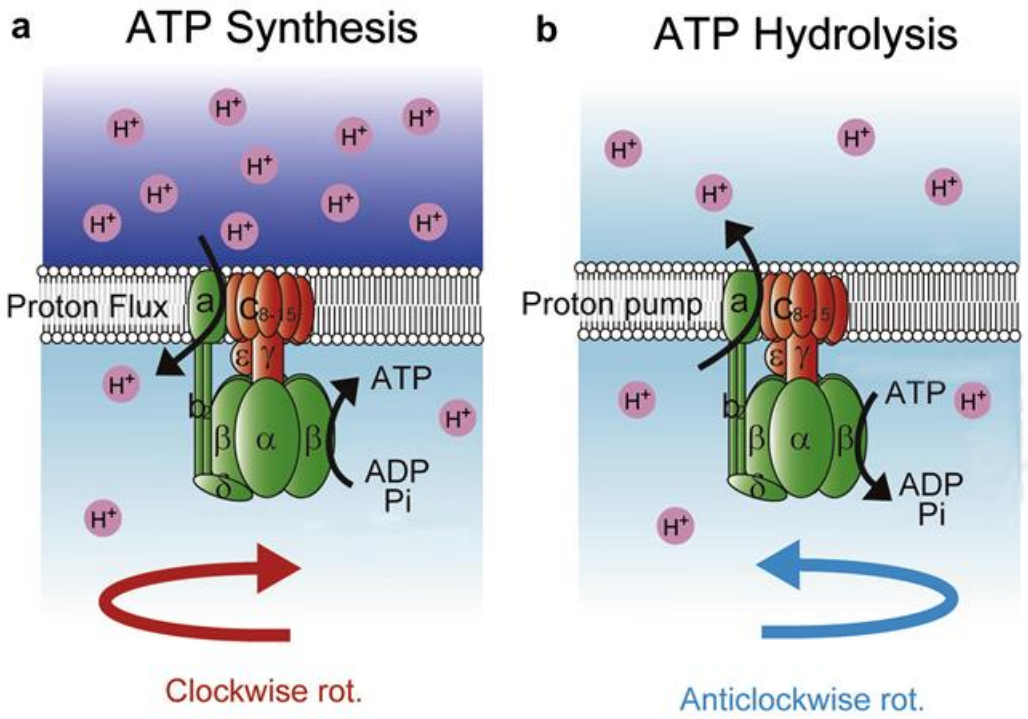

Figure 6 - The catalytic function of ATP synthase.[31]

1.6 Mitochondria in ageing and disease: the importance of reactive oxygen species (ROS)

Given the crucial nature of respiration and the important role played by mitochondria in signalling and homeostasis, it is unsurprising that mitochondrial dysfunction is implicated in many important medical conditions, including cancer,[32] diabetes[33] and mitochondrial myopathies such as ragged red fibre disease.[34] However, many of the most important effects of mitochondrial dysfunction arise indirectly from the generation of reactive oxygen species (ROS).

For many years it has been known that oxygen is both essential for life and toxic,[35] for the same reasons. As a powerful oxidant it plays a fundamental role in being the final destination for electrons from the electron transport chain. Inevitably such a powerful oxidant is also capable of doing considerable damage within the cell. Oxygen levels within tissue are much lower than atmospheric concentrations, and the sites where it is reduced are highly evolved to contain dangerous radical by-products. Even so high concentrations reduce the lifespan of many species and oxidative damage in response to normal atmospheric concentrations is measurable.

Oxidative damage is a major topic in biomedical fields, often implicated in degenerative diseases and illnesses associated with ageing,[36] in addition to various cardiovascular illnesses.[37] Mitochondria are known to be a major source of reactive oxygen species (ROS), with many redox active centres and electron transfer components. Among the most common ROS are superoxide and hydrogen peroxide. Although among the less reactive oxidative species generated, both can be converted by redox active centres to the hydroxyl radical, which reacts with biomolecules at a nearly diffusion limited pace.[38]

1.7 Free radical theory of ageing

Proposed by Denham Harman in 1954, the free radical theory of ageing proposes that the gradual damage which constitutes the ageing process arises ultimately from oxidative damage. Harman extended this in 1972 to suggest that superoxide radicals generated in metabolism are responsible for the most damage, and that maximum lifespan is ultimately determined by the rate of damage to the mitochondrial DNA.[39] The theory is difficult to prove or disprove conclusively and remains a matter of considerable debate, with attempts to provide definitive answers hampered by the complexities of the system studied and the limitations of the tools available to do so.

Chapter 2: Mitochondrial uncoupling and MitoPhotoDNP

2.1 Mitochondrial uncouplers

2.1.1 Endogenous uncouplers

The term 'mitochondrial uncoupling' describes a mechanism which allows protons to leak across the membrane without passing through ATP synthase (therefore uncoupling proton influx from ATP synthesis, **Figure 7**). The transfer of a proton across the electrochemical gradient is accompanied by a loss of potential energy, and where this is not used to drive ATP synthesis such energy is released as heat.

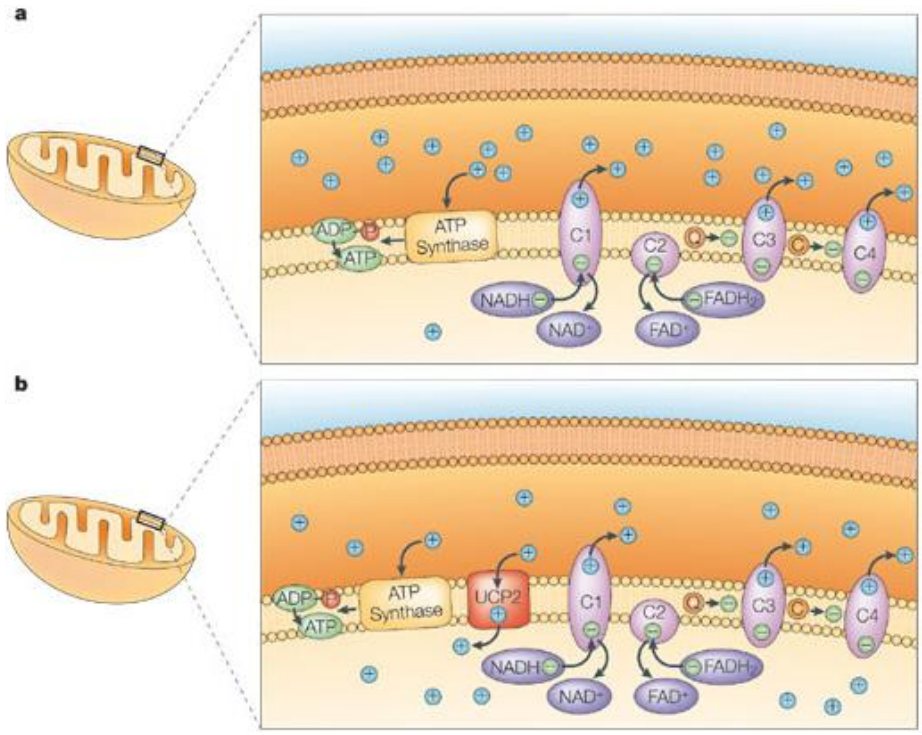

Figure 7 - The electron transport chain with (b) and without (a) uncoupling protein (UCP2) which allows protons to leak across the membrane.[40] Adapted by permission from Macmillan Publishers Ltd: Nat. Rev. Neurosci. Andrews, Z. B.; Diano, S.; Horvath, T. L., *6*, 829-40, **2005**. Copyright 2005.

Uncoupling is a naturally occurring phenomenon, and generating heat (hence maintaining homeostasis) is one important role. Another is to reduce the electrochemical gradient, and this impacts a range of other variables. The class of proteins involved (UCPs) have also been shown to be involved in fatty acid metabolism, insulin production and neuron function[40] and are believed to have other roles.[41] The uncoupling proteins have a specific role in regulation of the influx of calcium ions (an important signalling species within cells, **Chapter 11**) into mitochondria, via their ability to regulate membrane potential. By reducing mitochondrial membrane potential calcium influx is retarded or reversed and resulting cell death can be prevented.[42]

Reduction of the membrane potential is also important in limiting generation of ROS. These are caused by electron leakage from the electron transport chain to nearby molecular oxygen, generating the superoxide radical ($O_2^{\cdot-}$) which is catalytically converted to a mix of molecular oxygen and hydrogen peroxide (H_2O_2). Superoxide (and hence hydrogen peroxide) formation is

dependent on membrane potential.[43] Limited uncoupling as provided by the UCP proteins can therefore protect against oxidative damage (**Figure 8**).

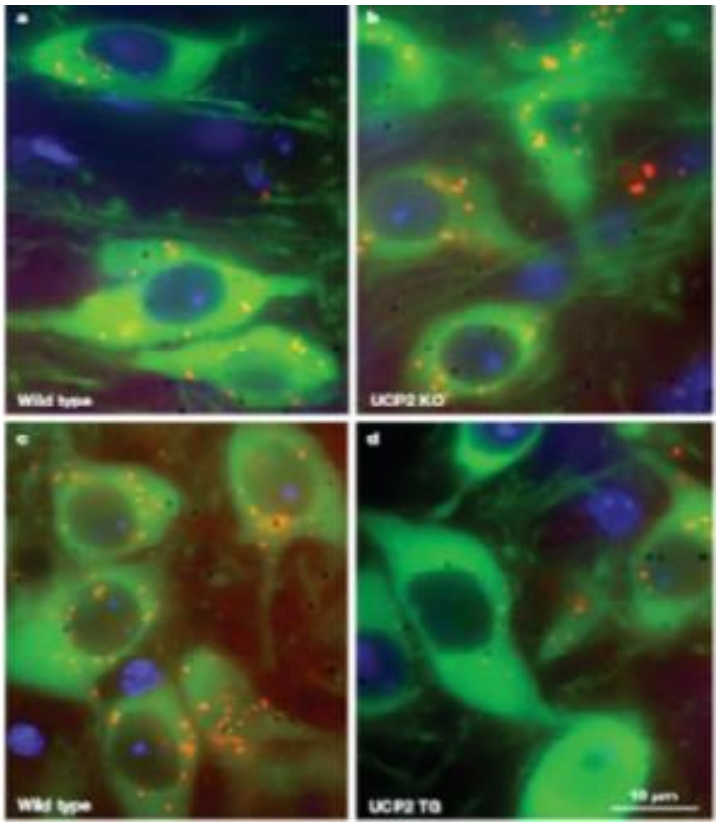

Figure 8[44] - Photomicrographs comparing tyrosine hydrolase neurons (green) wild type (a) and without UCP2 (b). ROS shown by red staining (ethidium, b). Higher exposure to the dye (c, d) compares wild type (c) with a transgenic cell containing human UCP2 (d). Republished with permission of the Society of Neuroscience from "Neurobiology of Disease Uncoupling Protein-2 Is Critical for Nigral Dopamine Cell Survival in a Mouse Model of Parkinson's Disease", Zane B. Andrews, Balazs Horvath, Colin J. Barnstable, John Elseworth, Lichuan Yang, M. Flynt Beal, Robert H. Roth, Russell T. Matthews, and Tamas L. Horvath, 25, 1, **2005**. Permission conveyed through Copyright Clearance Center, Inc.

2.1.2 Synthetic uncouplers

Uncoupling proteins are vastly complex proteins with very specific functions, but it is possible to reproduce the mitochondrial uncoupling with much simpler molecules. There are several mechanisms by which this can be done, and the simplest is direct proton cycling. The requirements are simple; the uncoupler must have a protonated form and a non-protonated form with a Pka close enough to 7 for a significant amount to be in the protonated form in the intermembrane space and the non-protonated form in the matrix. Any prospective uncoupler must also be able to cross the inner mitochondrial membrane in both its protonated and non-protonated forms (so the non-protonated form should be uncharged or heavily delocalised) and prove resilient enough to have a sustained effect. Several of the most commonly used uncouplers are shown below (**Fig. 9**)

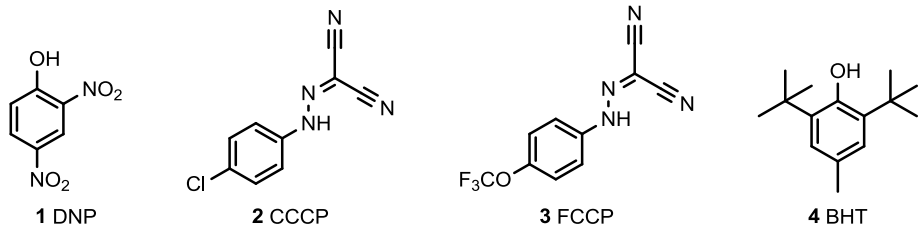

Figure 9 - A selection of common mitochondrial uncouplers.

Of the compounds shown (**Fig. 9**), 2,4-dinitrophenol **1** (DNP) is perhaps the best known. The compound itself is a weak lipophillic acid (pKa = 3.96),[45] and is partially protonated in the space between the inner and outer mitochondrial membranes. Upon crossing into the matrix (resting pH ~ 8)[46] the DNP is deprotonated, leaving a DNP anion **5** (**Fig. 10**). Aromaticity and conjugation with the nitro groups make the negative charge delocalised and diffuse, so it does not prevent the anion crossing the membrane. DNP uncouples directly via proton cycling and has a narrow therapeutic window, causing hyperthermia in the case of a large dose.

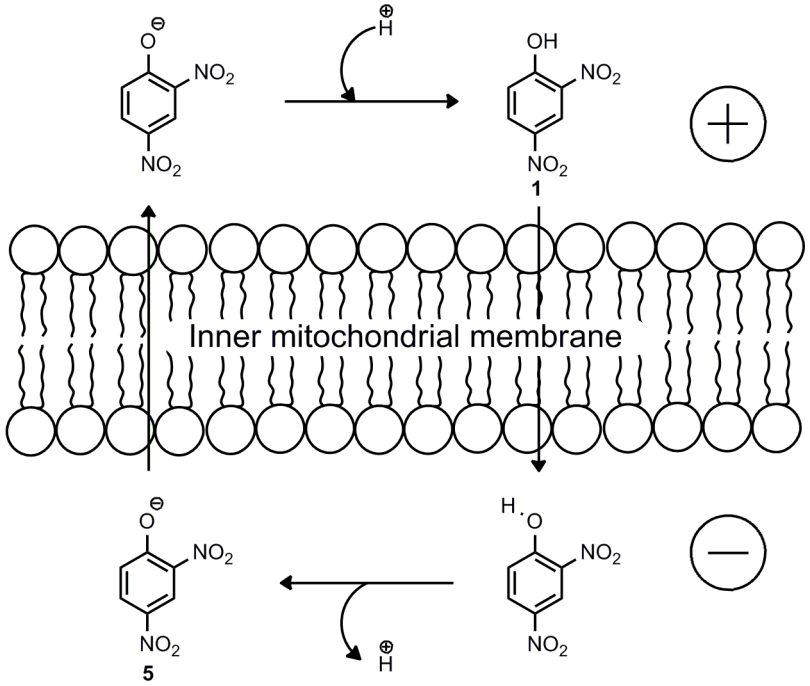

Figure 10 - DNP uncoupling of mitochondria by proton translocation.

Carbonyl cyanide *m*-chlorophenylhydrazone (CCCP) **2** and carbonylcyanide-*p*-trifluoromethoxyphenylhydrazone (FCCP) **3** are similar in both structure and function, with pKa of ~ 6.0 and 6.2 respectively.[47,48] In each case the acidic proton is the secondary amine attached to the aryl group. The deprotonation of CCCP **2** brings the entire molecule into conjugation, delocalising the charge over a large electronic surface and resulting in only a diffuse charge (**Scheme 1**). This allows $CCCP^-$ **6** to cross membranes.

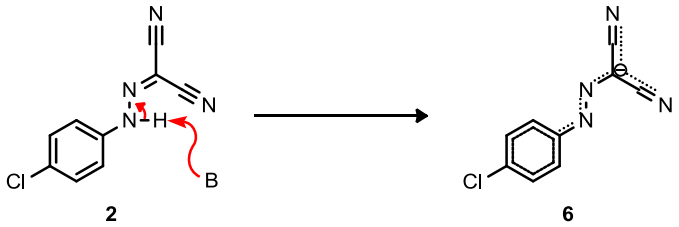

Scheme 1 - Charge delocalisation upon deprotonation of CCCP **2** to give $CCCP^-$ **6**.[49]

Butylated hydroxytoluene (BHT) **4**, works somewhat differently from DNP and FCCP. At low concentrations BHT induced uncoupling is through interaction with adenine nucleotide translocase (ANT)[50] through an unknown mechanism to uncouple the mitochondria. This pathway has a limited capacity, and produces weak uncoupling even when fully activated. This ANT dependent mechanism is not unique to BHT **4**; benzoic acid uncouples only through this mechanism. DNP **1** and CCCP **2** appear also to activate this pathway but this is overshadowed by their proton cycling properties, which are far better than BHT **4** and mask the effects of the ANT pathway. At higher concentrations BHT produces additional uncoupling through the proton cycling mechanism used by DNP **1**, CCCP **2** and FCCP **3**. The effect of combining a poor proton cycler such as BHT with the ANT mechanism is to give concentration dependent uncoupling over a much wider range of concentrations.[44]

Although the criteria for an effective uncoupler appear specific, some of these requirements (membrane permeability for polar molecules) are requirements of drugs in general, and compounds designed for other uses can act as uncouplers. DNP itself was not used for this purpose until many years after discovery,[51] and nimesulfide,[52] a non-steroidal anti-inflammatory drug, is another example. There are some possibilities for uncoupler design which better take advantage of the peculiar properties of mitochondria; in particular the membrane potential which drives ATP synthesis.

2.2 Targeted photoactivated uncoupler design

Our aim was to use the membrane potential to target a caged uncoupler to the mitochondria and then release it by irradiation with light. Thus, combining mitochondria targeting and a photolinker could allow selective mitochondrial accumulation and photorelease of an uncoupler. This would allow a small dose of inactive caged uncoupler to accumulate at the mitochondrial membrane and then be selectively activated. The caged uncoupler could be useful for temporal and spatially resolved studies on the mitochondria with imaging techniques. DNP **1** was chosen as the uncoupler in the caged uncoupler MitoPhotoDNP **7** (**Scheme 2**); its advantages include its properties being well characterised, the compound stable and the uncoupling kinetics relatively simple. Targeting would be achieved using a lipophilic cation, and alkyltriphenylphosphonium group (TPP). Photoactivated release of a phenol from an *o*-nitrobenzyl linker is quite well known and efficient and the synthesis not intrinsically difficult. Therefore this photolinker was chosen on the basis that it should be easy to link with the other components of the molecule and *o*-nitrobenzylic group is tolerant of a wide range of groups and substituents. An added advantage for both DNP and *o*-nitrobenzyl is that both have been used heavily in the past, potentially providing a lot of directly comparable data for both uncoupling studies and photocleavage. The TPP targeting group and the photolinker will now be discussed in detail.

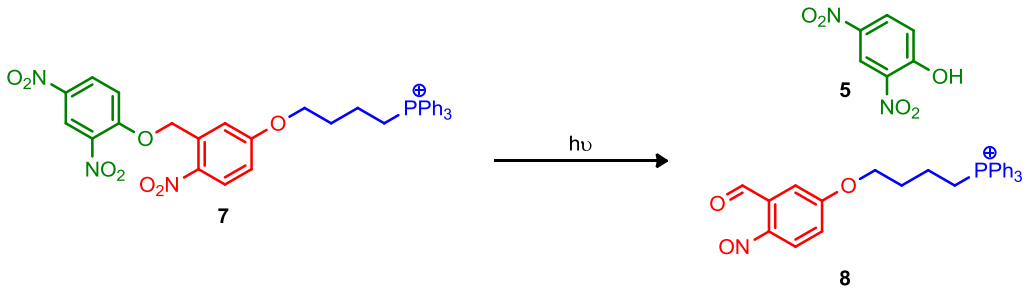

Scheme 2 - MitophotoDNP target **7**. The caged uncoupler, *o*-nitrobenzyl linker and the TPP targeting group are colour coded.

2.3 Lipophillic cations

Cell membranes are composed of lipids, with polar groups on the surface interacting with water molecules and long saturated alkyl chains within the membrane. Simple membranes self-assemble, as water-alkyl interactions are weaker than those between water molecules and charged groups or other water molecules, and so the molecules assemble in order to give the arrangement with minimal contact between water and lipophilic groups. Compounds added to the system will be found in equilibrium between the aqueous cytoplasm and hydrophobic membranes, with the position of this equilibrium determined by the properties of the compound. The equilibrium constant is expressed as a partition coefficient. A drug or probe will generally have to diffuse through several layers of each environment, so a compound which splits reasonably evenly between the two media is usually preferred for these. Because the probe molecules are diffusing in this manner they will generally be found in places other than their target, and this dispersion is accounted for in dosing.

If the drug or probe target is within the mitochondrial matrix or inner mitochondrial membranes then the charge gradient across the inner mitochondrial membrane provides an opportunity to concentrate compounds in the inner mitochondrial membrane or matrix.[53] Cations that are able to diffuse across the inner membrane will accumulate in accordance with the Nernst equation.[54] The primary difficulty with such an approach is that highly charged or polar compounds often struggle to get through membranes, and molecules targeted at inner mitochondrial processes need to diffuse through a number of these. As such, a very hydrophilic compound is unlikely to reach its target. Fortunately charged groups with diffuse charges stabilised by resonance or induction have less favourable interactions with water and are therefore more lipophilic. Alternatively, cations could be attached to otherwise very hydrophobic groups or molecules in order to balance out the effect of the cation. These effects can be modelled as giving the ion a large hydrophobic surface.[55]

Organophosphonium cations, particularly those with large lipophilic groups insulating the charge, are a good choice for targeting groups and there is literature precedence for use of alkyltriphenylphosphonium (TPP) groups for this purpose.[56] Previous studies have shown that the phosphonium group itself integrates into the membrane surface, but is also able to travel through it (**Fig 11**).[53]

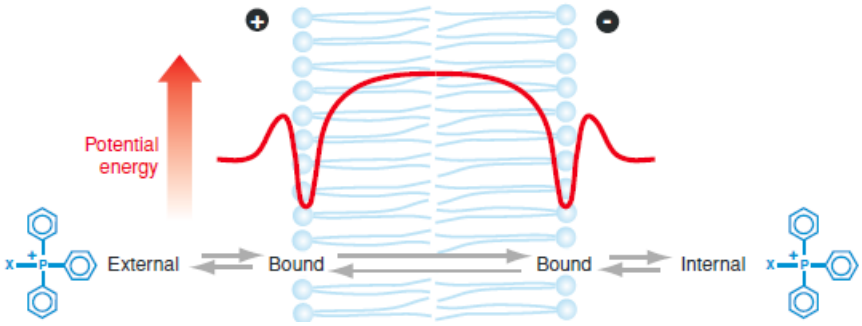

Figure 11 - Potential energy diagram for a lipophillic cation crossing a membrane.[53] Republished with permission of Annual Reviews, Inc, from "Targeting Antioxidants to Mitochondria by Conjugation to Lipophilic Cations", Murphy, M. P., & Smith, 47, **2006** permission conveyed through Copyright Clearance Center, Inc.

As a result concentrations on membranes surfaces are high but within the membrane the concentration is much lower, although a long alkyl chain between the charged head group and an attached drug may allow the active part of the drug to accumulate deeper in the membrane.[53] Bioactive organic molecules bearing TPP groups accumulate several hundred-fold in the mitochondrial matrix. Furthermore, one such compound, MitoQ, has been taken orally by patients in Phase II clinical studies for up to 1 year without problems, so TPP is well validated for biological use.

2.4 Photolinkers

The difficulty with such a targeting strategy is that the TPP ions will inhibit the proton cycling if attached to an uncoupler. This was an issue with MitoDNP **9** (**Figure 12**).[50] One way to overcome

this problem is to use a connection between the two components which can be broken by specific stimuli.

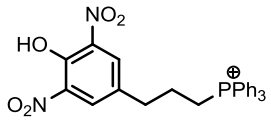

9

Figure 12 - MitoDNP[50]

Selecting the stimulus in question is challenging; the mitochondria is integrated with the biochemical pathways of the cell in a vastly complex manner not yet fully understood and as such it is difficult to find a stimulus which will break up a linker without impacting surrounding systems. One strategy is to use a photolinker, which can be cleaved on application of relatively intense light of specific wavelength. A laser beam can provide the correct energy to a small area of the cell where the targeted uncoupler is present. The wavelength specific nature of photoexcitation means that cellular components caught within the beam are unlikely to be very badly damaged if the photolinker is designed to cleave at a wavelength different from those which excite groups in proteins, lipids and sugars.

Design considerations for photolinkers are outlined by Adams and Tsein,[57] for whom the following properties are vital: the attached molecule should be unreactive when linked (or 'caged'), the molecule should be released in high yield and sufficiently quickly by wavelengths of light non-detrimental to the biological system used, and any side products generated should be both unreactive and unable to interact with the biological system. A small selection of photolinkers extensively used are shown below (**Fig. 13**).

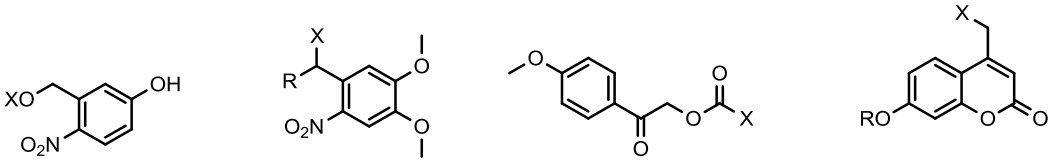

10 **11** **12** **13**

X = caged group R = H or alkyl

Figure 13 - A large range of photolinkers are used.[57,58,59,60] The selection presented is comprised of *ortho*-nitrobenzyl derivatives **10**, the related DMNPE analogues **11**, phenacyl ethers **12** and coumarins **13**.

Some common features are apparent; all have highly conjugated and mostly rigid structures. Either of these properties could be coincidental as rigid structures tend to be highly conjugated and vice versa, but in reality both are important. UV absorption (usually the wavelength region used for ease of handling) is typically high among conjugated, aromatic compounds, and a molecule with a rigid excited state will relax to ground state less easily due to Condon's rule (the limited geometries available restrict transitions available into lower energy levels). Many of the molecules are polar and some have highly polar excited states. Most are incapable of acting as acids or bases under physiological conditions. This is good as pH dependence would greatly complicate calculations of quantum yield and effective use.

Probably the most commonly used photocleavable linker is the *o*-nitrobenzyl group, which is optimally excited at 265 nm. A number of variants exist with a benzylic proton replaced. A general scheme for the photocleavage of such compounds is outlined below (**Scheme 3**).

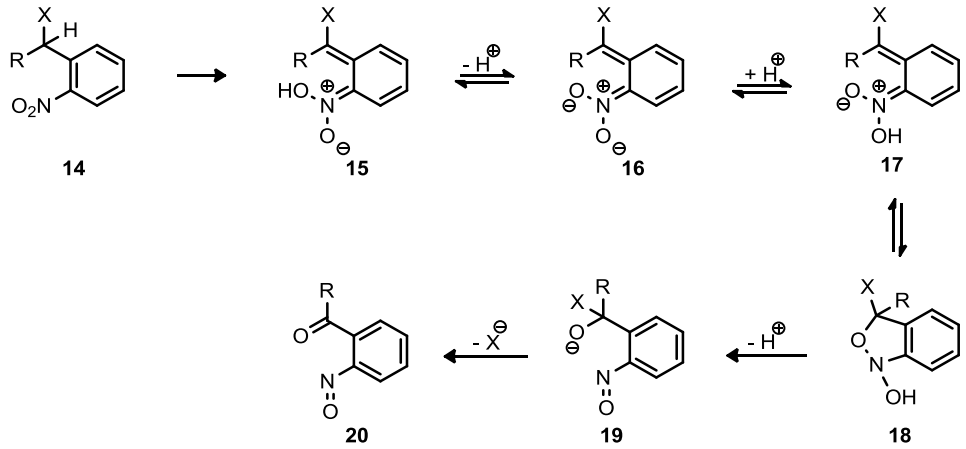

Scheme 3 – General photocleavage of *o*-nitrobenzyl compounds.[61]

The photoreaction starts with proton transfer to the nitro group in the excited state, at this point generating 2 geometrical isomers of the intermediate **15** if R and X are not identical. A proton is then transferred between the oxygens on the nitro group, giving **E** or **Z** *aci*-nitro intermediates **17** which can be observed and distinguished from one another, before forming a cyclic benzisoxazoline **18**. Both isomers then decay through cyclic state **18** into nitroso compound **19** which loses X to form the carbonyl **20**.

o-Nitrobenzyl groups have several advantages, such as being compatible with the functional groups for which photolinker are commonly used,[64] including primary amines which work poorly with other linkers. They are relatively easy to make and have reasonable photochemical properties,[62] which are unfortunately influenced by substituent, pH, solvent polarity and a host of other environmental factors.[55] A major advantage of these compounds is that their kinetic behaviour is relatively well understood and characterised. The disadvantage of *o*-nitrobenzyl derivatives is the undesirable reactivity of the nitrosobenzaldehyde products **20**.[63] DMNPE (**11**, R = Me) is an *ortho*-nitrobenzyl analogue with a longer photocleavage wavelength (365 nm), highlighting the impact of the methoxy groups adding electrons to the ring system. The release mechanism is analogous to that of other *o*-nitrobenzyl compounds.

Phenacyl ester derivatives such as **12** (**Fig. 13**) are used specifically where a carboxylic acid cleavage product is desired, and produce these in good yield and purity with a range of substrates.[64] These groups can also be used on phosphates[65] to good effect. They display high solubility in water and have been used as a photolinker in biotin/avidin systems.[66] 4-Methoxyphenacyl **12** is optimally excited at 280 nm, but can be excited at higher wavelengths.[50] High quantum yields are achieved for suitable substrates, and cleavage can be very fast.[64]

The final group listed in **Figure 13** are coumarin based. Low quantum yields are observed for carboxylic acids, but results are reasonable for uncaging cAMP and cGMP,[67] and amines can also be caged. Coumaryls can also be used to release sulfates,[67] alcohols and diols. The advantages of coumaryl chromophores is the high wavelength absorption maxima which are very substituent dependent, but can extend into the visible region. The group also gives rise to a fluorescent by-product, and gives fast release with the potential for two-photon excitation.

2.5 Iodo MitoPhotoDNP 7-I synthesis

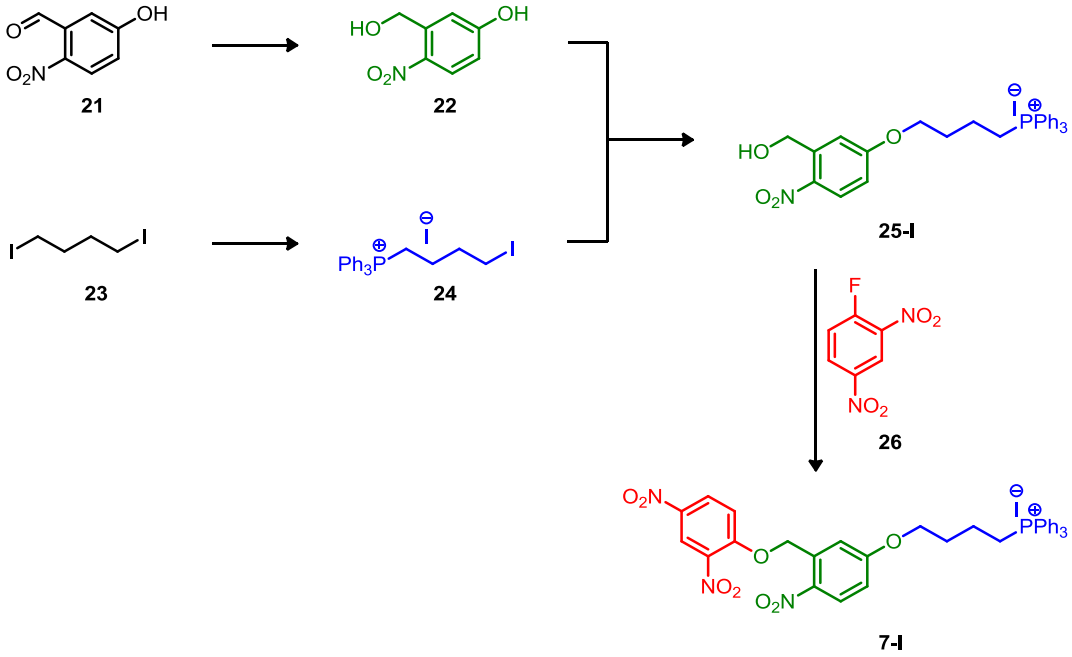

Scheme 4 - Overview of the route to MitoPhotoDNP.

The planned synthetic route to MitoPhotoDNP **7-I** uses a convergent synthesis following previous work within the group (**Scheme 4**).[68] The *ortho* nitrobenyl photocleavable group **22** (green) and the mitochondria targeting triphenylphosphonium salt **24** (blue) are prepared and linked to form phosphonium iodide salt **25-I** prior to addition of the DNP uncoupling moiety to form MitoPhotoDNP iodide **7-I**. Caroline Quin had previously prepared MitoPhotoDNP by the same route except that an alkyl bromide had been used instead of alkyl iodide **24**.[68] Her last two steps had suffered from low yields and more compound was required for testing.

In my hands, the commercially available benzaldehyde **21** was reduced to benzylic alcohol **22** using $NaBH_4$ in MeOH in high yield (**Scheme 5**).

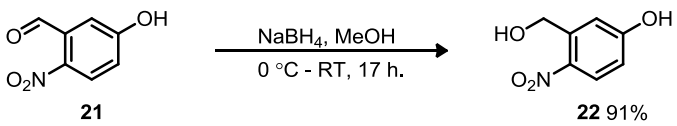

Scheme 5 - Reduction of benzaldehyde **21**.

The TPP iodide targeting group and linker was synthesised by substituting an iodide from 1,4-diodobutane **23** with triphenylphosphine, taking advantage of the poor solubility of charged

groups in PhMe to precipitate the TPP salt and give only the monosubstitution product **24** (**Scheme 6**).

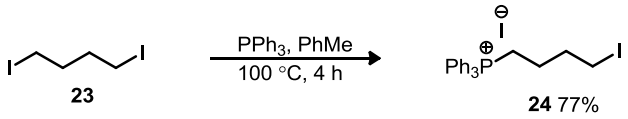

Scheme 6 - Targeting group synthesis

The phenol **22** and targeting group **24** were then coupled under basic conditions (**Scheme 7**) to give phosphonium salt **25-I**. Initially coupling in MeOH was problematic, with the difficulty of separating multiple phosphonium salt products exacerbated by the product proving unstable on silica. Switching the reaction solvent to dry MeCN and increasing the number of equivalents of phenol **22** from 1 to 1.7 resulted in near quantitative coupling.

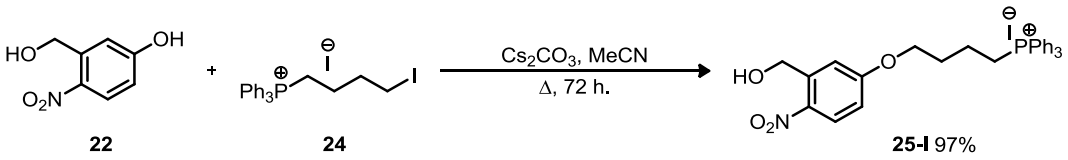

Scheme 7 - Coupling of the photoactivated and targeting groups

The final step of the synthesis was an S_NAr comprising attack by the benzylic alcohol **25-I** onto 1-fluoro-2,4-dinitrobenzene **26** under mild conditions (**Scheme 8**).

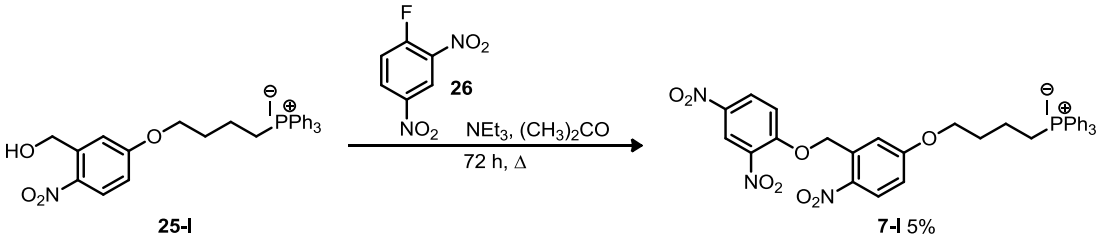

Scheme 8 - Addition of DNP uncoupling moiety.

The 1-fluoro-2,4-dinitrobenzene substrate **26** is ideal for this reaction as the *ortho* and *para* nitro groups stabilise the transition state leading to the Meisenheimer complex intermediate. Since the initial nucleophilic addition to generate this intermediate is usually the rate determining step, the highly electronegative fluorine also stabilises the transition state leading to this formal carbanion. Three solvents were tested for this transformation, with acetone proving the most effective, giving high conversion. The low solubility of phosphonium salt **25-I** hindering reaction in Et_2O, and MeCN gave a complex mixture of side products. Chromatographic purification proved challenging, with the MitoPhotoDNP iodide **7-I** eventually isolated in low yield.

2.6 MitoPhotoDNP Tetraphenylborate Salt synthesis

Following the difficulties experienced with the iodide salt **7-I**, the more crystalline tetraphenylborate salt was synthesised as an alternative (**Scheme 9**).

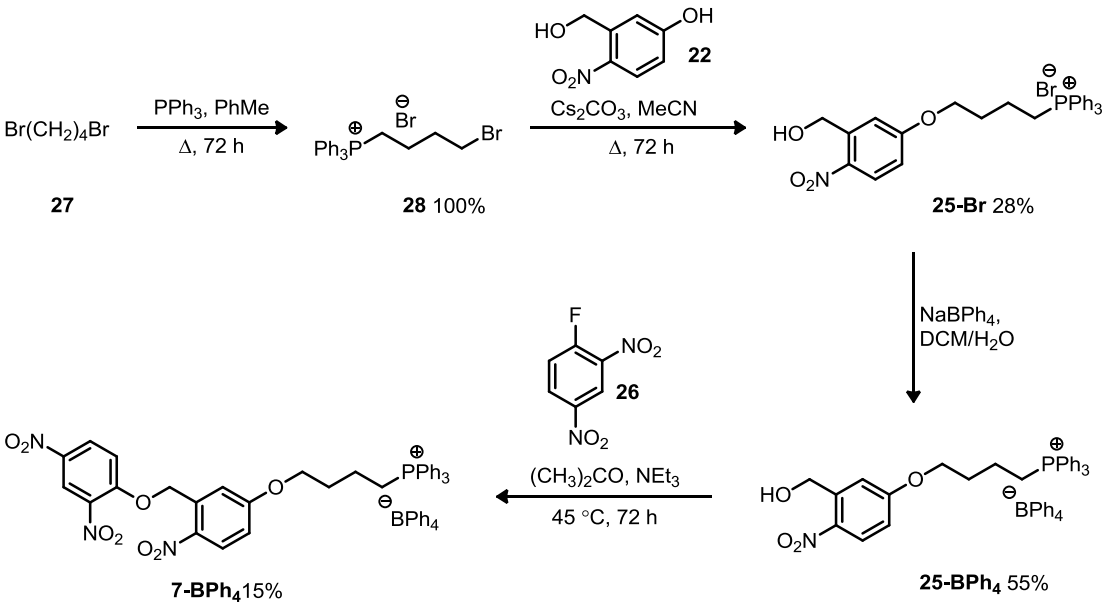

Scheme 9 - Tetraphenylborate synthesis.

The first two steps gave the same products as previously isolated by Caroline Quin. Using dibromobutane **27** substitution is significantly slower than using diiodide **23** due to the poorer leaving group but also higher yielding. The bromide **28** was coupled to phenol **22** to give alcohol **25-Br** then converted to the tetraphenylborate salt **25-BPh$_4$** prior to DNP addition to give MitoPhotoDNP tetraphenyl borate salt **7-BPh$_4$,** which crystallised following column chromatography. Unfortunately Dr Murphy's group in Cambridge showed that with this counterion MitoPhotoDNP is too hydrophobic and insoluble for uptake testing.

2.7 Alternate routes and variant compounds

Several alternate routes were investigated to circumvent the purification difficulties experienced in the synthesis of MitoPhotoDNP iodide **7-I**. The *p*-xylyl linker was considered on the assumption that the more rigid final product would prove easier to purify, and substitution at the benzyilc sites would be facile. Consequently, xylyl bromide **29** was converted into phosphonium salt **30**. However a complex mixture resulted from the attempted coupling to the *o*-nitrobenzyl group to give triphenylphosphonium bromide **31** (**Scheme 10**).

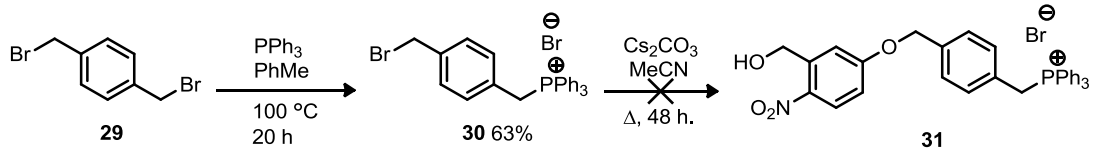

Scheme 10 - Attempted synthesis of more rigid p-xylyl derivative.

2.8 Uptake Testing

MitoPhotoDNP iodide **7-I** was tested for mitochondrial uptake by the group of Dr Michael P. Murphy (MRC, Cambridge), with the results shown below (**Figure 14**).

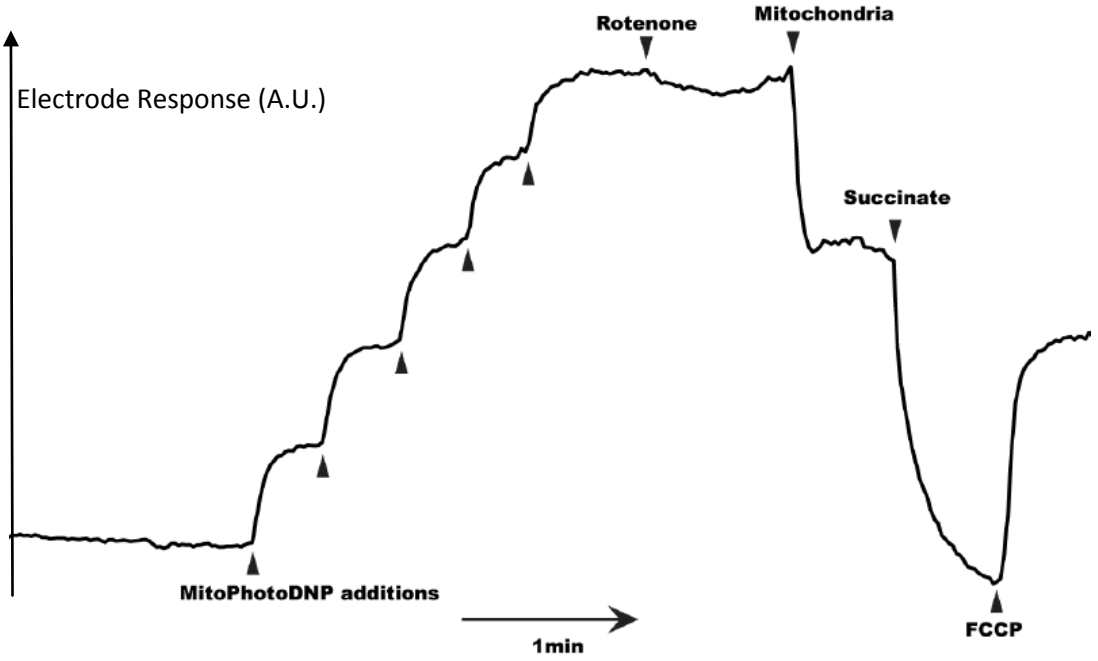

Figure 14 - Electrode response to the uptake of MitoPhotoDNP.

The response of an electrode selective for the triphenylphosphonium cation[69] is shown on the y-axis. Using an appropriately buffered solution at pH 7.2 and 37 ˚C, five sequential additions of MitoPhotoDNP allowed calibration of a linear response. Next Complex I of the electron transport chain was inhibited by addition the of pesticide rotenone,[70] which prevents development of a membrane potential in the rat liver mitochondria subsequently added. This means the decrease in electrode response can be attributed solely to MitoPhotoDNP accumulating by diffusion and partitioning into the membranes of the mitochondria. Succinate is then added to stimulate Complex II (succinate dehydrogenase), which is part of both the Krebs cycle and the electron

transport chain. This and bypasses the blockage of Complex I by rotenone. The electron transport chain begins to function and the electrode response then drops as most of the remaining free MitoPhotoDNP partitions into the mitochondrial matrix. The final addition of FCCP **3** (**Fig. 3**) uncouples the mitochondria eliminating the membrane potential, causing free MitoPhotoDNP concentrations to return towards the previous equilibrium position. The process is only semi-quantitative and drift means that the minimum prior to addition of FCCP **3** and the restored levels following FCCP **3** addition are lower than expected.

2.9 Effectiveness in cells

Following the successful demonstrations of mitochondrial uptake a post-doc in the group, Dr Stuart Caldwell, developed an efficient route to the MitoPhotoDNP bromide. Susan Chalmers from the group of Prof. John G. McCarron then tested MitoPhotoDNP bromide salt **7-Br** in colonic smooth muscle cells (**Fig. 15**).

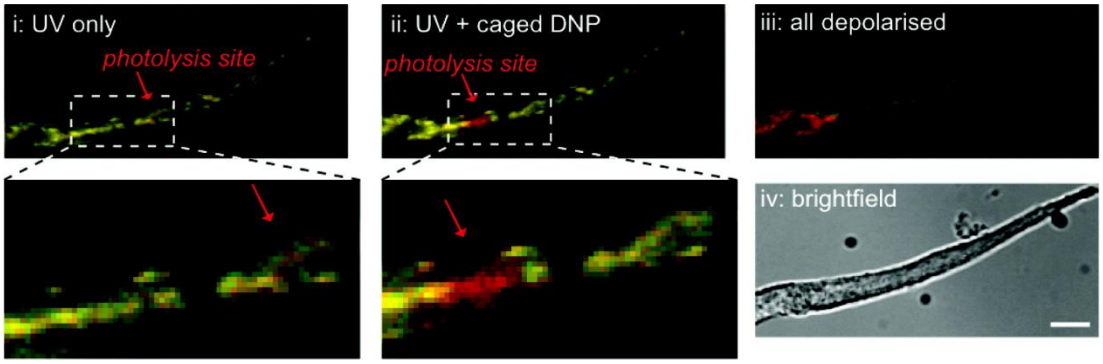

Figure 15[71] - Photolytic uncoupling of mitochondria in a whole cell - colours are artificial.

The cells were loaded with tetramethyl rhodamine ester (TMRE), a fluorescent dye which is dependent on membrane potential.[72] Panel **i** shows the effect of brief UV laser irradiation (355 nm for 85 ms) in the absence of MitoPhotoDNP **7**. 200 nM of MitoPhotoDNP **7-Br** was added and allowed to equilibrate. The same irradiation protocol was then applied (panel **ii**), with a loss of TMRE fluorescence shown in red at the site of photolysis. Rotenone and oligomycin were added resulting in total depolarisation (panel **iii**). The cell without colouring is also shown (panel **iv**). These results (in conjuction with appropriate controls) proved the effectiveness of the probe, and the work was subsequently published.[71]

Chapter 3: Design of a selective, quantitative superoxide probe

3.1 Types of small molecules probes used to study metabolism

3.1.1 Introduction to different types of probe

Limited information can be acquired from looking at the anatomy of cells, and the native chemical species are often engaged in multiple different pathways. The difficulties are exacerbated by the necessity of studying transient species and situations where a single species may engage in many processes dependent on timescale and concentration.[73] The obvious solution to understanding a complex system is to break it down into smaller parts, such as single pathways or cascades. One way to do this is to induce effects via mechanisms alien to normal cellular chemistry, or to measure an artificial species known to behave in a particular way. In essence, this is the role of the small molecule probe.

Various elaborate designs abound,[74] and 'chemical probe' is a descriptive rather than prescriptive term so over definition must be avoided, but some categorisation is possible. In particular, the distinction should be made between probes used to validate drug targets[75,76] and those used to interrogate cellular chemistry.[74,77,78] The latter are the focus of the following discussion. It should be noted that the term 'small molecule probe' can apply to any species significantly below the masses of biological polymers such as protein and RNA strands, including some molecules which are very large by the usual standards of a synthetic chemist, and covers any conceivable sensing or reporting mechanism. Some general points can be made relating to their design nonetheless.

There are two essential functions any such probe must display. These are sensing, the interaction which allows the species or phenomena being studied to be recognised by the probe, and reporting, any process by which a sensing event can be recognised by the investigator. Additionally, with the occasional exception[79] the response of probes to stimuli can be described as reversible, as in the case of ion chelators, or irreversible, usually where a chemical bond is formed.

Some of the same considerations applied in medicinal chemistry are important in probe design. Any probe intended to diffuse through the cytosol must have appropriate *solubility*, for example. Fortunately the requirements with respect to these properties are much less stringent than for drugs. Many probes are applied to cells or small fragments of organisms, and with techniques such as patch clamping not even membrane permeability is required. *Toxicity* is only a concern in so far as it occurs during the time course of the measurement. In order to reach the desired species on which it is to report a probe must have appropriate *stability*. Stability is contextual; a probe need only survive long enough to be useful. Often stability is related to *selectivity* for reaction with a particular species, especially in the case of irreversible reaction. However, selectivity might also be used to refer to different binding affinities for different ions. *Kinetics* is important and restricts the ability of the probe to report on dynamic and transient events. *Sensitivity* needs to be appropriate to the concentration of the species measured. Finally, in many cases it is desirable to *localise* probe distribution, to a particular compartment within the cell. To

better illustrate the interplay of these factors examples are described in the following sections (**3.1.3** - **3.1.6**). First, a brief explanation of fluorescence and associated phenomena is required.

3.1.2 FRET, PET and fluorescence[94,80]

Many probes use fluorescence as a reporting mechanism. Excitation is caused by absorption of a photon corresponding to the difference between ground and excited state energies, leading to the promotion of an electron between levels corresponding to molecular orbitals (**Figure 16**). Within these energy levels numerous rotational and vibrational levels exist. The 'S' and 'T' markers refer to 'singlet' and 'triplet', the spin states of the system, which are maintained on initial excitation. UV absorption results in the $S_0 \rightarrow S_x$ transition, with excitation to S_2 or higher not forbidden. Fluorescence refers to a spin allowed relaxation to a lower energy state by emission of a photon through the lowest vibrational level of S_1 to S_0. This is because fluorescence is slow compared to relaxation through vibration or internal conversion. As the rate of stimulated emission is proportional to the cube of emission frequency, only relatively high energy transitions occur in this fashion, and so $S_2 \rightarrow S_1$ is less likely to be fluorescent.

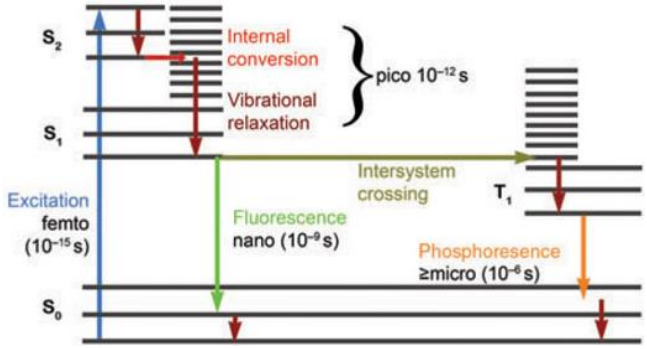

Figure 16 - Jablonski diagram. Reprinted by permission from Macmillan Publishers Ltd: Nature Methods, Lichtman and Conchello 2005, copyright 2005.[80]

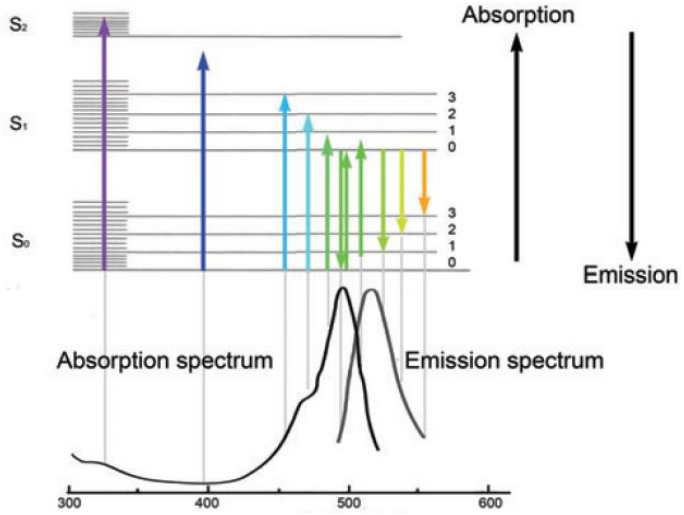

Figure 17 - The origin of absorption and emission ranges. Reprinted by permission from Macmillan Publishers Ltd: Nature Methods, Lichtman and Conchello 2005, copyright 2005.[80]

Although fluorescent relaxation is from the lowest energy S_1 level, higher vibrational or rotational energy levels may receive the electron prior to further non-radiative relaxation. Likewise, excitation can be to any rotational or vibrational level, and so a range of wavelengths are

absorbed and emitted, although each individual event corresponds to a transition of precise energy (**Figure 17**).

Many of the same considerations relevant to photo uncaging groups (**Section 2.4**) apply also to fluorophore design. In particular, UV absorption energies usually correspond to $\pi \rightarrow \pi^*$ transitions and so conjugated systems have the correct energies. Particularly in extended systems, the conjugation of multiple bonds allows absorption across more of the molecules' surface. These traits lend rigidity, limiting both the overlap of other energy levels which might allow non-radiative and limiting the excited state geometry available for such relaxation (see **Section 2.4**).

Because relaxation can also occur rapidly through interactions with neighbouring molecules, fluorescence has extraordinary environmental sensitivity. This has both positive and negative impacts on its use for detection. In **Figure 18** excitation of an electron from S_0 **32** to S_1 transfers electron density to the nitrogen, delocalising the charge over **33**. This excited species then forms hydrogen bonds with methanol giving a vibrational relaxation pathway which competes with, and quenches, fluorescence. The outcome of this competition, and hence the fluorescence quantum yield, is determined by the acidity of the solvent hydrogen bond. However, the emission wavelength is equally dependent on solvent hydrogen bond acidity and the dipolarity of the system. As a result both variables can be defined from the fluorescence spectra of the compound.[94]

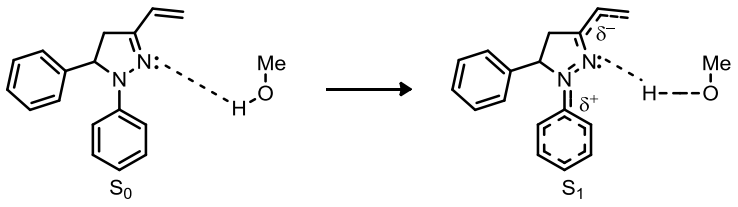

Figure 18 - Excitation of a fluorophore in a polar, acidic environment. Reproduced from de Silva *et al*.[94]

Fluorescence resonance energy transfer (FRET) is a non-radiative energy transfer mechanism by which excitation can be passed from one chromophore to another in close proximity, so long as the emission spectra of the excited donor overlaps with the absorption spectra of the acceptor (**Figure 19**).[81] The distance dependency is r^{-6}, so such mechanisms can be activated by a stimulus which changes the conformation of the molecule, giving a dramatic 'turn on' effect. They can also be used to modulate the wavelength of eventual emission. The first fluorophore can be common among a set of probes, allowing all to be excited simultaneously but with different subsequent emission wavelengths.[82]

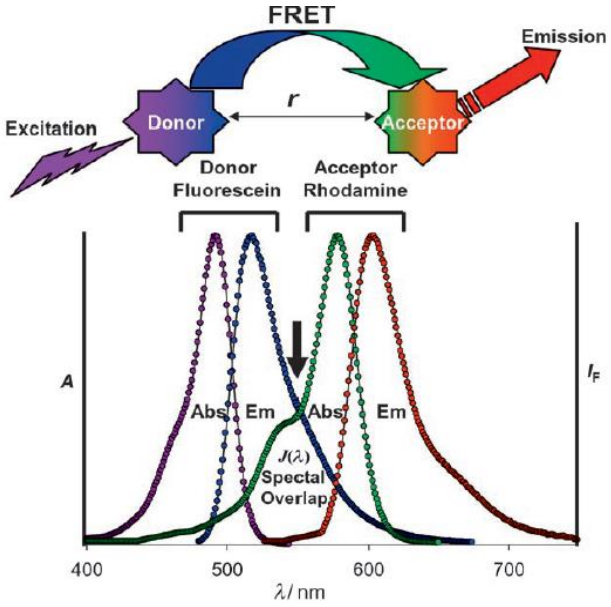

Figure 19 - A typical FRET system, with the required overlap marked by the arrow. Reproduced with permission from Sapsford *et al*.[83]

Photoinduced electron transfer (PET) is a common quenching mechanism utilised in probe design (**Figure 20**).[94] Excitation promotes an electron from the fluorophore HOMO into the fluorophore LUMO. An electron can then be transferred into the fluorophore HOMO from the PET donor HOMO, preventing radiative relaxation into the fluorophore HOMO. Changing the energy levels in such a way as to either make transfer from the donor HOMO geometrically impossible or reducing the energy of this level to make transfer unfavourable will remove the quenching mechanism and allow fluorescence.

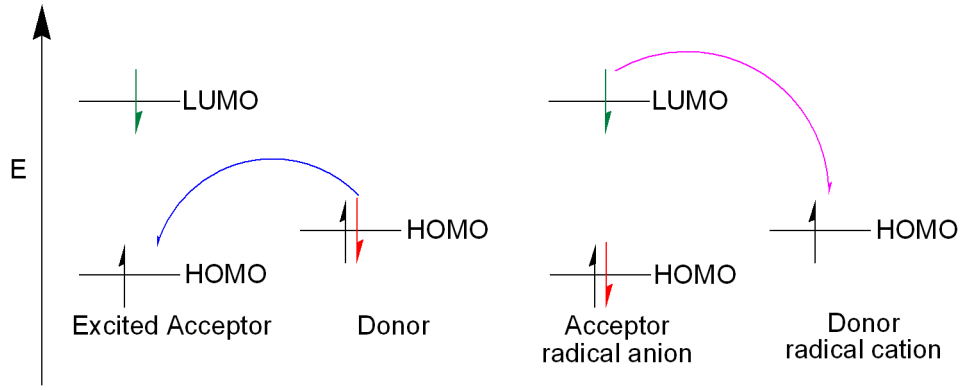

Figure 20 - PET mechanism. Adapted from de Silva *et al*.[94]

For a successful probe the fluorescence emission must change upon the sensor portion interacting with the target species. There are 2 changes likely, change in emission wavelength and change in brightness, and ideally both are desirable. A change in emission or excitation wavelength allows activated and unactivated forms to be separately imaged, and so be observed more accurately, a process referred to as ratiometric imaging. An increase in brightness on binding is preferred: a decrease in brightness also works in principle but in practice the sensitivity of such probes is more limited. Increased brightness helps maximise spatial resolution with light

microscopy, and is also important in order to minimise the quantity of dye required (and hence any disruption it may cause).

3.1.3 Reversible sensing of an abundant endogenous species: Calcium green FlAsH[88]

The first example of a chemical probe involves sensing a vital and abundant species in living cells. The pivotal role of Ca^{2+} ions within and between cells is detailed later (**Chapter 11**), but for the present it is sufficient to understand that it is among the most vital of signalling species, and that transient, localised variations in [Ca^{2+}] are crucial cellular events. Numerous probes exist for the purpose of calcium imaging,[84,85] and green flash (**Figure 21**) was designed specifically to report on transient microdomains of high calcium concentration.[86,88] The arsenic groups allow selective binding to a tetracysteine sequence expressed in specific proteins known to occur close to the phenomenon studied. The soft Lewis acid arsenic atoms bind strongly to the soft Lewis base sulfur atoms of cysteine, and strong binding and selectivity are achieved through the chelate effect, resulting in nearly all expressed tetra cysteine moieties binding fluorophore. Prior to binding the free arsenic groups quench fluorescence through either vibrational relaxation or photoinduced electron transfer (PET),[87] and so the restriction on movement and orbital geometry provided by tethering results in a four-fold increase in fluorescent emission, allowing successful tethering to be confirmed. Binding to Ca^{2+} then causes a further ten-fold increase in fluorescence, presumably restricting one or both of the aforementioned quenching mechanisms in the upper, ion chelating portion of the molecule. Lastly, excitation (488 nm) and emission (approx. 540 nm) are at wavelengths where few biomolecules absorb.

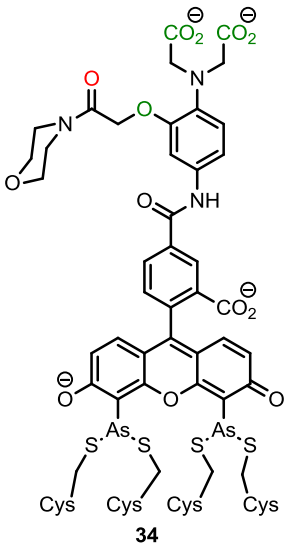

34

Figure 21 - The bound, active form of the calcium green FlAsH probe.[88] The coordination sites are shown in green (APTRA) and red (modified).

The calcium ion sensor component is based on the APTRA pentacoordinate magnesium chelator,[89] known to have low calcium affinity. A carboxylate was replaced with a morpholine amide, reducing the Lewis basicity of the coordination site to improve selectivity over Zn^{2+} (K_d = > 10 mM). Low affinity (K_d = 100 μM) means a greater range of [Ca^{2+}] can be distinguished prior to

saturation, and fast dissociation kinetics allows resolution of multiple events within a short time frame (**Figure 22**).

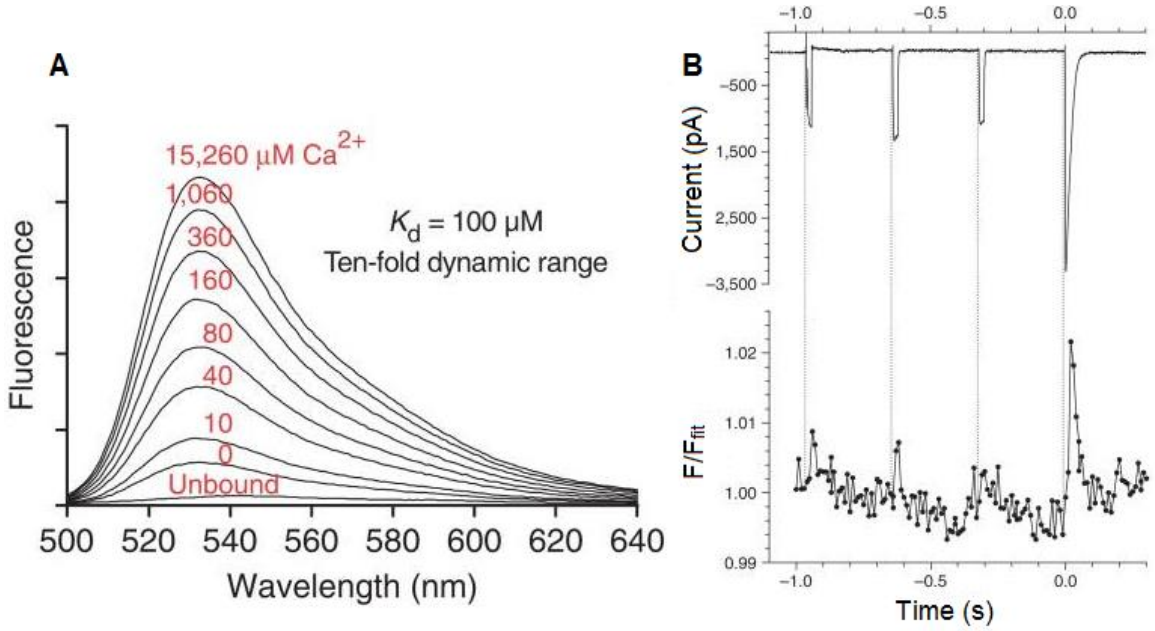

Figure 22 - The dynamic response range (A) and response times (B) demonstrate how low binding affinity produces ideal properties for measuring rapid concentration variations in an abundant species such as Ca2+. Adapted by permission from Macmillan Publishers Ltd: Nature Chemical Biology, Tour, O.; Adams, S. R.; Kerr, R. A.; Meijer, R. M.; Sejnowski, T. J.; Tsien, R. W.; Tsien, R. Y. 3, 423–431, copyright 2007.

3.1.4 Irreversible sensing of a toxic species at low concentration: Rhodamine based mercury probe

Quite different properties are desirable in a mercury probe. Where Ca^{2+} is ubiquitous and vital, Hg^{2+} is scarce and deadly. When looking for a rare species, an irreversible sensing approach is often desirable, allowing the reacted form concentration to build up over time and so improve detection. This is especially true in the case of an ion like mercury which does not perform a useful role; generally the role of a probe is to confirm the presence of Hg^{2+}, rather than investigate its interactions. Fine tuning kinetics and providing mechanisms to localise the probe is not especially important; selectivity and sensitivity become much more so, and stability and toxicity concerns may be greater if longer observation periods are required. Several rhodamine based probes[90,91] utilise cyclisation of thiosemicarbazide groups driven by the affinity of mercury for sulfur (**Scheme 11**). Mercury preferentially bonds with the thiocarbonyl following coordination in **36**, increasing reactivity towards the favoured 5-*exo*-*trig* cyclisation from the amide, which is activated by the α effect. Desulfurisation is then driven by the aromaticity of the furan product **38**.

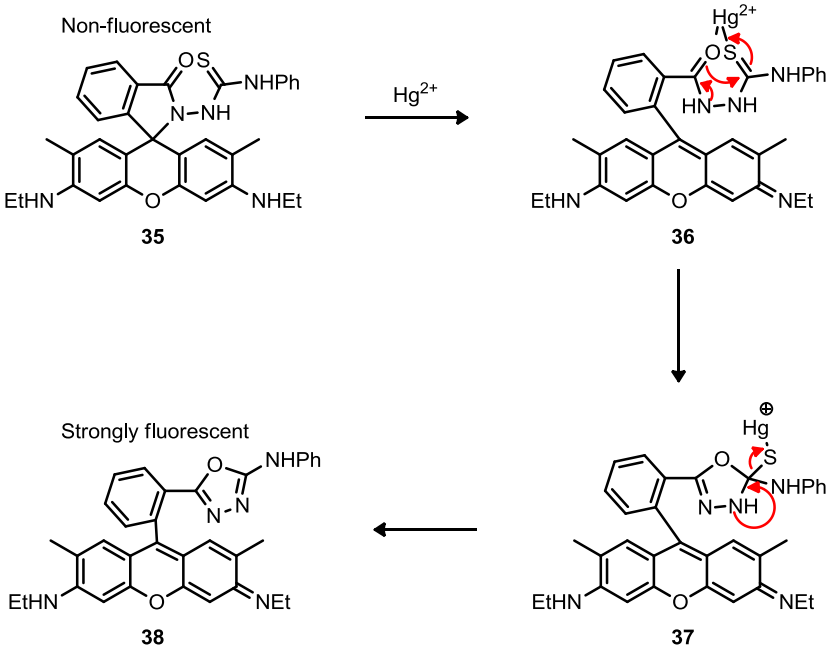

Scheme 11 - The mechanism of the Hg^{2+} sensing desulfurisation reaction.

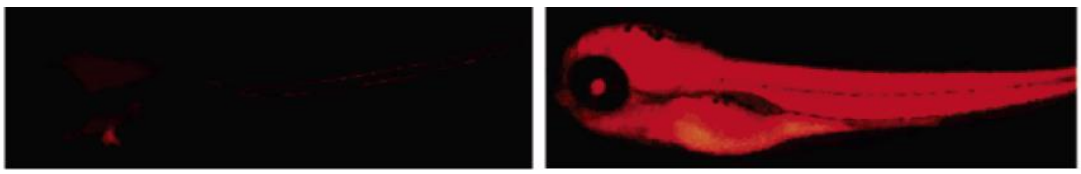

Figure 23 - Fluorescence of zebrafish before (left) and after (right) addition of $HgCl_2$. Adapted from Ko *et al*, J. Am. Chem. Soc., 128, 43, 2006.[90]

The applications of the probe are reflected in design elements; the non-fluorescent to fluorescent transition limits quantification accuracy but improves contrast, and the rhodamine dye has strong absorbance and high quantum yield (ϕ_f = 0.52), making rhodamine **38** detectable at 2 ppb.[74] With

an emission maximum of 577 nm biomolecule absorbance of the emission is negligible. **Figure 23** also demonstrates that the probe equilibrates through the organism, and as xanthene **35** is stable from pH 4-14, it should be active in virtually all cellular environments. The cyclisation used is selective for Hg^{2+}, and the probe gave minimal responses in the presence of other metal ions.

3.1.5 Irreversible sensing of a low abundance species: Dicarbonyl hydrogen peroxide probe

H_2O_2 is less ubiquitous than Ca^{2+} but of more subtle effect than Hg^{2+}. The most obvious reactivity of H_2O_2 is as an oxidising agent, a property shared by other ROS. Another property is used to distinguish it from other ROS. Many ROS are radicals, and less nucleophilic than the conjugate base of H_2O_2. The combination of high nucleophilicity and the presence of a hydroxide leaving group in H_2O_2 is exploited for selective detection. One fluorescein probe[93] uses the rapid Baeyer-Villiger reaction of benzil moieties[92] followed by hydrolysis to generate a fluorescein with a high quantum yield (ϕ_f = 0.8), and long excitation (495 nm) and emission (525 nm) wavelengths (**Scheme 12**). The standout feature of this probe is a 150-fold increase in brightness from benzil **39** to fluorescein **40**. While fluorescence and quenching observation is often serendipitous, in this case some rationale is given for the design: the reduction potential of the benzil group suggests a LUMO low enough to undergo donor PET quenching (**Section 3.1.2**) from the excited fluorophore.[93]

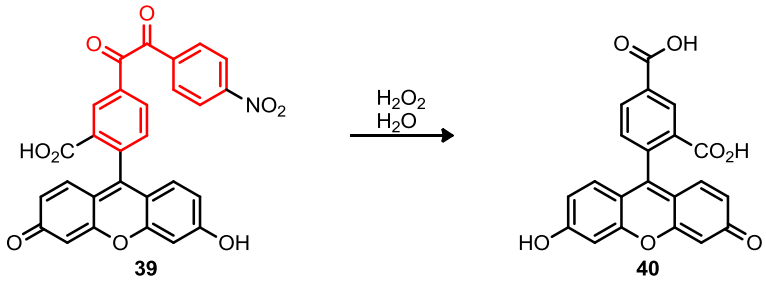

Scheme 12 - Activation of the fluorophore by H_2O_2.[93] The benzil moiety is marked in red.

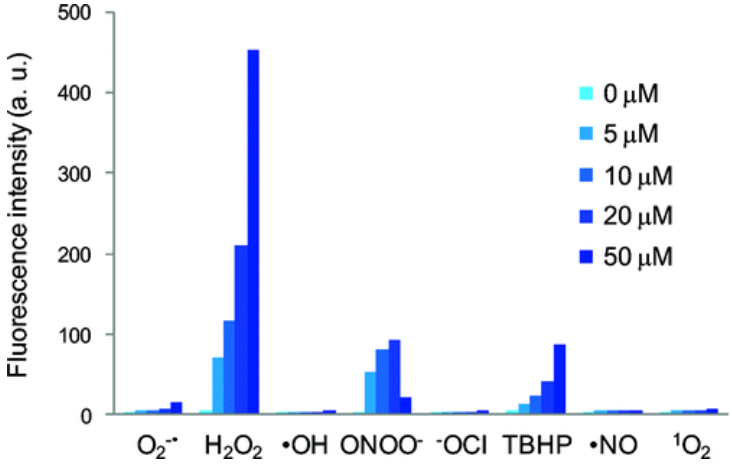

Figure 24 - Selectivity of probe **39** for hydrogen peroxide over other common ROS. Reproduced from Abo, M.; Urano, Y.; Hanaoka, K.; Terai, T.; Komatsu, T.; Nagano, T. *J. Am. Chem. Soc.* **2011**, *133*, 10629–10637.

Reasonable kinetics are also required as H_2O_2 is created and destroyed both regularly and in a localised fashion, and a moderate rate ($k = 4.2 \times 10^{-3} s^{-1}$, pseudo-1st order with 1000 fold excess of H_2O_2) was ideal as it does not disturb the steady state H_2O_2 concentration by competing with endogenous processes. The probe also reacts with alkylhydroperoxides and peroxynitrite (**Figure 24**), although the latter is a product of H_2O_2 and NO, and so the reaction could be considered an indirect measurement of H_2O_2. Fortunately, H_2O_2 is far more abundant than these species so the error induced by these side reactions is insignificant.

3.1.6 A targeted, quantitative and non-fluorescent hydrogen peroxide probe

The three previous examples provided all report by means of fluorescence. There are major advantages to this approach; numerous fluorophores are well characterised and often synthetically easy to obtain, it is non-invasive and extremely sensitive, simple experiments are (relatively) easy to do, and the output is visual, intuitively understandable, and gives dynamic responses and spatial distributions. For all these reasons and others most biological probes rely on fluorescence. As demonstrated previously however, the ideal properties of a probe are dependent on the measurement required, and fluorescence has drawbacks. In particular, it is extraordinarily sensitive to environmental factors,[94] and the cell is an extremely complex environment. Basic fluorescent measurements do not therefore allow quantification. Ratiometric probes can ameliorate some of the difficulties (**Chapter 11**), but a truly ratiometric probe is a non-trivial undertaking, and not a complete solution. Additionally, isolated mitochondria are known to be of limited comparative value when seeking to understand physiological systems (see **Section 3.2**). It is therefore necessary to examine the whole organism at once, which is not usually possible with optical techniques due to limited penetration. Where accurate quantification rather than spatial information is the goal alternatives to fluorescence should be considered.

One technique offering better quantification is LC/MS/MS, which was utilised for H_2O_2 quantification using MitoB, a probe developed and synthesised by the Hartley group and tested by the Murphy group at the MRC in Cambridge. The use of this probe is summarised in **Figure 25**. The arylboronic acid is attached to a triphenylphosphonium targeting moiety, which increases mitochondrial accumulation as described in **Section 2.3**. In *drosophila* calculations suggested 90% of the probe was within cells, and 98% of the cellular probe was within mitochondria.[95] The boronic acid from MitoB is then selectively attacked by the hydroperoxide anion,[96] which reacts substantially faster than H_2O_2, and is more prevalent within the mitochondrial matrix due to its higher pH in this environment. This results in four-fold faster conversion within the mitochondrial matrix versus the cytosol at the same concentration. Between the accumulation and preferential reaction of MitoB **41** the resulting MitoP/MitoB ratio is substantially indicative of mitochondrial H_2O_2 concentrations, with an error comparable with those inherent in such experiments regardless of detection method.

MitoB **41** and mitoP **42** diffuse freely across membranes[95] and so can be administered to whole organisms and the MitoB/MitoP ratio determined by extraction and extrapolated to quantitative

data, with deuterated analogues of both added to the homogenised organism to correct for detection variations. The cationic nature of the probes improves mass spectrometry detection.

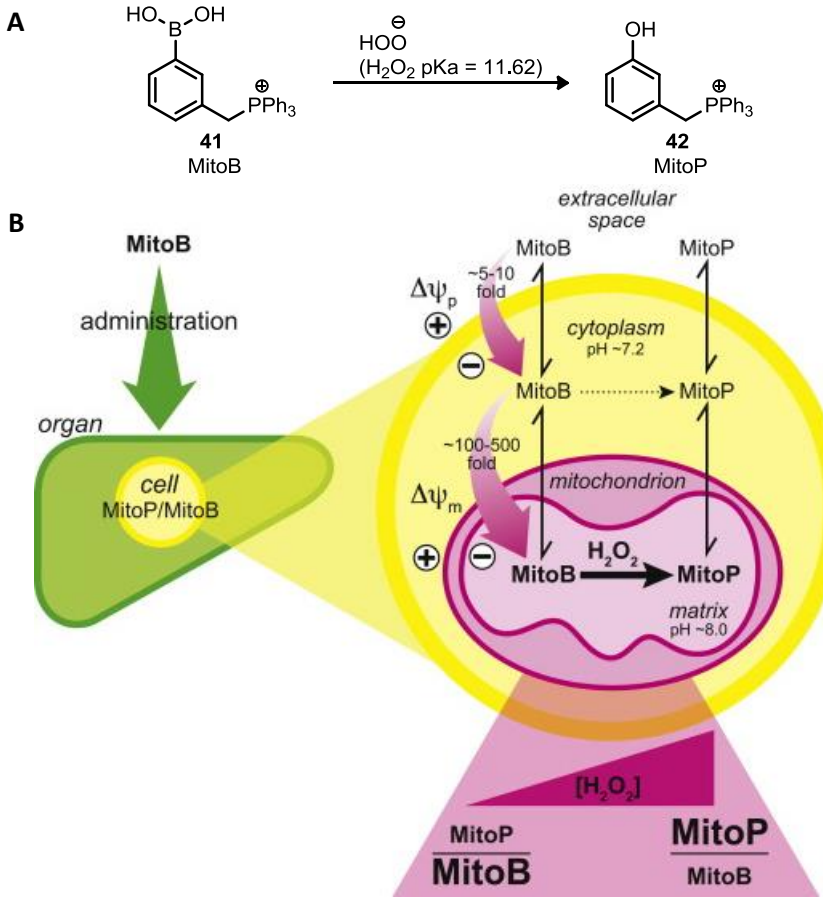

Figure 25 - The application and quantification of MitoB, reproduced with minor modifications from Cochemé, H. M.; Quin, C.; McQuaker, S. J.; Cabreiro, F.; Logan, A.; Prime, T. a; Abakumova, I.; Patel, J. V; Fearnley, I. M.; James, A. M.; Porteous, C. M.; Smith, R. a J.; Saeed, S.; Carré, J. E.; Singer, M.; Gems, D.; Hartley, R. C.; Partridge, L.; Murphy, M. P. *Cell metabolism* **2011**, *13*, 340–50.

3.2 Reactive oxygen species

3.2.1 What to measure?

Following the success of MitoB, my research involved using the same approach to measure another ROS, superoxide. Before describing the design of the probe it is necessary to consider the context, specifically to look in more detail at the generation and role of ROS.

The term ROS originally referred to a handful of oxygen-containing radicals, but the list of chemical species included has lengthened as it has become apparent that the sequences of biological reactions related to these radical species is very complex and often interlinked. The greater understanding of the cellular chemistry has resulted in a broadening of the definition to the point where both non-radicals and non-oxygen containing species are regularly described as ROS.[97] Many researchers working in the area are now suggesting that, if the term itself has not outlived its usefulness as a descriptor it is not specific enough to describe a target of study.[98] There are several reasons for this; one is that the term has now expanded to cover a range of very distinct chemical species with different specificity, different levels of reactivity and sometimes generated in different places. Therefore attributing an outcome to ROS is a poor description of

the likely actual pathway. Secondly, some ROS are now known to be useful or indeed essential, such as nitric oxide or H_2O_2, for signalling.[99]

Broadly the term ROS covers species that are capable either of causing oxidative damage or being converted by redox chemistry to a species which can do so. The majority of these species come from chain reactions initiated by superoxide,[100] and the radical chain generated from a single superoxide radical may span thousands of events.[106] The full details of the interactions of the myriad of ROS are both extremely complex and a matter of ongoing study but for the purposes of this summary the basics may be shown diagrammatically (**Figure 26**).

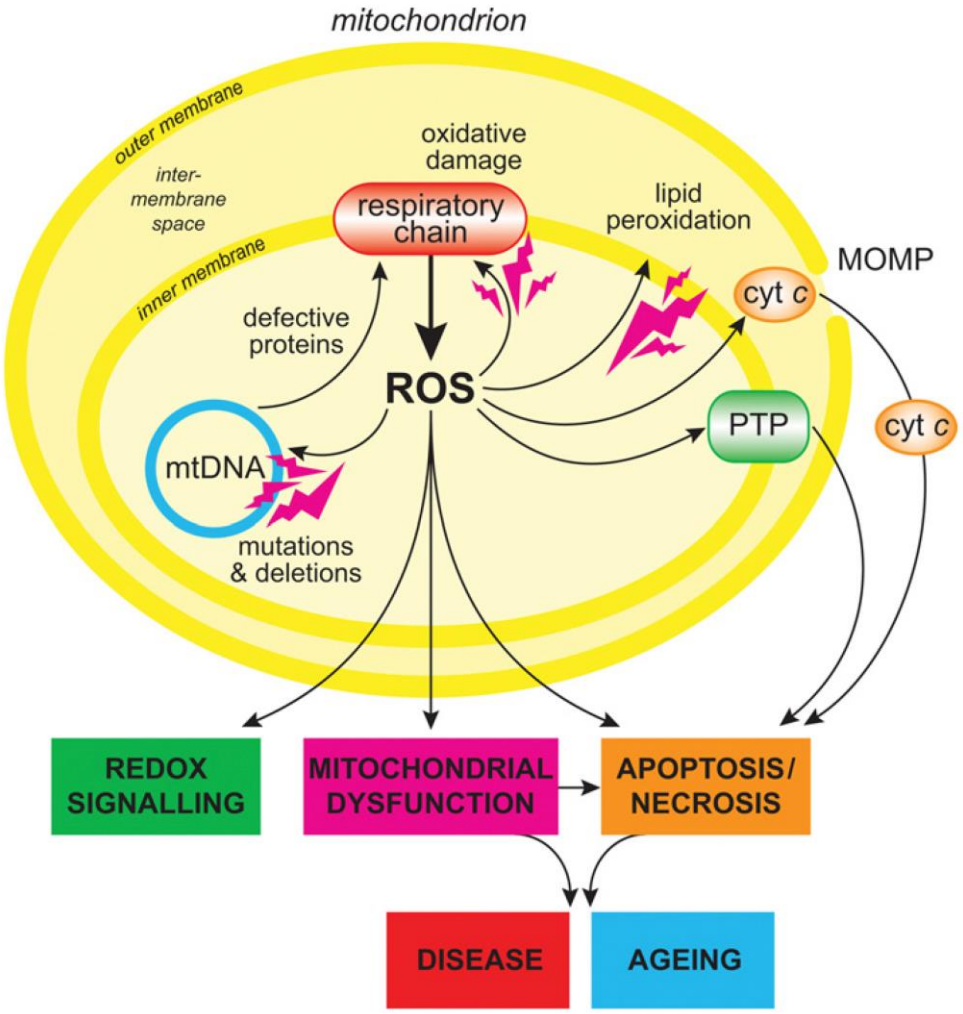

Figure 26[101] - This image was originally published in Biochemical Journal. Murphy, M. P. **2009**. How mitochondria produce reactive oxygen species; Biochemical Journal, 417, 1-13 © Portland Press Ltd.

A rough summary is as follows. The respiratory chain generates various ROS through initial production of superoxide. These ROS can then damage lipids, DNA and enzymes and cause cell or tissue death, being implicated in over 100 human or animal diseases.[106] However, some of these species also play an important role in cellular signalling pathways. Some 90% of ROS originate in the mitochondria,[102] and many are too short lived to diffuse significantly (**Figure 27**).

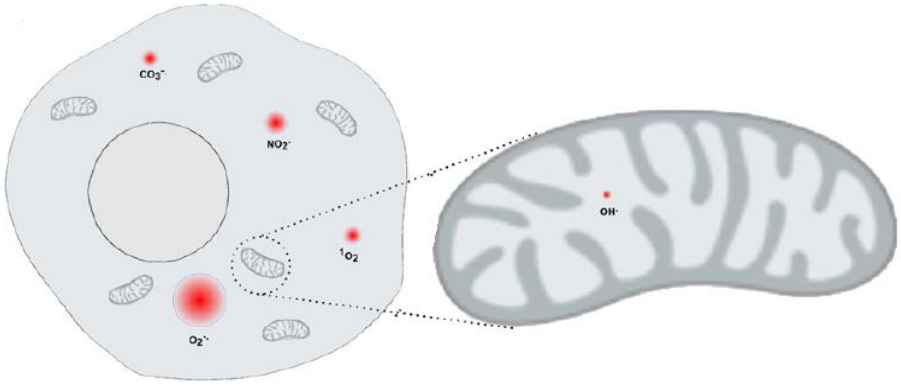

Figure 27 - Maximum diffusion distances estimated for various ROS within the cell.[103]

Ideally biomarkers could be used to observe the effects of oxidation, and this is a common approach. Increasingly, however, it has been realised that the role of some ROS is considerably more complex than initially surmised, and may in fact signal stress and mobilise protective responses in some cases.[104] Furthermore, some common biomarkers have been specifically shown to be problematic. For example, lipid peroxidation may be as much a measure of the antioxidant defence as anything else,[106] and similarly protein carbonylation represents protein turnover rates.[104]

An alternative would be to quantify the species causing individual types of oxidative damage events, but in many cases the terminal oxidant is the extremely reactive hydroxyl radical, which has the highest reduction potential of any known oxygen-centred radical (+2.31 V). This has an extremely low steady-state concentration owing to its ability to react at essentially diffusion limited pace with virtually any biomolecule,[105] meaning there is almost nothing to measure and the terminal oxidation is hardly selective anyway. Other species such as hydroperoxyl and alkylperoxyl radicals are also capable of causing damage by lipid peroxidation, but these are difficult to distinguish from each other and transient themselves.[106] Instead, the precursor to these reactive species, superoxide, was considered. This can lead directly to the hydroxyl radical via iron catalysed Haber-Weiss and Fenton chemistry (**Scheme 13**).

(a) $Fe^{3+} + O_2^{\cdot-} \rightarrow Fe^{2+} + O_2$
(b) $Fe^{2+} + H_2O_2 \rightarrow Fe^{3+} + {}^{\cdot}OH + {}^{-}OH$
(c) Overall reaction: $H_2O_2 + O_2^{\cdot-} \rightarrow {}^{\cdot}OH + {}^{-}OH + O_2$

Scheme 13 - Haber-Weiss and Fenton iron catalysed hydroxyl radical formation from H_2O_2 and $O_2^{\cdot-}$

While still difficult, it may be possible to measure superoxide. Superoxide is the product of one electron reduction of the diradical[107] O_2, which has two partially filled degenerate orbitals and correspondingly accepts only one electron at a time,[101] into an antibonding orbital.[106] Although the standard reduction potential for this process is negative, superoxide formation is favourable under physiological conditions due to the relative concentrations of O_2 and $O_2^{\cdot-}$ within the matrix, where tentative estimates suggest a superoxide concentration of 10-200 pM.[101] Superoxide is relatively unreactive, (although capable of damaging some Fe-S clusters),[38] but matrix $O_2^{\cdot-}$ is

limited by superoxide dismutase, an enzyme which converts the radical into H_2O_2 extremely rapidly (k is approx. 2.3 x 10^9 M^{-1} s^{-1}), a consideration not factored into the diffusion radius shown in **Figure 27**. When the effect of SOD, antioxidants and other defense mechanisms are considered alongside the difficulty of anionic superoxide crossing the inner mitochondrial membrane, multiple recent reviews have concluded that significant $O_2^{\cdot-}$ efflux from the matrix is improbable.[108,106] Since oxidative damage to mitochondrial DNA is postulated to be the limiting factor on human longevity according to the free radical theory of ageing, investigations can be limited to superoxide in the mitochondrial matrix. There is not currently any way of measuring matrix superoxide production or accurately determining its steady state concentration in the matrix of living organisms.[101]

3.2.2 How is superoxide produced?

Several sources of superoxide are known to exist within the mitochondrial matrix (**Figure 28**), although the mechanisms and extent of their activity under physiological conditions is poorly understood.[109,110]

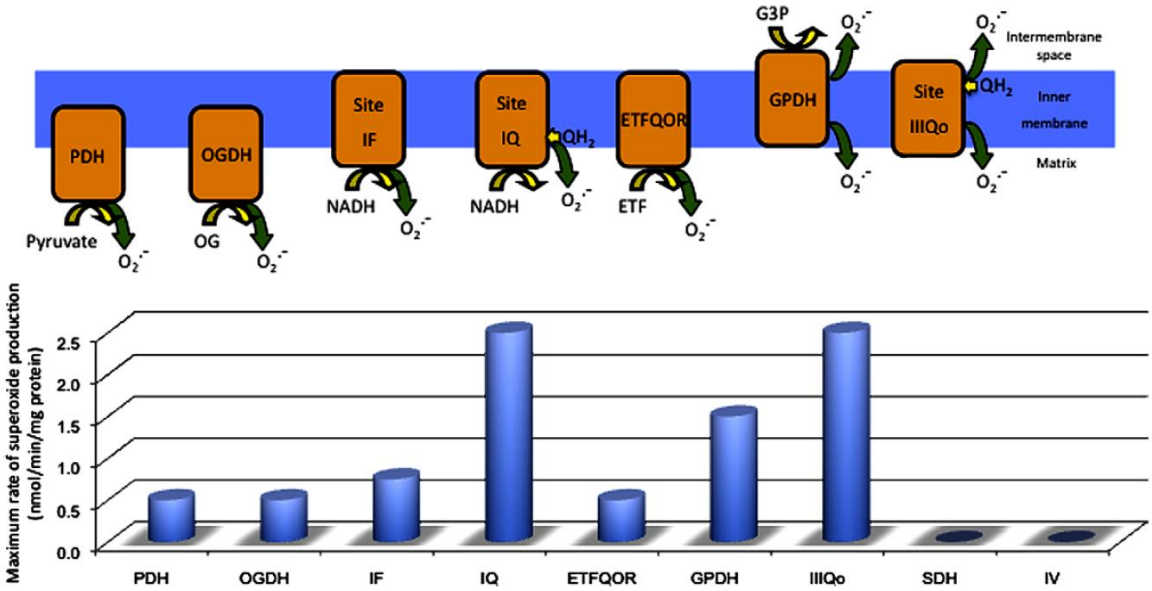

Figure 28[111] - The maximal rates of superoxide production at different sites in the mitochondria. It is not clear to what extent all of these are active in vivo. Superoxide production sites are pyruvate dehydrogenase (PDH), 2-oxo-glutarate dehydrogenase (OGDH), complex I NADH binding site (IF), complex I ubiquinone binding site (IQ), electron transferring flavoprotein ubiquinone oxidoreductase (ETFQOR), glycerol 3-phosphate dehydrogenase (GPDH) and complex III outer ubiquinone binding site (IIIQo).

The best understood of these are within the electron transport chain (see **Section 1.4**). Complex II produces superoxide in specific experimental conditions but is not believed to produce significant quantities *in vivo*, while the affinity of complex IV for partially reduced oxygen prevents escape of superoxide.[108] Complexes I and III are capable of superoxide production. An exhaustive description of these complexes is unnecessary, but as superoxide formation by complex I has been discussed in detailed reviews,[101,112] a brief outline of the process is provided for illustrative purposes.

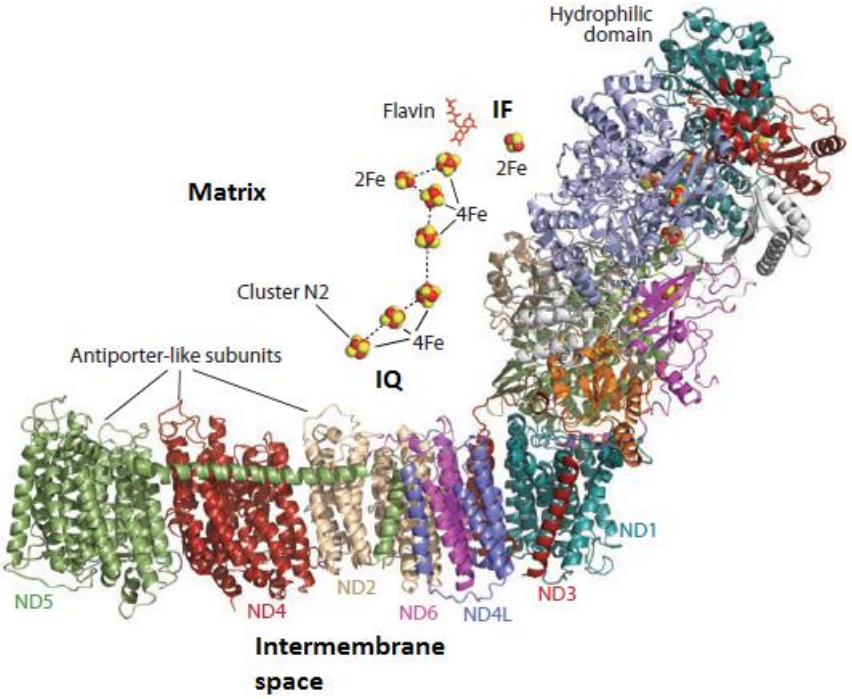

Figure 29 - The structure of mitochondrial complex I. The lower portion containing the antiporters is within the inner mitochondrial membrane. A hydrophilic arm points into the matrix. This contains the seven Fe-S clusters which compose the internal electron transport chain of Complex I. The NADH oxidation site (IF) has a flavin cofactor and is furthest from the membrane, while terminal ubiquinone reduction site N2 (IQ) is only 20 Å from the membrane. Republished with minor alterations with permission of Annual Reviews, Inc, from "Mitochondrial Complex I", Hirst, J. 82, **2012** permission conveyed through Copyright Clearance Center, Inc.

The reduction of oxygen to superoxide is believed to occur through an outer sphere mechanism, and so proximity is required. Only the entry (IF) and exit (IQ) of the complex I electron transport chain are accessible, as the Fe-S clusters are protected by the complex proteins (**Figure 29**).

The binding of NADH to the flavin (IF) at the peak of the complex I electron chain as drawn results in hydride transfer between the two, giving NAD^+. Binding and transfer is extremely rapid and reversible, with electron transfer by quantum tunnelling also extremely quick, and the rate limiting step is reduction of the ubiquinone at the lower energy site (IQ). It is possible to treat $NADH/NAD^+$ binding and hydride transfer as a pre-equilibrium, with the ratio essentially setting the relative levels of oxidised and reduced flavin. Superoxide production is favoured by a high $NADH/NAD^+$ ratio, as a greater proportion of IF sites are reduced and so able to reduce oxygen in turn. Interestingly, increasing the absolute NADH concentration rather than changing the $NADH/NAD^+$ ratio inhibits superoxide production by preventing access to the flavin site (oxygen reduction is very slow compared to NADH hydride transfer).

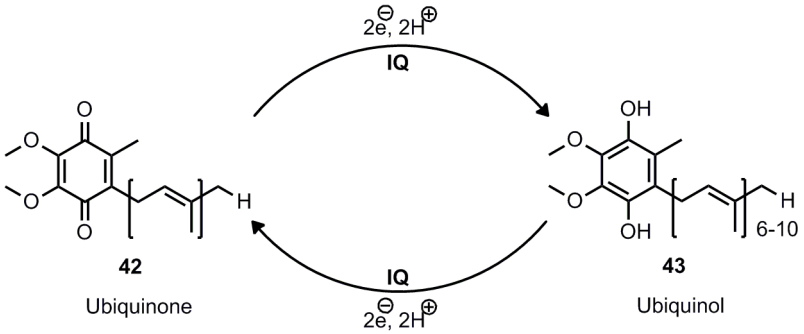

Scheme 14 - Reduction of ubiquinone at site IQ. The reverse oxidation process occurs under reverse electron transfer (RET) conditions.

Until recently it was suspected that IQ was also a significant superoxide source, as shown in **Figure 28**. This was considered to be particularly relevant during Reverse Electron Transfer (RET), where the mitochondrial chemiosmotic potential is sufficiently high to drive reverse transfer from a pool of ubiquinol (the reduced form of ubiquinone, **Scheme 14**) up the complex I electron transport chain. The absence of ubiquinone to react with the reduced N2 cluster would allow oxygen to do so instead. Underlining the developing nature of our knowledge of this area, recent evidence[113] appears to discount IQ as a superoxide source, showing superoxide reduction even under RET conditions occurs via the IF flavin.

The above description gives only a very simplified outline of the current understanding pertaining to complex I superoxide production. As the literature related to superoxide production is extremely extensive and the topic only tangentially related to the work undertaken no further description of superoxide production is attempted here, but may be found in both the recent reviews referenced throughout this section and in several others.[114,115]

3.3 Designing a probe for matrix superoxide quantification in whole organisms

3.3.1 What tools are available?

Several of the previously cited reviews explicitly emphasise the need for more information on superoxide, in fact our ability to quantify this species in the matrix under physiological conditions is very limited.[101] Most studies purporting to measure superoxide do so indirectly by measuring another species, usually H_2O_2. In many cases this is likely sufficient, but several assumptions are required. These include assuming that effectively all superoxide is converted to H_2O_2, and that all H_2O_2 comes from superoxide within the matrix (or at least that we can accurately correct for side reactions), and that no significant H_2O_2 degradation occurs prior to measurement.[101] We know that all three of these assumptions are certainly incorrect at least some of the time.[116,117,118] This does not of course mean that measuring H_2O_2 as an indicator of superoxide levels is invalid; in many cases it will likely give accurate data, but given our limited understanding of the mitochondrial matrix under physiological conditions it would be beneficial to measure the species of interest directly. In this respect many tools relying on specific damage markers are similarly limited by our understanding of their native roles and interactions. For example, when using

aconitase oxidation as a marker it should be noted that the iron released will take part in Fenton chemistry and modify the ROS balance present.[119]

Some tools for the direct measurement of superoxide do exist, and understanding the limitations of these is important in identifying new approaches to the problem. Many of the approaches have been reviewed[120] and the good and bad points of various detection schemes detailed. It is sufficient to note here that generally these approaches either display low selectivity or are very obviously unsuitable for *in vivo* application. A small selection of alternative superoxide probes are listed in a more recent review.[121] All rely on optical approaches, which limits the tissues in which they can be utilised. As mentioned earlier (**Section 3.1.5**), use of fluorescence as a quantification tool is limited by environmental sensitivity. In addition, the possibility of reabsorption of emitted photons by nearby probe molecules is relevant where selective uptake strategies could result in high local probe concentrations. Because of the limitations of the reporting technique, the compounds described in the following section are unsuitable for quantification of superoxide levels in a whole organism *in vivo*. However, the details of their function, and particularly their sensing moieties, can be used to design an alternative probe to do so.

3.3.2 A selective, oxidation resistant, 'turn on' fluorophore: Hydrocyanine dyes

The hydrocyanine probes developed by Murthy and coworkers[122] (**Scheme 15**) feature an extended conjugated system in the oxidised cyanine form **44**, which can be disrupted by reduction. The reduced form **45** is able to diffuse through membranes as it is uncharged. Subsequent oxidation by ROS results in a strongly fluorescent, membrane-impermeable probe.

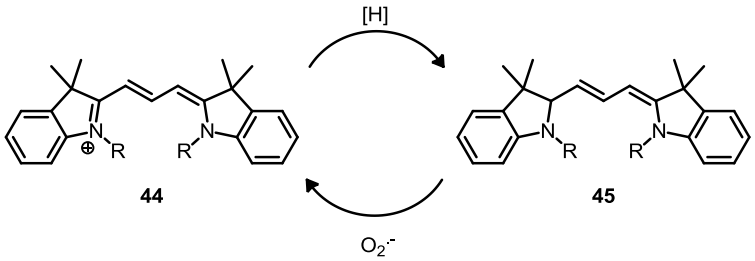

Scheme 15 - Interconversion of cyanine **44** (oxidised) and hydrocyanine **45** (reduced) by $NaBH_4$ or superoxide respectively. [122]

Cyanines **44** have several advantages as fluorophores. The extended conjugated system in the more fluorescent form **44** gives a long wavelength, low energy excitation (535-750 nm) and emission (560-830 nm), with the exact values dependent on the analogue used. The hydrocyanine form **45** is only weakly fluorescent, with oxidation producing a 100-fold increase in fluorescence intensity. The reduced moiety is quite resilient to auto-oxidation in aqueous environments, which is attributed to a lower driving force for oxidation compared to ethidium based probes (**Section 3.3.4**), for which this can be a limitation. Reasonably good selectivity for superoxide is reported (**Figure 30**) and believed to arise from two consecutive one electron oxidations. Importantly low reactivity with H_2O_2 is observed. Significant side reactions have been reported with indiscriminately reactive species such as the hydroxyl radical, but this is present only in

vanishingly low concentration (see **Section 3.2.1**). These probes are sensitive to nanomolar levels of radical oxidants.

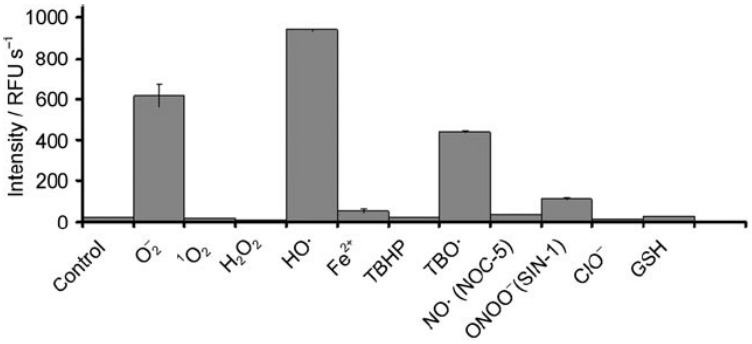

Figure 30 - The selectivity of Hydro-Cy3[122] for various ROS. Republished with permission from Kundu *et al*.[122] ©2009 Wiley-VCH Verlag GmbH & Co. KGaA, Weinheim

3.3.3 A ROS sensitive chemiluminescent probe: KEIO-BODIPY-KBI

An alternative to fluorescence as an optical reporting tool is showcased in Suzuki and coworkers'[123] chemiluminescent probe **46** for ROS. The energy emitted in this case is liberated by oxidation of the probe itself,[124] so no external stimulation is required. The chemiluminescent group was linked to an additional BODIPY fluorophore, with the idea of allowing transfer of excitation through chemiluminescence resonance energy transfer (CRET), which is functionally identical to FRET (see **Section 3.1.2**). Longer wavelength emission from the fluorophore is then less likely to be absorbed by biomolecules. This was the strategy originally pursued, but the probe synthesised emitted at a higher wavelength (545 nm) than the BODIPY fluorophore used, and so the emission was attributed to the whole probe acting as a single chromophore, exhibiting a strong response under superoxide generating conditions.

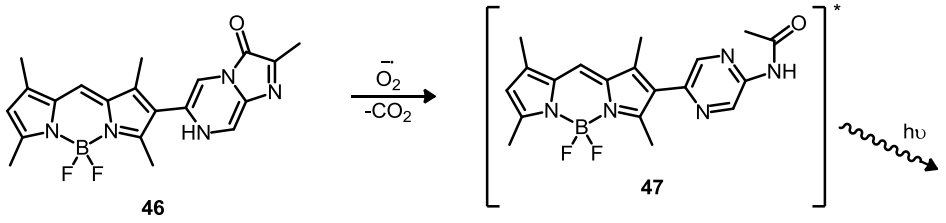

Scheme 16 - The chemiluminescent reaction of KEIO-BODIPY-KBI probe **46**.

High specificity is claimed but not fully demonstrated for this probe. The reported response to H_2O_2 was relatively strong, although this was attributed to the higher concentration of this oxidant under test conditions. A lower response was observed in the presence of catalase, which destroys H_2O_2, suggesting a 30:1 selectivity for superoxide over H_2O_2 assuming direct comparison is possible.

3.3.4 Unusual product selectivity and a targeted probe: MitoSOX

The use of hydrophenanthridines as probes is not an especially recent development. The parent phenanthridinium salts had long been used for a variety of purposes (see **Section 8.1.1**), and ethidium was known to undergo metabolic interactions *in vivo* in the 1970s.[125] By the mid 1980s oxidation of hydroethidine **48** (**Scheme 17**) was being used to infer the redox conditions in different areas of the cell.[126] This oxidation was attributed to ROS in 1990, with sensitivity to both H_2O_2 and $O_2^{\cdot-}$ observed.[127] In 2003 Kalyanaraman and coworkers observed during a study on redox sensitive dyes that superoxide addition appeared to lead to a different product to that produced from reaction with H_2O_2, hydroxyl radicals, peroxynitrite, cytochrome c and nitric oxide, although the actual structure was unknown.[128] Later work clarified the structure[129] and suggested a possible mechanism for this oxidation,[130,131] shown in **Scheme 17** and described below.

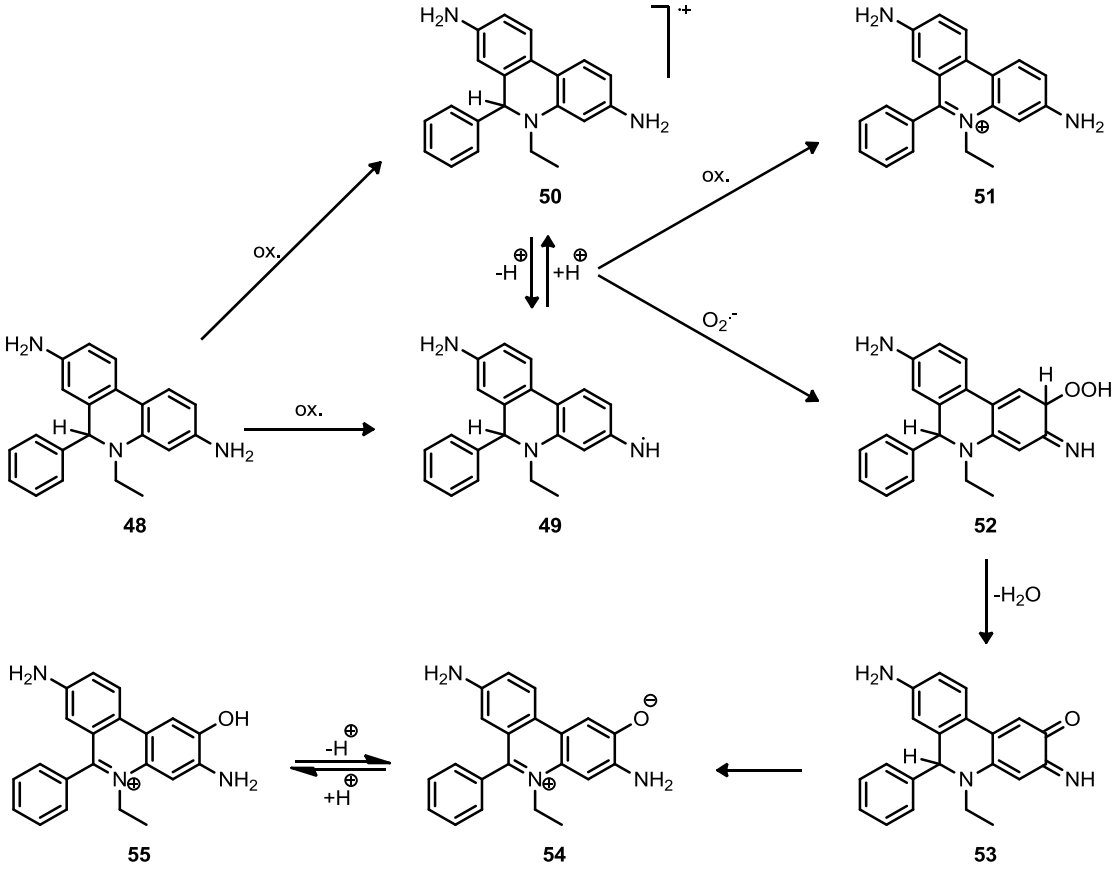

Scheme 17 - Oxidation of hydroethidine **48** makes both ethidium **51** and 2-OH-E^+ **55**.[130,131]

One electron oxidation of hydroethidine **48** gives aminyl radical **49** or radical cation **50**, which can interconvert via gain or loss of a proton. This rate of this initial step varies with oxidant and may be very fast, but is usually rate determining. Further one electron oxidation gives the parent ethidium **51**. Alternatively, in the presence of $O_2^{\cdot-}$ extremely rapid (k approx. 2 x 10^9 $M^{-1}s^{-1}$)[131] reaction with another $O_2^{\cdot-}$ produces peroxy adduct **52**, with water subsequently lost to form iminyl-quinone **53**. Tautomerisation, possibly via a reaction with a hydride donor or acceptor[130] gives phenoxide **54**, which is strongly favoured by the formation of an extended aromatic system. The conjugated, electron poor phenoxide **54** has a pKa of 7.4 and the protonated 2-hydroxyethidium (2-OH-E^+) **55** and deprotonated form **54** are roughly equal in concentration

within the cell. Two equivalents of oxidant are required in this pathway, however as many species can perform the original oxidation and $O_2^{\cdot-}$ is present at low concentrations, it is reasonable to assume that one superoxide radical gives one molecule of 2-OH-E^+ **55** under physiological conditions.

The key advantage of this mechanism is that extensive testing suggests that oxidation of hydroethidine **48** produces the 2-OH phenanthridinium product (2-OH-E^+) **55** only in the presence of $O_2^{\cdot-}$.[132,133] This selectivity is vital in detecting a species present only at low concentration. The Kalyanaraman group went on to suggest the red-shifted fluorescence of 2-OH-E^+ **55** relative to ethidium **51** could be used to distinguish the two,[130] and add a TPP cation to the end of a hexyl analogue to give MitoSOX **56** and ensure targeting to the mitochondria (**Fig. 27**). They abandoned this position on fluorescent quantification when it became clear that numerous fluorescent oxidation products were generated and interfered with quantification, and that the hydroethidium moiety was light sensitive, instead embracing HPLC quantification approaches.[134] Various other detection methods exist,[132,134] some of which may give sensitivity down to the atto molar level.[135]

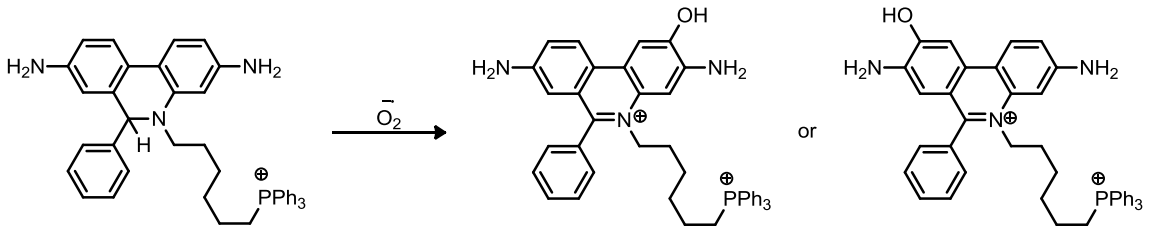

56 **57** **58**

Scheme 18 – The reaction of MitoSOX with superoxide gives rise to a product variously identified as the 2-OH phenanthridinium **57** or the 9-OH phenanthridinium **58**.

Beckman and coworkers attempted to use lower wavelength excitation to measure selectively superoxide formation in the mitochondrial matrix with MitoSOX.[136] Uptake and release in accordance with the membrane potential was demonstrated and the identity of the superoxide addition adduct was disputed. Beckman and co-workers claim the 9-OH analogue is produced, although it is labelled as the 2-OH compound, perhaps due to confusion surrounding the naming convention on phenanthridines. The different regioisomers have both recurred in the literature since, probably obscured by the related misnaming, and this uncertainty is further addressed in **Chapter 10**. Later work by the Beckman group uses MitoSOX for live cell imaging.[137]

When the creation of a mass spectrometry probe analogous to MitoB was investigated it was therefore considered that the creation of a deuterated analogue of MitoSOX **56** to correct for variations in uptake would allow quantification by mass spectrometry of superoxide production within the mitochondrial matrix of whole organisms. Unfortunately, no synthesis of MitoSOX had previously been published. In planning a route, the various literature approaches to 5,6-disubstituted dihydrophenanthridines were therefore considered and will be discussed in the next chapter.

Chapter 4: Making 5,6-disubstituted dihydrophenanthridines and phenanthridinium salts

4.1 Introduction to the synthesis of 5,6-disubstituted dihydrophenanthridines

Electron-rich 5,6-disubstituted dihydrophenanthridines like MitoSOX **56** are susceptible to oxidation and are generally prepared by reduction of the more stable 5,6-disubstituted phenanthridinium salts **60** or less commonly, the 6-substituent is introduced by addition of a formal carbanion or equivalent reagent to an *N*-alkylphenanthridinium **62** that is not substituted at C-6. These two disconnections are shown in **Scheme 19** and will be further discussed within the sections marked.

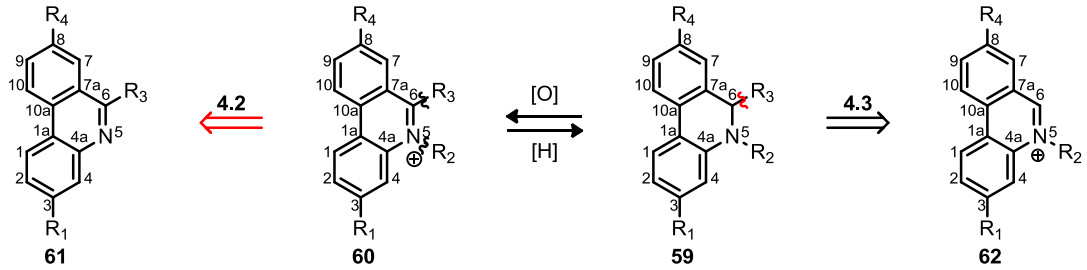

Scheme 19 - The initial disconnections used for the synthesis of a 5,6-disubstituted phenanthridinium salt **59**.

4.2 Disconnection one: the ubiquitous *N*-alkylation

Hydrogenation and most hydride reducing agents will reduce phenanthridiniums to dihydrophenanthridines, so the main challenge is accessing the parent 5,6-disubstituted phenanthridinium salt **60**. Given the many uses of 5,6-disubstituted phenanthridinium derivatives **60** (see **Section 8.1.1**), and the large number which have been synthesised, it is striking that *N*-alkylation of a 6-substituted phenanthridine is almost invariably the final step. Phenanthridines **61** are poor nucleophiles, so the early examples of *N*-alkylation and preparation of phenanthridiniums **60** bearing simple short *N*-alkyl chain used excess alkyl tosylates, bromides and iodides at elevated temperatures.[138,139,140] More recent syntheses mostly use triflates.[141,142] Synthetic approaches to the phenanthridine precursors **61** are much more varied, and a brief discussion of literature examples is organised in sections according to the retrosynthesis shown below (**Scheme 20**). Probably the most common disconnection is between C6 and C7a (red, **4.2.2**). Addition of a nucleophile to the C6 unsubstituted phenanthridine is also possible (green, **4.2.3**), as is intramolecular imine formation from a C6 ketone and a C4a amine (pink, **4.2.4**). A few recent methods use the more unusual N5-C4a disconnection (blue, **4.2.5**), with the C1a-C10a strategy most commonly applied to the synthesis of benzophenanthridine natural products (orange, **4.2.6**).

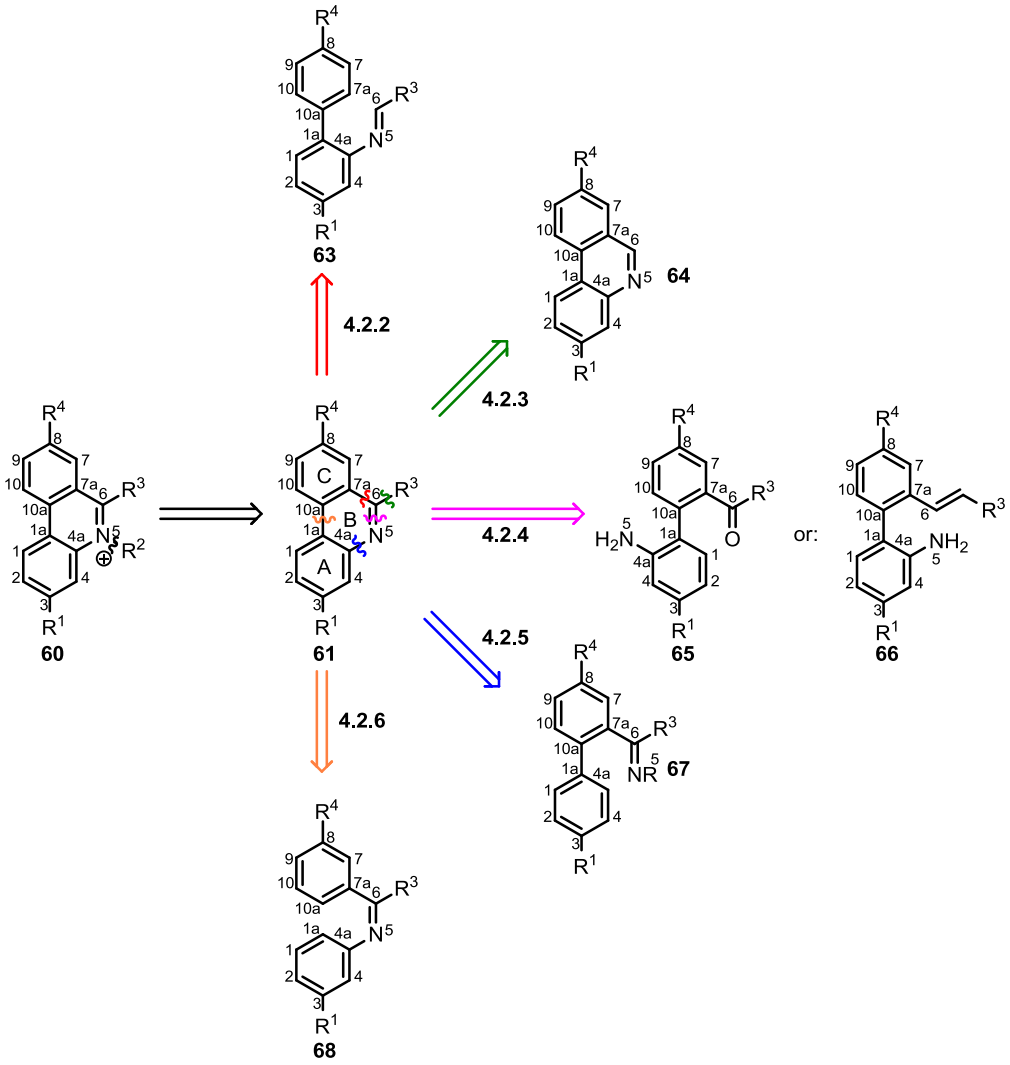

Scheme 20 - Common disconnections used in the synthesis of phenanthridines.

4.2.1 Forming the C6-C7a bond: intramolecular nucleophilic attack from an arene

The C6-C7a disconnection to give imine **63** is by far the most common retrosynthesis of 6-substituted phenanthridines **60**. In the forward direction this is nucleophilic addition to a polarised C=N which is an extremely common transformation and compatible with several classic heterocycle synthesis strategies. These include the Bischler-Napieralski reaction, sometimes called the Hubert-Pictet reaction ($ZnCl_2$, 250-300 °C) or Morgan-Walls cyclisation ($POCl_3$, 80-200 °C) depending on conditions (**Scheme 21**). Nucleophilic attack from the aromatic ring on an iminium chloride generated *in-situ* from amide **69** gives phenanthridine **70**, and is mechanistically similar to the Vilsmeier-Haack formylation (see **Section 11.4.1**).

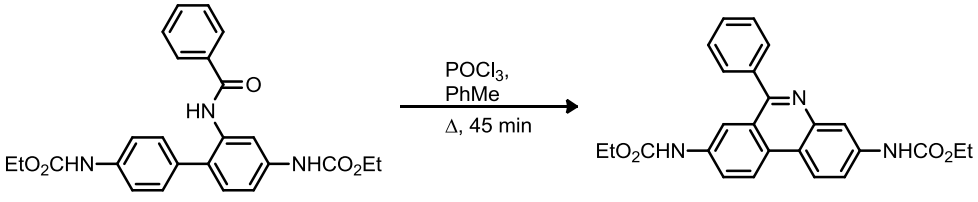

Scheme 21 - An example of the Morgan-Walls reaction from Lion *et al.*[143]

Another common way of forming phenanthridines is the Pictet-Spengler reaction (**Scheme 22**), e.g. imine (or iminium) formation from amine **71** and aldehyde **72** is followed by intramolecular nucleophilic attack in a 6-*endo-trig* cyclisation to give a dihydrophenanthridine. The dihydrophenanthridine oxidises under reaction conditions to give phenanthridine **73**.

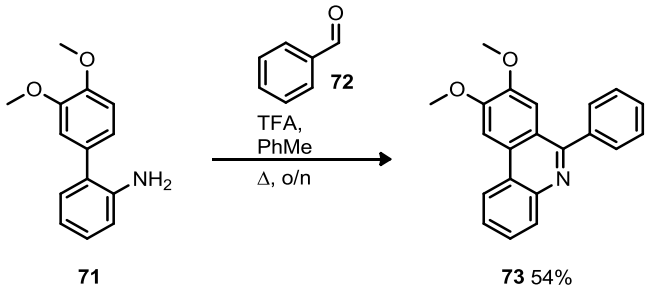

Scheme 22 - Phenanthridine synthesis by Pictet-Spengler reaction.

The Pictet-Spengler reaction is slightly different from the Bischler-Napieralski in that the C=N bond is formed in the same reaction as the C6-C7a bond. This is a relatively common theme among phenanthridine synthesis protocols. Intramolecular addition of an iminyl radical to an aromatic ring has also recently been used to effect the same transformation (**Scheme 23**) in a reaction between an aryl boronic or alkyl boronic acid **74** and a biaryl isocyanate **76**.[144] According to the mechanism proposed by Chatani and coworkers, reaction of boronic acid **74** with a one electron oxidant [Mn(III)] gave radical **75** which was trapped with isocyanobiphenyl **76** to give the carbon-centred radical **77**, which reacts to form the better stabilised phenyl radical **78**. Further oxidation to cation **79** followed by proton loss gives phenanthridine **80**.

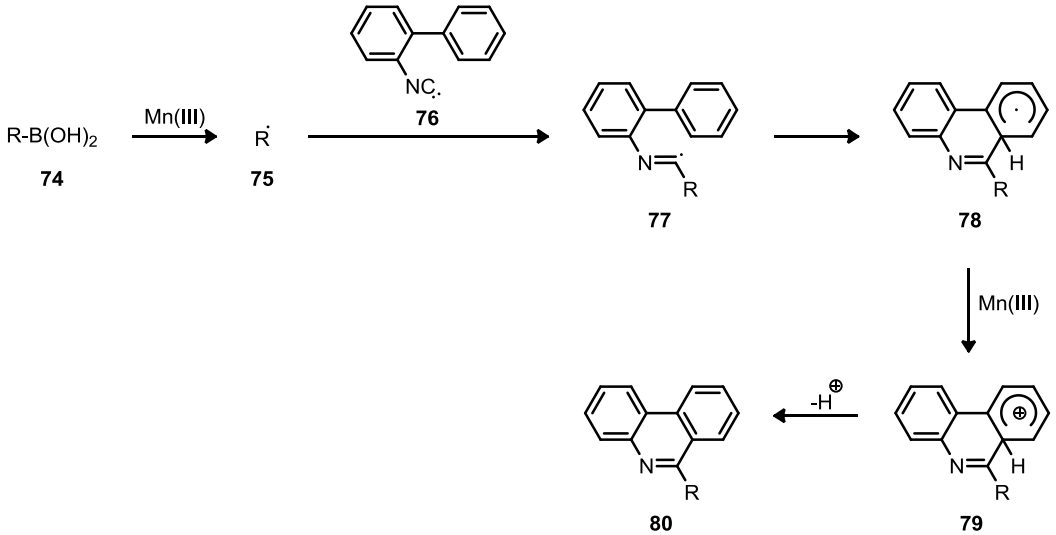

Scheme 23 - Mechanism proposed by Chatani and coworkers for the cyclisation of isocyanobiphenyl **76** to phenanthridine **80**.[144]

4.2.2 Addition of R3 to C6: nucleophilic attack on a phenanthridine

Nucleophilic addition to C6 is a common strategy for adding a range of R^3 groups. This is not a phenanthridine synthesis strategy so much as a functionalization, as the starting material **64** is a phenanthridine. Treating phenanthridine **81** which has no R^2 group with phenyllithium gives the 6-phenylphenanthridine **82**, following oxidation in the work up, which can be further substituted to 6,6 disubstituted hydrophenanthridine **83** (**Scheme 24**) under harsh conditions.[145] Addition to give the C6 phenyl derivative **82** can alternatively be achieved quantitatively under relatively mild conditions using a nickel catalysed arylzinc addition.[146]

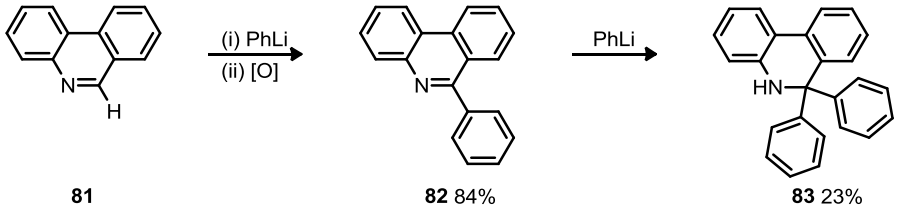

Scheme 24 - C6 funtionalisation of phenanthridine **81**.

Organometallic nucleophiles are not required, enolate addition also works well.[147] Surprisingly, C6 addition of an amine occurs in preference to reaction with an alkyl bromide, as evidenced by the formation of phenanthridinium **87a** by Cronin and coworkers.[148] This mechanism was proven by opening the five-membered ring, with the failure of the subsequent product to re-cyclise ruling out the Baldwin disallowed 5-*endo-trig* cyclisation. An interesting disproportionation was observed, presumably from intermediate **86**, which is reminiscent of the Cannizzaro reaction.

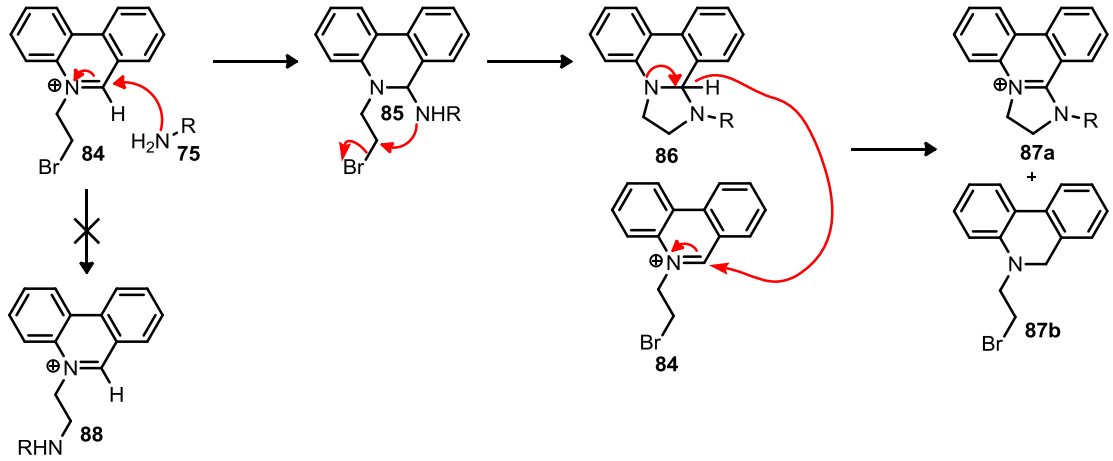

Scheme 25 - Unexpected C6 addition of an amine to phenanthridine.

4.2.3 N5-C6 condensation: cyclisation through imine formation

Compounds **92** closely related to phenanthridines can be made from biphenyls **91** with final intramolecular condensation of an amine onto a suitable ketone.[149] Imine formation is preceded by C1a-C10a bond formation via Suzuki coupling between aryl halides **89** and boronic acids **90**, while an acid sensitive amine protecting group allows deprotection and cyclisation to target **92** in one step (**Scheme 26**).

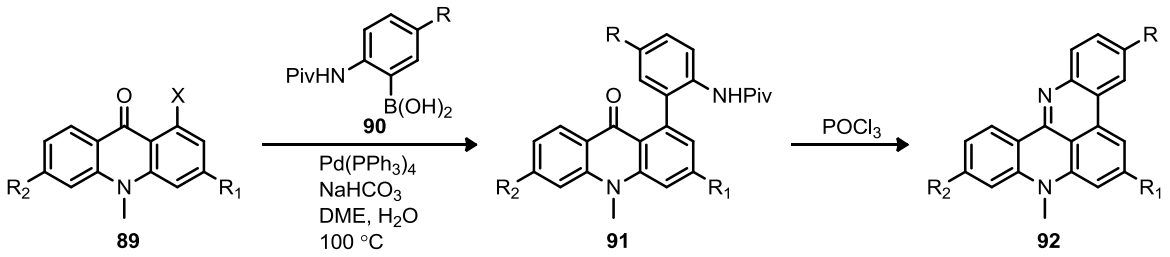

Scheme 26 - Suzuki coupling to form C1a-C10a followed by combined deprotection and cyclisation.[149]

Transition metal catalysed C-H activation followed by carboamination allows addition of more varied and complex C6 substituents and has been demonstrated with both free[150] (**Scheme 27**) and protected amines.[151]

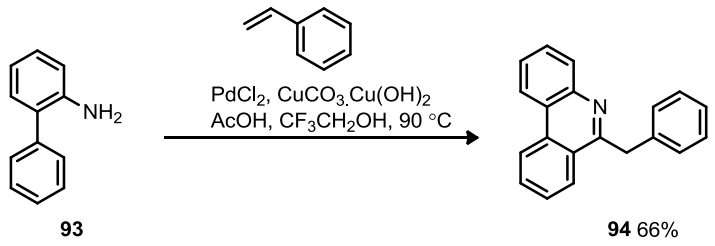

Scheme 27 - C-H activation and carboamination on unprotected biphenyl-2-ylamine **93**.[150]

An alternative formation of the imine is showcased in the work of Gallo and co-workers,[152] who use azides **95** as amino surrogates and a combination of a ruthenium catalyst, white light and heating to achieve a C-H amination and oxidation tandem reaction with the release of N_2 to give phenanthridines **96** (**Scheme 28**). Yields were variable and may reflect the difficulty of removing the side products reported.

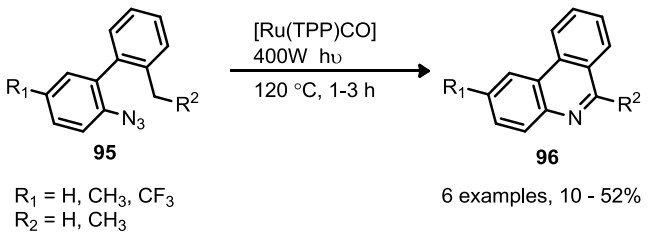

Scheme 28 - A ruthenium catalysed benzylic C-H amination and oxidation process.[152]

4.2.4 N5-C4a cyclisation: transition metal and radical induced cyclisation

Unlike the analogous C6-C7a bond formation on the other side of the heterocyclic B ring, N5-C4a cyclisation is comparatively rare. Presumably this reflects the ability of unsubstituted phenyl ring systems to undergo electrophilic substitution reactions, while leaving groups are generally required for the equivalent nucleophilic aromatic substitution. As a particularly electronegative element, nucleophilic attack on nitrogen is unusual and so formation of N5-C4a is rarely used to complete phenanthridine synthesis. Lautens and coworkers synthesise phenanthridines via an olefination-cyclisation cascade (**Scheme 29**), and propose formation of this bond by reaction of an imine with an aryl palladium (IV) species derived from the aryl triflate **97**.[153] A radical reaction not dissimilar to that used for C6-C7a bond formation has also been demonstrated as one outcome from photolysis of oxime carbamates.[154]

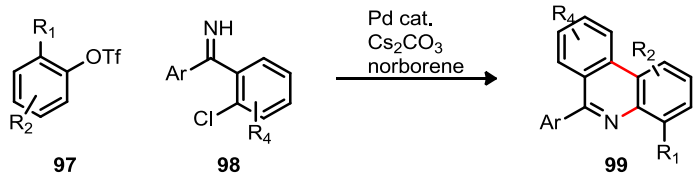

97 **98** **99**

Scheme 29 - Olefination-cyclisation, from Blanchot *et al*.[153] Bonds formed shown in red.

4.2.5 C1a-C10a: benzyne cyclisation and C-H activation

An unusual strategy for forming the C1a-C10a bond has been used to synthesise phenanthridine natural products lacking the C6 substituent. The phenanthridine moiety is found in numerous alkaloids,[155] and among these many are *N*-alkylated,[156] although not necessarily found in the quaternary salt form.[157] Naturally occurring benzophenanthridines are usually structurally and electronically different from ethidium-like phenanthridinium salts, and so different synthetic approaches are preferred. In particular, a benzyne cyclisation has been used in the synthesis of multiple benzophenanthridines alkaloids.[158,159] One example is the conversion of aryl halide **100** into benzophenanthridine **101** (**Scheme 30**).

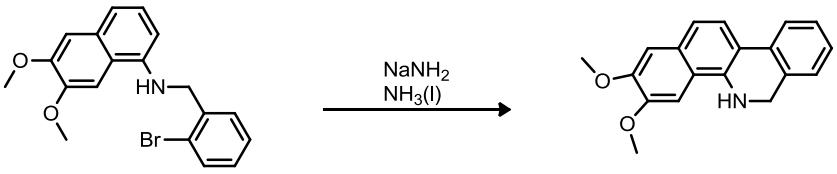

100 **101** 48%

Scheme 30 - Synthesis of a benzophenanthridine through benzyne cyclisation.[160]

The mechanistic steps of this type of cyclisation are shown in **Scheme 31**. First the amine **102** is deprotonated, then deprotonation of the CH of aryl halide **103** gives benzyne **104**. Nucleophilic attack from C1a (*ortho* to the amino group) onto the benzyne forms the C1a-C10a bond, in carbanion **105**. Protonation of anion **105** during the work up then gives the dihydrophenanthridine **106**, which is then oxidised to give phenanthridine **106**. Deprotonation of the amine **102** is required to activate ring A sufficiently to cyclise onto the benzyne.

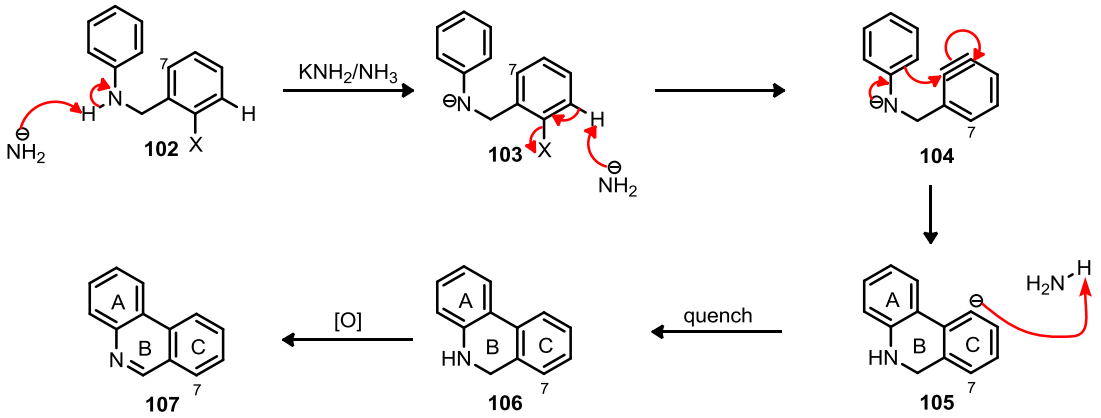

Scheme 31 - Benzyne cyclisation to a phenanthridine. The proton abstracted is shown on precursor **105**.

Subsequent investigation produced some mechanistic details: *N*-methylation prevented an analogous cyclisation, and deprotonation of only the amine alone did not produce cyclisation, showing that benzyne formation is necessary.[161] Substitution in the 7 position shown improves yield by favouring a conformation where the carbons of the A ring *ortho* to the nitrogen anion are close in space to the benzyne generated. The presence of alkoxy groups on the C ring are noted to favour side reactions because inductively withdrawing groups increase benzyne electrophilicity.[162] Changing conditions to LDA in THF at −78 °C improved the yield dramatically in some cases, and this was attributed to the bulkier base being prevented by steric hindrance from reacting further with the benzyne generated.[163] An alternative cyclisation of similar substrates was demonstrated by Nakanishi *et al* in the synthesis of drug candidate NK109, where the phenanthridine was closed by radical cyclisation instead.[164] More recently Peng *et al*[165] report cyclisation by a C-H activation mechanism (**Scheme 32**). Takeda *et al* have demonstrated this transformation occurring in tandem with prior *N*-arylation, however low to moderate yields resulted.[166]

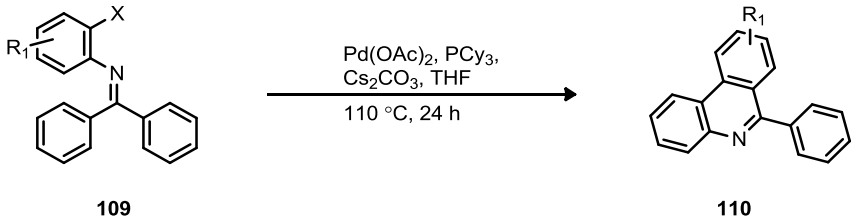

109 **110**

Scheme 32 - C-H activation and intramolecular cyclisation to form C1a-C10a.

4.3 Disconnection two: addition of a nucleophile to an *N*-alkylphenanthridinium

Preparation of 6-substituted phenanthridines **61** and *N*-alkylation to give 5,6-disubstituted phenanthridinium **60** is the most common way of accessing these compounds (**Scheme 19**). However, addition of carbanion equivalents to *N*-alkylphenanthridinium salts **62** also works. The practical difficulty of separating multiple *N*-alkylphenanthridinium salts in any mixture reduces the appeal of this approach. Furthermore the solubility of *N*-alkylphenanthridinium salts is usually low in the types of non-polar solvent often used for organometallic reagents. However, a range of benzophenanthridines have been synthesised by Nakanishi *et al* in this fashion (**Scheme 33**).[167] The methoxy adduct **111** (a pseudobase) forms the phenanthridinium **112** reversibly in solution,

avoiding solubility problems and allowing reaction with the Grignard nucleophile to form dihydrophenanthridine **113**. Even so, the authors note synthetic difficulties in preparing analogues in this way.

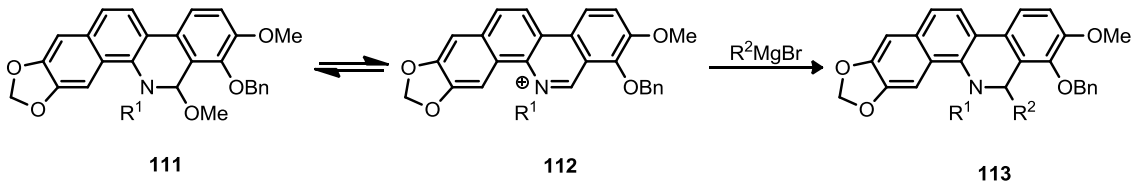

Scheme 33 - Grignard addition to a phenanthridinium salt.

The potential reversibility of nucleophilic additions to C6 can be utilised in sensor systems. Cronin and co-workers[168] developed a pH sensor based on cyclisations from groups such as malononitrile (pKa approx. 11)[169] which may or may not be nucleophiles in aqueous solution, depending on pH (**Scheme 34**). If the malononitrile is protonated the aromatic open form **114** is favoured. However, when the pH is reduced the neutral C6 adduct **115** is preferred despite the loss of aromaticity. This results in a fluorescent pH sensor, with change in absorbance and fluorescent properties upon acidification.

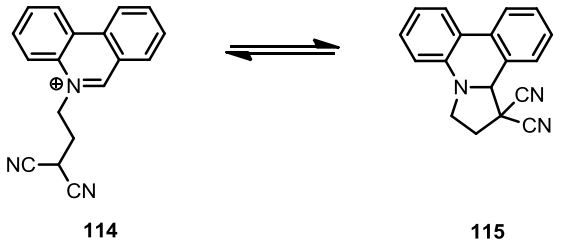

Scheme 34 - A pH dependent photoswitch based on reversible addition to the C6 position of the phenanthridinium.

Chen *et al*[170] take advantage of reversible addition to phenanthridinium salts in a combined coumarin-phenanthridinium heterocycle **116** which displays thermochromic properties upon cooling in MeOH.

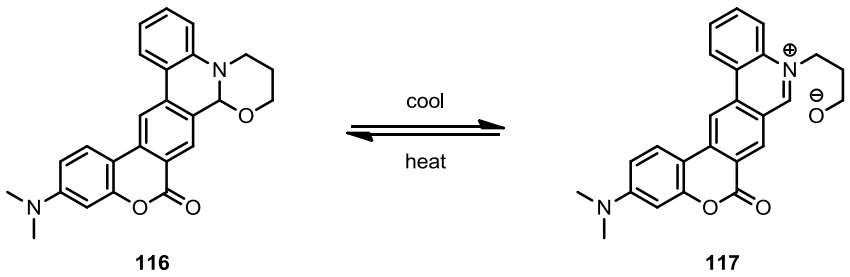

Scheme 35 - Coumarin-phenanthridinium combination **116** displays thermochromic properties.[170]

4.4 Direct access to 5,6-disubstituted dihydrophenanthridines

As previously discussed, according to the literature it is almost invariably necessary to *N*-alkylate a phenanthridine in order to make the corresponding 5,6-disubstituted phenanthridinium. Two recent exceptions exist: a single *N*-methyl hydrophenanthridine analogue **118** has been made via the Pictet-Spengler reaction, but the electronics of the precursor biphenyl **117** have been optimised and it is unclear that this strategy would be more generally applicable (**Scheme 36**).[171]

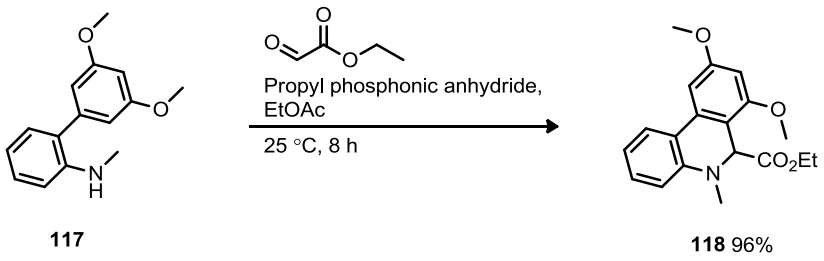

117 **118** 96%

Scheme 36 - Synthesis of an *N*-methyl hydrophenanthridine **118** by Pictet Spengler reaction.

Direct synthesis of dihydrophenanthridines with bulkier R groups has also been reported with what the authors describe as 'a hydride transfer/cyclisation/Dötz benzannulation cascade' (**Scheme 37**), but this requires R^2 and R^3 to be identical, and the starting material would likely prove challenging and sensitive. Additionally, while technically impressive the mechanistic complexity of this process would likely make optimisation very difficult.[172]

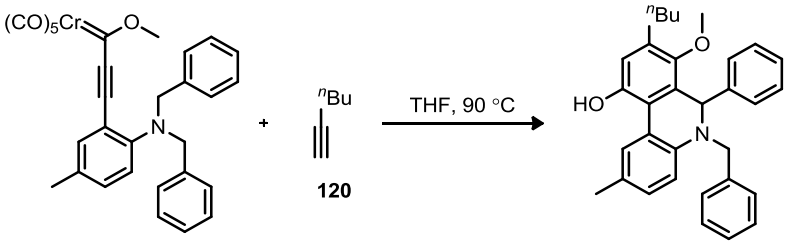

119 **120** **121** 72%

Scheme 37 - Dihydrophenanthridine synthesis via cascade reaction.[172]

Chapter 5: Synthesis of 3,8-Diamino-6-phenylphenanthridinium salts

5.1 Preparation of 9-Hydroxyphenanthridine for *N*-alkylation

Utilisation of MitoSOX **56** as a mass spectrometry superoxide probe required both deuterated and non-deuterated standards for the reaction product, believed to be the 9-OH compound **58** (See **Chapter 10**). Late addition of the TPP component would allow a late common synthetic intermediate. Conveniently, *N*-alkylation is by far the most common way of making these salts anyway, so a synthetic route to a protected 9-hydroxy phenanthridine precursor **126** was designed.

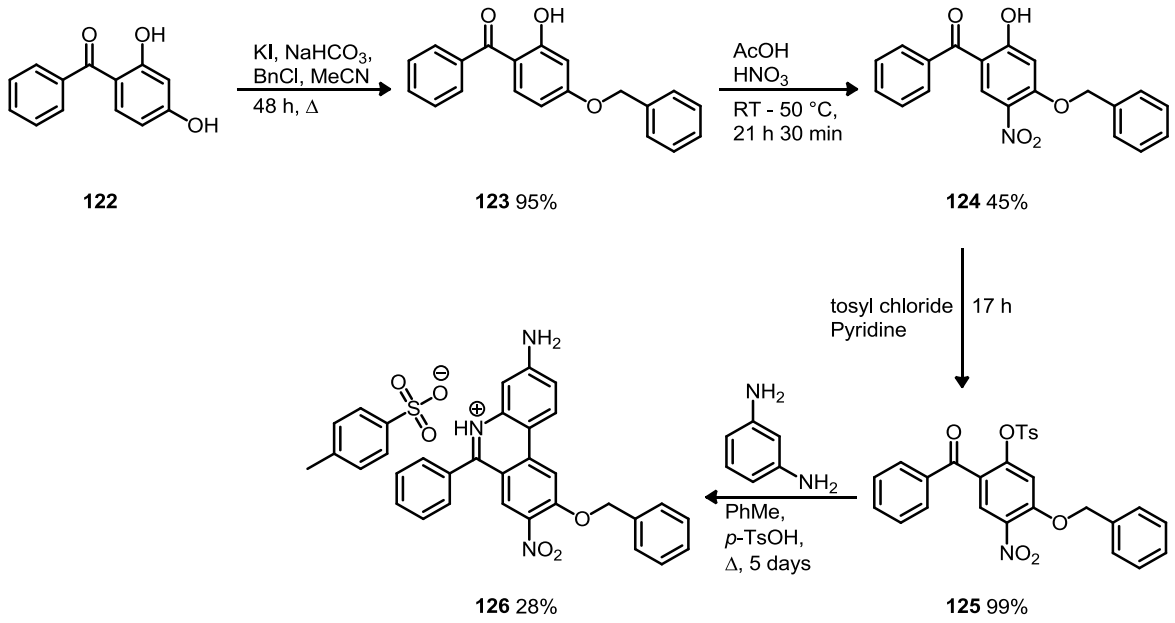

122 **123** 95% **124** 45%

126 28% **125** 99%

Scheme 38 - Synthesis of a precursor to 9-hydroxyphenanthridinium **126**.

The route (**Scheme 38**) is based on one originally attempted by Susan MacIntyre,[173] who had prepared benzophenones **123** and **124** starting with nitration of dihydroxybenzophenone **122**, benzyl protection of both phenols and then attempted selective deprotection. Disappointing yields resulting from low selectivity in nitration and deprotection steps were addressed by rearranging the synthesis.

The literature[174] and experience within the group suggested mono protection of 2,4-dihydroxybenzophenone **122** should be possible due to the low acidity of the phenolic hydroxyl group *ortho* to the ketone. Hydrogen bonding between 2-OH and C=O allows the 4-OH to be preferentially deprotonated. A single deprotonation increases the ring electron density and consequently disfavours diphenoxide formation, allowing the more acidic phenol to be protected selectively. This allowed near quantitative conversion of diol **122** into *para*-benzyloxy protected compound **123**. The same procedure cannot be used if C5 nitration precedes protection as the presence of the nitro group makes both phenols sufficiently acidic that either could be deprotonated, and like the ketone, the nitro group hydrogen bonds with an *ortho* phenol. Nitration of phenol **123** under mild conditions resulted in complete conversion of starting material **124** into a mixture of nitrobenzophenone **124** and an alternative nitrated side product in

a ratio of 4.2:1. The yield of the pure phenol **124** from the recrystallisation was limited due to the similarity of the side product.

Conversion of phenol **124** into aryl tosylate **125** was achieved overnight in pyridine. We reasoned that ketone **125** would react with 1,3-diaminobenzene to give phenanthridinium salt **126** when treated with acid. An initial attempt utilising Amberlyst 15 failed. When the mixture was heated under reflux with *p*-toluene sulfonic acid for 5 days under Dean-Stark conditions, a red solid with low solubility precipitated, the identity of which was eventually confirmed by washing with strong aqueous base, so that the ^{1}H NMR spectrum was not complicated by signals from *p*-toluene sulfonate (**Scheme 39**). This revealed the 7.30 ppm doublet (H1), which correlated with peaks for H2 and H4 in the COSY spectrum confirming the identity of phenanthridine **127**.

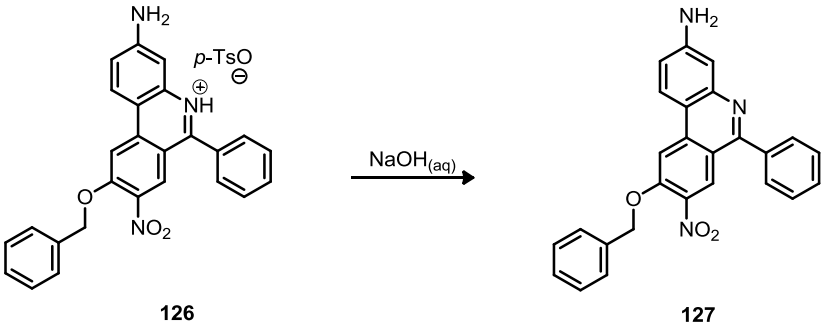

126 **127**

Scheme 39 - Neutralisation of phenanthridinium tosylate **126**.

The mechanism of this transformation is believed to involve the formation of both imine isomers **128** and **129** by removing water. The sterically less favoured isomer **129** then cyclises by nucleophilic attack from the *para* position of the dianiline ring on the aryl tosylate, with the resulting Meisenheimer complex **130** stabilised by the electron withdrawing properties of the *para* nitro group. Aromaticity is restored by loss of the tosylate from this. Restoration of aromaticity across the ring system then provides a strong driving force for deprotonation of **131**. Formation of phenanthridinines by this type of cyclisation is unprecedented (**Scheme 40**). The absence of a strong base rules out cyclisation via a benzyne[163] as used in the synthesis of Fagaronine[158] and recent analogues (see **Section 4.2.5**).[159] Attempts to use a higher boiling solvent, chlorobenzene, in the hope that higher temperatures would encourage isomerisation of the imine **128** and drive the reaction to completion were unsuccessful.

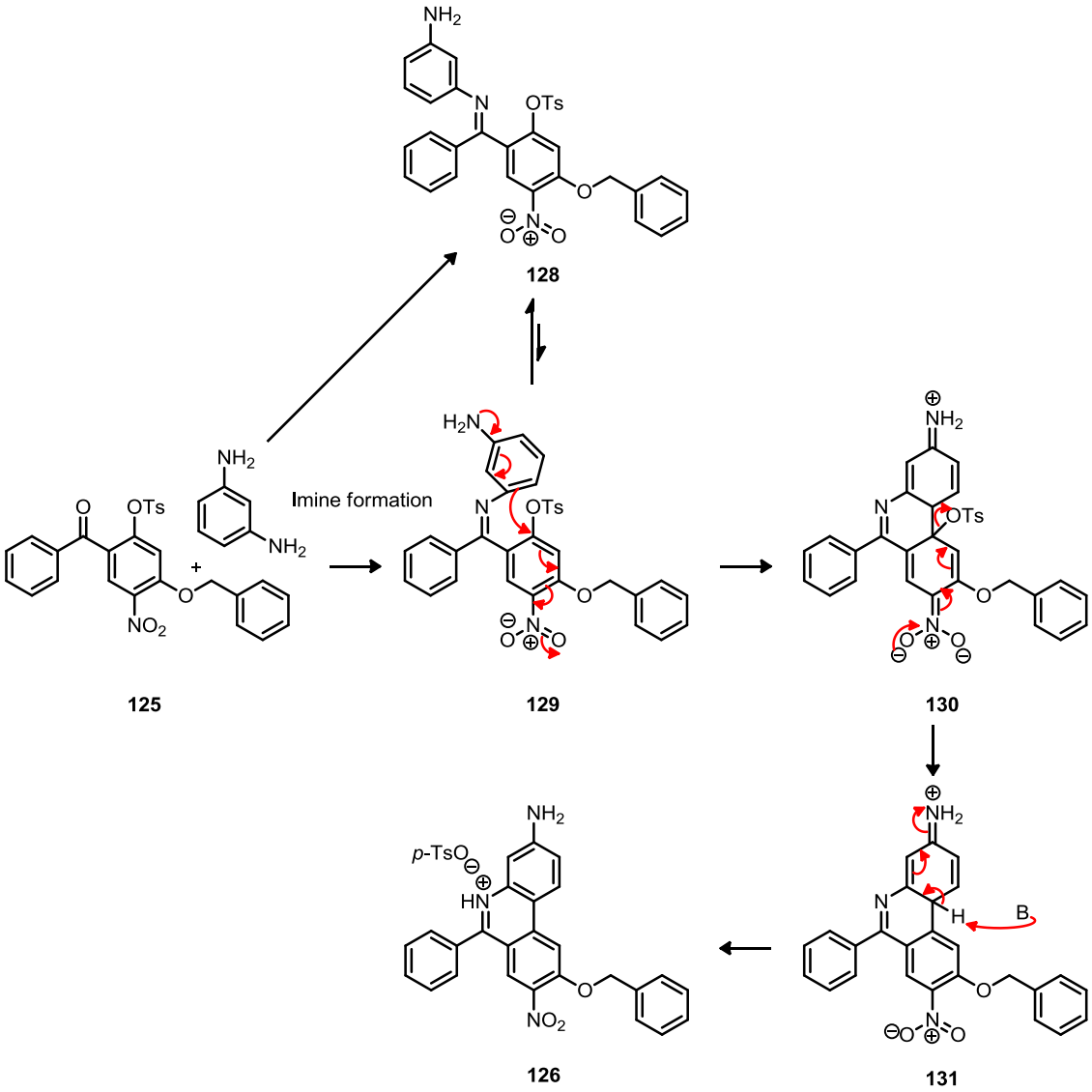

Scheme 40 - Postulated mechanism for cyclisation from benzophenone **125** to phenanthridinium **126**.

5.2 *N*-Alkylation of Phenanthridines

5.2.1 Introduction and phenanthridines

3,8-Diaminophenanthridine **133** is commercially available, so with 9-benzyloxy variant **127** in hand alkylation to give *N*-alkylphenanthridinium salts was attempted. Since the 3,8-diaminoprecursor is commercially available this is an ideal approach to MitoSOX. Avoiding synthesis of the heterocycle results in a short synthesis, with only protection of the 3,8-amino functionality and alkylation required (**Scheme 41**).

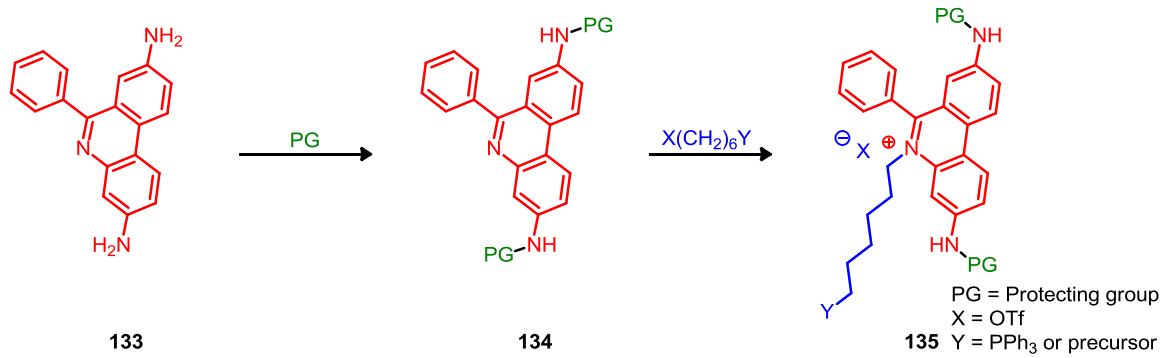

133 **134** **135**

Scheme 41 - Alkylation strategy for synthesis of *N*-alkylphenanthridinium salts **135**.

Commercially available phenanthridine **133** was protected as a variety of carbamates according to literature procedures (**Scheme 42**).[175] The Boc protected phenanthridine **137** was previously prepared by Stephen McQuaker, who attempted the alkylation with a variety of dihalides without success. Of the three additional carbamate-protected phenanthridines the methyl carbamate **139** proved very insoluble but the benzyl and ethyl analogues **138** and **140** were tractable.

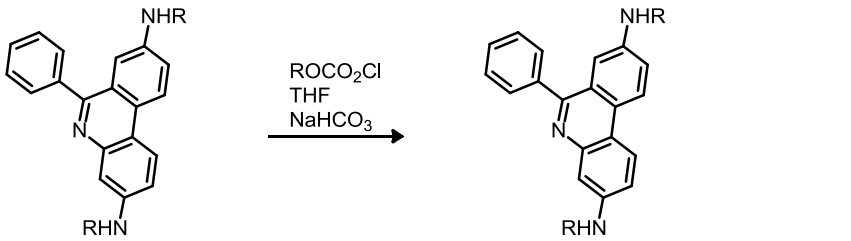

136

Scheme 42 - Carbamate protection of phenanthridine **136**

5.2.2 Alkylating agents

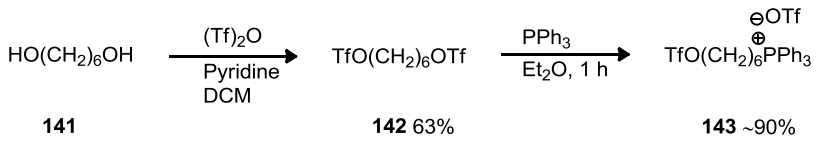

Scheme 43 - Synthesis of a monophosphonium triflate salt **143**.

Although there is literature precedent for use of alkyl dihalides,[176] phenanthridines are very poor nucleophiles[141] so triflate is the most commonly employed leaving group. Bis-triflate **142** was prepared according to a literature procedure from diol **141**, with a distinctive 2H *t* at 4.5 ppm in the ^{1}H NMR spectrum indicating success (**Scheme 43**).[177] On treatment with triphenylphosphine the insolubility of phosphonium cations in Et_2O allowed the mono-TPP salt **143** to be prepared exclusively. ^{1}H NMR spectroscopy showed yields in excess of 90% based on characteristic CH_2 groups adjacent to phosphonium and triflate groups, and material was used directly rather than isolated due to moisture sensitivity. This compound proved hugely more moisture sensitive than the parent *bis*-triflate **142**. This problem was independently experienced by the group of Robin Smith,[178] and was attributed to the charge improving association with water molecules, making hydrolysis more probable. The sensitivity of phosphonium triflate **143** required fresh preparation and laborious handling conditions, so monobenzyl triflate **146** was synthesised instead (**Scheme 44**).

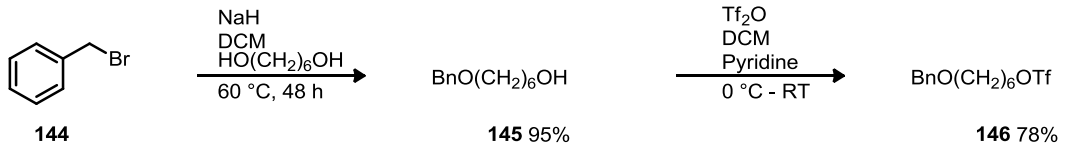

Scheme 44 - Synthesis of a monobenzyloxy alkyl triflate **146**.

One end of 1,6-hexanediol was benzylated, with the waxy solid being dried by azeotrope with PhMe prior to protection using a modified literature procedure.[179] No selectivity is achieved in this reaction and the statistical mixture results. It was quickly realised that most of the diol could be washed out, and the remainder would stick to the SiO_2 in the 1:1 petrol/Et_2O mixture which eluted the desired monobenzyl alcohol **145**. A sevenfold excess of 1,6-hexandiol was used with the excess removed by washing and filtration through SiO_2. This avoids generation of the more difficult to remove dibenzylated side product, and the diol could be recovered and reused if desired. Triflate formation then gave monobenzyl triflate **146** in good yield.

5.2.3 Alkylation experiments

Alkylation (**Scheme 45**) was attempted under various conditions, summarised in **Table 1**.

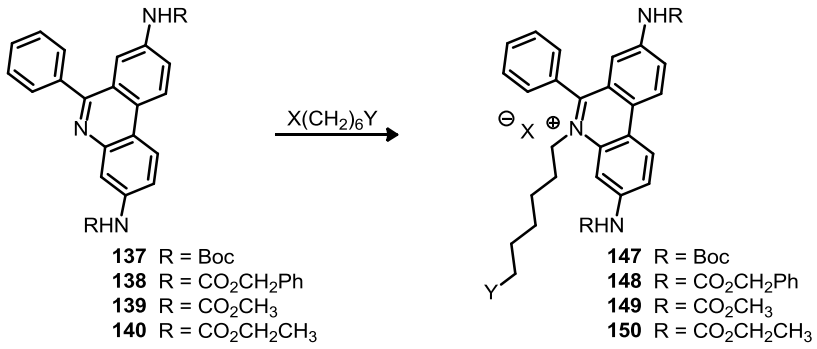

137 R = Boc
138 R = CO_2CH_2Ph
139 R = CO_2CH_3
140 R = $CO_2CH_2CH_3$

147 R = Boc
148 R = CO_2CH_2Ph
149 R = CO_2CH_3
150 R = $CO_2CH_2CH_3$

Scheme 45 - General scheme for the alkylation of protected 3,8-diaminophenanthridines

Table 1

Entry	Substrate	Triflate	T (˚C)	t (h)	Solv.	Base
I	**137**	**142**	RT - 120	20/3	$PhNO_2$	-
II	**138**	**142**	RT	1.5	THF	-
III	**138**	**142**	RT	72	THF	-
IV	**138**	**143**	RT	17	DCM	-
V	**138**	**143**	RT	17	$PhNO_2$	$NaHCO_{3(aq)}$
VI	**138**	**143**	reflux	17	CD_3CN	Proton sponge
VII	**138**	**143**	reflux	17	CD_3CN	-
VIII	**138**	**143**	RT	17	CD_3CN	-
IX	**138**	**143**	RT	17	d_6-DMSO	-
X	**138**	**146**	RT	60	CD_3CN	-
XI	**138**	**146**	RT - 100	60	d_6-DMSO	-
XII	**138**	**146**	RT	60	PhMe	-
XIII	**138**	**146**	125	17	d_6-DMSO	-
XIV	**138**	**146**	RT	21	$PhNO_2$	-
XV	**139**	**146**	RT	18.5	$PhNO_2$	-
XVI	**140**	**146**	RT	22	$PhNO_2$	-
XVII	**140**	**146**	RT	22	$PhNO_2$	$NaHCO_{3(aq)}$
XVIII	**140**	**143**	RT	17	$PhNO_2$	-
XIX	**140**	**143**	35	21	$PhNO_2$	-
XXI	**140**	**146**	RT	72	$PhNO_2$	[a]
XXII	**140**	**146**	70	16	$PhNO_2$	[a]

[a] 2,6-di*tert*butyl-4-methylpyridine

Nitrobenzene was the solvent of choice and is commonly used as the solvent for phenanthridine alkylation,[138] being polar enough to solubilise starting materials, products and the S_N2 transition state (which involves charge separation in this case) while being inert to most electrophiles due to electron deficiency. One indicator of alkylation is a *t* at around 4.5 ppm in the ^1H NMR spectrum, distinguished from the CH_2-1 peak at 4.5 ppm of triflates as a much broader signal.

The Boc protected phenanthridine **137** did not react with triflate **142** at RT; heating to 120 ˚C followed by cooling and addition of Et_2O resulted in precipitation of a mixture, possibly including

phenanthridinium **147** as a minor component (**I**). Similar results were achieved regardless of reaction time with benzylcarbamate **138** in THF (**II** and **III**). For the alkylation of TPP triflate **143** DCM was tested (**IV**) as it is not very hygroscopic and phosphonium salts tend to be soluble in chlorinated solvents, but little or no reaction was observed. Since elimination was a plausible competing reaction a base was introduced to re-activate any subsequently protonated phenanthridine; $NaHCO_{3(aq)}$ was tested based on literature precedent (**V**).[142] Following reaction a precipitate was observed, but no product. To eliminate decomposition during work up reaction in CD_3CN was followed by ^1H NMR spectroscopy. Heating to reflux caused decomposition (**VI** and **VII**), but entry **VIII** showed peaks at 4.5 and 4.1 ppm. These could be CH_2-1' and increase in size over 1 h, but heating overnight caused decomposition. Complicated mixtures uniformly resulted from these conditions at all time points. The procedure was repeated in d_6-DMSO due to the availability of literature data, allowing alkylation to be judged by comparison with the ethidium analogue prepared and assigned by Luedtke[180] - a shift to bring H7 upfield of H2/H9 would be considered characteristic of the phenanthridinium **148**. DMSO also allows higher temperatures if needed and the dispersion of the ^1H NMR peaks for the aromatic region in this solvent is helpful. No product was observed (**IX**).

The moisture sensitivity of triflate **143** was considered to be impeding progress. Repeating previous tests with triflate **146** (**X** - **XIII**) showed complete consumption of triflate, but no product **148**. Room temperature alkylation with triflate **146** in $PhNO_2$ did not result in reaction with benzyl carbamate **138** (**XIV**), but with methyl carbamate **139** gave a minor side product with an *ortho d* at 10 ppm and a broad *t* at 4.7 ppm in the ^1H NMR spectrum, suggesting phenanthridinium formation (**XV**). However, this was not successfully purified by chromatography or a Strata X-C ion exchange column.

Repetition with ethyl carbamate **140** and alkyl triflate **146** followed by repeated chromatography with both SiO_2 and C18 cartridges did give fractions which unambiguously contained an *N*-alkyl phenanthridinium **150** based on the characteristic broad *t* at 4.5 ppm (distinct in form from the sharp CH_2-OTf from triflate **146**), and amide broad singlets at 10 ppm in d_6-DMSO in the ^1H NMR spectrum (**XVI**). These amide peaks were present in duplicate in approximately 1:1 ratio, which was initially attributed to slow rotation of the amide giving rotamers on the NMR timescale as the benzyl CH_2 peak is present only once and integrates as if part of a single compound with the aromatic protons in the ^1H NMR spectrum. Including $NaHCO_{3(aq)}$ (**XVII**) afforded a fraction in which phenanthridinium **150** was the major component. This allowed more precise development of a TLC system, which was important as $PhNO_2$ is removed via initial chromatography of the reaction mixture. With evidence that the alkylation worked (if poorly), phosphonium triflate **143** was applied to the new conditions (**XVIII** - **XIX**). $NaHCO_{3(aq)}$ was omitted as experience had shown the moisture sensitivity of the alkylating agent by this point, with moderate conversion observed regardless of reaction time. On analysing fractions collected during chromatography of entries **XVIII** - **XIX** additional amide peaks were revealed to be an impurity rather than a rotamer when a trace sample from which they were absent was isolated. Faced with this purification problem

triflate **146** was again used, to avoid the complication of separating phosphonium salts from phenanthridinium salts.

Although $NaHCO_{3(aq)}$ appeared to improve conversion a base soluble in anhydrous $PhNO_2$ was considered preferable, with the caveat that very low nucleophilicity was required to prevent competition. 2,6-Di*tert*-butyl-4-methylpyridine was used, and after 72 h the desired product **150** appeared favoured by approximately a 63:37 ratio over the side product (**Scheme 46**). Repeated chromatography gave a 7% yield at a purity estimated to be around > 90% if residual DCM is ignored (**XXI**). Increasing the equivalents of triflate **146** and the temperature caused a loss of selectivity and a 1:1 ratio of the phenanthridinium **150** to side product (**XXII**).

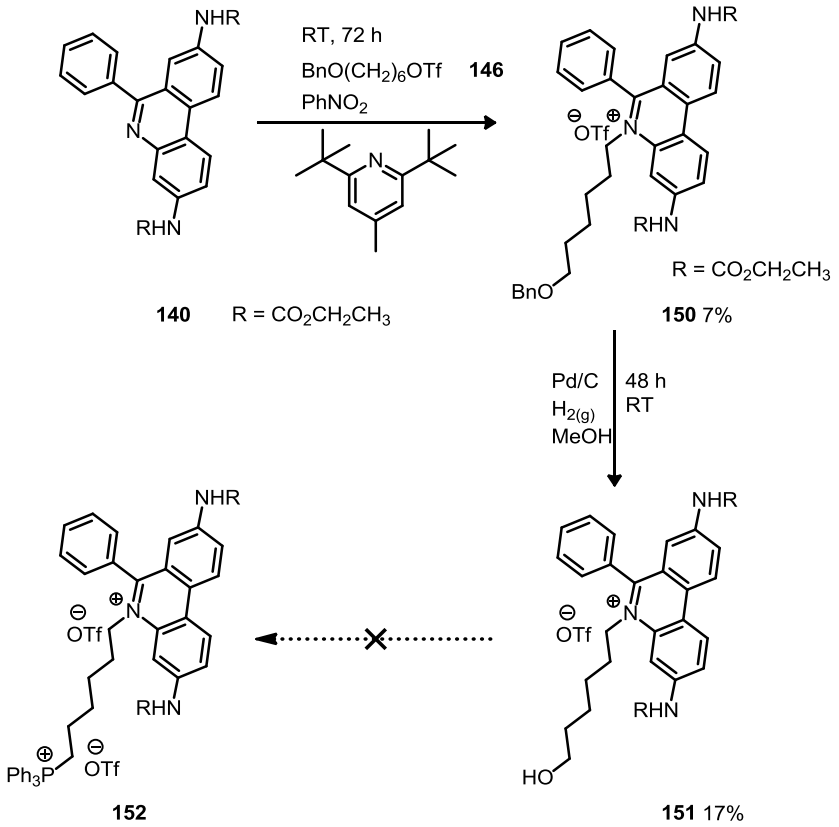

Scheme 46 - Alkylation and intended route to the MitoSOX precursor **152**.

Mixtures of phenanthridinium **150** and the side product from alkylation were subjected to hydrogenolysis to remove the benzyl protecting group. Clean deprotection resulted, and subsequent chromatography gave a 17% yield of alcohol **151**. Impure material was used for a small scale test of iodination (Appel reaction) and triphenylphosphine addition, confirming the conditions did not result in decomposition but unfortunately not that TPP salt **152** is formed. Small scale removal of ethyl carbamate by reflux in $HBr_{(aq)}$ gave better chromatographic separation, although unpredictable elution was still observed (see later). A single column yielded some fractions of approximately 90% purity, but the use of d_6-DMSO as an NMR solvent hid the CH_2 shift which would confirm the conversion from alcohol to bromide.

Particular note was made during the course of the above work of the difficulty inherent in purifying these compounds, with considerable streaking contributing to a situation where elution

rarely mimicked TLC. Acetone/EtOAc systems worked well on TLC but proved hopeless on silica column. Even the various DCM/MeOH systems often required washing with high percentages of MeOH and/or NEt_3 to recover the majority of material, which often adhered to the baseline but matched earlier fractions by NMR and TLC when recovered.

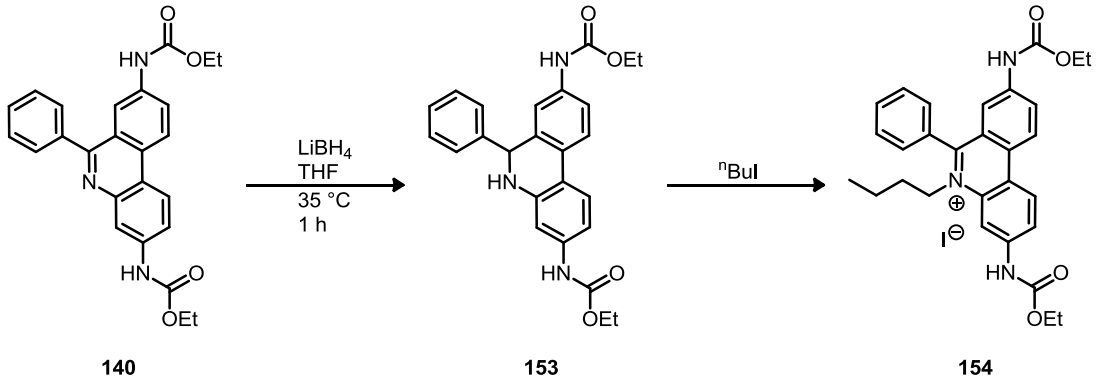

140 **153** **154**

Scheme 47 - Outline of a reduction-alkylation based synthesis of phenanthridinium iodide **154**.

When the difficulty of phenanthridine alkylation became apparent reduction of ethyl carbamate **140** to an amine and subsequent alkylation of hydrophenanthridine **153** was investigated (**Scheme 47**). Hydrogenation over Pd/C in AcOH (allowing reduction through the reactive iminium) was unsuccessful, so $LiBH_4$ was used. This is more reactive than $NaBH_4$ due to the higher Lewis acidity of Li^+,[181,182] and is soluble in ethereal solvents, from which *N*-alkylphenanthridinium **154** might be expected to precipitate were the steps combined. $LiBH_4$ does not reduce carbamates in numerous literature examples.[183] Reduction was confirmed by TLC and colour change. Additional aromatic peaks for the hydrophenanthridine **153** in the ^{1}H NMR spectrum including those at 7.6 ppm *d* (*J* = 9.2 Hz, H1/H10) and 6.64 ppm *dd* (*J* = 8.4, 2.1 Hz, H2/H9) are considerably upfield of where equivalent peaks are expected in the oxidised form **140**. Re-oxidation is rapid; at best a 3:1 ratio of **153**:**140** was observed by NMR spectroscopy (**Scheme 31**).

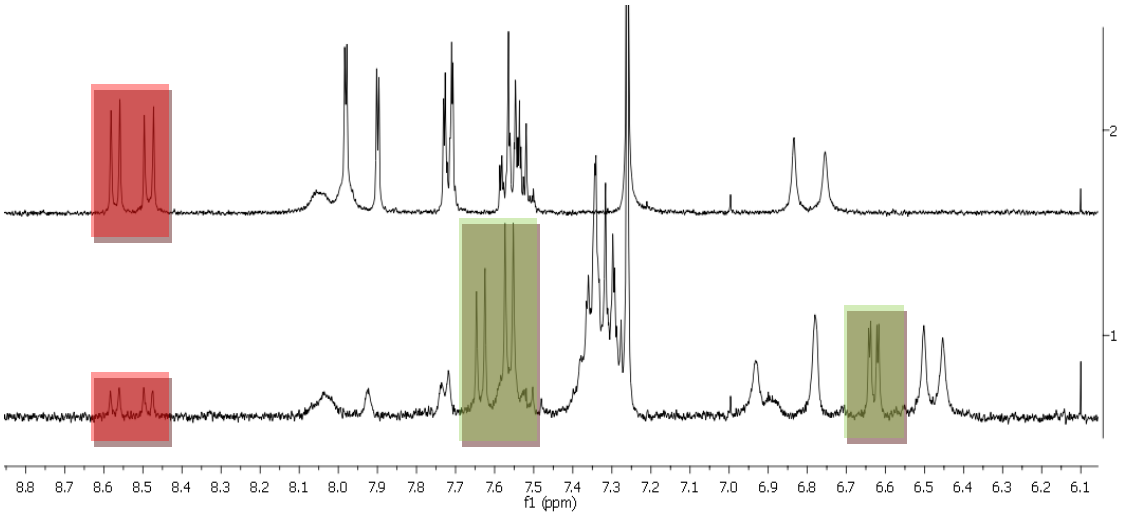

Figure 31 - Comparison of **140** (top) and post reduction mixture (bottom) containing mostly **153** in $CDCl_3$. The H1/H10 positions in each are highlighted, as is H2 in the reduced compound.

Alkylation was attempted on the mixture using iodobutane, but even with long (72 h) reaction times no alkylation was observed. It was increasingly apparent that the synthesis of *N*-alkylphenanthridinium salts was not trivial, so an alternative route was attempted.

5.3 Route to *N*-alkylphenanthridinium salts via Bischler-Napieralski cyclisation

An alternative synthesis attempts to build on a literature report of cyclisation directly to a phenanthridinium alkaloid precursor **155** via Bischler-Napieralski type cyclisation (**Scheme 48**).[184] This is analogous to the classic Morgan-Walls cyclisation to give phenanthridines (see **Section 4.2.1**).

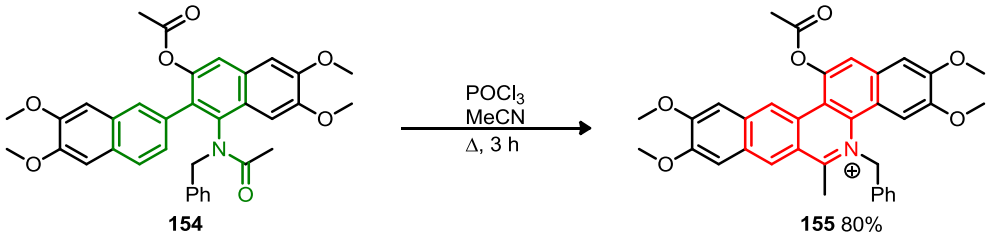

Scheme 48 - Literature example of a Bischler-Napieralski cyclisation to a phenanthridinium based alkaloid.[184]

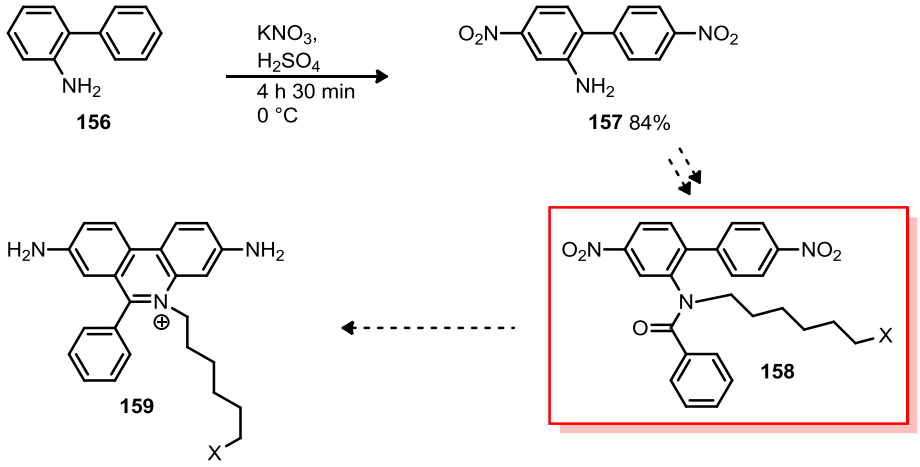

Scheme 49 - Synthesis of 3,8-diaminophenanthridinium salt **159** via Bischler-Napieralski reaction required access to key tertiary amide intermediate **158**.

Using the strategy outlined in **Scheme 49** intermediate **158** is the key precursor for the cyclisation reaction. 4,4-Dinitrobiphen-2-ylamine **157** was prepared from biphenyl-2-ylamine **156**, according to a literature procedure[143] using KNO_3 in H_2SO_4, which provides a powerful nitrating agent with lower water content than $HNO_{3(aq)}/H_2SO_{4(aq)}$.

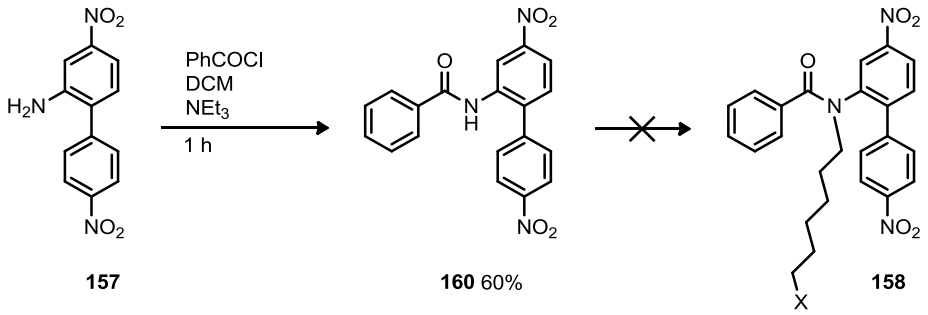

Scheme 50 - An amide formation and alkylation strategy did not allow access to intermediate **158**.

Using a large excess of KNO_3 (8 eq.) resulted in a mixture of double and possible triple nitrated aromatic rings even at low temperature, but reducing the amount of KNO_3 to 2.2 eq. gave clean conversion with no purification aside from an aqueous wash. The regiochemistry of nitration on

the aniline ring is consistent with the electron withdrawing effect of the aryl ammonium group generated in strongly acidic conditions. Amide formation by refluxing dinitrobiphen-2-ylamine **156** with benzoyl chloride in chlorobenzene as in Lion *et al* resulted in a mixture of products.[143] Mild alternative conditions[185] gave good conversion (**Scheme 50**) to amide **160**.

Amide **160** dissolved well only in DMSO or hot DMF, complicating the recovery of material. Quenching into water gave a very fine precipitate which did not reliably filter out, or stay settled enough to separate from the solution after centrifugation. Many attempts were made at the subsequent alkylation with increasingly harsh conditions, including heating amide **160** to 170 ˚C with 3 eq. sodium hydride and excess 1,6-dichlorohexane for 90 min. Use of iodide catalysis was tested, as were various alkylating agents including triflate **142**, 1,6-diiodohexane and an alkyl iodide bearing a THP-protected alcohol **162** synthesised via the Appel reaction (**Scheme 51**).

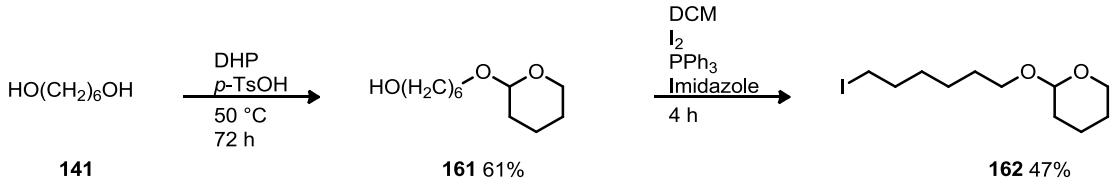

Scheme 51 - Synthesis of a mono-THP protected iodohexyl compound **162**.

Attempted alkylation of amide **160** resulted in various mixtures of numerous and diverse decomposition products under these conditions or indeed any more unusual procedures tested.[186,187] The alkylation of amide **160** was expected to be problematic, being very electron poor and because the tertiary amide **158** would be sterically congested. However, it was not fully appreciated how strained the desired product would be until the atropisomerism displayed by a less hindered carbamate **245** (**Scheme 77**) was later identified.

The original literature cyclisation[184] required heating to reflux in MeCN even when decorated with multiple donating groups (**Scheme 52**), so it was anticipated that reduction of the nitro groups on amide **160** would prove necessary. Reduction via transfer hydrogenation (**Scheme 52**) was tested on the dinitroamide **160**.

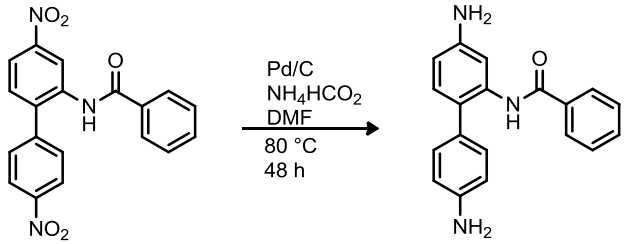

Scheme 52 - Reduction of dinitrobiphenyl **160** to give more nucleophilic biphenyl **163**.

The diamino compound **163** was confirmed by a uniform upfield shift in the aromatic protons in the ^{1}H NMR spectrum and the appearance of a 4H broad singlet at 3.8 ppm, but not purified or further characterised. To overcome alkylation difficulties the steps were rearranged, with benzoyl

protection following reductive amination. Aldehyde **164** was synthesised by Swern oxidation of alcohol **161** (**Scheme 53**).

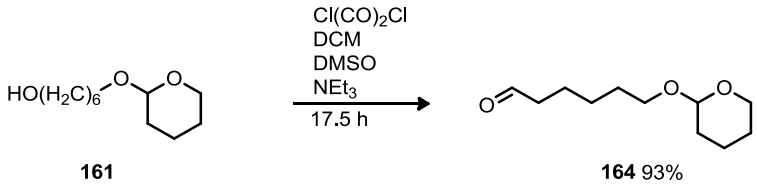

Scheme 53 - Swern oxidation to aldehyde **164**.

Attempts at reductive amination to convert primary amine **157** into secondary amine **165**, both *in-situ* and via isolation of imine **166** and reduction proved unsuccessful, as did an unusual procedure using the direct alkylation of the amine **157** with alcohol **161** (**Scheme 54**).[186]

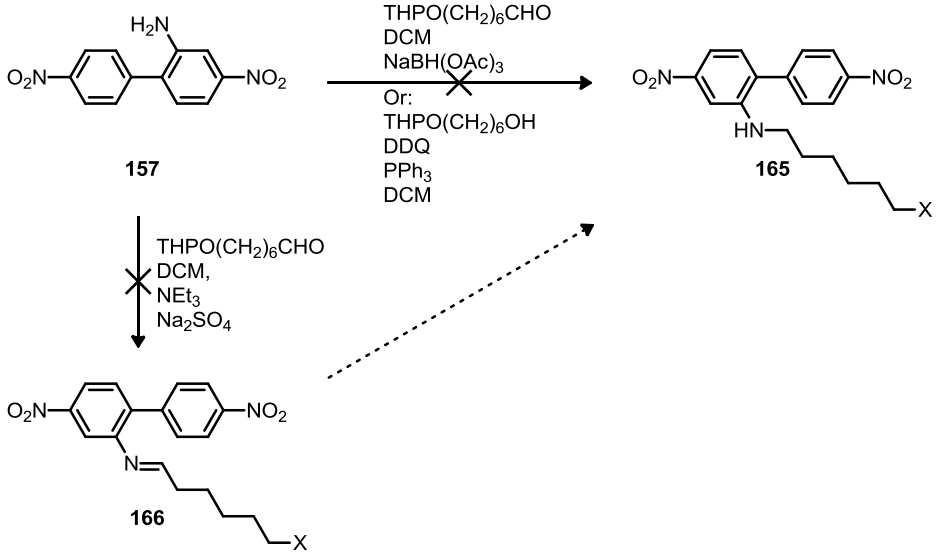

Scheme 54 - Different reductive amination protocols failed to access secondary amine **165**.

The reactivity of the aniline was proving problematic, so the more circuitous route of reaction with an acid chloride and subsequent reduction was investigated, for which several acylating agents were prepared (**Scheme 55**). Synthesis and isolation of the 7-membered cyclic anhydride **169** from a literature procedure[188] starting with adipic acid **167** proved problematic. Double acid chloride **170** was synthesised by reaction with thionyl chloride and reacted immediately with aniline **157**, resulting in a complex mixture of products. Mono methyl adipic acid was then used instead to generate acid chloride **171**.

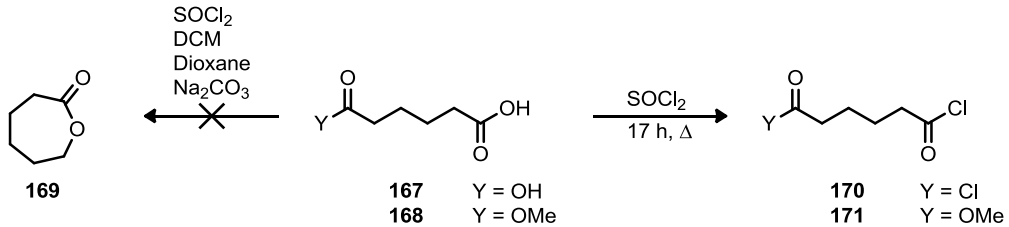

Scheme 55 - Preparation of acylating agents **170** and **171**.

Amine **157** was then reacted with acid chloride **171** to give amide **172** in good yield (**Scheme 56**). Ester **172** was hydrolysed to give acid **173**.

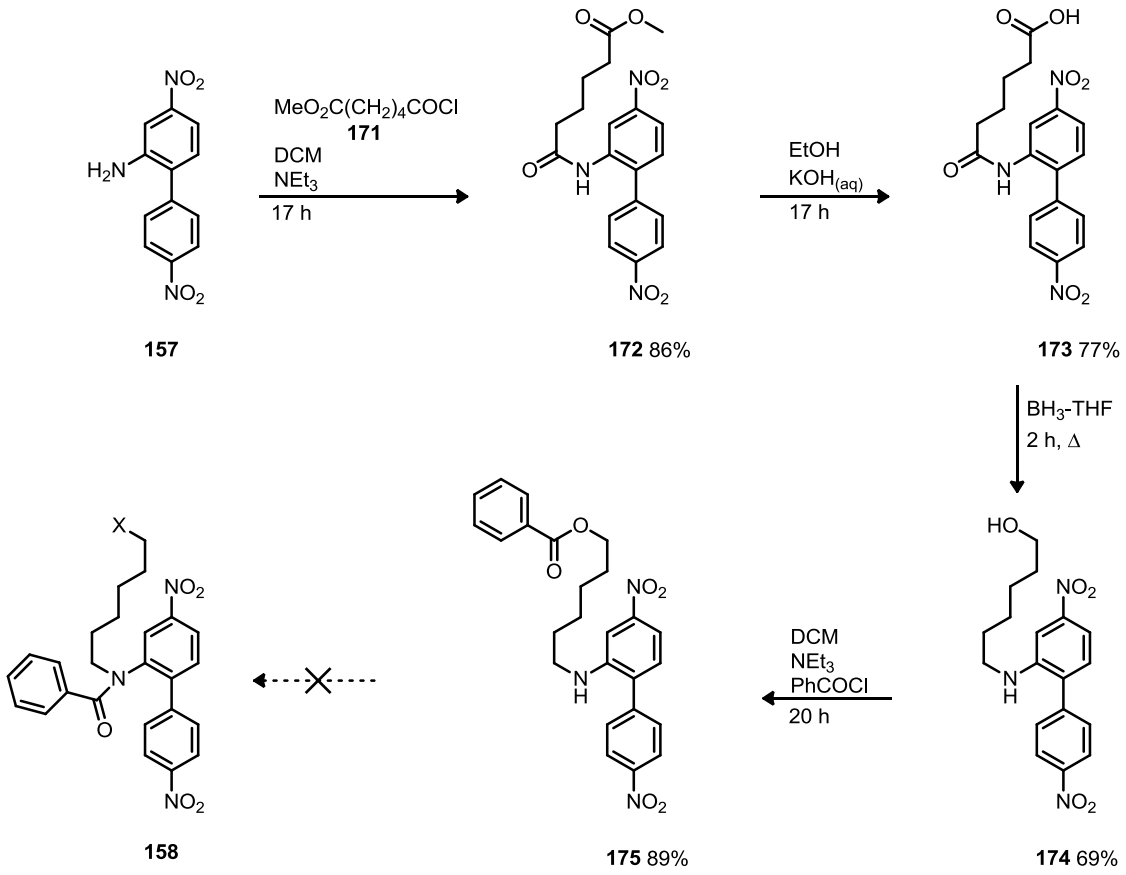

Scheme 56 - Secondary amine **175** was accessed by an acylation-reduction approach, but tertiary amide intermediate **158** remained elusive.

The next step was reduction of the amide using the neutral and electrophilic THF-borane reagent. The borane coordinates to the more Lewis basic position prior to reduction, and in the case of carboxylic acids forms a triacyloxyborane (**Scheme 57**).[189] Coordination to the acid generates complex **176**, or a related structure,[190] which decomposes to a structure **177** analogous to a mixed anhydride allowing rapid reduction. The expected result is that the aldehyde is generated then reduced in preference to the amide.[191] A hydride such as DIBALH would preferentially reduce the amide, risking cyclisation from the amine when the aldehyde is produced. There is strong literature precedent for borane tolerating aromatic nitro groups,[191,192] unlike reagents such as lithium aluminium hydride.

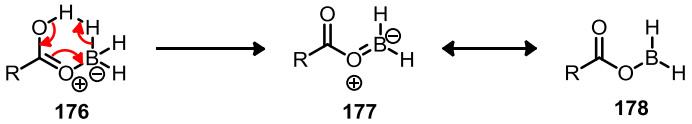

Scheme 57 - Triacyloxyborane **176** decomposes to a mixed anhydride **177**.[189]

An initial test of reduction of acid **173** with 4 eq. of borane and overnight reflux showed reduction of one nitro group in addition to the expected reaction. Reflux with 2 eq. overnight gave reduction of the acid to the alcohol without reaction at the amide. Returning to 4 eq. of borane and monitoring by TLC allowed for good conversion to alcohol **174**. Attempts to generate the amide

precursor **158** lead to benzoyl protection of the alcohol giving benzoate **175**, and subsequent deprotonation of this with LiHMDS and reaction with benzoyl chloride proved ineffective. Conversion directly to phenanthridinium was attempted via procedures reminiscent of the Pictet Spengler reaction, initially combining TMSCl with benzaldehyde **72** and alcohol **174,** before applying harsher literature Pictet-Spengler cyclisation and spontaneous oxidation conditions reported for the cyclisation of amine **156** to give phenanthridine **179**[193] using benzaldehyde in TFA at high temperature and in a sealed tube (**Scheme 58**).

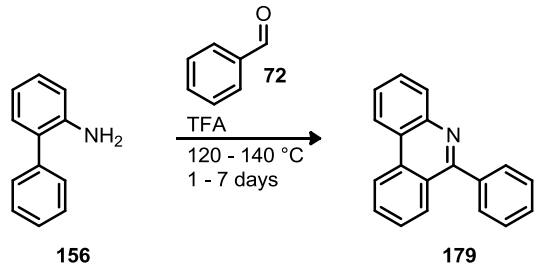

Scheme 58 - Literature Pictet-Spengler procedure.[193]

Although this literature example does not form an *N*-alkylphenanthridinium, the reaction occurs in neat TFA so it is reasonable to assume the reaction proceeds through an iminium intermediate. In reality only a TFA ester (identified by a downfield shift in the adjacent CH_2) was isolated (**Scheme 59**), probably due to the low reactivity of the aniline of dinitrobiphenyl derivative **33** towards electrophiles.

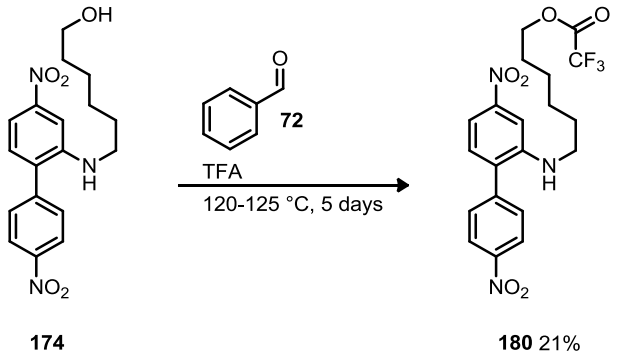

Scheme 59 - Pictet-Spengler attempt on secondary amine **174** gave only TFA ester **180**.

5.4 Summary

Having attempted multiple alkylation and cyclisation based routes, recurring difficulties were apparent. Alkylation of the consistently hindered and unreactive nitrogen was always problematic, exacerbated by the electron poor phenanthridines and biphenyl systems used.

Concurrent preliminary work on commercially available 3,8-diamino-6-phenylphenanthridinium salts by Dr Murphy's group at MRC in Cambridge suggested that the DNA intercalation observed made reproducible extraction challenging. On this basis the target was changed and required a bespoke phenanthridine heterocycle. Without the benefit of the commercially available 3,8-Diaminophenanthridine as a starting material for the new route and in light of the considerable difficulties encountered the alkylation work was abandoned. Similarly the biphen-2-ylamine routes were deemed to be too dependent on difficult alkylations and to offer limited scope for analogue synthesis. Therefore, when considering a new target alternative synthetic routes were investigated instead.

Chapter 6: A new targeted superoxide sensor design

6.1 Design and retrosynthesis

6.1.1 Avoiding DNA intercalation

In order to avoid DNA intercalation, it was necessary to modify the target probe. The structure was tweaked by exchanging the 3-amino group for a *tert*-butyl moiety, as shown in blue in superoxide probe target **181** (**Figure 32**). This should avert intercalation because the bulky substituent will make intercalation between DNA base pairs energetically unfavourable.

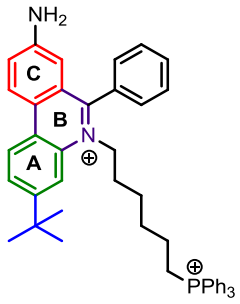

181

Figure 32 - Target phenanthridinium showing A, B, C labels for rings, with the blocking ^{t}Bu group in blue.

6.1.2 Synthetic route towards superoxide probe 181

The design of the new probe **181** imposed the requirement of selective substitution at the 3 and 8 positions. In addition, based on the failure of previous approaches a few guiding principles were identified for application in evaluating routes:

- Very electron poor aniline components should be avoided as they are unreactive, and sterically hindered versions even more so.
- The *N*-alkyl group should be appended prior to construction of the heterocyclic B-ring as *N*-alkylation of phenanthridines is a poor reaction.
- When constructing the B-ring, avoid loading one component of an intermolecular reaction with all the bulk of the C6- and *N*- substituents.
- The reaction to make the *N*-alkylphenanthridinium should be simple, clean, high yielding and close to the end of the synthesis, because the separation of different phenanthridinium compounds is difficult and their solubility is problematic.
- Demanding transformations that require extensive purification should occur prior to the construction of the *N*-alkylphenanthridinium for the same reasons.

Working from these principles, a new route was devised concluding the synthesis of phenanthridinium core **182** with intramolecular imine formation. This is a 6-*exo*-*trig* cyclisation to make a polyaromatic system, and should be highly favoured. Additionally, the phenanthridinium salt **182** would likely precipitate from a non-polar solvent allowing easy isolation. The precursor ketone **183** could be prepared with robust and reliable cross coupling chemistry such as the Suzuki reaction which would be used to form the C_{1a}-C_{10a} bond. The cross coupling could use either the combination of a *ortho*-halobenzophenone **185** with *ortho*-aminoarylmetal **187** or a 2-metalobenzophenone **184** with *ortho*-aminoaryl halide **186**. This route avoids tertiary amine or

amide formation, which had torpedoed previous routes. The R group can be introduced early, with a variety of methods available to access secondary amine **186** from aniline **188**. The 6-Ph substituent could be included by taking advantage of the commercial availability of benzophenones and the extensive literature on these substrates.

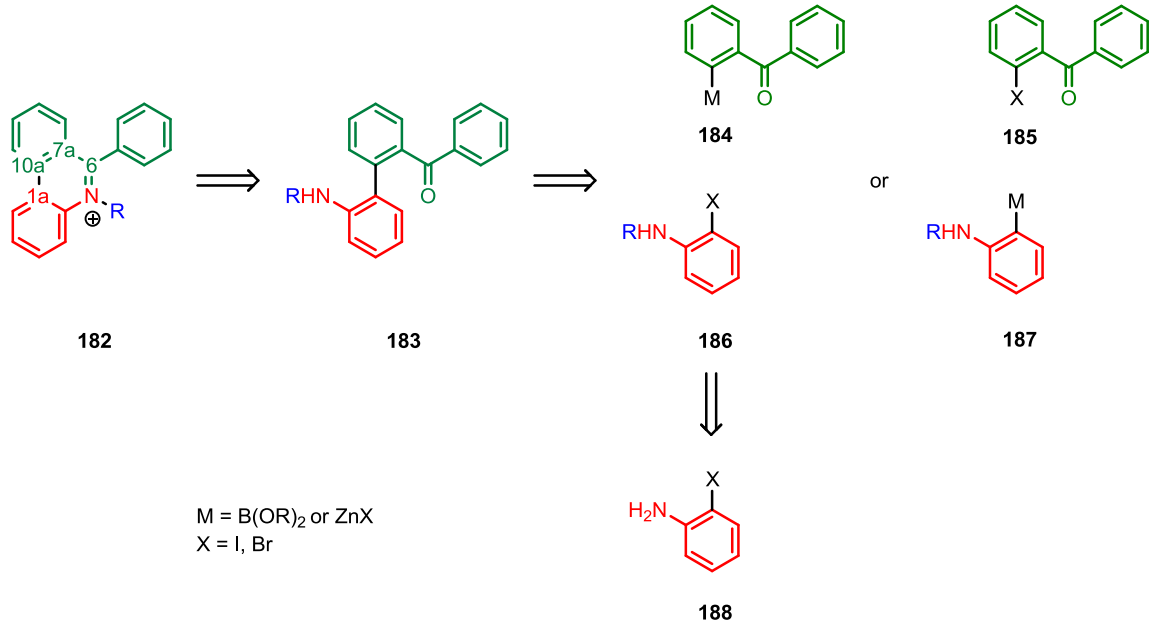

182 **183** **184** **185** **186** **187** **188**

Scheme 60 - Retrosynthesis for a proposed cross-coupling based synthesis. Unlike previous routes which relied upon C-N or C_6-C_{7a} bond formation for key steps, C_{1a}-C_{10a} is the critical transformation.

6.2 Suzuki cross coupling

6.2.1 Mechanism and ligand properties

Following assembly of the desired aromatic components they were to be linked to form the biaryl systems via palladium cross coupling chemistry, ideally the Suzuki coupling. The reaction itself was an obvious choice due to its ubiquity, robustness and substrate tolerance. An array of catalysts and conditions exist and three common catalysts which will be important in later discussion are $Pd(PPh_3)_4$ (tetrakis) **189** and (dppf)$PdCl_2$ **190**, which involve phosphine ligands, and PEPPSI-^{i}Pr **191**, which contains a *N*-heterocyclic carbene ligand (**Figure 33**).

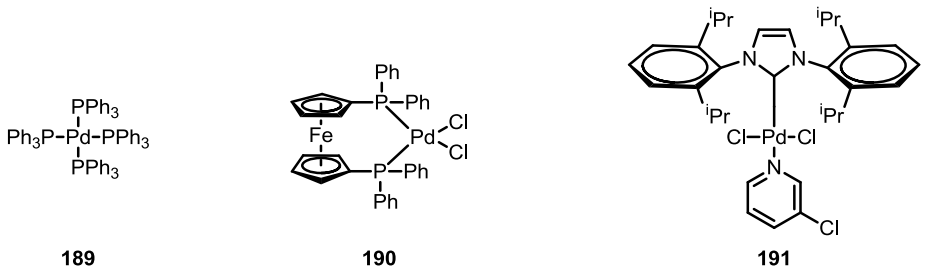

189 **190** **191**

Figure 33 - A selection of common palladium cross coupling catalyst systems.

A discussion of the mechanism and the choice of conditions is appropriate (**Scheme 61**).

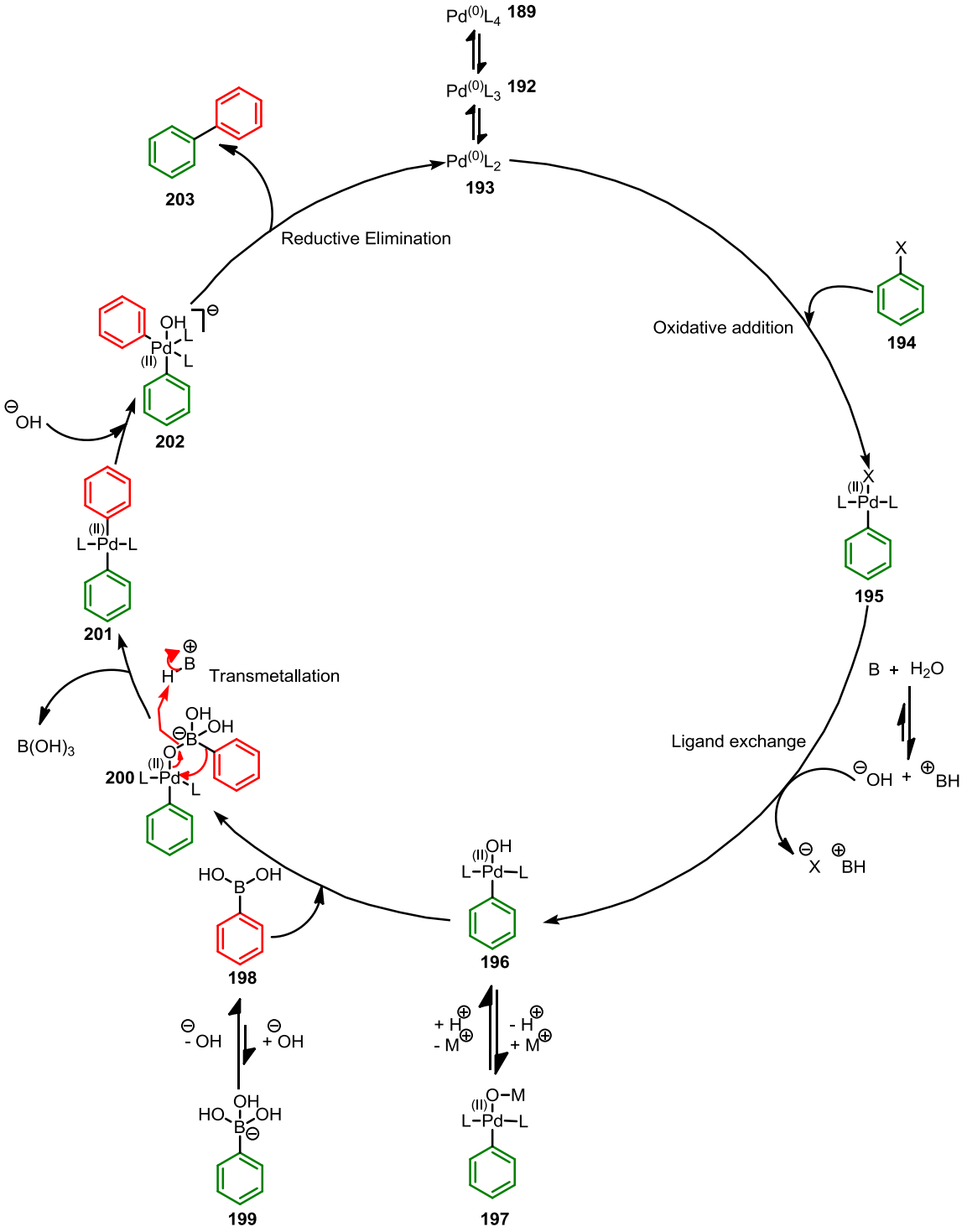

Scheme 61 - A simplified catalytic cycle for Suzuki coupling.

The precise nature of the catalytic $Pd^{(0)}L_n$ species varies and is a matter of debate, with $Pd^{(0)}L_2$ **193** and $Pd^{(0)}L$ both possible. The cycle shown above (**Scheme 61**) and described below is based on the tetrakis system (L = PPh_3). The metal has a full outer shell of d^{10} electrons in $Pd^{(0)}L_4$ **189** with repulsion reducing the bond strength and increasing ligand lability. Once one triphenylphosphine is lost the L_2 **193** and L_3 **192** forms equilibrate,[194] with L_2 species **193** considered catalytically active. Bidentate ligands such as dppf **190** are conceptually similar but the active $Pd^{(0)}$ species is generated from the dihalide $Pd^{(II)}$ salt rather than dissociating an additional bidentate ligand.[195] In

both cases the active species is usually a 14-electron complex which becomes 4 coordinate upon oxidative addition.

It is currently believed the active $Pd^{(0)}L_2$ species **193** undergoes oxidative addition inserting itself into the C-X bond of the aryl halide **194** via a concerted process to give a *cis* $Pd^{(II)}$ species. A theoretical study suggests this process is favoured by kinetics compared to insertion into an alkyl halide due to back bonding in the transition state resulting from interaction of the aromatic π system with X.[196] An exothermic isomerisation driven by the stability of the *trans* isomer[197] and probably occurring via ligand addition to form a trigonal bipyramidal transition state[200] leads to the observed *trans*[198,199] $Pd^{(II)}$ species **195**. This can be the rate determining step, especially for aryl chlorides. Substrate electronics influence the efficiency of this step, with electron poor aryl halides reacting more rapidly due to the electron rich nature of the neutral palladium species **193**, particularly where ligands are strongly donating.[200]

The halide is reversibly displaced by a nucleophilic ligand, usually hydroxide generated by a base reacting with water as shown in **Scheme 61** but fluoride is also frequently used.[201] This gives complex **196**, which undergoes faster transmetallation.[202,204] In the case of hydroxide the oxophillicity of the boron allows coordination prior to transmetallation in complex **200** and as a result the identity of the base counterion is important due to the potential competitive coordination of Pd-OH complex **196** by cations to form non-productive complex **197**.[203]

Due to the electron deficient nature of $Pd^{(II)}$ complexes transmetallation is a more facile process when an electron rich arylboronic acid is employed, and is disfavoured by donating ligands.[200] The arylboronic acid **198** is necessarily in equilibrium with the unreactive trihydroxyborate **199**, providing an upper limit to the acceleration provided by base.[201,204] The *trans* complex formed **201** is relatively stable[199,205] in the absence of base, with recent literature suggesting further coordination with hydroxide to give a pentacoordinate compound **202** which bypasses the requirement for *trans*/*cis* isomerisation prior to reductive elimination.[201,206] Analogous acceleration by a fifth ligand is precedented with a styrene promoter,[207] and fluoride is believed to behave similarly. Reductive elimination then occurs to give the biaryl product **203**, and this is most rapid when the electronic properties of the aryl groups are markedly different.[208] Electron rich ligands disfavour reductive elimination, while wide bite angle bidentate ligands sterically favour elimination.[209]

6.2.2 Mono-ligated palladium species

The previously shown catalytic cycle assumes $Pd^{(0)}L_2$ is the active catalyst. However, $Pd^{(0)}L$ is also possible. Bulky monodentate ligands are believed to form tricoordinate[210,211] intermediate **205** upon oxidative addition. The pathway to these intermediates is dependent mostly on the halide used (**Figure 34**).[212]

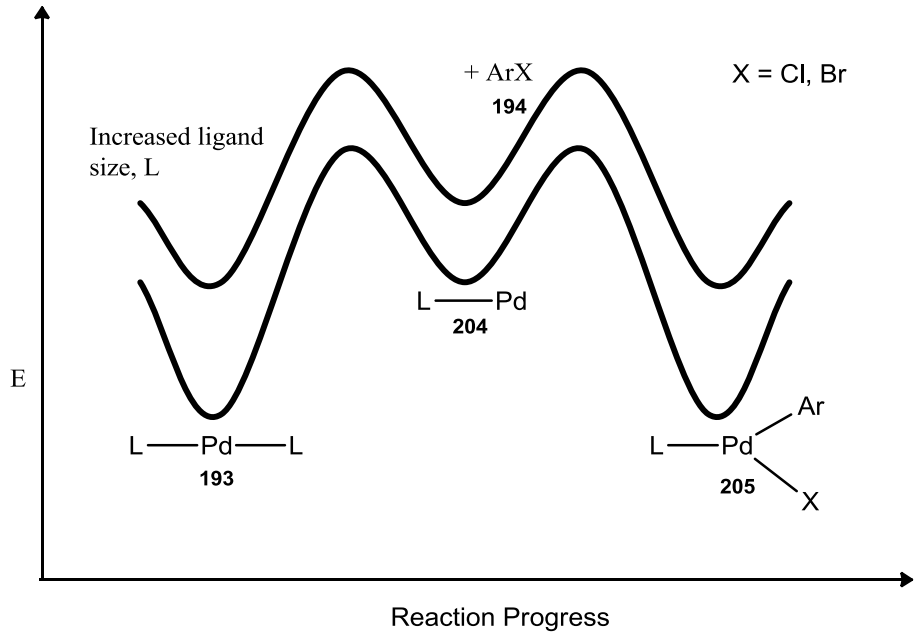

Figure 34 - The effect of ligand size on the generation of monoligated palladium species.[213]

The reaction coordinate diagram shows the dissociation of bicoordinate complex **193** to give monocoordinate complex **204** and oxidative addition to ArX **194** giving tricoordinate complex **205**. Increasing ligand bulk favours this dissociation by increasing the energy of the bicoordinate complex **193** more than the dissociated form **204**, as do specific interactions found in some ligands.[214] The nature of this process depends mostly on the halide used.[212]

In the case of aryl chlorides prior ligand dissociation from complex **193** gives **204**, a 12 electron species which undergoes rapid oxidative addition.[215,216] Aryl iodides react via the PdL_2 species, with one ligand then dissociating to form tricoordinate species **205**, which may then dimerise depending on ligand sterics.[217] Aryl bromides are variable; multiple mechanisms may occur in a substrate dependent fashion. Subsequent transmetallation may occur more easily to tricoordinate complexes,[214,218] and calculations on C-C and related C-N systems suggest they undergo reductive elimination more readily.[219,220,221]

6.2.3 *N*-Heterocyclic carbene catalysts

N-Heterocyclic carbene (NHC) ligands may also generate monocoordinate species **204**. NHC ligands represent an alternative to phosphine ligands. Originally believed to form PdL_2 complexes, it is now established that PdL complexes are the active species.[200,222] One example is the PEPPSI-^{i}Pr catalyst **191** (**Figure 33**). The core of the ligands themselves is an aromatic,[223] singlet,[224] bent

carbene stabilised by σ withdrawing and π donating nitrogen atoms.[225] While the reaction mechanism is broadly the same as when using phosphine ligands these complexes have important distinct properties. Bonding within NHC complexes varies depending on a range of subtleties.

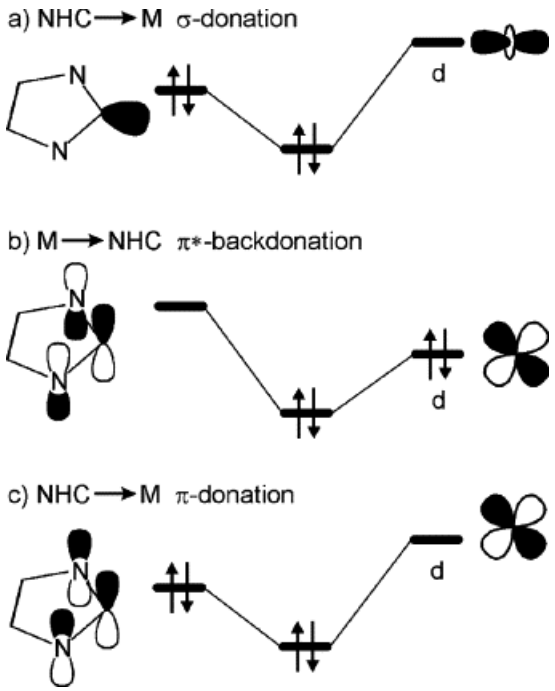

Figure 35 - The three major contributors to NHC-M bonding.[226]

There are three major bonding contributions to NHC metal complexes (**Figure 35**). Strong σ donation from the lone pair is the largest feature, providing more electron donation than phosphine ligands.[231] Of the remaining interactions metal → π^* backdonation is more important for d^{10} metal complexes.[227] A significant electrostatic component exists, particularly for cationic Pd species, but has proven difficult to quantify.[227] In the case of the PEPPSI family of commercially available catalysts activation is believed to occur through double transmetallation of the $Pd^{(II)}$ salt, and elimination to give $Pd^{(0)}$, then pyridine dissociation and oxidative addition, which is favoured by substituents increasing σ donation. Moderately bulky ligands improve either transmetallation or reductive elimination steps, with the effect of the pyridine ligand on the rate suggesting reattachment by this point.[228] NHC ligand based catalysts display high stability, allowing low catalyst loading.[229]

For testing purposes three catalytic systems were selected; the heavily used and studied $Pd(PPh_3)_4$ (tetrakis) **189**, $(dppf)PdCl_2$ **190**, selected as one of the more versatile bidentate catalysts,[230] and the most active[231] of the available PEPPSI-NHC catalysts, PEPPSI-^{i}Pr **191** (**Figure 33**).

6.3 Methods of constructing arylboron reagents

6.3.1 Miyaura Borylation:

Organometallics **185** and **186** are required for the cross-coupling and as discussed above organoboron compounds are ideal for this. The Miyaura reaction[283] is a way of converting aryl halides **194** to arylboronate esters **206** which uses a catalytic cycle mechanistically analogous to the Suzuki reaction to achieve borylation without the use of powerfully basic organometallic reagents (**Scheme 62**).

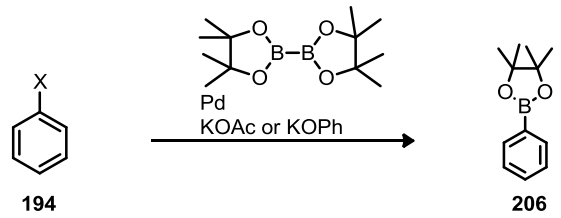

Scheme 62 - The Miyaura reaction.

Much of the prior discussion of the Suzuki mechanism is applicable here. The key difference is that these borylations go through a $L_nPd^{(II)}OAc$ complex. The hard Lewis base and soft Lewis acid combination may make this complex more reactive than the halide equivalent, with changes in geometry also implicated in some cases.[232] Pinacolboron acetate is produced as a by product. The weak base used limits hydroxide formation when water is present suppressing Suzuki coupling, although dry conditions are often required for good conversion. Various related procedures exist using different metals, different boronic esters and in one case *bis*-boronic acid.[233]

6.3.2 Lithium - halogen exchange followed by borylation

Organolithium and Grignard type reagents can be used to make arylboronates (**Scheme 63**). Rapid metal-halogen exchange on aryl halide **194** generates a highly nucleophilic organometallic species **207**, which attacks a suitable boronic ester to give the arylboronate salt **199**. Acidic workup then gives the boronic ester **198**. Literature studies generally focus on one reagent, but in essence both share distinctive properties and observations made of one type of reagent is often extended to the other in literature. Here the general overview and more extreme chemical properties of organolithiates are described, followed by more specific discussion of 'ate' complex decomposition in organomagnesium species.

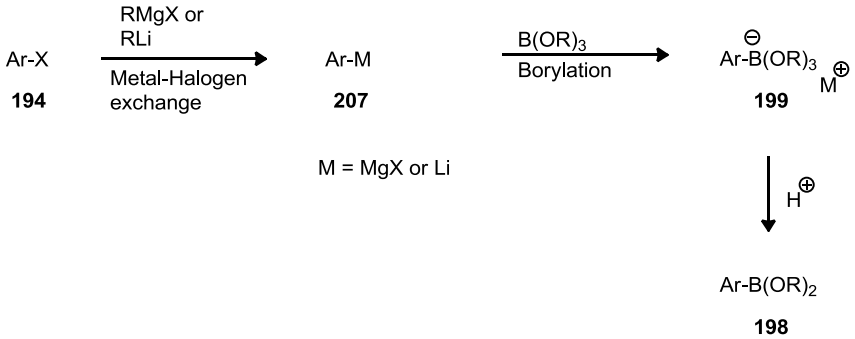

Scheme 63 - Metal halogen exchange followed by borylation.

The lithium-halogen exchange is an equilibrium process, with the position determined by the relative stability of the carbanions formed (**Figure 36**).[234] Increasing *s* character lowers the energy of the HOMO orbital so when exchanging an aryl halide with an alkyllithium species the transfer goes essentially to completion, because an aryllithium is more stable than an alkyllithium.

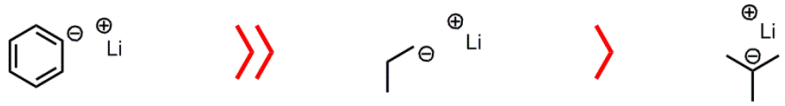

Figure 36 - Relative stability of carbanions

The mechanism of these exchanges is not completely understood. Complications include the aggregation of lithiated species, which is controlled by the sterics of the alkyl portion and varies with temperature, solvent and concentration.[235] In the absence of a Lewis base hexamers and tetramers predominate. Lithium ions (bonding is predominantly ionic)[236,237] form L_3 triangles.[237] Each lithium has at least four contacts, and is electron deficient in nature. The ^{n}butyllithium often used forms discrete octahedrons.[238] Addition of a Lewis base results in the positive lithium being stabilised by interaction with the base and reduces the aggregation, increasing reactivity.[235,237] The difference in reactivity is potentially enormous; Jones *et al*[239] show that dimeric ^{n}butyllithium is 8 orders of magnitude more reactive than tetrameric forms towards a terminal acetylene. In the same paper they estimate the monomer is at least 14 orders of magnitude more reactive than the tetramer towards the same substrate.[239] Such differences in already rapid transformations make identifying the active species challenging. Depending on the nature of the arylhalide **194** either a radical mechanism (SET) through radical anion **209** then neutral radical **211**, or an 'ate' complex such as **213** may be involved (**Figure 37**).

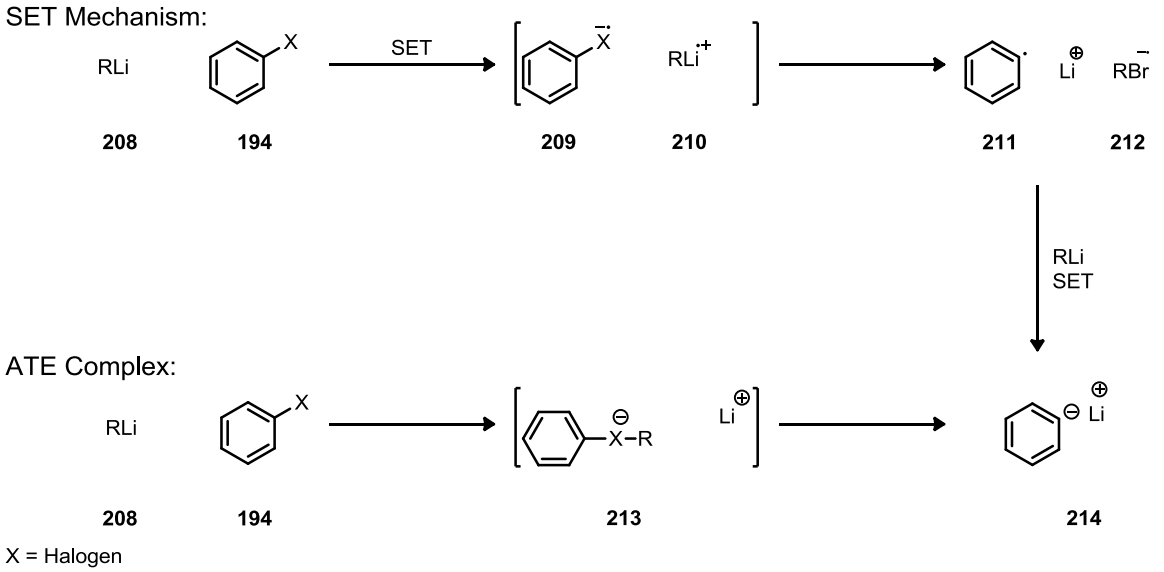

Figure 37 - SET (radical) and ATE (nucleophilic) mechanisms

Based on EPR spectroscopy,[240] cyclic radical probe studies,[241] and the isolation of characteristic products[242] radical mechanisms are known to occur, particularly at higher temperatures and where an alkyl bromide is the substrate.[243] Some 'ate' complexes have been isolated and are effective nucleophiles.[244] Studies on the effects of substituent electronics[245,246] and substrate

stoichiometry[247] on the kinetics of aryl halide exchange suggest this is the dominant mechanism. Evidence for one mechanism does not necessarily preclude the other; detection of radicals does not disprove the involvement of an 'ate' complex. Some iodine 'ate' complexes generate radicals during decomposition.[248]

Lithium - halogen exchange is a rapid process, occurring preferentially to deprotonation in some cases.[249] Organolithium species are reactive and in particular very basic (the conjugate acid of C_2H_5Li has a pKa of around 50 relative to water).[250] As such, low temperatures and short reaction times are preferable, and the exclusion of oxygen and water is vital.

Many of the mechanistic details pertaining to organolithium species are also relevant to magnesium halogen exchange processes; in particular an 'ate' complex is implicated. Some particular details have been elucidated by Hoffmann and co-workers.[45,251,252]

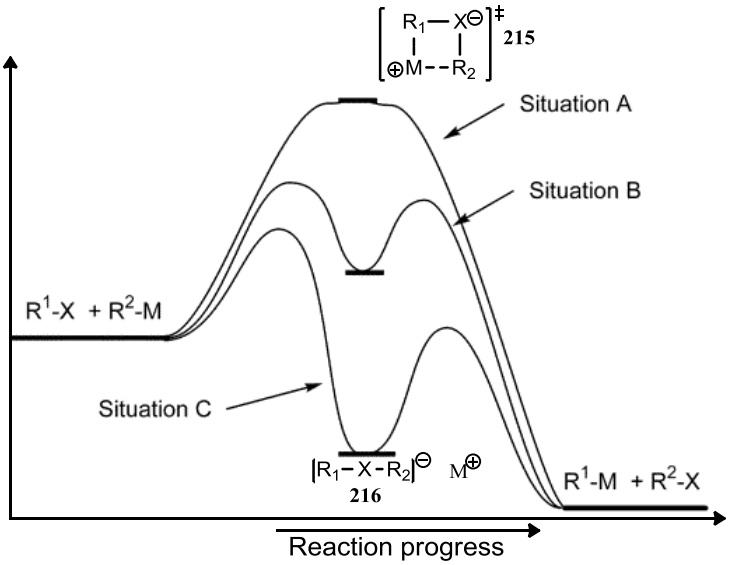

Figure 38 - The proposed 'ate' complex route to the exchange product. Diagram and proposed structures amalgamated from Hoffmann *et al*.[253]

If attached groups are sufficiently stabilising the 'ate' complex may take the form of an observable intermediate, either a solvent separated ion pair or dissociated ions **216** (**Figure 38**, Situation C). Otherwise a 'contact ion pair' **215** where the metal ion is more closely associated may be a transition state (Situation A). Alternatively, in Situation B 'ate' complex **215** is present only as a reactive intermediate and decomposes too rapidly to be observed. Situation C is also favoured by higher electron density at the magnesium centre, and hence by coordinating solvents.[254] However, even with very stable 'ate' complexes cationic species have a role in the final conversion to the Grignard reagent, with a bimolecular process 1st order with regard to total magnesium concentration observed.[253] Introduction of an electrophile in the presence of an 'ate' complex of this type may catalyse a chain radical process leading to Grignard formation.

6.4 Synthesis of benzophenones components

6.4.1 Synthesis of *ortho*-halobenzophenone component

Availability of 2-aminobenzophenone amine **217** and precedent[255] for synthesis of 2-iodobenzophenone **218** (**Scheme 64**) contributed to the decision to utilise Suzuki coupling.

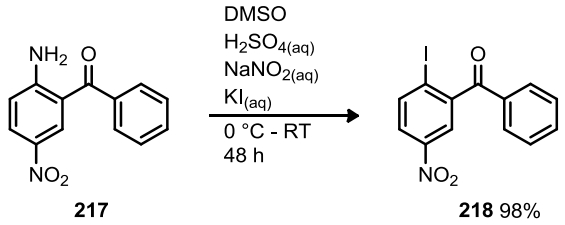

217 **218** 98%

Scheme 64 - Synthesis of benzophenone iodide **218**.

Diazotisation and quenching with potassium iodide gave near quantitative conversion with a procedure modified from literature.[255] The viscosity of the mixture and the quantity of gas generated meant mechanical stirring, a large flask and careful additions were necessary. The weak C-I bond and electron deficient aryl ring make this substrate ideal for the aryl halide component of Pd cross coupling reactions.

The synthetic plan was tested at this point by trial coupling reactions on iodobenzophenone **218**, initially with 4-methoxyphenylboronic acid **219** which is electron rich and should undergo transmetallation readily, with reductive elimination also favoured due to the electronic complementarity with iodobenzophenone **218**. The methoxybenzophenone **220** was isolated in an acceptable unoptimised yield (**Scheme 65**).

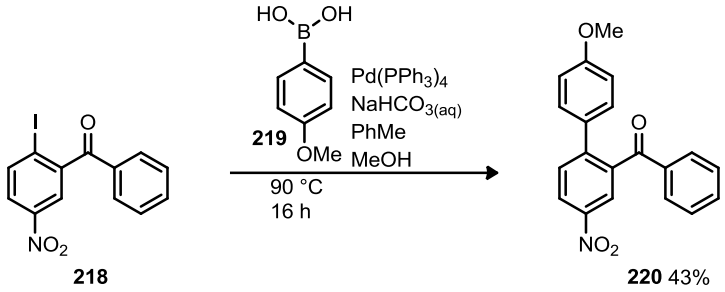

218 **220** 43%

Scheme 65 - Test Suzuki coupling of iodobenzophenone **218** with a methoxyarylboronic acid **219**.

In order to model the *ortho* substituent and establish the electronic of boronic acids or esters which could be used 2-nitrophenylboronic acid was coupled to benzophenone **218** (**Scheme 66**).

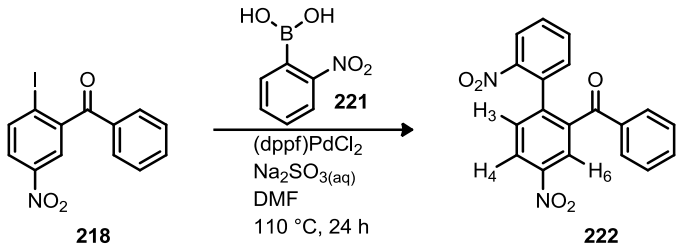

218 **222**

Scheme 66 - Test Suzuki coupling of iodobenzophenone **218** with a nitroarylboronic acid **221**.

The coupled benzophenone **222** was not isolated but inferred from the crude ^{1}H NMR spectrum by observation of H4 and H6, which were clustered together downfield of both H3 and their equivalent iodobenzophenone **218** peaks, a pattern consistent with benzophenone **222** and observed repeatedly in other analogues (**Chapter 8**).

Aryl bromide **223** was then used to test Negishi coupling conditions (**Scheme 67**). Successful lithiation of arylbromide **223** and transmetallation to Zn was followed by transfer into a reaction mixture with iodobenzophenone **218** and heating. A 64:36 ratio of starting iodobenzophenone **218** to 2-arylbenzophenone **225** was identified by ^{1}H NMR. No quenched arylzinc **224** was observed as a result of its volatility. Although optimisation would be required this demonstrated Negishi coupling to be possible with iodobenzophenone **218**.

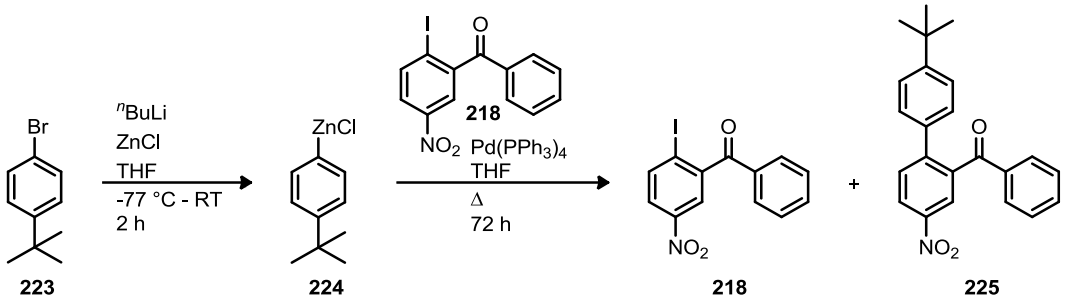

Scheme 67 - Test Negishi coupling of iodobenzophenone **218** with aryl bromide **223**.

6.4.2 *ortho*-metalobenzophenones

The alternative benzophenone-derived coupling partner would be an *ortho*-metalobenzophenone **185**. Some confusion surrounded the literature conditions[255] for magnesiation of iodobenzophenone **218**; the paper and the supporting information offer conflicting accounts of the reaction temperature. Testing first with iPrMgCl and PhMgCl at −40 ˚C (**Scheme 68**) a mixture of products was observed when either Grignard reagent was used followed by addition of borate **226**.

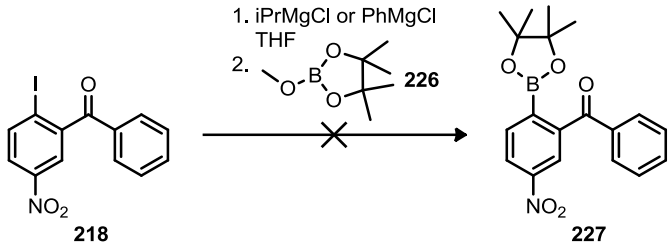

Scheme 68 - Metallation and borylation of iodobenzophenone **218**.

Chromatography allowed some of these fractions to be investigated, and it was observed that the aromatics signals typically shift substantially upfield in the ^{1}H NMR spectrum. This included a species with a *d* (*J* = 2.7 Hz, H6) and *dd* (*J* = 8.5, 2.7 Hz, H4) between 6.8 and 7.0 ppm, but the *ortho d* (H3) at 7.8 ppm. These peaks are close together in the iodobenzophenone **218**, probably because the H4 and H6 positions are conjugated to electron withdrawing groups, and the H3 position is *ortho* to iodine, which effects a downfield shift on the *ortho* position.[256] The opposite change in shift pattern would therefore be expected for successful magnesiation-borylation, and

this product appears more consistent with attack on a withdrawing group, to which both nitro and ketone groups are potentially susceptible. Broad singlets at 5.8 ppm and 4.9 ppm which exchanged upon D_2O shake were also observed in these mixtures. No dehalogenation product was observed.

Testing the more conservative SI conditions, exchange of iodine with iPrMgCl or PhMgCl at −78 ˚C followed by quenching with MeOH demonstrated that little or no exchange had occurred under these conditions (**Scheme 69**).

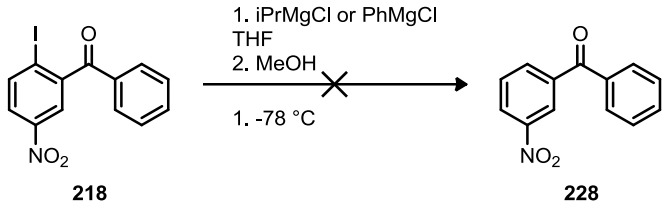

218 **228**

Scheme 69 - Metallation test of iodobenzophenone **218**.

With low temperature Grignard formation ineffective and side products apparently favoured over the formation of boronate ester **227** at higher temperature, Miyaura borylation was attempted instead (**Scheme 70**).

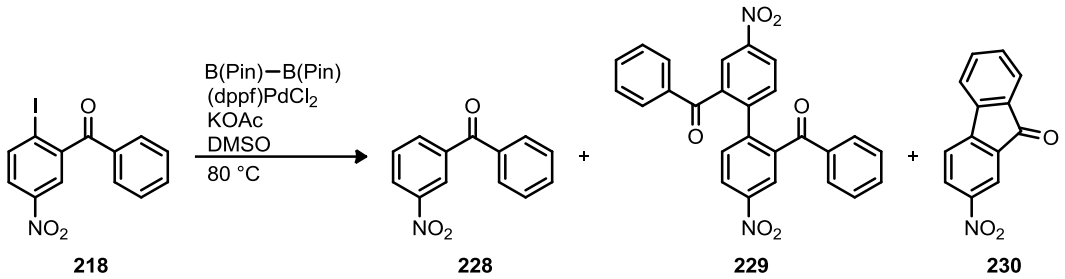

218 **228** **229** **230**

Scheme 70 - Product mixture from the attempted Miyaura borylation of iodobenzophenone **218**.

A complex mixture resulted from all attempts at these reactions, but the major products were identified. Using 1.1 eq. of bispinacolatodiboron, dehalogenated benzophenone **228** was identified as a minor component by comparison with literature data,[257] and the major component isolated and characterised as dimer **229**. This is believed to form through a Suzuki reaction between the iodide **218** and product **227**, although dimer **229** was also observed in **Scheme 107** where no borylated derivative could be formed. In order to favour the boronate ester **227**, the bispinaocolatodiboron equivalence was increased to 2 and the equivalence of KOAc reduced from 5 to a more normal 3, the concentration doubled and the catalyst loading halved. This resulted in a mixture including fluorenone **230**[258] (major) and dimer **229** (minor). The probable mechanism of fluorenone **230** formation can be ventured based on a very similar cyclisation with a palladacycle catalyst and fluorenone products, which is believed to occur through oxidative addition to $Pd^{(0)}$ followed by C-H activation, and reductive elimination.[259] The exact nature of such processes is a matter of ongoing debate, and a Heck-type mechanism is also conceivable.[260,261,262] The isolation of small, pure crystals of the fluorenone cyclisation product **230**, appeared to indicate that oxidative addition is followed by competing borylation and C-H activation based cyclisation of the

oxidative addition product. Rapid Suzuki coupling also competes once the arylboronate ester is present in significant quantities. Reduction of the temperature to 60 ˚C and reaction time to 3 h showed iodobenzophenone **218**, dimer **229** and fluorenone **230**, demonstrating that the Suzuki coupling is faster than the initial borylation and hence one of these side reactions will always be preferred, making Miyaura borylation unfeasible.

6.5 Synthesis of the *tert*-butylaryl component

6.5.1 Synthesis of *ortho*-(*N*-alkylamino)aryl halides

Ortho-(*N*-alkylamino)aryl halides were potential coupling partners and precursors to *ortho*-(*N*-alkylamino)arylmetals **186** (**Scheme 60**). *N*-Alkylation of aniline **188** with an alkyl halide was considered so alkyl bromide **232** was prepared via the Appel reaction. Reductive amination also appeared to be a good approach to preparing *N*-alkylaniline derivatives, so previously prepared alcohol **145** was oxidised to give aldehyde **231**. Numerous suitable procedures exist for oxidation of alcohol **145** to aldehyde **231**; a TEMPO oxidation protocol[263] was chosen as a mild, robust, cheap and quick approach (**Scheme 71**). The mechanism of this reaction is shown in **Scheme 72**.

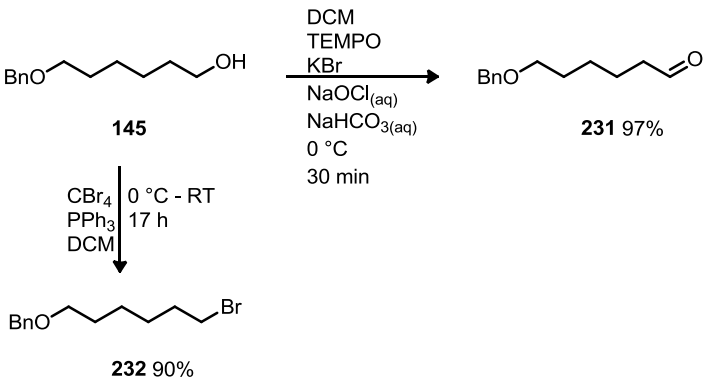

Scheme 71 - Synthesis of aldehyde **231** and bromide **232**.

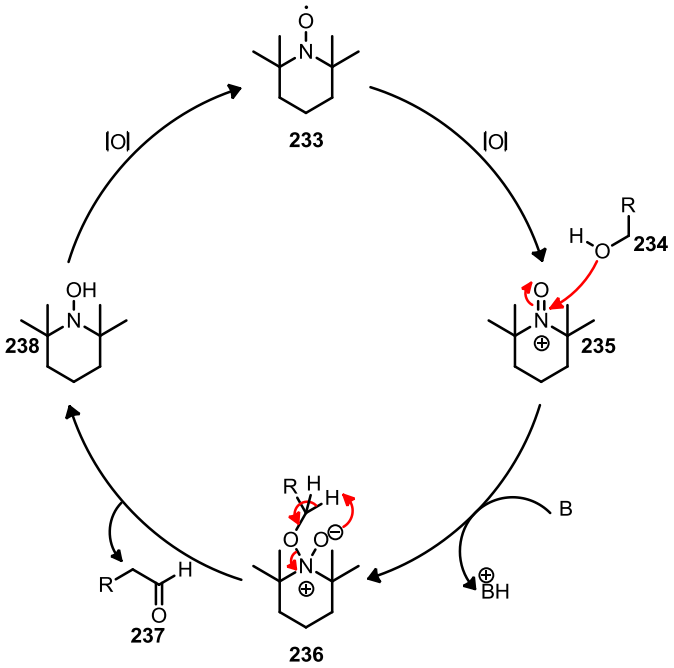

Scheme 72 - Postulated TEMPO oxidation mechanism.[264]

Oxidation of the TEMPO radical **233** generates a nitrosonium cation **235** which undergoes nucleophilic attack from the alcohol **234**, with deprotonation forming complex **236**. The resulting oxidation occurs by deprotonation to form the aldehyde **237** and eject the reduced cyclic hydroxylamine **238**. Re-oxidation occurs first to nitroxyl radical **233** then nitrosonium **235**. In the protocol NaOCl was added as the oxidant, but HOBr formed with KBr contributes significantly to

the oxidation rate.[265] Oxygen can be used as the oxidant with the correct co-catalyst.[266] Reaction is faster at pH 8.6 than at 12.7 (probably due to $^{-}$OBr partitioning mostly into the aqueous phase) and faster at 0 ˚C than RT (due to nitrosonium stability).[267] Benzyl ethers can oxidise to benzoates in systems containing NaOCl,[268] and the benzyl ester was observed as a side product in the ^{1}H NMR spectrum at levels of up to 15 - 20%, as identified by a 2H *t* at 4.35 ppm and 3 aromatic signals consistent is splitting and shift pattern to a phenyl group with an electron withdrawing substituent. Careful TLC monitoring and restricted reaction time and $NaOCl_{(aq)}$ equivalence eliminated this problem and allowed isolation in quantitative yield.

With these in hand the necessary amine **240** was prepared (**Scheme 73**). Literature conditions allowed near quantitative nitration of *tert*-butyl aryl bromide **223** to give nitroaryl **239**.[269] Dithionite reduction was attempted based on literature conditions.[270] This was initially successful, but proved unreliable. Reduction with an iron acid mixture proved more robust, giving aniline **240** in high yield.[271]

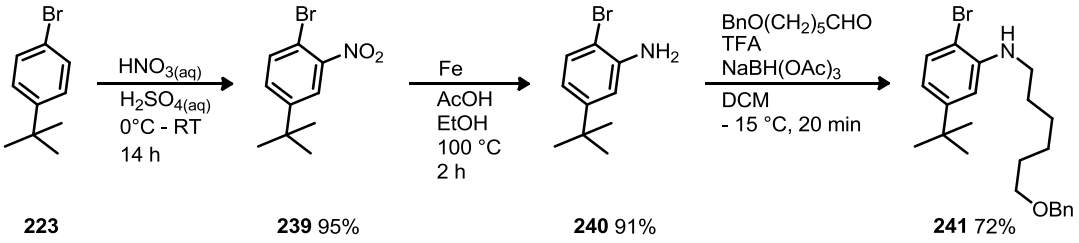

Scheme 73 - Bromide tBu coupling partner **240** synthesis.

Imine formation by stirring amine **240** and aldehyde **231** with Na_2SO_4 then reduction with $LiBH_4$ was ineffective, as was alkylation with alkyl bromide **232** at 80 ˚C in DMF with Cs_2CO_3, and at RT with NaH. Reductive amination with 2 eq. TFA produced a mixture of compounds.[272] $NaBH(OAc)_3$/DCE[273] gave very slow conversion and side products. An alternative TFA based procedure utilising much higher equivalence of TFA and later addition of aldehyde **231** in DCM gave rapid conversion to **241** in good yield.

6.5.2 Synthesis of *ortho*-(*N*-alkylamino)arylmetals

Attempts were then made to use metal - halogen exchange and nucleophilic attack from the subsequent organometallic species to form a boronic ester Suzuki precursor **242** (**Scheme 74**).

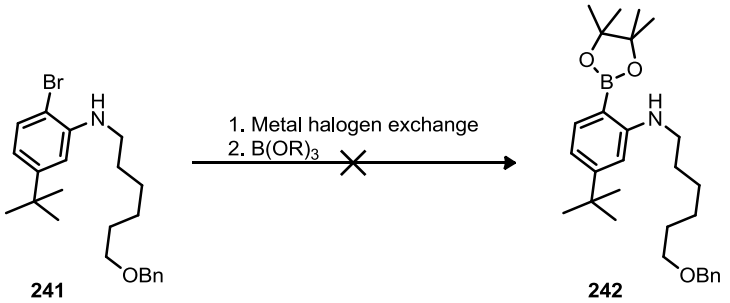

Scheme 74 - Borylation by metal halogen exchange on amine **241** was not successful.

Magnesium - halogen exchange *ortho* to a primary amine had previously been achieved by first deprotonating the amine.[274] Metallation of secondary aniline **241** was first attempted both with a combination of Grignard reagents; PhMgCl is used to effect deprotonation to form a 'magnesium amide'. The more reactive iPrMgCl is then used to transmetallate to give the aryl Grignard reagent[274] which can then be used for nucleophilic attack on a borate to give the Suzuki precursor. Use of the literature conditions returned starting material and a small quantity of a side product. Allowing the mixture of aryl bromide and Grignard reagents to stir at RT for 3 h prior to cooling and quenching with a boronic ester gave a 63:37 ratio of aniline **241** to the side product. From the mixture the ^{1}H NMR spectrum of this side product was observed to have an ABX coupling system shifted substantially downfield. Both the CH_2 *s* of a benzyl group at 4.5 ppm and CH_2 groups consistent with 1' (at 3.3 ppm) and 6' (at 3.5 ppm) positions were associated with this side product. The amino proton which is well defined and coupled to CH_2-1' in aniline **241** is missing however. Following chromatographic purification none of this side product was isolated. Both literature[275] and the experience of colleagues confirm that chromatographic purification of pinacolboronic esters is possible. Indeed complete hydrolysis of a pinacolboronate ester is a difficult transformation.[276] While it must be allowed that the electron-donation from the *ortho* group would accelerate protodeboronation, the coupling patterns observed in the reaction mixture and column fractions do not suggest this. On this basis, while the identity of the side product was not ascertained it was not believed to be the desired product.

When lithium halogen exchange was attempted no reaction was observed at −78˚C with less than 3 equivalents. It is possible that benzylic lithiation or directed lithiation occur. Warming a solution of aniline **241** and excess ^{n}butyllithium from −78˚C to −55 ˚C was noted to produce a green colour. Subsequent addition of boronate ester produced the same impurity as previously noted and numerous others. At this point the metal - halogen exchange was abandoned, and the Miyaura borylation reaction attempted instead (**Scheme 75**).

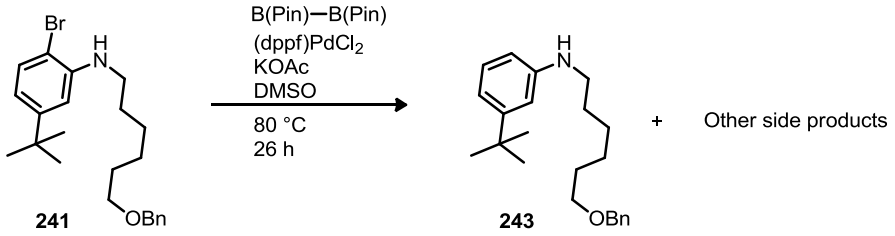

Scheme 75 - Miyaura borylation of secondary amine **241** gave dehalogenation product **243** among other side products.

Miyaura borylation of aryl bromide **241** resulted in complete conversion giving two products. The major one was identified as dehalogenated amine **243** on the basis of an apparent *t* with an *ortho* coupling constant (*J* = 8.1 Hz) which would represent the position *meta* to the amine, and a *meta* apparent *t* (*J* = 1.8 Hz) consistent with the position between the amine and the *tert*-butyl group. ^{11}B NMR confirmed the absence of boron from either product, proving the reaction to be unsuccessful.

Deviating from the original synthetic plan, a reductive amination of iodobenzophenone **218** with aniline **241** was then attempted (**Scheme 76**). Successful transformation to tertiary aniline **244** would give the desired trialkyl system which could then be linked, by Ullman coupling[277] for example.

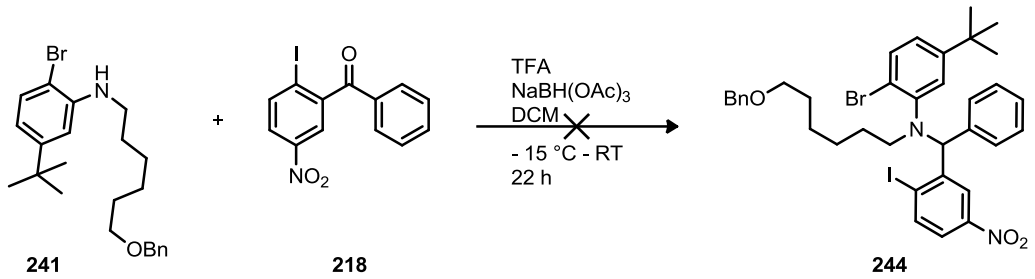

Scheme 76 - Reductive amination to give substrate **244**.

No reaction was observed, with starting materials **241** and **218** isolated. Alternatives to aniline **241** were then investigated.

6.5.3 Synthesis of *N*-alkyl-*N*-arylamides as precursors to the Suzuki Reaction

In order to simplify the transmetallation the aniline **241** was protected with Boc to give a carbamate (**Scheme 77**). this removes the most acidic hydrogen, and preventing formation of an anion at this position should improve the reactivity of the aryl bromide. Very hindered Suzuki couplings are well precedented.[210]

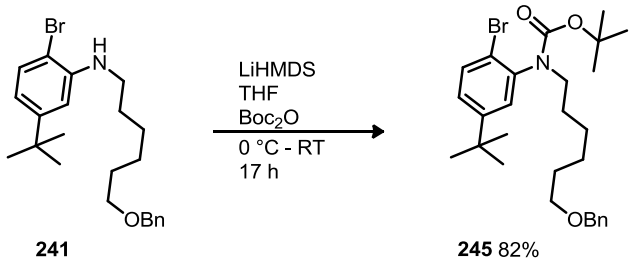

241 **245** 82%

Scheme 77 - Synthesis of tertiary amide **245**.

No reaction was observed when aniline **241** was heated to reflux with NEt_3, DMAP and di-*tert*-butyldicarbonate in DCM. Instead various strong bases were tested to deprotonate the aniline **241** prior to dicarbonate addition. Using 1.05 eq. of PhMgCl produced no reaction, however the equivalent reaction with 1.12 eq. ^{n}butyllithium gave good conversion, with some residual starting material but little decomposition. The procedure was refined by exchanging the ^{n}butyllithium with LiHMDS.[278] This allowed use of extra equivalents to drive the reaction to completion without lithiation giving rise to side products, and the isolation of the tertiary amide **245** in good yield. Minor side peaks were observed, alongside substantial broadening and inequivalent CH_2-1'. It was unclear if these represented an impurity or NMR timescale inequivalence due to sterics, so ^{1}H NMR at elevated temperature was compared to the RT data (**Figure 39**).

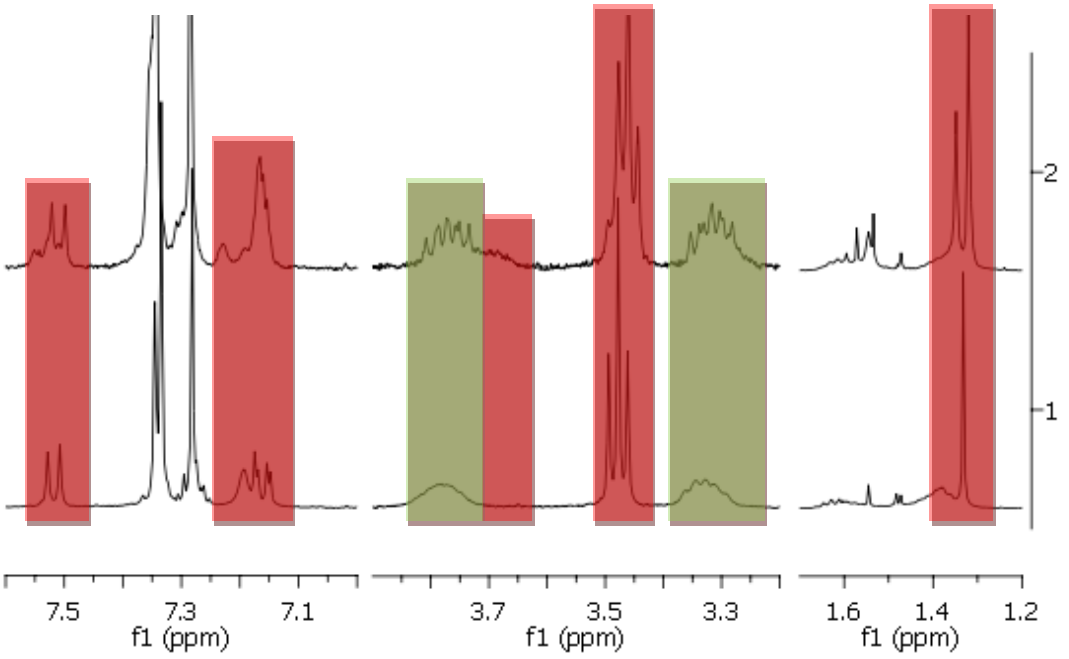

Figure 39 - Temperature controlled ^{1}H NMR spectra in $CDCl_3$ of tertiary amide **245**, showing RT (top) and 55 ˚C (bottom).

Two effects were identified. Axial chirality resulting in diastereotopic protons (green), which still do not interconvert at 55 ˚C, and geometrical isomers (red), which do. The origins of these effects are shown in **Figure 40**.

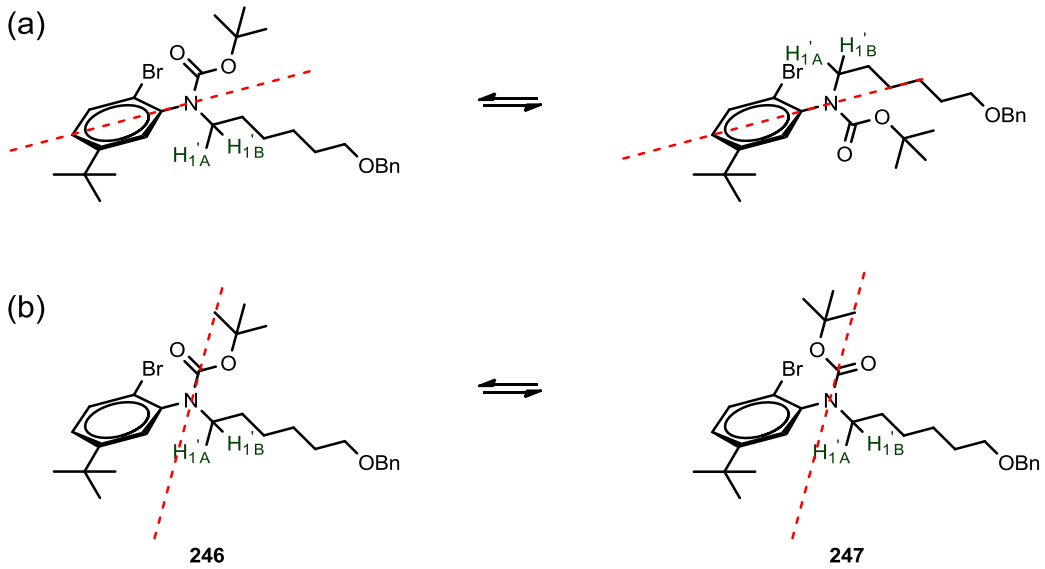

Figure 40 - Two types of asymmetry are present on the NMR timescale; axial chirality (a) along the C2-N bond, and geometrical isomers (b) where rotation around the amide bond is observed. Note the amide C2-N bond and the N-C1' bonds are out of the aryl ring plane (probably at approximately 90˚).

The diastereotopic protons arise from axial chirality. The relation of protons $H_1'_A$ and $H_1'_B$ to the ring and bromide atom differ and the rotation is too slow for these to interconvert on the NMR timescale, remaining so even at 90 ˚C. $H_1'_A$ and $H_1'_B$ therefore represent protons on one species inequivalent due to differences in environment. Geometrical isomerism in the form of slow rotation around the amide bond is the origin of the side peaks mentioned, and in this case these signals are the same proton in different species. These geometrical isomers **246** and **247** interconvert in a slow equilibrium process. Thus, unlike $H_1'_A$ and $H_1'_B$ the integrals of these signals are not required to be equal to one another. In this case one form is clearly favoured, but heating to 50 ˚C is sufficient to eliminate this effect, confirming one compound is present.

Both effects will in principle be eliminated if sufficient energy is provided to increase rotation speed until interconversion occurs on the NMR timescale. In the case shown the coalescence temperatures (T_c) cannot be established from the data obtained. If this was possible the difference in chemical shift can be related to a rate constant for rotation through the Gutowsky equation and the energetic barrier to the given rotation further approximated through the Eyring equation.[279]

Following confirmation that the tertiary amide **245** had been isolated pure, metal - halogen exchange of this substrate was investigated. Lithiation conditions were effective for amide **245** and this was confirmed by quenching the aryllithium into MeOH, giving dehalogenated amide **248** in good yield (**Scheme 78**).

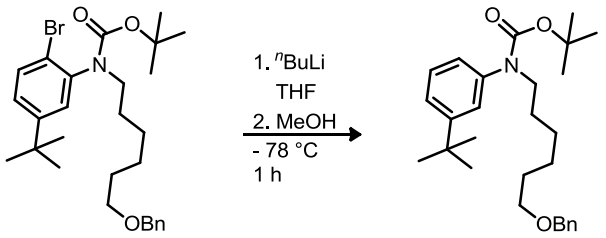

245 **248** 75%

Scheme 78 - Testing the metal-halogen exchange on tertiary amide **245**.

From the equivalent magnesiation with iPrMgCl at −30 ˚C only starting material was recovered. Repeat of the lithiation with *n*butyllithium and quenching with a boronate ester (**Scheme 79**) gave mostly the dehalogenation product **248** rather than arylboronate **249**, but chromatography showed several other side products, including one in which the ^{1}H NMR spectrum combined a broad 2H *t* at 3.65 ppm for CH_2N and a *dd* (1H, *J* = 8.5, 2.4 Hz) at 7.2 ppm suggesting a 1,2,4-substitution pattern for the aromatic ring. The lack of a large methyl *s* for a pinacol ester and the equivalence of $H_1'_A$ and $H_1'_B$ ruled out the desired product however. Another product observed as part of the mixture showed an aromatic *t* at 7.8 ppm (*J* = 8.1 Hz), consistent with the position *meta* to the amine in a dehalogenated product, and diastereotopic protons for the CH_2-1' position. Repeat reactions with trimethylborate as the quenching agent resulted in dehalogenation product.

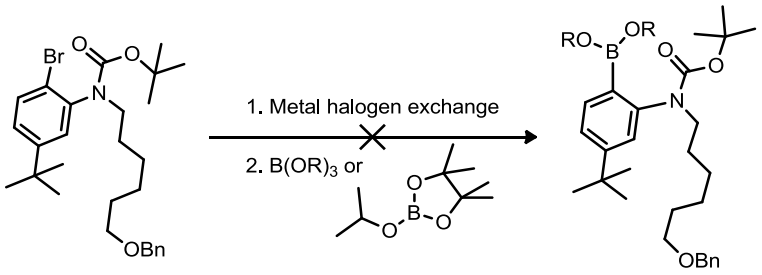

245 **249**

Scheme 79 - Attempted borylation of tertiary amide **245**.

Although some precedent exists for crowded positions adjacent to Boc groups failing to lithiate at −78 ˚C,[280] the dehalogenation product would appear to discount this possibility. Instead it was concluded that the reaction with borate esters is disfavoured by steric repulsion.

It was decided that replacing the bromine with a zinc chloride would by comparison clash far less with the *ortho* substituents, so a Negishi coupling was attempted (**Scheme 80**).

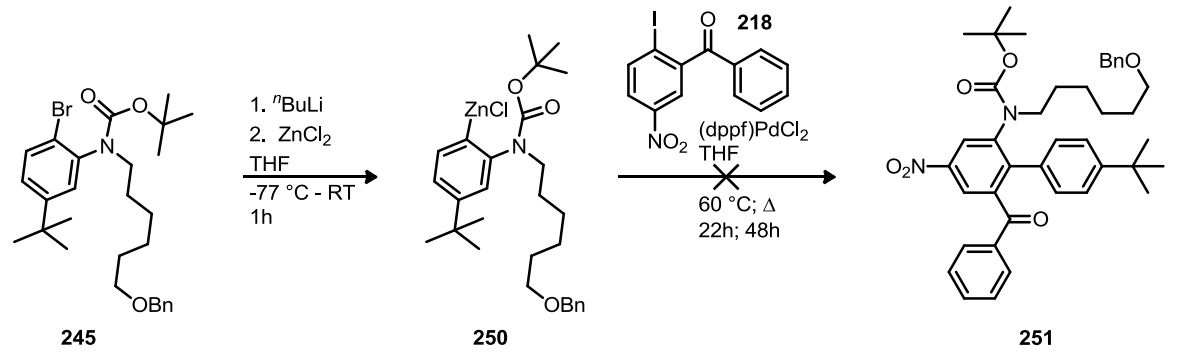

Scheme 80 - Unsuccessful transmetallation and Negishi coupling.

Treating aryl bromide **245** with ^{n}butyllithium then transmetallation to zinc and using the reaction mixture for a cross-coupling reaction with aryl iodide **218** gave only benzophenone starting material **218** and quenched amide **248**. The possibility of instead using tertiary amide **245** as the halide component was then investigated (**Scheme 81**). This was treated with 2-nitrophenylboronic acid **221**, in an attempt to synthesise biphenyl **252**. No reaction was observed and amide **245** was consequently abandoned.

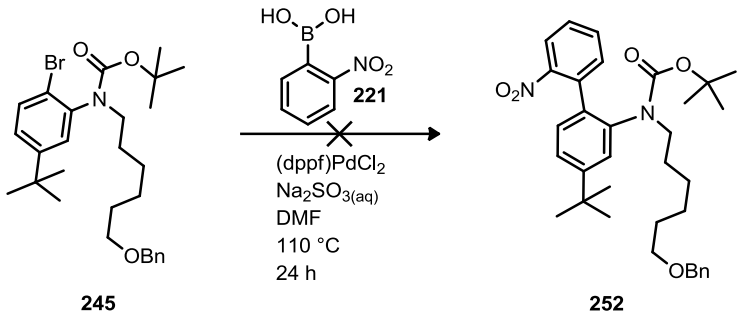

Scheme 81 - Unsuccessful test of Suzuki coupling with tertiary amide **245**.

Instead of using an additional protecting group, a secondary amide would provide a less strained alternative. This would prevent the amine interfering with Miyaura borylation, and secondary amides are surprisingly effective at directing lithiation.[281] Reduction could then be effected prior to cross-coupling, or if this proved problematic reasonable precedent exists for amide reduction in the presence of a ketone.[282] First a suitable acid chloride **254** was prepared from acid **253** (**Scheme 82**).

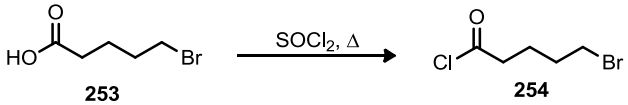

Scheme 82 - Preparation of acid chloride **254**.

Acid chloride **254** was used directly (**Scheme 83**) following preparation.

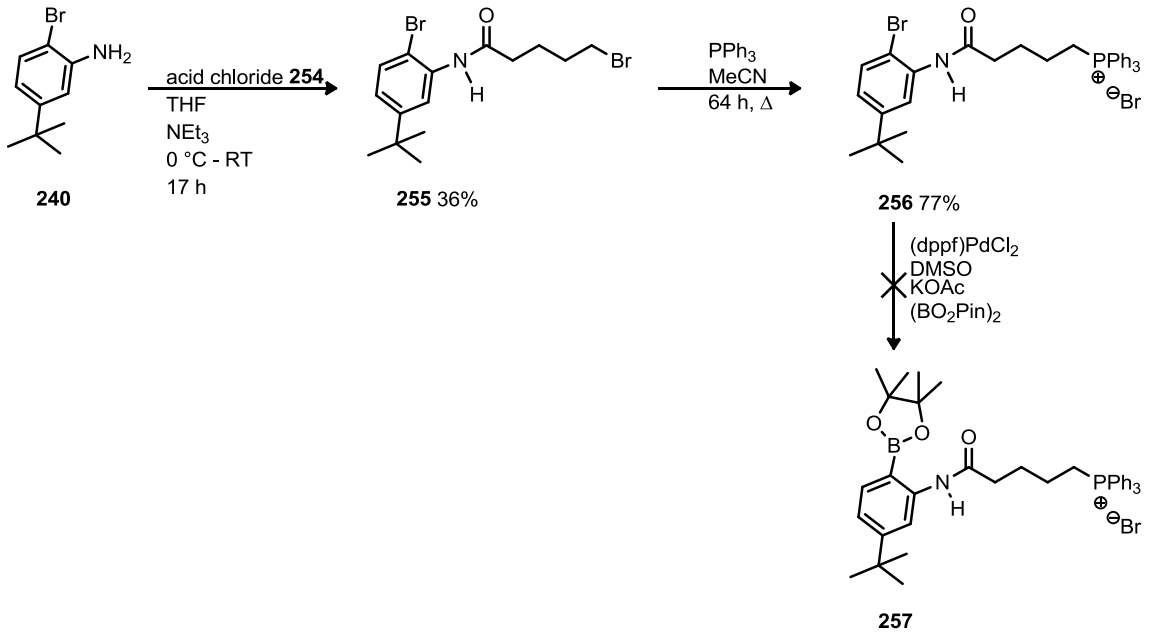

Scheme 83 - Synthesis of phosphonium amide **256**.

Synthesis of amide **255** proceeded in disappointing yield. However, subsequent formation of phosphonium salt **256** proved efficient. Miyaura borylation[283] then resulted in generation of side products; the most prominent appeared to lack the phosphonium salt as judged by the lack of the characteristic 2H *m* at 3.8 ppm in the ^{1}H NMR spectrum resulting from the CH_2 coupling to the adjacent ^{31}P. The aryl peaks were all subsumed into a broad *m* and so no coupling pattern could be deduced, but the significant downfield shift is inconsistent with conversion from a bromide to a boronate ester substituent. A variant without the phosphonium present was investigated (**Scheme 84**).

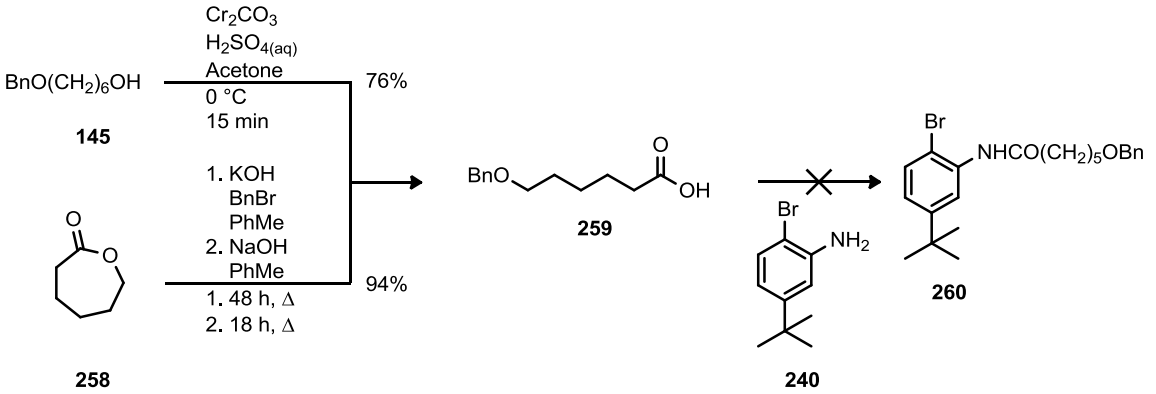

Scheme 84 - Alternate approaches to the synthesis of carboxylic acid **259** and unsuccessful formation of amide **260**.

The synthesis of amide **260** was approached by first producing carboxylic acid **259**, originally by Jones' oxidation[284] of the alcohol **145** in good yield. This was improved upon by an alternative 2 step procedure[285] from caprolactone **258** with initial hydrolysis and benzyl protection of both acid and alcohol groups, followed by ester hydrolysis for selective deprotection to acid **259**. Subsequent formation of an acid chloride and amide formation from amine **240** resulted in a

mixture. Later EDCI coupling conditions appeared to give slow reaction. A 1:1 mixture of starting material **240** and a side product was obtained. The side product gave a downfield shift of around 0.3 ppm in the ^{1}H NMR spectrum in the *dd* signal assigned *para* to the amine but a much smaller shift of 0.1 ppm in the *d* assigned *meta* to the amine. These integrated reasonably with peaks assigned as CH_2-1' and CH_2-6'. This is consistent with the amide **260**, although the material was not isolated or further pursued as this approach was abandoned in favour of S_NAr, an alternative route which had been performed in parallel and which was felt to offer more novelty and versatility. This will be discussed in the next chapter.

Chapter 7: Phenanthridinium-based sensor by nucleophilic aromatic substitution

7.1 New synthetic plan

During the development of the Suzuki coupling an alternative approach was conceived (**Scheme 85**). This retained nitro reduction of phenanthridinium **262** to give the aniline in the 8 position of probe **261** but envisaged an 6-*exo-trig* cyclisation by S_NAr from a benzophenone derived imine (N5) to a halogen-substituted C4a. The electronics of imine **263** are appropriate as the rate-determining step of S_NAr is nucleophilic addition to form a carbanion, which is stabilised by electron withdrawing groups such as the 7a imine and especially the 8 nitro group, both of which are conjugated to the 4a position. Fluorine was used as the halide because the carbanion is inductively stabilised by the leaving group, and fluorine provides more effective stabilisation due to its greater electronegativity relative to the other halides.[286] The alkylamine **264** is separately synthesised allowing the chain and triphenylphosphonium targeting group to be introduced by formation of imine **263** from biphenyl **265**. The aryl-aryl bond of biphenyl **265**, which becomes C_{1a}-C_{10a} in probe **261** would be formed by Suzuki coupling of benzophenone **218** with *ortho*-fluoroarylboronate **266**, previously formed by borylation of aryl fluoride **267**.

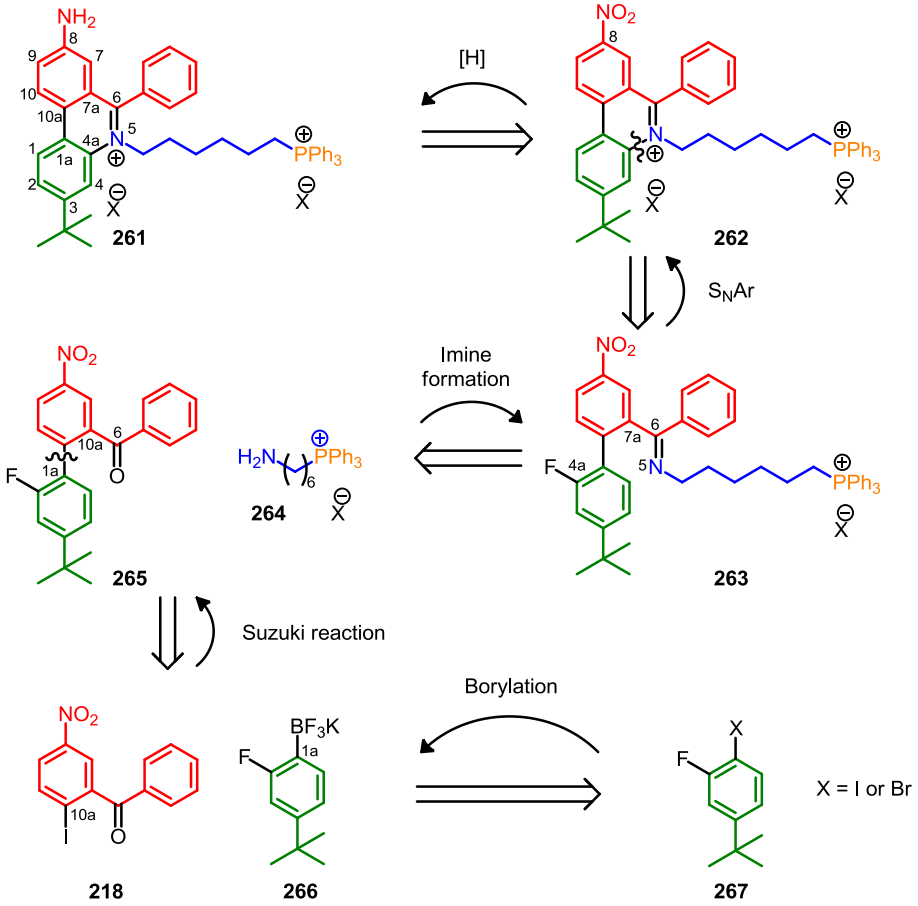

Scheme 85 – Retrosynthesis of S_NAr route, atoms numbered as positioned in probe **261**.

The route outlined in **Scheme 85** has several advantages. The late addition of alkylamine **264** results in a more convergent synthesis, and imine formation is well precedented on a huge range

of substrates, various benzophenones included.[287] The 2-fluoroarylboron component **266** is also a far less sterically demanding substrate than the previously synthesised alkyl anilines (**Chapter 6**).

7.2 Aryl fluoride synthesis

Synthesis of the appropriate aryl halides **267** was required in order to test this route. Aryl fluorides are an obvious choice of electrophile for S_NAr reactions. Aromatic fluorination is a relatively challenging transformation at a laboratory scale, due to harsh conditions and hazardous, difficult to manage reagents and side products. Taking advantage of the commercial availability of aryl fluorides a route using Friedel-Crafts alkylation of 2-fluorohalobenzenes **268** and **269** was investigated. Consideration of both Hammett parameters[288] and the influence of the halides on ^{13}C NMR shifts[289] suggested C5 is the more nucleophilic position, but the differences between C4 and C5 are small. It was believed that steric interactions may favour formation of the C4 substituted aryl fluoride **271**. A variety of Friedel-Crafts alkylation conditions were used to probe the regiochemistry of the reaction (**Scheme 86**).

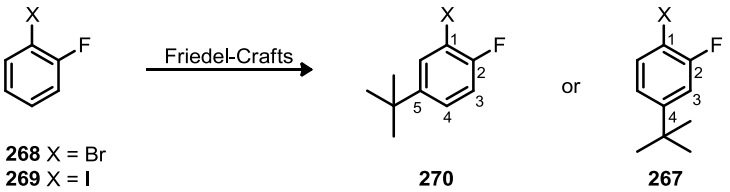

268 X = Br
269 X = I

270 **267**

Scheme 86 - Friedel-Crafts alkylation, possible regiochemistry.

Rapid conversion was achieved with a 3% loading of $AlCl_3$ in ^tBuCl at 0 ˚C. When applied to 1-bromo-2-fluorobenzene **268** the C5 substituted arylbromide **272** was the major product, but the 4-*tert*-butylaryl bromide product was observed as a minor product (**Scheme 87**).

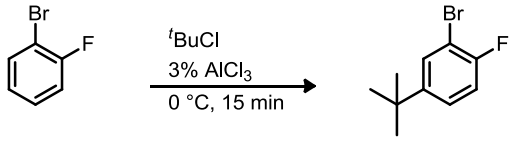

268 **272** 75%

Scheme 87 - Friedel-Crafts alkylation on the bromoaryl substrate **268** gave mostly C5 selectivity.

When repeated with the 1-iodo-2-fluorobenzene **269** the procedure gave near quantitative conversion to the C5 substituted aryliodide **273** (**Scheme 88**).

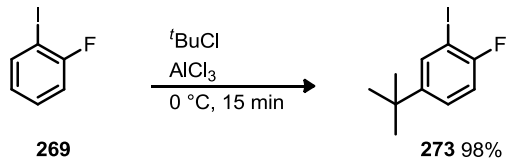

269 **273** 98%

Scheme 88 - Friedel-Crafts alkylation on the iodoaryl substrate **269** gave complete C5 selectivity.

These results prove the desired regiochemistry to be the less favoured outcome for the Friedel-Crafts alkylation, due to the influence of the fluoride group on electrophilic substitution. On this basis it was decided that the fluoride should be introduced after the *tert*-butyl group. Effective electrophilic fluorination protocols rely on the formation of organometallic nucleophiles,[290] difficult to do selectively in the presence of an aryl bromide. With the electron rich aryl bromide **223** unsuitable for S_NAr reactions and with regiocontrol of fluorination vital the Balz-Schiemann

reaction appeared to be the most viable approach. Aniline **240** was used to provide the desired regiochemistry (**Scheme 89**).

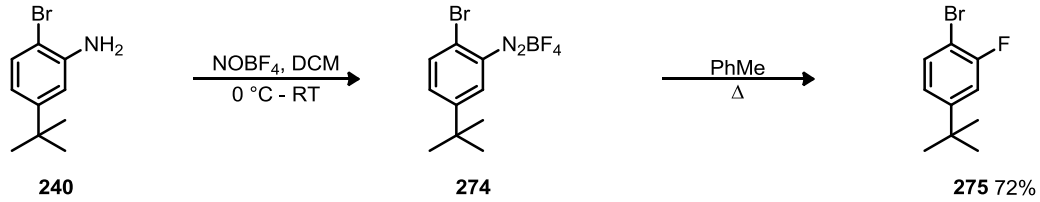

240 **274** **275** 72%

Scheme 89 - Synthesis of the fluoroaryl substrate **275**.

The Balz-Schiemann reaction actually involves two steps, with diazonium tetrafluoroborate **274** formed and then thermally decomposed. Initially a combination of $HBF_{4(aq)}$ and $NaNO_2$ was reacted with aniline **240** to form the diazonium tetrafluoroborate **274** in 51% yield after washing with $HBF_{4(aq)}$ and Et_2O. Due to the low solubility of diazonium salt **274** subsequent pyrolysis under reflux in PhMe gave only a low yield of aryl fluoride **275** (24%). DMSO was tested as a solvent for pyrolysis, giving clean conversion to a non-fluorinated product assumed to be the phenolic derivative. This is consistent with a literature study showing incorporation of the oxygen from DMSO, forming phenols due to a preassociation of the solvent molecule prior to generation of the aryl cation.[291]

Although diazonium salt **274** had been isolated in reasonable yield, the combination of poor solubility in PhMe, toxic reagents and the potentially explosive intermediate made this procedure undesirable. Instead, the diazonium tetrafluoroborate salt **274** was formed with $NOBF_4$ in DCM, then PhMe added and the DCM removed under vacuum before pyrolysis to give aryl fluoride **275** in good yield.[292,293] Scale up was carried out in batches for safety reasons. Various details of the reaction mechanism remain obscure. There are two alternate pathways for decomposition broadly accepted in the literature (**Scheme 90**).[294]

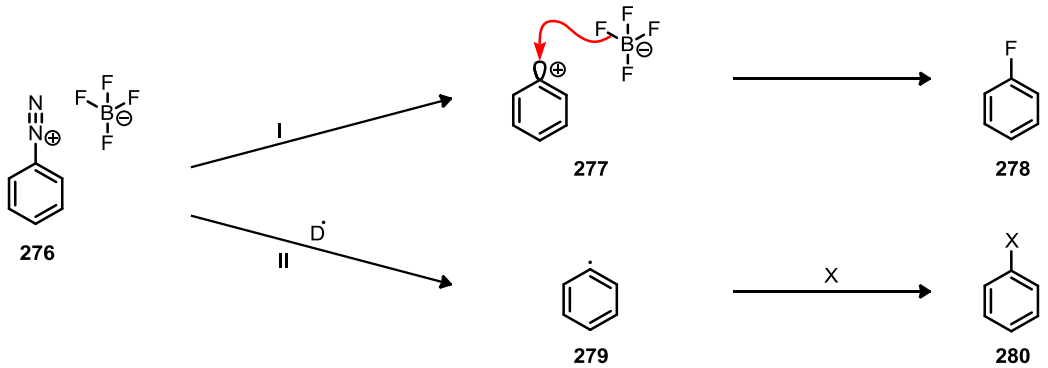

276 **277** **278** **279** **280**

Scheme 90 - Alternate dediazoniation pathways.[295] D· is a radical donor, X = electrophile.

Balz-Schiemann products arise from the heterolytic pathway (**I**), where the C-N bond of the diazonium tetrafluoroborate ion pair **276** is broken, resulting in an ion pair between nitrogen and the reactive phenyl cation[296] **277** which reacts with a nucleophile within a local solvation sphere to give aryl fluoride **278**.[297] The nucleophile has been shown to be BF_4^- rather than F^-.[298] Heterolytic decomposition is favoured by electron donating substituents which destabilise the arenediazonium **276** and stabilise the cation **277**. These reactions are favoured by oxygen rich

atmospheres which suppress the homolytic pathway (**II**), in which the aryldiazonium salt **276** decomposes to the phenyl radical **279**, which reacts with an electrophile and undergoes SET to give neutral species **280**.[299] Many reactions of this type exist, with some mechanistic variation.[300] The homolytic pathway can result from solvent acting as a nucleophile prior to decomposition to the phenyl radical **279**. Since the homolytic pathway[301] can result in protodediazoniation and aryl homocoupling in addition to formation of the desired product non-nucleophilic solvents are preferred, and basic conditions avoided.[302]

Evidence for the Balz-Schiemann going through the heterolytic pathway (**I**) can be seen in the biaryl product composition seen when the reaction takes place in the presence of other aryl groups, with regiochemistry defined by ring electronics and influenced by substituents (**Scheme 91**).[303] The Gomberg - Bachmann reaction uses diazonium salts to produce biphenyls under neutral or basic conditions via a radical mechanism and correspondingly does not show the same selectivity in product composition.[304] One study of diazonium tetrafluoroborate pyrolysis in the solid phase observed the Balz-Schiemann reaction accelerates in a fashion reminiscent of a chain reaction, leading the authors to propose a mechanism where radicals are generated following decomposition to an ion pair.[305]

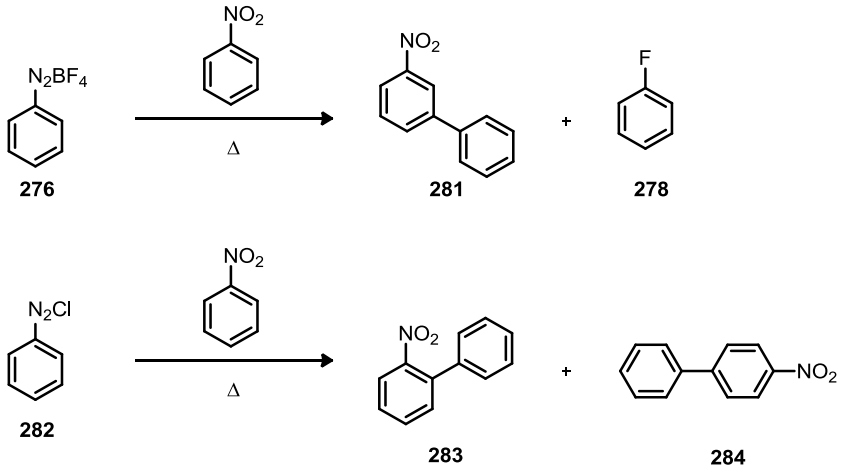

Scheme 91 - Products observed from pyrolysis of diazonium tetrafluoroborate **276** (top) and chloride **282** (bottom).[303]

7.3 Borylation of 2-fluoroarylhalides

The aryl bromide **275** was to be converted to a boronate using a lithium-halogen exchange. Conditions for the lithiation and conversion to the potassium trifluoroborate salt were tested on 1-bromo-2-fluorobenzene **268** (**Scheme 92**).

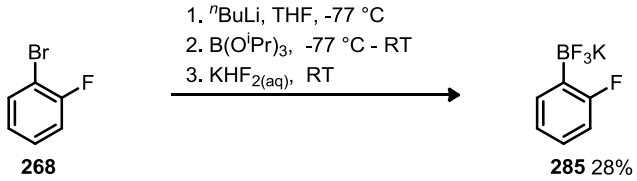

268 **285** 28%

Scheme 92 - Lithiation condition testing

The aryllithium species is generated at low temperature from *ortho* arylbromide **268** to avoid side reactions, including solvent decomposition. Triisopropylborate was used as the boronate source, forming the arylboronate ester which was converted to the stable trifuoroborate salt **285** by stirring in $KHF_{2(aq)}$. Trifluoroborate salt **285** was crystallised from acetone. Formation of the aryltrifluoroborate **285** avoids the formation of boronate trimers sometimes seen in boronic acid synthesis.[213] Although these react similarly to the monomers, analysis and yield calculation is less precise where multiple species are present. The trifluoroborate salts undergo slow hydrolysis to the boronic acid prior to cross-coupling, with side reactions suppressed by the low concentration of the boronic acid.[306] The procedure was repeated with aryl bromide **275** (**Scheme 93**). Lithiating aryl bromide **275** and borylating then quenching into a KHF_2 solution gave clean conversion to trifluoroborate salt **266** without the need for recrystallisation.

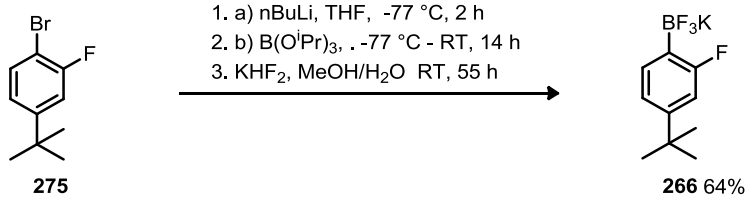

275 **266** 64%

Scheme 93 - Synthesis of the potassium trifluoroborate coupling partner

7.4 Suzuki coupling to form *ortho*-arylbenzophenone 265

The coupling of arylmetal **266** and benzophenone **218** was expected to be challenging due to both having *ortho* substituents, so time was spent identifying appropriate cross-coupling conditions. For testing purposes three catalytic systems were selected; the heavily used and studied $Pd(PPh_3)_4$ (tetrakis) **189**, one of the more versatile bidentate catalysts (dppf)$PdCl_2$ **190**,[230] and the most active[231] of the available PEPPSI-NHC catalysts, PEPPSI-^{i}Pr **191** (**Figure 33**). The need for alcoholic solvents was anticipated based on the solubility of the potassium trifluoroborate salts **266** and **285**. Since hydrolysis to the boronic acid precedes transmetallation low water content could inhibit reaction; use of a hygroscopic solvent also eliminated this concern. EtOH was used over MeOH allowing a greater thermal range without changing solvents. The temperature (78 ˚C) and catalyst loading (3%) are within the normal range for Suzuki coupling. DIPEA was used as the base with the exception of the PEPPSI ^{i}Pr example where K_2CO_3 was initially used in line with the

PEPPSI use guide.[307] The model potassium aryl trifluoroborate salt **285** was initially used as a test substrate and coupled to iodobenzophenone **218** with all three catalysts with the intention of making ketone **286** (**Scheme 94**).

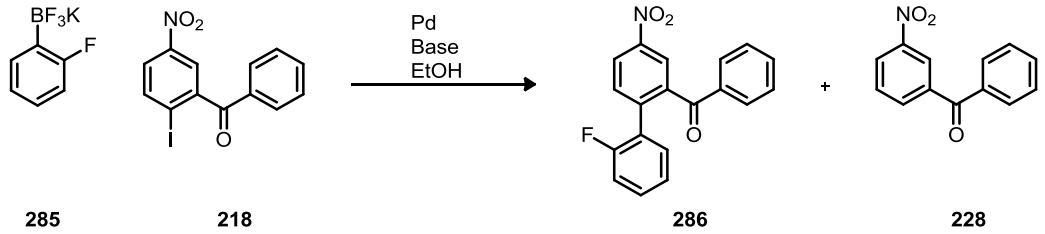

285 **218** **286** **228**

Scheme 94 - Cross coupling test reaction.

Little reaction was observed using $Pd(PPh_3)_4$ **189**, and as this catalyst was also the least stable it was not further tested. Both dppf **190** and PEPPSI-^{i}Pr ligands **191** consumed the starting material, giving one spot by TLC. Subsequent ^{1}H NMR spectra showed two compounds, one of which could be readily identified as benzophenone **286** due to ^{19}F coupling on the fluorinated aromatic ring. These proved inseparable by flash chromatography. HPLC was used to isolate the other product as the dehalogenated compound **228**.

Isolation of the dehalogenated material suggested problems with the transmetallation or reductive elimination steps. Trifluoroboronate **266** is more electron rich (aiding transmetallation) and more electronically divergent from iodobenzophenone **218** (aiding reductive elimination) than the test substrate **285**. It was decided that *N,N*-diisopropylethylamine (DIPEA) should be used as the base for both catalysts in the hope that β-hydride elimination would aid reduction of $Pd^{(II)}$ salts to $Pd^{(0)}$.[308] DIPEA is also more soluble and less likely to reduce the available water content, and the conjugate acid is less likely to interact with Pd-OH prior to transmetallation. PEPPSI-^{i}Pr was tested in the coupling of iodobenzophenone **218** and trifluoroborate salt **266** and the biaryl **265** was isolated in good yield (**Scheme 95**). The dppf catalyst **190** also worked but the reaction was marginally less clean.

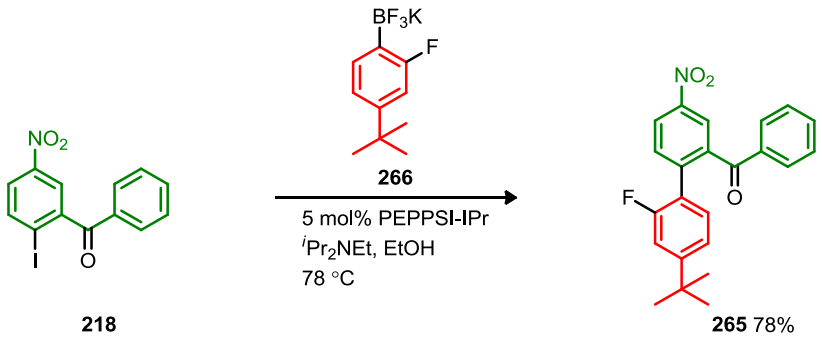

218 **265** 78%

Scheme 95 - The Suzuki coupling of iodobenzophenone **218** and potassium aryltrifluoroborate **266**.

7.5 Imine formation and S_NAr to complete phenanthridinium core

7.5.1 Imine formation

With the key C1a-C10a bond made the remaining key transformations were the formation of the imine and intramolecular nucleophilic displacement of the fluoride ion to give the phenanthridinium core. The sequence was tested using benzophenone **265** and hexylamine to make imine **287**, which could then be cyclised (**Scheme 96**). Heating in MeCN at 80 ˚C or at 150 ˚C in a sealed tube under microwave irradiation gave no reaction, and heating benzophenone **265** to 90˚C in neat hexylamine also gave only starting material. However, using an excess of hexylamine with titanium tetrachloride converted benzophenone into imine **287** in acceptable yield following purification.

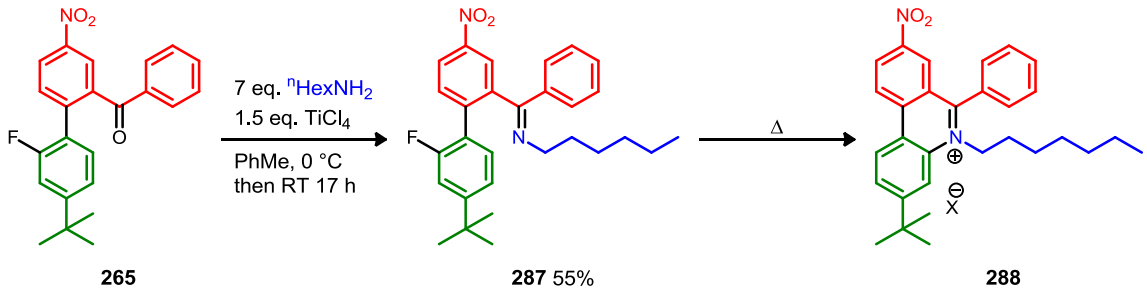

Scheme 96 - Formation of imine **287** followed by heating gives cyclisation to phenanthridinium salt **288**.

The imine retained the dual 1,2,4-trisubstituted systems of benzophenone **265** in the ^{1}H NMR spectrum (**Figure 41**). H4 and H6 showed a significant upfield shift, while H3 scarcely moved. This suggests a change in the electronics of the group at C1.

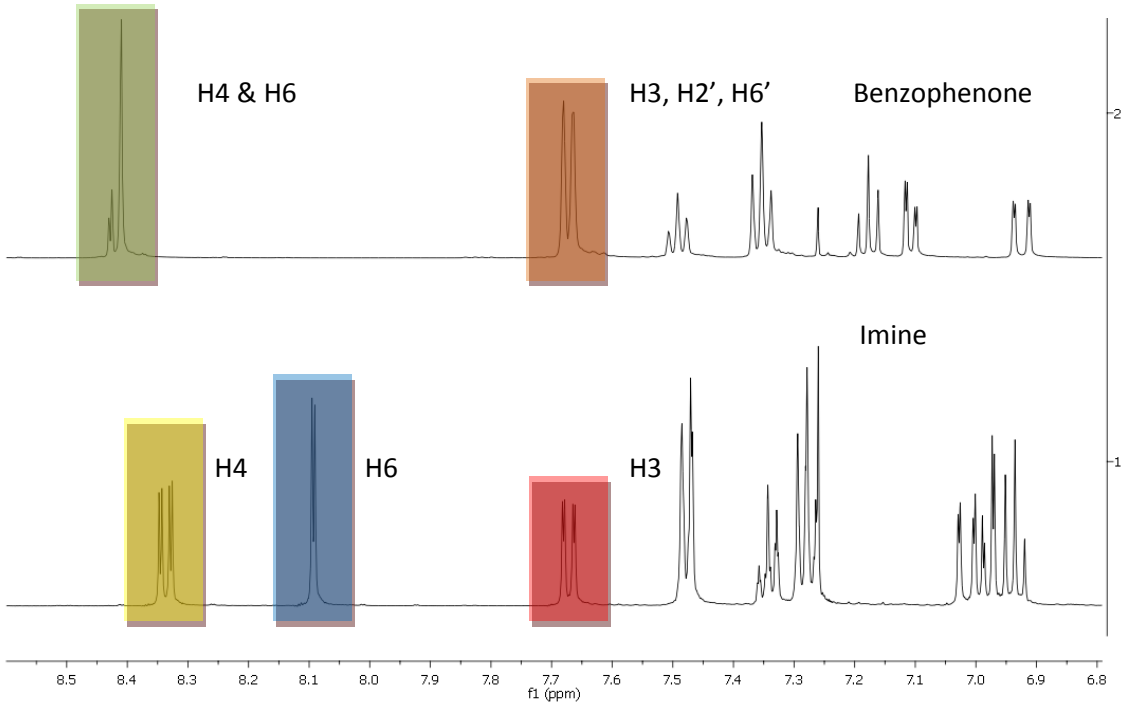

Figure 41 - Benzophenone **265** (top) vs imine **287** (bottom), with key shifts highlighted.

The difference in chemical shift between H4 and H6 in ^{1}H NMR spectrum of the imine **287**, but not in that of benzophenone **265**, perhaps indicates that the hexyl chain forces the phenyl group into

a different conformation relative to the other ring of the benzophenone. The H-F couplings in the ^{1}H NMR spectrum of the imine **287** were confirmed using ^{19}F decoupled ^{1}H NMR spectroscopy and showed that the fluoride had been retained in the same position as in the starting benzophenone **265**. Interestingly, the *ortho* F appears to couple with both C3 and H3 of the neighbouring C ring, demonstrated by the small additional C(H) - F coupling in the sp^2 region of the ^{13}C NMR spectrum and the loss of the smaller splitting of the *dd* assigned to H3 in the ^{19}F decoupling experiment. Imine **287** shares structural features with literature compounds exhibiting this phenomenon, which in those cases was attributed to N lone pair - F repulsion locking the F in close proximity to C/H to which it couples.[309] This is consistent with the observation of a pair of ddd at 3.0 - 3.5 ppm that were identified as diastereotopic protons at CH_2N resulting from hindered rotation about the bond linking the two rings of the biaryl unit.

7.5.2 Cyclisation

There are very few examples of imines displacing an aryl halide intramolecularly. However, an intramolecular S_NAr was attempted by heating the crude imine **287** with 3 eq. TMSCl in $CDCl_3$ at 60 ˚C for 1 h prior to ^1H NMR analysis. The resulting ^1H NMR spectrum showed a few interesting features:

- Additional methylsilane peaks were apparent in the 0.0 - 0.5 ppm region.
- The aromatic region matched the pattern of the imine, but the benzophenone rings in particular showed strong downfield shifts. Also, peaks assumed to be H5'' and H6'' of the A-ring were separated.
- The broad peak at 4.5 - 5.0 ppm characteristic of CH_2N^+ in the phenanthridinium salts was not observed.

These were considered consistent with TMS-iminium salt **289**, although hardly conclusive evidence (**Figure 42**).

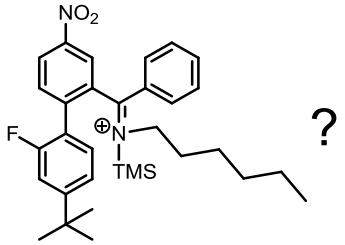

289

Figure 42 - Possible TMS-iminium adduct **289.**

Following work up and short-path vacuum distillation of this reaction mixture in a kugelrohr apparatus, ^1H NMR spectroscopy showed peaks characteristic of *N*-alkyl phenanthridinium salts, including a broad singlet at 5 ppm. Attempting to cyclise pure imine **287** at 200 ˚C in nitrobenzene resulted in isolation of phenanthridine **290** (a small amount of which was isolated for characterisation purposes) and no phenanthridinium **288** (**Scheme 97**).

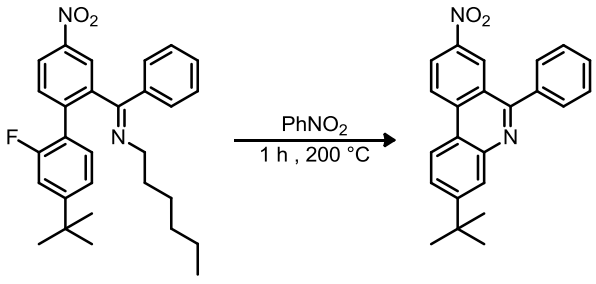

287 **290** 26%

Scheme 97 - High temperature cyclisation of imine **287**.

Cyclisation of imine **287** (**Scheme 97**) was next investigated by heating the solid to 100 ˚C in a kugelrohr apparatus for 1 h, causing the material to discolour. Addition of $CDCl_3$ followed by removal by distillation and heating for a further hour gave complete conversion of starting material to a mixture containing no ^{19}F-^1H coupling in the ^1H NMR spectrum and no ^{19}F according

to ^{19}F decoupled ^{1}H NMR spectroscopy (**Figure 43**). These clearer spectra resolved a peak corresponding to CH_2N at 3.3 ppm as a 2H *t*. This was inconsistent with a phenanthridinium **288**, but consistent with amine **292**, which would result from hydroxide attack to give a pseudobase **291** (see **Section 4.3**) and opening. COSY analysis shows H6'' to be considerably downfield of H3'' and H5'' (**Figure 43**), which is as expected for this position, *meta* to both donating groups and conjugated to a stronger withdrawing group than before in the form of the ketone. Based on this evidence, these peaks were assigned to the hydrolysis product **292**.

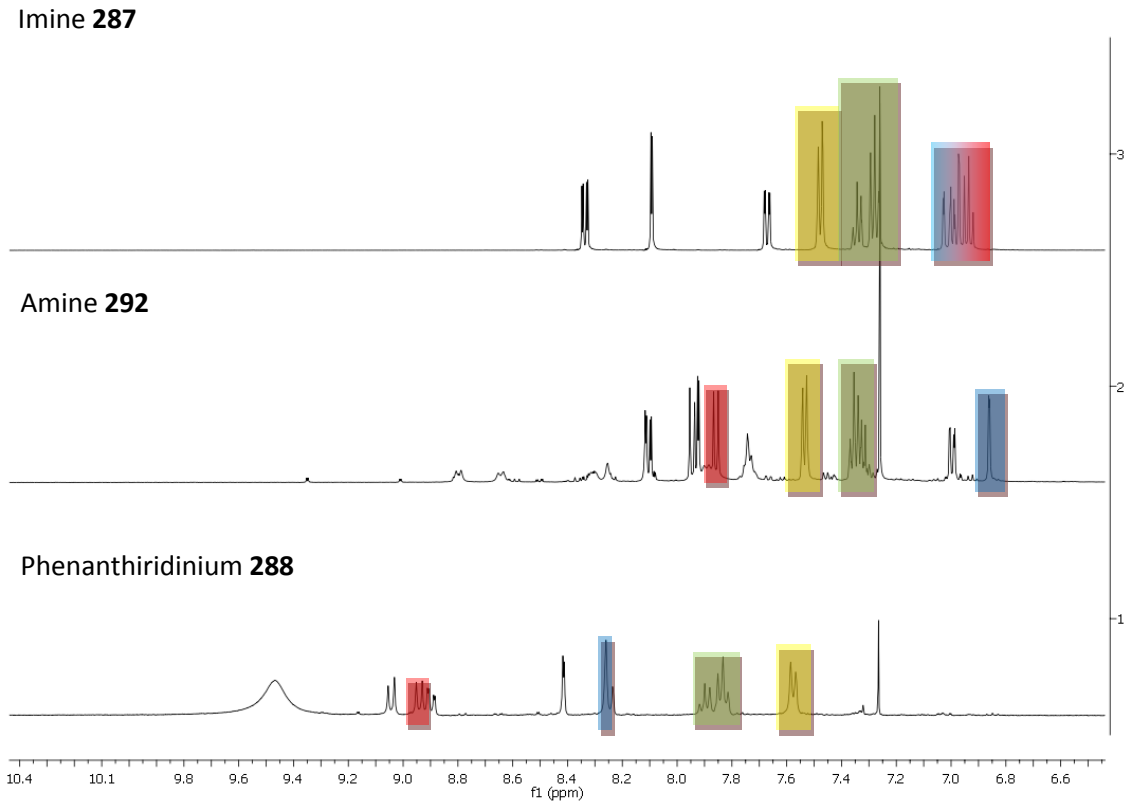

Figure 43 - heating imine (top) results in a mixture containing predominantly amine **292** (middle), which then cyclises to the *N*-alkylphenanthridinium salt **288** on addition of TFA.

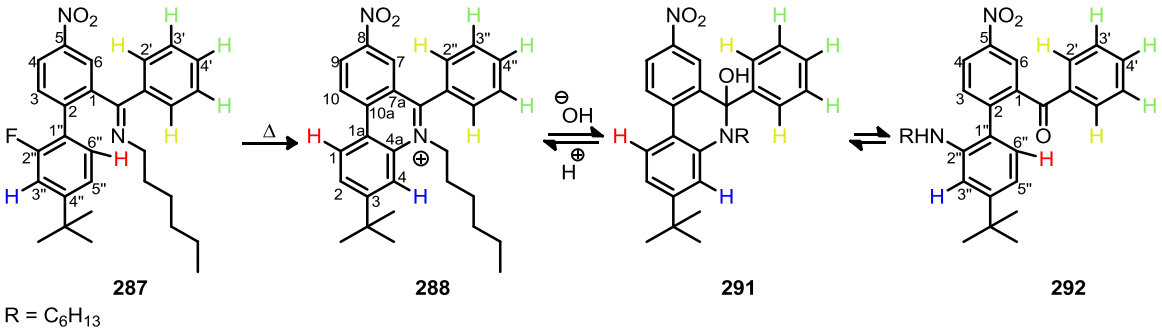

Scheme 98 - The cyclisation of imine **287** and subsequent products. Protons are colour coded to the ^{1}H NMR spectra shown above (**Figure 43**).

As loss of fluorine had been observed, the eventual fate of the fluoride anion was of interest. It was considered that formation of fluorosilicates in the glass may drive the hydrolysis reaction, providing water and destabilising the salt. To test this theory the kugelrohr cyclisation experiment was repeated twice in the presence of chromatography grade SiO_2. On both occasions the imine **287** reacted somewhat more slowly, as expected in the presence of an acidic additive. Trace

quantities of phenanthridinium **288** were formed alongside a greater range of side products. Comparison of the results with and without SiO_2 (**Figure 44**) indicated that omission of SiO_2 was preferable.

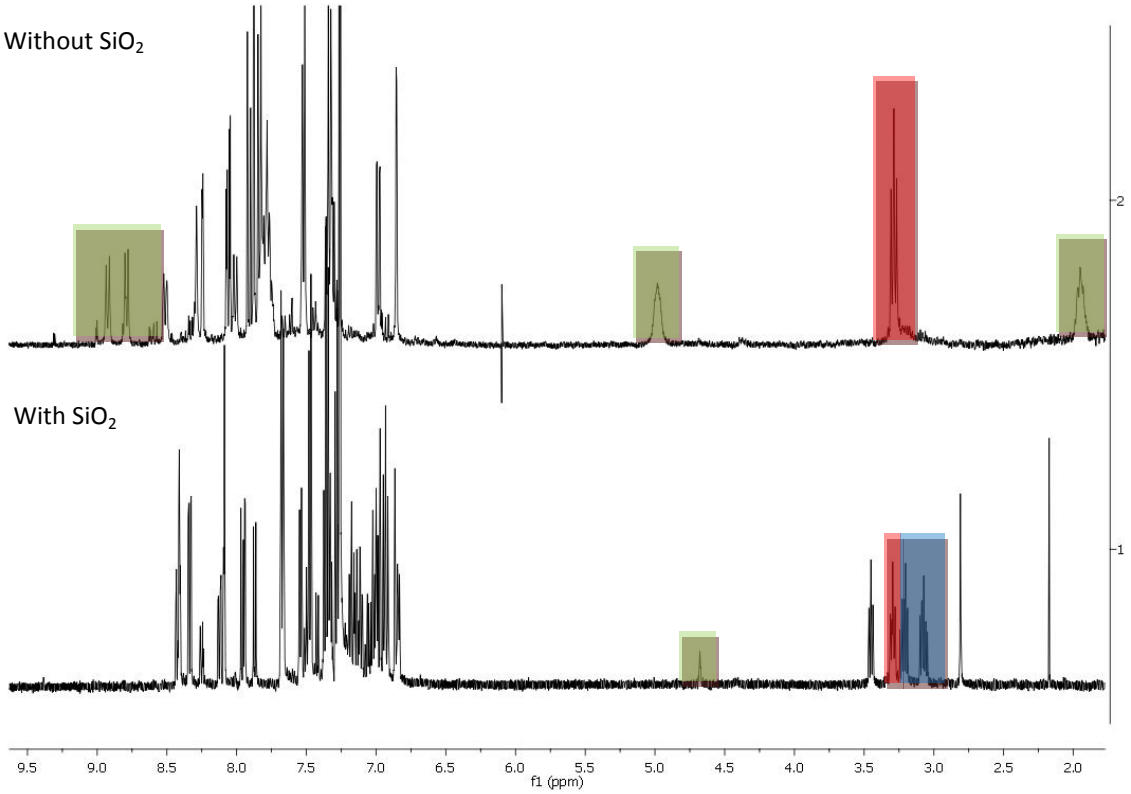

Figure 44 - Comparison of cyclisation for 1 h from $CHCl_3$, with and without SiO_2. Green boxes indicate phenanthridinium peaks, red is the open form and blue the SM.

It was expected that acidic conditions would push the equilibrium to favour phenanthridinium **288** over pseudobase **291** and ketone **292** by favouring dehydration and limiting availability of hydroxide or neutral water for hydrolysis to the amine **292**. Electron-rich phenanthridiniums would show greater hydrolytic stability as the electrophilicity of the iminium would decrease so it was decided to treat with acid after the cyclization and reduce the nitro group under acidic conditions.

7.6 Scale up and completion of the probe

The Suzuki coupling of trifluoroborate salt **266** and iodobenzophenone **218** was repeated on a large scale and benzophenone **265** isolated in a 95% crude yield (**Scheme 99**). This unpurified material was used to prepare imine **287**, which was not purified following work-up, but was heated in a kugelrohr at 100 °C for 1 h. The resulting mixture was treated with TFA to ensure conversion to the phenanthridinium salt **288**, and immediately hydrogenated over Pd/C using TFA as solvent. The mixture was neutralised and dried with K_2CO_3. An ion exchange procedure converted the material to mesylate. This gave the target aminophenanthridinium salt **293** in 47% yield from benzophenone **265** and a 45% overall yield from iodobenzophenone **218**.

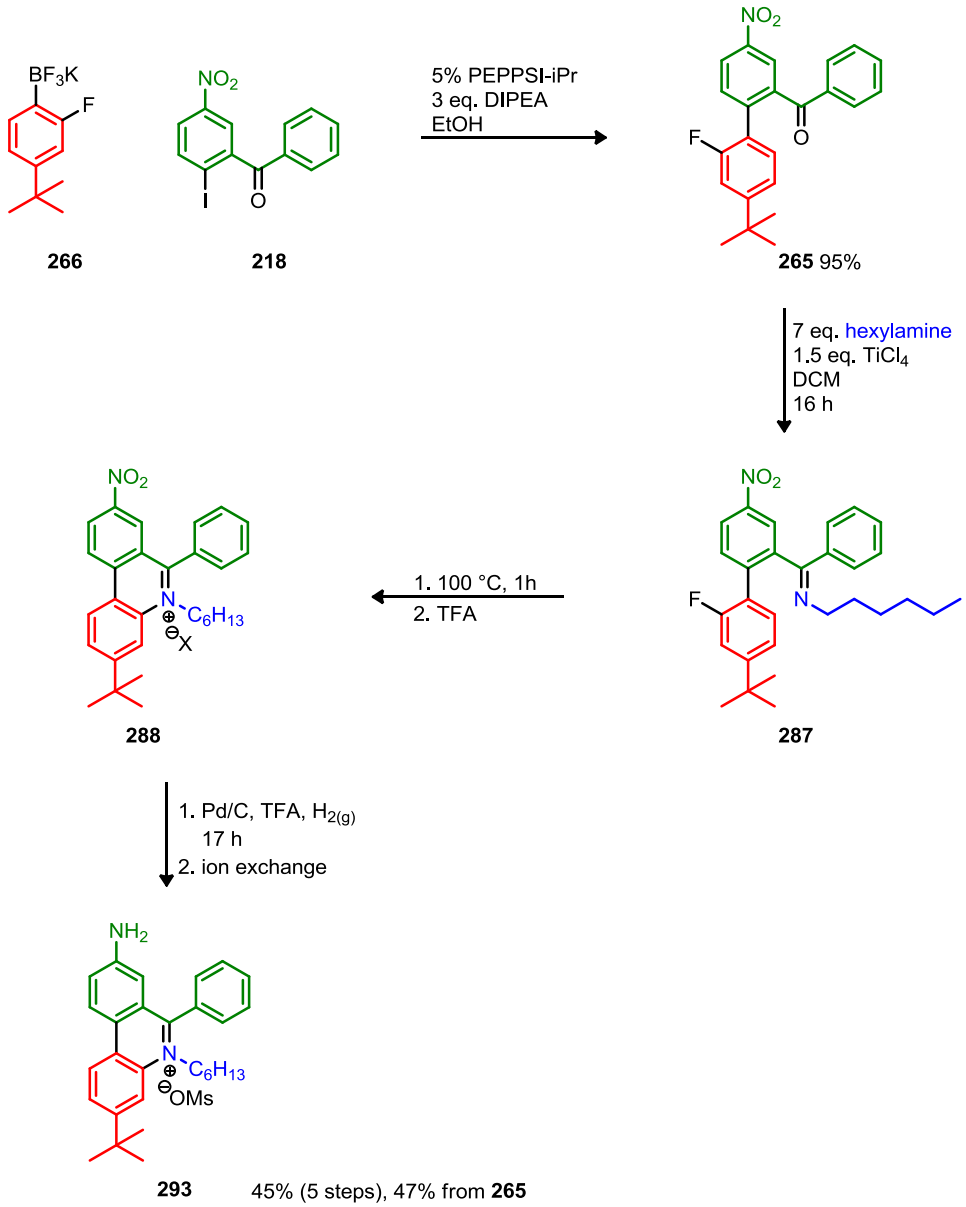

Scheme 99 - The final synthesis of the ^{t}Bu superoxide probe model **293**.

Phenanthridinium **293** was a precursor to a potential untargeted superoxide sensor **294**, so reduction to the latter was tested and reacted rapidly with $NaBH_4$. Re-oxidation proved very rapid and so isolation of the reduced form required development of a specific protocol (**Scheme 100**).

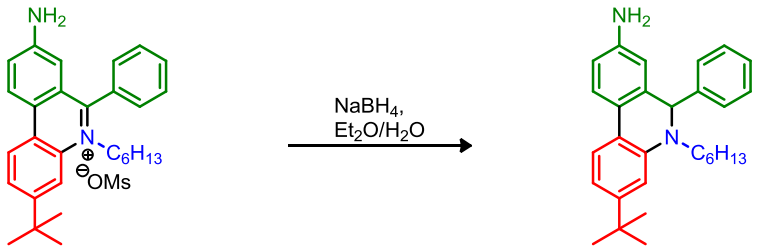

293 **294**

Scheme 100 - Reduction of superoxide probe precursor **293** to superoxide probe **294**.

The oxidised form **293** was added to a degassed biphasic system of H_2O and Et_2O through which argon is constantly bubbled. Excess $NaBH_4$ was added and the bright orange colour of the aqueous phase was lost, then the system sealed and shaken for 10 min. Without opening the vessel, the Et_2O layer is carefully syringed out into another vessel sealed and under argon, then additional degassed Et_2O used to repeat the process. A high flow of argon was then used to evaporate the Et_2O. When taken up and in degassed $CDCl_3$ ^1H NMR spectroscopy showed complete reduction, although rapid re-oxidation subsequently occurred. Since the dihydrophenanthridine **294** could be prepared from phenanthridinium **293**, the phenanthridinium **294** was submitted for testing by the group of Dr Michael P. Murphy at the MRC, Cambridge. The results of these tests will be discussed in **Chapter 9**. Since we had now developed a new route to N-alkylphenanthridiniums, we decided to exemplify this methodology, and this will be discussed in the next chapter.

Chapter 8: Methodology exemplification

8.1 Why exemplify this methodology?

8.1.1 The uses of *N*-alkylphenanthridinium salts

N-Alkylphenanthridinium heterocycles have a considerable multitude of uses aside from their potential as superoxide probes, such as DNA intercalating[132,180,310] dyes (such as ethidium bromide) and trypanocidal drugs[311] e.g. Samorin. The combination of appropriate redox properties and intercalation allows phenanthridinium salts to be used in the study of the redox and electron transport properties of DNA.[176,139] Phenanthridinium salts function as allosteric inhibitors of acetylcholine esterase.[312] Related alkaloids display potential anti-tumour properties. These are reliant on the planar, cationic nature of the heterocycles,[313] and can occur through Topoisomerase inhibition.[314,315] They have also been shown to exhibit antibiotic properties.[316,317]

8.1.2 Methodology scope and novelty

In addition to the previously mentioned features, the route described in **Chapter 7** also has considerable chemical novelty - S_NAr reactions utilising an *N*-alkyl imine nucleophile are extremely rare, but a few examples do exist.[318,319] The same reaction with an acyclic *N*-alkyl imine nucleophile, however, is almost unprecedented - only one literature example was found.[320]

Despite their many applications, extant synthetic routes to phenanthridinium salts are limited, and rely on *N*-alkylation almost without exception (see **Sections 4.1**-**4.3**). A synthetic route to structural analogues without this often messy and slow transformation would allow the properties of phenanthridinium salts to be investigated and tuned more easily to meet the range of applications mentioned, and is therefore of considerable practical value.

Following optimisation the imine cyclisation in **Chapter 7** gave near quantitative conversion to the *N*-alkylphenanthridinium salt **288**. The efficiency of this transformation was gratifying, and further work was undertaken to illustrate the electronic and steric tolerance of the cyclisation with a view towards providing a practical, general and convergent route to these important substrates. **Scheme 101** outlines how our strategy allows access to a phenanthridinium salt **295** in just three steps from an arylboron **296**, alkylamine **297** and benzophenone **298**. Many analogues of each of these components are available commercially, and far more are identified in the literature. Furthermore, the chemistry used to access the precursor imines (Suzuki coupling, imine formation) is well understood, well precedented and generally robust.

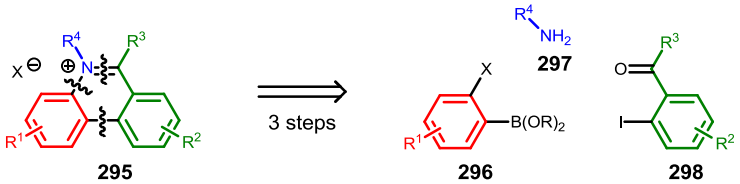

Scheme 101 - A generalised approach to the synthesis of 5,6-disubstituted *N*-alkylphenanthridinium salts.

8.2 Target selection for methodology exemplification

Subsequently targets were selected to exemplify the reaction and explicate its utility (**Figure 45**), focusing particularly on showing variation in electronics, sterics and substitution pattern while starting from a small palette of available or readily synthesised compounds.

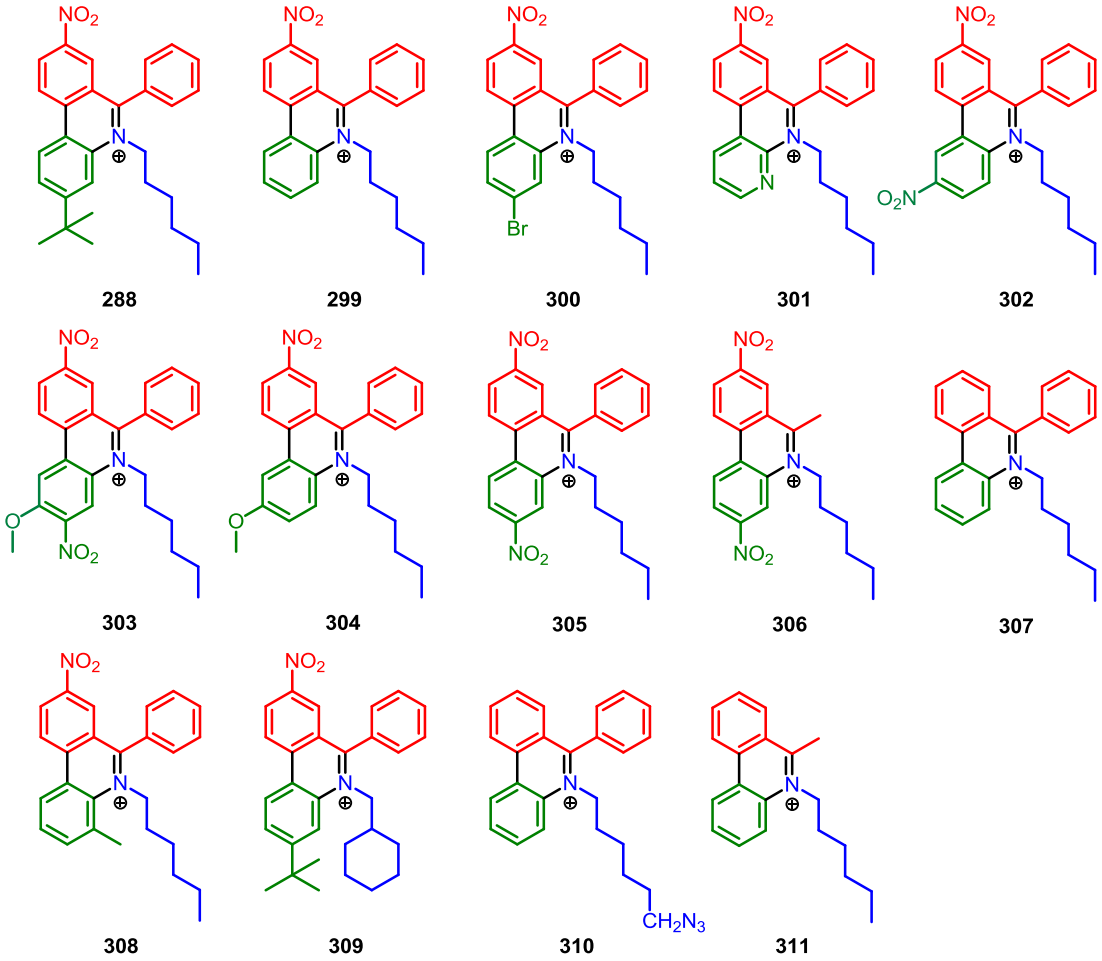

Figure 45 - Selected exemplification targets

The 6 points of variation in the core structure give a diversity of objective compounds commensurate to the scope and utility to be demonstrated; compounds **299**, **302**, **303**, **304**, **305** and **307** to probe the electronics of the system, **308** and **309** the steric tolerance, **306** and **311** the importance of the phenyl substituent. The remaining targets show either diversification routes (**300** and **310**) or in the case of **301** access to a novel structure which would require a convoluted synthetic route if constructed via alkylation protocols.

8.3 Precursor synthesis

8.3.1 Synthesis of precursor arylboron 296 components

Maximising the use of commercially available components such as the range of 2-fluorophenylboronic acids and previously synthesised components such as iodobenzophenone **218** was also considered during target selection. As such, the 2-haloaryl boronic acids used to couple with the precursor benzo and acetophenones **298** were mostly purchased from commercial sources (**Figure 46**).

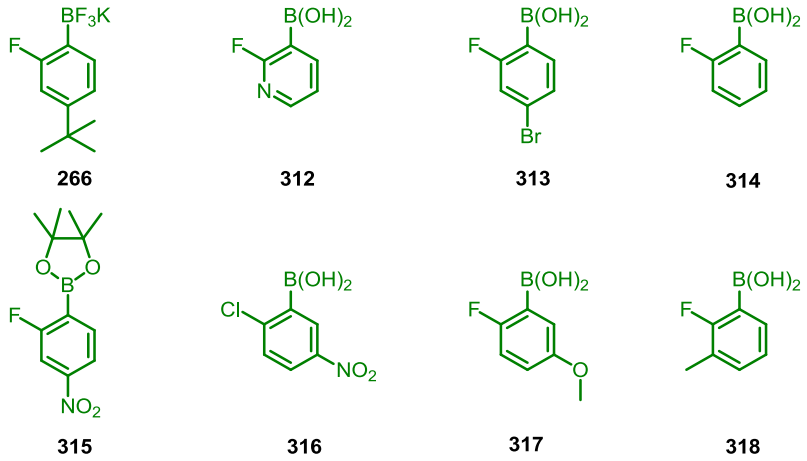

Figure 46 - The arylmetal components. With the exception of **266** and **315**, these are commercially available.

As potassium trifluoroborate salt **266** had already been synthesised, only pinacolborate **315** required preparation. Grignard formation with PhMgBr then borylation was attempted according to a literature procedure[321] but this gave a mixture of products (**Scheme 102**).

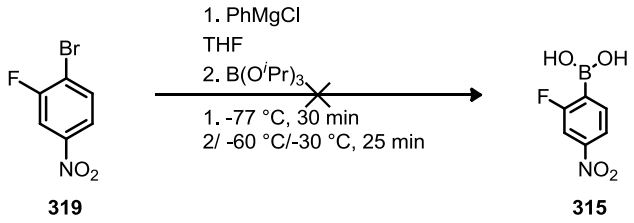

Scheme 102 - Attempted synthesis of arylboronate **315** by Grignard formation and quenching with a boronate electrophile.

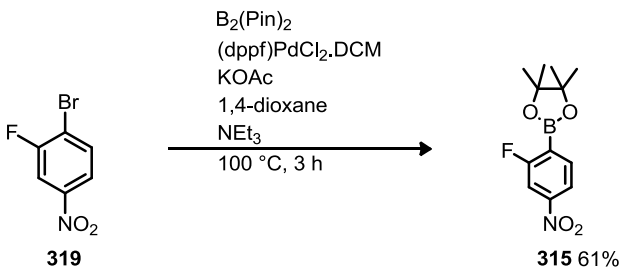

Scheme 103 - Palladium catalysed borylation giving the 2-fluoro-4-nitroarylboronate ester **315**.

Instead pinacolboronate **315** was synthesised via Miyaura borylation (**Scheme 103**), using a modified literature procedure.[322] 0.15 eq. of NEt_3 is added to activate the catalyst by β-hydride elimination.[308] Quantitative conversion was observed; however repeated chromatography proved

necessary to remove the boronate byproducts. Recrystallisation of the pinacolboronate ester gave clean material in a lower yield.

The potassium trifluoroborate salt **320** was also synthesised, by subjecting the crude reaction mixture from Miyuara borylation to $KHF_{2(aq)}$ and recrystallising from acetone (**Scheme 104**). Unfortunately this gave the salt **320** in low yield.

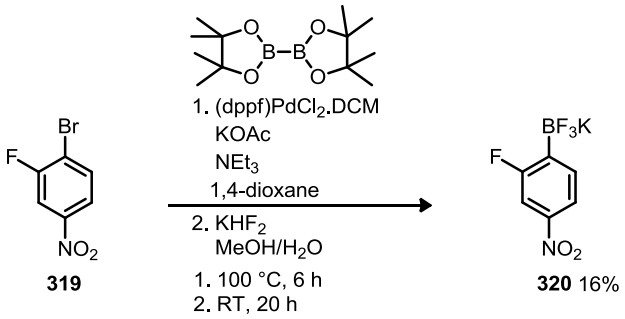

Scheme 104 - Palladium catalysed borylation giving the potassium trifluoroborate salt **320**.

8.3.2 Synthesis of precursor arylhalide component

For the most part 2-iodo-4-nitrobenzophenone **218** was used as the aryl halide component, supplemented by 2-bromoacetophenone **321**, and 2-iodobenzophenone **322**, and 2-bromo-4-nitroacetophenone **323** (**Figure 47**).

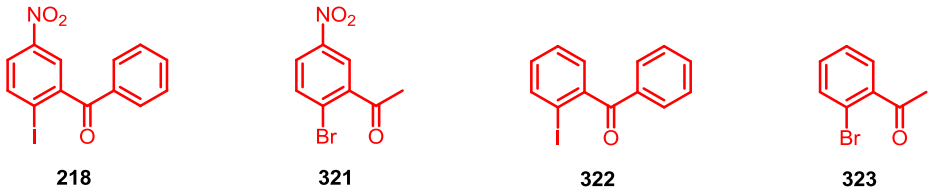

Figure 47 - Selected benzophenone precursors.

The synthesis of 2-iodo-4-nitrobenzophenone **218** has been described already (see **Chapter 5**) and ketones **322** and **323** were purchased. 2-Bromonitroacetophenone **321** was synthesised by nitration of 2-bromoacetophenone **323**. Three sets of conditions were tested: $KNO_3/H_2SO_{4(aq)}$, $Ac_2O/HNO_{3(aq)}$ and $AcOH/HNO_{3(aq)}$. Acetophenone **323** proved too deactivated for the milder conditions so the $H_2SO_{4(aq)}/KNO_3$ conditions were scaled up, and stopped at around 85-90% completion due to side product formation. Chromatography gave the desired compound in moderate yield (**Scheme 105**).

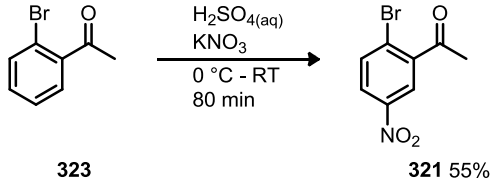

Scheme 105 - Synthesis of 4-nitroacetophenone **321**.

8.3.3 Suzuki cross coupling to give biaryl precursors

A range of biaryls **324** - **333** (**Figure 48**) were then prepared by Suzuki coupling (**Scheme 106** and **Table 2**), with conditions used initially based on those previously used for benzophenone **265** (**Section 7.4**). Although the reagents are the same the conditions used varied (**Table 2**). These reactions can be divided into 2 categories: microwave and non-microwave reactions. The former was developed as a response to difficulties in getting particularly electron-poor arylboronates such as nitroarene **315** to cross couple, where higher temperatures are necessary. Transmetallation is usually the rate limiting step in the case of the NHC catalysts used, and electron poor arylboronates undergo this reaction less readily. The microwave is a fast and efficient way of achieving higher temperatures, and reaction was further aided by higher concentrations. More specific microwave effects have previously been claimed, but a recent review suggests there is no evidence of this.[323]

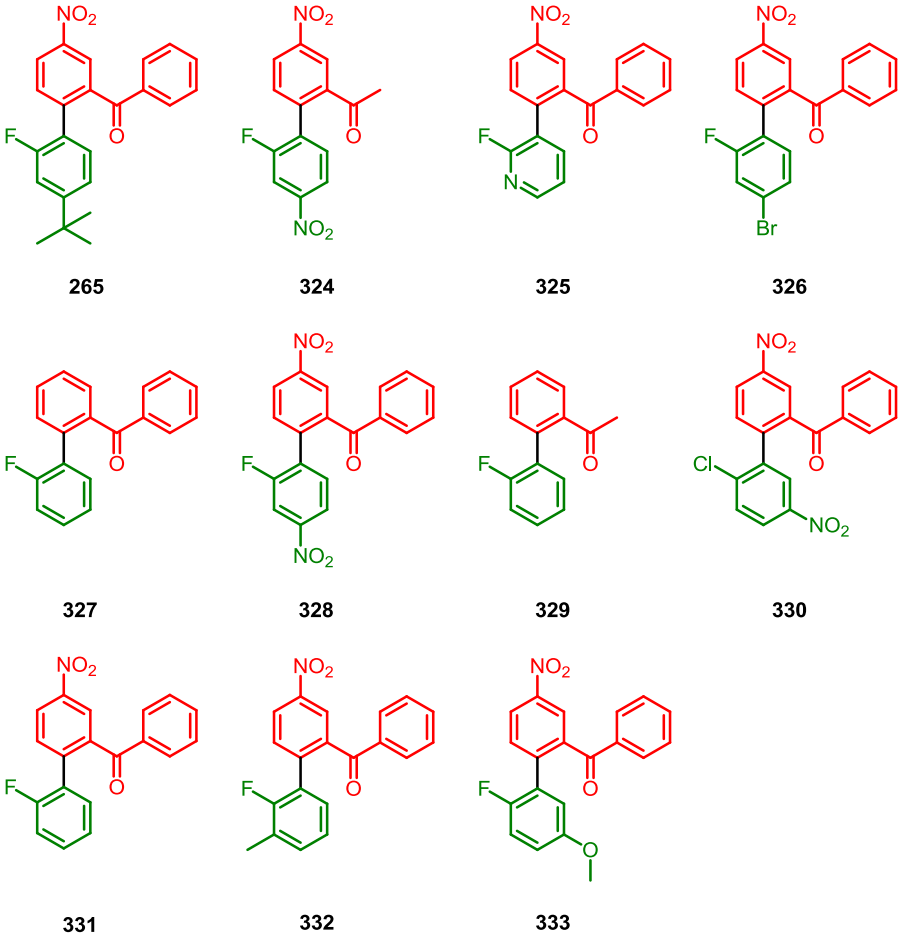

Figure 48 - Cross coupling aryl halide and transmetallation partners.

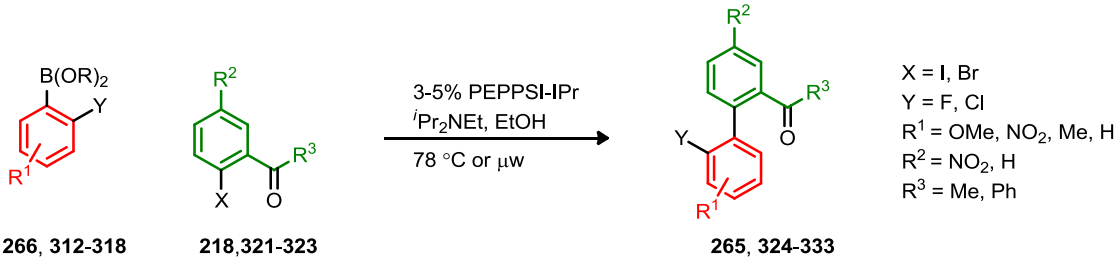

266, **312-318** **218**,**321-323** **265**, **324-333**

Scheme 106 - Generalised Suzuki coupling outline.

Table 2 - Summary of Suzuki reaction conditions and product yields.

Target	[ArX]	t (h)	$ArBX_n$ eq.	cat.	T (˚C)	μwave	Purification	Yield
265	0.12	4	1.12	6%	78	N	Chromatography	78%
324	0.41	0.17	1.03	5%	125	Y	Chromatography	40%
325	0.28	1	1.00	5%	125	Y	Chromatography	53%
326	0.10	22	1.11	3%	78	N	Chromatography	55%
327	0.25	16	1.00	3%	78	N	Chromatography	76%
328	0.19	0.5	1.03	5%	100	Y	Chromatography	99%
329	0.34	1	1.00	5%	125	Y	Chromatography	84%
330	0.28	0.16	1.00	5%	125	Y	Chromatography	56%
331	0.20	16	1.00	3%	78	N	Precipitation	49%
332	0.16	22	1.00	3%	78	N	Crystallised	66%
333	0.15	22	1.00	3%	78	N	Crystallised	83%

The conditions described for ^{t}butyl benzophenone **265** were used as a starting point. The 6% catalyst loading appeared to give near quantitative conversion, but chromatography entailed substantial loses. Purification difficulties were observed with several substrates.

Nitroacetophenone **321** reacted readily under microwave conditions, giving a 3 - 4:1 ratio of the 3,8-Dinitroacetophenone **324** to an acetophenone derived impurity. Purification proved difficult, giving a moderate yield. Coupling to give heterocyclic benzophenone derivative **325** was attempted under thermal conditions, but only unreacted benzophenone **218** was recovered in large quantities. As the pyridylboronic acid **312** has a reported melting point of 172 ˚C[324] and no aqueous wash was utilised in work up it was assumed that deboronation had destroyed the transmetallating component as pyridyl boronic acids are prone to decomposition.[214] It is also possible that the pyridyl **312** competes with the weakly binding 3-chloropyridine ligand. Raising the reaction temperature with the microwave showed the Suzuki coupling to be faster than decomposition at 125 ˚C, allowing pyridylbenzophenone **325** to be isolated, although chromatography proved challenging.

The coupling of bromoarylboronic acid **313** with 2-iodo-5-nitrobenzophenone **218** to give bromobenzophenone **326** posed a challenge; although electron poor 2-iodo-5-nitrobenzophenone **218** was likely to undergo oxidative addition more rapidly than the bromide, the bromoarylbenzophenone **326** is also a good Suzuki coupling substrate and is present in higher concentrations as the reaction nears completion. Originally an excess of the iodobenzophenone **218** was used, but it was established that this starting material was chromatographically

inseparable from the bromobenzophenone **326**. Some success was achieved by sonicating the chromatographed mixture in an Et_2O/Pet. ether mixture in which the product **326** was sparingly soluble, resulting in precipitation of the product as a fine white solid. Multiple failures to repeat this procedure with a later batch of material suggested that the conditions required are very precise and difficult to achieve reproducibly. Instead it proved necessary to use an excess of arylboronic acid **313** to consume fully the 2-iodo-5-nitrobenzophenone **218**. This generated another impurity, identified as benzophenone dehalogenation product **228** (**Scheme 70**), which could be removed by chromatography.

Coupling to give unsubstituted 2-arylbenzophenone **327** worked under thermal (76%) conditions. The equivalent acetophenone **329** required harsher conditions, producing a good yield only after extensive microwave heating.

Since arylboronate **315** was synthesised by the Miyaura reaction, an attempt was made to combine Miyaura and Suzuki reactions to synthesise dinitrobenzophenone **328** by changing the Miyaura catalyst to PEPPSI-^{i}Pr and then adding the Suzuki reagents and a small amount of water after 16 h, but a complicated mixture containing little or no product resulted. Suzuki coupling of isolated arylboronate **315** with iodobenzophenone **218**, under thermal conditions proved sluggish. Microwave irradiation of a 0.1 M solution of each component to 120 ˚C for 10 mins gave rapid conversion and mostly the dinitrobenzophenone **328**. Dropping to 100 ˚C for 30 min reduced side product generation. Adjusting the conditions to 100˚C/30 min at 0.2 M concentration of iodobenzophenone **218** gave higher conversion and a yield of 99% after chromatography.

Synthesis of aryl chloride **330** was problematic. The PEPPSI-^{i}Pr catalyst can affect oxidative addition on C - Cl bonds, and the electronics of the product **330** favour this and disfavour transmetallation from the arylboronate **316**. Standard thermal conditions proved ineffective while microwave heating to 125 ˚C for 1 h with 1.1 eq. 2-chloro-5-nitrophenylboronic acid **316** gave side products in addition to chlorobenzophenone **330**. Reducing the number of equivalents of chloroboronic acid **316** to 0.9 and reaction time to 10 min gave little purity change. A ratio of 3:1 for product to homocoupled benzophenone **229** resulted (**Scheme 107**). This suggests transmetallation is sufficiently slow for competitive $Pd^{(II)}$ reduction. Increasing the number of equivalents substantially to counteract this would risk further cross coupling of the chlorobenzophenone **330** with arylboronic acid **316**, so a moderate yield of 56% was accepted.

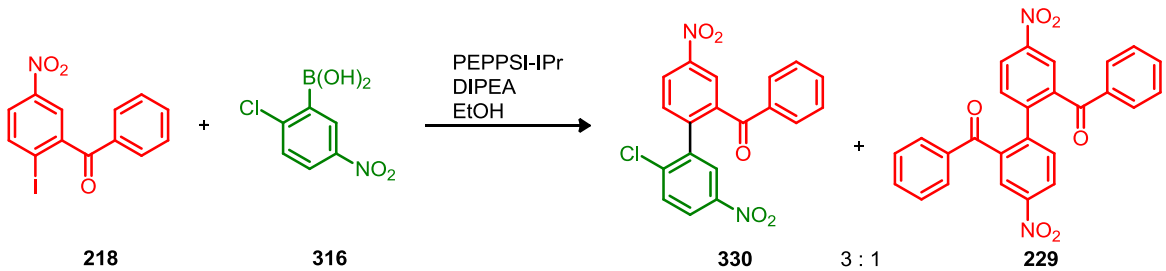

Scheme 107 - Products of chloroarylboronic acid **316** and iodobenzophenone **218** cross coupling.

Synthesis of 2-arylbenzophenone **331** from iodobenzophenone **218** and 2-fluorophenylboronic acid **314** proved easier. Thermal conditions gave near quantitative conversion to mononitrobenzophenone **331** on a small scale. An unexpected shortage of 2-fluorophenylboronic acid **314** meant only 0.9 equivalents could be used, and subsequent Suzuki coupling resulted in a mixture of compounds. Separation proved challenging, with chromatography followed by precipitation as described for bromobenzophenone **326** giving a moderate yield of mononitrobenzophenone **331**. Both methylbenzophenone **332** and methoxybenzophenone **333** were synthesised by Suzuki coupling in a near quantitative fashion thermally, being recrystallised from $CHCl_3$ to remove inorganic impurities prior to the methodology steps.

8.3.4 Nitration of 2-(5''-methoxy-2''-fluorophenyl)-5-nitrobenzophenone 333

To investigate the interplay of electron donating and withdrawing groups and to produce a precursor to the 2-hydroxyphenanthridinium MitoSOX standard desired for the superoxide probe project (**Chapter 10**) the dinitro compound **334** above was among the target precursors for the phenanthridiniums. Rather than modify the Suzuki precursor it was felt that the electronics of the ring systems might be distinct enough to allow regioselective nitration (**Scheme 109**). Although the major features of electrophilic aromatic substitutions and nitration in particular are understood, some details are recently discovered or disputed.[325,326,327] Preassociation of the nitronium ion and the arene substrate occurs, through an ionic (π) complex or via SET to give two radicals, depending on the nature of the reactants. Either then give the σ-complex which precedes product.[328] The ease of rearranging these associated states explains the observed high regioselectivity but low substrate selectivity.[329] Various nitration conditions were attempted.

Initial attempts to nitrate methoxyarene **333** with $AcOH/HNO_{3(aq)}$ proved this system to be insufficiently reactive, with no reaction observed after 1 h. Nitration in a biphasic mixture using $H_2SO_{4(aq)}/KNO_3$ resulted in spontaneous decomposition to an insoluble black residue, believed to be composed of sulfonylation products.

The nitronium salt NO_2BF_4 is a common, powerful nitrating agent. This was tested on the rationale that addition of 1 equivalent at –42 °C in MeCN followed by slow warming would result in preferential reaction at the more electron rich site and give dinitro compound **334**. Practical and theoretical problems became apparent - NO_2BF_4 is sufficiently hygroscopic to be extremely difficult to weigh on a sub 50 mg scale, and sparingly soluble. The reaction with methoxyarene **333** is rapid and exothermic, so the degree of local temperature control achieved with an external dry ice bath is debatable. The handling properties of NO_2BF_4 made using the correct equivalence challenging, and excesses resulted in further nitration and isolation of trinitro arene **335** showed it to have been formed in a 2:1 ratio (^{1}H NMR) to the dinitrobenzophenone target **334**, although the absence of methoxybenzophenone **333** from the mixture was considered encouraging. The regiochemistry of trinitrobenzophenone **335** was confirmed through analysis of C-F coupling in the ^{13}C NMR spectra; in this case the C(H)-F coupling on the penta-substituted aryl ring was 28 ppm, too large to be any position but adjacent to F.[330] When addition in MeCN solution was

attempted fewer equivalents of the reagent were added due to the low solubility of NO_2BF_4; a mixture of methoxybenzophenone **333** and dinitrobenzophenone **334** resulted (**Scheme 108**).

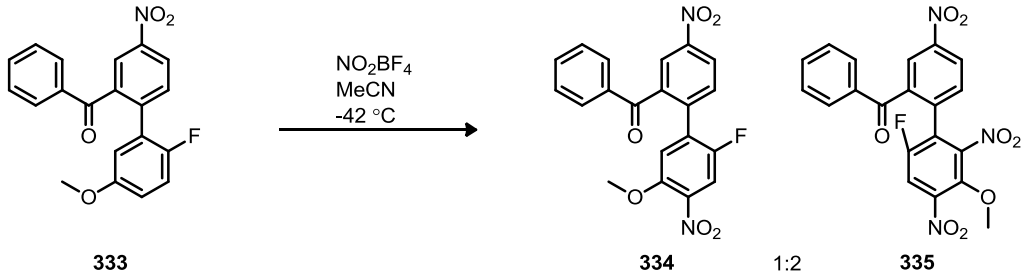

Scheme 108 - Trinitroaryl **335** was observed in a 2:1 ratio to desired dinitroaryl **334** when NO_2BF_4 was used as the nitrating agent.

These practical difficulties motivated the use of an $Ac_2O/HNO_{3(aq)}$ system. $Ac_2O/HNO_{3(aq)}$ is known to be a more powerful nitrating combination than $AcOH/HNO_{3(aq)}$.[331,332] Inclusion of DCM aided the solubility of methoxyarene **333** in acetic anhydride prior to $HNO_{3(aq)}$ and optimisation of the reaction time to 2 h at 0 °C allowed isolation of the dinitrobenzophenone **334** in 72% yield (**Scheme 109**).

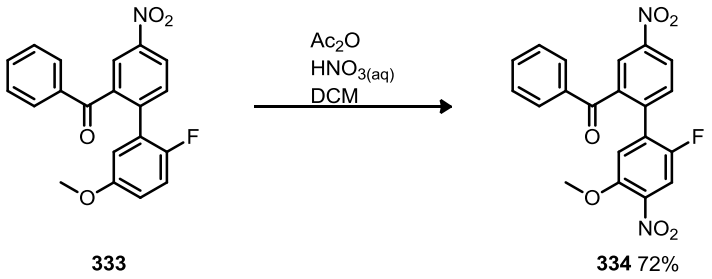

Scheme 109 - Selective nitration of lower benzophenone ring.

8.3.5 Alternate alkylating groups

Having assembled a range of 2-arylbenzophenones for imine formation a number of amines and amine precursors were selected as condensation partners (**Figure 49**).

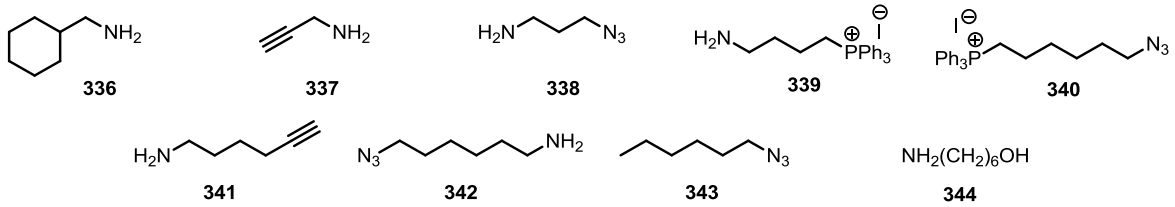

Figure 49 - Alternative alkyl groups investigated. Compound **338** was provided by Stuart Caldwell.

Compounds **336**, **337** and **344** are commercially available. To produce the final superoxide probe target **261** either the $^{+}PPh_3$ or a surrogate should be substituted on the end of the alkyl chain. Unsurprisingly, therefore 4-aminobutylphosphonium iodide **339** was the first substrate investigated. Nucleophilic substitution using $NH_{3(aq)}$ in MeCN was performed on the iodobutylphosphonium iodide **24** synthesised previously (**Section 2.5**, **Scheme 6**). This gave a mixture, with a colleague having a similar result using condensed $NH_{3(l)}$. Instead using sodium azide as the nucleophile 4-azidophosphonium salt **345** was prepared quantitatively. Reduction of this alkyl azide proved difficult, with Staudinger reduction using PPh_3 in DCM appearing to result in several products. Investigation showed iminophosphorane in the ^{1}H NMR spectrum alongside side products when hydrolysis was omitted. When reduction with $LiAlH_4$ in THF was tested azidoalkylphosphonium salt **345** was destroyed. Hydrogenation with $Pd/C/H_{2(g)}$ showed amine **339** in the ^{1}H NMR spectrum, but the initial choice of AcOH prevented precipitation and complicated isolation. Switching to MeOH and using a high catalyst loading (0.24 eq. of 10% Pd/C) with the azidobutylphosphonium salt **345** gave near quantitative conversion to the aminobutylphosphonium salt **339** (**Scheme 110**).

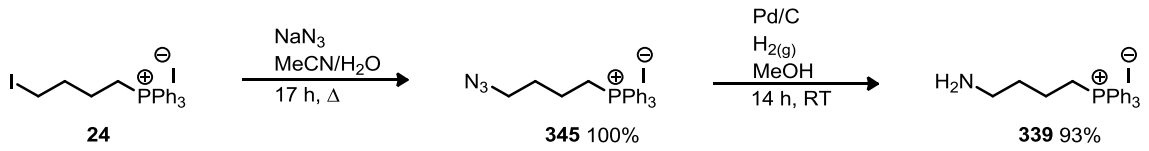

Scheme 110 - Synthesis of aminobutylphosphonium salt **339**.

6-Azidohexylphosphonium iodide **340** was synthesised through the same nucleophilic substitution as used to synthesise phosphonium salt **345** from the iodoalkyl precursor **348** acquired from Stephen McQuaker (**Scheme 52**). The simple hexylazide **343** and 1,6-diazidohexane **349** were similarly prepared from the alkyl bromides **346** and **347**.

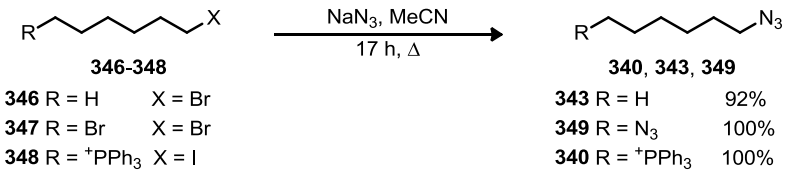

346 R = H X = Br
347 R = Br X = Br
348 R = $^{+}PPh_3$ X = I

343 R = H 92%
349 R = N_3 100%
340 R = $^{+}PPh_3$ 100%

Scheme 111 - Synthesis of azidoalkyl compounds **340**, **343** and **349**. 6-Azidohexylphosphonium iodide **348** was provided by Stephen McQuaker.

The 1,6-azidohexane **349** was reduced (**Scheme 53**) with the two-phase Staudinger procedure which allows monoreduction as previously discussed in **Section 11.4.3**, **Scheme 142**.

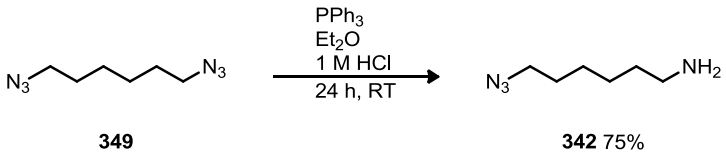

349 **342** 75%

Scheme 112 - Monoreduction of 1,6-diazohexane **349**.

Difficulties were encountered in the synthesis of alkyne **341**, where use of hydrazine produced alkene side products. An alternative procedure use AcOH and $NaBH_4$ was successful,[333] but purification by ion exchange gave a poor yield (**Scheme 113**).

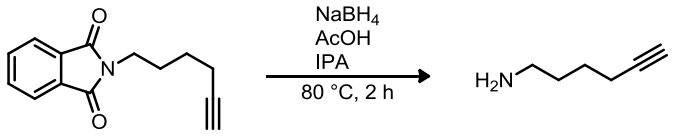

350 **341** 14%

Scheme 113 - Deprotection to yield alkyne **341** proved low yielding.

With a range of simple amines in hand, imine formation was investigated.

8.3.6 Imine formation

Imine **287** had been prepared from benzphenone **265** using $TiCl_4$ in DCM or PhMe. $TiCl_4$ is a powerful dehydrating agent due to the oxophilicity of the Ti^{4+} ion and the favourability of TiO_2 formation. The high Lewis acidity of $TiCl_4$ allows it to coordinate to carbonyls[334] activating these to nucleophilic attack. It has been suggested the active species in imine formation is an alkylamino complex of titanium (IV),[335] certainly a colour change is observed on combination with hexylamine in PhMe or DCM.

A series of *N*-hexylimine derivatives (**Scheme 114**, **Figure 50**) were synthesised under conditions similar to those used for the original benzophenone imine **287**. Use of PhMe was convenient as 1 M $TiCl_4$ in PhMe is bright orange, so the quality of the reagent is easily assessed. The excess of amine, which was usually around 7 eq.,[335] was reduced where the amine required synthesis. Between 1.5 and 2.0 eq. $TiCl_4$ was used. The variation in $TiCl_4$ and concentration were decided pragmatically: where problems with stirring were observed PhMe was added, incomplete conversion after approx. 24 h was taken to mean more $TiCl_4$ was required. The original substrate **265** gave several products in the imine formation procedure, which required chromatography to separate. However, the unpurified mixture reacted to produce the desired phenanthridinium products cleanly, so the imines were not purified following work up. More electron rich ketones gave cleaner conversion to the imine, while electron poor ketones cyclised rapidly following imine formation to produce a mixture. As the overlapping signals in the ^1H NMR spectrum often obsfuscated important aromatic peaks, reaction completion was confirmed by loss of starting

material peaks, including movement of H4/H6 (**Section 7.5**, **Figure 41**). The diastereotopic CH_2-1 peaks at 3.0 - 3.5 ppm were also considered a useful indicator.

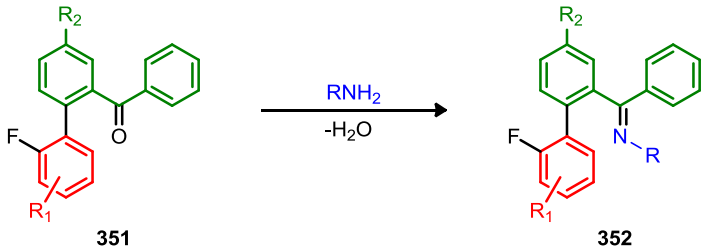

351 **352**

Scheme 114 - Imine formation outline.

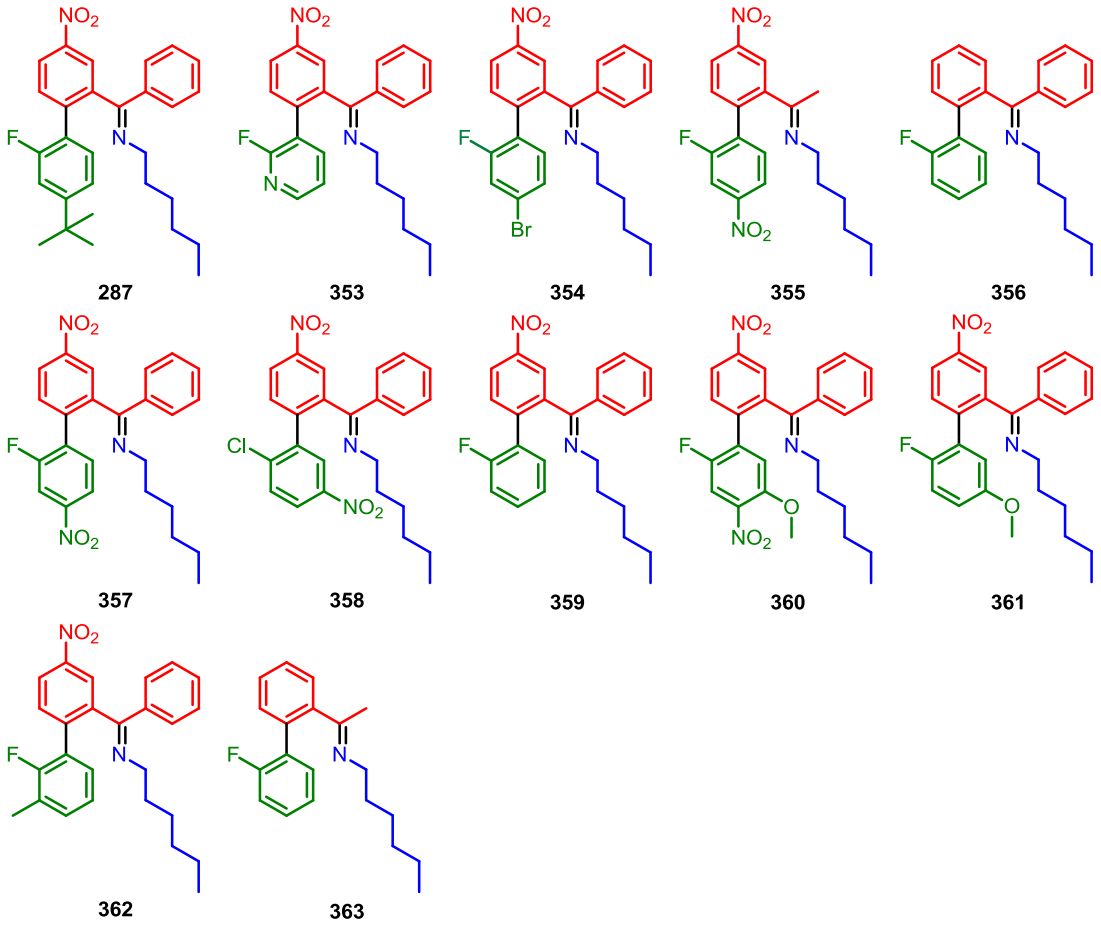

287 **353** **354** **355** **356**

357 **358** **359** **360** **361**

362 **363**

Figure 50 - The imine precursors targets.

The work up procedure developed with experience, as the quantity of TiO_2 produced in quenching, the residual hexylamine and the vulnerability of the product to hydrolysis made identification of the correct procedure challenging.

The conversion of acetophenone **329** to imine **363** did not proceed well and there were large quantities of SM present after work up, but it is not known if this represents incomplete conversion or facile hydrolysis.

Overall the imines **353** - **362** formed from hexylamine could be prepared efficiently using $TiCl_4$, but the $TiCl_4$ solutions have short shelf lives, and the moisture sensitivity makes a usually routine

transformation the most technically demanding of the route. Although effective in the previous synthesis, $TiCl_4$ has limited functional group tolerance, so the range of amines that could be used was explored briefly. Bulky cyclohexylmethylamine reacted with benzophenone **265** to give imine **364** (**Scheme 114**). Similarly, the azido functionality in amine **342** was tolerated and the imine **365** formed easily (**Scheme 115**). On the other hand imine formation with amines **336** - **341**, **343** and **344** failed when $TiCl_4$ was used as the Lewis acid. A range of other conditions including $MgSO_4$, PhMe/TsOH, $BF_3.OEt_2$, $Ti(O^iPr)_4$ and $CH(OEt)_3$ were then investigated. However, all were unsuccessful.

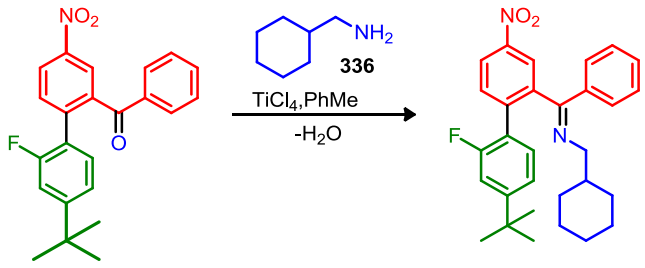

265 **364**

Scheme 115 - Synthesis of cyclohexylmethylimine **364**.

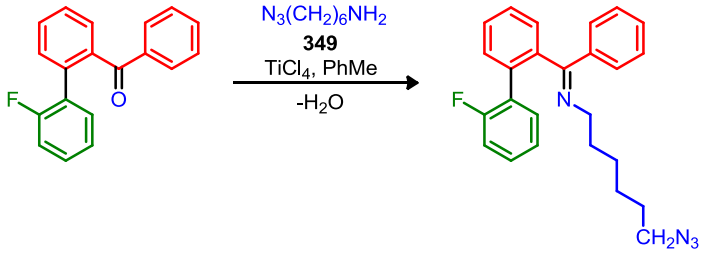

327 **365**

Scheme 116 - Synthesis of azidohexylimine **365**.

Attempts were also then made to form the imine with an aza-Wittig reaction using alkyl azides **340** and **343** with PPh_3 or PBu_3 and benzophenone **265** (**Scheme 117**). Following a trial with benzophenone **265**, azide **343** and PPh_3 in THF in the microwave at 100 °C, the iminophosphorane product of the Staudinger reaction was identified by a signal at 3.08 ppm, which was a *dt* (*J* = 18.3, 7.4 Hz) and is consistent with literature values for the methylene unit of $Ph_3P{=}NCH_2$.[336] This was observed in the presence of benzophenone **265**, showing the iminophosphoranes generated to be insufficiently reactive with the ketone to produce imine **287**.

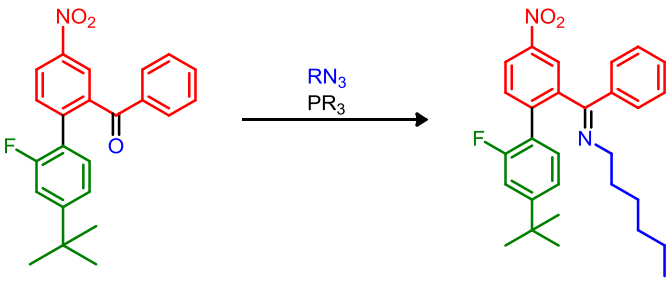

265 **287**

Scheme 117 - Outline of the attempted aza-Wittig reactions.

8.4 Cyclisation

8.4.1 Solvent free thermal cyclisation

With the crude imines **287** and **353** - **365** in hand, the limits of the cyclisation procedure were established. The procedure developed for the preparation of the superoxide probe precursor **288** involved heating under an inert atmosphere in a kugelrohr apparatus at atmospheric pressure. At the beginning of the reaction the imine is loaded as a solution in chloroform, which quickly evaporates leaving a layer of imine on the hot glass surface.

The utility of these conditions were tested using the substrates believed to be most electronically and sterically demanding, methoxybenzophenone imine **361** and 3''-methylbenzophenone imine **362**, respectively. The conjugation of methoxy group in imine **361** disfavours reaction *para* to this group. This is demonstrated by considering the contribution of minor resonance form **366**, which displays the increase in electron density at C2'' in exaggerated fashion (**Scheme 118**). Unsurprisingly the reaction is slower than with the benzophenone imine **287**, However, forcing conditions (2 h 45 min at 100 ˚C, then 3 h at 125 ˚C) were successful and gave the phenanthridinium **304** in a 3:1 ratio over an impurity. Chromatography using 2% MeOH, 1% NEt_3 in DCM gave the N-hexylphenanthridinium **304** in a yield of 47% over two steps from the benzophenone **366**. The ^{1}H NMR spectrum of the impurity displayed a pattern for the aromatic protons that is characteristic of a phenanthridinium salt and so it was assumed to be elimination product **367**.

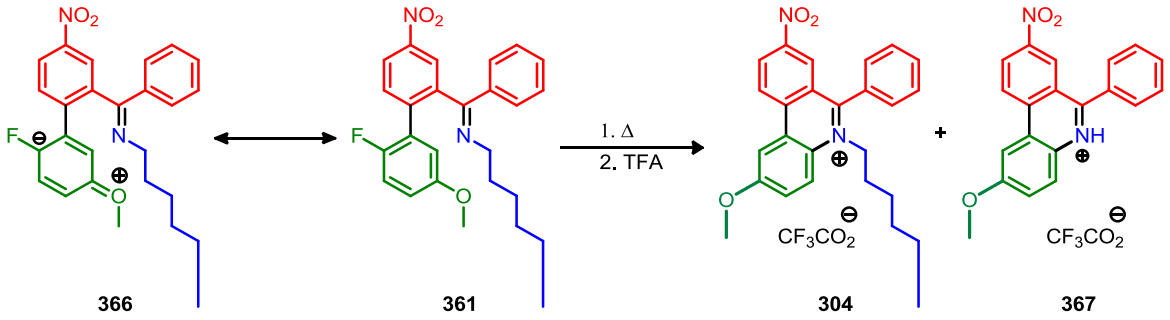

Scheme 118 - The cyclisation of 5''-methoxybenzophenone imine **361**, with the contributing resonance form **366**, and suspected elimination product phenanthridinium **367**.

When imine formation was tested with sterically challenging 3''-methylbenzophenone **332** two products resulted, with the expected benzophenone imine **362** favoured 3:1 over a related fluorinated compound which did not show inequivalent protons at CH_2N. Initial heating (100 ˚C, 1 h) in the kugelrohr increased the ratio of imine **362** to the unidentified side product of imine formation, but did not give significant conversion to the *N*-alkylphenanthridinium salt. When the reaction temperature was increased to 150 ˚C for 2 h 30 min, cyclisation and elimination of the *N*-alkyl side chain occurred together to give phenanthridine **368**, and this elimination was driven to completion by heating for 3 h at 200 ˚C (**Scheme 119**). A small quantity was purified for characterisation purposes.

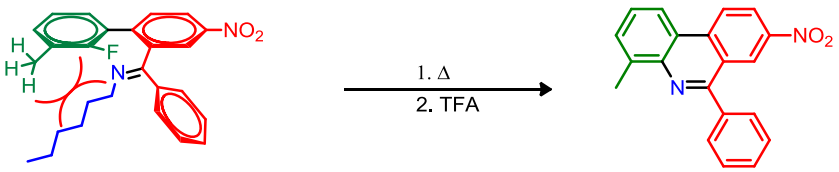

362 **368** 11%

Scheme 119 - The steric hindrance to cyclisation of 3''-methylbenzophenone imine **362**, as shown by the red arcs.

8.4.2 Microwave-assisted cyclisations to give phenanthridinium salts in aprotic solvents

It was clear that the method of cyclisation was not appropriate for imine **362** and had to be improved. Furthermore, solid material heats unevenly and chars, and this would be problematic for many of the the imines **353**-**365** as they would not be liquid at 100 ˚C given that most of the benzophenones melted at a higher temperature than this. It was also thought that other researchers would be more likely to make use of a more conventional procedure.

Consequently, microwave heating in a range of solvents was tested. 1 mg/mL solutions of imine **287** were heated in sealed tubes at 100 °C for 1 h using a 50 W microwave. No protic solvents were investigated because most of these are moderately nucleophilic and may compete with the desired reaction. The reactions in acetone and in toluene gave side products. Reactions in dichloromethane and THF did not go to completion, but the THF mixture contained only starting imine and product. The reaction in MeCN gave complete conversion, but had traces of side product, so the procedure was optimised to 2 h in THF at 100 °C. It is not surprising that reaction in the most polar solvent gave fastest conversion since the conjectured transition state (S_NAr) is more polar than the ground state.

8.4.3 Optimisation of individual cyclisations and results

With the start point for optimisation chosen, 20 mg portions of benzophenone imines were weighed by difference (due to the oily or foam-like nature of the imines) into 1 mL solvent and sonicated into solution or suspension. Small variations in molar concentration are unimportant considering the high dilution and intramolecular reaction. Following microwave heating the solvent was removed under vacuum, then a sample taken up in deuterated solvent and approx. 0.05 mL d-TFA added. Conditions were assessed based on conversion as observed by ^{1}H NMR spectroscopy, with final conditions then applied to the conversion of 100 mg in 5 mL of solvent.

The work up procedure used for the scaled up microwave conditions involved removing the reaction solvent under reduced pressure and re-dissolving the residue in dry Et_2O, then precipitating the phenanthridinium salt with excess ethereal HCl. Difficulties achieving reasonable spectra were common features of the phenanthridinium work, due to broad aromatic peaks attributed to aggregation effects such as π stacking, so the solvent used for the definitive spectra vary with the substrate. The conditions for the final cyclisations and the combined yields over imine formation and cyclisation steps are summarised in **Table 3**.

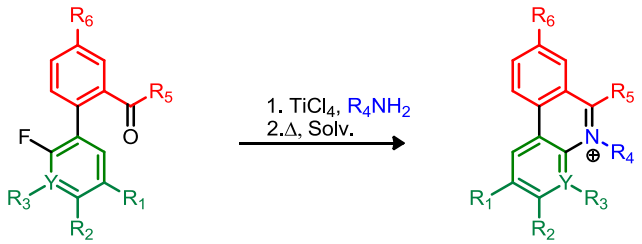

265, **324-333** **288**, **299-310**

Scheme 120 - Imine formation/cyclisation overview.

Table 3 - Imine formation/cyclisation combined yield - conditions refer to cyclisation.

n°	R_1	R_2	Y	R_3	R_4	R_5	R_6	X	Solv.	T (˚C)	t (h)	%
288	H	tBu	C	H	C_6H_{13}	Ph	NO_2	F	THF	100	2	85
299	H	H	C	H	C_6H_{13}	Ph	NO_2	F	THF	100	2	84
300	H	Br	C	H	C_6H_{13}	Ph	NO_2	F	THF	100	2	100
301	H	H	N	H	C_6H_{13}	Ph	NO_2	F	THF	100	0.5	98
302	NO_2	H	C	H	C_6H_{13}	Ph	NO_2	Cl	THF	100	0.5	86
303	OMe	NO_2	C	H	C_6H_{13}	Ph	NO_2	F	THF	100	2	74
304	OMe	H	C	H	C_6H_{13}	Ph	NO_2	F	-	100*	2	47
305	H	NO_2	C	H	C_6H_{13}	Ph	NO_2	F	-	-#	-	97
306	H	NO_2	C	H	C_6H_{13}	Me	NO_2	F	-	-#	-	100†
307	H	H	C	H	C_6H_{13}	Ph	H	F	MeCN	110	1.5	68
308	H	H	C	Me	C_6H_{13}	Ph	NO_2	F	MeCN	110	10	79
309	H	tBu	H	H	C_7H_{13}	Ph	NO_2	F	MeCN	110	1.5	75
310	H	H	C	H	$C_6H_{12}N_3$	Ph	H	F	MeCN	110	1.5	78

* Original kugelrohr conditions.

Cyclisation complete on work up of imine formation.

† Compound isolated as enamine

Upon scale up of the test cyclisation in THF at 100 °C for 2 h imine **287** gave good conversion to phenanthridinium **288**. Cyclisations to electronically similar 8-nitrophenanthridiniums **299** and **300** gave good yields under these conditions, with the variation in the yield dictated mostly by the imine formation step.

The 2''-fluoro-3''-azabenzophenone imine **353** gave rapid reaction; most of the material cyclised during work up, with 30 min of microwave heating ensuring complete conversion. Ascertaining the nature of this compound posed a quandary; isolation of the double chloride salt was envisaged on addition of HCl. No sign of this species was observed by mass spectrometry suggesting that the final isolated form is the single salt. Chlorobenzophenone imine **358** rapidly cyclised to give phenanthridinium **302**, despite the poorer chloride leaving group. This salt proved hygroscopic and required additional drying, resulting in a small loss in yield.

The cyclisation to 2-methoxy-3-nitro phenanthridinium **303** proceeded in good yield under the THF/100 ˚C conditions. This is consistent with the summation of the Hammett parameters.[288] Even though the methoxy group is electron-donating and directly conjugated to the site of nucleophilic attack, the inductive withdrawing effect of the *meta* NO_2 group dominates. No impurities were observed so the lower yield is probably the result of losses on handling and drying. In the absence of the electron withdrawing group, the electron-donation of the methoxy dominates and the reaction is demanding. An attempt was also made to replace the kugelrohr method for synthesis of C2-OMe substrate **304**, but similar conversion was achieved under microwave heating.

Both the dinitroacetophenone **324** and analogous 3,8-dinitrobenzophenone **328** gave quantitative conversion to product without an explicit cyclisation step; for dinitroacetophenone **324** the neutral product enamine **369** is easier to isolate, although the expected phenanthridinium **306** is formed in acid (**Scheme 121**).

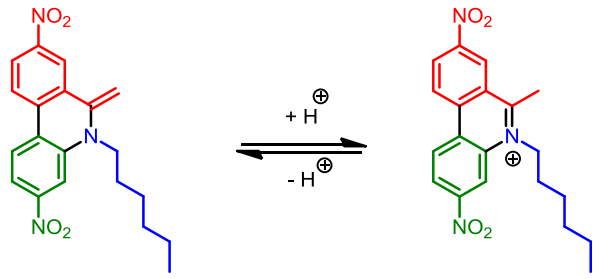

369 **306**

Scheme 121 - Enamine **369** is isolated from imine formation, but reversibly forms phenanthridinium **306** on acidification.

Cyclisation of imine **356** derived from benzophenone **327** to phenanthridinium **307** with unsubstituted A and C rings demonstrated the unsuitability of using THF at 100 ˚C for less activated substrates. Longer reaction times in this solvent resulted in decomposition. Testing at an increased temperature of 110 ˚C in THF and MeCN revealed the MeCN to be superior for slower cyclisations. High conversion was observed, with a 97% yield over the cyclisation step.

Following the earlier failure to form 4-methylphenanthridinium **308** by heating imine **362** formed from benzophenone **332** under the solvent-less conditions, this substrate was re-investigated under microwave conditions. No product was observed at 100 ˚C in THF, but increasing the temperature to 125 ˚C did give sluggish conversion and decomposition. Using MeCN as the solvent at 110 °C provided a breakthrough, converting the majority of the imine **362** into 4-methylphenanthridinium **308** in 1 h. Increasing the temperature to 120 ˚C produced impurities, and longer reaction times at 110 °C gave a mixture of the starting imine **362**, 4-methylphenanthridinium **308** and phenanthridine **368**. Driving the reaction to completion (14 h, MeCN, 110 ˚C) proved detrimental; more of phenanthridine **368** was observed (see **Scheme 119**, **Section 8.4.1**). Iterative testing showed that 10 h at 110 ˚C in MeCN gave the best ratio of product to starting imine **362** and phenanthridine **308**. Purification on an ion exchange column gave the 4-methylphenanthridinium **308** in a high yield.

By contrast the other sterically challenging substrate *N*-cyclohexylmethyl imine **364** cyclised with relative alacrity in MeCN at 110 °C. The alternative of using THF at 100 ˚C was sluggish compared to the *N*-hexyl derivative **287**, and significant impurities were generated. Loading the crude mixture from the MeCN reaction onto SiO_2 and subsequent washing with DCM allowed impurities to be removed while the acidic silica prevented hydrolysis of the phenanthridinium salt **309**. Addition of 0.5% NEt_3 to DCM then allowed rapid elution of the open form, which was cyclised with HCl to give the phenanthridinium chloride in good yield. Azido-phenanthridinium **310** required similar chromatographic purification due to decomposition of the imine **365** derived from the benzophenone **327** (perhaps via a process analogous to the Schmidt rearrangement). The incorporation of an azido group and would allow functionalization via the Huisgen cycloadddition.

8.5 Further modifications of phenanthridinium products

The synthesis of 3-bromophenanthridinium **300** offered the possibility of synthesising a DNA targeting H_2O_2 probe **370** based on the group's previous work.[95] Conceptually the hydrolysis of a boronic ester **370** would give a small group in plane with the ring and capable of H bonding, mimicking the 3-NH_2 group important to intercalation. Reaction with H_2O_2 at DNA could be monitored by fluorescence (**Scheme 122**). The empty orbital of the boron may well quench the fluorescence of the phenanthridinium probe **371**, but even if it did not formation of the phenol would give a considerable Stokes shift, allowing ratiometric measurement.

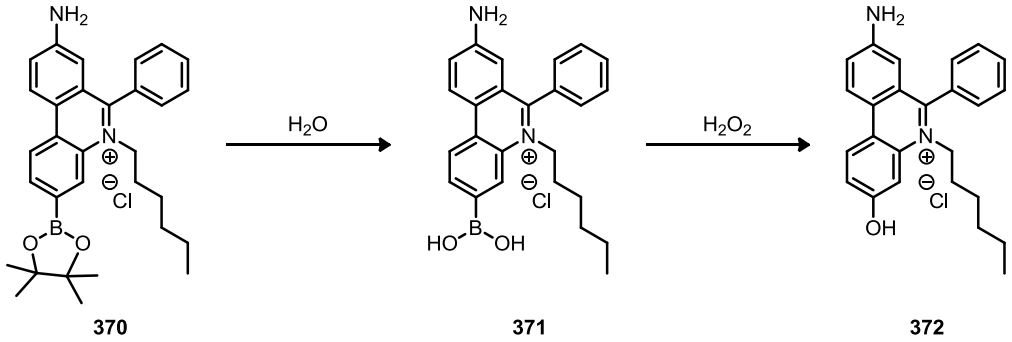

Scheme 122 - The hydrolysis of boronic ester **370** to potential DNA-localised hydrogen peroxide probe **371**, and reaction with hydrogen peroxide to form 3-hydroxyphenanthridinium **372**.

The bromophenanthridinium salt **300** was reduced using an Iron/acid procedure under mild conditions at 40 ˚C (**Scheme 123**), to give 8-aminophenanthridinium **373**, a versatile precursor due to the aryl bromide functionality.

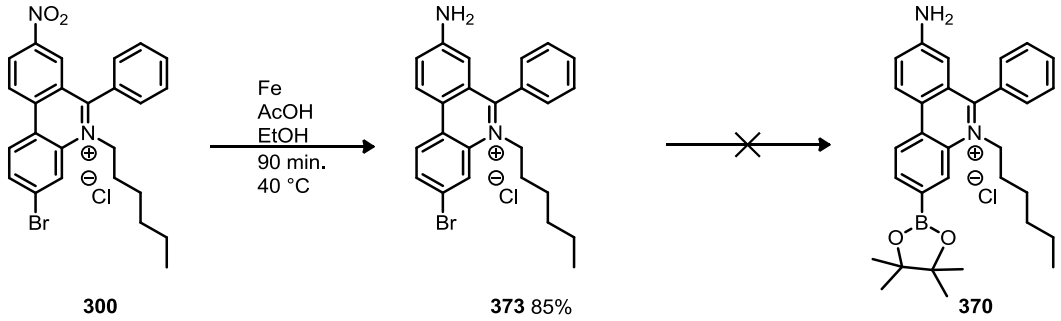

Scheme 123 - Iron reduction of the 3-bromophenanthridinium **300**.

Trial Miyaura borylation reactions were unsuccessful; in dioxane solubility proved low. Reaction in DMSO gave difficulties in recovery of the material. Given time and thorough screening of conditions, testing of alternative procedures,[337] and investigation of options such as protecting the aniline or borylation before cyclisation, it is anticipated that synthesis of hydrogen peroxide probe **370** should be achievable.

Small scale reduction of 3-azaphenanthridinium **301** gave a 60% yield of the 8-amino-3-azaphenanthridinium **374** (**Scheme 124**), identified by ^{1}H NMR spectroscopy (**Figure 51**).

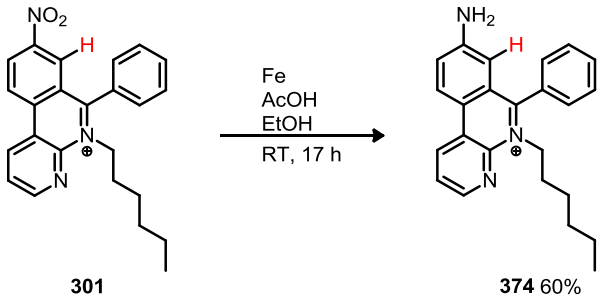

301 **374** 60%

Scheme 124 - Small scale reduction of azaphenanthridinium **301**.

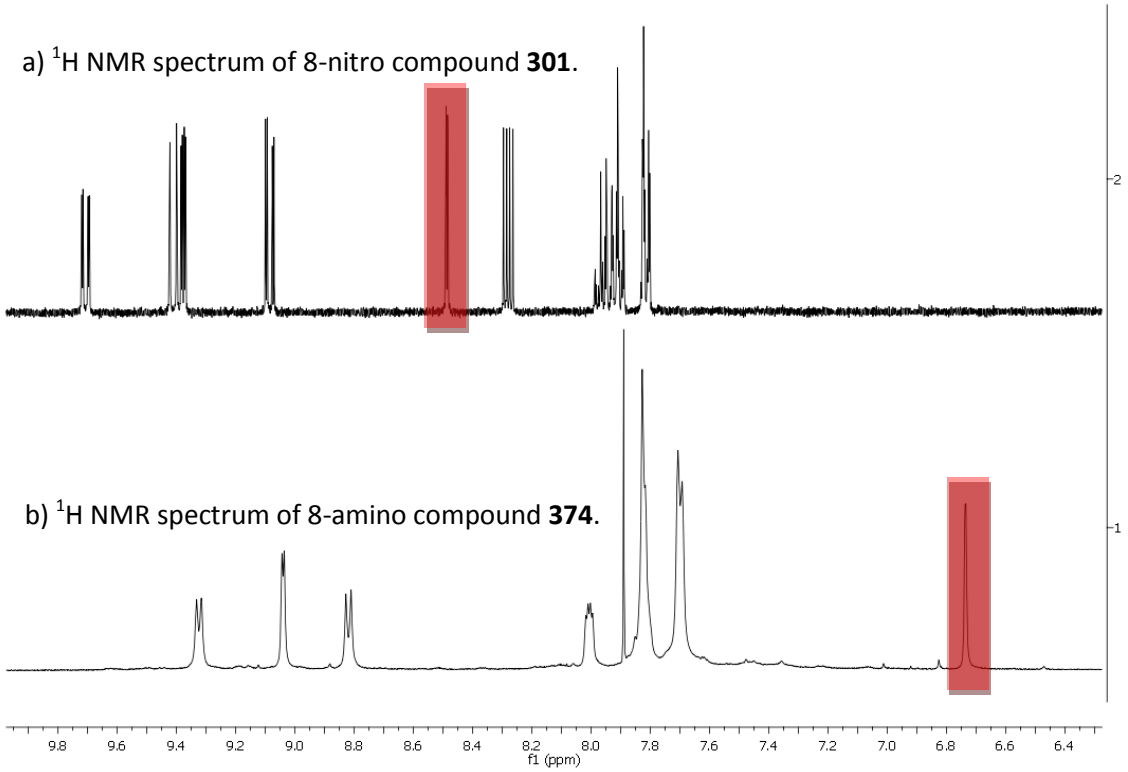

Figure 51 - Comparison between pre and post reduction material.

The overall upfield shift is consistent with the nitro reduction, but the most characteristic change is the large upfield shift of H7 (red), which is particularly pronounced in 8-amino substrates, and is mirrored in the ^{13}C spectrum. Time constraints did not allow this reaction to be repeated and further characterisation data to be acquired.

Enamine **369** was reduced under similar conditions to the aza-phenanthridinium **301**, then the mixture was acidified so that the phenanthridinium partitioned into the aqueous layer. Neutralising the aqueous layer, and then reducing the mixture in a two-phase system of water and $CHCl_3$ using $NaBH_4$ led to isolation of dihydrophenanthridine **375** in low yield (**Scheme 125**). In $CDCl_3$ the reduced form proved stable for several days.

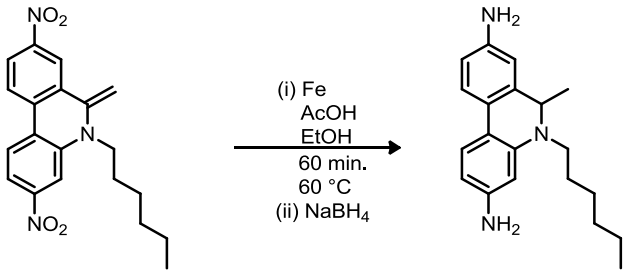

369 **375** 18%

Scheme 125 - Enamine reduction. The product is isolated in the reduced form due to $NaBH_4$ in the work up.

In addition to modifying the products of the cyclisation, some more thought was given to the mechanism. In the original plan an S_NAr mechanism had been assumed to operate, and some features of this mechanism are now described in greater detail.

8.6 Nucleophilic aromatic substitution mechanism

Nucleophilic aromatic substitution (S_NAr) is a reasonably well understood process, with the accepted mechanism shown in **Figure 52**. The nucleophile **377** approaches the aromatic electrophile and attacks the δ^+ carbon attached to the 'X' group, breaking the aromaticity of the ring system **376**. This forms species **378**, which is the first transition state. The formation of **TS1** is usually (but not invariably)[338] the rate determining step. A conjugated electron withdrawing group is generally considered necessary[339] except perhaps in the presence of a very powerful nucleophile[340] or perhaps with the aid of an alternate single electron transfer (SET) mechanism.[343] This withdrawing group stabilises the formally anionic ring system, and the capacity of this group to stabilise charge will strongly affect **TS1**. The degree of polarisation of C-X and the capacity of the leaving group to stabilise the anion will also contribute, as does the nucleophilicity of the attacking group.[341] Intermediate **379**, known as the Meisenheimer complex, is formed with a full bond to both nucleophile and leaving group. These have pyramidal geometry at C1 and in some cases can be isolated as stable salts.[342] A further (usually) lower energy barrier exists to **TS2**, **380**, which represents the dissociation of the leaving group as an anion, allowing the complex to re-aromatise and give aromatic product **381**.

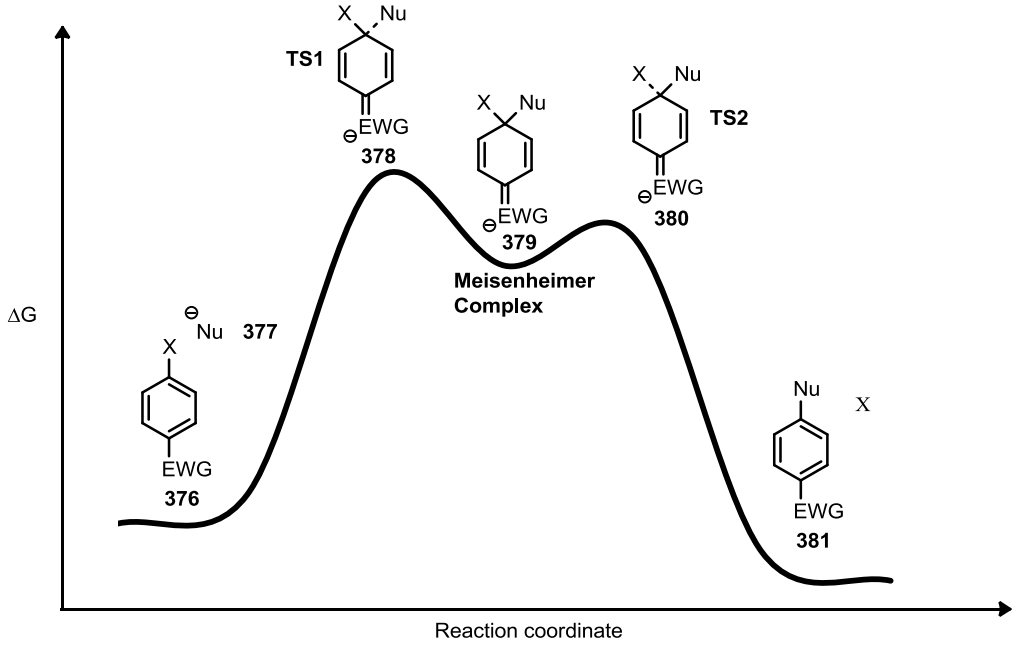

Figure 52 - Generic S_NAr reaction coordinate diagram.

That nucleophilic attack as the rate limiting step is an inversion of the order normally encountered in both S_N1 and S_N2 mechanisms, and as such the leaving group characteristics which favour these (such as weak C-X bonding) do not apply. The greater polarisation and charge stabilisation of **TS1** offered by fluorine means that it is favoured over Cl as a leaving group in S_NAr (k_F/k_{Cl} may be as high as 1300), although it is probably poorer with regard to the actual leaving step **TS2**.[343] Complicating this simplistic picture is the importance of solvent and hydrogen bonding, particularly with amine nucleophiles, with *ortho*-nitro groups increasing reactivity through

hydrogen bonding with the nucleophile in **TS1**.[344] In some cases specific solvent hydrogen bonding effects may also be relevant.[345]

The addition of hydrogen bonding and additional solvent molecules does produce a more complex picture of S_NAr, and these systems are less understood. One particular situation outlined in **Figure 53** arises where amine nucleophiles are used in the presence of a weak base and formation of **TS2** is rate-limiting. In this case general base catalysis is observed (**Figure 53**).[345,346] Nucleophilic attack from the amine **382** on arene **376** generates an ammonium species **384**. Both the ammonium and hydrogen bonding interaction with the departing nucleophile will stabilise **383** and **384**, so deprotonation is required to increase electron density at the pyramidal carbon and proceed to the rate determining **TS2**. The involvement of multiple molecules of amine in a cyclic arrangement with the zwitterionic Meisenheimer complex is suggested by Isanbor and Babatunde[346] with George and coworkers also implicating an additional molecule of ethanolamine in Meisenheimer complex decomposition in S_NAr reactions on fluoronitrobenzenes.[347]

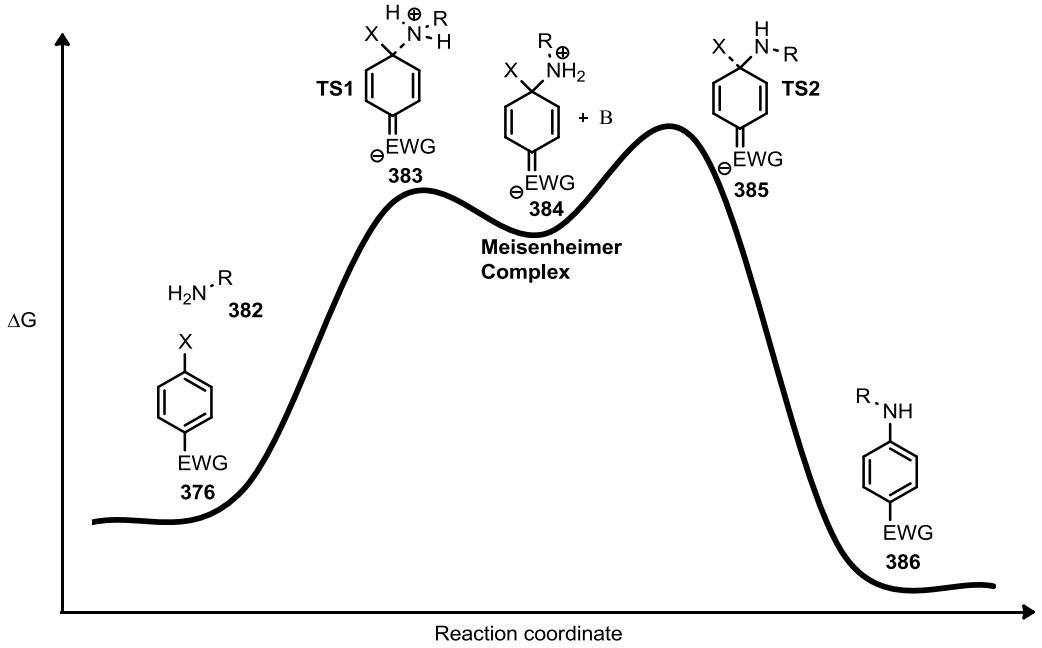

Figure 53 - **TS2** limited, base catalysed S_NAr.

Both models shown (**Figure 52** and **Figure 53**) feature a Meisenheimer complex, and theoretical studies consistently find this intermediate in a variety of conditions.[341,345,347,348,349] A few exceptions exist, with a brief communication[350] by Iwata and coworkers implicating a concerted process through a transition state equivalent to **TS2** in **Scheme 126** in the formation of the minor *para* regioisomer in reaction of ammonia with a polyfluorobenzene.

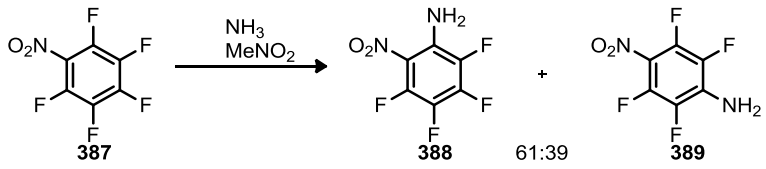

Scheme 126 - Calculations by Iwata and co-workers suggest that formation of *para* isomer **389** is concerted.[350]

Goryunov *et al* were able to take advantage of the favourable formation of Si-F bond in a leaving group to give concerted reaction between Me_3SiPMe_2 and polyfluoroarenes (**Scheme 127**).[351]

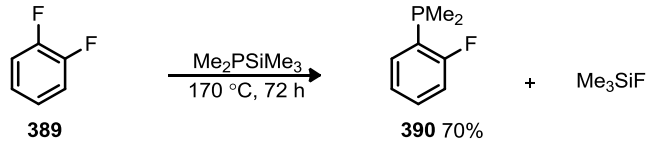

389 **390** 70%

Scheme 127 - Typical example of the concerted S_NAr conditions given by Goryunov *et al*.[351]

Some calculations support the idea of concerted displacement in particular circumstances, for non-first row leaving groups,[352] with the observation that Meisenheimer complexes formed from iodoarenes are unstable,[348] and that gas phase calculations suggest heavier halides require multiple withdrawing groups to form Meisenheimer complexes.[353] It should be noted that even relatively favourable S_NAr processes often require considerable heating; reaction of 2,4-dichloropyridine with aqueous ammonia requires heating to 150-175 °C. As pyridine provides a level of activation analogous to a nitro substituent,[343] the theoretical reactivity of weakly activated aryl bromides and iodides is probably unimportant as reaction is unlikely to occur; at least when using aryl fluorides or favourable, activated substrates a Meisenheimer complex should be assumed.

8.7 The mechanism of imine cyclisation: a computational study

8.7.1 Mechanistic uncertainty

Originally envisaged as an S_NAr, another mechanistic pathway is hypothetically possible for the cyclisation shown; 6π electrocyclisation.[354]

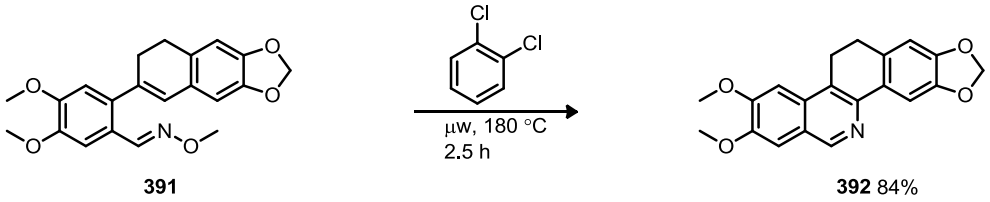

Scheme 128 - Literature 6π electrocyclisation example.[354]

Curly-arrow representations of both mechanisms results in resonance structures of the Meisenheimer complex (**Figure 54**), illustrating the similarity of the pathways. The fundamental difference is the orbitals involved; S_NAr originating from the imine lone pair, electrocyclisation from the C=N π bond. This difference has repercussions for the transition state geometry but cannot be convincingly distinguished experimentally. Dr Hans Senn investigated the reaction computationally to ascertain the correct mechanism, and provided all of the data and much of the interpretation for the following section.

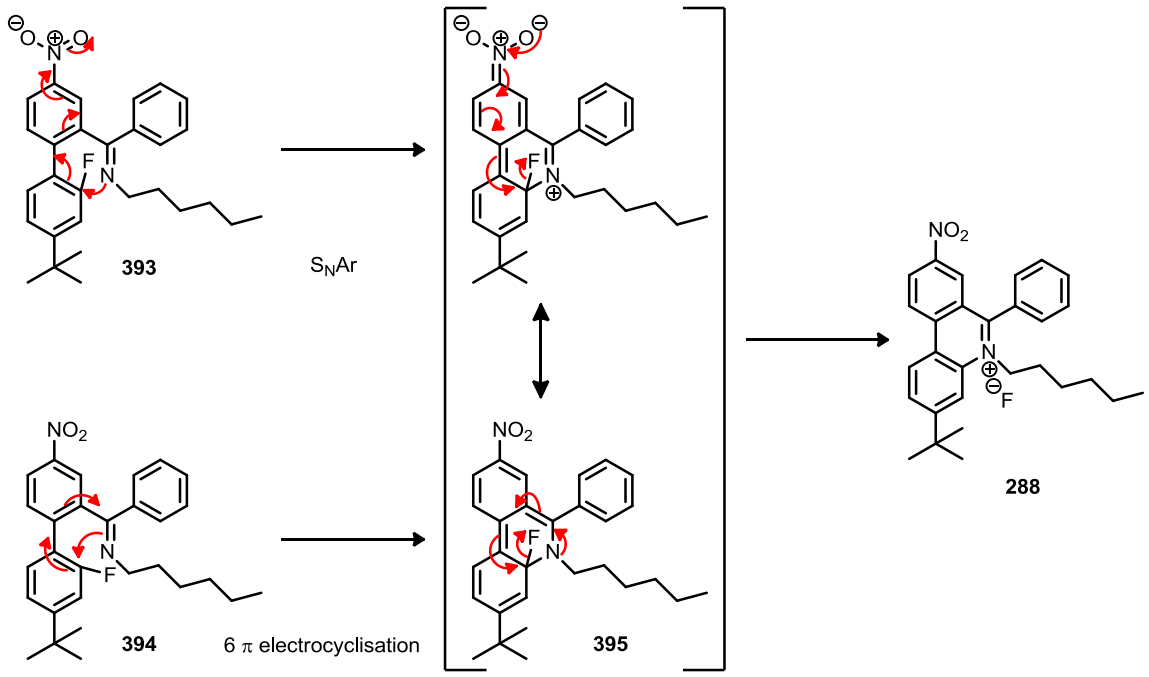

Figure 54 - Suggested S_NAr (top) and electrocyclisation (bottom) mechanisms give rise to the same Meisenheimer complex-like structure **395** according to a curly arrow model.

8.7.2 The calculated pathway and energy values

The *N*-alkyl chain was modelled as an ethyl group to reduce the complexity of the calculations. Structures **397a**-**h** for a number of structural analogues (**Table 4**) were calculated using DFT modelling, with possible intermediates identified. With the exception of **c**, **d** and **h** these analogues had substituents on the A and C rings that matched compounds synthesised. The pathway considered involved conversion of the imine **396** into Meisenheimer complex **398** via transition state **397**. The Meisenheimer complex then collapses to a close ion pair **399**, which can then dissociate to solvent separated ion pair **401** or recombine to give the adduct of **400** of counterion addition to the iminium ion. The last structure is analogous to the pseudobase discussed in **Section 4.3**, **Scheme 35**.

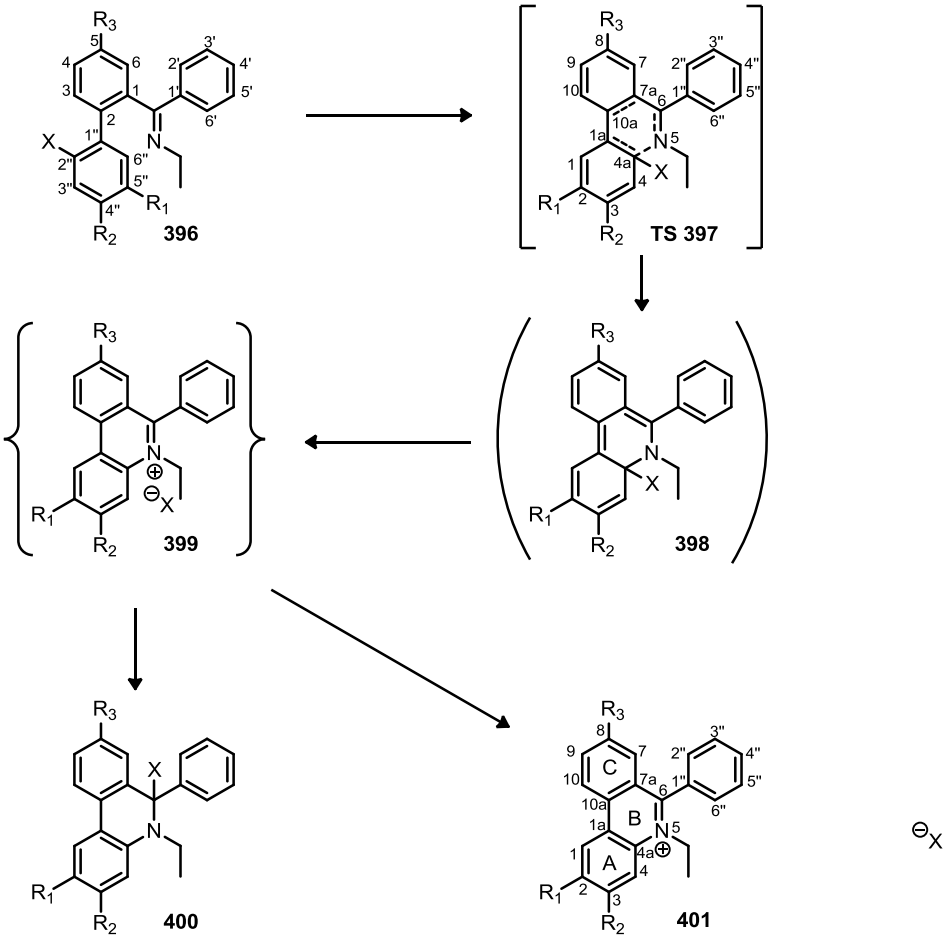

Scheme 129 - The species and pathway identified by DFT calculations.[355]

Table 4 - The range of substrates investigated in the computational study

Substrate	X	R_1	R_2	R_3
a	F	H	H	H
b	F	H	H	NO_2
c	F	H	NO_2	H
d	F	NO_2	H	H
e	F	OMe	H	H
f	F	H	NO_2	NO_2
g	F	OMe	H	NO_2
h	Cl	H	H	H

The pathway identified was shown to be an S_NAr process (**Scheme 129**) based on transition state geometry, but with a twist. The Meisenheimer complex **398** is unstable and dissociates spontaneously into ion pair **399**. Depending on the interplay of ion solvation enthalpy and C-X bond strength, the ion pair **399** can separate to form a solvent separated ion pair **401** (an entropic rather than enthalpically favoured process), or form an unusual C6-X adduct **400**.

Table 5 - DFT calculation results. The N5-C4a and C4a-X distances refer to **TS 397**, and are numbered as would be normal for the product phenanthridinium salts **401**.

		Δ*G* / (kJ mol^{-1})			*d*‡ / Å	
396	**TS 397**	**399**	**401**	**400**	**N5–C4a**	C4a–X
a	103	–65	–81	–79	1.85	**1.40**
b	98	–57	–74	–84	1.88	**1.39**
c	93	–60	–72	–93	1.87	**1.39**
d	72	-52	-71	-89	1.96	**1.37**
e	115	–70	–90	–78	1.84	**1.41**
f	90	–51	–59	–88	1.88	**1.39**
g	112	–61	–77	–76	1.87	**1.40**
h	120	–126	–133	[b]	1.88	**1.87**
a$_{vac}$[c]	**112**	**80**[d]	**440**	**–80**	**1.81**	**1.39**

[a] Calculated at M06-2X/def2-TZVP+ level in polarizable continuum MeCN (ε_r = 22.5) for T = 383 K, p = 320 kPa. **[b]** The 6-chlorophenanthridine **400g** is not a stable minimum, but dissociates into the ion pair **399g** during structure optimization. **[c]** Calculated in vacuum. **[d]** Energy of **398a$_{vac}$**. In vacuum, the ion pair **399a$_{vac}$** is not stable, but collapses to **398a$_{vac}$**.

Although the mechanistic pathway is consistent over the substrates, the stability of the solvent separated ion pair **401** versus halide adduct **400**, transition state energy and bond lengths vary (**Table 5**). For those substrates synthesised activation energies (90 - 112 kJmol^{-1}) correlate well to the reaction conditions. **Figure 55** shows a reaction coordinate diagram based on the calculated values for **f**.

Figure 55 - A Reaction coordinate diagram for cyclisation of benzophenone imine **396f** to phenanthridinium salt **401f**, based on DFT calculations.

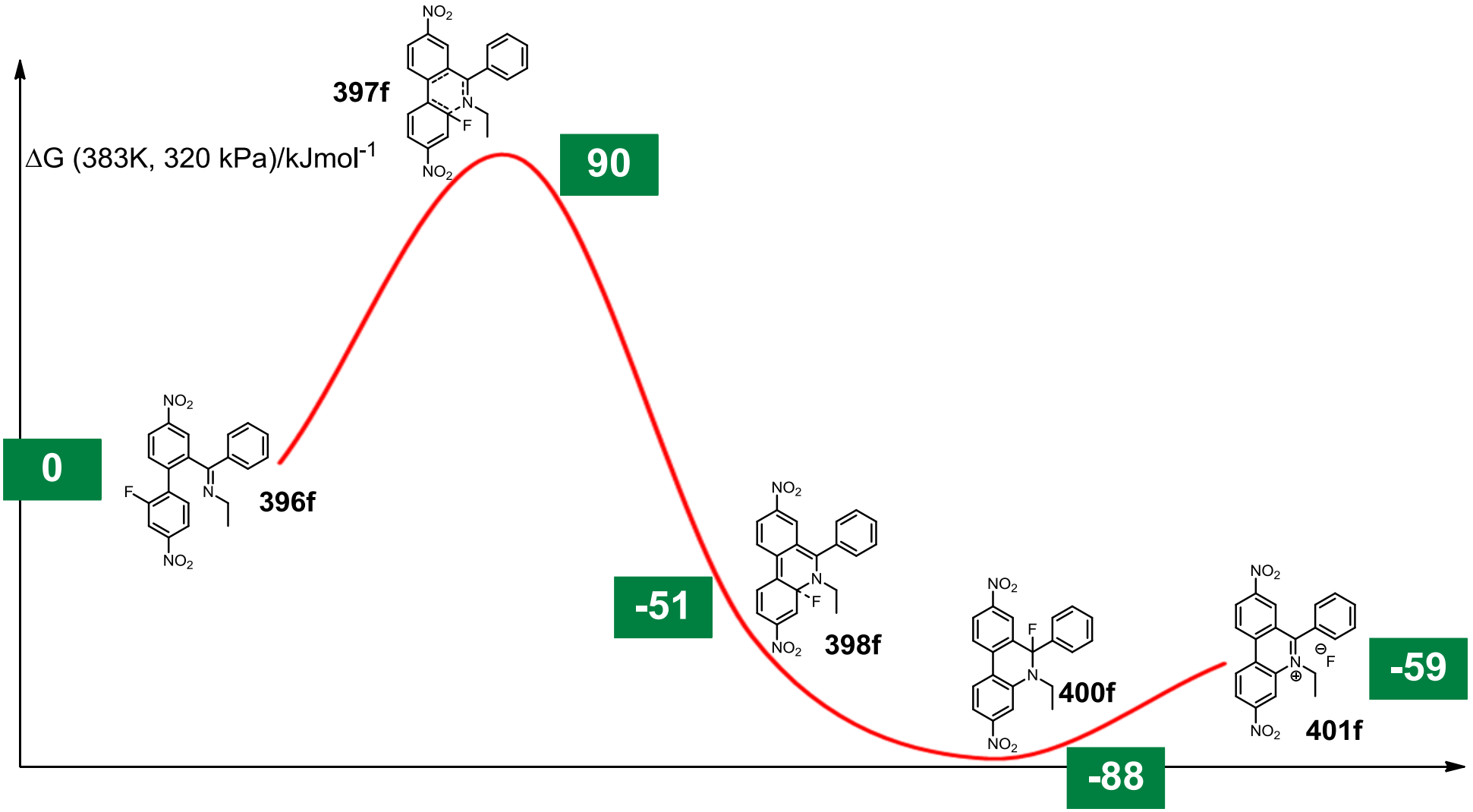

The calculated structures of **396**-**401** will now be considered in order and related to the experimental observations, and the task of distinguishing between the electrocyclisation and SNAr mechanisms.

8.7.3 The Calculated Conformations of Imines 396a-h

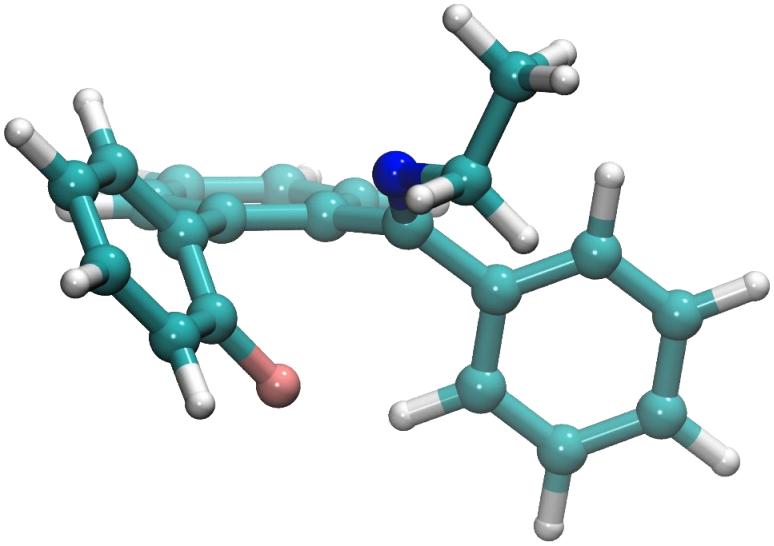

Figure 56 - Calculated conformation of **396a**.

The calculated conformation of the imine **396a** corresponds well with the ^{1}H NMR data (**Figure 56**). The orientation of the phenyl ring face on to the C-ring is consistent with the upfield ^{1}H NMR shift of H6 (8.1 ppm vs 8.3 ppm for H4). The electrophilic fluoroarene A ring is out of plane of the C ring by -54˚ in **396a,** which limits conjugation between the rings and in more substituted analogues, reduces the effect that groups on one ring have on the other. Considerable steric congestion suggests a high barrier to rotation about the N- CH_2 bond, demonstrated by the inequivalent methylene protons. Comparing Hirschfeld charges for **a** and **h** show the C-Cl to be less polarised revealing a less δ^+ C2". Thus, the more electronegative halogen atom lowers σ^*_{CX}, so that the aryl fluoride is more reactive.

8.7.4 The Calculated Structure of Transition State 397a

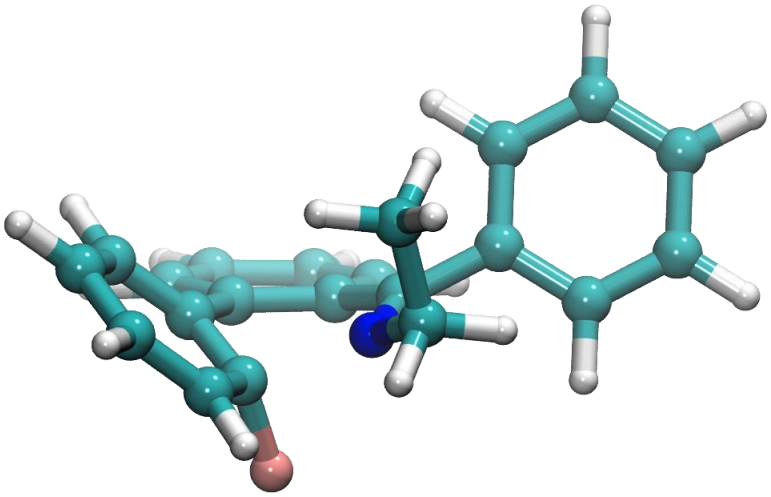

Figure 57 - Calculated transition state structure (TS) **397a**.

The TS structure **397a** represents an 'early' transition state as it is closer in structure to **396a** than product phenanthridinium **401a**, with the electrophilic A ring still -37˚ out of plane of the C ring (**Figure 57**). A shorter N-C4a distance suggests the vacuum transition state **397a$_{vac}$** is later. The key feature is that the lone pair of N5 points at C4a at 125˚ from the ring plane of ring A (numbering see **Scheme 129**), which is consistent with the S_NAr mechanism and inconsistent with an electrocyclisation. This will be discussed in more detail in **Section 8.7.7**. The F is shifted out of plane of the A ring by 36˚ giving pyramidal geometry, and the C-F bond lengthened due to loss of conjugation, although the 'early' nature of the TS is underlined by the average C4a-F bond length of around 1.39 Å for transition state structures **397a**-**h** being equivalent to a full sp^3 C-F bond.[356] The nearby C=C bond is lengthened from 1.39 Å to 1.42 Å, but C=N is almost unchanged (1.28 Å from 1.27 Å), which is again consistent with the S_NAr mechanism and inconsistent with an electrocyclisation. Nitro groups on the electrophilic A ring have a stronger effect than those on the C ring even if *meta* to F (**397b** vs **397c**, **Table 5**), consistent with their strong inductive effect.[357] Comparing **397d** and **397f** shows the extent of the TS stabilisation provided by resonance from nitro groups on the different rings, with the long N5-C4a bond length in **397d** suggesting this stabilisation allows an especially early TS. These results show the extent to which the biphenyl torsion angle reduces the effect of conjugated groups from the C ring on the TS energy.

8.7.5 The Calculated Structure of ion pairs 399a and 401a

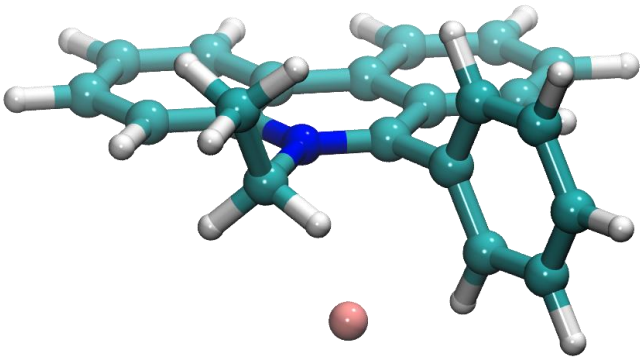

Figure 58 - The ion close and solvent separated ion pairs **399a** and **401a**.

The structure shown (**Figure 58**) represents both ion pairs, **399a** and **401a**. These are stabilised by aromaticity across the A, B and C phenanthridinium rings, providing a planar structure (**Figure 58**). Separation of the close ion pair **399** to give solvent separated ion pair **401** is enthalpically disfavoured; however the entropic contribution from dissociating the ions is large enough to favour ion pair separation in solution. The conformation shows the C6-phenyl ring to be at an angle of close to 90˚ from the plane of the phenanthridinium, is characteristic of these salts. This conformation is consistent with the ^{1}H NMR spectra of the product chloride salt **307**, where H2'' and H6'' are upfield of H3'' and H5''. This is due to the loss of conjugation and mesomeric interaction with the electron poor phenanthridinium caused by the lack of orbital overlap between the respective π systems of the phenanthridinium and the phenyl ring in the conformation shown. In contrast to the transition state **397**, the product **401** is destabilised by electron poor substituents. The position of electron donating or withdrawing substituents appears to have less influence on the energies of these planar, conjugated species than in **397** or **400**.

8.7.6 The Calculated Structure of fluoride pseudo-base 400a

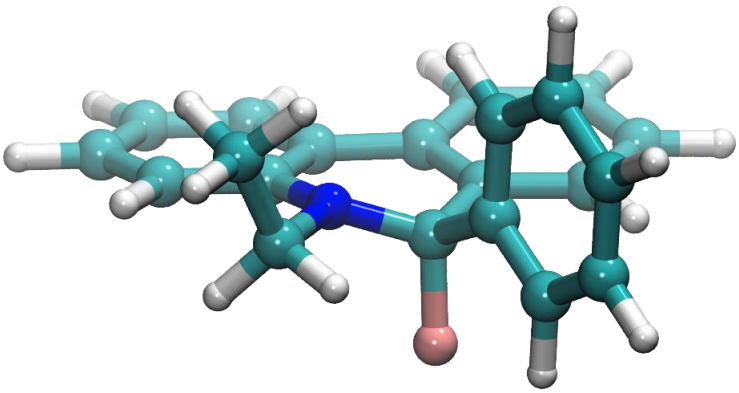

Figure 59 - Unexpected halide intermediate **400a**.

Halide addition at C6 of the ion pair **399** gives an adduct analogous to the pseudobases proposed in **Section 4.3**, **Scheme 35**. This unusual C6-halide adduct (**Figure 59**) is enthalpically favoured, and in some cases this preference overcomes the entropic drive for solvent separed ion pair **401**. This

tends to occur where electron withdrawing substituents destabilise the phenanthridinium and make C6 more δ^+. Phenanthridinium substituents are very influential; dinitrophenanthridinium fluoride adduct **400f** is quite strongly favoured compared to solvent separated ion pair **401f** (-29 $kJmol^{-1}$). In comparison the 2-methoxy phenanthridinium fluoride adduct **400e** is less favoured than the solvent separated ion pair **401e** (+ 12 $kJmol^{-1}$). The pseudobase species neutralises charge and relieves the strain caused by the clashing 5 and 6 substituents, but the most important stabilising element is C-F bond strength. Chloride adduct **400g** is unstable and dissociates to **399g**. The solvation of the Cl^- anion is weaker than the equivalent solvation of F^-, however the difference between the strength of the C-Cl bond and a C-F bond in the halide adduct more than offsets the differences in anion solvation energy. During the synthesis a chloride counter ion is added on work up, so the the isolation of solely the ion pair product **401** is consistent with the results of these calculations. In addition, the chloride anion is added to the work up as HCl, which forms the much weaker acid HF. The relatively weak acidity of HF is a reflection of the favourability of the H-F bonds, and the enthalpic gain from generating this relatively low energy side product would also favour the formation of the solvent separated ion pair **401**.

8.7.7 Natural Bond Orbital analysis:

The pyramidal geometry and the bond lengths of transition state **397** leave little doubt this is a S_NAr type process. Further evidence was acquired through Natural Bond Orbital analysis, producing a model with localised orbitals rather molecular orbitals. This is displayed in **Figure 60**.

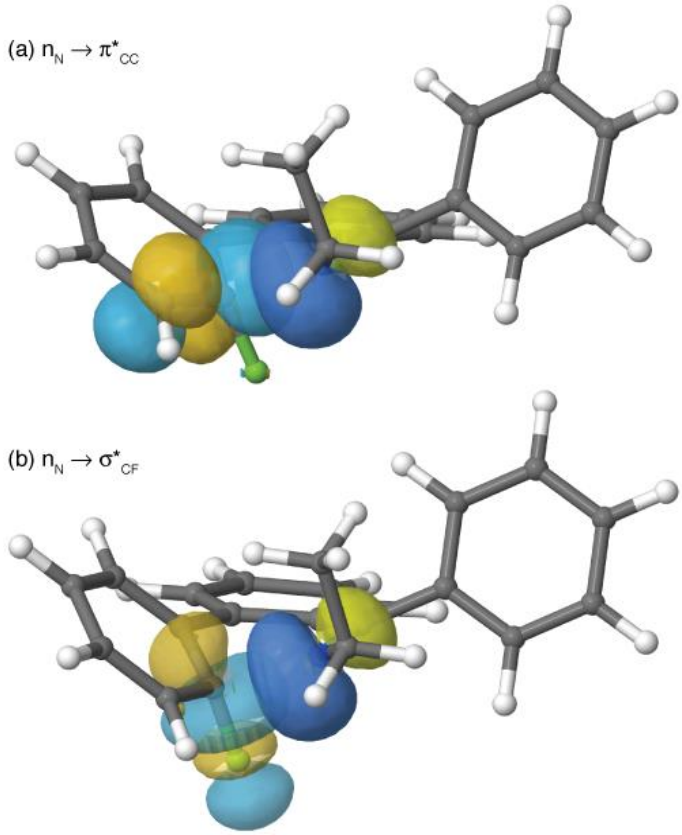

Figure 60 - Imine lone pair (n_N) interacting with π^* and σ^* orbitals.[358]

Both of the interactions shown in **Figure 60** are highly favourable; donation of 0.4e from the lone pair to the π^* (C4=C4a) aryl antibonding orbital is the largest interaction. This is clear in **Figure 60** from the degree of overlap. Donation primarily to the aryl π^* orbital denotes an S_NAr mechanism. The donation to the C4a-F antibonding σ^* orbital is also significant, and weaker when X = Cl than when X = F. None of the π C=N affiliated orbitals have significant overlap with the electrophilic A ring. The transition state represents formation of the C4a-N5 bond and is essentially a Meisenheimer complex, with no intermediates between this and close ion pair **399**. The reaction is therefore concerted, which represents a considerable mechanistic novelty, with extant studies showing unstable Meisenheimer complexes doing so only where additional stabilisation of F^- reduces the barrier to the C-F bond breaking.[351,359]

The relative energies of the calculated transition states **397a**-**g** correspond well with the experimental conditions for these cyclisations. The S_NAr mechanism and calculated structures perhaps hint at why 3''-methylbenzophenone imine **362** was more difficult to cyclise than *N*-methylcyclohexane imine derivative **364** - S_NAr allows for the R substituent of the imine to be directed away from the reaction site in a way impossible in 6π electrocyclisation, and for a C3 methyl substituent in either mechanism.

Chapter 9: A novel mitochondria-targeted probe for superoxide

9.1 Testing of the 8-amino-3-^{t}butyl-6-phenyldihydrophenanthridine probe

Testing of the precursor **293** to superoxide probe **294** was carried out by Dr Murphy's group at the MRC in Cambridge. Following the procedure developed in Glasgow, Angela Logan reduced the phenanthridinium **293** with $NaBH_4$ in Et_2O-water so that the product dihydrophenanthridine **294** partitioned into the Et_2O layer. Separation of layers and removal of Et_2O gave a single product by HPLC. Dissolving the dihydrophenanthridine in EtOH, diluting with buffer and then reaction with superoxide generated from xanthine from xanthine oxidase[360] gave no oxidation products. Neither phenanthridinium **293** nor hydroxyphenanthridinium **402** were produced.

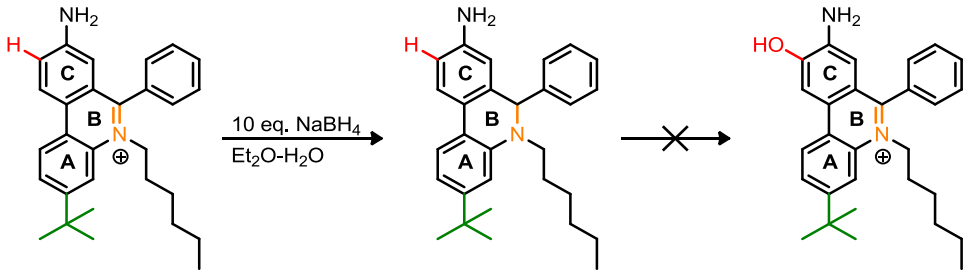

293 **294** **402**

Scheme 130 - The reaction of model probe **293** with superoxide, with the expected substitution shown in red, the redox active iminium in orange and the ^{t}Bu group which prevents intercalation in green.

Based on the work of collaborators[136] it was believed that the regiochemistry of superoxide reaction would give the 9-OH compound **402**. On consulting the literature it was apparent that the regiochemistry of the superoxide reaction was disputed and attack at the C-2 was proposed by some authors.[129] A detailed description of this issue and the assignment of phenanthridinium salts generally is provided in **Chapter 10**, but the potential site of reactivity at C-2 was blocked in dihydrophenanthridine **294**.

9.2 A new probe design

Having considered the available literature (**Chapter 10**) it was decided that a new probe design should allow reaction at 2 and 9 positions, while preferably being electronically similar to MitoSOX and preventing intercalation. We envisaged that aniline alkylation with a bulky group such as ^{t}Bu would achieve this. The *N*-^{t}Bu analogue was discounted as it might block both sites and would have low stability in acid; a robust molecule would allow easy handling and increase the variety of conditions available for work up and purification. It was desirable to have an electronic rich substrate to improve the challenging alkylation. The small tweak of inserting a CH_2 into the design (using neopentyl groups) gave a much more robust molecule (**Figure 61**), while decreasing the steric hindrance to reaction at C2.

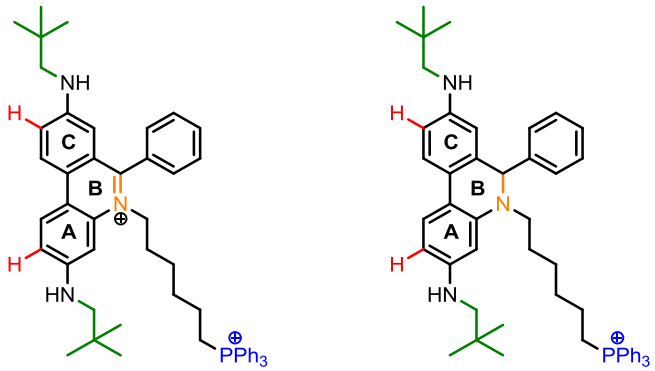

Figure 61 - The improved targeted superoxide probe **404**, MitoBNH and its phenanthridinium precursor **403** are shown. Potential substitution sites are shown in red, the targeting group in blue, the bulky neopentyl groups in green and the redox active iminium site in orange.

9.3 Synthesis of the model phenanthridinium

Prior difficulties had emphasised the difficulty of *N*-alkylation of electron-poor phenanthridines and purification of their phosphonium analogues. The model untargeted bisneopentylethidium (BNE) analogue **405** was synthesised as a model compound (**Scheme 131**).

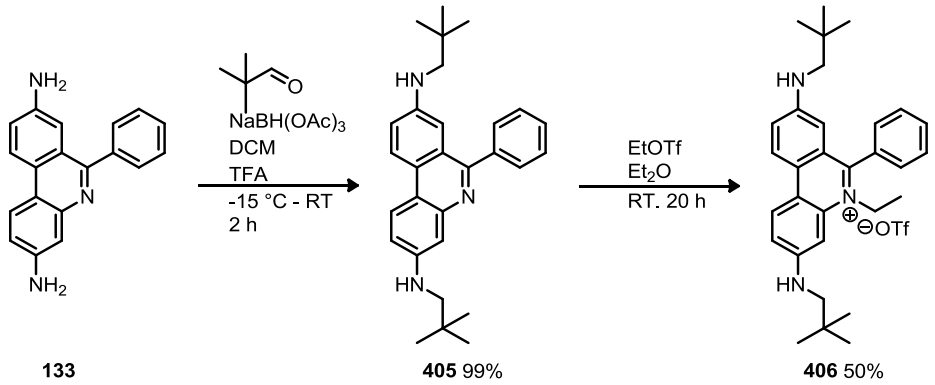

Scheme 131 - Synthesis of a model neopentyl ethidium superoxide probe **406**.

Reductive amination was investigated for alkylation of 3,8-diaminophenanthridine **133** using Pd/C and H_2 according to a literature procedure.[361] Imine π bonds are weaker than comparable carbonyls and undergo reversible iminium formation, allowing their reduction where Pd/H_2 alone is usually insufficient for carbonyl reduction.[362] Less than 10% conversion was observed. Instead the TFA/acetoxyborohydride procedure used previously for used in synthesis of secondary aniline **241** (**Section 6.5.1**) was applied to 3,8-diaminophenanthridine **133,** giving quantitative conversion to neopentyl derivative **405**. Alkylation with EtOTf followed by chromatography gave ethidium derivative **406** in 50% yield. The key feature here is that the *N*-alkylamino groups at C-3 and C-8 are strongly electron-donating making the *N*-alkylation of the phenanthridine using it favourable, but the neopentyl groups discourage alkylation of the pendant amines. Purification via recrystallisation in IPA also gives ethidium derivative **406**, which is intensely purple.

Although synthesised to test conditions, phenanthridinium **406** has potential uses as a non-intercalating ethidium analogue. The oxidised version can be detected easily by mass spectrometry so the corresponding dihydrophenanthridine could function as an untargeted probe for ROS which react with phenanthridiniums in a characteristic fashion, such as nitric oxide. It is anticipated that the group will investigate the utility of this compound in future.

9.4 Synthesis of MitoBNH

Given previous difficulties with the phosphonium compound **142**, the triflate **408** of 1-bromohexan-1-ol **407** was selected as the alkylating agent of choice and synthesised (**Scheme 132**) using the same procedure as for triflates **142** and **146**.

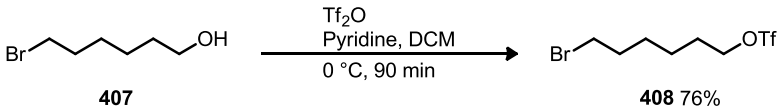

407 **408** 76%

Scheme 132 - Synthesis of bromohexyltriflate **408**.

The synthesis of the final probe is shown below (**Scheme 133**). Dry Et_2O was chosen for the alkylation reaction as experience suggested that the phenanthridinium cationic products would precipitate. Alkylation of bisneopentylphenanthridine **405** worked, giving bisneopentylhexidium alkyl bromide **409**. Unfortunately the material proved partially soluble in Et_2O and so chromatography was necessary but insufficient for complete purification, giving 90 - 95% purity on a small scale. On the expectation that the dication produced by replacement of the bromide with phosphonium would result in phenanthridinium **403** being insoluble in PhMe or Et_2O, less pure bromide **409** was used in the scaled up addition to form the phosphonium salt **403**. Chromatography, ion exchange and precipitation did not give complete purification and so HPLC was employed to isolate the phenanthridinium **403**, giving a disappointing yield.

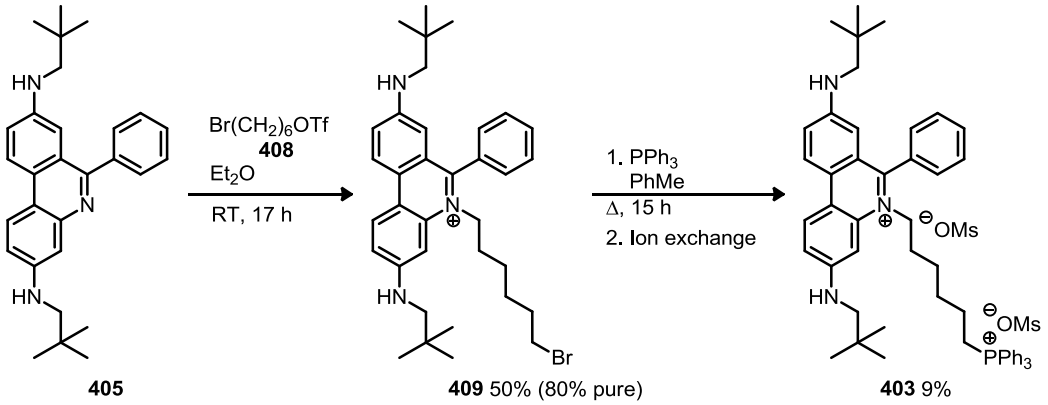

405 **409** 50% (80% pure) **403** 9%

Scheme 133 - Synthesis of MitoBNH precursor **403**.

The d-15 phosphonium analogue **410** (**Figure 62**) was required as an internal standard for mass spectrometry calibration, and was synthesised on a smaller scale via the same route but using d_{15}-PPh_3. This compound was isolated (4%) by HPLC, but a small of excess methanesulfonic acid was present following ion exchange and the material was contaminated on washing.

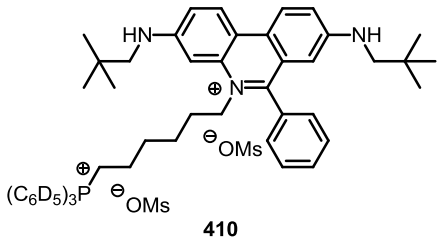

410

Figure 62 - The deuterated mass spectrometry standard **410**.

Chapter 10: Assignment of the proton NMR of phenanthridinium salts

10.1 Why spectral assignment is important

Review of the literature associated with MitoSOX **56** suggests some confusion exists as to the regiochemistry of superoxide addition. Chang[363] names the product as the 2-hydroxyphenanthridinium **57** while displaying the 9-hydroxy analogue **58** (**Figure 63**). The original literature suggests attack at the 2-position, and some spectral evidence has been offered for this conclusion by Zhao *et al*.[129] The site of addition critically affects the synthesis of the MS standards and the design of analogues of MitoSOX.

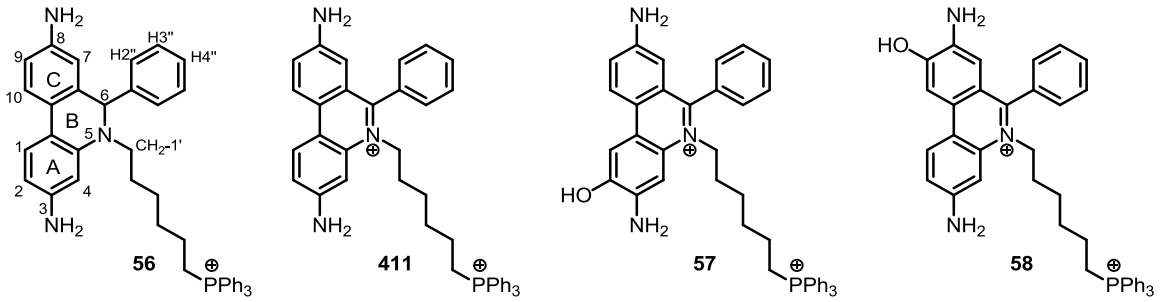

Figure 63 - MitoSOX and potential oxidation products.

The issue was therefore re-examined. A paper by Beckman and co-workers[136] compares the COSY correlation spectrum obtained from MitoSOX **56** to the spectrum of the superoxide oxidation product. The COSY of the superoxide addition product allows assignment of one spin system unambiguously, which is either H1-H2-H4 for product **58** or H10-H9-H7 for product **57** depending on the regiochemistry of addition (**Table 6**).

Table 6 - The potential assignments of the 1,2,4 spin system identified by COSY. All other aromatic peaks are within a 7.6 - 8.0 ppm range.

δ (ppm)	Multiplicity	Assignment:	
		57	**58**
6.2	d	H7	H4
7.4	s	H4	H7
7.5	dd	H9	H2
8.4	d	H10	H1

It is then stated that the signal from either H2 or H9 of dihydrophenanthridine **56** has been lost and that definitive assignment of the regiochemistry is limited by the impossibility of distinguishing the A and C ring systems. As H9 was believed to be the more reactive position, the superoxide product was identified as 9-hydroxyphenanthridinium **58**. Although logical within the scope of the work presented the more illuminating comparison of the addition product to the generic oxidation product **411** is missed; these systems are more electronically comparable. It was anticipated that if A and C rings were distinguished in a more definitive fashion then the regiochemistry of superoxide addition could likewise be ascertained by comparison with literature data.

10.2 Assignment of 3,8-dinitrophenanthridinium salt 305

The steps used to assign phenanthridinium ring protons are detailed below alongside some commentary on the electronic features of phenanthridinium salts as inferred from the NMR spectroscopy data. The trends and assignments observed are in agreement with the detailed study presented by Leudkte *et al*.[180]

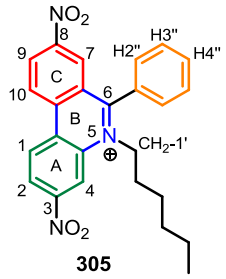

305

Figure 64 - Numbering of 3,8-dinitrophenanthridinium **305**.

Phenanthridinium salts show characteristic NMR features which aid assignment of the protons of the A and C rings. ^{1}H NMR shifts are variable depending on conditions, but the order of the peaks is consistent. An assignment of 3,8-dinitrophenanthridinium **305** (**Figure 64**) illustrates these (**Figure 65**).

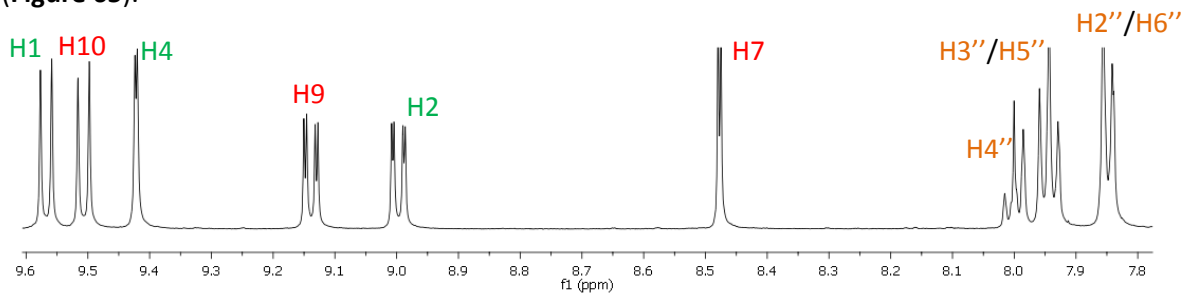

Figure 65 - ^{1}H NMR spectra in CD_3OD, assigned with the aid of the 2D spectra presented in **Figure 66** - **Figure 68**.

The H7 proton signal is important in assignment of the C ring spin system, and as a result key to differentiating the A and C spin systems. This is because it displays a large upfield shift relative to other phenanthridinium signals. The presence of an 8-amino moiety exaggerates this shift in other compounds, which may be as far upfield as 6.0 ppm in more electron rich phenanthridinium salts than 3,8-dinitrophenanthridinium **305**. One explanation for this behaviour is that the 6-Ph ring sits at an angle close to 90˚ to the plane of the phenanthridinium heterocycle, allowing the ring π system to shield H7.

The assignment of H7 itself can in the case of phenanthridinium **305** be confirmed by HMBC correlation to a quaternary ^{13}C peak at 168 ppm, which is too far downfield to credibly represent any position but C6, and which correlates further to H2''/H6'' itself (**Figure 66**).

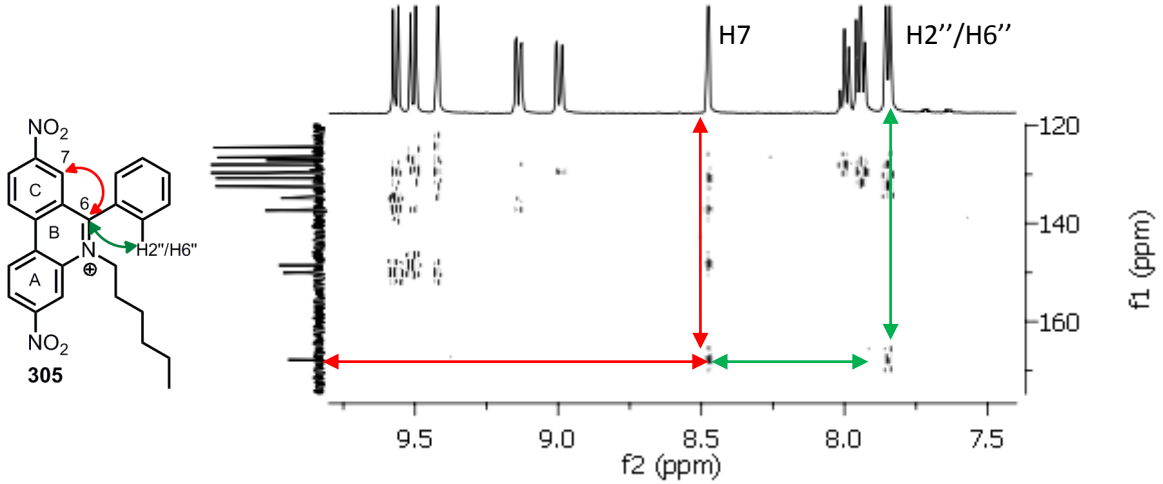

Figure 66 – HMBC of dinitrophenanthridinium **305** in CD_3OD. The **H7 – C6** and **C6 – H2''/H6''** correlations are highlighted. f1 corresponds to the 1D ^{13}C spectrum, while f2 corresponds to the 1D ^{1}H NMR spectrum.

Having identified H7, the attached carbon C7 can be identified from HSQC (**Figure 67**). There are a few distinctive features worthy of comment. Firstly, as demonstrated in **Figure 67**, many of the phenanthridinium ^{1}H NMR shifts suggest very electronically distinct protons, yet the ^{13}C NMR spectra suggest the attached carbons are fairly similar electronically. The strong downfield shift of H1/H10 is a recurring feature of the phenanthridinium core regardless of substitution pattern, and can probably be attributed to the influence of the neighbouring A/C ring π system through space. Similarly, the upfield shift of the C4 in the ^{13}C NMR is characteristic. Indeed in more electron rich examples this may be below 100 ppm, giving values rarely seen in aromatic systems in the absence of metallic substituents or the heavy atom effect.

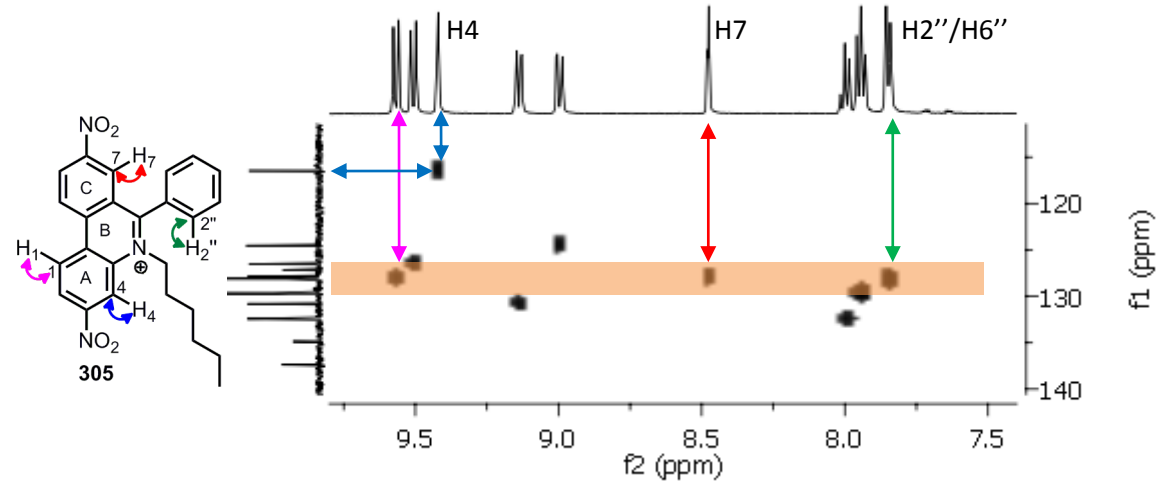

Figure 67 – HSQC of dinitrophenanthridinium **1** in CD_3OD.

Having distinguished H7 from H4, COSY spectra can then be used to link the other signals to these and hence differentiate the large *ortho d* of H1 from that of H10 and the *dd* of H2 from that of H9 by following the correlations around the ring systems (**Figure 68**).

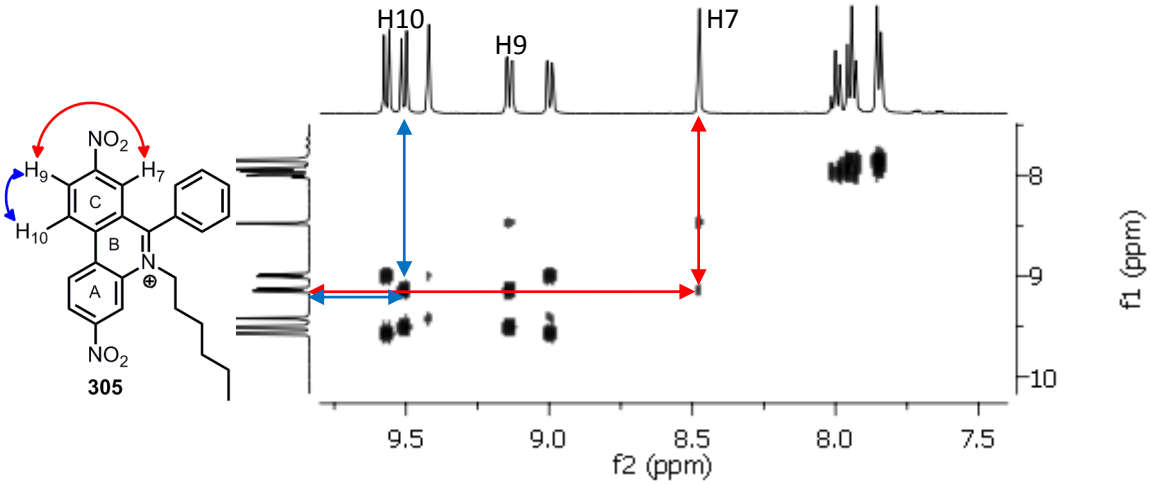

Figure 68 – COSY spectrum of 3,8-dinitrophenanthridinium **305** in CD_3OD. The assignment of H9 and H10 from H7 is illustrated.

Following analysis of the 2D spectra shown the A and C ring systems can therefore be unambiguously differentiated. In practice COSY correlation spectroscopy is usually sufficient as the position of H7 and H4 are often readily apparent. Similarly, placement of H1 relative to H10 and H2 relative to H9 are general, excepting where the electronic effect of a substituent exerts a disproportionate influence on one or the other ring system.

10.3 **The assignment of 3,8-diaminophenanthridinium salt 406**

It was desirable that the ^{1}H NMR of the phenanthridinium precursor **403** to the final superoxide probe be described as thoroughly and accurately as possible in order to provide an analogue for identifying the superoxide reaction product with final probe **404** and any other potential side products. For this neopentylethidium **406** (**Table 7**) was employed as a model because the ring system is extremely similar to that of the phenanthridinium precursor to the final probe, and was characterised by COSY, HMBC and HSQC correlation spectroscopy. In addition to the correlations already described HMBC correlations from the CH_2-1' triplet at around 4.5 ppm to H4 allowed the identity of H4 to be assigned. Accordingly the identity of H7, already acknowledged within the literature for electronically similar systems,[180,364] was established unambiguously. The ^{1}H (**Figure 69**) and ^{13}C NMR assignments are presented below (**Table 7**).

Table 7 - Structure and ^{13}C assignment of *bis*neopentylethidium **406**.

Pos.	ppm	
C1	124.17	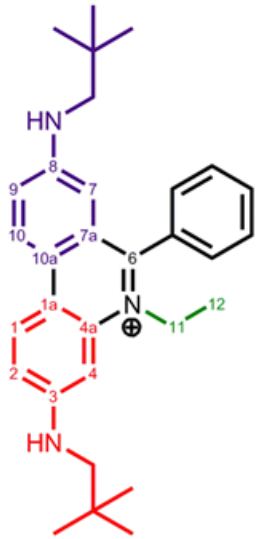
C1a	117.43	
C2	117.30	
C3	152.30	
C4	98.30	
C4a	134.80	
C6	157.40	
C7a	124.73	
C7	105.50	
C8	147.64	
C9	128.15	
C10	122.06	
C10a	128.99	
C11	49.49	
C12	14.48	

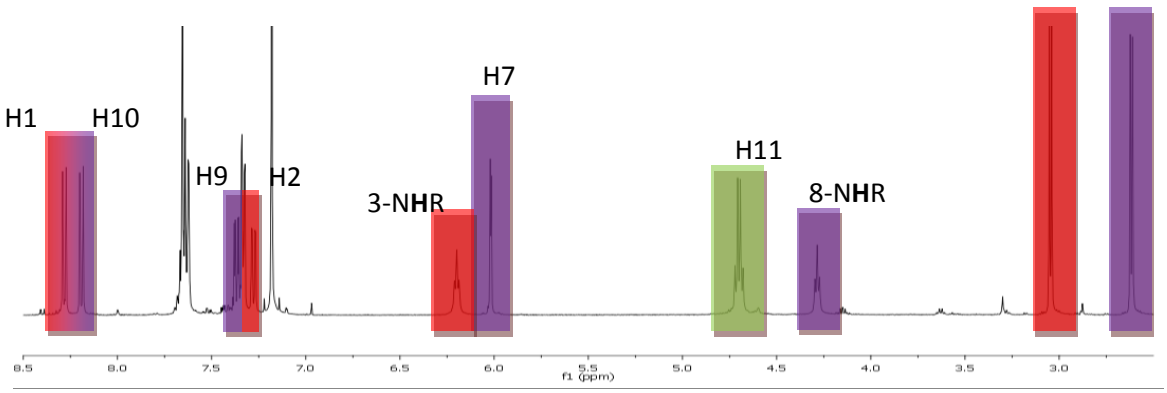

Figure 69 - Assigned ^{1}H NMR spectrum of *bis*neopentylethidium **406**.

One unusual feature of this spectrum is the two neat 1H *t* observed for the amines, probably due to steric hindrance slowing exchange. The 2 ppm shift difference illustrates the difference in

electronics between the A and C ring systems. With H7 identified, re-examination of both Beckman[136] and Zhao's[129] 2D NMR data demonstrate that attack occurs in the 2 position, and the correct structure of the product is phenanthridinium **57**.

10.4 General features of the ^{1}H NMR spectra of phenanthridinium salts

10.4.1 Orientation of the C6-Ph ring

The conformation adopted by the C6-Ph group relative to the phenanthridinium unit is reflected in both ^{1}H and ^{13}C NMR spectra, in the unusual order of the signals. In a ring system conjugated to an electron poor iminium substituent such as a phenanthridinium core, it is reasonable to expect the *ortho* (H2''/H6'') and *para* (H4'') signals to have similar chemical shifts and both to be downfield of the *meta* protons (H3''/H5'') due to the mesomeric contribution of the electron poor substituent. Instead H4'' is the most downfield shifted signal, followed by H3''/H5'', with the *ortho* H2''/H6'' signals invariably displaying the lowest chemical shift of these phenyl group protons, because the phenyl group is twisted out of conjugation (**Figure 70**). This is consistent with the unconjugated phenanthridinium core influencing these shifts in a predominantly inductive fashion.

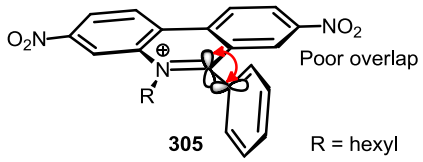

Figure 70 - Poor *p* orbital overlap from the C6-phenyl to the phenanthridinium core.

10.4.2 Assigning protons of an unsubstituted A ring

Substrates which do not display the ABX (3,8 substitution) patterns provided additional challenges, making distinguishing H1/H4 and H2/H3 difficult. NOESY correlations allow these signals to be distinguished by correlating H1/H10 and H4/CH_2-1'.

10.5 Substituent Effects

The existence of strong substituent effects can disrupt the established order of peaks; these are consistent with the known donating or withdrawing capability of the groups in question. A few substrates with difficult to interpret electronic influences are discussed in the following pages.

10.5.1 Assigning H1 and H4 of 2-Methoxy-3,8-dinitro-5-(hex-1'-yl)-6-phenylphenanthridinium chloride 303

One exotic example is the 2-methoxy-3-nitrophenanthridinium **303**. In the absence of substituents H1 would be the more downfield signal, however 2-OMe and 3-NO_2 move the H1 and H4 peaks upfield and downfield respectively. Basing an assignment on the balance of two unquantified, competing, and variable effects is dubious, so NOESY correlation spectroscopy was used to acquire a definitive answer.

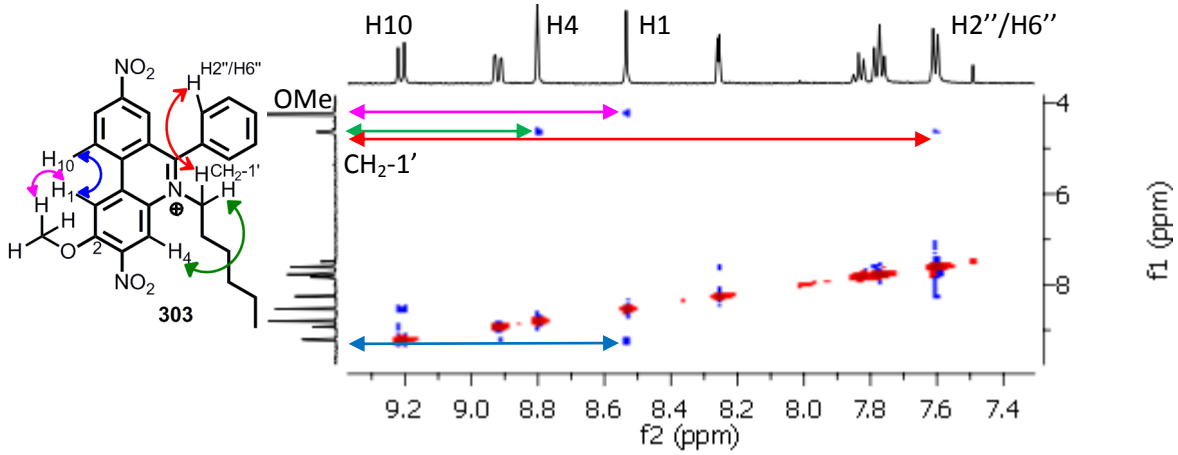

Figure 71 - NOESY spectrum in $CDCl_3$, with 'real' correlations (negative signals) to other protons in blue. The observed correlations are shown on the structure.

The correlation from H10 (9.2 ppm *d*, *ortho* coupling) and 2-OMe (4.2 ppm, *s*) identify H1 as the 4th signal from the left (approx. 8.5 ppm), and correlation from CH_2-1' (4.7 ppm) gives additional confirmation by identifying H4. Correlation between H2''/H6''and CH_2-1' is also visible.

10.5.2 Assigning H1 and H3 of 4-aza-5-(hex-1'-yl)-6-phenyl-8-nitrophenanthridinium chloride 301

The pyridine ring system in 4-azaphenanthridinium **301** means many of the previously identified patterns would not necessarily be expected to apply. If it is assumed that the chemical shift patterns observed in simple pyridines is replicated, H3 would be shifted up to 1 ppm downfield relative to H1 before the influence of the larger conjugated system is considered.[365] H1 itself would be expected still to display a downfield shift. The rationale for this observation is unlikely to be abolished by a change in the nature of the ring aromatic system, although the magnitude of the shift may vary. Again, even if numbers could be placed on these two effects a simple additive approach does not necessarily account for larger changes to the heterocycle electronics induced by the pyridine. NOESY correlation spectroscopy allowed these protons to be identified.

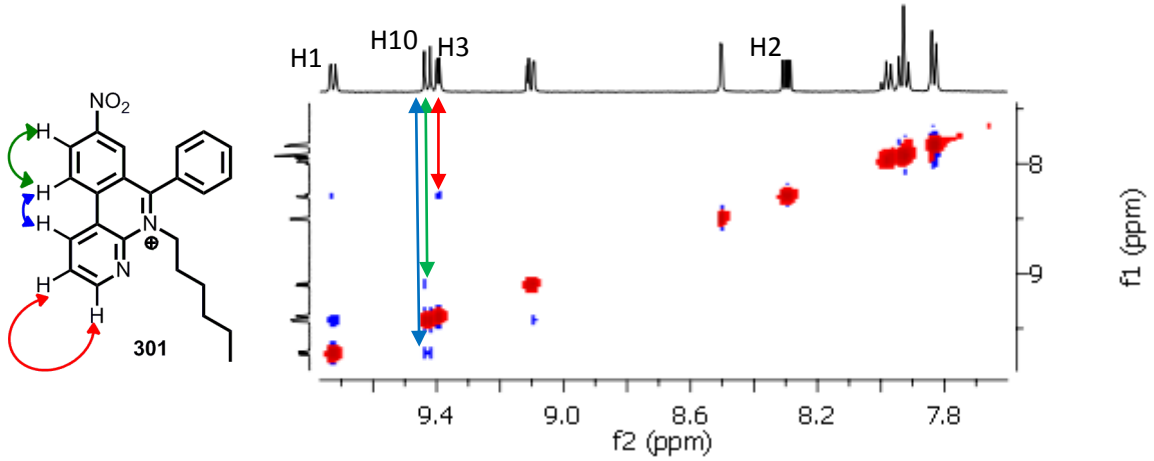

Figure 72 - NOESY of 4-azaphenanthridinium **301** in CD_3OD with 'real' correlations (negative signals) to other protons in blue. The observed correlations are shown on the structure.

H10 is readily identified (9.4 ppm, *d*, *ortho* coupling) and gives a correlation to H1, more than 0.3 ppm downfield of H3. As expected H2 is shifted upfield (1.2 ppm from H1), and is upfield even of H7. This is supported by the ^{1}H NMR spectrum coupling pattern as relatively small *ortho* couplings of 4 - 6 Hz are common from the position (H3) adjacent to the nitrogen of the pyridine (shown by the red arrow in **Figure 72**).

10.5.3 Coalescence of 3-*tert*butyl-5-(cyclohexylmethylamino)-6-phenyl-8-nitrophenanthridinium chloride

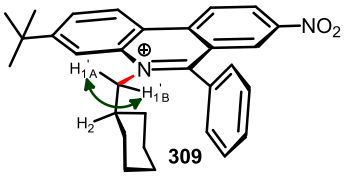

Figure 73 - Fluxional behaviour on the ^{1}H NMR timescale based on slow rotation around N5-CH-1' resulting in slow interconversion of H'$_{1A}$ and H'$_{1B}$ is observed for phenanthridinium **309**.

Hindered phenanthridinium **309** showed distinctive fluxional behaviour, due to slow rotation around N5-C1'. CH_2-1' was variably present as two broad singlets H'$_{1A}$ and H'$_{1B}$ (**Figure 74**) or absent in room temperature spectra, a result of rotation interchanging the position of these protons on a timescale close to that of the NMR relaxation. The signal was resolved by increasing the temperature, resulting in coalescence (**Figure 74**). The ^{13}C spectra also showed an unusually broad aromatic signal believed to represent C2''/C6'' - higher temperatures (70 ˚C in d_6-DMSO) producing an acceptable spectra.

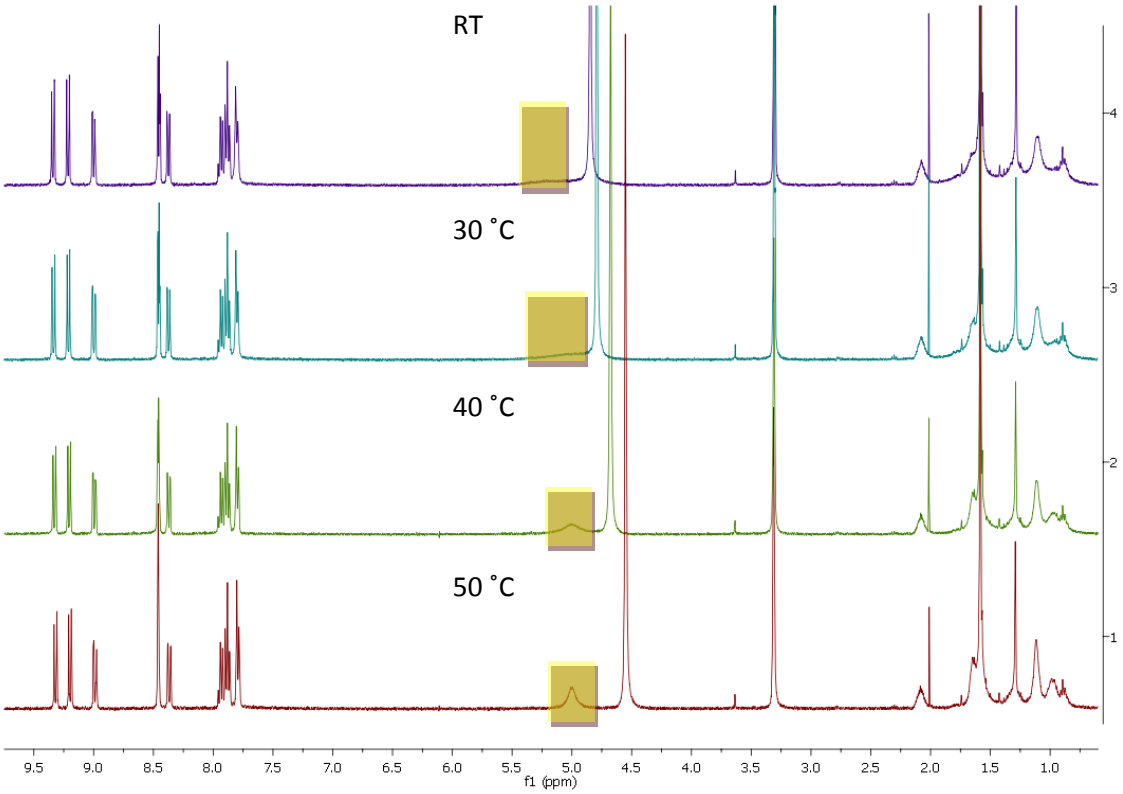

Figure 74 - ^{1}H spectra of phenanthridinium **309** in CD_3OD from RT to 50 ˚C with the appearance of CH_2-1' highlighted.

Chapter 11: A targeted and ratiometric fluorescent calcium sensor

11.1 Calcium and the mitochondria

11.1.1 Why is calcium relevant?

As with many components within the cell, the mitochondria orchestrate a number of other processes in addition to their vital role in providing energy for cellular processes. Of particular interest and discussed here is the role of the mitochondria in calcium signalling. The calcium dication is responsible for the regulation of a remarkable variety of cellular and extra-cellular processes. Calcium is the single most abundant metal in many animals; in humans it is responsible for bone structure, muscle contraction (including heartbeat), regulation of ATP synthesis in some cells and signalling for a vast number of different processes, possibly including cell mitosis.[366] Signals may be local, through the cell or indeed between cells. Concentration curves over the timespan of a signal can assume different shapes and the lifetime of a signal itself can vary greatly depending on the process; exocytosis can be triggered in microseconds but transcription may take minutes or even hours.[367] Calcium signalling is therefore a topic of considerable depth and discussion here is limited to two specific contexts: the role of mitochondria in calcium signalling and the importance of such signalling in smooth muscle contraction.

The specific functions of mitochondria in ion handling in general and calcium signalling specifically is a result of the chemiosmotic potential and resulting charge gradient across the inner mitochondrial membrane creating conditions different from those experienced elsewhere in the cell. Mitochondria have been identified as crucial elements in calcium signalling control in nearly all cell types.[368] The formation of ATP and control of calcium ion concentration are intrinsically linked, with calcium ions being maintained in steep concentration excesses in organelles such as the endoplasmic reticulum and Golgi apparatus via ATP powered calcium pumps.[369,370]

11.1.2 Calcium regulation within the mitochondria

A concise (if simplified) summary of calcium regulation within the mitochondria is illustrated in **Figure 75** and is interpreted as follows; a sodium proton exchanger pumps out sodium ions, driven by proton influx due to the chemiosmotic potential. This sodium can then re-enter via an exchanger coupled to calcium efflux. This calcium removal is balanced by a uniporter transporting calcium ions into the mitochondria.[371,372,373] Within the matrix the calcium is present in at least two forms: free calcium, often referred to as $[Ca^{2+}]_m$, and as an insoluble phosphate salt (believed to be either hydroxyapatite or tricalcium phosphate).[371] The phosphate ions are transferred to the matrix in the form of phosphoric acid. The solubility of this salt is strongly pH dependent and addition of a protonophore leads to acidification and dramatic rises in $[Ca^{2+}]_m$.[374] The formation of this salt acts as a buffer on matrix calcium ion concentration.

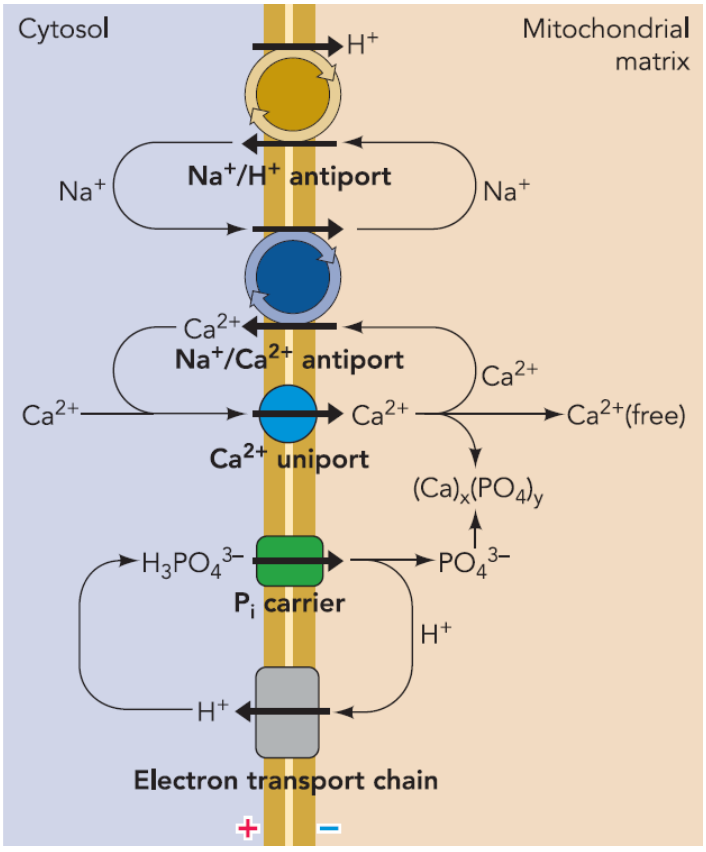

Figure 75 - Illustration of calcium homeostatis regulation within the mitochondria. Reproduced from Szabadkai and Duchen, 2008.[368]

The contributions of the antiports and buffering is shown in **Figure 76**. Calcium ion matrix $[Ca^{2+}]_m$ concentration can rise in a linear fashion at low concentration, acting as a messenger to stimulate enzymes such as NADH dehydrogenases and the Kreb's cycle, increasing ATP output.[3,375] Since extramitochondrial calcium rises as a result of many processes which consume ATP, this calcium feedback mechanism is regulating metabolism. Above this concentration range phosphate buffering ensues, and is so effective that a 50 fold increase in total matrix calcium causes an increase of $[Ca^{2+}]_m$ of less than 50%.[376] Calcium efflux within this range is dependent on phosphate concentration and pH rather than calcium concentration, as shown by the relatively flat activity of the antiport. The uniporter by contrast increases in activity as a 3.5 power of extramitochondrial

concentration ($[Ca^{2+}]_e$), combining with the buffering to allow the mitochondria to control the local cytosol calcium concentration ($[Ca^{2+}]_c$), maintaining a concentration known as the 'set point', with a value of 0.78 μM under normal conditions.[371]

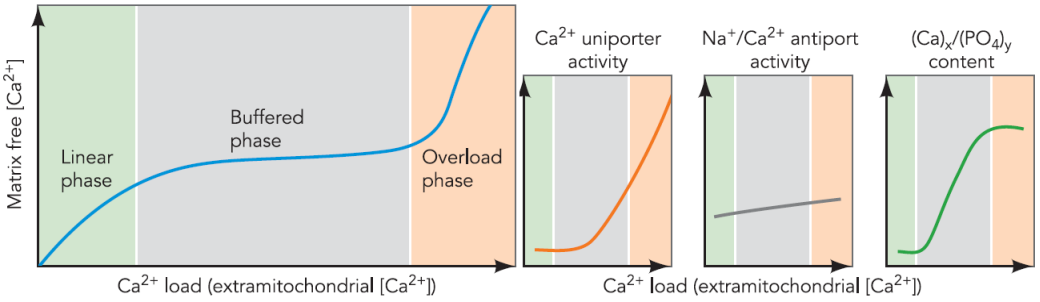

Figure 76 - Free matrix calcium concentrations as a function of extramitochondrial calcium concentration, compared to the relative activity of known regulation mechanisms as a function of extramitochondrial calcium concentration.

In the 3rd 'overload' phase the buffering capacity of the phosphate salts is exceeded, leading to linear rises in $[Ca^{2+}]_m$. When this occurs calcium is released alongside low molecular weight ions and compounds, and additional solute enters, causing swelling and rupturing of the membrane. This is known as the permeability transition and has been investigated as a possible trigger for cell death via release of cytochrome c and other proteins with similar effects, through opening of a non-selective pore in both mitochondrial membranes.[368] Loss of calcium homeostasis is an important step in cell death.[371] This includes apoptotic death as well as necrotic (traumatic) destruction of cells. There is some evidence that in some cases even within the cell death process the majority of mitochondria continue to function in order to provide the energy for the programmed cell death.[377]

An interesting example of Ca^{2+} mediated cell death occurs where glutamate has accumulated in response to anoxia or ischemia. In this case depolarising mitochondria to prevent uptake of calcium in the mitochondria has been shown to protect neurons.[42] In this case the relationship between the cytosolic calcium ion concentration $[Ca^{2+}]_c$ and cell death is not obvious, since similar concentrations from other sources do not trigger cell death. There is some evidence that the specific entry point for calcium in this case (NMDA gated channels) results in higher localised concentrations near receptors which cause nitrous oxide production (NO), which combines with the calcium concentration to trigger depolarisation and cell death.[378] This highlights the importance of transient and local Ca^{2+} concentration variations, and the interactions of mitochondria and other organelles are vital in these events. Mitochondria also support calcium ion signalling by allowing the generation of microdomains of differing calcium ion concentration. This involves both active uptake and calcium release and the provision of ATP allowing other organelles to modulate their calcium uptake. Examples of direct involvement include the reduction of calcium ion concentration following depolarisation in signalling, which is achieved through the sodium/calcium exchange at the inner mitochondrial membrane.[368]

11.2 Calcium signalling in the sarcoplasmic reticulum of smooth muscle

11.2.1 Smooth muscle

As a tissue where energy consumption and the associated metabolic rate are directly tied to function and vary accordingly, muscle is of particular interest in the study of metabolism. Three types of muscle exist, and these are different at the cellular level: skeletal, cardiac and smooth muscle. Both skeletal and cardiac muscle produce short, powerful contractions (albeit repetitively in the case of cardiac muscle), by contrast smooth muscle produces a longer, sustained contraction. We have no conscious control over smooth muscle contraction, which respond to autonomic nervous signals and local stimuli, and are flexible, with a fusiform shape. This dependence on local stimulus and different mode of action allows smooth muscle to perform different roles, such as lining most blood vessels (not large arteries) and regulating their diameter to maintain pressure or contracting rhythmically in a peristaltic fashion to force matter through the digestive tract. Smooth muscle also plays an important structural role, helping to maintain the positioning and shape of internal organs. Calcium concentration plays an important role in muscle contraction through 'excitation contraction coupling', and so variation in patterns of contraction are likely to be reflected in the pattern of calcium signalling,[379] in which a specialised organelle called the sarcoplasmic reticulum is heavily involved.

11.2.2 Calcium signalling and the sarcoplasmic reticulum

Both the sarcoplasmic reticulum, which is a type of endoplasmic reticulum found in smooth muscle, and the endoplasmic reticulum are in general strongly associated with mitochondria. There are two types of endoplasmic reticulum (rough and smooth) and their combined roles include numerous functions including synthesis of membranes, lipids, steroids and proteins and detoxification of drugs in addition to calcium storage and signalling functions. Calcium related interaction between mitochondria and the endoplasmic reticulum is believed to have an important role in stress related cell death.[368] The sarcoplasmic reticulum is a more specialised organelle, with a primary role in calcium storage and signalling and is found in muscle tissue, with calcium release being a major component of the 'excitation contraction coupling' which stimulates muscle contraction.[380] The calcium gradient is maintained via active transport[381] (Ca^{2+}-ATPase enzymes such as SERCA) which requires a constant supply of ATP; for this reason mitochondria are often found close to the sarcoplasmic reticulum,[368] and release ATP at specific sites, generating local high concentrations of ATP.[382] In these regions the calcium releasing channels from both organelles are directly linked.[383] Calcium concentrations also control the shape and position of mitochondria, for example causing migration of mitochondria onto the surface of the endoplasmic reticulum.[384] Although present in all muscle, the role of the sarcoplasmic reticulum may vary somewhat between muscle cell types.

Referring to the diagram shown (**Figure 77**), the interplay of calcium and the sarcoplasmic reticulum in smooth muscle contraction can be described as follows. The sarcoplasmic reticulum uses active transport to contribute to calcium regulation by removing it from the surrounding cytoplasm (1), which allows muscle relaxation (2). Calcium signals are then stimulated, modified

or amplified by this calcium being released in response to stimuli (3). The excitability of the membrane to further stimulus is then modified via calcium sensitive channels for other ions (4), and calcium released directly to extrusion pumps in the plasma membrane (5). The sarcoplasmic reticulum interacts strongly with mitochondria in smooth muscle (99.4% of mitochondria is within 30 nm of the sarcoplasmic reticulum, with 82% totally surrounded by it),[385] producing various microdomains of different calcium ion concentration and exchanging calcium with the mitochondria depending on the situation (6).

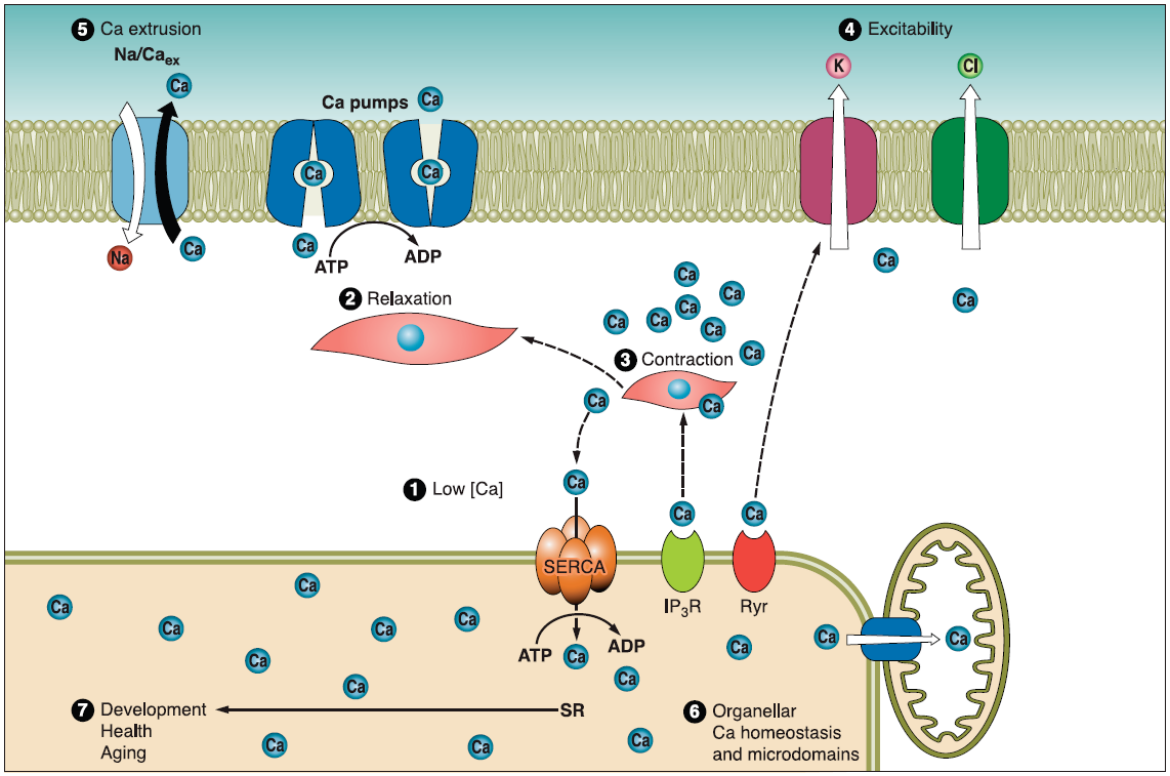

Figure 77 - Calcium and the sarcoplasmic reticulum in smooth muscle contraction.[386]

The proximity of the mitochondria and the release points for calcium ions in the sarcoplasmic reticulum leads to the mitochondrial calcium transporter taking up calcium ions much faster than would normally be expected, due to high local concentrations.[386] It has been suggested that by decreasing feedback from the calcium sensors in the sarcoplasmic reticulum stimulating the release the calcium efflux is maximised. Release channels include IP_3R and RyR receptors, which release calcium ions in response to messenger concentration and in a fashion mediated by a number of other factors. IP_3R features a channel activated by binding of inositol triphosphate and mediated in activity by calcium ion concentration, providing a feedback mechanism,[385] and are also found outside of the sarcoplasmic reticulum. IP_3R channels are not randomly distributed but are clustered in groups across the sarcoplasmic reticulum, allowing various local concentrations to exist in a cell on a transient basis. The RyR (ryanodine sensitive release) channels are much larger and bind less specifically, being activated and deactivated directly by calcium binding in the protein. As a result the channel is stimulated by micromolar concentrations of calcium ions but deactivated at millimolar concentrations.[387] The channel exists in a few different isoforms, with different calcium sensitivity, with RyR1 and RyR2 possibly aggregating together.[388] Of these, RyR1 is the more sensitive, possibly amplifying the calcium signal until RyR2 is activated, leading to a

large calcium efflux known as a 'spark'. A third RyR3 is far more evenly distributed and may be an inhibitor[389] under normal physiological conditions, although it can function as a release channel in the correct circumstances.[390]

11.2.3 Calcium induced calcium release in smooth muscle contraction

The collection of positive feedback mechanisms referred to as 'calcium induced calcium release' (CICR) are important in numerous cell types. They are believed to be involved in smooth muscle contraction, although the contribution from different Ca^{2+} sources probably varies somewhat. Various permutations are set out in Jaggar *et al*[390] and discussed in a review by Berridge.[391] An outline of the mechanisms involved is illustrated in **Figure 78** as follows. (1) An external messenger such as acetylcholine activates a membrane receptor releasing the signalling molecule inositol triphosphate (labelled $InsP_3$ in **Figure 78**) into the cytosol. (2) Synchronously through various mechanisms high extra-cellular Ca^{2+} leaks into the cytoplasm, reducing membrane polarisation and increasing $[Ca^{2+}]_c$, which is sequestered into the sarcoplasmic reticulum (3). The $InsP_3$ channel IP_3R precipitates a Ca^{2+} 'spark', (4), which is then amplified by positive feedback cycles from both IP_3R and RyR channels (5). Increasing Ca^{2+} results in contraction of the muscle (6), with SERCA and the functionally analogous PMCA pumping Ca^{2+} into the SR and extracellular space respectively (7). Local increases in Ca^{2+} also activate potassium channels, which hyperpolarise the cell to prevent further excitation in a negative feedback mechanism limiting contraction (8). In some cells Ca^{2+} may also activate chloride channels which depolarise the cell and allow further Ca^{2+} accumulation from the extracellular space (9). It should be noted that while these mechanisms are all known to exist in some form, their relative importance or even involvement is variable and not well understood.[392,393,394,395]

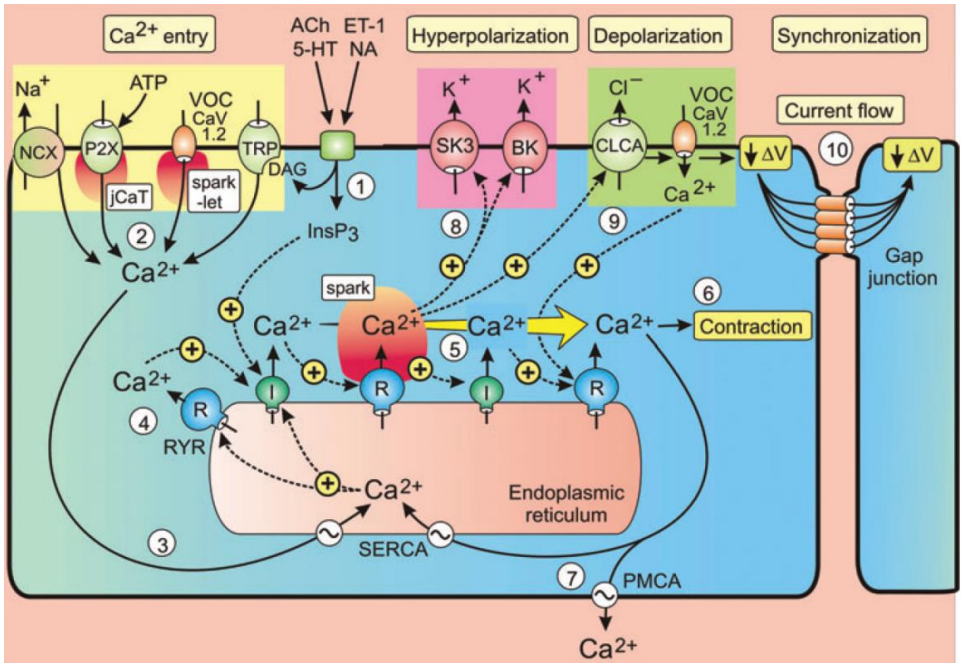

Figure 78 - Calcium induced contraction in smooth muscle. ©2008 The Author. Journal compilation. ©2008 The Physiological Society[391]

In some cells it is possible that the final chloride induced Ca^{2+} influx initiates contraction, however it is not clear that global (full cytoplasm) increase in calcium ion concentration is required to open

chloride channels, with both major ion channel types able to generate substantial local increases in calcium ion concentration. These local increases allow for selective activation of calcium sensors based on a number of factors. Because loss of the high local concentration is rapid due to diffusion, selective activation of receptors with high association constants over slower receptors with comparable dissociation constants is possible. The localised nature of these sparks also allows spatial resolution.[395]

The interaction of mitochondria and the sarcoplasmic reticulum is expressed through various channels in carefully defined positions themselves modulated by several variables. Localised microdomains selectively activate and in turn activate further receptors and organelles. These are based on the selectivity of receptors which can be modulated up or down by both calcium ion concentration and other factors. Coupling this to the potential for receptors to be selectively activated based on association constant and calcium signalling within cells clearly constitutes an immensely complicated system. This is only very roughly elucidated here and varies considerably between cell types. The remarkable control and regulation of calcium within the smooth muscle cell allows a single species to act as a messenger selectively for a huge variety of processes and highlights the challenges and potential of designing sensors for such a system.

11.3 Design of a ratiometric intracellular ion probe

11.3.1 Probe design features

With the importance of probes for calcium ions clear, there is some potential for combining a mitochondria-targeting group with a calcium ion sensor in the same way as targeting DNP decouplers is potentially useful. However, with calcium ions involved in so many ion channels, organelles and individual signalling pathways there is also great utility in other targeting strategies. For this reason the synthesis of a fluorescent calcium sensor which can be easily conjugated to various targeting groups was planned. The fluorophore and binding groups are based on extant probes[396,397] modified to allow easy attachment of different targeting groups (**Scheme 134**).

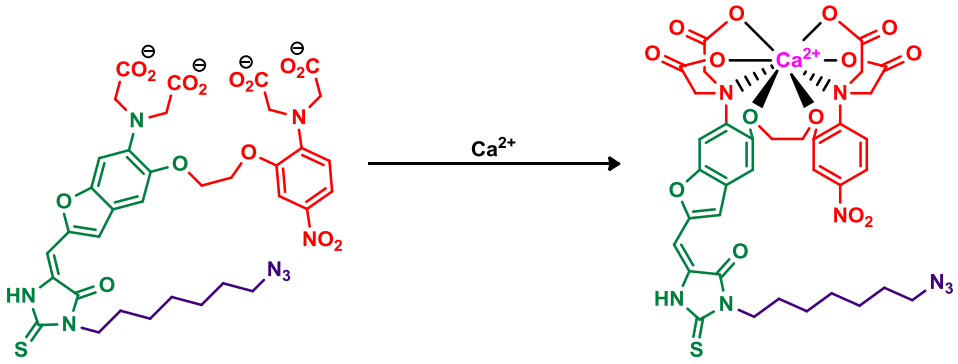

Scheme 134 - Ion sensor target divided roughly into components; the ionophore (red), fluorophore (green) and targeting handle (purple).

Sensor precursor **412** has an azide for attachment to different targeting groups by click chemistry.[398] It is based on the benzofuran fluorophore Fura red due to the large stokes shift on Ca^{2+} observed with this fluorophore, which allows ratiometric imaging.[399] This is attached through a conjugated system to a polydentate (octacoordinate) calcium chelator. Binding to calcium changes the bond angles from the coordinating groups to the tertiary amine, removing these from conjugation and changing the electronic properties of the ion sensor. Through conjugation this electronic change is passed to the fluorophore (**Scheme 134**), and here a difference in electronics translates to different excitation and fluorescence wavelengths.

The chelating section of the molecule is based on Tsein's 1,2-bis(o-aminophenoxy)ethane-*N*,*N*,*N*',*N*'-tetraacetic acid (BAPTA) Ca^{2+} sensors[396] as used in the Fura type indicators,[73] although with the important addition of a nitro group on one ring. The reasoning for this is the dramatic increase in dissociation constant observed upon addition of an electron withdrawing substituent to Fluo-4.[400] The intention is that the probe should have high selectivity but relatively low affinity to achieve a large dynamic reporting range and image specifically high local, transient Ca^{2+} concentrations. The probe is also ratiometric, due to the different absorption wavelength exhibited by chelating and non-chelating fura indicators.

11.3.2 Planned forward synthesis

The modular synthesis illustrated below shares many common features with other syntheses of BAPTA type probes, in particular that of Grynkiewicz, Poenie and Tsein.[396]

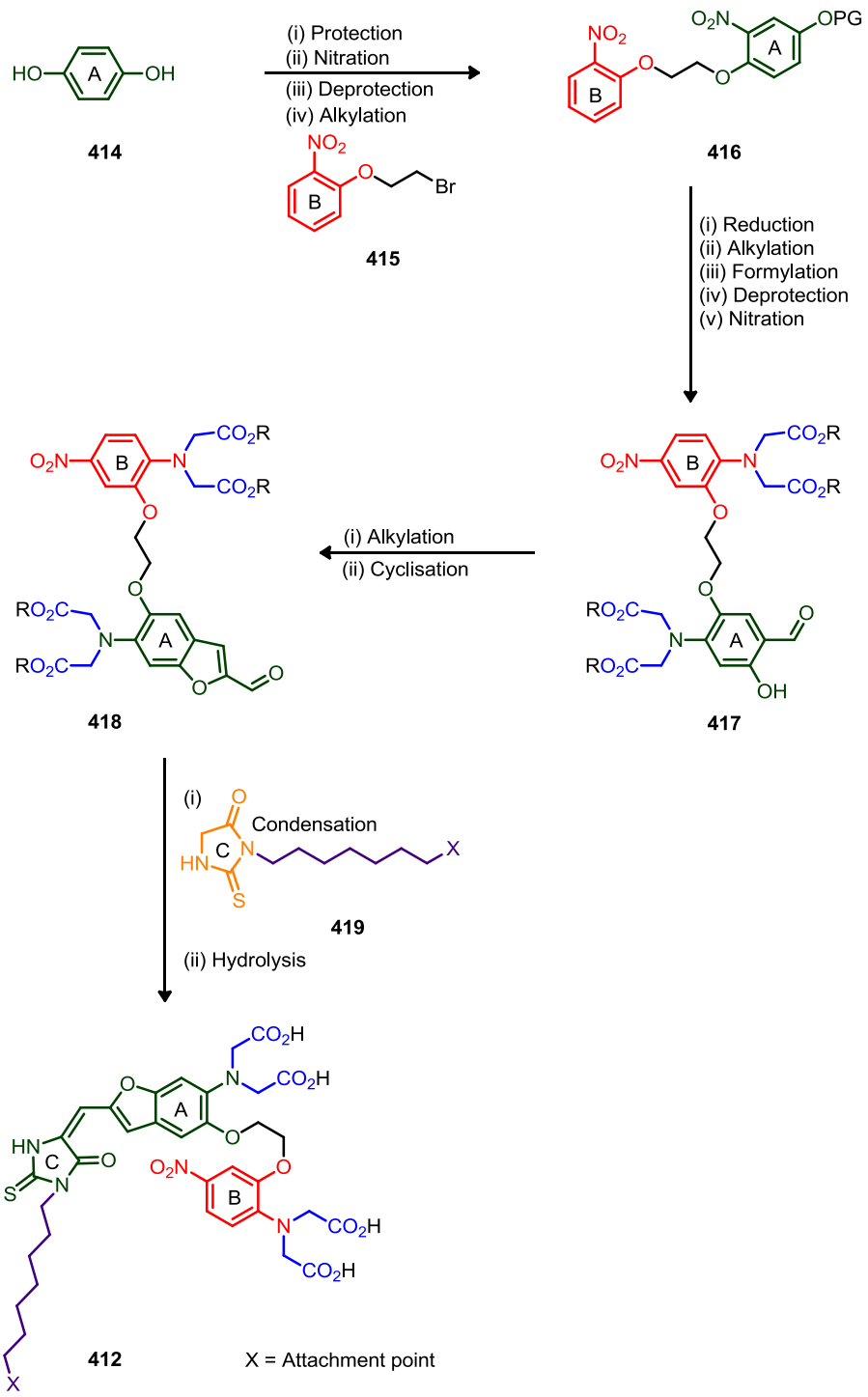

Scheme 135 - Intended forward synthesis.

The two core rings A and B form the basis of the fluorophore and the binding modulating group respectively and are constructed by applying well established chemistry to hydroquinone **414** through a series of protection, nitration, and deprotection then linked by alkylation with nitroarene **415** to form BAPTA precursor **416**. Reduction of the nitro groups in this precrusor is followed by alkylation to add the chelating arms, followed by formylation of the more electron-

rich ring and deprotection to give aldehyde **417**. The placement of the last nitration step is restricted to quite late in the synthesis due to electronics, in particular the need for the formylation of ring B to deactivate this ring and improve nitration selectivity for ring A. Alkylation of aldehyde **417** with an aldehyde surrogate and condensatory cyclisation to give fura red precursor **418**, with further condensation to connect thiohydantoin **419** forming ring C. Hydrolysis of the ester groups to give calcium sensor **412** as a tetra-acid would then complete then initial synthesis. An appropriate attachment point for the targeting group is also simultaneously attached with the thiohydantoin. There are a range of options for this group, with the typical example being an azido group as a precursor to copper-catalysed Huisgen cycloaddition.[398]

11.4 Synthesis of a ratiometric Ca^{2+} ion sensor

11.4.1 Synthesis and linking of phenol components

The synthesis of the phenolic components (**Scheme 136**) and formation of the BAPTA skeleton were all carried out on large scale, allowing purification via non-chromatographic techniques such as crystallisation.

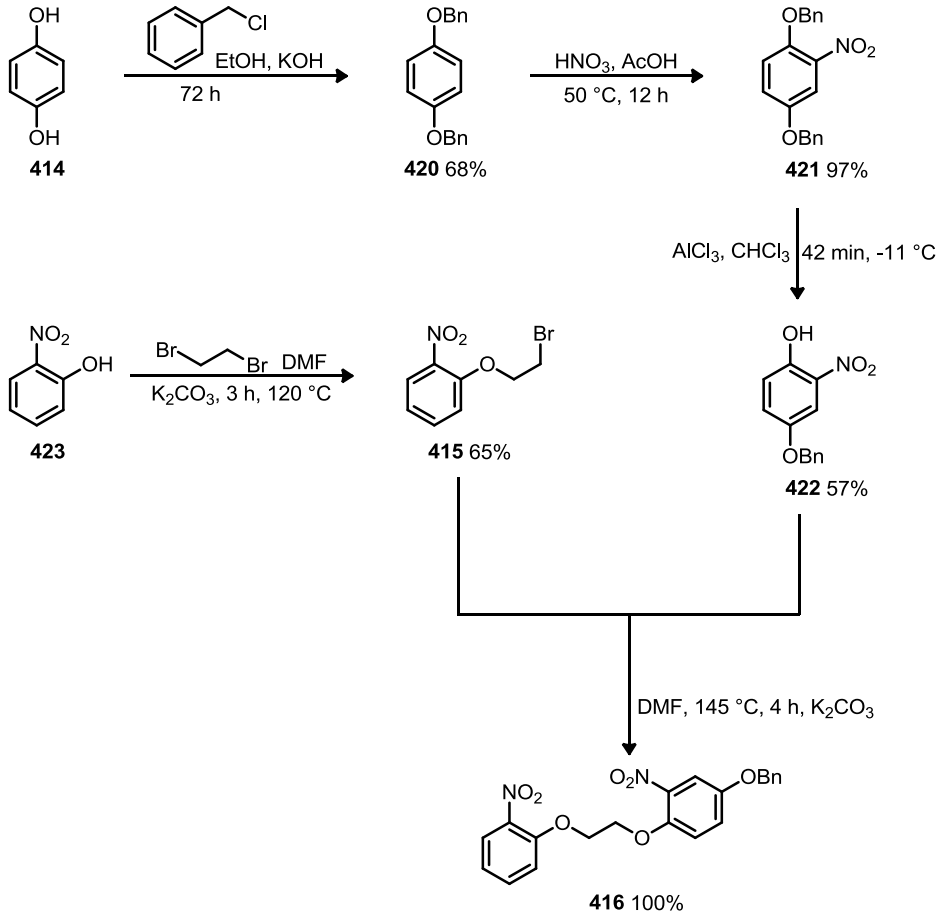

Scheme 136 - BAPTA skeleton construction

Benzyl protection of hydroquinone **414** to give dibenzylated phenol **420** works with benzyl chloride or bromide, although mechanical stirring proved necessary due to the viscosity of the suspension. The ethanol used was distilled from KOH prior to use due to the observation of a brown residue in a small scale trial which was attributed to additives in this solvent.

The benzyl ether **420** is sufficiently electron rich for nitration using nitric and acetic acid with modest heating to give nitroarene **421**. This approach is considerably milder than more common nitric/sulphuric acid mixes as the rate equation for such an electron rich ring system would be zeroth order with respect to the aromatic component. The rate is dependent only on nitronium ion formation and this species is immediately consumed. Consequently the mixture is less oxidising. This may be important in avoiding oxidation to a quinone-type structure.[331] The acetic acid also serves to moderate the acidity of nitric acid.

Deprotection to give phenol **422** using TFA and chloroform proved slow, unreliable and difficult to purify. An alternative was investigated which made use of the *ortho*-nitro group to chelate a strong Lewis acid with an adjacent ether and so promote the deprotection of the phenol in this position through complex **424** (**Scheme 137**). The result is benzyl chloride and the aluminium phenoxide **425**, which subsequently hydrolyses in acidic solution to the desired phenol product.

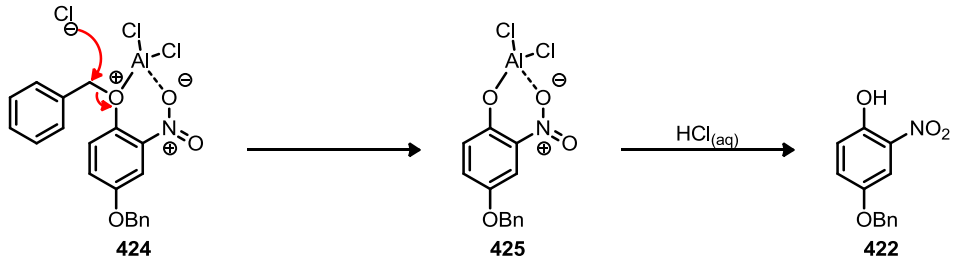

Scheme 137 - Lewis acid catalysed deprotection.

The conditions used are modified from a literature procedure;[401] an initial small scale trial showed that the reaction worked well and gave good conversion. On scale up concentration was increased and the temperature was lowered to compensate for the change in heat loss characteristics of the exothermic reaction with the increased scale and concentration. The starting material was completely consumed and selectivity for the phenol **422** is about 5:1 over alternate phenolic products. The yield was limited by the repeated recrystallisation needed to remove side products, which had similar solubilities to the product.

The bromide **415** was synthesised in moderate yield by reacting phenol **423** with dibromoethane in DMF, with similar conditions then used to link bromide **415** to phenol **422** to give biaryl **416**. The initial attempt at this reaction contained dibromoethane and dimer **426** was isolated as a byproduct (**Scheme 138**).

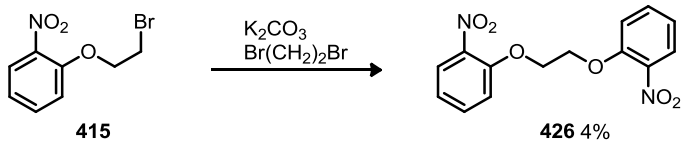

Scheme 138 – Small quantities of dimer **426** resulted from leftover dibromoethane in the coupling of nitroarenes **415** and **422**.

Removal of leftover dibromoethane on scale up by distillation under reduced pressure from the product **415** allowed the subsequent coupling to form **416** to proceed quantitatively.

Material generated from the large scale early synthesis was then transformed over a number of steps to the fluorophore precursor (**Scheme 139**). These steps proved more problematic and required more development.

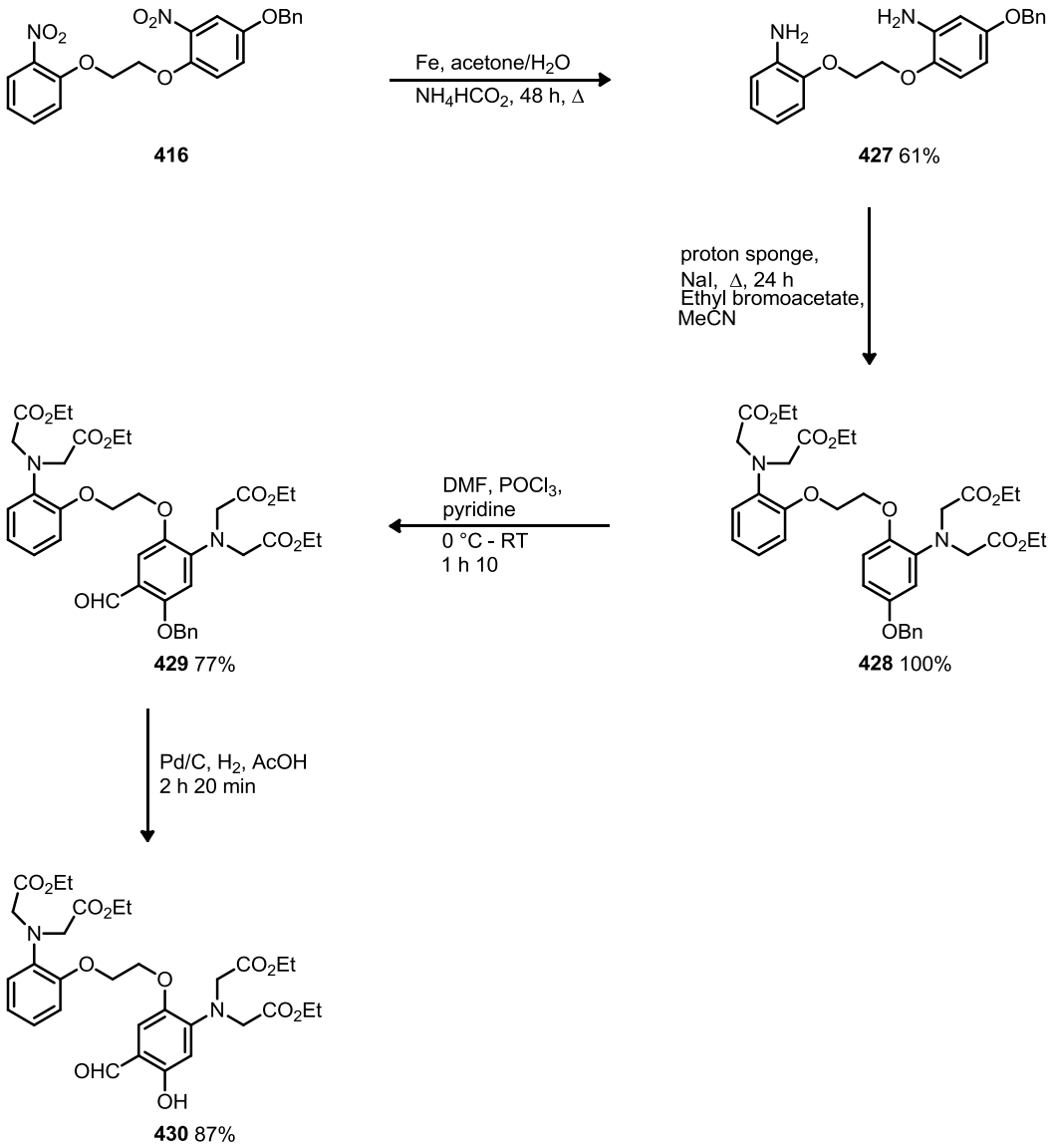

Scheme 139 - Continuation of the synthesis towards the fluorophore

The reduction of the dinitro precursor **416** is complicated by the need to preserve the benzyl ether. Several conditions were evaluated in search of a replacement for hydrogenation over the Pt/C, reagent which was used in the synthesis of Tsein's original ion sensor[396] due to the expense of using this reagent on a large scale. Sodium dithionite[402] in THF was tested, but no reaction was observed. Palladium on carbon with ammonium formate as a hydrogen source was also tested because it was hoped the reactivity of the nitro and benzyl groups would be sufficiently different as to allow reduction of the nitro group without deprotection. Small scale experiments quickly showed that complete reduction without deprotection was impossible under the conditions used.

As an alternative, iron in aqueous acid is a well-established reagent for reduction of nitroarenes. Initial tests in ethanol based on procedures previously used within the group[403] proved unsuccessful, but replacement of the ethanol with an acetone/water mix[404] gave clean conversion to dianiline **427** and acceptable yields after the solvent ratio was modified to better suit the substrate **416**.

The 'arms' of the molecule were then attached to dianiline **427**, which is a potentially problematic reaction due to the need to ensure complete reaction and thus avoid difficult to remove impurities without risking generation of quaternary ammonium salts. Some variability in yields was seen in earlier attempts at this reaction, which may be explained by the subsequent observation that product **428** is somewhat sensitive to moderate heat and possibly prolonged exposure to light. Use of a large excess of reagents and careful drying of all reagents used allowed for eventual quantitative conversion to tetra-ester **428**.

Formylation was achieved with the Vilsmeier-Haack reaction,[405] for which the mechanism is shown below (**Scheme 140**).

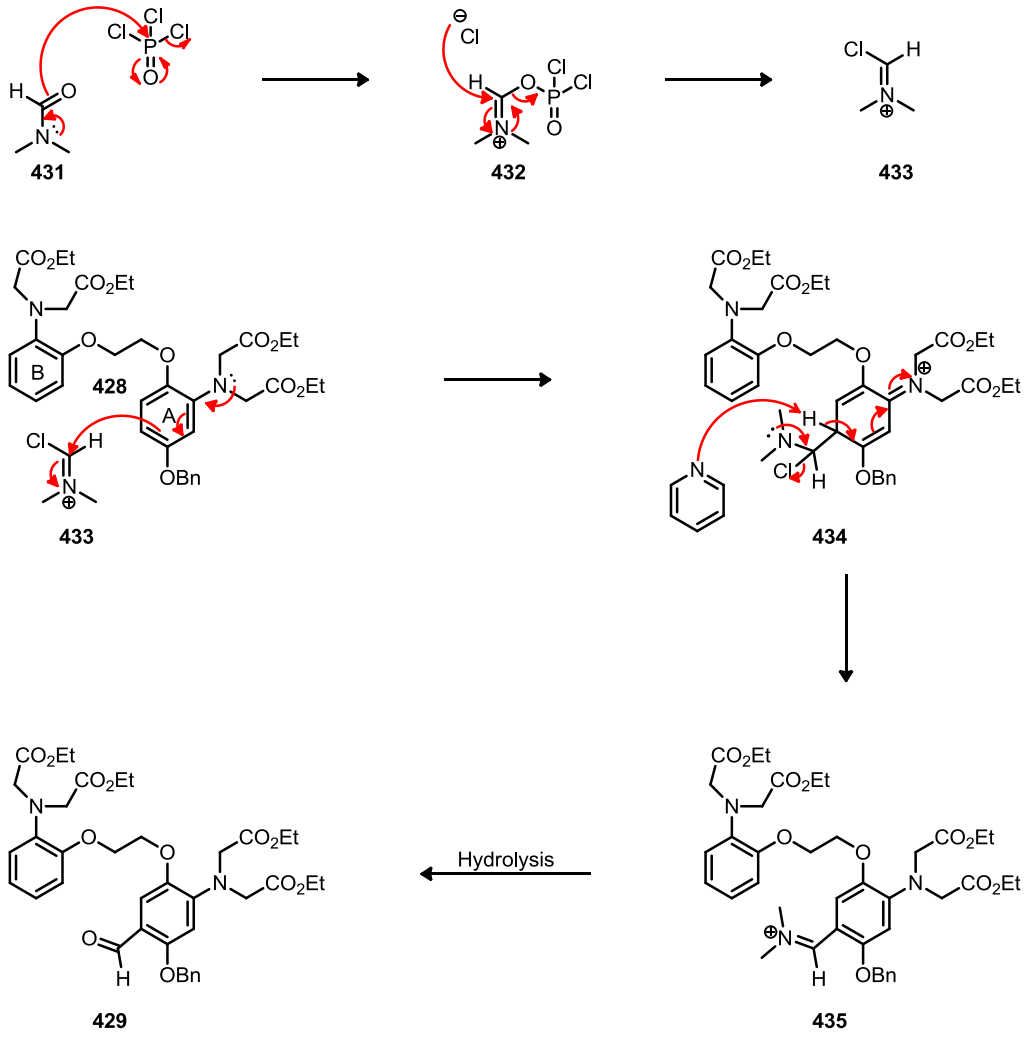

Scheme 140 - The Vilsmeier-Haack formylation mechanism.

First the Vilsmeier reagent **433** is generated through nucleophilic attack by the oxygen atom of DMF **431** on the phosphorus atom, which subsequently loses a chloride. The resulting iminium phosphoryl chloride **432** is attacked by the chloride to form the iminium chloride **433**, aided by the energetically favourable formation of the strong phosphorus-oxygen double bond. Once formed the reagent undergoes nucleophilic attack from the more electron rich aromatic ring of tetraester **428**. The regiochemistry of addition is controlled by the *ortho* and *para* directing amino group and benzyl ether on the A ring, which both donate most strongly to the same positions. Since the position *ortho* to the amino group is sterically crowded selective reaction *para* to this group is favourable. The amine then ejects the chloride to reform the iminium structure **435**, and a hydrogen ion is readily lost from the site of reaction due to the lower energy of the resulting aromatic system. The iminium ion **435** is hydrolysed in aqueous work up to give the desired aldehyde **429**.

In Tsein's synthesis the major alternative formylation site on the B ring is blocked by a methyl group absent in our target, so formylation of the tetraester compound **428** required optimisation of conditions. Variation of conditions and equivalents showed that it was possible to formylate in only the desired position using additional equivalents of $POCl_3$ for a short period of time (monitored by TLC), giving aldehyde **429** in high yield.

Deprotection of benzyl ether **429** proved difficult; initially transfer hydrogenation with ammonium formate appeared effective, but proved unreliable on a larger scale and lead to decomposition. This was attributed to the acidic ammonium and an alternative hydrogen source was investigated, 1,4-cyclohexadiene, but no reaction was observed.

Lewis acids were also investigated, starting with a procedure using magnesium bromide and reputed to be quite specific for benzyl groups next to an aldehyde in a similar manner to the earlier aluminium trichloride deprotection.[406] However benzyl ether **429** showed poor solubility in the specific solvent system used for this reaction, and no reaction was observed. Aluminium trichloride gave deprotection but other phenolic side products. The ability of this reagent to generate $HCl_{(aq)}$ in the presence of moisture and potentially cleave ether links meant that generation of impurities was difficult to control. Nevertheless some material was brought through with this system.

Replacing the earlier transfer hydrogenation procedures with hydrogen gas and using a purer batch of starting material and a rigorous freeze/thaw degassing procedure prior to saturating the solvent with $H_{2(g)}$ gave phenol **430** in good yield.

11.4.2 Nitration: addition of the binding modulating group

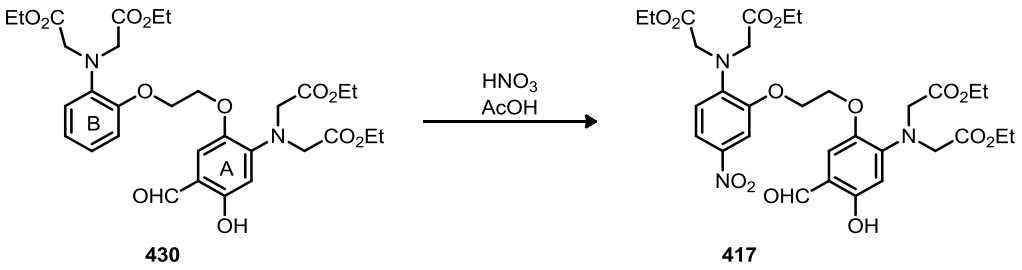

Scheme 141 - Attempted nitration of the B ring.

The addition of a nitro group *para* to the amino group on ring B, which was on the less substituted ring system was a vital part of the initial design of the synthesis, but the exact position of the step in the synthesis is somewhat flexible. Since literature precedent for nitration at this stage exists the procedure was tested.[407]

Given the earlier experience with acidic reagents for the deprotection, it was not surprising to observe considerable decomposition of the starting material when heated in a nitric acid/acetic acid mixture. Compared to the literature synthesis this reaction was of small scale, and so controlling the equivalents of nitric acid was problematic. Following this result the nitration step was postponed to later in the synthesis.

11.4.3 Thiohydantoin heterocycle synthesis

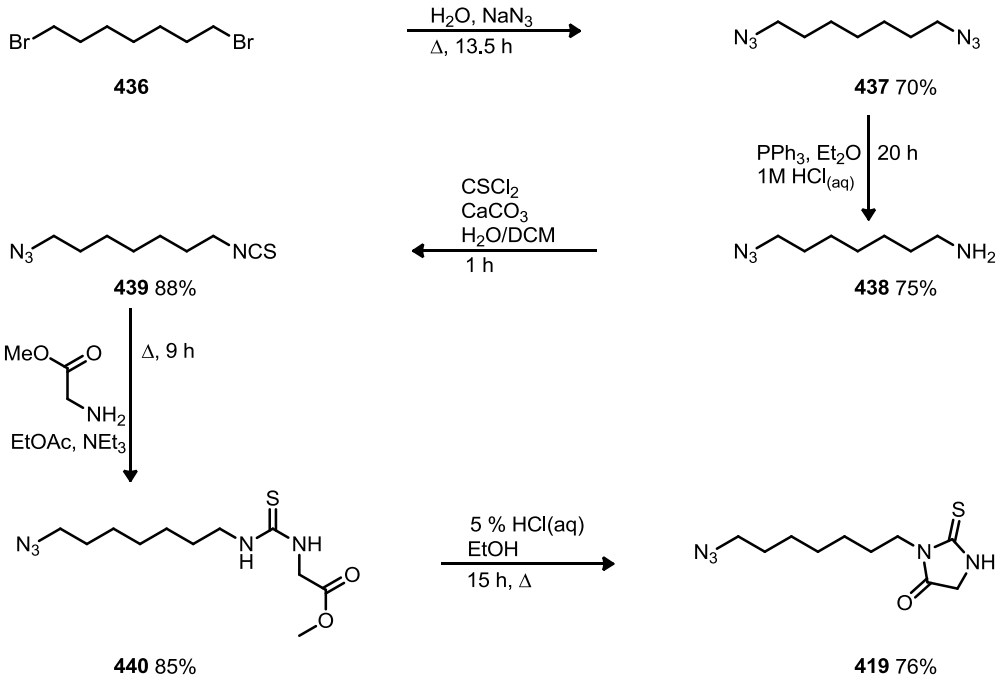

Scheme 142 - Synthesis of the thiohydantoin heterocycle **419**.

The thiohydantoin coupling partner **419** for later in the sequence was completed (**Scheme 142**), beginning from 1,7-dibromoheptane **436** and following a literature route to the amine[408] **438** in which the diazo compound **437** is formed by reaction with sodium azide in water. Although most

literature routes make use of DMF to improve mixing this proved unnecessary. This was followed by Staudinger reduction of one azido group featuring a biphasic Et_2O/aqueous acid system. The amine formed is protonated and thus dragged into the acidic aqueous layer, preventing over-reduction.

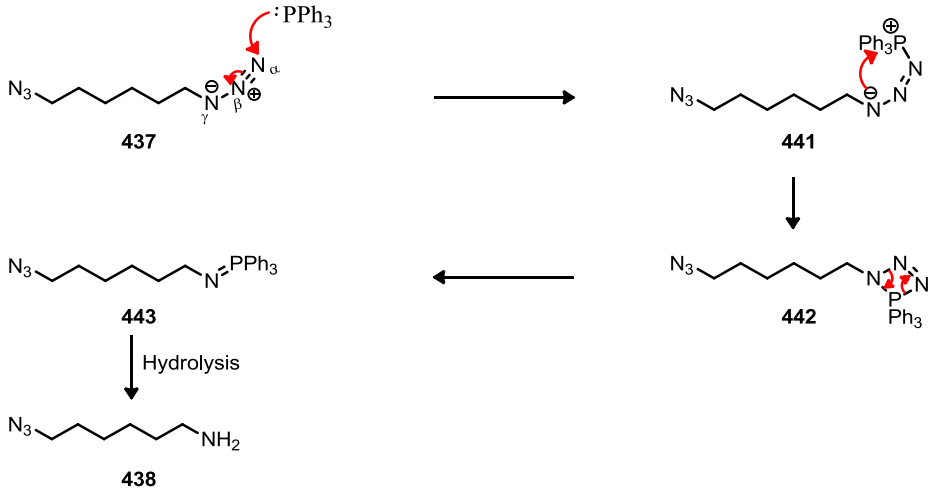

Scheme 143 – Mechanism of the Staudinger reduction.

The Staudinger reaction mechanism (**Scheme 143**) has been investigated computationally in the literature.[409,410] These studies suggest the phosphine nucleophile attacks the α nitrogen atom of the azide **437** on the same side as the γ nitrogen atom with the attached R group to give a *cis* phosphazide due to stabilising interactions between the phosphine and the γ nitrogen atom. The resulting triphenylphosphonium salt **441** is subsequently attacked by the γ negative nitrogen atom to form a 4-membered intermediate **442**,[409] which decomposes, extruding N_2 to give the iminophosphorane. It is noted[409,410] that the energies of these transition states and intermediates are very close in the pathway and the reaction may be concerted in some cases. The resulting iminophosphorane can then undergo hydrolysis to give the amine **438**.

The isothiocyanate **439** was then formed in good yield by gradual addition of thiophosgene to a stirring mixture of mono azide **438**. It was hoped that reaction with glycine methyl ester hydrochloride would lead directly to closed ring system **419**,[411] but instead the open chain compound **440** was isolated. Different ring closing strategies were attempted, with stirring in DCM with SiO_2 proving unsuccessful, and *p*-toluenesulfonic acid in toluene giving lower yields than the aqueous acid/EtOH system shown in the scheme. The desired heterocycle was then isolated in good yield by recrystallisation. The completed heterocycle was used by Dr Stuart Caldwell and Laura Martin to make the intended fluorophore in advancing the calcium sensor synthesis and a separate project, respectively.

11.4.4 Benzofuran formation

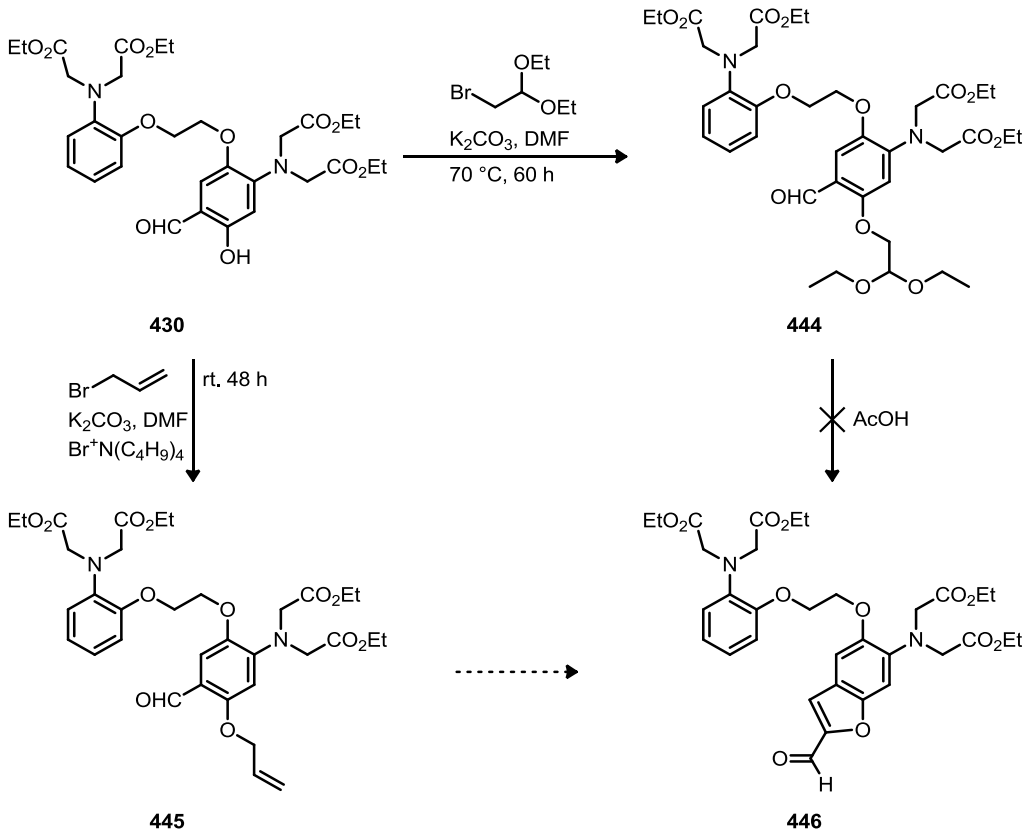

Scheme 144 - Routes investigated towards formation of the benzofuran.

Following the decision to delay nitration, benzofuran formation was instead attempted. The combination of the diethyl acetal alkylating agent and the subsequent acid catalysed condensation are well precedented in literature.[412] However, this is often a low yielding reaction. Initial alkylation proved difficult, perhaps due to thermal decomposition of the starting material **430**. A slower reaction at lower temperature appeared to yield some product **444** as part of a complex mixture, identified by a set of symmetrical multiplets at 3.9-3.6 ppm and a *t* at 4.8 ppm in the ^{1}H NMR spectrum ($CDCl_3$). Cyclisation was attempted both by stirring in acetic acid and using $HCl_{(aq)}$/MeOH, but niether gave any of the desired product **446**. Consequently, this route to the benzofuran product **446** was abandoned.

Failure of the cyclisation represented a considerable difficulty; the substrate **430** is unsuitable for adaptation to a route mimicking the synthesis of related ion sensors. An alternative strategy of allylation to give allyl ether **445** then dihydroxylation and oxidative cleavage was investigated (**Scheme 144**). The first step was attempted on small scale (0.07 mmol) and the correct product was identified as part of a mixture due to the distinctive allyl signals (**Figure 79**), with the H_C-H_D geminal coupling of very similar size to the J_4 coupling between H_A and H_C and H_D giving the appearance of a dq structure, consistent with literature examples.[413] The yield was estimated by ^{1}H NMR to be around 44%. No further work was carried out on this route.

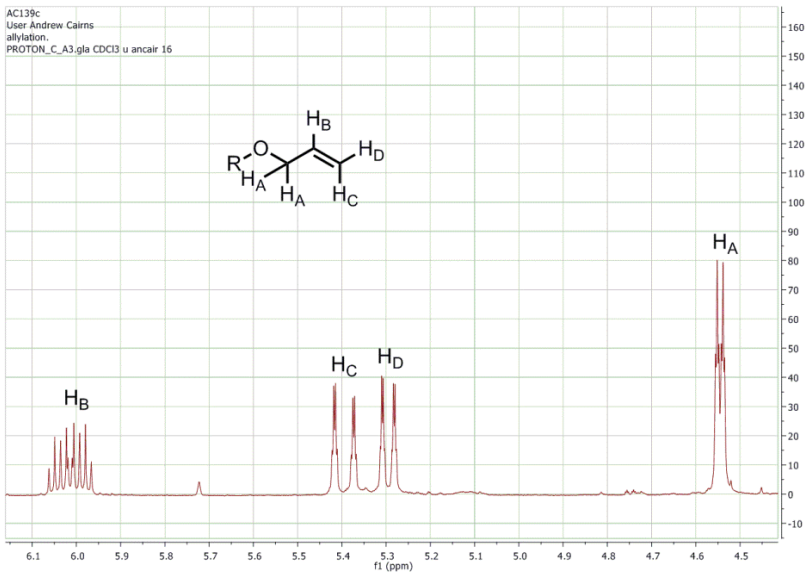

Figure 79 - Characteristics signals in partial ^{1}H NMR spectrum of tetraester **445** indicating the presence of an allyl group.

11.4.5 Further work

Work on the above route was halted at this point as Dr Stuart Caldwell pursued an alternative route, before eventually building on the route outlined to complete the synthesis of the final probe with a KDEL peptide sequence for retention in the sarcoplasmic reticulum attached (**Figure 80**).

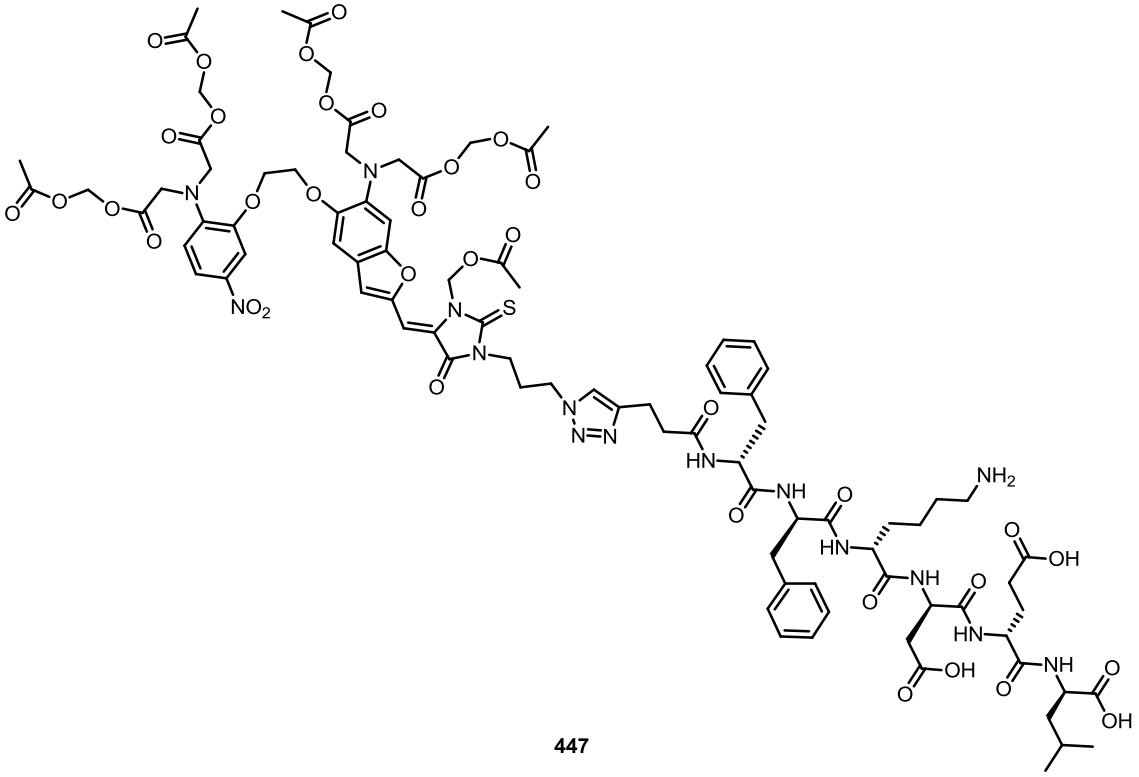

447

Figure 80 - A sarcoplasmic reticulum targeted ratiometric calcium probe.

The structure and route are mostly as previously described, with the exception of the heterocycle where a shorter chain has been utilised to aid purification.

Chapter 12: Thesis summary and future work

12.1 Summary

Synthesis of a photoactivated uncoupler **7-I** was completed (**Figure 81**) and subsequently used by collaborators to demonstrate mitochondria uptake. The probe was then shown to allow selective uncoupling of mitochondria on UV stimulation.

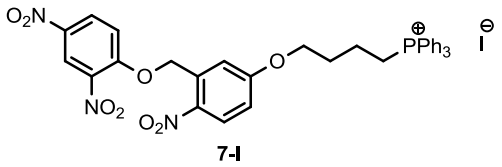

Figure 81 - MitophotoDNP iodide salt

The synthesis of a ratiometric, targetable calcium sensor was completed up to intermediate **430** (9 steps), alongside a thiohydantoin heterocycle **419** synthesised in 5 steps (**Figure 82**). A co-worker has subsequently completed the probe synthesis based on this route, with the resulting probe shows good binding and optical responses in testing.

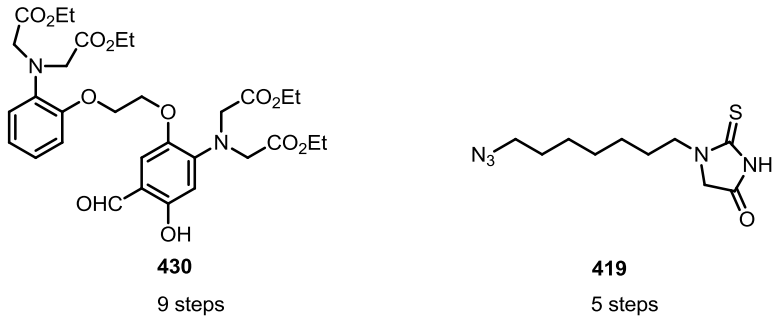

Figure 82 - The BAPTA intermediate **430** and thiohydantoin heterocycle **419**.

Numerous routes to 5,6-disubstituted phenanthridinium salts were investigated towards the synthesis of a mitochondrially targeted superoxide probe and hydroxylated standards. In the course of this work a novel cyclisation was developed based on intramolecular S_NAr giving access to 9-benzyloxyphenanthridinium salt **126**.

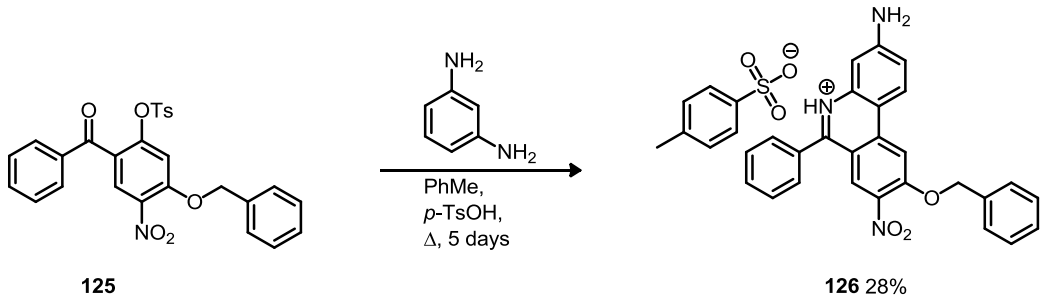

Scheme 145 - Novel cyclisation to 9-OH phenanthridine **126**.

Rapid and high-yielding access to 5,6-disubstituted phenanthridinium salts **289** and **299**-**310** was then achieved through forming benzophenones **265**, **324**-**333** via Suzuki coupling and converting these to imines with the alkylamine. The nitrogen atom of the imine then undergoes cyclisation onto the aryl fluoride in an intramolecular S_NAr upon heating. This transformation was shown to

have good steric and electronic tolerance in the synthesis of 13 phenanthridinium analogues with 6 structural diversification points (**Scheme 146**). Subsequent DFT calculations by a colleague showed this reaction proceeds in a concerted fashion and as such represents a considerable mechanistic novelty.

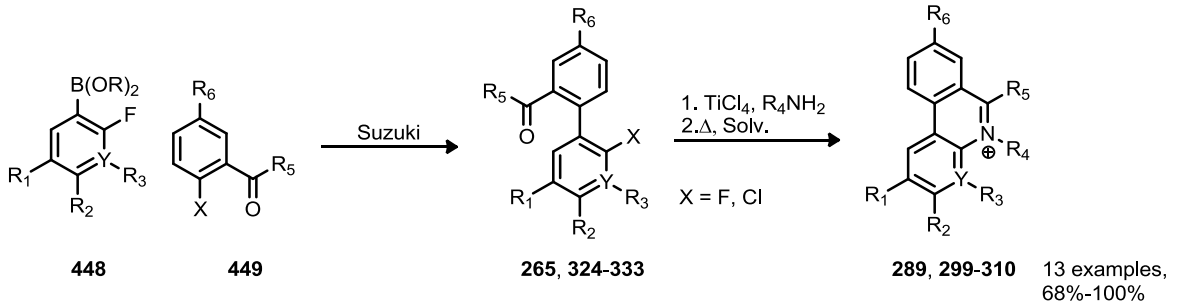

Scheme 146 - Precursors **448** and **449** allow access to benzophenones **265** and **324** - **333**. The imine formation and cyclisation by intramolecular S_NAr gives the 5,6-disubstituted phenanthridinium salts **289** and **299** - **310** in high yield.

Efforts towards a new probe for mitochondrial superoxide led to the synthesis of 3-*tert*butyl-dihydrophenanthridine **294**, which does not intercalate into DNA upon oxidation. This concept was refined and lead to the development of neopentyl ethidium **406** and the targeted analogue MitoBNH **404** and its deuterated analogue **410**.

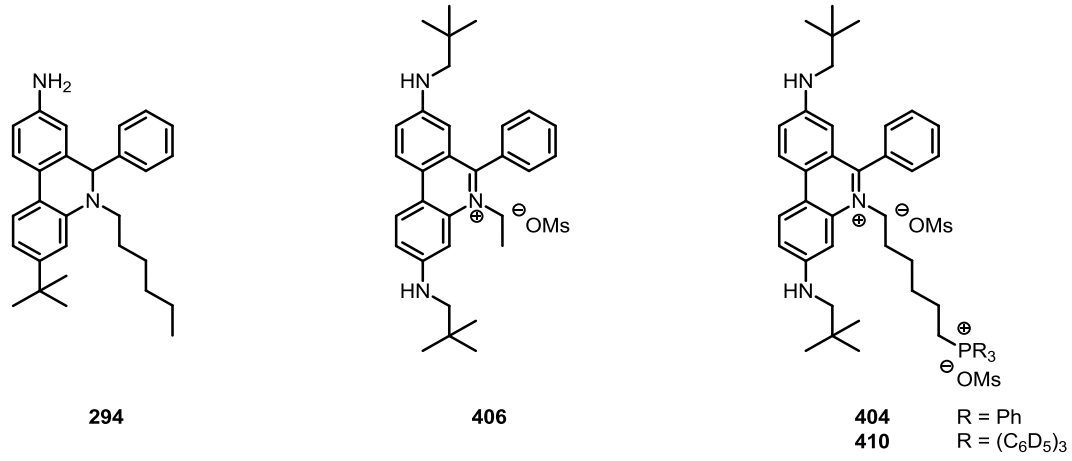

Figure 83 - The non DNA-intercalating probes synthesised.

12.2 Future work

With regard to MitoPhotoDNP **7** and the ratiometric Ca^{2+} sensor it is hoped these will be appropriately utilised by collaborators, and the designs could be used to deliver alternative payloads or target different organelles, respectively.

The cyclisation to the 9-benzyloxyphenanthridinium **126** may provide rapid access to substituted 6-phenylphenanthridines, if higher yields and milder conditions could be achieved. The key to improving this reaction is likely to be found in reducing the imine isomerisation energy, and to this end an *N*-coordinating additive may prove helpful.

Numerous diversifications and expansions may be possible on the fruitful imine S_NAr cyclisation. The C6 functionalisation opportunities offered by the enamine **369** may be worthy of investigation, allowing additional flexibility in decorating these important heterocycles. Many analogues are likely to be accessible via the methodology developed, including C6 unsubstituted variants. Improving or replacing the $TiCl_4$ imine formation would be desirable, especially if the aza-Wittig reaction could be made to work with a less stabilised phosphine or without the C6 substituent in order to consolidate the imine formation step into the cyclisation procedure. Replacing the alkylamine with hydrazine or hydroxylamine may allow low temperature cyclisation due to the α effect, and the products may give interesting optical and particularly photolytic properties.

Most obviously, the methodology will be utilised to access further probe systems, and to this end work is ongoing within the group to complete the DNA targeted H_2O_2 probe **371**.

Some further work is required to re-synthesise the MitoBNH deuterated standard, and then access the 2-hydroxymitoBNH controls. It is hoped that when these are available collaborators will be able to use these probes for accurate *in vivo* quantification of superoxide. The neopentylethidium model **406** is independently of interest, with the intention being to make a deuterated standard and use the combination for quantifying superoxide more generally.

Chapter 13: Experimental

^{1}H NMR were obtained using Bucker-ACS 60 spectrometers operating at 500 and 400 MHz respectively, ^{13}C NMR spectra at 126 and 101 MHz accordingly. All coupling constants are recorded in Hz and reported uncorrected. DEPT was used to assign C, CH, CH_2 and CH_3. 2D techniques including COSY, HSQC, HMBC, NOESY and ^{19}F equivalents and decoupled protons were used to aid assignment. The ^{19}F spectra for trifluoroboronate salt **266** was corrected using CF_3CO_2H as an external standard. EI and CI mass spectra were obtained using the (M Station) JEOL JMS-700 spectrometer. Some ESI spectra were collected on a Bruker MicroTOF-Q in Glasgow, others by an LTQ Orbitrap XL by the National Mass Spectrometry Service Centre in Swansea. IR Spectra were obtained with a Shimadzu FTIR 8400S. Alumina for chromatography was deactivated by saturation with deionised water followed by drying at 150 °C for 72 h. Ethanol for the synthesis of 1,4-bis(benzyloxy)-2-nitrobenzene was distilled from KOH. Acetone was dried by stirring with 4 angstrom molecular sieves or distilled from $CuSO_4$. All dry triethylamine was distilled from CaH_2 and stored over KOH. Dry solvents Hexylamine was distilled from CaH_2 and stored over KOH. Pyridine was distilled from CaH_2. All glassware for reactions involving anhydrous conditions was dried in an oven at 250 °C or flame dried under vacuum, with dry solvents collected from a Puresolv solvent purification system. A CEM Explorer PSL set to a maximum power of 50W, maximum ramp time of 20 min (never reached) and a 15 atm pressure cut off was used for the microwave reactions. All NEt_3 was distilled from CaH_2 and stored over KOH. Pyridine was distilled from CaH_2. Allyl bromide was distilled $MgSO_4$ in a dark environment and kept covered in storage to protect from light. NaI used was previously dried by heating under vacuum at 100 °C for 6 h.

5-(Hydroxy-2-nitrobenzyl)methanol **22**

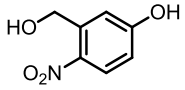

22

$NaBH_4$ (2.38 g, 62.9 mmol, 1.90 eq.) was added over 45 min to a stirred solution of 5-hydroxy-2-nitrobenzaldehyde (5.06 g, 33.0 mmol, 1.00 eq.) in MeOH (100 mL) at 0 °C under argon. After 17 h the reaction was quenched into H_2O. MeOH was removed and the aqueous concentrated under reduced pressure, leaving a yellow solid. This was partitioned between Et_2O and 0.5 M $HCl_{(aq)}$, then the aqueous re-extracted with Et_2O (x 3). The combined organic extracts were dried ($MgSO_4$) and filtered, then the solvent was removed under reduced pressure and the solid dried under high vacuum to give benzylic alcohol **22** as a solid (4.68 g, 91%). δ_H (400 MHz, CD_3OD): 8.08 (1H, d, *J* = 9.0 Hz, H3), 7.26 (1H, s, H6), 6.78 (1H, dd, *J* = 8.9, 2.4 Hz, H4), 4.94 (2H, s, C**H**$_2$OH). In agreement with values from Caroline Quin's thesis.[414]

4-Iodobut-1-yltriphenylphosphonium iodide **24**

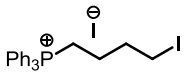

24

Triphenylphosphine (9.18 g, 35.0 mmol, 1.00 eq.) was dissolved in dry PhMe (40 mL). This was added slowly to a stirred solution of 1,4-diiodobutane (5.0 mL, 38 mmol, 1.1 eq.) in dry PhMe (160 mL) under argon which was then heated to 100 °C in the dark for 4 h. A white solid was formed which was then vacuum filtered and washed with Et_2O then hot PhMe and dried under vacuum to give the phosphonium salt **24** as a powder (15.4 g, 26.9 mmol, 77%). δ_H (400 MHz, $CDCl_3$): 7.92 - 7.78 (9H, m, $^+$P**Ph**$_3$), 7.74 - 7.68 (6H, m, $^+$P**Ph**$_3$), 3.90 - 3.80 (2H, m, $CH_2C\mathbf{H}_2{}^+PPh_3$), 3.35 (2H, t, *J* = 6.1 Hz, $IC\mathbf{H}_2CH_2$), 2.24 (2H, quintet, *J* = 6.6 Hz, $ICH_2C\mathbf{H}_2CH_2$), 1.83 (2H, sextet, *J* = 7.8 Hz, $CH_2C\mathbf{H}_2CH_2{}^+PPh_3$). δ_C ($CDCl_3$, 100 MHz): 135.25 (d, *J* = 3.0 Hz, CH), 133.65 (d, *J* = 10.1 Hz, CH), 130.61 (d, *J* = 12.6 Hz, CH), 117.68 (d, *J* = 86.2 Hz, C), 32.58 (d, *J* = 17.0 Hz, CH_2), 23.16 (d, *J* = 3.6 Hz, CH_2), 21.85 (d, *J* = 51.4 Hz, CH_2), 7.29 (CH_2). IR (ATR cm^{-1}): 2890 (CH), 2859 (CH), 1588 (C_{Ar}=C_{Ar}), 1484 (C_{Ar}=C_{Ar}), 1433 (P-Ph). MS (NSI^+): 445 (M^+, 100%), 289 (M^+–HI –H_2–C_2H_4).

{4-[3'-(Hydroxymethyl)-4'-nitrophenoxy]butyl}triphenylphosphonium iodide **25-I**

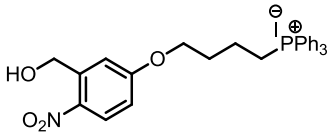

25-I

Phenol **22** (1.18 g, 7.21 mmol, 1.00 eq.), phosphonium salt **24** (2.49 g, 4.35 mmol, 0.60 eq.), and Cs_2CO_3 (1.48 g, 4.53 mmol, 0.63 eq.) were stirred and heated under reflux and argon in dry MeCN (20.0 mL) for 72 h. After cooling DCM was added, then the solution decanted off. The residual solvent was removed under reduced pressure, and the material dissolved in DCM and washed with 1 M $NaOH_{(aq)}$. The aqueous washings were extracted with DCM (x 2). The combined organics were then dried ($MgSO_4$), then filtered and the solvent removed to give phosphonium salt **25-I** as a yellow foam (2.57 g, 97%). δ_H (400 MHz, $CDCl_3$): 8.03 (1H, d, *J* = 9.1 Hz, H5'), 7.81 - 7.75 (9H, m, $^+$P**Ph**$_3$), 7.71 - 7.65 (6H, m, $^+$P**Ph**$_3$), 7.48 (1H, d, *J* = 2.8 Hz, H2'), 6.73 (1H, dd, *J* = 9.1, 2.8 Hz, H6'), 4.70 (2H, s, $C\mathbf{H}_2OH$), 4.29 (2H, t, *J* = 6.1 Hz, $OC\mathbf{H}_2CH_2$), 3.75 - 3.65 (2H, m, $CH_2C\mathbf{H}_2{}^+PPh_3$), 2.19 (2H, quintet, *J* = 6.6 Hz, $OCH_2C\mathbf{H}_2CH_2$), 1.85 (2H, sextet, *J* = 7.8 Hz, $CH_2C\mathbf{H}_2CH_2{}^+PPh_3$). δ_C ($CDCl_3$, 100 MHz): 163.12 (C), 142.71 (C), 139.45 (C), 135.27 (d, *J* = 2.9 Hz, CH), 133.66 (d, *J* = 10.0 Hz, CH), 130.63 (d, *J* = 12.6 Hz, CH), 127.35 (CH),117.80 (d, *J* = 86.2 Hz, C), 113.60 (CH), 67.21 (CH_2), 61.66 (CH_2), 29.03 (d, *J* = 16.7 Hz, CH_2), 22.33 (d, *J* = 51.3 Hz, CH_2), 18.95 (d, *J* = 3.8 Hz, CH_2). IR (ATR cm^{-1}): 3320 (OH), 3053 (C_{Ar}-H), 2932 (CH), 2864 (CH), 1613 (C_{Ar}=C_{Ar}), 1584 (C_{Ar}=C_{Ar}), 1576 (C_{Ar}=C_{Ar}), 1506 (NO_2), 1433 (P-Ph). MS (FAB/NOBA), m/z: 486 [M^+ (phosphonium cation), 100%], 317 ($C_{22}H_{22}P^+$, 83), 262.1 ($^+PPh_3$, 53). HRMS: 486.1834. $C_{29}H_{29}O_4NP$ requires 486.1829.

{4-[3-(2”,4”-dinitrophenoxymethyl)-4’nitrophenoxy]butyl}triphenylphosphonium iodide **7-I**

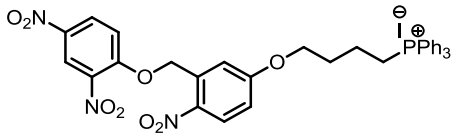

7-I

Benzylic alcohol **25-I** (712 mg, 1.16 mmol, 1.00 eq.), 1-fluoro-2,4-dinitrobenzene **26** (0.60 mL, 5.0 mmol, 4.3 eq.) were combined and stirred in dry acetone (15.0 mL) under argon. Dry triethylamine (0.40 mL, 2.9 mmol, 2.5 eq.) was then added and the mixture heated to 45 °C for 72 h in the dark. The solvent was removed under reduced pressure and the material dissolved in DCM and washed with 0.5 M $NaOH_{(aq)}$ (x 3). The DCM layer was then dried ($MgSO_4$), filtered and the solvent removed under reduced pressure. The material was then dissolved in minimal DCM and precipitated with addition of Et_2O (x 2), then this process repeated to give a brown foam (706 mg). Column chromatography on 244 mg of this material using gradient elution [MeCN - EtOAc (10:3 - 10.1), then MeCN – MeOH (20:1 - 1:1)] on deactivated alumina gave the DNP derivative **7-I** as a yellow foam (13 mg, 5%). δ_H (400 MHz, $CDCl_3$): 8.87 (1H, d, *J* = 2.8 Hz, H3”), 8.52 (1H, d, *J* = 9.3, 2.8 Hz, H5”), 8.27 (1H, d, *J* = 9.2 Hz, H6”), 7.94 - 7.84 (6H, m, $^+$P**Ph**$_3$), 7.82 - 7.76 (3H, m, $^+$P**Ph**$_3$), 7.74 - 7.65 (6H, m, $^+$P**Ph**$_3$), 7.58 (1H, d, *J* = 2.7 Hz, H2’), 7.50 (1H, d, *J* = 9.3 Hz, H5’), 7.06 (1H, dd, *J* = 9.1, 2.8 Hz, H6’), 5.79 (2H, s, C**H**$_2$OAr”), 4.37 (2H, t, *J* = 6.2 Hz, OC**H**$_2$CH$_2$), 4.15 - 4.00 (2H, m, CH$_2$C**H**$_2^+$PPh$_3$), 2.28 (2H, quintet, *J* = 6.8 Hz, OCH$_2$C**H**$_2$CH$_2$), 1.96 - 1.85 (2H, m, CH$_2$C**H**$_2$CH$_2^+$PPh$_3$). δ_C ($CDCl_3$, 100 MHz): 163.93 (C), 156.00 (C), 140.57 (C), 139.07 (C), 138.45 (C), 135.00 (d, *J* = 3.0 Hz, CH), 133.72 (d, *J* = 10.0 Hz, CH), 130.44 (d, *J* = 12.5 Hz, CH), 129.85 (CH), 128.43 (CH), 122.42 (CH), 118.30 (d, *J* = 85.9 Hz, C), 115.30 (CH), 114.50 (CH), 114.07 (CH), 69.41 (CH_2), 68.02 (CH_2), 29.07 (d, *J* = 17.0, CH_2), 21.95 (d, *J* = 50.5 Hz, CH_2), 19.18 (d, *J* = 4.0 Hz, CH_2). IR (NaCl, DCM cm^{-1}): 3054 (C_{Ar}-H), 2987 (CH), 2924 (CH), 2854 (CH), 1606 (C_{Ar}=C_{Ar}), 1519 (C_{Ar}=C_{Ar}), 1438 (P-Ph). MS (NSI$^+$): 652 [M$^+$ (phosphonium cation), 100%]. HRMS: 652.1834. $C_{35}H_{31}O_8N_3P$ requires 652.1843.

4-Bromobut-1-yltriphenylphosphonium bromide **28**

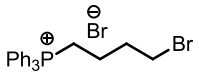

28

A stirred mixture of triphenylphosphine (2.73 g, 10.4 mmol, 1.00 eq.) and 1,4-dibromobutane (1.50 mL, 12.6 mmol, 1.21 eq.) in dry PhMe (35 mL) was then heated to reflux under argon for 72 h. The mixture was allowed to cool and filtered. The solid collected was washed with Et_2O and hot PhMe, then dissolved in MeOH. The solvent was removed under reduced pressure to give solid **28** (4.30 g, 100%). δ_H (400 MHz, $CDCl_3$): 7.91 - 7.85 (6H, m, $^+$P**Ph**$_3$), 7.83 - 7.77 (3H, m, $^+$P**Ph**$_3$), 7.74 - 7.68 (6H, m, $^+$P**Ph**$_3$) 4.02 - 3.94 (2H, m, CH$_2$C**H**$_2^+$PPh$_3$), 3.59 (2H, t, *J* = 5.9 Hz, BrC**H**$_2$CH$_2$), 2.33 (2H, quintet, *J* = 6.5 Hz, BrCH$_2$C**H**$_2$CH$_2$), 1.86 (2H, sextet, *J* = 7.8 Hz, CH$_2$C**H**$_2$CH$_2^+$PPh$_3$). Compound is commercially available.[415]

{4-[3'-(Hydroxymethyl)-4'-nitrophenoxy]butyl}triphenylphosphonium bromide **25-Br**

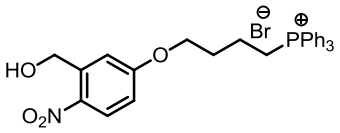

25-Br

Phenol **22** (829 mg, 5.08 mmol, 1.00 eq.), phosphonium salt **28** (1.81 g, 4.50 mmol, 0.89 eq.), and Cs_2CO_3 (1.48 g, 4.53 mmol, 0.89 eq.) were stirred under reflux and argon in dry MeCN (20.0 mL) for 72 h. The mixture was partitioned between H_2O and EtOAc, then the aqueous was re-extracted with EtOAc (x 4). The mixture was then dried ($MgSO_4$) and the solvent removed under reduced pressure. The material was then dissolved in minimal DCM and precipitated with Et_2O. Repeating this process gave triphenylphosphonium salt **25-Br** (706 mg, 28%) which was used without further purification.

{4-[3'-(Hydroxymethyl)-4'-nitrophenoxy]butyl}triphenylphosphonium tetraphenylborate **25-BPh_4**

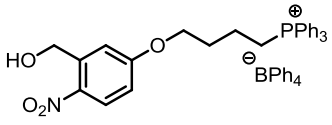

25-BPh_4

Benzylic alcohol **25-Br** (706 mg, 1.26 mmol, 1.00 eq.) and $NaBPh_4$ (450 mg, 1.31 mmol, 1.04 eq.) were dissolved in a biphasic mixture of DCM (50 mL) and H_2O (50 mL). The layers were separated then the DCM layer was partitioned with H_2O. The organic layer was dried ($MgSO_4$), filtered and the solvent removed under reduced pressure. The sample was dissolved in minimal DCM and precipitated with MeOH, giving salt **25- BPh_4** (574 mg, 55%) as a brown foam sufficiently pure for the next step. δ_H (400 MHz, $CDCl_3$): 8.14 (1H, d, *J* = 9.1 Hz, H5'), 7.46 - 7.23 (23H, m, **Ph**$_4B^-$, $^+$P**Ph**$_3$), 7.11 (1H, d *J* = 2.7 Hz, H2'), 6.98 - 6.86 (8H, m, **Ph**$_4B^-$), 6.82 - 6.74 (4H, m, **Ph**$_4B^-$), 6.70 (1H, dd, *J* = 9.1, 2.8 Hz, H6'), 5.02 (2H, s, C**H**$_2$OH), 3.76 (2H, t, *J* = 5.4 Hz, OC**H**$_2$CH$_2$), 2.12 - 2.00 (2H, m, CH$_2$C**H**$_2^+$PPh$_3$), 1.65 - 1.35 (4H, m, OCH$_2$C**H**$_2$C**H**$_2$CH$_2^+$PPh$_3$).

{4-[3'-(2",4"-Dinitrophenoxymethyl)-4'nitrophenoxy]butyl}triphenylphosphonium tetraphenylborate **7-BPh_4**

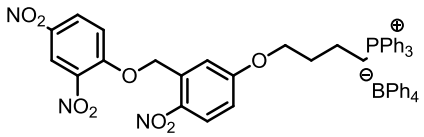

7-BPh_4

A stirred mixture of benzylic alcohol **25-BPh_4** (574 mg, 0.71 mmol, 1.00 eq.), 1-fluoro-2,4-dinitrobenzene **26** (0.5 mL, 4.0 mmol, 5.6 eq.) and dry NEt_3 (0.15 mL, 1.1 mmol, 1.5 eq.) in dry acetone (10.0 mL) under argon was heated to 45 °C for 72 h in the dark. The solvent was removed under reduced pressure and the material dissolved in DCM and washed with 0.2 M $NaOH_{(aq)}$ (x 3). The DCM layer was then dried ($MgSO_4$), filtered and the solvent removed under reduced pressure. The material was redissolved in minimal DCM and precipitated with excess MeOH. The residual solution was decanted off and the solid dried under vacuum. Following column chromatography [SiO_2, dry loaded with DCM, EtOAc/MeOH (10:1)] the solvent mix was allowed to partially

evaporate over 4 days, resulting in formation of needle shaped brown crystals (104 mg, 15%) of probe **7-BPh$_4$**. δ_H (400 MHz, $CDCl_3$): 8.86 (1H, d, *J* = 2.9 Hz, H3''), 8.59 (1H, dd, *J* = 9.3, 2.9 Hz, H5''), 8.29 (1H, d, *J* = 9.2 Hz, H6''), 7.94 - 7.87 (3H, m, $^+$P**Ph**$_3$), 7.86 - 7.72 (13H, $^+$P**Ph**$_3$, H5'), 7.34 (1H, d, *J* = 2.6 Hz, H2'), 7.22 - 7.16 (8H, m, **Ph**$_4$B$^-$), 7.13 (1H, dd, J = 9.2, 2.8 Hz, H6') 6.93 (8H, t *J* = 6.9 Hz, **Ph**$_4$B$^-$), 6.80 (4H, t *J* = 6.9 Hz, **Ph**$_4$B$^-$), 5.88 (2H, s, C**H**$_2$OAr''), 4.23 (2H, t, *J* = 6.0 Hz, OC**H**$_2$CH$_2$), 3.74 - 3.61 (2H, m, CH$_2$C**H**$_2^+$PPh$_3$), 1.98 (2H, quintet, *J* = 6.4 Hz, OCH$_2$C**H**$_2$CH$_2$), 1.76 (2H, sextet, *J* = 7.6 Hz, CH$_2$C**H**$_2$CH$_2^+$PPh$_3$). MS (NSI$^+$): 652 [M$^+$ (phosphonium cation), 100%]. HRMS: 652.1836. $C_{35}H_{31}O_8N_3P$ requires 652.1843. MS (NSI$^-$): 319 [M$^-$ (tetraphenyl borate anion), 100%]. HRMS: 319.1664. $C_{24}H_{20}B$ requires 319.1664.

4-Bromomethyltriphenylphosphonium bromide **30**

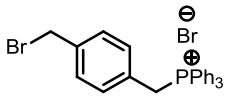

30

A solution of triphenylphosphine (307 mg, 1.17 mmol, 1.00 eq.) in dry PhMe (2.0 mL) which was added slowly to a stirring solution of α,α'-dibromoxylene **29** (616 mg, 2.34 mmol, 2.00 eq.) in dry PhMe (10.0 mL) at 100 °C under and argon. After 20 h the mixture was allowed to cool and the precipitate was collected and washed with Et_2O and hot PhMe. After drying under vacuum salt **30** was collected as a solid (379 mg, 63%). δ_H (400 MHz, $CDCl_3$): 7.82 - 7.71 (9H, m, $^+$P**Ph**$_3$), 7.69 - 7.60 (6H, m, $^+$P**Ph**$_3$), 7.18 - 7.08 (4H, m, H2,3,5,6), 5.50 (2H, d, *J* = 14.2 Hz, ArC**H**$_2^+$PPh$_3$), 4.40 (2H, s, ArC**H**$_2$Br). Data matches previous spectra by Stephen McQuaker.[416]

2-Benzoyl-5-(benzyloxy)phenol **123**

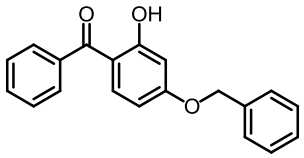

123

2,4-dihydroxybenzophenone **122** (5.00 g, 23.4 mmol, 1.00 eq.), KI (5.84 g, 35.2 mmol, 1.50 eq.) and $NaHCO_3$ (3.05 g, 36.3 mmol, 1.55 eq.) were combined and stirred under argon in dry MeCN (30 mL). Benzyl chloride (3.3 mL, 29 mmol, 1.2 eq.) was added, followed by additional dry MeCN (30 mL). The reaction mixture was then heated under reflux and argon for 48 h. The contents of the flask were washed out with additional DCM, and the solvent removed from all the material. The solid was then washed with DCM and the organic extracts dried ($MgSO_4$) then filtered and the solvent removed under reduced pressure to give benzyl ether **123** (6.74 g, 95%). A small portion was crystallised for analysis (acetone/water), giving needles. δ_H (400 MHz, $CDCl_3$): 12.68 (1H, s, PhO**H**), 7.64 (2H, d, *J* = 7.6 Hz, H2', H6'), 7.60 - 7.46 (4H, m, H3, H3', H4', H5'), 7.46 - 7.32 (5H, m, Ph), 6.61 (1H, d, *J* = 2.5 Hz, H6), 6.49 (1H, dd, *J* = 9.0, 2.4, H4), 5.13 (2H, s, OC**H$_2$**Ph). δ_C (100 MHz, $CDCl_3$): 200.04 (C), 166.27 (C), 165.29 (C), 138.26 (C), 135.85 (C), 135.32 (CH), 131.48 (CH), 128.85 (CH), 128.73 (CH), 128.34 (CH), 128.30 (CH), 127.54 (CH), 113.33 (C), 107.89 (CH), 102.12 (CH), 70.29 (CH_2). IR (ATR cm^{-1}): 3032 (C_{Ar}-H), 2091, 1643 (C=O), 1597 (C_{Ar}=C_{Ar}), 1505 (C_{Ar}=C_{Ar}), 1342 (Ph-

OH). MS (EI^+): 304 (M^+, 95%), 91 ($C_7H_7^+$, 100). HRMS: 304.1098. $C_{20}H_{16}O_3$ requires 304.1099. MP: 118 °C.

2-Benzoyl-5-benzyloxy-4-nitrophenol **124**

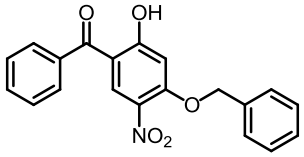

124

Phenol **123** (1.04 g, 3.41 mmol, 1.00 eq.) was suspended stirring in AcOH (6.6 mL) under argon, then $HNO_{3(aq)}$ (0.42 mL, 6.6 mmol, 1.9 eq., 70%) was added dropwise. After 4 h 30 min stirring under argon the reaction mixture was heated to 50 ˚C and developed a red colour. After a further 17 h the mixture was poured into water, then extracted with chloroform (x 2) and the combined organics dried by azeotrope in PhMe and the solvent removed under reduced pressure. A mixture of 4-nitro and 6-nitro compounds (4.2:1) resulted, from which dropwise addition of water to the compound dissolved in acetone caused precipitation to give 4-nitrophenol **124** (517 mg, 45%). δ_H (400 MHz, $CDCl_3$): 12.95 (1H, s, PhO**H**), 8.39 (1H, s, H3), 7.69 - 7.65 (2H, m, H2', H6'), 7.65 - 7.62 (1H, m, H4'), 7.55 (2H, t, *J* = 7.5 Hz, H3', H5'), 7.49 (2H, d, *J* = 7.3 Hz, H2'', H6''), 7.42 (2H, t, *J* = 7.1 Hz, H3'', H4'', H6''), 6.70 (1H, s, H6), 5.27 (2H, s, O C**H**$_2$Ph). ^{13}C NMR (101 MHz, $CDCl_3$) δ 199.60, 168.65, 158.57, 136.71, 134.49, 132.95, 132.72, 132.04, 128.99, 128.86, 128.65, 128.56, 126.97, 111.70, 102.89, 71.54. Data matches previous characterisation by Susan Macintyre.[173]

2'-Benzoyl-5'-benzyloxy-4'-nitrophenyl 4-methylbenzene-1-sulfonate **125**

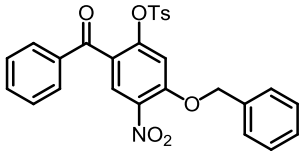

125

Nitrophenol **124** (2.01 g, 5.73 mmol, 1.00 eq.) and para-methylbenzenesulfonyl chloride (1.42 g, 7.47 mmol, 1.30 eq.) were combined stirring in dry pyridine (10.0 mL), then any residual solid washed in with additional dry pyridine (23.0 mL). The reaction mixture was then stirred at RT for 17 h. The solvent was removed under reduced pressure, and the solids dissolved in DCM and washed with water (x 2), then the solvent was removed from the collected organics which were then dried by azeotrope in PhMe. Tosylate **125** was isolated (2.86 g, 99%). δ_H (400 MHz, $CDCl_3$): 7.98 (1H, s, H3'), 7.61 - 7.53 (3H, m, H2'', H4'', H6''), 7.53 - 7.38 (9H, m, H2, H6, H3'', H5'', OCH$_2$**Ph**), 7.29 (1H, s, H6'), 7.14 (2H, d, *J* = 8.1 Hz, H3, H5), 5.31 (2H, s, OC**H**$_2$Ph), 2.36 (3H, s, C**H**$_3$Ar). δ_c (100 MHz, $CDCl_3$): 190.36 (C), 154.43 (C), 150.49 (C), 146.21 (C), 136.18 (C), 134.28 (C), 133.61 (CH), 131.12 (C), 129.95 (CH), 129.90 (CH), 128.94 (CH), 128.73 (CH), 128.50 (CH), 128.43 (CH), 128.33 (CH), 127.28 (CH), 124.98 (C), 110.48 (CH), 71.92 (CH_2), 21.73 (CH_3). Data matches previous characterisation by Susan Macintyre.[173]

9-(Benzyloxy)-8-nitro-6-phenylphenanthridin-3-amine **127**

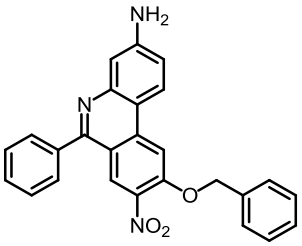

127

Tosylate **125** (303 mg, 0.60 mmol, 1.00 eq.) was combined with 1,3-phenylenediamine (408 mg, 3.77 mmol, 6.29 eq.) and *p*-toluenesulfonic acid (96 mg, 0.50 mmol, 0.84 eq.) in PhMe (30 mL) within a dean stark apparatus, and heated under reflux stirring under argon for 120 h. The material was then filtered, and the filter cake washed with organic solvents (MeOH x 3, DCM, x 1), isolating the salt form **126** (130 mg, 28%), which was then washed with 7M $NaOH_{(aq)}$ to give phenanthridine **127** as a red solid for characterisation purposes. δ_H (400 MHz, d_6-DMSO): 7.94 (1H, s, H7), 7.69 - 7.62 (3H, m, H2', H4', H6'), 7.59 (1H, s, H10), 7.53 (2H, d, *J* = 7.9 Hz, H2'', H6''), 7.48 - 7.41 (4H, m, H3', H5', H3'', H5''), 7.38 - 7.33 (1H, t, *J* = 7.4 Hz, H4''), 7.30 (1H, d, *J* = 9.3 Hz, H1), 7.0 (1H, dd, *J* = 9.3, 2.2 Hz, H2), 6.93 (1H, d, *J* = 2.2 Hz, H4), 6.52 (2H, d, br, D_2O, N**H**$_2$), 5.46 (2H, s, OC**H**$_2$Ph). δ_c (100 MHz, d_6-DMSO): 153.03 (C), 150.55 (C), 152.52 (C), 150.05 (C), 148.22 (C), 137.89 (C), 136.02 (C), 134.32 (C), 130.05 (CH), 128.87 (CH), 128.71 (CH), 128.53 (CH), 128.05 (CH), 128.01 (CH), 127.29 (CH), 125.53 (CH), 121.06 (CH), 118.45 (C), 115.92 (C), 109.05 (CH), 102.58 (CH), 102.53 (CH), 70.38 (CH_2). IR (ATR cm^{-1}): 3341 (NH), 3171 (NH), 1636 (C=N), 1597 (C_{Ar}=C_{Ar}), 1528 (NO_2). MS (FAB): 422.4 [$(M+H)^+$, 100%], 329.2 [$(M - C_6H_7N)^+$, 73], 307.2 [$(M - C_7H_7 - NO_2 + Na)^+$, 74]. HRMS: 422.1501. $C_{26}H_{19}N_3O_3$ requires 422.1505. MP (as tosylate salt): 245 - 248 °C.

3,8-Bis(carbobenzylamino)-6-phenylphenanthridine **138**

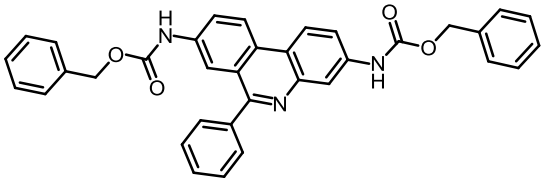

138

3,8-Diamino-6-phenylphenanthridine **133** (108 mg, 0.378 mmol, 1.00 eq.) was dissolved in THF (2.0 mL) and cooled to 0 ˚C stirring under argon. $NaHCO_3$ (84 mg, 1.0 mmol, 2.6 eq.) was added followed by dropwise addition of benzyl chloroformate (3.0 mL, 21 mmol, 2.3 eq.), after which the mixture was allowed to warm to RT and stirred under argon for 72 h. The mixture was quenched into water then extracted with Et_2O (x 2). The organic layer was washed repeatedly with water then dried ($MgSO_4$), filtered and the solvent removed under reduced pressure. Column chromatography [SiO_2, dry loaded in THF, Pet. ether/EtOAc (1:1)] gave phenanthridine **138** as a solid (172 mg, 82%). R_f = 0.64 in Pet. ether/EtOAc (1:1). ^{1}H NMR (500 MHz, $CDCl_3$) δ 8.45 (d, *J* = 9.1 Hz, H10), 8.37 (d, *J* = 9.0 Hz, H1), 8.01 (1H, d, br, *J* = 8.3 Hz, H9), 7.98 (1H, d, *J* = 2.2 Hz, H4), 7.92 (1H, d, br, *J* = 8.7 Hz, H2), 7.87 (1H, d, *J* = 2.2 Hz, H7) 7.65 (2H, dd, *J* = 7.8, 1.5 Hz, H2'', H6''), 7.50 - 7.43 (3H, m, H3'', H4'', H5''), 7.41 (2H, dd, *J* = 7.8, 1.3 Hz, H2''', H6'''), 7.39 - 7.29 (8H, m, H3''', H4''', H5''', Ph'), 7.13 (2H, s, br, NH), 5.23 (2H, s, 8-$NHCO_2C$**H**$_2$), 5.19 (2H, s, 3-$NHCO_2C$**H**$_2$). ^{13}C NMR (126 MHz, $CDCl_3$) δ 161.28 (C), 153.31 (C), 143.83 (C), 139.39 (C), 138.05 (C), 136.39 (C), 135.94

(C), 135.83 (C), 129.57 (CH), 129.44 (C), 128.82 (CH), 128.64 (CH), 128.62 (CH), 128.41 (CH), 128.28 (CH), 125.22 (C), 123.06 (CH), 122.62 (CH), 119.64 (CH), 119.10 (CH), 117.90 (CH), 116.80 (CH), 67.22 (CH_2). IR (ATR cm^{-1}): 3294 (N-H), 3059 (C_{Ar}-H), 3034 (C_{Ar}-H), 1703 (C=O), 1622 (C=N), 1587 (C_{Ar}=C_{Ar}), 1547 1587 (C_{Ar}=C_{Ar}), 1517 (C_{Ar}=C_{Ar}), 1056 (C-O). MS (NSI^+): 1107 [$(2M+H)^+$, 33%], 554 [$(M+H)^+$, 100]. HRMS: 554.2066. $C_{35}H_{28}N_3O_4$ requires 554.2076. MP: 93 - 95 ˚C.

3,8-Bis(carbomethoxyamino)-6-phenylphenanthridine **139**

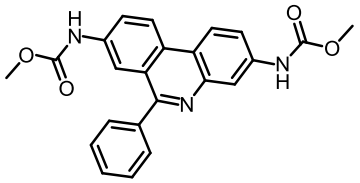

139

3,8-Diamino-6-phenylphenanthridine **133** (510 mg, 1.79 mmol, 1.00 eq.) in dry pyridine (3.0 mL) was cooled to 0 ˚C stirring under argon. Methyl chloroformate (0.55 mL, 7.1 mmol, 4.0 eq.) was added dropwise then the mixture heated to RT and stirred under argon for 20 h. The mixture was filtered, washed with water then the solid filtered and washed with MeOH. The solvent was removed under reduced pressure then the solid residue washed with 1 M $NaOH_{(aq)}$, filtered and acidified with 1 M $HCl_{(aq)}$ then dissolved in MeOH and the solvent removed under reduced pressure. The solid was dried by azeotrope with PhMe to give methylcarbamate **139** as the orange hydrochloride salt (649 mg, 83%). For analysis a sample (21 mg) of the salt was loaded onto a strata WCX ion exchange resin in MeOH and washed with further MeOH, then eluted with 7 M NH_3/MeOH solution and removing the solvent under reduced pressure (19 mg, quant.). ^{1}H NMR (500 MHz, CD_3OD) δ 8.48 (1H, d, *J* = 8.9 Hz, H10), 8.40 (1H, d, *J* = 8.9 Hz, H1), 8.12 (1H, d, *J* = 2.2 Hz, H4), 8.07 (1H, d, *J* = 1.7 Hz, H7), 7.88 (1H, dd, *J* = 8.9, 1.7 Hz, H9), 7.74 (1H, dd, *J* = 8.9, 2.0 Hz, H2), 7.67 - 7.62 (2H, m, H2', H6'), 7.60 - 7.54 (3H, m, H3', H4', H5'), 3.80 (3H, s, 8-$NHCO_2C\mathbf{H}_3$), 3.73 (3H, s, 3-$NHCO_2C\mathbf{H}_3$). ^{13}C NMR (126 MHz, CD_3OD) δ 161.49 (C), 154.94 (C), 154.91 (C), 142.90 (C), 139.18 (C), 139.07 (C), 137.64 (C), 129.35 (CH), 128.90 (C), 128.58 (CH), 128.02 (CH), 124.81 (C), 123.01 (CH), 122.45 (CH), 122.17 (CH), 119.20 (CH), 119.09 (CH), 115.96 (CH), 51.24 (CH_3). IR (ATR cm^{-1}, as HCl salt): 3221 (N-H), 3056 (C_{Ar}-H), 2954 (C-H), 1729 (C=O), 1701 (C=O), 1622 (C=N), 1586 (C_{Ar}=C_{Ar}), 1575 (C_{Ar}=C_{Ar}), 1525 (C_{Ar}=C_{Ar}), 1071 (C-O). MS (NSI^+): 1204 [$(3M+H)^+$, 9%], 803 [$(2M+H)^+$, 49], 402 [$(M+H)^+$, 100]. HRMS: 402.1446. $C_{23}H_{20}N_3O_4$ requires 402.1448. MP (as HCl salt): Decomposition above 325 ˚C.

3,8-Bis(carboethoxyamino)-6-phenylphenanthridine **140**

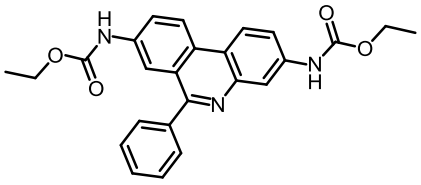

140

3,8-Diamino-6-phenylphenanthridine **133** (4.05 g, 14.2 mmol, 1.00 eq.) was dissolved in THF (112 mL) and cooled to – 11 ˚C stirring under argon. $NaHCO_3$ (2.92 g, 34.8 mmol, 2.45 eq.) was added followed by dropwise addition of ethyl chloroformate (3.3 mL, 35 mmol, 2.4 eq.), after which the

mixture was stirred for 3 h then allowed to warm to RT and stirred under argon for 44 h. The mixture was quenched into MeOH then the solvent removed under reduced pressure. The residue was partitioned between ETOAc and 1 M $NH_{3(aq)}$, and the organic layer washed with water (x 3) and concentrated under reduced pressure, then 1 M $HCl_{(aq)}$ was added and the mixture cooled to ~5 ˚C for 16 h. The mixture was filtered and washed with EtOAc, then the filter cake dissolved in DCM/MeOH/1 M $NH_{3(aq)}$ and the solvent removed under reduced pressure. The residue was dissolved in EtOAc and washed with water (x 2), dried ($MgSO_4$), filtered and the solvent removed under reduced pressure, giving bisethyl carbamate **140** as a yellow solid (5.82 g, 95%). ^{1}H NMR (400 MHz, DMSO) ^{1}H NMR (400 MHz, DMSO) δ 10.02 (1H, s, br, 8-N**H**CO_2Et), 9.98 (1H, s, 3-N**H**CO_2Et), 8.73 (1H, d, *J* = 9.1 Hz, H10), 8.63 (1H, d, *J* = 9.1 Hz, H1), 8.31 (1H, d, br, *J* = 1.6 Hz, H4), 8.22 (1H, d, *J* = 2.1 Hz, H7), 7.96 (1H, dd, *J* = 9.0, 2.0 Hz, H9), 7.81 (1H, dd, *J* = 8.9, 2.2 Hz, H2), 7.74 - 7.67 (2H, m, H2', H6'), 7.65 - 7.53 (3H, m, H3', H4', H5'), 4.19 (2H, q, *J* = 7.1 Hz, 8-NHCO$_2$C**H**$_2$CH$_3$), 4.11 (2H, q, *J* = 7.1 Hz, 3-NHCO$_2$C**H**$_2$CH$_3$), 1.29 (3H, t, *J* = 7.1 Hz, 8-NHCO$_2$CH$_2$C**H**$_3$), 1.22 (3H, t, *J* = 7.1 Hz, 8-NHCO$_2$CH$_2$C**H**$_3$). ^{13}C NMR (101 MHz, DMSO) δ 160.38 (C), 153.59 (C), 153.55 (C), 143.29 (C), 139.51 (C), 139.28 (C), 137.89 (C), 129.54 (CH), 128.58 (CH), 128.20 (CH), 124.39 (C), 123.11 (CH), 122.79 (CH), 122.70 (CH), 118.92 (CH), 118.46 (C), 116.44 (CH), 115.05 (CH), 60.35 (CH_2), 14.50 (CH_3), 14.43 (CH_3). IR (ATR cm^{-1}): 3293 (N-H), 2917 (C-H), 2852 (C-H), 1707 (C=O), 1620 (C=N), 1590 (C_{Ar}=C_{Ar}), 1549 (C_{Ar}=C_{Ar}), 1522 (C_{Ar}=C_{Ar}), 1071 (C-O). MS (EI$^+$): 429 ($M^{+\cdot}$, 70%), 383 ($M^{+\cdot}$ – C_2H_5OH, 100), 336 [$(M – H)^+$ – $2C_2H_5OH$, 80], 310 [$(M – H)^+$ – $2C_2H_5OH$ – CO, 63], 295 (37). HRMS: 429.1688. $C_{25}H_{23}O_4N_3$ requires 429.1689. MP: 128 - 132 ˚C. This compound is known in literature.[417]

1,6-Hexanetrifluoromethanesulfonyl **142**

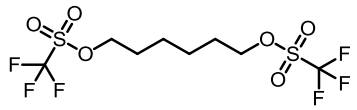

142

Triflic anhydride (10.0 g, 35.4 mmol, 1.00 eq.) was weighed under argon then dissolved in dry DCM (30 mL) and stirred at 0 ˚C under argon. Dry pyridine (2.8 mL, 35 mmol, 0.98 eq.) was added followed by 1,6-hexanediol **141** (1.70 mg, 14.4 mmol, 0.41 eq.). After stirring under argon at RT for 35 min the reaction mixture was quenched and washed with water (x 2) and the organic layer dried ($MgSO_4$), filtered and the solvent removed under reduced pressure. The residue was redissolved in Et_2O and filtered through a combination of SiO_2 and $MgSO_4$. Product **142** was isolated as an oil (3.44 g, 63%). δ_H (400 MHz, $CDCl_3$): 4.55 (4H, t, *J* = 6.28 Hz, C**H**$_2$OTf), 1.94 - 1.79 (4H, m, C**H**$_2$CH$_2$OTf), 1.55 - 1.48 (4H, m, C**H**$_2$CH$_2$CH$_2$OTf) δ_c (100 MHz, $CDCl_3$): 118.64 (q, *J* = 254 Hz), 29.04, 24.58. ^{1}H NMR data agrees with literature.[177]

6-Trifluoromethylsulfonylhex-1-yltriphenylphosphonium trifluoromethylsulfonate **143**

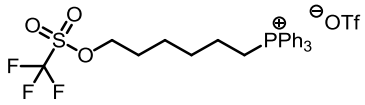

143

Triflate **142** (197 mg, 0.515 mmol, 1.00 eq.) was dissolved in dry Et_2O (2.6 mL) and stirred under argon. Triphenylphosphine (124 mg, 0.43 mmol, 0.83 eq., previously dried by azeotrope in PhMe) was added and the mixture stirred for 1 h. The solvent was then removed under reduced pressure. The resulting solid **143** (318 mg) was of > 90% estimated purity by ^{1}H NMR. ^{1}H NMR (500 MHz, $CDCl_3$) δ 7.91 - 7.61 (15H, m, PPh_3), 4.61 - 4.52 (2H, m, CH_2-6), 3.48 - 3.30 (2H, m, CH_2-1), 1.93 - 1.76 (2H, m, CH_2-5), 1.75 - 1.32 (6H, m, CH_2-2, CH_2-3, CH_2-4).The stability of this compound was too poor to collect further data.

6-Benzyloxyhexan-1-ol **145**

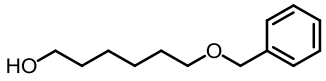

145

1,6-Hexanediol **141** (49.34 g, 417.4 mmol, 7.075 eq.) was melted and dried by azeotrope with PhMe, which was removed under reduced pressure. Dry DMF (120 mL) was added and the reaction cooled to 0 ˚C stirring under argon. NaH (60% dispersion in mineral oil, 2.52 g, 63.0 mmol, 1.07 eq.) was added portionwise, then after 30 min stirring followed by dropwise addition of benzyl bromide (7.0 mL, 59 mmol, 1.0 eq.). After 10 min stirring the mixture was heated to 60 ˚C for 48 h. The solvent was then removed under reduced pressure. Column chromatography [SiO_2, loaded with Pet. ether, Pet. ether/Et_2O (1:1)] gave alcohol **145** as an oil (11.71 g, 95%). R_f = 0.11 Pet. ether/EtOAc (3:1). ^{1}H NMR (400 MHz, $CDCl_3$) δ 7.39 - 7.24 (5H, m, Ph), 4.50 (2H, s, C**H**$_2$Ph), 3.64 (2H, t, *J* = 6.4 Hz, C**H**$_2$OH), 3.47 (2H, t, *J* = 6.6 Hz, C**H**$_2$OBn), 1.70 - 1.52 (4H, m, CH_2-2, CH_2-5), 1.47 - 1.33 (4H, m, CH_2-3, CH_2-4), 1.22 (1H, s, br, OH). ^{13}C NMR (126 MHz, $CDCl_3$) δ 138.64, 128.36, 127.64, 127.51, 72.89, 70.33, 62.97, 32.72, 29.72, 26.02, 25.58. Data is consistent with literature values.[418]

6-Benzyloxyhex-1-yltrifluoromethanesulfonate **146**

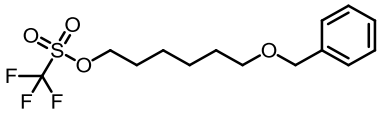

146

Trifluoromethanesulfonic anhydride (10 g, 35 mmol, 1.3 eq.) was dissolved with stirring in dry DCM (55 mL) and cooled to 0 ˚C under argon. Addition of dry pyridine (2.8 mL, 35 mmol, 1.3 eq.) was followed by allowing the mixture to warm to RT and adding alcohol **145** (5.58 g, 26.8 mmol, 1.00 eq.), then stirring for 2 h under argon. The mixture was diluted with DCM and washed with water (x 2). The washings were extracted with DCM and the combined organics dried ($MgSO_4$), filtered, the solvent removed under reduced pressure and the residue washed through a small plug of SiO_2 with dry Et_2O, then the solvent removed under reduced pressure to give trifluoromethanesulfonyl **146** as a brown oil (7.15 g, 78%). ^{1}H NMR (400 MHz, $CDCl_3$) δ 7.39 - 7.27

(5H, m, Ph), 4.53 (2H, t, *J* = 6.5 Hz, C**H**$_2$OSO$_2$CF$_3$), 4.50 (2H, s, OC**H**$_2$Ph), 3.48 (2H, t, *J* = 6.4 Hz, C**H**$_2$OBn), 1.83 (2H, quin., *J* = 6.9 Hz, CH$_2$-2), 1.63 (2H, *J* = 6.8 Hz, CH$_2$-5), 1.48 - 1.40 (4H, m, CH$_2$-3, CH$_2$-4). ^{1}H NMR matches literature values.[419]

3,8-Bis(carboethoxyamino)-5-(6'-benzyloxyhex-1'-yl)-6-phenylphenanthridinium trifluoromethanesulfonate **150**

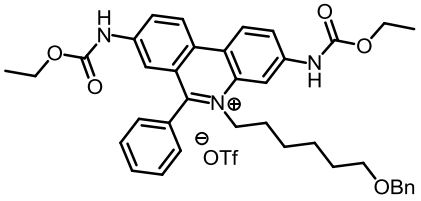

150

Phenanthridine **140** (208 mg, 0.484 mmol, 1.00 eq.) and 2,6-di*tert*butyl-4-methylpyridine (283 mg, 1.38 mmol, 2.87 eq.) were combined under argon then trifluoromethanesulfonate **146** (704 mg, 2.07 mmol, 4.31 eq.) was added as a solution in dry PhNO$_2$ (3.0 mL). After 72 h stirring under argon the mixture was transferred to SiO$_2$ in DCM and washed with additional DCM, followed by elution with DCM/MeOH (9:1). Repeated column chromatography [SiO$_2$, loaded in DCM, DCM/MeOH gradient elution (33:1) - (3:2)] gave a soft yellow residue which was 2:1 Phenanthridinium **150** to DCM by weight (26 mg, 7%). ^{1}H NMR (400 MHz, CDCl$_3$) δ 9.08 (1H, s, br, 3-N**H**CO$_2$Et), 8.55 (1H, d, br, *J* = 1.2 Hz, 8-N**H**CO$_2$Et), 8.34 (1H, d, *J* = 9.4 Hz, H1), 8.31 (1H, s, br, H4), 8.28 (1H, d, *J* = 9.3 Hz, H10), 8.13 (1H, dd, br, *J* = 9.2, 1.4 Hz, H2), 8.06 (1H, dd, *J* = 9.1, 2.1 Hz, H9), 7.75 (1H, d, *J* = 1.8 Hz, H7), 7.72 - 7.62 (3H, m, H3'', H4'', H5''), 7.38 (2H, dd, *J* = 7.5, 1.7 Hz, H2'', H6''), 7.29 - 7.13 (5H, m, OCH$_2$**Ph**), 4.62 (2H, s, br, CH$_2$-1'), 4.37 (2H, s, OC**H**$_2$Ph), 4.11 (2H, q, *J* = 7.1 Hz, 3-NHCO$_2$C**H**$_2$CH$_3$), 4.02 (2H, q, *J* = 7.1 Hz, 8-NHCO$_2$C**H**$_2$CH$_3$), 3.31 (2H, t, *J* = 6.4 Hz, CH$_2$-6'), 1.83 (2H, s, br, CH$_2$-2'), 1.48 - 1.38 (2H, m, CH$_2$-5'), 1.29 - 1.10 (4H, m, CH$_2$-3', CH$_2$-4'), 1.23 (3H, t, *J* = 7.1 Hz, 3-NHCO$_2$CH$_2$C**H**$_3$), 1.14 (3H, t, *J* = 7.1 Hz, 8-NHCO$_2$C**H**$_2$CH$_3$). ^{13}C NMR (126 MHz, CDCl$_3$) δ 161.94 (C), 154.07 (C), 153.58 (C), 143.36 (C), 140.03 (C), 138.63 (C), 133.92 (C), 131.83 (CH), 130.77 (C), 130.59 (C), 130.39 (CH), 129.83 (CH), 128.27 (CH), 128.03 (CH), 127.54 (CH), 127.44 (CH), 127.39 (CH), 125.02 (C), 124.38 (CH), 122.70 (CH), 120.89 (C), 120.67 (q, *J* = 320.3 Hz, CF$_3$), 118.07 (CH), 106.65 (CH), 72.87 (CH$_2$), 70.03 (CH$_2$), 61.61 (CH$_2$), 61.51 (CH$_2$), 54.79 (CH$_2$), 29.53 (CH$_2$), 29.24 (CH$_2$), 26.09 (CH$_2$), 25.28 (CH$_2$), 14.24 (CH$_3$), 14.21 (CH$_3$). IR (ATR cm^{-1}): 3259 (N-H), 2943 (C-H), 2858 (C-H), 1727 (C=O), 1622 (C=N), 1596 (C$_{Ar}$=C$_{Ar}$), 1552 (C$_{Ar}$=C$_{Ar}$), 1519 (C$_{Ar}$=C$_{Ar}$). MS (NSI$^+$): 620 [M$^+$ (phenanthridinium cation), 100%]. HRMS: 620.3104. C$_{38}$H$_{42}$N$_3$O$_5$ requires 620.3119. MP: 73 - 85 ˚C.

3,8-Bis(carboethoxyamino)-5-(1'-hexan-6-ol)-6-phenylphenanthridinium trifluoromethanesulfonate **151**

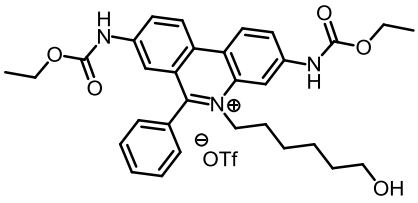

151

Phenanthridinium salt **150** (260 mg, 0.338 mmol, 1.00 eq.) was combined in MeOH (3.0 mL) with 10% palladium on carbon (50 mg, 0.047 mmol, 0.14 eq.), then the solution frozen in $N_{2(l)}$, exposed to vacuum and then sealed and warmed to until the mixture melted. This process was repeated (x 2), then $H_{2(g)}$ bubbled through the solution for 20 min and the reaction stirred at RT under $H_{2(g)}$ for 20 h. The mixture was filtered through celite, eluting with DCM and MeOH, then dried ($MgSO_4$), filtered and the solvent removed under reduced pressure. Column chromatography [SiO_2, loaded in DCM followed by gradient elution DCM/MeOH (50:1) - (8:1)] gave alcohol **151** as a yellow foam (40 mg, 17%). R_f = 0.25 DCM/MeOH (17:3). ^{1}H NMR (400 MHz, DMSO) δ 10.57 (1H, s, br, 3-N**H**CO_2Et), 10.28 (1H, s, br, 8-N**H**CO_2Et), 9.08 (1H, d, *J* = 9.4 Hz, H1), 9.02 (1H, d, *J* = 9.2 Hz, H10), 8.68 (1H, s, br, H4), 8.26 (1H, dd, *J* = 9.3, 2.0 Hz, H2), 8.14 (1H, dd, *J* = 9.2, 1.9 Hz, H9), 7.86 - 7.73 (6H, m, H7, Ph), 4.53 (2H, s, br, CH_2-1'), 4.32 (1H, t, *J* = 5.1 Hz, OH), 4.26 (2H, q, *J* = 7.1 Hz, 3-NHCO$_2$C**H**$_2$CH$_3$), 4.09 (2H, q, *J* = 7.1 Hz, 8-NHCO$_2$C**H**$_2$CH$_3$), 1.97 (2H, s, br, CH_2-2'), 1.51 - 1.36 (2H, s, br, CH_2-5'), 1.35 - 1.09 (4H, m, CH_2-3', CH_2-4'), 1.32 (3H, t, *J* = 7.1 Hz, 3-NHCO$_2$CH$_2$C**H**$_3$), 1.20 (3H, t, *J* = 7.1 Hz, 8-NHCO$_2$CH$_2$C**H**$_3$). (ATR cm^{-1}): 3058 (C_{Ar}-H), 2939 (C-H), 2870 (C-H), 1729 (C=O), 1623 (C=N), 1596 (C_{Ar}=C_{Ar}), 1553 (C_{Ar}=C_{Ar}), 1519 (C_{Ar}=C_{Ar}). MS (ESI$^+$): 530 [M$^+$ (phenanthridinium cation), 100%]. HRMS: 530.2664. $C_{31}H_{36}N_3O_5$ requires 530.2649.

5-Nitro-2-(4'-nitrophenyl)aniline **157**

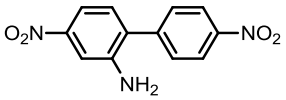

157

Biphenyl-2-ylamine **156** (13.8 g, 81.3 mmol, 1.00 eq.) was dissolved in concentrated $H_2SO_{4(aq)}$ (98%, 170 mL) at 0 ˚C with mechanical stirring. After the initial heat from neutralisation had dissipated KNO_3 (16.2 g, 161 mmol, 1.98 eq.) was added portion wise over 20 min. The mixture was then kept at 0 ˚C stirring for 4 h 30 min before being quenched slowly into ice water then basified with $NaOH_{(aq)}$ (7 M). The suspension formed was filtered. The filter cake was dissolved in acetone and solvent removed under reduced pressure. The solid was washed repeatedly with water to remove inorganic impurities, then transferred in acetone and dried by azeotrope in PhMe (x 3) before being dried under vacuum at 80 ˚C for 6 h. To give amine **157** as an orange solid (17.1 g, 84%). δ_H (400 MHz, d_6-DMSO): 8.33 (2H, d, *J* = 8.8 Hz, H3', H5'), 7.76 (2H, d, *J* = 8.8 Hz, H2', H6'), 7.65 (1H, d, *J* = 2.4 Hz, H6), 7.45 (1H, dd, *J* = 8.4, 2.4 Hz, H4), 7.29 (1H, d, *J* = 8.4 Hz, H3), 5.76 (2H, s, N**H$_2$**). δ_c (400 MHz, d_6-DMSO): 148.21 (C), 146.75 (C), 146.66 (C), 144.61 (C), 131.24 (CH), 129.95 (CH), 129.03 (C), 123.95 (CH), 110.36 (CH), 109.03 (CH). IR (ATR cm^{-1}): 3470 (NH), 3381 (NH), 3106 (C_{Ar}-H), 3086 (C_{Ar}-H), 1632 (C_{Ar}=C_{Ar}), 1597 (C_{Ar}=C_{Ar}), 1501 (NO_2), 1337 (NO_2). MS (CI) 260 [(M+H)$^+$, 9%), 230, 200 [(M+H)$^+$ – $H_2N_2O_2$, 27], 113, (47), 85 (73), 71 (100). HRMS: 260.0672.

$C_{12}H_{10}O_4N_3$ requires 260.0671. MP: 199 - 205 ºC. Compound has been previously synthesised but limited data was reported.[143]

N-[5'-Nitro-2'-(4''-nitrophenyl)phenyl]benzamide **160**

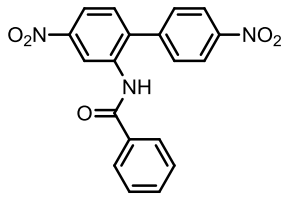

160

Adapted from a literature procedure.[185] Dry NEt_3 (0.15 mL, 1.1 mmol, 1.1 eq.) was added to a solution of amine **157** (295 mg, 0.99 mmol, 1.00 eq.) in dry DCM (8.4 mL) stirring under argon, followed by dropwise addition of benzoyl chloride (180 µL, 1.55 mmol, 1.57 eq.). After 1 h stirring under argon the mixture was quenched into 0.5 M $HCl_{(aq)}$, then extracted into DCM and washed (0.5 M $HCl_{(aq)}$ x 1, 0.5 M $NaOH_{(aq)}$ x 2). The collected organic layer was dried ($MgSO_4$), filtered, then the solvent removed under reduced pressure and the solid dried by azeotrope in PhMe and then further evaporated with $CHCl_3$. The material was crystallised (acetone/water) to give the amide **160** (267 mg, 74%) as a solid. δ_H (400 MHz, d_6-DMSO): 10.52 (1H, s, br, N**H**CO), 8.59 (1H, d, *J* = 2.4 Hz, H6'), 8.41 (2H, d, *J* = 8.8 Hz, H3'', H5''), 8.36 (1H, dd, *J* = 8.6, 2.4, H4'), 7.94 - 7.88 (4H, m, H2'', H2, H6, H6''), 7.88 (1H, d, *J* = 8.6 Hz, H3'), 7.69 (1H, tt, *J* = 7.4 Hz, 1.3 Hz, H4) 7.64 - 7.56 (2H, m, H3, H5). δ_c (400 MHz, d_6-DMSO): 165.76 (C), 147.42 (C), 147.04 (C), 144.52 (C), 141.61 (C), 136.49 (C), 133.79 (C), 131.89 CH), 131.71 (CH), 129.82 (CH), .128.44 (CH), 127.64 (CH), 123.63 (CH), 121.98 (CH), 121.02 (CH). IR (ATR cm^{-1}): 3214 (CON-H), 1645 (C=O), 1597 (C_{Ar}=C_{Ar}), 1510 (NO_2), 1341 (NO_2). MP: 232 °C. MS (ESI^-): 362 [$(M–H)^–$, 100]. HRMS: 362.0767. $C_{19}H_{12}N_3O_5$ requires 362.0782.

6-(Tetrahydropyran-2'-yloxy)hexan-1-ol **161**

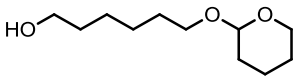

161

Previously dried by azeotrope with PhMe, 1,6-hexanediol **141** (40.0 g, 338 mmol, 4.02 eq.) was melted at 60 ˚C stirring under argon. Addition of *para* toluenesulfonic acid monohydrate (3.0 g, 16 mmol, 0.2 eq.) appeared to cause some precipitation, so the mixture was heated to 90 ˚C and allowed to cool back to 50 ˚C prior to addition of 3,4-dihydropyran (7.7 mL, 84 mmol, 1.0 eq.) and stirring for 72 h at this temperature under argon. The reaction mixture was washed repeatedly with water then the solvent removed under reduced pressure. Column chromatography [SiO_2, Pet. ether/EtOAc (1:1)] gave the alcohol **161** as an oil (10.3 g, 61%). Pet. ether/EtOAc (1:1) R_f = 0.39. δ_H (400 MHz, $CDCl_3$): 4.57 (1H, dd, *J* = 4.5, 2.8 Hz, H2'), 3.86 (1H, ddd, *J* = 11.1, 7.3, 3.6 Hz, H6'$_{ax}$), 3.78 - 3.69 (1H, m, C**H**^{A}H^{B}OTHP), 3.68 - 3.61 (2H, m, CH_2OH), 3.54 - 3.47 (1H, m, H6'$_{eq}$), 3.39 (1H, m, CH^A**H**^{B}OTHP), 1.89 - 1.76 (1H, m, H3') 1.76 - 1.67 (1H, m), 1.67 - 1.47 (8H, m, CH_2), 1.47 - 1.34 (4H, m, CH_2), 1.28 (1H, s, br, O**H**). ^{1}H NMR data agrees with literature.[420]

2- (6'-Iodohex-1'-yloxy)tetrahydropyran **162**

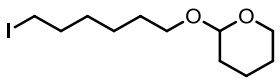

162

Triphenylphosphine (2.62 g, 10.0 mmol, 2.13 eq.) and imidazole (664 mg, 9.75 mmol, 2.07 eq.) were dried by azeotrope in PhMe then dissolved in dry DCM (30 mL). Iodine (2.55 g, 9.96 mmol, 2.12 eq.) was added at 0 ˚C to the stirring solution. After 15 min the mixture was warmed to RT and alcohol **161** (950 mg, 4.70 mmol, 1.00 eq.) was added dropwise in DCM (1.0 mL). The mixture was then stirred under argon for 4 h, then quenched into water and extracted in DCM. The solvent was removed under reduced pressure. Column chromatography [SiO_2, Pet. ether/EtOAc (19:1)] gave iodide **162** as an oil (620 mg, 42%). R_f = 0.58 Pet. ether/EtOAc (19:1). δ_H (400 MHz, $CDCl_3$): 4.57 (1H, dd, *J* = 4.4, 2.8 Hz, H1), 3.92 - 3.81 (1H, ddd, *J* = 11.0, 7.3, 3.4 Hz, $H6_{ax}$), 3.74 (1H, dt, *J* = 9.6, 6.7 Hz, C**H**^{A}H^{B}OTHP), 3.54 - 3.47 (1H, m, $H6_{eq}$), 3.39 (1H, dt, *J* = 9.6, 6.5 Hz, CH^A**H**^{B}OTHP), 3.19 (2H, t, *J* = 7.1 Hz, CH_2I), 1.90 - 1.78 (3H, m, C**H**$_2$$CH_2I$, 1 of CH_2) 1.76 - 1.67 (1H, m, 1 of CH_2), 1.66 - 1.48 (6H, m, 3 x CH_2), 1.48 - 1.35 (4H, m, 2 x CH_2). δ_C (100 MHz, $CDCl_3$): 98.80, 67.31, 62.29, 33.37, 30.67, 30.22, 29.43, 25.40, 25.14, 19.60, 6.97. ^{1}H and ^{13}C NMR match literature data.[421]

6-(Tetrahydropyran-2'-yloxy)hexanal **164**

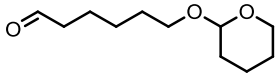

164

Oxalyl chloride (10.0 mL, 120 mmol, 2.9 eq.) was added at –78˚C to DCM (160 mL) stirring under argon. After 10 min DMSO (8.5 mL, 120 mmol, 2.9 eq.) was syringed into the mixture which was then stirred for a further 40 min. Alcohol **161** (8.3 g, 41 mmol, 1.0 eq.) was then added as a DCM solution (80 mL) and the reaction allowed to stir at −78 ˚C under argon for 2 h. NEt_3 (30.0 mL, 215 mmol, 5.24 eq.) was then added and the reaction allowed to warm to RT overnight. The mixture was washed with 0.5 M $HCl_{(aq)}$, which was back extracted with DCM. The combined organics were washed with water, then dried ($MgSO_4$), filtered and the solvent removed under reduced pressure. The residue was washed through SiO_2 with Et_2O, then dried ($MgSO_4$), filtered and the solvent removed under reduced pressure, giving aldehyde **164** as an oil (7.7 g, 93%). (400 MHz, $CDCl_3$): 9.77 (1H, t, *J* = 1.7 Hz, C(O)**H**), 4.60 - 4.54 (1H, m, H2'), 3.92 - 3.81 (1H, m, H6'), 3.80 - 3.69 (1H, m, C**H**^{A}H^{B}OTHP) 3.58 - 3.45 (1H, m, H6'), 3.43 - 3.35 (1H, m, CH^A**H**^{B}OTHP), 2.45 (2H, td, *J* = 7.3, 1.8 Hz, C**H**$_2$C=O), 1.9 - 1.3 (12H, m, CH_2). Data consistent with literature.[422]

Methyl 5-{[5'-nitro-2'-(4''-nitrophenyl)phenyl]carbamoyl}pentanoate **172**

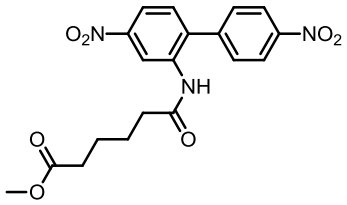

172

6-Methoxy-6-oxohexanoic acid **171** (1.0 mL, 5.8 mmol, 2.0 eq.) was dissolved in $SOCl_2$ (3.0 mL, 41.2 mmol, 7.1 eq.) and heated stirring under reflux and argon for 13 h. The $SOCl_2$ was then removed under reduced pressure. Some of this material (1.0 g, 5.6 mmol, 1.9 eq.) was dissolved in dry DCM (3.0 mL) and added dropwise to a stirring solution of amine **157** (772 mg, 2.98 mmol, 1.00 eq.) in dry DCM (30 mL) under argon. After 17 h stirring the mixture was quenched into water, then the layers separated and the organic layer washed with 0.5 M $HCl_{(aq)}$ (x 1) and 0.5 M $NaOH_{(aq)}$ (x 2), then dried ($MgSO_4$) and filtered. The solvent was evaporated off at atmospheric pressure then traces removed under vacuum. The mixture was then dry loaded onto celite in DCM. Column chromatography [SiO_2, Pet. ether/EtOAc, gradient elution (7:3 to 3:7)] gave 1.02 g (86%) gave amide as a solid **172**. δ_H (400 MHz, $CDCl_3$): 9.10 (1H, d, *J*= 1.8 Hz, H6') 8.40 (2H, d, *J* = 8.8, H3'', H5''), 8.09 (1H, dd, *J* = 8.4, 2.3 Hz, H4') 7.76 (2H, d, *J* = 8.8 Hz, H2'', H6''), 7.43 (1H, d, *J* = 8.4 Hz, H3'), 7.24 (1H, s, br, N**H**CO), 3.65 (3H, s, $CO_2C\mathbf{H}_3$), 2.33 (2H, t, *J* = 7.0 Hz, $C\mathbf{H}_2CO_2Me$) 2.28 (2H, t, *J* = 6.9 Hz, $C\mathbf{H}_2CONH$), 1.72 - 1.59 (4H, m, $NCOCH_2C\mathbf{H}_2C\mathbf{H}_2CH_2CO_2Me$). δ_C (100 MHz, $CDCl_3$): 173.83 (C), 170.99 (C), 148.46 (C), 148.16 (C), 143.05 (C), 136.45 (C), 135.68 (C), 130.70 (CH), 130.06 (CH), 124.59 (CH), 119.54 (CH), 118.03 (CH), 51.66 (CH_3), 36.96 (CH_2), 33.42 (CH_2), 24.59 (CH_2), 24.01 (CH_2). IR (ATR cm^{-1}): 3225 (NH_2), 3086 (C_{Ar}-H), 2940 (C-H), 2862 (C-H), 1728 (C=O), 1651 (C=O), 1597 (C_{Ar}=C_{Ar}), 1528 (C_{Ar}=C_{Ar}), 1505 (NO_2), 1335 (NO_2). MS (FAB/NOBA): 402 [$(M+H)^+$, 62%], 370 [$(M+H)^+$ – MeOH, 13], 154 (100). HRMS (FAB): 402.1298 requires 402.1301 $C_{19}H_{20}O_7N_3$. MP: 154 - 156 °C.

Methyl 5-N-{[5'-nitro-2'-(4''-nitrophenyl)phenyl]carbamoyl}pentanoic acid **173**

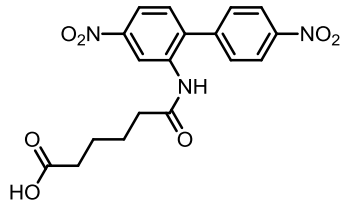

173

Ester **172** (199 mg, 0.50 mmol, 1.00 eq.) was suspended in ethanol (2.5 mL) and 7 M $KOH_{(aq)}$ was added (0.25 mL, 1.8 mmol, 3.5 eq.). The solution was then stirred for 17 h at RT under argon and quenched into water. The mixture was extracted with Et_2O and EtOAc (x 2). The aqueous layer was acidified with 0.5 M $HCl_{(aq)}$ and the precipitate filtered off. After drying the solid was dissolved in acetone then dried ($MgSO_4$) and filtered. After removal of solvent under reduced pressure the product **173** was collected as a beige solid (147 mg, 77%).δ_H (400 MHz, CD_3OD): 8.50 (1H, d, *J* = 2.3 Hz, H6'), 8.35 (2H, d, *J* = 8.8 Hz, H3'', H5''), 8.20 (1H, dd, *J* = 8.5, 2.3 Hz, H4'), 7.67 (2H, d, *J* = 8.8 Hz, H2'', H6''), 7.63 (1H, d, *J* = 8.5 Hz, H3'), 2.30 (2H, t, *J* = 7.1 Hz, $C\mathbf{H}_2CO_2H$), 2.27 (2H, t, *J* = 7.1 Hz, $C\mathbf{H}_2CONH$), 1.66 - 1.49 (4H, m, $CH_2C\mathbf{H}_2C\mathbf{H}_2CH_2$). δ_c IR (ATR cm^{-1}): 3233 (NH), 3086 (C_{Ar}-H), 3032 (C_{Ar}-

H), 2940 (C-H), 2870 (C-H), 1705 (C=O), 1659 (C=O), 1597 (C_{Ar}=C_{Ar}), 1528 (C_{Ar}=C_{Ar}), 1505 (NO_2), 1335 (NO_2). MP: 187 °C. Used without further analysis.

6-{[5'-Nitro-2'-(4''-nitrophenyl)phenyl]amino}hexan-1-ol **174**

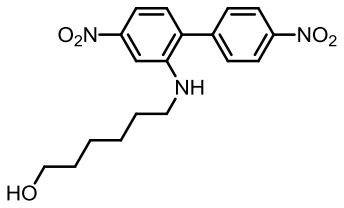

174

BH_3-THF (24.6 mL of a 1 M solution, 24.6 mmol, 4.01 eq.) was added dropwise to a stirred solution of carboxylic acid **173** (2.38 g, 6.14 mmol, 1.00 eq.) in dry THF (30 mL) under argon. The mixture was then heated to reflux for 2 h. On cooling the solution was quenched into MeOH and filtered through $MgSO_4$ eluting with DCM and $CHCl_3$. The solvent was then removed under reduced pressure and the material dried by azeotrope with PhMe. Column chromatography [SiO_2, Pet. ether/EtOAc (1:1)] and drying under high vacuum gave **174** as a red solid (1.53 g, 69%). R_f = 0.41 in Pet. ether. ether/EtOAc (1:1). δ_H (400 MHz, $CDCl_3$): 8.36 (2H, d, *J* = 8.8 Hz, H3'', H5''), 7.61 (2H, d, *J* = 8.8 Hz, H2'', H6''), 7.63 - 7.60 (1H, m, H4'), 7.50 (1H, d, *J* = 2.2 Hz, H6'), 7.18 (1H, d, *J* = 8.2 Hz, H3'), 3.95 (1H, t, D_2O ex., *J* = 5.1 Hz, N**H**R), 3.65 (2H, td, *J* = 6.4, 5.3 Hz, C**H**$_2$OH), 3.18 (2H, td, *J* = 7.1, 5.4 Hz, C**H**$_2$NHR), 1.65 - 1.52 (4H, m, C**H**$_2$CH$_2$NH, C**H**$_2$CH$_2$OH), 1.45 - 1.35 (4H, m, CH$_2$CH$_2$C**H**$_2$-C**H**$_2$), 8.36 (1H, t, *J* = 5.3 Hz, O**H**). δ_c (400 MHz, $CDCl_3$): 149.47 (C), 147.72 (C), 145.84 (C), 144.37 (C), 130.53 (CH), 130.52 (C), 130.00 (CH), 124.57 (CH), 117.70 (CH), 104.97 (CH), 62.75 (CH_2), 43.77 (CH_2), 32.53 (CH_2), 28.89 (CH_2), 26.85 (CH_2), 25.46 (CH_2). IR (ATR cm^{-1}): 3626 (OH), 3356 (NH), 3109 (C_{Ar}-H), 2932 (C-H), 2862 (C-H), 1597 (C_{Ar}=C_{Ar}), 1512 (NO_2), 1335 (NO_2). MS (FAB): 360 [$(M+H)^+$, 100%], 154 (44). HRMS (FAB): 360.1560. $C_{18}H_{22}O_5N$ requires 360.1559. MP: 75 - 76 °C.

6'-{[5''-Nitro-2''-(4'''-nitrophenyl)phenyl]amino}hexan-1'-yl benzoate **175**

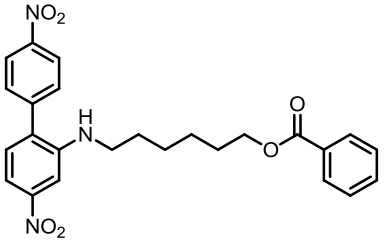

174

Alcohol **174** (542 mg, 1.51 mmol, 1.00 eq.) was dissolved in dry DCM (22 mL) stirring under argon. Dry NEt_3 (0.25 mL, 1.8 mmol, 1.2 eq.) was added, followed by benzoyl chloride (160 µL, 1.38 mmol, 0.914 eq.). The mixture was stirred for 20 h at RT under argon, then quenched into 1 M $NaOH_{(aq)}$ and extracted with DCM. The organic layer was washed with 1 M $HCl_{(aq)}$ and 1 M $NaOH_{(aq)}$, dried ($MgSO_4$), filtered and the solvent removed under reduced pressure. Column chromatography [SiO_2, loaded in minimal DCM, gradient elution with Pet. ether/EtOAc (4:1) - (1:1)] gave ester **175** as an orange solid (572 mg, 89%). R_f = 0.8 in Pet. ether/EtOAc (1:1). ^{1}H NMR (500 MHz, $CDCl_3$) δ 8.37 (2H, d, *J* = 8.9 Hz, H3''', H5'''), 8.04 (dd, *J* = 8.4, 1.3 Hz, H2, H6), 7.66 - 7.60 (3H, m, H4'', H2''', H6'''), 7.57 (1H, tt, *J* = 7.4, 1.4 Hz, H4), 7.52 (1H, d, *J* = 2.2 Hz, H6''), 7.45 (2H,

dd, *J* = 7.9, 7.5 Hz, H3, H5), 7.20 (1H, d, *J* = 8.2 Hz, H3''), 4.34 (2H, t, *J* = 6.6 Hz, CH_2-1'), 3.97 (1H, t, *J* = 5.2 Hz, NH), 3.21 (2H, dt, *J* = 5.5, 7.1 Hz, CH_2-6'), 1.86 - 1.76 (2H, quin., *J* = 6.6 Hz, CH_2-2'), 1.69 - 1.61 (2H, quin., *J* = 7.3 Hz, CH_2-5'), 1.56 - 1.41 (4H, m, CH_2-3', CH_2-4'). ^{13}C NMR (126 MHz, $CDCl_3$) δ 166.61 (C), 149.44 (C), 147.70 (C), 145.79 (C), 144.32 (C), 132.91 (CH), 130.54 (CH), 130.34 (C), 129.97 (CH), 129.49 (CH), 128.36 (CH), 124.56 (CH), 111.72 (CH), 104.95 (CH), 64.66 (CH_2), 43.74 (CH_2), 28.87 (CH_2), 28.61 (CH_2), 26.66 (CH_2), 25.68 (CH_2). IR (ATR cm^{-1}): 3405 (N-H), 2952 (C-H), 2936 (C-H), 2927 (C-H), 2857 (C-H), 1706 (C=O), 1614 (C_{Ar}=C_{Ar}), 1600 (C_{Ar}=C_{Ar}), 1585 (C_{Ar}=C_{Ar}), 1516 (NO_2), 1344 (NO_2). MS (NSI^+): 949 [$(2M+Na)^+$, 16%], 502 [$(M+K)^+$, 29], 486 [$(M+Na)^+$, 65], 464 [$(M+H)^+$, 100]. HRMS: 464.1814. $C_{25}H_{26}N_3O_6$ requires 465.1848. MP: 83 - 85˚ C.

6-{[5'-nitro-2'-(4''-nitrophenyl)phenyl]amino}hexan-1-yl trifluoroethanoate **180**

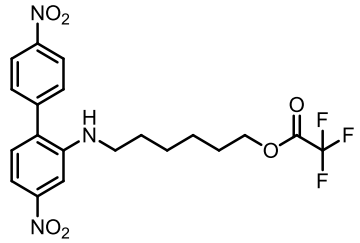

180

Alcohol **174** (49 mg, 0.13 mmol, 1.0 eq.) and benzaldehyde (30 µL, 0.29 mmol, 2.2 eq.) were combined in TFA (0.3 mL) then sealed in an argon flushed tube and heated to 120 ˚C for 2 days, then 125 ˚C for a further 3 days. The solvent was then removed under reduced pressure. Column chromatography gave trifluoroacetic ester **180** as a brown oil (13 mg, 21%). ^{1}H NMR (500 MHz, $CDCl_3$) δ 8.38 (2H, d, *J* = 8.9 Hz, H3'', H5''), 7.67 - 7.60 (3H, m, H2'', H6'', H4'), 7.52 (1H, d, *J* = 2.2 Hz, H6'), 7.21 (1H, d, *J* = 8.2 Hz, H3'), 4.37 (2H, t, *J* = 6.6 Hz, CH_2-1), 3.97 (1H, s, NH), 3.21 (2H, t, *J* = 7.1 Hz, CH_2-6), 1.83 - 1.74 (2H, m, CH_2-2), 1.68 - 1.60 (2H, m, CH_2-5), 1.50 - 1.39 (4H, m, CH_2-3,4). ^{13}C NMR (126 MHz, $CDCl_3$) δ 157.52 (q, *J* = 42.2 Hz, C), 149.44 (C), 147.72 (C), 145.73 (C), 144.30 (C), 130.57 (CH), 129.97 (CH), 124.55 (CH), 114.50 (q, *J* = 285.6 Hz, CF_3), 111.80 (CH), 104.94 (CH), 67.91 (CH_2), 43.71 (CH_2), 28.83 (CH_2), 28.01 (CH_2), 26.54 (CH_2), 25.29 (CH_2). IR (ATR cm^{-1}): 2934 (C-H), 2856 (C-H), 1784 (C=O), 1722, 1614 (C_{Ar}=C_{Ar}), 1597 (C_{Ar}=C_{Ar}), 1517 (NO_2), 1341 (NO_2). MS ($APCI^+$): 456 [$(M+H)^+$, 100%], 356 [$(M+H)^+ - CF_3CO_2H$], 260 [$(M+H)^+ - CF_3CO_2H - C_7H_{12}$]. HRMS: 456.1369. $C_{20}H_{21}F_3N_3O_6$ requires 456.1377.

2-Iodo-5-nitrobenzophenone **218**

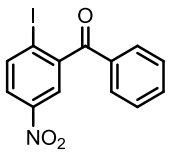

218

2-amino-5-nitrobenzophenone **217** (15.0 g, 42.5 mmol, 1.00 eq.) was dissolved in DMSO (300 mL). $H_2SO_{4(aq)}$ (30%, 300mL) was added to the stirring mixture at 0 ˚C over 5 min and the mixture stirred at this temperature for 30 min. A 3.7 M solution of $NaNO_{2(aq)}$ (70 mL, 260 mmol, 6.1 eq.) was added dropwise and the mixture stirred for 3 h at 0 ˚C. $KI_{(aq)}$ was added dropwise as an 5.6 M solution (90 mL, 500 mmol, 12 eq.) and the mixture allowed to warm to RT and stir for 48 h. The

reaction mixture was then diluted (H_2O) and extracted with EtOAc. The combined organics were washed sequentially with saturated $NaHCO_{3(aq)}$, saturated $NaS_2O_{3(aq)}$ and water before drying ($MgSO_4$), filtering and removal of solvent under reduced pressure. This gave benzophenone **218** as a yellow solid (21.4 g, 98%). ^{1}H NMR (500 MHz, $CDCl_3$) δ 8.16 (1H, d, *J* = 8.6 Hz, H3), 8.12 (1H, d, *J* = 2.6 Hz, H6), 8.02 (1H, dd, *J* = 8.6, 2.7 Hz, H4), 7.82 - 7.78 (2H, dd, *J* = 8.4, 1.3 Hz, H2', H6'), 7.68 (1H, ddt, *J* = 7.8, 7.0, 1.3 Hz, H4), 7.52 (2H, t, *J* = 7.8 Hz, H3', H5'). ^{13}C NMR (126 MHz, $CDCl_3$) δ 195.10 (C), 147.88 (C), 146.04 (C), 141.28 (CH), 134.71 (CH), 134.65 (C), 130.60 (CH), 129.21 (CH), 125.32 (CH), 123.00 (CH), 100.81 (C). Consistent with literature data.[255]

2-(4''-Methoxybenzene)-5-nitrobenzophenone **220**

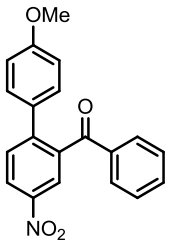

220

Benzophenone **218** (101 mg, 0.286 mmol, 1.00 eq.), 4-methoxyphenylboronic acid **219** (68 mg, 0.45 mmol, 1.5 eq.), $NaHCO_3$ (83 mg, 0.99 mmol, 3.4 eq.), PhMe (2.8 mL) and MeOH (0.3 mL) were combined and under argon and frozen with $N_{2(l)}$, then placed under vacuum and melted. This process was repeated twice, then $Pd(PPh_3)_4$ was added (34 mg, 0.030 mmol, 0.10 eq.) and the mixture heated to 90 ˚C stirring under argon for 16 h. The mixture was partitioned between Et_2O and water, then the aqueous further extracted with Et_2O and the combined organics dried ($MgSO_4$), filtered and the solvent removed under reduced pressure. Column chromatography [SiO_2, Pet. ether/EtOAc (7:1)] gave the coupled biaryl **220** as a thick yellow oil (41 mg, 43%). R_f = 0.24, Pet. ether/EtOAc (7:1). ^{1}H NMR (400 MHz, $CDCl_3$) δ 8.39 (1H, dd, *J* = 8.5, 2.4 Hz, H4), 8.35 (1H, d, *J* = 2.3 Hz, H6), 7.64 (3H, apparent d, *J* = 8.6 Hz, H3, H2', H6'), 7.48 (1H, tt, *J* = 7.5, 1.3 Hz, H4'), 7.33 (1H, t, *J* = 7.8 Hz, H3', H5'), 7.22 (2H, d, *J* = 8.8 Hz, H2'', H6''), 6.78 (2H, d, *J* = 8.8 Hz, H3'', H5''), 3.74 (3H, s, OCH_3). ^{13}C NMR (101 MHz, $CDCl_3$) δ 196.50 (C), 160.20 (C), 147.08 (C), 146.50 (C), 139.82 (C), 136.34 (C), 133.78 (CH), 131.11 (CH), 130.47 (C), 130.32 (CH), 130.00 (CH), 128.63 (CH), 124.99 (CH), 124.02 (CH), 114.35 (CH), 55.40 (CH_3). (ATR cm^{-1}): 3065 (C_{Ar}-H), 2961 (C-H), 2934 (C-H), 2837 (C-H), 1663 (C=O), 1604 (C_{Ar}=C_{Ar}), 1579 (C_{Ar}=C_{Ar}), 1516 (NO_2), 1342 (NO_2). MS (Cl^+): 334 [$(M+H)^+$, 100%], 304 [$(M+H)^+$ – OCH_3, 62]. HRMS: 334.1081. $C_{20}H_{16}O_4N$ requires 334.1079.

3-Nitrobenzophenone **228**

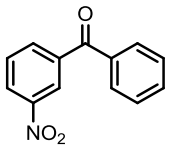

228

Iodobenzophenone **218** (107 mg, 0.300 mmol, 1.00 eq.), trifluoroborate salt **285** (70 mg, 0.35 mmol, 1.2 eq.), PEPPSI-^{i}Pr catalyst (4.0 mg, 0.0059 mmol, 0.02 eq.) and K_2CO_3 (124 mg, 0.900 mmol, 3.00 eq.) were combined under argon then the flask evacuated and refilled with argon (x 2). EtOH (degassed with argon, 4 mL) was added and the mixture stirred under reflux and argon for 18 h. The mixture was then diluted with Et_2O and filtered through celite then dried ($MgSO_4$), filtered and the solvent removed under reduced pressure. Nitrobenzophenone **228** was estimated to be 65% of the crude by ^{1}H NMR; a sample was separated from the residue, which included dimer **229**, by HPLC [C12, gradient elution; MeOH/0.1% $HCO_2H_{(aq)}$ (60:40) for 8 min, then gradient to (95:5) by 30 min.] for characterisation purposes. RT = 19.2 min. R_f = 0.24 in Pet. ether/EtOAc (5:1). ^{1}H NMR (500 MHz, $CDCl_3$) δ 8.66 - 8.59 (1H, m, H2), 8.48 - 8.42 (1H, m, H6), 8.15 (1H, dd, *J* = 7.7, 1.0 Hz, H4), 7.84 - 7.78 (2H, m, H2', H6'), 7.71 (1H, t, *J* = 7.9 Hz, H5), 7.67 (1H, t, *J* = 7.5 Hz, H4'), 7.54 (2H, t, *J* = 7.8 Hz, H3', H5'). ^{13}C NMR (126 MHz, $CDCl_3$) δ 194.30 (C), 148.27 (C), 139.25 (C), 136.44 (C), 135.56 (CH), 133.51 (CH), 130.16 (CH), 129.78 (CH), 128.89 (CH), 126.86 (CH), 124.87 (CH). MS (EI^+): 227 ($M^{+\cdot}$, 65%), 105 ($C_6H_5CO^+$, 100). HRMS: 227.0584. $C_{13}H_9O_3N$ requires 227.0582. Consistent with literature data.[257]

t:	0.1% HCO_2H (%):	MeOH (%):	Flow (mL):	RT (min):
0	40	60	15.0	**228** 19.24
8	40	60	15.0	**229** 27.29
30	5	95	15.0	
50	5	95	15.0	
55	50	50	15.0	
58	50	50	1.0	

2,2'-Dibenzoyl-4,4'-dinitrobiphenyl **229**

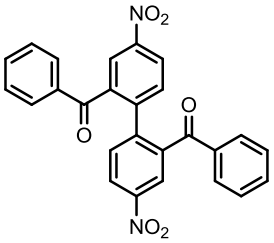

229

Iodobenzophenone **218** (1.00 g, 2.83 mmol, 1.12 eq.), PEPPSI-^{i}Pr catalyst (96 mg, 0.14 mmol, 0.05 eq.) and arylboronic acid **316** (510 mg, 2.53 mmol, 1.00 eq.) were divided evenly between two microwave tubes (10.0 mL) under argon. The tubes were opened to vacuum, then refilled with argon. This process was repeated twice then *N,N*-diisopropylethylamine (1.45 mL, 8.32 mmol, 3.29 eq.) and degassed ethanol (10.0 mL) were split between the tubes. Each tube was heated to 125 ˚C for 10 min. After cooling the mixtures were combined and partitioned between DCM and 1 M $HCl_{(aq)}$ then the aqueous layer extracted (DCM x 2). The combined organics were dried ($MgSO_4$),

filtered and the solvent removed under reduced pressure. Column chromatography [SiO_2, Pet. Ether/EtOAc (15:1), after drying loading onto celite] gave dimer **229** as a yellow solid (24 mg, 2%). ^{1}H NMR (500 MHz, $CDCl_3$) δ 8.36 (2H, dd, *J* = 8.5, 2.4 Hz, H5, H5'), 8.27 (2H, d, *J* = 2.3 Hz, H3, H3'), 7.64 (4H, dd, *J* = 8.4, 1.2 Hz, H2'', H6''), 7.61 (2H, d, *J* = 8.5 Hz, H6, H6'), 7.40 (2H, tt, *J* = 7.5, 1.3 Hz, H4''), 7.31 (4H, dd, *J* = 8.2, 7.5 Hz, H3'', H5''). ^{13}C NMR (126 MHz, $CDCl_3$) δ 194.35 (C), 146.83 (C), 145.02 (C), 139.09 (C), 135.64 (C), 133.98 (CH), 132.41 (CH), 130.31 (CH), 128.57 (CH), 125.01 (CH), 124.22 (CH). (ATR cm^{-1}): 1667 (C=O), 1597 (C_{Ar}=C_{Ar}), 1526 (NO_2), 1346 (NO_2). MS (APCI$^+$): 453 [$(M+H)^+$, 100%]. HRMS: 453.1086. $C_{26}H_{17}N_2O_6$ requires 453.1081.

6-Benzyloxyhexen-1-al **231**

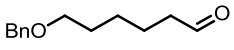

231

Alcohol **145** (11.5 g, 55.0 mmol, 1.00 eq.) was dissolved in DCM (550 mL) and cooled to 0 ˚C then KBr (1.30 g, 10.9 mmol, 0.198 eq.) added, followed by TEMPO (88 mg, 0.56 mmol, 0.010 eq.) and a combination of $NaOCl_{(aq)}$ (assumed 4%, 100 mL, 56.9 mmol, 1.03 eq.) and $NaHCO_{3(aq)}$ (140 mL, 160 mmol, 2.91 eq.). The mixture was stirred for 2 h, then additional $NaOCl_{(aq)}$ (23.0 mL, 13.1 mmol, 0.238 eq.) was added. The mixture was stirred for 2 h with addition of $NaOCl_{(aq)}$ (9.0 mL, 5.12 mmol, 0.0936 eq. in total), then the biphasic mixture separated and the aqueous extracted with DCM. The combined organics were dried ($MgSO_4$), filtered and the solvent removed under reduced pressure to give aldehyde **231** as an oil (11.05 g, 97%). ^{1}H NMR (400 MHz, $CDCl_3$) δ 9.79 (1H, t, *J* = 1.8 Hz, CH_2C**H**O), 7.40 - 7.30 (5H, m, Ph), 4.52 (2H, s, OC**H**$_2$Ph), 3.50 (2H, t, *J* = 6.5 Hz, CH_2-5), 2.46 (2H, td, *J* = 7.4, 1.7 Hz, CH_2-1), 1.74 - 1.60 (4H, m, CH_2-2, CH_2-4), 1.50 - 1.39 (2H, m, CH_2-3). ^{13}C NMR (126 MHz, $CDCl_3$) δ 202.83 (CH), 138.67 (C), 128.51 (CH), 127.77 (CH), 127.68 (CH), 73.08 (CH_2), 70.16 (CH_2), 43.98 (CH_2), 29.65 (CH_2), 25.97 (CH_2), 22.03 (CH_2). Consistent with literature data.[423]

6-Benzyloxy-1-bromohexane **232**

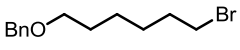

232

Alcohol **145** (1.50 g, 7.17 mmol, 1.00 eq.) was dissolved in dry DCM (26 mL) with stirring under argon and cooled to 0 ˚C. CBr_4 (3.05 g, 9.18 mmol, 1.28 eq.) and PPh_3 (2.44 g, 9.30 mmol, 1.30 eq.) were added successively, then the mixture stirred under argon for 20 min before being allowed to warm to RT and stir for a further 17 h. The mixture was washed with brine and water, dried ($MgSO_4$), filtered and the solvent removed under reduced pressure. Column chromatography [SiO_2, Pet. ether/Et_2O (99:1)] followed by vacuum distillation to remove $CHBr_3$ gave alkyl bromide **232** as an oil (1.76 g, 91%). ^{1}H NMR (500 MHz, $CDCl_3$) δ 7.37 - 7.26 (5H, m, Ph), 4.50 (2H, s, OC**H**$_2$Ph), 3.47 (2H, t, *J* = 6.5 Hz, CH_2-6), 3.40 (2H, t, *J* = 6.8 Hz, CH_2-1), 1.86 (2H, tt, *J* = 6.9, 6.8 Hz, CH_2-5), 1.63 (2H, tt, *J* = 7.0, 7.0 Hz, CH_2-2), 1.50 - 1.36 (4H, m, CH_2-3, CH_2-4). ^{13}C NMR (126 MHz, $CDCl_3$) δ 138.74 (C), 128.51 (CH), 127.78 (CH), 127.67 (CH), 73.07 (CH_2), 70.34 (CH_2), 34.05 (CH_2), 32.90 (CH_2), 29.73 (CH_2), 28.15 (CH_2), 25.57 (CH_2). Data is consistent with literature.[424]

2-Nitro-4-*tert*butylbromobenzene **239**

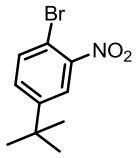

239

A solution of $HNO_{3(aq)}$ (1.0 mL, 16 mmol, 1.4 eq.) in $H_2SO_{4(aq)}$ (98%, 2mL) was added to stirring 4-*tert*butylbenzene at 0 ˚C. The mixture was allowed to gradually warm to RT and stirred under argon for 14 h. The reaction mixture was then partitioned with Pet. ether, and the aqueous re-extracted with Pet. ether. The combined organics were washed with brine then dried ($MgSO_4$), filtered and the solvent removed under reduced pressure to give nitroarene **239** as a yellow oil (2.82 g, 95%). ^{1}H NMR (400 MHz, $CDCl_3$) δ 7.83 (1H, d, *J* = 2.4 Hz, H3), 7.64 (1H, d, *J* = 8.5 Hz, H6), 7.48 – 7.42 (1H, dd, *J* = 8.5, 2.4 Hz, 1H), 1.34 [9H, s, $C(CH_3)_3$]. Consistent with literature data.[270]

2-Amino-4-*tert*butylbromobenzene **240**

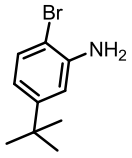

240

Bromobenzene **239** (3.5 g, 14 mmol, 1.0 eq.) was dissolved in a mixture of AcOH (60 mL) and EtOH (60 mL), and iron fillings (4.06 g, 72.6 mmol, 5.34 eq.) added, then the mixture stirred and heated to 100 ˚C for 2 h under argon. The mixture was cooled then basified with $NaOH_{(aq)}$ (7 M) and extracted with EtOAc (x 2). The combined organics were washed with brine then dried ($MgSO_4$), filtered and the solvent removed under reduced pressure. The brown oil was dried by azeotrope with PhMe then dissolved in Pet. ether and dry loaded onto SiO_2, washed with pet. ether and eluted with Et_2O, then dried ($MgSO_4$), before filtering and removal of the solvent under reduced pressure, giving aniline **240** as a red oil (2.80 g, 91%). ^{1}H NMR (400 MHz, $CDCl_3$) δ 7.31 (1H, d, *J* = 8.4 Hz, H6), 6.79 (1H, d, *J* = 2.3 Hz, H3), 6.66 (1H, dd, *J* = 8.4, 2.3 Hz, H5), 4.02 (2H, s, br, NH_2), 1.27 [9H, s, $C(CH_3)_3$]. ^{13}C NMR (101 MHz, $CDCl_3$) δ 151.97 (C), 143.59 (C), 132.10 (CH), 117.17 (CH), 113.27 (CH), 106.41 (C), 34.56 (C), 31.31 (CH_3). Consistent with literature data.[425]

2-(6'-Benzyloxyhexylamino)-*tert*butylbromobenzene **241**

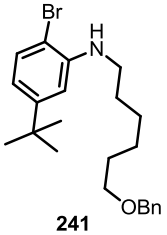

241

Aniline **240** (6.0 g, 26 mmol, 1.0 eq., dried by azeotrope with PhMe) was cooled to –15 ˚C under argon then dry TFA (34 mL) added and the material agitated and warmed until the material dissolved, then cooled to –15 ˚C. $NaBH(OAc)_3$ (12.0 g, 56.6 mmol, 2.18 eq.) was added and the mixture stirred for 30 min, then aldehyde **231** (10.1 g, 48.6 mmol, 1.87 eq., dried by azeotrope

with PhMe) was added portion wise as a solution in dry DCM (135 mL). After 20 min the mixture was quenched into $NaOH_{(aq)}$ (7 M) and extracted with DCM (x 2), then the combined organics dried ($MgSO_4$), filtered and the solvent removed under reduced pressure. Column chromatography [SiO_2, Pet. ether/Et_2O (20:1)] gave secondary amine **241** as an orange oil (7.86 g, 72%). R_f = 0.30 in Pet. ether/Et_2O (10:1). ^{1}H NMR (500 MHz, $CDCl_3$) δ 7.36 - 7.26 (5H, m, Ph''), 7.31 (1H, d, *J* = 8.5 Hz, H6), 6.64 (1H, d, *J* = 2.2 Hz, H3), 6.59 (1H, dd, *J* = 8.3, 2.3 Hz, H5), 4.51 (2H, s, OC**H**$_2$Ph), 4.18 (1H, t, *J* = 5.0 Hz, NH), 3.48 (2H, t, *J* = 6.5 Hz, CH_2-6'), 3.16 (2H, dt, *J* = 7.0, 5.3 Hz, CH_2-1'), 1.75 - 1.61 (4H, m, CH_2-2', CH_2-5'), 1.48 - 1.41 (4H, m, CH_2-3', CH_2-4'), 1.29 [9H, s, $C(CH_3)_3$]. ^{13}C NMR (126 MHz, $CDCl_3$) δ 151.87 (C), 144.60 (C), 138.68 (C), 131.69 (CH), 128.36 (CH), 127.64 (CH), 127.51 (CH), 114.92 (CH), 108.69 (CH), 106.69 (C), 72.94 (CH_2), 70.30 (CH_2), 43.84 (CH_2), 34.73 (C), 31.32 (CH_3), 29.73 (CH_2), 29.31 (CH_2), 27.02 (CH_2), 26.07 (CH_2). (ATR cm^{-1}): 3408 (N-H), 2933 (C-H), 2854 (C-H), 1588 (C_{Ar}=C_{Ar}), 1511 (C_{Ar}=C_{Ar}). MS (CI$^+$): 420 [(^{81}BrM+H)$^+$, 96%], 418 [(^{79}BrM+H)$^+$, 100]. HRMS: 420.1711 and 418.1748. $C_{23}H_{33}ON^{81}Br$ and $C_{23}H_{33}ON^{79}Br$ require 420.1728 and 418.1746 respectively.

2-[N-(6'-benzyloxyhexylamino)-*tert*-butylcarbamate]-4-*tert*-butylbromobenzene **245**

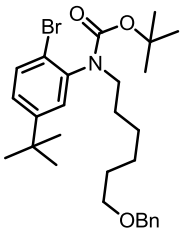

245

Aniline **241** (5.425 g, 12.79 mmol, 1.000 eq.) and di-*tert*-butyl dicarbonate (5.66 g, 25.9 mmol, 2.02 eq.) were combined in dry THF (65 mL) at 0 ˚C under stirring under argon. Lithium hexamethyldisilazide (1.0 M in THF, 20.0 mL, 20 mmol, 1.6 eq.) was added over 10 min, then the mixture was allowed to warm to RT and stirred for 3 h. The reaction was cooled back to 0 ˚C and additional Lithium hexamethyldisilazide (5.0 mL, 5.0 mmol, 0.4 eq.) and di-*tert*-butyl dicarbonate (3.0 g, 14 mmol, 1.1 eq.) added, then the reaction allowed to warm to RT and stirred under argon for 17 h. The solvent was removed under reduced pressure, then the residue triturated with warm Et_2O and filtered. The combined organics were washed with $NaHCO_{3(aq)}$ and brine, then dried ($MgSO_4$), filtered and the solvent removed under reduced pressure. Hexamethylsilazide was distilled out of the product under high vacuum at 50 ˚C. Column chromatography [SiO_2, Pet. ether/Et_2O gradient from (20:1) - (10:1), using ceric ammonium molybdate solution to visualise residual hexamethyldisilazide] gave carbamate **245** as a pink oil (5.42 g, 82%). R_f = 0.17 in Pet. ether/Et_2O (5:1). ^{1}H NMR (400 MHz, $CDCl_3$) δ 7.54 - 7.45 (1H, m, H6), 7.37 - 7.26 (5H, m, Ph), 7.22 - 7.11 (2H, m, H5, H3), 4.51 - 4.46 (2H, m, OC**H**$_2$Ph), 3.81 - 3.63 (1H, m, CH_2-1'$_A$), 3.50 - 3.40 (2H, m, CH_2-6'), 3.34 - 3.21 (1H, m, CH_2-1'$_B$), 1.67 - 1.46 (8H, m, CH_2-2', CH_2-3', CH_2-4', CH_2-5'), 1.43 - 1.24 [18H, m, $C(CH_3)_3$ x 2]. Spectrum is complex due to the appearance of atropisomers on an NMR timescale - limited coalescence seen at 90 ˚C. ^{13}C NMR (101 MHz, DMSO, recorded at 90 ˚C) δ 153.39, 151.32, 148.46, 140.71, 138.85, 132.31, 127.95, 127.69, 127.13, 127.01, 125.45, 119.61, 83.62, 79.01, 71.96, 69.69, 34.11, 30.76, 29.14, 27.92, 27.26, 26.15, 25.41. (ATR cm^{-1}): 2967 (C-H), 2936 (C-H), 2862 (C-H), 1697 (C=O). MS (CI$^+$): 520 [(^{81}BrM+H)$^+$, 17%], 518 [(^{79}BrM+H)$^+$, 18], 464

[(^{81}BrM+H)$^+$ – C(CH$_3$)$_3$, 100], 462 [(^{79}BrM+H)$^+$ – C(CH$_3$)$_3$, 100], 420 [(^{81}BrM+H)$^+$ – C(CH$_3$)$_3$ – CO$_2$, 30], 418 [(^{79}BrM+H)$^+$ – C(CH$_3$)$_3$ – CO$_2$, 32], 382 [(M–H)$^+$ – Br – C(CH$_3$)$_3$, 22]. HRMS: 520.2263 and 518.2258. $C_{28}H_{41}O_3N^{81}Br$ and $C_{28}H_{41}O_3N^{79}Br$ require 520.2285 and 518.2270.

2-[*N*-(6'-benzyloxyhexylamino)-*tert*-butylcarbamate]-4-*tert*-butylbenzene **248**

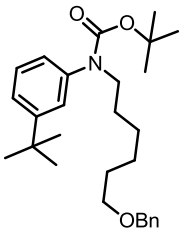

248

Bromobenzene **245** (96 mg, 0.19 mmol, 1.00 eq.) was dissolved in dry THF (1.0 mL) under argon and the stirring solution cooled to –78 ˚C. ^{n}Butyllithium (2.5 M in hexane, 90 µL, 0.23 mmol, 1.2 eq.) was added and the mixture stirred under argon for 1 h. MeOH (0.3 mL) was added then the mixture partitioned between Et_2O and water then the organic layer dried ($MgSO_4$), filtered and the solvent removed under reduced pressure. Column chromatography [SiO_2, Pet. ether/Et_2O (5:1)] gave carbamate **248** as an oil (61 mg, 75%). R_f = 0.43 in Pet. ether/Et_2O (2:1). ^{1}H NMR (500 MHz, $CDCl_3$) δ 7.29 - 7.13 (7H, m, Ph, H1, H3), 7.10 (1H, s, br, H5), 6.91 (1H, d, *J* = 7.3 Hz, H6), 4.42 (2H, s, OC**H**$_2$Ph), 3.54 (2H, apparent *t*, *J* = 7.5 Hz, CH_2-6'), 3.38 (2H, t, *J* = 6.6 Hz, CH_2-1'), 1.57 - 1.44 (4H, m, CH_2-2', CH_2-5'), 1.41 - 1.19 [22H, m, CH_2-3', CH_2-4', C(CH$_3$)$_3$ x 2]. MS (EI$^+$): 439 (M$^{+\cdot}$, 20%), 339 (M$^{+\cdot}$ – $^{\cdot}$CO$_2$ – $^{\cdot}$C$_4$H$_8$, 90), 248 ((M$^{+\cdot}$ – $^{\cdot}$CO$_2$ – $^{\cdot}$C$_4$H$_8$ – $^{\cdot}$C$_7$H$_7$, 51), 161 (PhN$^+$H$_2$C$_5$H$_9$, 100). HRMS: 439.3090. $C_{28}H_{41}O_3N$ requires 439.3086.

2-(5'-bromopentanamide)-*tert*butylbromobenzene **255**

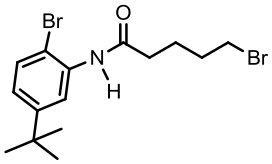

255

5-Bromopentanoic acid **253** (900 mg, 4.97 mmol, 1.13 eq.) was dissolved in $SOCl_2$ and heated to reflux stirring under argon for 70 h. The $SOCl_2$ was removed by distillation then the residue dissolved in dry THF (10 mL). The mixture was cooled to 0 ˚C then a solution of bromoaniline **240** (1.0 g, 4.4 mmol, 1.0 eq.) in dry THF (30 mL) was added. The mixture was allowed to warm gradually to RT and stirred under argon for 17 h. The mixture was then quenched into $NaHCO_{3(aq)}$ and extracted into Et_2O. The organic layer was washed with $NaHCO_{3(aq)}$, brine and water then dried ($MgSO_4$), filtered and the solvent removed under reduced pressure. Column chromatography [SiO_2, dry loaded onto celite with Et_2O, Pet. ether/Et_2O (10:1)] to give amide **255** as an oil (621 mg, 36%). R_f = 0.08 Pet. ether/Et_2O (5:1). ^{1}H NMR (500 MHz, $CDCl_3$) δ 8.43 (1H, s, br, H3), 7.58 (1H, s, br, NH), 7.43 (1H, d, *J* = 8.5 Hz, H6), 7.01 (1H, dd, *J* = 8.5, 2.2 Hz, H5), 3.45 (2H, t, *J* = 6.5 Hz, CH_2-5'), 2.48 (2H, t, *J* = 7.1 Hz, CH_2-2'), 2.04 - 1.84 (4H, m, CH_2-3', CH_2-3'), 1.31 [9H, s, C(CH$_3$)$_3$]. ^{13}C NMR (126 MHz, $CDCl_3$) δ 170.61 (C), 152.20 (C), 135.27 (C), 131.65 (CH), 122.65 (CH), 119.54 (CH), 110.24 (C), 36.86 (CH_2), 35.01 (C), 33.15 (CH_2), 32.09 (CH_2), 31.31 (CH_3), 24.04 (CH_2).

(ATR cm^{-1}): 3279 (N-H), 2961 (C-H), 2907 (C-H), 2868 (C-H), 1667 (C=O), 1574 (C_{Ar}=C_{Ar}), 1518 (C_{Ar}=C_{Ar}).

5-[(2-Bromo-5-*tert*-butylbenzene)carbamoyl]butyltriphenylphosphonium bromide **256**

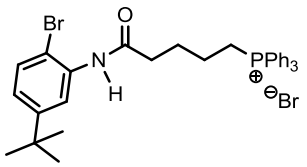

256

Bromide **255** (543 mg, 1.39 mmol, 1.00 eq.) was dried by azeotrope with PhMe then dissolved in dry MeCN (3.0 mL) and transferred into triphenylphosphine (dried by azeotrope with PhMe, 720 mg, 2.75 mmol, 1.98 eq.) under argon, then additional dry MeCN (2.0 mL) added and the mixture stirred under reflux and argon for 64 h. The mixture was cooled, the solvent removed under reduced pressure and the residue dissolved in DCM and precipitated by addition to Et_2O, then the solvent decanted off and the process repeated. The residue was loaded onto SiO_2 in DCM and washed with further DCM, then eluted with DCM/MeOH, dried ($MgSO_4$), filtered and the solvent removed under educed pressure, giving triphenylphosphonium bromide **256** as a white solid (700 mg, 77%). ^{1}H NMR (500 MHz, $CDCl_3$) δ 8.89 (1H, s, NH), 7.91 - 7.58 (16H, m, PPh_3, H6'), 7.36 (1H, d, *J* = 8.4 Hz, H3'), 6.98 (1H, dd, *J* = 8.4, 2.2 Hz, H4'), 3.87 - 3.76 (2H, m, CH_2-1), 2.86 (2H, t, *J* = 6.6 Hz, CH_2-4), 2.10 (2H, quin., *J* = 6.5 Hz, CH_2-2), 1.85 - 1.74 (2H, m, CH_2-3), 1.24 [9H, s, $C(CH_3)_3$]. ^{13}C NMR (126 MHz, $CDCl_3$) δ 171.52 (C), 151.16 (C), 135.59 (C), 135.00 (d, *J* = 3.0 Hz, CH), 133.73 (d, *J* = 10.0 Hz, CH), 131.82 (CH), 130.48 (d, *J* = 12.6 Hz, CH), 123.37 (CH), 122.61 (CH), 118.21 (d, *J* = 86.0 Hz, CP), 113.85 (C), 35.31 (CH_2), 34.66 (C), 31.19 (CH_3), 25.92 (d, *J* = 16.9 Hz, CH_2), 22.58 (d, *J* = 50.5 Hz, CH_2), 21.45 (d, *J* = 4.0 Hz, CH_2). (ATR cm^{-1}): 2963 (C-H), 2870 (C-H), 1674 (C=O), 1574 (C_{Ar}=C_{Ar}), 1520 (C_{Ar}=C_{Ar}). MS (NSI^+): 574 [$^{81}BrM^+$ (phosphonium cation), 100%], 572 [$^{79}Br\ M^+$ (phosphonium cation), 97]. HRMS: 574.1682 and 572.1705. $C_{33}H_{36}{}^{81}BrNOP$ and $C_{33}H_{36}{}^{79}BrNOP$ require 574.1693 and 572.1712 respectively. MP: 91 - 95 ˚C.

6-Benzyloxyhexanoic acid **259**

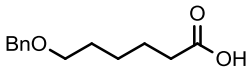

259

Based on the procedure of *Lermer et al*,[426] ε-capralactone **258** (5.0 mL, 45 mmol, 1.0 eq.) was dissolved stirring in dry PhMe (120 mL) under argon, then KOH (12.5 g, 223 mmol, 4.95 eq.) and benzyl bromide (26.5 mL, 223 mmol, 4.95 eq.) added and the mixture heated under reflux for 48 h. After cooling the mixture was diluted and partitioned between Et_2O and water, then the aqueous further extracted with Et_2O (x 2). The solvent was removed from the combined organics under reduced pressure, then PhMe (15 mL) and $NaOH_{(aq)}$ (5.0 M, 45 mL, 225 mmol, 5.0 eq.) added and the mixture heated with stirring under reflux for 18 h. After cooling the mixture was partitioned with Et_2O and water, then the aqueous further extracted with Et_2O (x 3), acidified with a mixture of 1 M $H_2SO_{4(aq)}$ and ice then extracted with DCM (x 3). The chlorinated extracts were combined, dried ($MgSO_4$), filtered and the solvent removed under reduced pressure to give acid **259** as a yellow oil (9.46 g, 95%). ^{1}H NMR (400 MHz, $CDCl_3$) δ 7.45 - 7.10 (5H, m, Ph), 4.55 - 4.45

(2H, m, OC**H**$_2$Ph), 3.54 - 3.44 (2H, m, CH_2-6), 2.43 - 2.32 (2H, m, CH_2-2), 1.75 - 1.59 (4H, m, CH_2-3, CH_2-5), 1.52 - 1.39 (2H, m, CH_2-4). ^{13}C NMR (101 MHz, $CDCl_3$) δ 178.68 (C), 138.69 (C), 128.51 (CH), 127.78 (CH), 127.67 (CH), 73.07 (CH_2), 70.21 (CH_2), 33.87 (CH_2), 29.54 (CH_2), 25.87 (CH_2), 24.65 (CH_2). Data consistent with literature values.[426]

2-Fluoro-5-*tert*-butylphenyliodide **273**

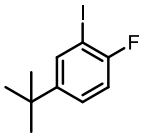

273

2-fluorophenyliodide **269** (260 µL, 2.23 mmol, 1.00 eq.) and *tert*-butyl chloride (372 µL, 0.338 mmol, 1.47 eq.) were combined and cooled to 0 ˚C stirring under argon. $AlCl_3$ (9 mg, 0.07 mmol, 0.03 eq.) was added, then the mixture stirred for 15 min and quenched into ice water, then combined with $Na_2S_2O_{3(aq)}$ and shaken until colourless then extracted with DCM (x 2). The organics were washed with brine, dried ($MgSO_4$), filtered and the solvent removed under reduced pressure, giving aryl iodide **273** as an oil (610 mg, 98%). ^{1}H NMR (400 MHz, $CDCl_3$) δ 7.71 (1H, dd, *J* = 6.0, 2.4 Hz, H6), 7.31 (1H, ddd, *J* = 8.7, 4.8, 2.4 Hz, H4), 6.98 (1H, dd, *J* = 8.6, 7.8 Hz, H3), 1.29 [9H, s, $C(CH_3)_3$]. ^{13}C NMR (126 MHz, $CDCl_3$) δ 159.80 (d, *J* = 243.5 Hz, CF), 149.05 (d, *J* = 3.5 Hz, C), 136.37 (d, *J* = 1.2 Hz, CH), 127.20 (d, *J* = 6.9 Hz, CH), 115.04 (d, *J* = 23.3 Hz, CH), 81.08 (d, *J* = 24.9 Hz, C), 34.44 (C), 31.48 (CH_3). ^{19}F NMR (377 MHz, $CDCl_3$) δ −99.20 - −99.25 (m). (ATR cm^{-1}): 2963 (C-H), 2907 (C-H), 2870 (C-H), 1493 (C_{Ar}=C_{Ar}). MS (EI$^+$): 278 ($M^{+\cdot}$, 98%), 263 ($M^{+\cdot}$ – $^{\cdot}CH_3$, 100), 235 ($M^{+\cdot}$ –$^{\cdot}CH_3$ x 3, 35), 136 ($C_9H_9F^{+\cdot}$, 39). HRMS: 277.9965. $C_{10}H_{12}FI$ requires 277.9968.

2-Bromo-5-*tert*-butylphenyldiazonium tetrafluoroborate **274**

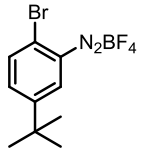

274

2-amino-4-*tert*-butylbromobenzene **240** (976 mg, 4.28 mmol, 1.00 eq.) was added dropwise to a stirring solution of $HBF_{4(aq)}$ (48%, 5.0 mL, 38 mmol, 8.9 eq.). After 30 min the mixture was cooled to 0 ˚C then $NaNO_{2(aq)}$ (5.1 M, 2.0 mL, 10 mmol, 2.4 eq.) was added dropwise. After 30 min stirring the mixture was shaken then allowed to warm to RT and stirred for 2 h. Precipitation with Et_2O followed by vacuum filtration, washing with $HBF_{4(aq)}$ then drying under vacuum gave the diazonium salt **274** as a beige solid (719 mg, 51%). ^{1}H NMR (400 MHz, d_6-DMSO) δ 8.94 (1H, d, *J* = 1.9 Hz, H6), 8.25 (1H, dd, *J* = 8.8, 2.3 Hz, H4), 8.22 (1H, d, *J* = 8.6 Hz, H3), 1.33 [9H, s, $C(CH_3)_3$]. The very low solubility and probable explosive nature of this compound hindered further characterisation.

2-Fluoro-4-*tert*-butylphenylbromide **275**

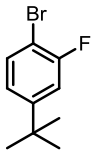

275

$NOBF_4$ (313 mg, 2.70 mmol, 1.32 eq.) was dissolved in stirring, dry DCM (10.0 mL), at 0 ˚C under argon. After 30 min 2-Amino-4-*tert*butylphenylbromide **240** (471 mg, 2.04 mmol, 1.00 eq.) was added dropwise and the mixture allowed to warm to RT under argon for 13 h. PhMe (10.0 mL) was added then the DCM removed carefully under vacuum. The suspension was heated to reflux for 2 h stirring under argon, then cooled and the solvent removed under reduced pressure. Column chromatography (SiO_2, Pet. ether) gave aryl fluoride **275** as an oil (341 mg, 72%). ^{1}H NMR (500 MHz, $CDCl_3$) δ 7.46 (1H, apparent t, *J* = 7.9 Hz, H6), 7.16 (1H, dd, *J* = 10.9, 2.2 Hz, H3), 7.06 (1H, dd, *J* = 8.4, 2.1 Hz, H5), 1.32 [9H, s, $C(CH_3)_3$]. ^{13}C NMR (126 MHz, $CDCl_3$) δ 159.01 (d, *J* = 245.9 Hz, CF), 153.49 (d, *J* = 5.9 Hz, C), 132.95 (CH), 122.49 (d, *J* = 3.2 Hz, CH), 113.94 (d, *J* = 22.4 Hz, CH), 105.51 (d, *J* = 20.8 Hz, C), 34.88 (d, *J* = 1.4 Hz, C) 31.21 (CH_3). ^{19}F NMR (470 MHz, $CDCl_3$) δ −108.22 (dd, 10.8, 7.4 Hz). ν_{Max}(ATR)cm^{-1}: 2963 (C-H), 2870, (C-H), 1566 (C_{Ar}=C_{Ar}), 1481, 1404 (C-F). MS (EI$^+$): 232 (^{81}BrM$^{+\cdot}$, 22%), 230 (^{79}BrM$^{+\cdot}$, 22%), 217 [(^{81}BrM+H)$^+$ – $^{\cdot}CH_3$, 77], 215 [(^{79}BrM+H)$^+$ – $^{\cdot}CH_3$, 77], 84 (100). HRMS: 232.0078 and 230.0110. $C_{10}H_{12}{}^{81}$BrF requires 232.0086, $C_{10}H_{12}{}^{79}$BrF requires 230.0106.

Potassium 2-Fluorophenyltrifluoroborate **285**

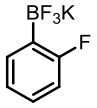

285

2-Fluorophenylbromide **268** (0.62 mL, 5.7 mmol, 1.0 eq.) was dissolved stirring in dry THF (15.0 mL) under argon and cooled to –77 ˚C. ^{n}butyllithium (2.5 M in hexane, 2.50 mL, 6.25 mmol, 1.10 eq.) was added over 20 min, then the mixture stirred for 65 min. Triisopropxyborate (2.65 mL, 11.5 mmol, 2.01 eq.) was added and the mixture stirred for a further 30 min before warming to RT and stirring for a further 30 min. The mixture was poured into $KHF_{2(aq)}$ (0.85 M, 30.0 mL, 25.5 mmol, 4.48 eq.) and stirred for 17 h under argon. The solvent was removed under reduced pressure, triturated with Et_2O and filtered. The filter cake was dissolved in acetone then dried ($MgSO_4$), filtered and the solvent removed under reduced pressure. Crystallisation from acetone gave trilfuoroborate salt **285** as a solid (317, 28%). ^{1}H NMR (400 MHz, DMSO) δ 7.34 (1H, t, *J* = 5.3 Hz, H6), 7.11 - 7.03 (1H, m, H4), 6.91 (1H, td, *J* = 7.2, 0.7 Hz, H5), 6.79 (1H, t, *J* = 8.6 Hz, H3). ^{13}C NMR (126 MHz, DMSO) δ 165.60 (dd, *J* = 239.0, 0.8 Hz, CF), 134.08 (dq, *J* = 13.4, 2.6 Hz, CH), 127.06 (d, *J* = 8.0 Hz, CH), 122.35 (d, *J* = 2.4 Hz, CH), 113.59 (d, *J* = 25.9 Hz, CH). (ATR cm^{-1}): 3078 (C_{Ar}-H), 3057 (C_{Ar}-H), 1616 (C_{Ar}=C_{Ar}), 1566 (C_{Ar}=C_{Ar}). Data is consistent with literature values.[427]

Potassium 2-Fluoro-4-*tert*-butylphenyltrifluoroboronate **266**

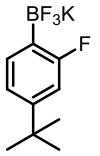

266

Aryl bromide **275** (5.88 g, 25.5 mmol, 1.00 eq.) was dissolved in dry THF (100 mL) and cooled to –77 ˚C. 1.6 M ^{n}butyllithium (21.0 mL, 33.6 mmol, 1.32 eq.) was added to the stirring mixture dropwise over 50 min, then the mixture allowed to stir for 90 min. Triisopropylborate (12.0 mL, 50.5 mmol, 1.98 eq.) was added dropwise over 10 min and the mixture allowed to warm to RT and stir for 14 h. The mixture was quenched into a KHF_2 (10.0 g, 128 mmol, 5.0 eq.) solution [MeOH/H_2O (1:1)] and allowed to stir for 55 h then the solvent removed under reduced pressure. The residue was dissolved in acetone and filtered, then the filtrate concentrated. Crystallisation from acetone gave Potassium trifluoroborate salt **266** (4.22 g, 64%). ^{1}H NMR (500 MHz, Acetone) δ 7.45 (1H, apparent t, *J* = 7.3 Hz, H6), 7.03 (1H, ddd, *J* = 7.7, 1.7, 0.9 Hz, H5), 6.87 (1H, dd, *J* = 11.8, 1.6 Hz, H3) [$C(CH_3)_3$]. ^{13}C NMR (126 MHz, Acetone) δ 168.23 (d, *J* = 235.0 Hz, CF), 152.83 (d, *J* = 7.2 Hz, C), 135.87 (dq, *J* = 13.2, 2.6 Hz, CH), 121.19 (CH), 112.49 (d, *J* = 27.3 Hz, CH), 35.86 (d, *J* = 1.8 Hz, C), 32.71 (CH_3). ^{19}F NMR [470 MHz, $(CD_3)_2CO$] δ −107.63 - −107.79 (m), −137.84- −138.49 (m). ν_{Max}(ATR)cm^{-1}: 2965 (C-H), 1624, 1551 (C_{Ar}=C_{Ar}), 1398. MS (NSI^{-}): 219 (M^{-} (trifluoroborate anion), 100%), 149 ($M^{-}-H_3BF_3$, 59). HRMS: 219.0971. $C_{10}H_{12}BF_4$ requires 219.0974. MP: > 250 ˚C.

2-(2''-Fluorophenyl)-5-nitrobenzophenone **286**

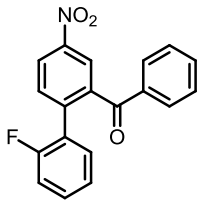

286

Iodobenzophenone **218** (1.29 g, 3.65 mmol, 1.00 eq.), PEPPSI-^{i}Pr catalyst (72 mg, 0.11 mmol, 0.03 eq.) and arylboronic acid **314** (450 mg, 3.65 mmol, 1.00 eq.) were combined under argon and the reaction vessel was opened to vacuum, then refilled with argon. This process was repeated twice then *N,N*-diisopropylethylamine (1.90 mL, 10.9 mmol, 2.99 eq.) and degassed ethanol (18.0 mL) added. The mixture was heated to reflux stirring for 16 h. After cooling the mixture was filtered through celite eluting with DCM and the solvent removed under reduced pressure. After column chromatography [SiO_2, Pet. ether/Et_2O gradient (99:1) to (9:1)] the solvent was removed under reduced pressure and the material suspended in Pet. ether/Et_2O (9:1) then sonicated. Ketone **286** precipitated as an amorphous solid (570 mg, 49%). ^{1}H NMR (400 MHz, $CDCl_3$) δ 8.44 (1H, dd, *J* = 8.4, 2.4 Hz, H4), 8.41 (1H, dd, *J* = 2.4, 0.5 Hz, H6), 7.71 - 7.67 (3H, m, H3, H2', H6'), 7.52 (1H, ddt, *J* = 8.0, 6.9, 1.3 Hz, H4'), 7.40 - 7.35 (2H, m, H3', H5'), 7.30 - 7.23 (2H, m, H4'', H6''), 7.11 (1H, td, *J* = 7,8, 1.1 Hz, H5''), 6.95 (1H, ddd, J = 10.2, 8.9, 1.0 Hz, m, H3''). ^{13}C NMR (101 MHz, $CDCl_3$) δ 195.11 (d, *J* = 1.1 Hz, C), 158.91 (d, *J* = 247.8 Hz, CF), 147.18 (C), 141.69 (C), 140.57 (d, *J* = 1.0 Hz, C), 136.19 (C), 133.68 (CH), 132.53 (d, *J* = 1.4 Hz, CH), 131.18 (d, *J* = 2.6 Hz, CH), 130.99 (d, *J* = 8.3 Hz, CH), 129.99 (CH), 128.58 (CH), 126.05 (d, *J* = 14.8 Hz, C), 125.09 (CH), 124.60 (d, *J* = 3.7 Hz, CH),

124.15 (CH), 115.90 (d, *J* = 21.8 Hz, CH). ^{19}F NMR (377 MHz, $CDCl_3$) δ −115.11 - −115.20 (m). ν_{Max}(ATR)cm^{-1}: 3067 (C_{Ar}-H), 1667 (C=O), 1597 (C_{Ar}=C_{Ar}), 1582 (C_{Ar}=C_{Ar}), 1522 (NO_2), 1348 (NO_2). MS (EI$^+$): 321 ($M^{+\cdot}$, 39), 227 ($M^{+\cdot}$ – C_6H_5F, 37), 105 ($PhCO^+$, 100), 77 (Ph^+, 39). MP: 108 - 110 ˚C. HRMS: 321.0807. $C_{19}H_{12}O_3NF$ requires 321.0801.

2-(2''-Fluoro-4''-*tert*-butylphenyl)-5-nitrobenzophenone **265**

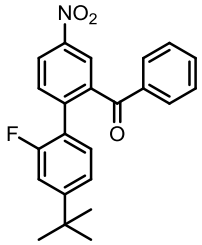

265

Iodobenzophenone **218** (431 mg, 1.22 mmol, 1.00 eq.), PEPPSI-^{i}Pr catalyst (51 mg, 0.08 mmol, 0.06 eq.) and potassium trifluoroborate salt **266** (353 mg, 1.37 mmol, 1.12 eq.) were combined under argon then the reaction vessel was opened to vacuum, then refilled with argon. This process was repeated twice then *N,N*-diisopropylethylamine (0.74 mL, 4.2 mmol, 3.4 eq.) and degassed ethanol (10.0 mL) added. The mixture was heated to reflux stirring for 4 h. After cooling the mixture was partitioned between Et_2O and H_2O, then the aqueous re-extracted with Et_2O. The combined organics were washed with brine, then dried ($MgSO_4$), filtered through celite eluting with Et_2O and the solvent removed under reduced pressure. Column chromatography [SiO_2, Pet. Ether/EtOAc (8:1), loaded in $CHCl_3$] gave ketone **265** as a pale straw coloured oil (357 mg, 78%). R_f = 0.26 in Pet. ether/EtOAc (5:1). ^{1}H NMR (500 MHz, $CDCl_3$) δ 8.44 - 8.39 (2H, m, H4, H6), 7.67 (3H, d, br, *J* = 7.8 Hz, H3, H2', H6'), 7.49 (1H, apparent t, *J* = 7.4 Hz, H4'), 7.35 (2H, apparent t, *J* = 7.7 Hz, H3', H5'), 7.18 (1H, apparent t, *J* = 8.1 Hz, H6''), 7.11 (1H, dd, *J* = 8.1, 1.8 Hz, H5''), 6.92 (1H, dd, *J* = 12.4, 1.7 Hz, H3''), 1.23 [9H, s, $C(CH_3)_3$]. ^{13}C NMR (126 MHz, $CDCl_3$) δ 195.21 (d, *J* = 1.1 Hz, C), 158.66 (d, *J* = 246.7 Hz, CF), 155.27 (d, *J* = 6.9 Hz, C), 146.85 (C), 141.83 (C), 140.31 (C), 136.24 (C), 133.31 (CH), 132.33 (d, *J* = 1.2 Hz, CH), 130.55 (d, *J* = 3.1 Hz, CH), 129.79 (CH), 128.33 (CH), 124.98 (CH), 124.11 (CH), 122.73 (d, J = 15.5 Hz, C), 121.43 (d, *J* = 3.0 Hz, CH), 112.80 (d, *J* = 22.4 Hz, CH), 34.82 (d, *J* = 1.4 Hz, C), 30.94 (CH_3). ^{19}F NMR (470 MHz, $CDCl_3$) δ −115.57 - −115.66 (m). ν_{Max}(ATR)cm^{-1}: 2964 (CH), 1670 (C=O), 1606 (C_{Ar}=C_{Ar}), 1582 (C_{Ar}=C_{Ar}), 1523 (NO_2), 1349 (NO_2). MS (EI$^+$): 377 ($M^{+\cdot}$, 64%), 362 ($M^{+\cdot}$ – $\cdot CH_3$, 100). HRMS (EI$^+$): 377.1426. $C_{23}H_{20}FNO_3$ requires $M^{+\cdot}$ 377.1427.

N-hexyl imine of 2-(2''-Fluoro-4''-*tert*butylphenyl)-5-nitrophenyl(phenyl)benzophenone **287**

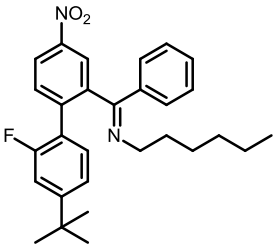

287

Benzophenone **265** (1.01 g, 2.66 mmol, 1.00 eq.) and dry hexylamine (2.45 mL, 18.6 mmol, 6.97 eq.) were combined stirring under argon at 0 ˚C in dry PhMe (20.0 mL) then titanium tetrachloride (0.44 mL, 4.0 mmol, 1.5 eq.) was added over 5 min. The reaction was allowed to warm to RT and allowed to stir for 17 h. The mixture was quenched into H_2O, with the residue washed out with Et_2O. The layers were separated and the aqueous was then extracted (Et_2O, x 2) then the combined organics washed (brine) and dried ($MgSO_4$), then filtered and the solvent removed under reduced pressure. The imine **287** was purified by chromatography [SiO_2, Pet. ether/Et_2O (20:1)] and isolated as a solid (665 mg, 54%). R_f = 0.26 Pet. Ether/Et_2O (20:1). ^{1}H NMR (500 MHz, $CDCl_3$) δ 8.34 (1H, dd, *J* = 8.5, 2.4 Hz, H4), 8.09 (1H, d, *J* = 2.4 Hz, H6), 7.67 (1H, dd, *J* = 8.5, 1.8 Hz, H3), 7.52 - 7.44 (2H, m, H2', H6'), 7.34 (1H, tt, *J* = 7.3, 1.3 Hz, H4'), 7.31 - 7.24 (2H, m, H3', H5'), 7.02 (1H, dd, *J* = 12.4, 1.7 Hz, H3''), 6.98 (1H, dd, *J* = 8.1, 1.8 Hz, H5''), 6.94 (1H, apparent t, *J* = 8.0 Hz, H6''), 3.26 - 3.18 (1H,m, $H1_A$'''), 3.08 (1H, ddd, *J* = 13.6, 7.8, 5.7 Hz, $H1_B$'''), 1.63 - 1.53 (1H, m, $H2_A$'''), 1.45 - 1.33 (1H, m, $H2_B$'''), 1.32 - 1.15 (15H, m, H3''', H4''', H5''', tBu), 0.85 [3H, t, *J* = 7.1 Hz, $C(CH_3)_3$]. ^{13}C NMR (126 MHz, $CDCl_3$) δ 164.11 (C), 159.13 (d, *J* = 247.1 Hz, CF), 155.28 (d, *J* = 6.8 Hz, C), 147.26 (C), 141.92 (C), 139.50 (C), 138.16 (C), 132.48 (d, *J* = 2.6 Hz, CH), 130.13 (CH), 129.94 (d, *J* = 2.9 Hz, CH), 128.29 (CH), 128.15 (CH), 124.05 (CH), 123.36 (CH), 122.72 (d, *J* = 14.6 Hz, C), 121.20 (d, *J* = 3.1 Hz, CH), 113.12 (d, *J* = 22.5 Hz, CH), 54.39 (CH_2), 34.97 (d, *J* = 1.4 Hz, C). 31.80 (CH_2), 31.14 (CH_3), 30.93 (CH_2), 27.29 (CH_2), 22.72 (CH_2), 14.19 (CH_3). ^{19}F NMR (377 MHz, $CDCl_3$) δ −116.01 (dd, *J* = 12.4, 7.8 Hz). ν_{Max}(ATR)cm^{-1}: 2958 (C-H), 2932 (C-H), 2859 (C-H), 1624 (C=N), 1578 (C_{Ar}=C_{Ar}), 1524 (NO_2), 1346 (NO_2). MS (EI$^+$): 460 ($M^{+\cdot}$, 7%), 441 ($C_{29}H_{33}N_2O_2^{+\cdot}$, 7), 403 ($C_{25}H_{24}FN_2O_2^+$, 22), 84 ($C_6H_{12}^{+\cdot}$, 100). HRMS: 460.2527. $C_{29}H_{33}FN_2O_2$ requires 460.2526. MP: decomp.

3-*tert*-Butyl-6-phenyl-8-nitrophenanthridine **290**

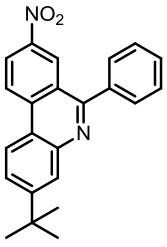

290

Imine **287** (10 mg, 0.02 mmol, 1.0 eq.) was heated to 200 ˚C stirring in dry nitrobenzene (1.0 mL) for 1 h, then cooled and the solvent removed under reduced pressure. The resulting mixture was dissolved in MeOH and $HCl_{(aq)}$ (1 M, approx. 1:1), and the solvents removed under reduced pressure. The salt was loaded onto a Strata SCX ion exchange column, then washed with additional MeOH. The material was then eluted with 7 M NH_3 in MeOH, and the solvent removed

under reduced pressure to give traces of phenanthridine **290** (2 mg, 26%). ^{1}H NMR (500 MHz, $CDCl_3$) δ 9.01 (1H, d, *J* = 2.3 Hz, H7), 8.81 (1H, d, *J* = 9.1 Hz, H10), 8.63 (1H, dd, *J* = 9.1, 2.4 Hz, H9), 8.58 (1H, d, *J* = 8.7 Hz, H1), 8.30 (1H, d, *J* = 2.0 Hz, H4), 7.86 (1H, dd, *J* = 8.7, 2.1 Hz, H2), 7.77 - 7.73 (2H, m, H2', H6'), 7.65 - 7.57 (3H, m, H3', H4', H5'), 1.48 [s, 9H, $C(CH_3)_3$]. ^{13}C NMR (126 MHz, $CDCl_3$) δ 161.51 (C), 155.02 (C), 145.97 (C), 145.23 (C), 138.70 (C), 137.58 (C), 129.84 (CH), 129.60 (CH), 129.07 (CH), 126.93 (CH), 126.46 (CH), 125.21 (CH), 124.52 (C), 124.29 (CH), 124.02 (CH), 122.65 (CH), 120.24 (C), 35.48 (C), 31.40 (CH_3). ν_{Max}(ATR)cm^{-1}: 2965 (C-H), 1616 (C=N), 1589 (C_{Ar}=C_{Ar}), 1537 (C_{Ar}=C_{Ar}), 1516 (NO_2), 1341 (NO_2). MS (EI^+): 356 ($M^{+\cdot}$, 59%), 341 ($M^{+\cdot}$ – $^{\cdot}CH_3$, 100), 326 ($M^{+\cdot}$ – C_2H_6, 49), 311 [($M^{+\cdot}$ – $^{\cdot}NO_2$, 60], 295 ($M^{+\cdot}$ – CH_4, $^{\cdot}HNO_2$, 34). HRMS: 356.1526. $C_{23}H_{20}N_2O_2$ requires 356.1525.

3-*tert*-Butyl-5-(hex-1'-yl)-6-phenyl-8-nitrophenanthridinium chloride **288**

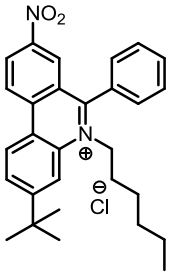

288

Benzophenone **265** (500 mg, 1.33 mmol, 1.00 eq.) and dry hexylamine (1.05 mL, 9.31 mmol, 7.00 eq.) were combined stirring under argon at 0 ˚C in dry PhMe (5.0 mL) then a 1 M solution of titanium tetrachloride in dry PhMe (2.00 mL, 2.00 mmol, 1.50 eq.) was added over 5 min. The reaction was allowed to warm to RT and allowed to stir for 40 h. The mixture was quenched into 1 M $K_2CO_{3(aq)}$ then filtered through celite and extracted into DCM (x 3). The combined organics were acidified (0.55 M $HCl_{(aq)}$). The acidic aqueous extracts were further extracted (DCM, x 2), then the organic extracts recombined and basified in 1 M $K_2CO_{3(aq)}$. The organic layers were dried ($MgSO_4$), then filtered and the solvent removed under reduced pressure. From the crude yield of 623 mg of extremely viscous brown oil, a portion (100 mg, 0.22 mmol, 1.00 eq.) was weighed by difference onto a spatula and sonicated into a microwave tube (10 mL) containing dry THF (5.0 mL). The tube was filled with argon and sealed then heated to 100 ˚C for 2 h. After cooling the material was transferred to a round bottom flask with DCM and the solvent removed under reduced pressure. The residue was dissolved in dry Et_2O then precipitated with 2 M ethereal HCl (1.00 mL, 2.00 mmol, 9.09 eq.). The precipitate was allowed to settle, then the bulk of the solvent syringed out and the remainder removed under reduced pressure, isolating the phenanthridinium chloride **288** as a brown foam (87 mg, 85%). ^{1}H NMR (400 MHz, 0.75 mL CD_3CN + 0.05 mL CF_3CO_2D) δ 8.96 (d, *J* = 9.2 Hz, H10), 8.86 (1H, d, *J* = 9.1 Hz, H1), 8.71 (1H, dd, *J* = 9.2, 2.3 Hz, H9), 8.16 - 8.05 (3H, m, H2, H4, H7), 7.72 - 7.67 (1H, m, H4''), 7.67 - 7.61 (2H, m, H3'', H5''), 7.51 - 7.46 (2H, m, H2'', H6''), 4.68 - 4.56 (2H, m, CH_2-1'), 1.85 – 1.76 (2H, m, CH_2-2''), 1.34 [s, 9H, $C(CH_3)_3$], 1.20 - 1.09 (2H, m, CH_2-3'), 1.00 (4H, m, CH_2-4', CH_2-5'), 0.63 (3H, t, *J* = 7.0 Hz, CH_3-6'). ^{13}C NMR (126 MHz, 0.75 mL CD_3CN + 0.05 mL CF_3CO_2D) δ 164.32 (C), 158.62 (C), 147.28 (C), 138.16 (C), 134.94 (C), 132.03 (CH), 129.95 (CH), 129.68 (CH), 129.62 (CH), 128.22 (CH), 127.91 (CH), 125.60 (CH), 125.38 (C), 125.19 (CH), 123.51 (C), 117.03 (CH), 116.30 (C), 55.26 (CH_2), 35.86 (C), 30.33 (CH_2), 29.89 (CH_3), 28.82 (CH_2),

25.66 (CH_2), 21.79 (CH_2), 12.84 (CH_3) . ν_{Max}(ATR)cm^{-1}: 2956 (C_{Ar}-H), 2927 (C_{Ar}-H), 2870 (C_{Ar}-H), 1620 (C=N), 1588 (C_{Ar}=C_{Ar}), 1539 (C_{Ar}=C_{Ar}), 1342 (NO_2). MS (ESI^+): 441 [M^+ (phenanthridinium cation), 100%]. HRMS: 441.2516. $C_{29}H_{33}N_2O_2$ requires 441.2537.

3-*tert*-Butyl-5-(hex-1'-yl)-6-phenyl-8-aminophenanthridinium chloride **293**

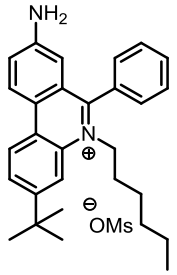

293

Benzophenone **265** (500 mg, 1.33 mmol, 1.00 eq.) and dry hexylamine (1.23 mL, 9.31 mmol, 7.16 eq.) were combined stirring under argon at 0 ˚C in dry DCM (10.0 mL) then titanium tetrachloride (0.22 mL, 2.0 mmol, 1.5 eq.) was added over 5 min. The reaction was allowed to warm to RT and allowed to stir for 15 h. The remaining mixture was quenched into H_2O and partitioned with DCM then the aqueous layer was re-extracted (DCM x 2). The combined organics were washed with brine and dried by filtration through a hydrophobic frit, then the solvent removed under reduced pressure. The residue was dissolved in dry $CHCl_3$ and transferred to a kugelrohr bulb. The $CHCl_3$ was evaporated at atmospheric pressure and the oil allowed to heat at 100 ˚C under argon for 110 min. The oil was then dissolved in $CHCl_3$ and TFA (10:1), which were removed under reduced pressure to give the cyclised nitro product. This was dissolved in TFA (18.0 mL) and 10% Pd/C (349 mg, 0.33 mmol, 0.25 eq.) added, then the mixture stirred while a balloon of $H_{2(g)}$ was used to degas the solution. The mixture was allowed to stir for 2 h at RT under a $H_{2(g)}$ atmosphere, then concentrated. The residue was diluted and neutralised by addition of DCM and K_2CO_3 respectively, then filtered through a combination of celite and K_2CO_3 with additional DCM. The material was purified by chromatography (SiO_2, loaded and washed with DCM, then eluted with DCM/MeOH). The counterion was then exchanged to mesylate on an Amberlite IR-401 column, giving the final salt **293** as a red foam (315 mg, 47%). ^{1}H NMR (500 MHz, $CDCl_3$) δ 8.60 (1H, d, *J* = 9.0 Hz, H1), 8.43 (1H, d, *J* = 9.1 Hz, H10), 8.03 (1H, d, *J* = 1.4 Hz, H4), 7.96 (1H, dd, *J* = 8.8, 1.5 Hz, H2), 7.84 (1H, dd, *J* = 8.9, 1.7 Hz, H9), 7.76 - 7.68 (3H, m, H3'', H4'', H5''), 7.47 - 7.41 (2H , m, H2'', H6''), 6.34 (1H, d, *J* = 2.2 Hz, H7), 5.43 (2H, s, br, NH_2), 4.80 - 4.60 (2H, m, br, CH_2-1'), 2.59 (3H, s, O_3SCH_3), 1.96 - 1.79 (2H, m, br, CH_2-2'), 1.46 [9H, s, $C(CH_3)_3$], 1.32 - 1.10 (6H, m, CH_2-3', CH_2-4', CH_2-5'), 0.79 (3H, t, *J* = 7.0 Hz, CH_2-6'). ^{13}C NMR (126 MHz, $CDCl_3$) δ 160.63 (C), 153.78 (C), 150.31 (C), 131.65 (CH), 131.61 (C), 131.29 (C), 129.97 (CH), 129.40 (CH), 128.67 (CH), 128.16 (CH), 127.03 (C), 126.32 (C), 125.03 (C), 123.60 (CH), 123.51 (CH), 115.13 (CH), 110.53 (CH), 54.30 (CH_2), 39.46 (CH_3), 35.80 (C), 31.15 (CH_3), 30.89 (CH_2), 29.72 (CH_2), 26.28 (CH_2), 22.27 (CH_2), 13.84 (CH_3). ν_{Max}(ATR)cm^{-1}: 3333 (NH), 3210 (NH), 2959 (C-H), 2932 (C-H), 2866 (C-H), 1609 (C=N). MS (NSI^+): 411 [M^+ (phenanthridinium cation), 100%], 327 [$(M+H)^+ - C_6H_{12}$, 25]. HRMS: 411.2803. $C_{29}H_{35}N_2$ requires 411.2795.

2-Fluoro-4-nitrophenyl-4,4,5,5-tetramethyl-1,3,2-dioxoborolane **315**

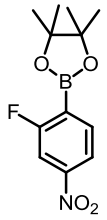

315

Aryl bromide **319** (1.88 g, 8.55 mmol, 1.00 eq.), bis(pinacolato)diboron (2.24 g, 8.82 mmol, 1.03 eq.), anhydrous potassium acetate (2.71 g, 27.6 mmol, 3.23 eq.) and (dppf)$PdCl_2$.DCM (150 mg, 0.18 mmol, 2 mol%) were combined and opened to vacuum, then refilled with argon. The cycle was repeated (x 2) then dry 1,4-dioxane (65 mL) added and the reaction heated to 100 ˚C and stirred under argon for 3 h. The mixture was filtered through celite, dried ($MgSO_4$), filtered and the solvent removed under reduced pressure. Column chromatography [SiO_2, gradient from Pet. ether to Pet. ether/EtOAc (6.7:1)] gave impure boronate ester (2.01 g), of which a portion (1.81 g) was chromatographed again [SiO_2, gradient from Pet. ether to Pet. ether/EtOAc (6.7:1)] to give boronate ester **315** as a solid (1.27 g, 61%). ^{1}H NMR (500 MHz, $CDCl_3$) δ 8.00 (1H, dd, *J* = 8.2, 2.0 Hz, H5), 7.92 (1H, dd, *J* = 8.2, 5.8 Hz, H6), 7.88 (1H, dd, *J* = 8.7, 2.0 Hz, H3), 1.38 (12H, s, CH_3 x 4). ^{13}C NMR (101 MHz, $CDCl_3$) δ 166.69 (d, *J* = 255.5 Hz, CF), 150.99 (d, *J* = 9.2 Hz, C), 137.82 (d, *J* = 8.5 Hz, CH), 118.42 (d, *J* = 3.6 Hz, CH), 110.93 (d, *J* = 29.4 Hz, CH), 84.84 (C), 24.88 (CH_3). ^{19}F NMR (377 MHz, $CDCl_3$) δ −98.70 (dd, *J* = 8.6, 5.8 Hz). ν_{Max}(ATR)cm^{-1}: 2978 (C-H), 2932 (C-H), 1611 (C_{Ar}=C_{Ar}), 1524 (NO_2), 1341 (NO_2). MS (APCI$^+$): 268 [(M+H)$^+$, 100%]. HRMS: 268.1149. $C_{12}H_{16}BFNO_4$ requires 268.1151. MP: 73 - 77 ˚C.

Potassium 2-fluoro-4-nitrophenyltrifluoroborate **320**

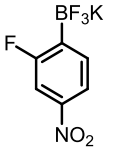

320

Bromide **319** (2.00 g, 9.09 mmol, 1.00 eq.), bis(pinacolato)diboron (2.58 g, 10.1 mmol, 1.12 eq.), dry KOAc (2.78 g, 28.3 mmol, 3.12 eq.) and (dppf)$PdCl_2$.DCM (150 mg, 0.184 mmol, 0.0202 eq.) were placed under vacuum then the vessel refilled with argon. This process was repeated (x 2), then dry 1,4-dioxane (65 mL) was added and the mixture heated with stirring under argon to 100 ˚C for 6 h, with dry NEt_3 (0.20 mL, 1.4 mmol, 0.16 eq.) added at 60 ˚C. After cooling to 50 ˚C the mixture was vacuum filtered through celite and $MgSO_4$ eluting with $CHCl_3$, then the solvent removed from the filtrate under reduced pressure. The residue was dissolved in MeOH/water (1:1) then KHF_2 added (16 g, 205 mmol, 22.5 eq.) and the solution stirred for 20 h. The mixture was concentrated under reduced pressure and the residue dissolved in acetone and filtered. The filtrate was concentrated, and the potassium trifluoroborate salt **320** crystallised from hot acetone as a beige solid (367 mg, 16%). ^{1}H NMR (500 MHz, Acetone) δ 7.82 (1H, ddd, *J* = 8.1, 2.1, 0.7 Hz, H5), 7.72 (1H, apparent t, br, *J* = 6.3 Hz, H6), 7.62 (1H, dd, *J* = 8.6, 1.8 Hz, H3). ^{13}C NMR (101 MHz, DMSO) δ 164.79 (d, *J* = 243.7 Hz, CF), 146.93 (d, *J* = 9.2 Hz, C), 134.85 (dq, *J* = 13.9, 2.6 Hz, CH), 117.67 (d, *J* = 2.8 Hz, CH), 109.11 (d, *J* = 31.7 Hz, CH). (ATR cm^{-1}): 1528 (NO_2), 1360 (NO_2). MS

(NSI$^-$): 208 [M$^-$ (trifluoroborate anion)]. HRMS: 208.0195. $C_6H_3BF_4NO_2$ requires 208.0198. MP: > 250 ˚C.

2-Bromo-5-nitroacetophenone **321**

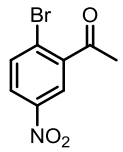

321

2-Bromoacetophenone **323** (2.00 g, 10.1 mmol, 1.00 eq.) was added to a solution of KNO_3 (1.26 g, 12.5 mmol, 1.23 eq.) in $H_2SO_{4(aq)}$ (10 mL) stirring at 0 ˚C. The mixture was allowed to stir warming to RT for 70 min, and was then quenched (H_2O) and extracted with DCM (x 2). The combined organics were dried ($MgSO_4$), filtered and the solvent removed under reduced pressure. Column chromatography [SiO_2, Pet. ether/EtOAc (7:1)] gave nitroacetophenone **321** as a solid (1.34 g, 55%). R_f = 0.34 in Pet. ether/EtOAc (7:1). ^{1}H NMR (500 MHz, $CDCl_3$) δ 8.28 (1H, d, *J* = 2.7 Hz, H6), 8.12 (1H, dd, *J* = 8.7, 2.7 Hz, H4), 7.82 (1H, d, *J* = 8.7 Hz, H3), 2.67 (3H, s, $COCH_3$). ^{13}C NMR (101 MHz, $CDCl_3$) δ 198.87 (C), 147.06 (C), 142.39 (C), 135.27 (CH), 126.22 (C), 125.98 (CH), 123.83 (CH), 30.19 (CH_3). ν_{Max}(ATR)cm^{-1}: 3095 (C_{Ar}-H), 3073 (C_{Ar}-H), 1709 (C=O), 1604 (C_{Ar}=C_{Ar}), 1568 (C_{Ar}=C_{Ar}), 1523 (NO_2), 1355 (NO_2). MS (EI$^+$): 245 (^{81}BrM$^{+\cdot}$, 22%), 243 (^{79}BrM$^{+\cdot}$, 26), 230 [(^{81}BrM+H) – $^{\cdot}CH_3$, 82], 228 [(^{79}BrM+H) – $^{\cdot}CH_3$, 100], 184 [(^{81}BrM$^{\cdot}$+H) – $^{\cdot}CH_3$ – $^{\cdot}NO_2$, 24], 182 [(^{79}BrM$^{\cdot}$+H) – $^{\cdot}CH_3$ – $^{\cdot}NO_2$, 26]. HRMS: 244.9514. $C_8H_6{}^{81}BrNO_3$ requires 244.9511. MP: 85 - 87 ˚C.

2-(2'-Fluoro-4'-nitrophenyl)-5-nitroacetophenone **324**

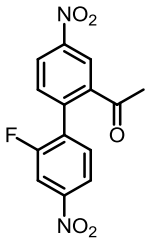

324

Bromoacetophenone **321** (1.00 g, 4.10 mmol, 1.00 eq.), PEPPSI-^{i}Pr catalyst (140 mg, 0.21 mmol, 0.05 eq.) and arylboronic acid **315** (1.13 g, 4.22 mmol, 1.03 eq.) were divided evenly between two microwave tubes (10 mL) under argon. The tubes were opened to vacuum, then refilled with argon. This process was repeated twice then *N,N*-diisopropylethylamine (2.00 mL, 11.4 mmol, 2.79 eq.) and degassed ethanol (10.0 mL) were split between the tubes. Each tube was heated to 125 ˚C for 10 min. After cooling the mixtures were filtered through celite eluting with DCM and the solvent removed under reduced pressure. The residue was redissolved then partitioned (DCM/1 M $HCl_{(aq)}$) then the aqueous layer extracted (DCM x 2). The combined organics were dried ($MgSO_4$), filtered and the solvent removed under reduced pressure. Additional boronic acid (200 mg, 0.75 mmol, 0.18 eq.), *N,N*-diisopropylethylamine (1.00 mL, 5.74 mmol, 1.40 eq.), PEPPSI-^{i}Pr catalyst (50 mg, 0.07 mmol, 0.02 eq.) and ethanol (10.0 mL) was added and the mixture divided then the previous processes repeated. Column chromatography [SiO_2, Pet. Ether/ EtOAc (5:1)] gave ketone **324** as a solid (499 mg, 40%). R_f = 0.23 in Pet. Ether/ EtOAc (5:1). ^{1}H NMR (500 MHz, $CDCl_3$) δ 8.65 (1H, d, *J* = 2.3 Hz, H6), 8.46 (1H, dd, *J* = 8.4, 2.3 Hz, H4), 8.17 (1H, dd, *J* = 8.4, 1.9 Hz,

H5'), 7.99 (1H, dd, *J* = 9.5, 2.2 Hz, H3'), 7.56 (1H, d, *J* = 8.4 Hz, H3), 7.51 (dd, *J* = 8.2, 7.4 Hz, H6'), 2.62 (s, 3H). ^{13}C NMR (126 MHz, $CDCl_3$) δ 198.04 (d, *J* = 0.6 Hz, C), 158.38 (d, *J* = 251.0 Hz, CF), 148.90 (d, *J* = 8.7 Hz, C), 148.12 (C), 139.95 (C), 138.97 (C), 134.19 (d, *J* = 16.0 Hz, C), 132.89 (CH), 131.01 (d, *J* = 3.3 Hz, CH), 126.41 (CH), 123.64 (CH), 120.03 (d, *J* = 3.7 Hz, CH), 111.65 (d, *J* = 27.4 Hz, CH), 28.44 (CH_3). ^{19}F NMR (470 MHz, $CDCl_3$) δ −111.05 (dd, *J* = 9.6, 7.2 Hz). ν_{Max}(ATR)cm^{-1}: 3111 (C_{Ar}-H), 3078, (C_{Ar}-H), 3057 (C_{Ar}-H), 1699 (C=O), 1609 (C_{Ar}=C_{Ar}), 1580 (C_{Ar}=C_{Ar}), 1510 (NO_2), 1346 (NO_2). MS (EI$^+$): 304 ($M^{+\cdot}$, 62%), 289 ($M^{+\cdot}$ – $^{\cdot}CH_3$, 100), 285 ($M^{+\cdot}$ – $^{\cdot}$F 9), 243 ($M^{+\cdot}$ – F$^{\cdot}$ – CH_2CO, 22) 213 ($C_{14}H_{10}FO^+$, 15). HRMS: 304.0491. $C_{14}H_9FN_2O_5$ requires 304.0495. MP: 123 - 124 ˚C.

2-(2''-Fluoro-3''-pyridyl)-5-nitrobenzophenone **325**

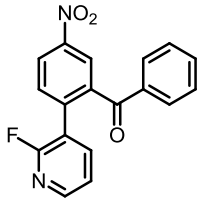

325

Iodobenzophenone **218** (1.00 g, 2.83 mmol, 1.00 eq.), PEPPSI-^{i}Pr catalyst (100 mg, 0.15 mmol, 0.05 eq.) and arylboronic acid **312** (400 mg, 2.84 mmol, 1.00 eq.) were divided evenly between two microwave tubes (10 mL) under argon. The tubes were then opened to vacuum, then refilled with argon. This process was repeated twice then *N,N*-diisopropylethylamine (1.46 mL, 8.38 mmol, 2.96 eq.) and degassed ethanol (10 mL) were split between the tubes. Each tube was heated to 125 ˚C for 1 h in a microwave. After cooling the mixtures were combined and filtered through celite with DCM and the solvent removed under reduced pressure. The residue was partitioned between DCM and 1 M $HCl_{(aq)}$ then the aqueous layer extracted (DCM x 2). The combined organics were dried ($MgSO_4$), filtered and the solvent removed under reduced pressure. Column chromatography [SiO_2, Pet. Ether/EtOAc gradient from (7:1) to (5:1)]. The benzophenone **325** was isolated as a solid (480 mg, 53%). R_f = 0.14 in Pet ether/EtOAc (5:1). ^{1}H NMR (400 MHz, $CDCl_3$) δ 8.46 (1H, dd, *J* = 8.4, 2.4 Hz, H4), 8.42 (1H, d, *J* = 2.2 Hz, H6), 8.15 (1H, ddd, *J* = 4.9, 1.9, 1.2 Hz, H4''), 7.77 - 7.65 (4H, m, H3, H6'', H2', H6'), 7.56 (1H, ddt, *J* = 8.0, 6.8, 1.3 Hz, H4'), 7.45 - 7.38 (2H, m, H3', H5'), 7.20 (1H, ddd, *J* = 7.4, 4.9, 1.8 Hz, H5''). ^{13}C NMR (101 MHz, $CDCl_3$) δ 194.67 (C), 159.30 (d, *J* = 238.7 Hz, CF), 148.26 (d, *J* = 14.8 Hz, CH), 147.43 (C), 141.47 (d, *J* = 3.5 Hz, CH), 140.45 (C), 139.85 (d, *J* = 4.5 Hz, C), 135.85 (C), 134.05 (CH), 132.44 (d, *J* = 0.8 Hz, CH), 129.99 (CH), 128.80 (CH), 125.35 (CH), 124.29 (CH), 121.73 (d, *J* = 4.4 Hz, CH), 121.01 (d, *J* = 30.4 Hz, C). ^{19}F NMR (377 MHz, $CDCl_3$) δ −68.76 (d, *J* = 9.5 Hz). ν_{Max}(ATR)cm^{-1}: 3069 (C_{Ar}-H), 3062 (C_{Ar}-H), 1668 (C=O), 1607 (C_{Ar}=C_{Ar}), 1583 (C_{Ar}=C_{Ar}), 1523 (NO_2), 1351 (NO_2). MS (EI$^+$): 322 ($M^{+\cdot}$, 100%), 245 (M^+ – Ph, 20), 121 ($C_6H_3NO_2^{+\cdot}$, 40), 105 ($PhCO^+$, 87), 77 (Ph^+, 37). HRMS: 322.0750. $C_{18}H_{11}O_3N_2F$ requires 322.0754. MP: 125 -127 ˚C.

2-(2''-Fluoro-4''-bromophenyl)-5-nitrobenzophenone **326**

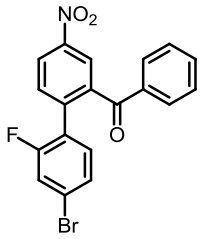

326

Iodobenzophenone **218** (1.45 g, 4.11 mmol, 1.00 eq.), PEPPSI-^{i}Pr catalyst (94 mg, 0.14 mmol, 0.03 eq.) and arylboronic acid **313** (1.00 g, 4.57 mmol, 1.11 eq.) were combined under argon and the reaction vessel was opened to vacuum, then refilled with argon. This process was repeated twice then *N,N*-diisopropylethylamine (2.4 mL, 14 mmol, 3.4 eq.) and degassed ethanol (40 mL) added. The mixture was heated to reflux stirring for 22 h. After cooling the mixture was filtered through celite eluting with DCM and the solvent removed under reduced pressure. The residue was partitioned between DCM and 1 M $HCl_{(aq)}$ then the aqueous layer further extracted (DCM x 2). The combined organics were dried ($MgSO_4$), filtered and the solvent removed under reduced pressure. Column chromatography [SiO_2, Pet. ether/EtOAc (15:1)]. Gave ketone **326** as a yellow solid (896 mg, 55%). R_f = 0.32 in Pet. ether/EtOAc (5:1). ^{1}H NMR (400 MHz, $CDCl_3$) δ 8.43 (1H, dd, *J* = 8.4, 2.4 Hz, H4), 8.39 (1H, d, *J* = 2.3 Hz, H6), 7.75 - 7.68 (2H, m, H2', H6'), 7.65 (1H, d, *J* = 8.4 Hz, H3), 7.57 (1H, ddt, *J* = 8.0, 7.0, 1.3 Hz, H4'), 7.41 (2H, t, *J* = 7.7 Hz, H3', H5'), 7.28 (1H, dd, *J* = 8.3, 1.6 Hz, H5''), 7.19 - 7.12 (2H, m, H3'', H6''). ^{13}C NMR (101 MHz, $CDCl_3$) δ 194.82 (d, *J* = 0.7 Hz, C), 158.56 (d, *J* = 252.3 Hz, CF), 147.20 (C), 140.69 (C), 140.36 (C), 135.94 (C), 133.96 (CH), 132.42 (d, *J* = 0.6 Hz, CH), 132.02 (d, *J* = 3.3 Hz, CH), 130.06 (CH), 128.74 (CH), 128.07 (d, *J* = 3.7 Hz, CH), 125.29 (CH), 125.21 (d, *J* = 15.1 Hz, C), 124.21 (CH), 123.64 (d, *J* = 9.5 Hz, C), 119.62 (d, *J* = 25.1 Hz, CH). ^{19}F NMR (470 MHz, $CDCl_3$) δ −112.25 (apparent t, *J* = 8.7 Hz). ν_{Max}(ATR)cm^{-1}: 3088 (C_{Ar}-H), 3071 (C_{Ar}-H), 1668 (C=O), 1605 (C_{Ar}=C_{Ar}), 1582 (C_{Ar}=C_{Ar}), 1524 (NO_2), 1350 (NO_2). MS (EI^+): 401 ($^{81}BrM^{+\cdot}$, 26%) 399 ($^{79}BrM^{+\cdot}$, 30), 353 ($M^{+\cdot} - NO_2^{\cdot}$, 30), 105 ($PhCO^+$, 100), 77 ($Ph^+$, 34). HRMS: 398.9902 and 400.9877. $C_{19}H_{11}O_3NBrF$ requires 398.9906 and 400.9888. MP: 101 -105 ˚C.

2-(2''-Fluorophenyl)-benzophenone **327**

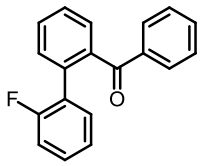

327

Iodobenzophenone **218** (1.41 g, 4.57 mmol, 1.00 eq.), PEPPSI-^{i}Pr catalyst (76 mg, 0.11 mmol, 0.03 eq.) and arylboronic acid **314** (563 mg, 4.55 mmol, 1.00 eq.) were combined under argon and the reaction vessel was opened to vacuum, then refilled with argon. This process was repeated twice then *N,N*-diisopropylethylamine (1.91 mL, 11.0 mmol, 2.75 eq.) and degassed ethanol (18.0 mL) added. The mixture was heated to reflux stirring for 16 h. After cooling the mixture was filtered through celite eluting with DCM and the solvent removed under reduced pressure. The residue was taken up in Et_2O then dried ($MgSO_4$), filtered and the solvent removed under reduced pressure. Column chromatography [SiO_2, Pet. ether/EtOAc (12:1)] gave ketone **327** as a clear oil

(958 mg, 76%). R_f = 0.24 Pet. ether/EtOAc (12:1). ^{1}H NMR (500 MHz, $CDCl_3$) δ 7.71 - 7.67 (2H, m, H2', H6'), 7.62 - 7.55 (2H, m, H6, H4), 7.51 - 7.47 (2H, m, H3, H5), 7.43 (1H, ddt, *J* = 7.9, 6.8, 1.3 Hz, H4'), 7.35 - 7.29 (2H, t, *J* = 7.7 Hz, H3', H5'), 7.24 (apparent td, *J* = 7.6, 1.8 Hz, H6''), 7.17 - 7.13 (1H, m, H4''), 7.05 (1H, apparent td, *J* = 7.5, 1.3 Hz, H5''), 6.88 (1H, ddd, *J* = 10.1, 8.4, 1.2 Hz, H3''). ^{13}C NMR (101 MHz, $CDCl_3$) δ 197.70 (d, *J* = 1.1 Hz, C), 159.20 (d, *J* = 246.3 Hz, CF), 139.34 (d, *J* = 0.8 Hz, C), 137.49 (C), 135.39 (C), 132.83 (CH), 131.60 (d, *J* = 3.2 Hz, CH), 131.24 (d, *J* = 1.2 Hz, CH), 130.65 (CH), 130.06 (CH), 129.59 (d, *J* = 8.1 Hz, CH), 129.32 (CH), 128.17 (CH), 128.10 (d, *J* = 15.1 Hz, C), 127.66 (CH), 124.19 (d, *J* = 3.7 Hz, CH), 115.53 (d, *J* = 22.3 Hz, CH). ^{19}F NMR (470 MHz, $CDCl_3$) δ −115.75 (ddd, *J* = 10.0, 7.7, 5.2 Hz). ν_{Max}(ATR)cm^{-1}: 3061 (C_{Ar}-H), 3030 (C_{Ar}-H), 1663 (C=O), 1595 (C_{Ar}=C_{Ar}), 1582 (C_{Ar}=C_{Ar}), 1501 (C_{Ar}=C_{Ar}). MS (EI$^+$): 276 ($M^{+\cdot}$, 89%), 257 ($M^+ - F^\cdot$, 38), 199 ($M^{+\cdot} - Ph^\cdot$, 100), 170 ($C_{12}H_{10}O^{+\cdot}$, 62). HRMS: 276.0946. $C_{19}H_{13}OF$ requires 276.0950.

2-(2''-Fluoro-4''-nitrophenyl)-5-nitrobenzophenone **328**

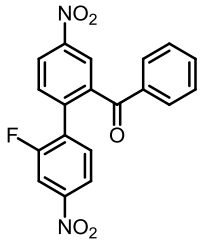

328

Iodobenzophenone **218** (995 mg, 2.82 mmol, 1.00 eq.), PEPPSI-^{i}Pr catalyst (105 mg, 0.15 mmol, 0.05 eq.) and arylboronate **315** (706 mg, 2.64 mmol, 0.94 eq.) were divided evenly into three microwave tubes (10 mL) and each reaction vessel was opened to vacuum, then refilled with argon. This process was repeated twice then *N,N*-diisopropylethylamine (1.56 mL, 8.96 mmol, 3.18 eq.) and degassed ethanol (15.0 mL) divided between them. Each tube was sealed and heated to 100 ˚C for 30 min in a microwave. After cooling the material was combined in DCM and filtered through a celite/K_2CO_3 mixture and the solvent removed from the filtrate under reduced pressure. The material was dry loaded onto celite in DCM then column chromatography [SiO_2, Pet. Ether/DCM, (1:1)] gave ketone **328** as a solid (962 mg, 99%). R_f = 0.14 DCM/Pet. ether (6:4). ^{1}H NMR (500 MHz, $CDCl_3$) δ 8.50 (1H, dd, *J* = 8.4, 2.4 Hz, H4), 8.44 (1H, d, *J* = 2.3 Hz, H6), 8.07 (1H, dd, *J* = 8.4, 2.1 Hz, H5''), 7.87 (1H, dd, *J* = 9.4, 2.2 Hz, H3''), 7.74 (2H, d, *J* = 8.5 Hz, H2', H6'), 7.69 (d, *J* = 8.4 Hz, H3), 7.63 - 7.58 (1H, tt, *J* = 7.5, 1.2 Hz, H4'), 7.52 (1H, dd, *J* = 8.4, 7.4 Hz, H6''), 7.46 (2H, m, H3', H5'). ^{13}C NMR (126 MHz, $CDCl_3$) δ 194.07 (d, *J* = 1.1 Hz, C), 158.42 (d, *J* = 252.3 Hz, CF), 148.95 (d, *J* = 8.6 Hz, C), 147.76 (C), 140.49 (d, *J* = 0.9 Hz, C), 139.37 (C), 135.77 (C), 134.02 (CH), 132.86 (d, *J* = 15.6 Hz, C), 132.22 (d, *J* = 1.3 Hz, CH), 131.74 (d, *J* = 3.2 Hz, CH), 129.92 (CH), 128.74 (CH), 125.30 (CH), 124.24 (CH), 119.47 (d, *J* = 3.8 Hz, CH), 111.62 (d, *J* = 27.4 Hz, CH). ^{19}F NMR (470 MHz, $CDCl_3$) δ −110.18 (dd, *J* = 9.3, 7.7 Hz). ν_{Max}(ATR)cm^{-1}: 3090 (C_{Ar}-H), 1667 (C=O), 1597 (C_{Ar}=C_{Ar}), 1522 (NO_2), 1346 (NO_2). MS (CI$^+$): 367 [$(M+H)^+$, 100%], 228 [$(PhCOC_6H_4NO_2+H)^+$, 92]. HRMS: 367.0722. $C_{19}H_{12}O_5NF$ requires 367.0730. MP: 143 -144 ˚C.

2-(2'-Fluorophenyl)acetophenone **329**

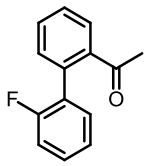

329

Bromoacetophenone **323** (800 mg, 4.02 mmol, 1.00 eq.), PEPPSI-^{i}Pr catalyst (136 mg, 0.20 mmol, 0.05 eq.) and aryl boronic acid **314** (562 mg, 4.02 mmol, 1.00 eq.) were divided evenly between two microwave tubes (10 mL) under argon. The tubes were opened to vacuum, then refilled with argon. This process was repeated twice then *N,N*-diisopropylethylamine (2.10 mL, 15.6 mmol, 3.88 eq.) and degassed ethanol (12.0 mL) were split between the tubes. Each tube was heated to 125 ˚C for 1 h. After cooling the mixtures were filtered through celite with DCM and the solvent removed under reduced pressure. The residue was redissolved then partitioned (DCM/1 M $HCl_{(aq)}$) then the aqueous layer extracted (DCM x 2). The combined organics were dried ($MgSO_4$), filtered and the solvent removed under reduced pressure. Column chromatography [SiO_2, Pet. Ether/EtOAc (15:1)] gave ketone **329** as a clear oil (725 mg, 84%). R_f = 0.32 in 7:1 Pet. Ether/ EtOAc. ^{1}H NMR (400 MHz, $CDCl_3$) δ 7.69 (1H, ddd, *J* = 7.6, 1.4, 0.5 Hz, H6), 7.55 (1H, td, *J* = 7.5, 1.4 Hz, H4), 7.46 (1H, td, *J* = 7.6, 1.3 Hz, H5), 7.40 - 7.31 (2H, m, H3, H4'), 7.29 (1H, dd, *J* = 7.6, 1.8 Hz, H6'), 7.22 (td, *J* = 7.5, 1.2 Hz, H5'), 7.15 - 7.08 (1H, m, H3'). ^{13}C NMR (101 MHz, $CDCl_3$) δ 202.17 (C), 159.27 (d, *J* = 245.8 Hz, CF), 140.28 (C), 134.36 (C), 131.48 (CH), 131.17 (CH), 131.12 (d, *J* = 3.3 Hz, CH), 129.72 (d, *J* = 8.1 Hz, CH), 128.72 (d, *J* = 15.5 Hz, C), 128.39 (CH), 128.08 (d, *J* = 2.0 Hz, CH), 124.52 (d, *J* = 3.6 Hz, CH), 115.64 (d, *J* = 22.3 Hz, CH), 29.14 (CH_3). ^{19}F NMR (377 MHz, $CDCl_3$) δ −116.23 - −116.33 (m). ν_{Max}(ATR)cm^{-1}: 3063 (C_{Ar}-H), 1688 (C=O), 1595 (C_{Ar}=C_{Ar}), 1568 (C_{Ar}=C_{Ar}), 1499 (C_{Ar}=C_{Ar}). MS (EI^{+}): 214 ($M^{+\cdot}$, 57%), 199 ($C_{13}H_8FO^{+}$, 100), 170 ($C_{12}H_{10}O^{+\cdot}$, 42). HRMS: 214.0791. $C_{14}H_{11}FO$ requires 214.0794.

2-(2''-Chloro-5''-nitrophenyl)-5-nitrobenzophenone **330**

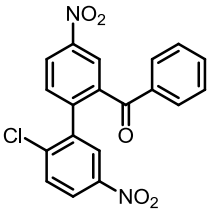

330

Iodobenzophenone **218** (1.00 g, 2.83 mmol, 1.12 eq.), PEPPSI-^{i}Pr catalyst (96 mg, 0.14 mmol, 0.05 eq.) and arylboronic acid **316** (510 mg, 2.53 mmol, 1.00 eq.) were divided evenly between two microwave tubes (10.0 mL) under argon. The tubes were opened to vacuum, then refilled with argon. This process was repeated twice then *N,N*-diisopropylethylamine (1.45 mL, 8.32 mmol, 3.29 eq.) and degassed ethanol (10.0 mL) were split between the tubes. Each tube was heated to 125 ˚C for 10 min. After cooling the mixtures were combined and partitioned between DCM and 1 M $HCl_{(aq)}$ then the aqueous layer extracted (DCM x 2). The combined organics were dried ($MgSO_4$), filtered and the solvent removed under reduced pressure. Column chromatography [SiO_2, Pet. Ether/EtOAc (15:1), after drying loading onto celite]. Ketone **330** was isolated as a solid (540 mg, 56%). ^{1}H NMR (500 MHz, $CDCl_3$) δ 8.50 (1H, dd, *J* = 8.4, 2.4 Hz, H4), 8.48 (1H, d, *J* = 2.3 Hz, H6),

8.16 (1H, d, *J* = 2.6 Hz, H6''), 8.13 (1H, dd, *J* = 8.7, 2.7 Hz, H4''), 7.72 (2H, dd, *J* = 8.5, 1.4 Hz, H2', H6'), 7.64 (1H, dd, *J* = 8.4, 0.5 Hz, H3), 7.59 (1H, ddt, *J* = 7.8, 7.1, 1.3 Hz, H4'), 7.52 (1H, d, *J* = 8.7 Hz, H3''), 7.37 (2H, t, br, *J* = 7.9 Hz, H3', H5'). ^{13}C NMR (126 MHz, $CDCl_3$) δ 194.03 (C), 147.63 (C), 146.45 (C), 143.25 (C), 140.09 (C), 139.32 (C), 138.79 (C), 135.84 (C), 134.11 (CH), 132.60 (CH), 130.80 (CH), 130.15 (CH), 128.89 (CH), 126.11 (CH), 125.66 (CH), 124.75 (CH), 124.62 (CH). ν_{Max}(ATR)cm^{-1}: 3057 (C_{Ar}-H), 1670 (C=O), 1597 (C_{Ar}=C_{Ar}), 1574 (C_{Ar}=C_{Ar}), 1530 (NO_2), 1348 (NO_2). MS (EI$^+$): 385 [(^{37}ClM+H)$^+$, 35%], 383 [(^{35}ClM+H)$^+$, 100]. HRMS: 385.0416 and 383.0432. $C_{19}H_{11}ClN_2O_5$ requires 385.0413 and 383.0435. MP: 115 - 116 ˚C.

2-(2''-Fluoro-3''-methylphenyl)-5-nitrobenzophenone **332**

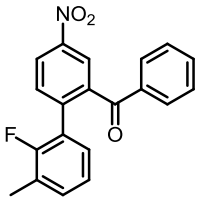

332

Iodobenzophenone **218** (688 mg, 1.95 mmol, 1.00 eq.), PEPPSI-^{i}Pr catalyst (41 mg, 0.06 mmol, 0.03 eq.) and arylboronic acid **318** (300 mg, 1.95 mmol, 1.00 eq.) were combined under argon then the reaction vessel was opened to vacuum, then refilled with argon. This process was repeated twice then *N,N*-diisopropylethylamine (1.02 mL, 5.85 mmol, 3.00 eq.) and degassed ethanol (12.0 mL) added. The mixture was heated to reflux stirring for 22 h. After cooling the mixture was filtered through celite eluting with DCM and the solvent removed under reduced pressure. The material was the redissolved in Et_2O, dried with $MgSO_4$ and ethereal HCl (2 M) added to precipitate the diisopropylethylamine as a salt, which was then removed by filtration. The solvent was then removed from the filtrate under reduced pressure and the solid recrystallised from $CHCl_3$ and washed with $CHCl_3$ to give ketone **332** as a brown solid (430 mg, 66%). R_f = 0.29 [SiO_2, Pet. ether/EtOAc (9:1)]. ^{1}H NMR (500 MHz, $CDCl_3$) δ 8.42 (1H, dd, *J* = 6.2, 2.4 Hz, H4), 8.41 (1H, d, *J* = 2.5 Hz, H6), 7.69 - 7.64 (3H, m, H3, H2', H6'), 7.50 (1H, ddt, *J* = 7.9, 7.0, 1.3 Hz, H4'), 7.35 (2H, apparent t, *J* = 8.0 Hz, H3', H5'), 7.10 - 7.02 (2H, m, H4'', H6''), 6.97 (1H apparent t, *J* = 7.5 Hz, H5''), 2.14 (3H, d, *J* = 2.2 Hz, CH_3). ^{13}C NMR (126 MHz, $CDCl_3$) δ 195.24 (C), 157.34 (d, *J* = 246.3 Hz, CF), 147.08 (C), 142.13 (C), 140.46 (C), 136.27 (C), 133.53 (CH), 132.49 (CH), 132.45 CH), 129.87 (CH), 128.58 (d, *J* = 2.5 Hz, CH), 128.44 (CH), 125.71 (d, *J* = 15.7 Hz, C), 125.40 (d, *J* = 17.7 Hz, C) , 125.03 (CH), 124.18 (CH), 124.07 (d, *J* = 4.3 Hz, CH), 14.56 (d, *J* = 4.3 Hz, CH_3). ^{19}F NMR (377 MHz, $CDCl_3$) δ −119.51 (apparent td, *J* = 6.9, 2.2 Hz). ν_{Max}(ATR)cm^{-1}: 1670 (C=O), 1597 (C=C_{Ar}), 1582 (C=C_{Ar}), 1524 (NO_2), 1348 (NO_2). MS (EI$^+$): 335 ($M^{+\cdot}$, 97%), 320 ($M^{+\cdot}$ – $^{\cdot}CH_3$, 55), 258 ($M^{+\cdot}$ – $Ph^{\cdot}$, 43), 183 ($C_{13}H_8F^{+\cdot}$, 42), 105 ($PhCO^+$, 85), 86 (100). HRMS (EI$^+$): 335.0954. $C_{20}H_{14}FNO_3$ requires $M^{+\cdot}$ 335.0958. MP: 140 - 145 ˚C.

2-(2''-Fluoro-5''-methoxyphenyl)-5-nitrobenzophenone **333**

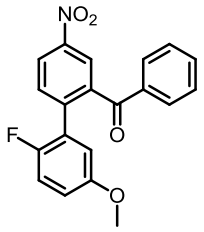

333

Iodobenzophenone **333** (625 mg, 1.77 mmol, 1.00 eq.), PEPPSI-^{i}Pr catalyst (36 mg, 0.05 mmol, 0.03 eq.) and arylboronic acid **317** (301 mg, 1.77 mmol, 1.00 eq.) were combined under argon then the reaction vessel was opened to vacuum, then refilled with argon. This process was repeated twice then *N,N*-diisopropylethylamine (0.93 mL, 5.3 mmol, 3.0 eq.) and degassed ethanol (12.0 mL) added. The mixture was heated to reflux stirring for 22 h. After cooling the mixture was filtered through celite eluting with DCM and the solvent removed under reduced pressure. The material was the redissolved in Et_2O, dried with $MgSO_4$ and ethereal HCl (2 M) added to precipitate the diisopropylethylamine as a salt, which was then removed by filtration. The solvent was then removed from the filtrate under reduced pressure and the solid recrystallised from $CHCl_3$ then washed with $CHCl_3$ to give ketone **333** as a brown solid (517 mg, 83%). R_f = 0.20 [Pet. ether/EtOAc (9:1)]. ^{1}H NMR (500 MHz, $CDCl_3$) δ 8.43 (1H, dd, *J* = 8.4, 2.4 Hz, H4), 8.40 (1H, d, *J* = 2.3 Hz, H6), 7.70 (3H, apparent t, *J* = 8.7 Hz, H3, H2', H6'), 7.53 (1H, tt, *J* = 7.4, 1.3 Hz, H4'), 7.39 (2H, apparent t, *J* = 7.8 Hz, H3', H5'), 6.89 - 6.84 (1H, m, H3''), 6.78 - 6.74 (2H, m, H4'', H6''), 3.72 (s, 3H). ^{13}C NMR (101 MHz, $CDCl_3$) δ 195.13 (C), 155.80 (d, *J* = 2.0 Hz, C), 153.25 (d, *J* = 240.3 Hz, CF), 147.13 (C), 141.66 (C), 140.54 (C), 136.14 (C), 133.74 (CH), 132.46 (d, *J* = 1.0 Hz, CH), 130.00 (CH), 128.60 (CH), 126.32 (d, *J* = 16.5 Hz, C),125.12 (CH), 124.10 (CH), 116.58 (d, *J* = 23.9 Hz, CH), 116.13 (d, *J* = 8.0 Hz, CH), 115.70 (d, *J* = 2.5 Hz, CH), 55.93 (CH_3). ^{19}F NMR (377 MHz, $CDCl_3$) δ −126.33 (dt, *J* = 9.6, 4.8 Hz). ν_{Max}(ATR)cm^{-1}: 2951 (CH), 2934 (CH), 2845 (CH), 1672 (C=O), 1595 (C=C_{Ar}), 1578 (C=C_{Ar}), 1518 (C=C_{Ar}), 1499 (NO_2), 1346 (NO_2). MS (EI$^+$): 351 ($M^{+\cdot}$, 90%), 279 ($M^{+\cdot}$ – NO_2 – C_2H_2, 30), 274 ($M^{+\cdot}$ – $Ph^{\cdot}$, 25), 227 ($PhCOC_6H_4NO_2^{+\cdot}$, 25), 167,149 ($O_2NC_6H_3CO^{+\cdot}$, 100) 105 ($PhCO^+$, 97), 77 (Ph^+, 45). HRMS: 351.0902. $C_{20}H_{14}O_4NF$ requires 351.0907. MP: 100 - 102 ˚C.

2-(2''-Fluoro-4''-nitro-5''-methoxyphenyl)-5-nitrobenzophenone **334**

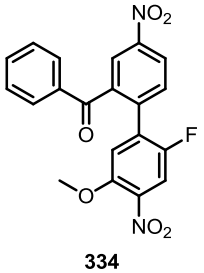

334

Benzophenone **218** (749 mg, 2.13 mmol, 1.00 eq.), acetic anhydride (20 mL) and DCM (10.0 mL) were combined and cooled to 0 ˚C. Concentrated nitric acid (2.0 mL, 44 mmol, 21 eq.) was added and the mixture allowed to stir for 2 h then quenched into $NaOH_{(aq)}$ (1 M) and extracted (DCM, x 2). The organic layer was dried ($MgSO_4$), filtered and the solvent removed under reduced pressure. The residue was then dissolved in minimal hot EtOAc and precipitated by addition of pet. ether, then left to settle (12 h). The solvent was decanted off and the solid triturated with hot

EtOAc. Nitrated benzophenone **334** was isolated as a brown solid (604 mg, 72%). ^{1}H NMR (400 MHz, $CDCl_3$) δ 8.48 (1H, dd, *J* = 8.4, 2.4 Hz, H4), 8.42 (1H, d, *J* = 2.3 Hz, H6), 7.76 - 7.68 (3H, m, H3, H2', H6'), 7.60 (1H, ddt, *J* = 8.0, 7.0, 1.3 Hz, H4'), 7.55 (1H, d, *J* = 8.8 Hz, H3''), 7.49 - 7.41 (2H, m, H3', H5'), 7.00 (1H, d, *J* = 5.9 Hz, H6''), 3.89 (s, 3H). ^{13}C NMR (101 MHz, $CDCl_3$) δ 194.56 (C), 151.45 (d, *J* = 244.8 Hz, CF), 149.60 (d, *J* = 2.7 Hz, C), 147.75 (C), 140.75 (C), 139.48 (d, *J* = 0.9 Hz, C), 139.06 (d, *J* = 8.1 Hz, C), 135.78 (C), 134.37 (CH), 132.33 (d, *J* = 1.3 Hz, CH), 132.01 (d, *J* = 16.7 Hz, C), 130.09 (CH), 128.98 (CH), 125.40 (CH), 124.18 (CH), 116.20 (d, *J* = 2.5 Hz, CH), 113.66 (d, *J* = 28.3 Hz, CH), 57.29 (CH_3). ^{19}F NMR (377 MHz, $CDCl_3$) δ −122.91 (dd, *J* = 8.8, 6.0 Hz). ν_{Max}(ATR)cm^{-1}: 3069 (C_{Ar}-H), 1668 (C=O), 1595 (C_{Ar}=C_{Ar}), 1522 (NO_2), 1346 (NO_2). MS (EI$^+$): 396 ($M^{+\cdot}$, 100%), 105 ($PhCO^+$, 59), 77 (Ph^+, 31). HRMS: 396.0751. $C_{20}H_{13}O_6N_2F$ requires 396.0758. MP: 143 - 144 ˚C.

2-(2''-Fluoro-4''-nitro-5''-methoxy-6''-nitrophenyl)-5-nitrobenzophenone **335**

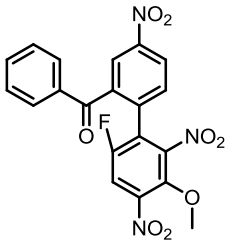

335

Benzophenone **218** (100 mg, 0.284 mmol, 1.00 eq.) was dissolved in MeCN (2.0 mL) and stirred under argon and cooled to – 42 ˚C. NO_2BF_4 was added (approx. 2 eq.) and the reaction warmed to 0 ˚C then stirred for 10 min. The mixture was quenched into water then extracted with DCM. The organic layer was dried ($MgSO_4$), filtered and the solvent removed under reduced pressure. ^{1}H NMR showed the major product to be the double nitrated benzophenone **335**, and a characterisation sample was acquired by column chromatography [SiO_2, Pet. ether/EtOAc (7:1)]. R_f = 0.20 in Pet. ether/EtOAc (7:1). ^{1}H NMR (400 MHz, $CDCl_3$) δ 8.50 (1H, dd, *J* = 8.3, 2.3 Hz, H4), 8.47 (1H, dd, *J* = 2.3, 0.5 Hz, H6), 7.86 (1H, d, *J* = 8.0 Hz, H3''), 7.75 (2H, dd, *J* = 8.4, 1.3 Hz, H2', H6'), 7.68 (1H, ddt, *J* = 7.9, 7.0, 1.4 Hz, H4'), 7.64 (1H, dd, *J* = 8.3, 0.5 Hz, H3), 7.56 - 7.50 (2H, t, *J* = 7.7 Hz, H3', H5'), 4.00 (3H, s, OCH_3). ^{13}C NMR (101 MHz, $CDCl_3$) δ 193.14 (C), 153.84 (d, *J* = 252.1 Hz, CF), 148.23 (C), 146.39 (C), 143.27 (d, *J* = 8.6 Hz, C), 143.01 (d, *J* = 4.3 Hz, C), 139.75 (C), 135.53 (C), 134.15 (CH), 133.82 (C), 132.14 (CH), 130.19 (CH), 128.89 (CH), 126.89 (C), 126.10 (CH), 125.43 (CH), 114.45 (d, *J* = 28.2 Hz, CH), 65.32 (CH_3). ^{19}F NMR (377 MHz, $CDCl_3$) δ −110.49 (d, *J* = 8.0 Hz). (ATR cm^{-1}): 3077 (C_{Ar}-H), 1668 (C=O), 1595 (C_{Ar}=C_{Ar}), 1528 (NO_2), 1343 (NO_2). MS (CI$^+$): 442 [$(M+H)^+$, 100%], 412 [$(M+2H)^+ - OCH_3$, 49]. HRMS: 442.0694. $C_{20}H_{13}O_8N_3F$ requires 442.0687.

4-Azidobutyltriphenylphosphonium iodide **345**

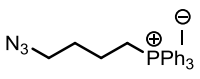

345

Phosphonium iodide **24** (955 mg, 1.67 mmol, 1.00 eq.) and NaN_3 (404 mg, 6.22 mmol, 3.72 eq.) were dissolved in a combination of MeCN (3.5 mL) and water (0.9 mL) then stirred and heated to 80 ˚C for 2 h. The mixture was then cooled and partitioned between DCM and water, then the aqueous re-extracted with DCM and the combined organics washed with brine then the solvent

removed under reduced pressure to give triphenylphosphonium salt **345** as a solid (820 mg, quant.). ^{1}H NMR (400 MHz, $CDCl_3$) δ 7.83 - 7.70 (9H, m, $^{+}PPh_3$), 7.70 - 7.60 (6H, m, $^{+}PPh_3$), 3.81 - 3.68 (2H, m, CH_2-1), 3.37 (2H, t, *J* = 6.2 Hz, CH_2-4), 1.96 (2H, quin., *J* = 6.9 Hz, CH_2-2), 1.75 - 1.62 (2H, m, CH_2-3). ^{13}C NMR (101 MHz, $CDCl_3$) δ 135.28 (d, *J* = 3.1 Hz, CH), 133.83 (d, *J* = 10.0 Hz, CH), 130.68 (d, *J* = 12.6 Hz, CH), 118.11 (d, *J* = 86.1 Hz, C), 50.71 (d, *J* = 1.2 Hz, CH_2), 29.31 (d, *J* = 16.7 Hz, CH_2), 22.71 (d, *J* = 51.0 Hz, CH_2), 19.96 (d, *J* = 3.9 Hz, CH_2). (ATR cm^{-1}): 3075 (C_{Ar}-H), 3055 (C_{Ar}-H), 2945 (C_{Ar}-H), 2936 (C_{Ar}-H), 2893 (C_{Ar}-H), 2868 (C_{Ar}-H), 2097 (N_3), 1587 (C_{Ar}=C_{Ar}). MS (NSI^{+}) 289 [M^{+} (phosphonium cation), 100%]. HRMS: 360.1627. $C_{22}H_{23}N_3P$ requires 360.1624. MP: 142 - 144 °C.

4-Aminobutyltriphenylphosphonium iodide **339**

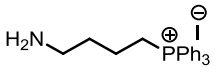

339

Phosphonium salt **345** (836 mg, 1.72 mmol, 1.00 eq.) and 10% Pd/C (220 mg, 0.207 mmol, 0.120 eq.) were combined in MeOH (8.0 mL) and degassed by bubbling $H_{2(g)}$ through the solution. The mixture was then stirred under a $H_{2(g)}$ atmosphere for 14 h. The mixture was filtered through celite eluting with MeOH, then the solvent removed under reduced pressure. The residue was re-dissolved in DCM then dried ($MgSO_4$), filtered and the solvent removed under reduced pressure to give amine **339** as a solid (736 mg, 93%). ^{1}H NMR (500 MHz, $CDCl_3$) δ 7.88 - 7.57 (15H, m, $^{+}PPh_3$), 4.05 (2H, s, br, NH_2), 3.74 - 3.58 (2H, m, CH_2-1), 2.81 (2H, t, *J* = 6.7 Hz, CH_2-4), 2.02 - 1.89 (2H, m, CH_2-2), 1.78 - 1.64 (2H, m, CH_2-3). ^{13}C NMR (126 MHz, $CDCl_3$) δ 135.07 (d, *J* = 2.8 Hz, CH), 133.78 (d, *J* = 10.0 Hz, CH), 130.57 (d, *J* = 12.5 Hz, CH), 118.02 (d, *J* = 86.0 Hz, C), 39.97 (CH_2), 31.14 (CH_2), 22.66 (d, *J* = 50.4 Hz, CH_2), 20.06 (CH_2). (ATR cm^{-1}): 3378 (N-H), 3051 (C_{Ar}-H), 3008 (C_{Ar}-H), 2989 (C_{Ar}-H), 2867 (C_{Ar}-H), 1587 (C_{Ar}=C_{Ar}). MS (ESI^{+}): Matches data acquired by a colleague.[416]

1-Azidohexane **343**

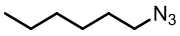

343

Bromohexane **346** (2.0 g, 12 mmol, 1.0 eq.) was dissolved in MeCN (25 mL), then NaN_3 (2.35 g, 36.2 mmol, 3.01 eq.) and water (6 mL) added and the reaction stirred under reflux for 17 h. The mixture was partitioned between brine and Et_2O then the organic layer washed with water (x 3) and dried ($MgSO_4$), filtered and the solvent removed under reduced pressure to give azide **343** as an oil (1.40 g, 92%). ^{1}H NMR (500 MHz, $CDCl_3$) δ 3.26 (2H, t, *J* = 7.0 Hz, CH_2-1), 1.60 (2H, quin., *J* = 7.2 Hz, CH_2-2), 1.45 - 1.27 (6H, m, CH_2-3, CH_2-4, CH_2-5), 0.91 (3H, t, *J* = 7.0 Hz, CH_2-6). ^{13}C NMR (126 MHz, $CDCl_3$) δ 51.75 (CH_2), 31.51 (CH_2), 29.01 (CH_2), 26.58 (CH_2), 22.65 (CH_2), 14.04 (CH_3). Consistent with literature data.[428]

1,6-Diazidohexane **349**

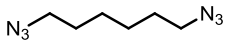

349

1,6-Dibromohexane **347** (1.90 mL, 12.4 mmol, 1.00 eq.) was added to a stirring solution of NaN_3 (4.96 g, 76.3 mmol, 6.15 eq.) in water (50 mL) and heated to reflux for 68 h. After cooling the mixture was extracted with Et_2O (x 2), and the combined organic extracts dried ($MgSO_4$), filtered and the solvent removed under reduced pressure. Azide **349** was isolated as a clear oil (2.10 g, quant.). ^{1}H NMR (500 MHz, $CDCl_3$) δ 3.28 (4H, t, *J* = 6.9 Hz, CH_2-1, CH_2-6), 1.67 - 1.57 (4H, m, CH_2-2, CH_2-5), 1.46 - 1.38 (4H, m, CH_2-3, CH_2-4). ^{13}C NMR (126 MHz, $CDCl_3$) δ 51.55 (CH_2), 28.92 (CH_2), 26.49 (CH_2). Consistent with literature data.[429]

6-Azidohexyltriphenylphosphonium Iodide **348**

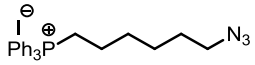

340

Triphenylphosphonium iodide **348** (100 mg, 0.167 mmol, 1.00 eq.) and NaN_3 (45 mg, 0.69 mmol, 4.2 eq.) were combined in a mixture of MeCN (0.5 mL) and water (0.1 mL) and heated to 80 ˚C with stirring for 2 h. The mixture was partitioned with water and $CHCl_3$ then the organic layer dried ($MgSO_4$), filtered and the solvent removed under reduced pressure, giving azide **340** as a solid (89 mg, quant.). ^{1}H NMR (500 MHz, $CDCl_3$) δ 7.92 - 7.54 (15H, m, $^+PPh_3$), 3.66 - 3.50 (2H, m, CH_2-1), 3.17 (2H, t, *J* = 6.8 Hz, CH_2-6), 1.72 - 1.53 (4H, m, CH_2-2, CH_2-5), 1.52 - 1.41 (2H, m, CH_2-4), 1.38 - 1.28 (2H, m, CH_2-3). ^{13}C NMR (126 MHz, $CDCl_3$) δ 135.11 (d, *J* = 3.0 Hz, CH), 133.54 (d, *J* = 10.0 Hz, CH), 130.52 (d, *J* = 12.6 Hz, CH), 117.90 (d, *J* = 86.0 Hz, C), 51.16 (CH_2), 29.75 (d, *J* = 16.0 Hz, CH_2), 28.33 (CH_2), 26.10 (CH_2), 22.96 (d, *J* = 50.4 Hz, CH_2), 22.39 (d, *J* = 4.3 Hz, CH_2). (ATR cm^{-1}): 3053 (C_{Ar}-H), 2936 (C-H), 2859 (C-H), 2091 (N_3), 1587 (C_{Ar}=C_{Ar}). Matches data acquired by a colleague.[416]

1-Azido-6-aminohexane **342**

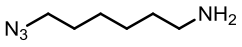

342

1,6-Diazidohexane **349** (7.47 g, 44.4 mmol, 1.00 eq.) was dissolved in Et_2O (150 mL), and combined with 1 M $HCl_{(aq)}$ (150 mL). Triphenylphosphine (13.2 g, 50.3 mmol, 1.13 eq.) was added and the mixture stirred for 24 h. The layers were then separated and the aqueous basified with 7 M $NaOH_{(aq)}$ and extracted with Et_2O (x 2). The combined organics were dried ($MgSO_4$), then filtered and the solvent removed under reduced pressure to give amine **342** as a clear oil (4.74 g, 75%). ^{1}H NMR (500 MHz, $CDCl_3$) δ 3.26 (2H, t, *J* = 6.9 Hz, CH_2-1), 2.70 (2H, t, *J* = 6.9 Hz, CH_2-6), 1.67 – 1.56 (2H, apparent quin. *J* = 7.1 Hz, CH_2-2), 1.46 (2H, quin., *J* = 7.0 Hz, CH_2-5), 1.42 – 1.32 (4H, m, CH_2-3, CH_2-4), 1.15 (2H, s, br, NH_2). ^{13}C NMR (126 MHz, $CDCl_3$) δ 51.64 (CH_2), 42.29 (CH_2), 33.86 (CH_2), 29.00 (CH_2), 26.79 (CH_2), 26.61 (CH_2). Consistent with literature data.[429]

Aminohex-5-yne **341**

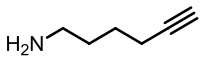

341

Phthalimide **350** (5.0 g, 22 mmol, 1.0 eq.) was dissolved in IPA (25 mL) and water (15 mL) then $NaBH_4$ added (4.17 g, 110 mmol, 5.00 eq.) and the mixture stirred for 18 h. AcOH (100 mL) was then added and the mixture heated to 80 ˚C for 2 h. The material was loaded onto a previously acidified column of IR-120 resin (65 g), washed with water then eluted with $NH_{3(aq)}$. The aqueous was extracted into Et_2O, then from the organic into 1 M $HCl_{(aq)}$ then the solvent removed under reduced pressure and the residue recrystallised from IPA to give amine **341** (300 mg, 14%). ^{1}H NMR (500 MHz, CD_3OD) δ 3.00 - 2.94 (2H, m, CH_2-1), 2.31 - 2.25 (3H, m, CH_2-2, CH_2-6), 1.85 - 1.76 (2H, m, CH_2-3), 1.66 - 1.58 (2H, m, CH_2-4). ^{13}C NMR (126 MHz, CD_3OD) δ 84.00, 70.39, 40.34, 27.65, 26.39, 18.56. Consistent with literature data.[430]

4-Methyl-6-phenyl-8-nitrophenanthridine **368**

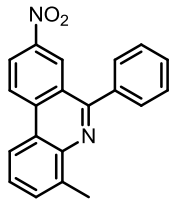

368

Imine **362** (100 mg, 0.24 mmol, 1.00 eq.) was weighed and sonicated into dry MeCN (5.0 mL) in a microwave tube (10 mL), which was sealed and heated to 110 ˚C in a microwave for 10 h. After cooling the solvent was removed under reduced pressure then the residue dissolved in dry Et_2O and precipitated with 2 M ethereal HCl (1.00 mL, 2.00 mmol, 8.33 eq.). The solvent was removed under reduced pressure then the mixture dissolved in MeOH and loaded onto a Strata WCX ion exchange column. The column was washed with additional MeOH before elution with NaOAc/MeOH (15 mg/mL). The solvent was removed under reduced pressure and replaced with dry $CHCl_3$ then the solution filtered and the solvent removed under reduced pressure. The product **368** was sequentially recrystallised from MeOH and dry $CHCl_3$, then isolated as a white solid (8 mg, 11%). ^{1}H NMR (500 MHz, $CDCl_3$) δ 9.11 (1H, d, *J* = 2.3 Hz, H7), 8.83 (1H, d, *J* = 9.1 Hz, H10), 8.61 (1H, dd, *J* = 9.1, 2.4 Hz, H9), 8.50 (1H, d, *J* = 8.1 Hz, H1), 7.86 - 7.79 (2H, m, H2', H6'), 7.75 (1H, d, *J* = 7.0 Hz, H3), 7.69 - 7.57 (4H, m, H2, H3', H4', H5'), 2.90 (s, 3H). ^{13}C NMR (126 MHz, $CDCl_3$) δ 159.49 (C), 146.08 (C), 143.93 (C), 139.05 (C), 138.06 (C), 131.74 (CH), 130.35 (CH), 129.54 (CH), 128.87 (CH), 127.61 (CH), 124.98 (CH), 124.51 (CH), 124.23 (C), 123.89 (CH), 122.31 (C), 120.66 (CH), 18.51 (CH_3). ν_{Max}(ATR)cm^{-1}: 2918 (C_{Ar}-H), 1614 (C=N), 1602 (C_{Ar}=C_{Ar}), 1590 (C_{Ar}=C_{Ar}), 1571 (C_{Ar}=C_{Ar}), 1531 (NO_2), 1336 (NO_2). MS (APCI): 315 ([M+H]$^+$, 100%). HRMS: 315.1129. $C_{20}H_{14}N_2O_2$ requires 315.1128. MP: 242 -243 ˚C.

5-(Hex-1'-yl)-6-phenyl-8-nitrophenanthridinium chloride **299**

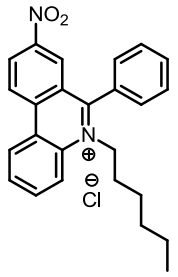

299

Benzophenone **286** (253 mg, 0.79 mmol, 1.00 eq.) and dry hexylamine (0.73 mL, 5.5 mmol, 7.0 eq.) were combined stirring under argon at 0 ˚C in dry PhMe (3.0 mL) then 1 M titanium tetrachloride in dry PhMe (1.18 mL, 1.18 mmol, 1.49 eq.) was added over 5 min. The reaction was allowed to warm to RT and allowed to stir for 72 h. The mixture was quenched into brine then filtered and extracted into Et_2O (x 1) and DCM (x 2). The combined organics were dried ($MgSO_4$), then filtered and the solvent removed under reduced pressure. From the crude yield of 272 mg of extremely viscous brown oil, a portion (101 mg, 0.25 mmol, 1.00 eq.) was weighed by difference onto a spatula and sonicated into a microwave tube (10 mL) containing dry THF (5.0 mL). The tube was filled with argon and sealed then heated in a microwave to 100 ˚C for 2 h. The solution was filtered and the residue eluted with $CHCl_3$ and MeOH, then the solvent removed under reduced pressure, then the residue triturated with pet. ether, which was filtered. The residue and filter cake were recombined in $CHCl_3$ and the solvent removed under reduced pressure. The residue was then redissolved in dry Et_2O and precipitated with ethereal HCl (1.00 mL, 2.00 mmol, 7.69 eq.), then allowed to settle for 15 h. The solid was partitioned between Et_2O and 1 M $NaOH_{(aq)}$ then the aqueous re-extracted (Et_2O x 1, $CHCl_3$ x 2). The organic fractions were recombined, then ethereal HCl (1.00 mL, 2.00 mmol, 7.69 eq.) and PhMe were added and the solvent removed under reduced pressure, isolating the phenanthridinium chloride **299** as brown solid (103 mg, 84%). ^{1}H NMR (500 MHz, CD_3CN + 0.05 mL CF_3CO_2D): 9.12 (1H, t, *J* = 9.0 Hz, H10), 9.07 (1H, d, *J* = 7.9 Hz, H1), 8.87 (1H, d, *J* = 8.6 Hz, H9), 8.48 (1H, d, *J* = 8.3 Hz, H4), 8.26 (1H, s, H7), 8.21 (1H, apparent t, br, *J* = 7.2 Hz, H3), 8.14 (1H, apparent t, br, *J* = 7.1 Hz, H2), 7.83 (1H, t, *J* = 7.2 Hz, H4''), 7.77 (2H, t, *J* = 6.8 Hz, H3'', H5''), 7.63 (2H, d, *J* = 6.9 Hz, H2'', H6''), 4.71 (2H, s, br, CH_2-1'), 2.00 - 1.89 (2H, m, CH_2-2'), 1.30 - 1.04 (6H, m, CH_2-3', CH_2-4', CH_2-5'), 0.75 (3H, t, *J* = 6.9 Hz, CH_2-6'). ^{13}C NMR (101 MHz, 0.75 mL CD_3OD + 0.05 mL CF_3CO_2D) δ 166.13 (C), 149.03 (C), 140.13 (C), 136.62 (C), 135.59 (CH), 133.53 (CH), 132.71 (CH), 131.58 (C), 131.45 (CH), 131.07 (CH), 130.03 (CH), 129.10 (CH), 127.37 (C), 127.35 (CH), 127.31 (C), 127.04 (CH), 122.28 (CH), 57.07 (CH_2), 31.94 (CH_2), 30.71 (CH_2), 27.20 (CH_2), 23.35 (CH_2), 14.17 (CH_3). ν_{Max}(ATR)cm^{-1}: 3067 (C_{Ar}-H), 2953 (C-H), 2926, (C-H), 2857 (C-H), 1620 (C=N), 1589 (C_{Ar}=C_{Ar}), 1537 (NO_2), 1341 (NO_2). MS (NSI$^+$): 385 [M^+ (phenanthridinium cation), 100%], 301 (M^+ – C_6H_{10}, 15). HRMS: 385.1916. $C_{25}H_{25}N_2O_2^+$ requires 385.1911. MP: 190 - 192 ˚C.

3-Bromo-5-(hex-1'-yl)-6-phenyl-8-nitrophenanthridinium chloride **300**

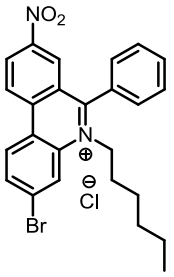

300

Benzophenone **326** (530 mg, 1.32 mmol, 1.00 eq.) and dry hexylamine (1.75 mL, 13.2 mmol, 10.0 eq.) were combined stirring under argon at 0 ˚C in dry PhMe (5.0 mL) then 1 M titanium tetrachloride in dry PhMe (1.86 mL, 1.86 mmol, 1.41 eq.) was added. The reaction was allowed to warm to RT and allowed to stir for 15 h, at which point additional 1 M titanium tetrachloride in PhMe was added (0.50 mL, 0.50 mmol, 0.38 eq.). After stirring for an additional 20 h the mixture was quenched into 1 M $K_2CO_{3(aq)}$ then filtered and extracted into DCM (x 3). The combined organics were acidified (0.55 M $HCl_{(aq)}$). The acidic aqueous extracts were further extracted (DCM, x 2), then the organic extracts recombined and basified in 1 M $K_2CO_{3(aq)}$. The organic layers were dried ($MgSO_4$), then filtered and the solvent removed under reduced pressure. From the crude yield of 656 mg of extremely viscous brown oil, a portion (102 mg, 0.20 mmol, 1.00 eq.) was weighed by difference onto a spatula and sonicated into a microwave tube (10 mL) containing dry THF (5.0 mL). The tube was filled with argon and sealed then heated in a microwave to 100 ˚C for 2 h. After cooling the material was transferred to a round bottom flask with $CHCl_3$ and the solvent removed under reduced pressure. The residue was dissolved in dry Et_2O then precipitated with 2 M ethereal HCl (1.00 mL, 2.00 mmol, 10.0 eq.). The precipitate was allowed to settle, then the bulk of the solvent syringed out and the remainder removed under reduced pressure, then the solid triturated with dry Et_2O, $CHCl_3$ and MeOH consecutively. The solvent was removed under reduced pressure, isolating the phenanthridinium chloride **300** was isolated as an off-white solid (103 mg, 100%). ^{1}H NMR (400 MHz, CD_3OD) δ 9.25 (1H, d, *J* = 9.2 Hz, H10), 9.09 (1H, d, *J* = 8.9 Hz, H1), 8.93 (1H, dd, *J* = 9.2, 2.2 Hz, H9), 8.79 (1H, d, *J* = 1.4 Hz, H4), 8.33 – 8.27 (2H, m, H2, H7), 7.85 (1H, t, *J* = 7.5 Hz, H4''), 7.79 (2H, t, *J* = 7.3 Hz, H3'', H5''), 7.68 (2H, d, *J* = 7.4 Hz, H2'', H6''), 4.87 - 4.72 (2H, m, CH_2-1'), 2.00 - 1.86 (2H, m, CH_2-2'), 1.31 - 1.03 (6H, m, CH_2-3', CH_2-4', CH_2-5'), 0.81 - 0.72 (3H, t, *J* = 7.2 Hz, CH_2-6'). ^{13}C NMR (126 MHz, 0.75 mL CD_3OD + 0.05 mL CF_3CO_2D) δ 167.34 (C), 149.26 (C), 139.82 (C), 137.15 (C), 136.11 (CH), 133.68 (CH), 131.89 (CH), 131.25 (C), 131.06 (CH), 129.97 (C), 129.91 (CH), 129.29 (CH), 128.83 (CH), 127.30 (C), 127.02 (CH), 126.36 (C), 124.82 (CH), 57.10 (CH_2), 31.76 (CH_2), 30.55 (CH_2), 27.00 (CH_2), 23.15 (CH_2), 13.92 (CH_3). ν_{Max}(ATR)cm^{-1}: 2955 (C-H), 2930 (C-H), 2857 (C-H), 1618 (C=N), 1603 (C_{Ar}=C_{Ar}), 1589 (C_{Ar}=C_{Ar}), 1533 (NO_2), 1518 (C_{Ar}=C_{Ar}), 1341 (NO_2). MS (ESI$^+$): 465 [^{81}BrM$^+$ (phenanthridinium cation), 100%], 463 [^{79}BrM$^+$ (phenanthridinium cation), 98]. HRMS: 463.1011 and 465.0986. $C_{25}H_{24}BrN_2O_2$ requires 463.1016 and 465.0996. MP: 160 - 165 ˚C.

4-Aza-5-(hex-1'-yl)-6-phenyl-8-nitrophenanthridinium chloride **301**

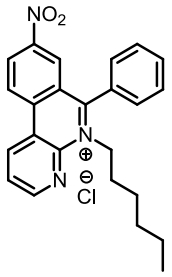

301

Benzophenone **325** (520 mg, 1.61 mmol, 1.00 eq.) and dry hexylamine (1.50 mL, 11.4 mmol, 7.05 eq.) were combined stirring under argon at 0 ˚C in dry PhMe (5.0 mL) then 1 M titanium tetrachloride in dry PhMe (2.40 mL, 2.40 mmol, 1.49 eq.) was added over 5 min. The reaction was allowed to warm to RT and allowed to stir for 20 h. The mixture was quenched into H_2O, then filtered through celite with DCM and partitioned between DCM and 1 M $HCl_{(aq)}$, then the aqueous layer was re-extracted (DCM x 2). The combined organics were washed with 1 M $HCl_{(aq)}$ then $NaHCO_{3(aq)}$ and dried ($MgSO_4$) then filtered and the solvent removed under reduced pressure. From the crude yield of 631 mg of brown solid a portion (100 mg, 0.25 mmol, 1.00 eq.) was weighed by difference onto a spatula and sonicated into a microwave tube (10 mL) containing dry THF (5.0 mL). The tube was filled with argon and sealed then heated in a microwave to 100 ˚C for 30 min then cooled and transferred to a round bottomed flask in dry $CHCl_3$, then the solvent removed under reduced pressure. The residue was dissolved in dry Et_2O then precipitated with 2 M ethereal HCl (1.00 mL, 2.00 mmol, 8.13 eq.). The solvent was removed under reduced pressure, then the solid triturated with pet. ether and dried under reduced pressure. The salt **301** was isolated as a solid (106 mg, 98%). ^{1}H NMR (400 MHz, CD_3OD) δ 9.71 (1H, dd, *J* = 8.5, 1.7 Hz, H1), 9.41 (1H, d, *J* = 9.1 Hz, H10), 9.38 (1H, dd, *J* = 4.4, 1.7 Hz, H3), 9.08 (1H, dd, *J* = 9.1, 2.3 Hz, H9), 8.49 (1H, d, *J* = 2.0 Hz, H7), 8.28 (1H, dd, *J* = 8.4, 4.4 Hz, H2), 7.97 (1H, t, *J* = 7.4 Hz, H4''), 7.91 (2H, t, *J* = 7.3 Hz, H3'', H5''), 7.85 - 7.79 (2H, d, *J* = 7.4 Hz, H2'', H6''), 5.12 - 5.02 (2H, m, CH_2-1'), 2.08 - 1.97 (2H, m, CH_2-2'), 1.40 - 1.16 (6H, m, CH_2-3', CH_2-4', CH_2-5'), 0.87 (3H, t, *J* = 7.1 Hz, CH_2-6'). ^{13}C NMR (126 MHz, $CDCl_3$) δ 167.29 (C), 153.69 (CH), 147.66 (C), 144.54 (C), 138.75 (C), 136.83 (CH), 132.35 (CH), 130.23 (CH), 129.73 (CH), 129.62 (C), 128.77 (CH), 128.02 (CH), 127.77 (CH), 126.80 (CH), 126.32 (C), 121.51 (C), 54.80 (CH_2), 30.65 (CH_2), 29.78 (CH_2), 26.47 (CH_2), 22.28 (CH_2), 13.86 (CH_3). ν_{Max}(ATR)cm^{-1}: 3064 (C_{Ar}-H), 2956 (C-H), 2931 (C-H), 2926 (C-H), 1623 (C=N), 1604 (C_{Ar}=C_{Ar}), 1592 (C_{Ar}=C_{Ar}), 1538 (NO_2), 1518 (C_{Ar}=C_{Ar}), 1343 (NO_2). MS (ESI$^+$): 418 [M^+ (phenanthridinium cation) + MeOH, 62%], 386 [M^+ (phenanthridinium cation), 100], 302 [(M^+ (phenanthridinium cation) – C_6H_{12}, 69). HRMS: 386.1857. $C_{24}H_{24}N_3O_2^+$ requires 386.1863. MP: 188 - 189 ˚C.

2,8-Dinitro-5-(hex-1'-yl)-6-phenylphenanthridinium chloride **302**

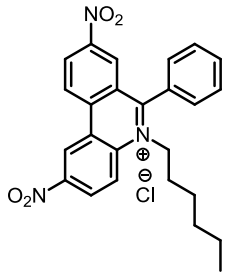

302

Benzophenone **330** (300 mg, 0.78 mmol, 1.00 eq.) and dry hexylamine (0.60 mL, 4.6 mmol, 5.9 eq.) were combined stirring under argon at 0 ˚C in dry PhMe (3.0 mL) then 1 M titanium tetrachloride in dry PhMe (0.98 mL, 0.98 mmol, 1.3 eq.) was added over 5 min. The reaction was allowed to warm to RT and allowed to stir for 20 h. A sample (0.1 mL) was quenched into H_2O, partitioned between DCM and water and the organic separated and the solvent removed under reduced pressure. Proton NMR confirmed the reaction was complete. The remaining mixture was quenched into H_2O, then filtered through celite with DCM and partitioned between DCM and 1 M $HCl_{(aq)}$, then the aqueous layer was re-extracted (DCM x 2). The combined organics were washed with 1 M $HCl_{(aq)}$ then $NaHCO_{3(aq)}$ and dried ($MgSO_4$) then filtered and the solvent removed under reduced pressure. From the crude yield of 336 mg of brown solid a portion (100 mg, 0.21 mmol, 1.00 eq.) was weighed by difference onto a spatula and sonicated into a microwave tube (10 mL) containing dry THF (5.0 mL). The tube was filled with argon and sealed then heated in a microwave to 100 ˚C for 30 min then cooled and transferred to a round bottomed flask in dry $CHCl_3$, then the solvent removed under reduced pressure. The residue was dissolved in dry Et_2O then precipitated with 2 M ethereal HCl (1.00 mL, 2.00 mmol, 9.35 eq.). The solvent was removed under reduced pressure. The solid was dissolved in DCM, dried ($MgSO_4$) and filtered, then the solvent removed under reduced pressure. The salt **302** was isolated as a solid (91 mg, 86%). ^{1}H NMR [500 MHz, CD_3CN/CF_3CO_2D (10:1)] δ 9.82 (1H, d, *J* = 2.3 Hz, H1), 9.27 (1H, d, *J* = 9.1 Hz, H10), 8.95 (1H, dd, *J* = 9.1, 2.2 Hz, H9), 8.84 (1H, dd, *J* = 9.5, 2.2 Hz, H3), 8.66 (1H, d, *J* = 9.5 Hz, H4), 8.29 (1H, d, *J* = 2.2 Hz, H7), 7.86 (1H, t, *J* = 7.5 Hz, H4''), 7.79 (2H, t, *J* = 7.5 Hz, H3'', H5''), 7.63 (2H, d, *J* = 7.3 Hz, H2'', H6''), 4.79 - 4.66 (2H, m, CH_2-1'), 1.99 - 1.88 (2H, m, CH_2-2'), 1.30 - 1.03 (6H, m, CH_2-3', CH_2-4', CH_2-5'), 0.75 (3H, t, *J* = 7.2 Hz, CH_2-6'). ^{13}C NMR [126 MHz, CD_3CN/CF_3CO_2D (10:1)] δ 167.94 (C), 148.39 (C), 148.15 (C), 138.14 (C), 137.68 (C), 132.56 (CH), 131.23 (CH), 129.83 (CH), 129.38 (C), 128.56 (CH), 128.09 (CH), 127.42 (CH), 126.64 (C), 126.35 (C), 126.25 (CH), 123.34 (CH), 121.76 (CH), 56.45 (CH_2), 30.31 (CH_2), 28.88 (CH_2), 25.61 (CH_2), 21.89 (CH_2), 12.99 (CH_3). ν_{Max}(ATR)cm^{-1}: 3099 (C_{Ar}-H), 2957 (C-H), 2927 (C-H), 2857 (C-H), 1601 (C=N), 1578 (C_{Ar}=C_{Ar}), 1526 (NO_2), 1494 (NO_2), 1342 (NO_2), 1326 (NO_2). MS (NSI$^+$): 430 [M^+ (phenanthridinium cation), 100%]. HRMS: 430.1752. $C_{25}H_{24}N_3O_4^+$ requires 430.1761. MP: 260 - 263 ˚C.

2-Methoxy-3,8-dinitro-5-(hex-1'-yl)-6-phenylphenanthridinium chloride **303**

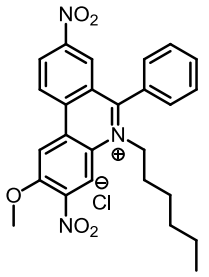

303

Benzophenone **334** (501 mg, 1.26 mmol, 1.00 eq.) and dry hexylamine (1.17 mL, 8.86 mmol, 7.03 eq.) were combined stirring under argon at 0 ˚C in dry PhMe (5.0 mL) then a 1 M solution of titanium tetrachloride in dry PhMe (1.90 mL, 1.90 mmol, 1.51 eq.) was added over 5 min. The reaction was allowed to warm to RT and allowed to stir for 40 h. The mixture was quenched into H_2O, filtered through celite with DCM and partitioned between DCM and 0.5 M $HCl_{(aq)}$, then the aqueous layer was re-extracted (DCM x 2). The combined organics were dried ($MgSO_4$) then filtered and the solvent removed under reduced pressure. From the crude yield of 572 mg of brown solid a portion (100 mg, 0.21 mmol, 1.00 eq.) was was weighed by difference onto a spatula and sonicated into a microwave tube (10 mL) containing dry THF (5.0 mL). The tube was filled with argon and sealed then heated in a microwave to 100 ˚C for 2 h. The solvent was removed under reduced pressure, then the residue dissolved in dry Et_2O and precipitated with 2 M ethereal HCl (1.00 mL, 2.00 mmol, 9.52 eq.). The precipitate was allowed to settle, then the bulk of the solvent syringed out and the process repeated. After the remaining solvent was removed under reduced pressure the phenanthridinium salt **303** was isolated as a powder (80 mg, 74%). ^{1}H NMR (400 MHz, 0.75 mL CD_3CN + 0.05 mL CF_3CO_2D) δ 9.31 (1H, d, *J* = 9.2 Hz, H10), 9.02 (1H, dd, *J* = 9.2, 2.2 Hz, H9), 8.90 (1H, s, H4), 8.64 (1H, s, H1), 8.36 (1H, d, *J* = 2.2 Hz, H7), 7.94 (1H, t, *J* = 7.5 Hz, H4''), 7.87 (2H, t, *J* = 7.3 Hz, H3'', H5''), 7.71 (2H, d, *J* = 7.1 Hz, H2'', H6''), 4.79 - 4.71 (2H, m, CH_2-1'), 4.36 (3H, s, OCH_3), 2.06 - 1.91 (2H, m, CH_2-2'), 1.39 - 1.10 (6H, m, CH_2-3', CH_2-4', CH_2-5'), 0.84 (3H, t, *J* = 7.1 Hz, CH_2-6'). ^{13}C NMR (126 MHz, 0.75 mL DMSO + 0.05 mL CF_3CO_2D) δ 163.79 (C), 151.64 (C), 147.82 (C), 143.26 (C), 136.31 (C), 131.79 (CH), 129.70 (C), 129.63 (CH), 129.28 (CH), 129.06 (C), 128.44 (C), 128.36 (CH), 127.13 (CH), 127.06 (CH), 126.81 (C), 117.75 (CH), 109.21 (CH), 58.14 (CH_3), 55.44 (CH_2), 29.90 (CH_2), 28.53 (CH_2), 25.19 (CH_2), 21.47 (CH_2), 13.16 (CH_3). ν_{Max}(ATR)cm^{-1}: 3018 (C_{Ar}-H), 2954 (C-H), 2922 (C-H), 2917 (C-H), 2853 (C-H), 1621 (C=N), 1595 (C_{Ar}=C_{Ar}), 1537 (NO_2), 1521 (C_{Ar}=C_{Ar}), 1501 (C_{Ar}=C_{Ar}), 1350 (NO_2). MS (ESI$^+$): 460 [M^+ (phenanthridinium cation), 100%]. HRMS: 460.1846. $C_{26}H_{26}N_3O_5^+$ requires 460.1867. MP: 195 - 198 ˚C.

2- Methoxy-5-(hex-1'-yl)-6-phenyl-8-nitrophenanthridinium trifluoroacetate **304**

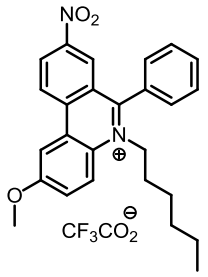

304

Benzophenone **333** (102 mg, 0.29 mmol, 1.00 eq.) and dry hexylamine (0.27 mL, 2.0 mmol, 7.1 eq.) were combined stirring under argon at 0 ˚C in dry PhMe (1.0 mL) then titanium tetrachloride (0.42 mL, 0.4 mmol, 1.5 eq.) was added. The reaction was allowed to warm to RT and allowed to stir for 20 h. The mixture was quenched into H_2O and extracted into diethyl ether (x 2). The combined organics were dried ($MgSO_4$), then filtered and the solvent removed under reduced pressure. The crude yield of 114 mg was transferred in dry $CHCl_3$ into a kugelrohr bulb and the chloroform distilled out, then the oil heated at 100 ˚C for 2 h 45 min, then at 125 ˚C for 3 h. TFA was added then evaporated off under reduced pressure. The mixture was partitioned from a water/TFA mixture with DCM (x 3), and $CHCl_3$ (x 3). The organics were combined and the solvent removed under reduced pressure. Following column chromatography [SiO_2, loaded and washed in DCM then eluted with DCM/MeOH/NEt_3 (97:2:1)]. The solvent was removed under reduced pressure and replaced with $CHCl_3$ then the compound dried ($MgSO_4$). The mixture was filtered, then TFA was added then and the solvent removed under reduced pressure. The phenanthridinium trifluoroacetate **304** was isolated as brown oil (70 mg, 47%). ^{1}H NMR (500 MHz, $CDCl_3$) δ 9.08 (1H, d, *J* = 9.1 Hz, H10), 8.77 (1H, dd, *J* = 9.1, 2.1 Hz, H9), 8.39 (1H, d, *J* = 9.6 Hz, H4), 8.34 (1H, d, *J* = 2.2 Hz, H7), 8.27 (1H, d, *J* = 2.5 Hz, H1), 7.86 - 7.82 (1H, m, H4''), 7.78 (2H, t, *J* = 7.8 Hz, H3'', H5''), 7.74 (1H, dd, *J* = 9.6, 2.6 Hz, H3), 7.65 (2H, d, *J* = 7.7 Hz, H2'', H6''), 4.94 - 4.79 (2H, m, CH_2-1'), 4.10 (3H, s, OCH_3), 1.93 (2H, quin, *J* = 7.9 Hz, CH_2-2'), 1.34 - 1.08 (6H, m, CH_2-3', CH_2-4', CH_2-5'), 0.81 (3H, t, *J* = 7.2 Hz, CH_2-6'). ^{13}C NMR (126 MHz, $CDCl_3$) δ 161.75 (C), 160.61 (C), 147.64 (C), 137.85 (C), 132.43 (CH), 130.11 (C), 129.73 (C), 129.57 (CH), 128.84 (CH), 128.05 (C), 127.74 (CH), 126.39 (CH), 125.70 (C), 124.60 (CH), 122.64 (CH), 106.64 (CH), 56.82 (CH_3), 56.09 (CH_2), 30.76 (CH_2), 30.05 (CH_2), 26.19 (CH_2), 22.26 (CH_2), 13.74 (CH_3). ν_{Max}(ATR)cm^{-1}: 2958 (C-H), 2920 (C-H), 2850 (C-H), 1777 (TFA), 1731 (TFA), 1614 (C=N), 1541 (C_{Ar}=C_{Ar}), 1592 (C_{Ar}=C_{Ar}), 1348 (NO_2). MS (NSI$^+$): 415 [M^+ (phenanthridinium cation), 100%]. HRMS: 415.2005, $C_{26}H_{27}N_2O_3^+$ requires 415.2016.

3,8-Dinitro-5-(hex-1'-yl)-6-phenylphenanthridinium chloride **305**

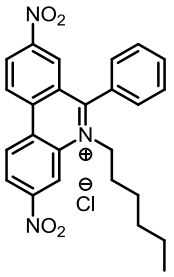

305

Benzophenone **328** (390 mg, 1.06 mmol, 1.00 eq.) and dry hexylamine (1.00 mL, 7.57 mmol, 7.14 eq.) were combined stirring under argon at 0 ˚C in dry PhMe (5.5 mL) then a 1 M solution of titanium tetrachloride in dry PhMe (1.60 mL, 1.60 mmol, 1.51 eq.) was added over 5 min. The reaction was allowed to warm to RT and allowed to stir for 48 h. The mixture was quenched into H_2O, and the resulting precipitate washed with Et_2O, $CHCl_3$, DCM, MeCN and MeOH and the organics combined and washed with brine and extracted DCM (x 1), Et_2O (x 1), and $CHCl_3$ (x 4). The combined organics were dried ($MgSO_4$) then filtered and the solvent removed under reduced pressure. From the crude yield of 504 mg of brown solid a portion (100 mg, 0.22 mmol, 1.00 eq.) was transferred to a round bottom flask with DCM and the solvent removed under reduced pressure. The residue was dissolved in dry Et_2O then precipitated with 2 M ethereal HCl (1.00 mL, 2.00 mmol, 9.09 eq.). The precipitate was allowed to settle, then the bulk of the solvent syringed out and the remainder removed under reduced pressure, isolating the phenanthridinium chloride **305** as a powder (95 mg, 97%). ^{1}H NMR (500 MHz, CD_3OD) δ 9.58 (1H, d, *J* = 9.2 Hz, H1), 9.52 (1H, d, *J* = 9.1 Hz, H10), 9.44 (1H, d, *J* = 1.9 Hz, H4), 9.15 (1H, dd, *J* = 9.1, 2.3 Hz, H9), 9.01 (1H, dd, *J* = 9.1, 1.9 Hz, H2), 8.49 (1H, d, *J* = 2.2 Hz, H7), 8.01 (1H, t, *J* = 7.5 Hz, H4''), 7.96 (2H, t, *J* = 7.5 Hz, H3'', H5''), 7.86 (2H, d, *J* = 7.8 Hz, H2'', H6''), 5.10 - 4.99 (2H, m, CH_2-1'), 2.20 - 2.08 (2H, m, CH_2-2'), 1.49 - 1.40 (2H, m, CH_2-3'), 1.36 - 1.23 (4H, m, CH_2-4', CH_2-5'), 0.92 (3H, t, *J* = 7.1 Hz, CH_2-6'). ^{13}C NMR (126 MHz, CD_3OD) δ 170.05 (C), 152.37 (C), 150.81 (C), 139.67 (C), 137.15 (C), 134.72 (CH), 133.09 (CH), 132.01 (C), 131.97 (CH), 131.93 (C), 130.41 (CH), 130.32 (CH), 130.17 (CH), 129.44 (C), 128.82 (CH), 126.82 (CH), 118.76 (CH), 58.12 (CH_2), 32.68 (CH_2), 31.39 (CH_2), 27.95 (CH_2), 24.16 (CH_2), 15.01 (CH_3). ν_{Max}(ATR)cm^{-1}: 2955 (C-H), 2928 (C-H), 2859 (C-H), 1618 (C=N), 1591 (C_{Ar}=C_{Ar}), 1537 (C_{Ar}=C_{Ar}), 1518 (NO_2), 1343 (NO_2). MS (NSI$^+$): 430 [M^+ (phenanthridinium cation), 100%]. HRMS: 430.1754. $C_{25}H_{24}N_3O_4$ requires 430.1761. MP: 189 ˚C.

3,8-Dinitro-5-(hex-1'-yl)-6-methylene-5-hydrophenanthridine **369**

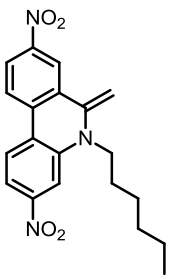

369

Benzophenone **324** (426 mg, 1.40 mmol, 1.00 eq.) and dry hexylamine (1.45 mL, 11.0 mmol, 7.58 eq.) were combined stirring under argon at 0 ˚C in dry PhMe (5.0 mL) then a 1 M solution of

titanium tetrachloride in dry PhMe (2.70 mL, 2.70 mmol, 1.93 eq.) was added over 5 min. The reaction was allowed to warm to RT and allowed to stir for 19 h. The mixture was quenched into H_2O, then filtered through celite with DCM and partitioned between DCM and 1 M $HCl_{(aq)}$, then the aqueous layer was re-extracted (DCM x 2). The combined organics were washed with 1 M $HCl_{(aq)}$ then $NaHCO_{3(aq)}$ and dried ($MgSO_4$) then filtered and the solvent removed under reduced pressure. The enamine **369** was isolated as a purple solid (523 mg, quant.). ^{1}H NMR (400 MHz, $CDCl_3$) δ 8.62 (1H, d, *J* = 2.3 Hz, H7), 8.22 (1H, dd, *J* = 8.9, 2.3 Hz, H9), 8.03 (1H, d, *J* = 8.9 Hz, H10), 7.96 (1H, d, *J* = 8.7 Hz, H1), 7.74 (1H, dd, *J* = 8.7, 2.2 Hz, H2), 7.69 (1H, d, *J* = 2.1 Hz, H4), 4.96 (1H, d, *J* = 3.1 Hz, NC=CH_{trans}), 4.39 (1H, d, *J* = 3.2 Hz, NC=CH_{cis}), 3.83 - 3.69 (2H, m, CH_2-1'), 1.83 (2H, quint., J = 7.8 Hz, CH_2-2'), 1.56 - 1.47 (2H, m, CH_2-3'), 1.47 - 1.36 (4H, m, CH_2-4', CH_2-5'), 0.95 (3H, t, *J* = 7.1 Hz, CH_2-6'). ^{13}C NMR (101 MHz, $CDCl_3$) δ 149.91 (C), 148.41 (C), 142.18 (C), 141.83 (C), 133.65 (C), 132.01 (C), 125.05 (CH), 124.37 (CH), 123.72 (C), 123.54 (CH), 120.68 (CH), 113.94 (CH), 108.01 (CH), 86.80 (CH_2), 48.23 (CH_2), 31.50 (CH_2), 26.69 (CH_2), 24.43 (CH_2), 22.75 (CH_2), 14.11 (CH_3). ν_{Max}(ATR)cm^{-1}: 2957 (C-H), 2926 (C-H), 2856 (C-H), 1603 (C_{Ar}=C_{Ar}), 1578 (C_{Ar}=C_{Ar}), 1520 (NO_2), 1339 (NO_2). MS (APCI$^+$): 368 [(M+H)$^+$, 100). HRMS: 368.1603. $C_{20}H_{22}N_3O_4^+$ requires 368.1605. MP: 169 - 171 ˚C.

5-(Hex-1'-yl)-6-phenylphenanthridinium chloride **307**

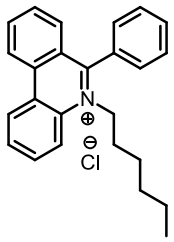

307

Benzophenone **327** (594 mg, 2.15 mmol, 1.00 eq.) and dry hexylamine (2.00 mL, 15.1 mmol, 7.04 eq.) were combined stirring under argon at 0 ˚C in dry PhMe (5.0 mL) then titanium tetrachloride (0.35 mL, 3.2 mmol, 1.5 eq.) was added over 5 min. The reaction was allowed to warm to RT and allowed to stir for 72 h. The mixture was quenched into brine, and extracted with diethyl ether (x 1), EtOAc (x 1) and DCM (x 5). The combined organics were dried ($MgSO_4$) then filtered and the solvent removed under reduced pressure. From the crude yield of 537 mg of brown oil a portion (100 mg, 0.28 mmol, 1.00 eq.) was weighed by difference onto a spatula and sonicated into a microwave tube (10 mL) containing dry MeCN (5.0 mL). The tube was filled with argon and sealed then heated in a microwave to 110 ˚C for 90 min. After cooling the material was transferred to a round bottom flask with DCM and the solvent removed under reduced pressure. The residue was dissolved in dry Et_2O then precipitated with 2 M ethereal HCl (1.00 mL, 2.00 mmol, 7.14 eq.) The precipitate was allowed to settle, then the bulk of the solvent syringed out and the remainder removed under reduced pressure, isolating the phenanthridinium salt **307** as a white solid (102 mg, 68%). ^{1}H NMR (500 MHz, 0.75 mL CD_3CN + 0.05 mL CF_3CO_2D) δ 9.01 (1H, d, *J* = 7.6 Hz, H1), 8.94 (1H, d, *J* = 8.1 Hz, H10), 8.40 (1H, d, *J* = 8.0 Hz, H4), 8.21 (1H, apparent t, *J* = 7.3 Hz, H9), 8.12 - 8.00 (2H, m, H2, H3), 7.80 - 7.67 (4H, m, H8, H2'', H3'', H5''), 7.61 - 7.50 (3H, m, H7, H2'', H6''), 4.74 - 4.55 (2H, m, CH_2-1'), 2.00 - 1.85 (2H, m, CH_2-2'), 1.30 - 1.18 (2H, m, CH_2-3'), 1.16 - 1.00 (m, CH_2-4', CH_2-5'), 0.74 (3H, t, *J* = 7.0 Hz, CH_2-6'). ^{13}C NMR (101 MHz, 0.75 mL CD_3CN + 0.05 mL

CF_3CO_2D) δ 164.01 (C), 137.53 (CH), 135.04 (C), 133.91 (C), 132.91 (CH), 132.38 (CH), 131.46 (CH), 130.79 (C), 130.48 (CH), 130.13 (CH), 129.43 (CH), 128.11 (CH), 126.37 (C), 125.74 (C), 124.68 (CH), 122.83 (CH), 120.39 (CH), 54.86 (CH_2), 30.31 (CH_2), 28.97 (CH_2), 25.64 (CH_2), 21.83 (CH_2), 12.85 (CH_3). ν_{Max}(ATR)cm^{-1}: 3051 (C_{Ar}-H), 2953 (C-H), 2926 (C-H), 2861 (C-H), 1609 (C=N), 1584 (C_{Ar}=C_{Ar}), 1574 (C_{Ar}=C_{Ar}). MS (NSI$^+$): 340 [M^+ (phenanthridinium cation], 100%], 256 (M^+ – C_6H_{12}, 52). HRMS: 340.2058. $C_{25}H_{26}N^+$ requires 340.2060. MP: 194 - 195 ˚C.

4- Methyl-5-(hex-1'-yl)-6-phenyl-8-nitrophenanthridinium chloride **308**

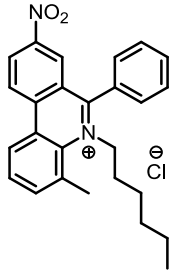

308

Benzophenone **332** (526 mg, 1.57 mmol, 1.00 eq.) and dry hexylamine (1.45 mL, 11.0 mmol, 7.01 eq.) were combined stirring under argon at 0 ˚C in dry PhMe (5.0 mL) then titanium tetrachloride (0.26 mL, 2.4 mmol, 1.5 eq.) was added. The reaction was allowed to warm to RT and allowed to stir for 72 h. The mixture was quenched into brine then filtered and extracted into diethyl ether (x 1) and DCM (x 2). The combined organics were dried ($MgSO_4$), then filtered and the solvent removed under reduced pressure. From the crude yield of 695 mg of extremely viscous brown oil, a portion (100 mg, 0.24 mmol, 1.00 eq.) was weighed by difference onto a spatula and sonicated into a microwave tube (10 mL) containing dry MeCN (5.0 mL). The tube was filled with argon and sealed then heated in a microwave to 110 ˚C for 10 h. After cooling the material was transferred to a round bottom flask with DCM and the solvent removed under reduced pressure. The residue was dissolved in dry Et_2O then precipitated with 2 M ethereal HCl (1.00 mL, 2.00 mmol, 8.33 eq.). The precipitate was allowed to settle, then the bulk of the solvent syringed out and the remainder removed under reduced pressure, then the residue loaded onto a Strata WCX column in MeOH, then the column washed with additional MeOH before elution with NaOAc/MeOH (15 mg/mL). The solvent was removed under reduced pressure and replaced with $CHCl_3$ then the compound dried ($MgSO_4$) and the solution filtered then the solvent removed under reduced pressure. The phenanthridinium chloride **308** was isolated as brown oil (77 mg, 79%). ^{1}H NMR (500 MHz, CD_3OD) δ 9.31 (1H, d, *J* = 9.2 Hz, H10), 9.10 (1H, dd, *J* = 7.6, 1.9 Hz, H1), 9.00 (1H, dd, *J* = 9.2, 2.3 Hz, H9), 8.48 (1H, d, *J* = 2.3 Hz, H7), 8.14 - 8.06 (2H, m, H2, H3), 8.00 - 7.94 (1H, m, H4''), 7.93 - 7.85 (4H, m, H2'', H3'', H5'', H6''), 5.05 (2H, t, *J* = 6.9 Hz, CH_2-1'), 3.07 (3H, s, $ArCH_3$), 1.54 (2H, quintet, *J* = 7.7 Hz, CH_2-2'), 1.08 - 1.00 (2H, m, CH_2-3'), 0.99 - 0.84 (4H, m, CH_2-4', CH_2-5'), 0.71 (3H, t, *J* = 7.2 Hz, CH_2-6'). ^{13}C NMR (126 MHz, CD_3OD) δ 169.05 (C), 148.88 (C), 140.64 (C), 139.63 (CH), 137.15 (C), 134.20 (CH), 133.25 (C), 132.45 (C), 132.11 (CH), 131.72 (CH), 131.43 (CH), 131.07 (CH), 129.26 (CH), 128.59 (C), 126.88 (CH), 126.82 (C), 125.11 (CH), 61.15 (CH_2), 31.75 (CH_2), 31.02 (CH_2), 26.66 (CH_2), 24.53 (CH_3), 23.02 (CH_2), 14.00 (CH_3). ν_{Max}(ATR)cm^{-1} (TFA salt): 2961 (C-H), 2930 (C-H), 2862 (C-H), 1778 (TFA), 1732 (TFA), 1622 (C=N), 1586 (C_{Ar}=C_{Ar}), 1539 (C_{Ar}=C_{Ar}), 1348 (NO_2).

MS (ESI^+): 399 [M^+ (phenanthridinium cation), 100%]. HRMS: 399.2050. $C_{26}H_{27}N_2O_2^+$ requires 399.2067.

3-*tert*-Butyl-5-(cyclohexylmethylamino)-6-phenyl-8-nitrophenanthridinium chloride **309**

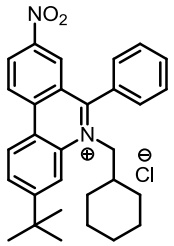

309

Benzophenone **265** (360 mg, 0.95 mmol, 1.00 eq.) and cyclohexylmethylamine **336** (0.90 mL, 6.9 mmol, 7.3 eq.) were combined stirring under argon at 0 ˚C in dry PhMe (5.0 mL) then a 1 M solution of titanium tetrachloride in dry PhMe (1.50 mL, 1.50 mmol, 1.50 eq.) was added over 5 min. The reaction was allowed to warm to RT and allowed to stir for 20 h. The mixture was quenched into H_2O, then filtered through celite with DCM and partitioned between DCM and 0.5 M $HCl_{(aq),}$ then the aqueous layer was re-extracted (DCM x 2). The combined organics were washed with 1 M $HCl_{(aq)}$ then $NaHCO_{3(aq)}$ and dried ($MgSO_4$) then filtered and the solvent removed under reduced pressure. From the crude yield of 445 mg of brown solid four portions (total of 80 mg, 0.16 mmol, 1.00 eq.) were weighed by difference onto a spatula and sonicated into microwave tubes (10 mL) containing dry MeCN (1.0 mL). The tubes were filled with argon and sealed then heated in a microwave to 110 ˚C for 90 min then cooled and the solvent removed under reduced pressure. Following column chromatography of the combined residues [SiO_2, loaded in and washed with DCM and eluted with DCM/NEt_3 (200:1)] the combined organics were concentrated under reduced pressure then washed (1 M $HCl_{(aq)}$ x 2), and dried ($MgSO_4$). After filtration 2 M ethereal HCl (1.00 mL, 2.00 mmol, 12.5 eq.) was added to the filtrate and the solvent removed under reduced pressure, to give phenanthridinium salt **309** as a brown solid (63 mg, 75%). R_f = 0.21 in DCM/NEt_3 (100:1). ^{1}H NMR (400 MHz, CD_3OD, 50˚C) δ 9.32 (1H, d, *J* = 9.2 Hz, H10), 9.20 (1H, d, *J* = 8.8 Hz, H1), 8.99 (1H, dd, *J* = 9.2, 2.2 Hz, H9), 8.49 - 8.43 (2H, m, H4, H7), 8.37 (1H, dd, *J* = 8.8, 1.4 Hz, H2), 7.94 (1H, t, *J* = 7.4 Hz, H4''), 7.88 (2H, t, *J* = 7.3 Hz, H3'', H5''), 7.79 (2H, d, *J* = 7.0 Hz, H2'', H6''), 5.00 (2H, s, br, CH_2-N), 2.08 (1H, m, CH_2-1'), 1.73 - 1.49 (2H, m, CH_2-2'$_A$), 1.59 [9H, s, C(CH_3)], 1.40 - 0.82 (8H, m, CH_2-2'$_B$, CH_2-4', CH_2-5'). ^{13}C NMR (126 MHz, DMSO, 70 ˚C) δ 164.57 (C), 157.00 (C), 146.73 (C), 137.58 (C), 135.08 (C), 131.65 (CH), 129.94 (C), 129.49 (CH), 129.31 (CH), 128.89 (CH), 128.82 (CH), 127.30 (CH), 125.55 (C), 125.31 (CH), 125.03 (CH), 123.00 (C), 117.19 (CH), 59.46 (CH_2), 38.29 (CH), 35.65 (C), 30.32 (CH_3), 29.88 (CH_2), 24.82 (CH_2). ν_{Max}(ATR)cm^{-1}: 2926 (C-H), 2853 (C-H), 1621 (C=N), 1587 (C_{Ar}=C_{Ar}), 1540 (C_{Ar}=C_{Ar}), 1343 (NO_2). MS (ESI^+): 453 [M^+ (phenanthridinium cation), 100]. HRMS: 453.2523. $C_{30}H_{33}N_2O_2^+$ requires 453.2537.

5-(6'-Azidohex-1'-yl)-6-phenylphenanthridinium chloride **310**

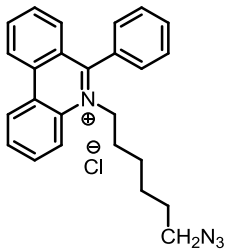

310

Benzophenone **327** (414 mg, 1.49 mmol, 1.00 eq.) and 6-azidohex-1-ylamine (1.00 g, 7.86 mmol, 5.28 eq.) were combined stirring under argon at 0 ˚C in dry PhMe (7.0 mL) then 1 M titanium tetrachloride in dry PhMe (1.70 mL, 1.70 mmol, 1.14 eq.) was added over 5 min. After 15 h a sample (0.1 mL) was quenched into H_2O, partitioned between DCM and water and the organic separated and the solvent removed under reduced pressure. This process was repeated at 21 h, at which point the starting material was shown to be consumed by proton NMR. The mixture was quenched into water then filtered through celite with DCM, then partitioned between DCM and 1 M $HCl_{(aq)}$. The aqueous was extracted with DCM (x 2) then the collected organics washed with 1 M $HCl_{(aq)}$, followed by $NaHCO_{3(aq)}$. The organic layers were dried ($MgSO_4$), then filtered and the solvent removed under reduced pressure. From the crude yield of 571 mg of brown oil a portion (100 mg, 0.25 mmol, 1.00 eq.) was weighed by difference onto a spatula and sonicated into a microwave tube (10 mL) containing dry MeCN (5.0 mL). The tube was filled with argon and sealed then heated in a microwave to 110 ˚C for 90 min. After cooling the residue was dissolved in MeOH and loaded onto a Strata SCX ion exchange column and washed (MeOH) then eluted (15 mg/mL NaOAc in MeOH). The solution was partitioned between $CHCl_3$ and 1 M $HCl_{(aq)}$, then the organic layer washed (1 M $HCl_{(aq)}$ x 2). The organic layer was dried ($MgSO_4$), filtered and ethereal HCl (1.00 mL, 2.00 mmol, 7.75 eq.) was added, then the solvent removed under reduced pressure. The phenanthridinium chloride **310** was isolated as a brown oil (79 mg, 78%). ^{1}H NMR (400 MHz, 0.75 mL $CDCl_3$ + 0.05 mL CF_3CO_2D) δ 8.99 (1H, dd, *J* = 8.1, 1.7 Hz, H1), 8.93 (1H, d, *J* = 8.5 Hz, H10), 8.40 (1H, d, *J* = 8.3 Hz, H4), 8.30 (1H, ddd, *J* = 8.5, 7.2, 1.5 Hz, H9), 8.20 - 8.11 (2H, m, H2, H3), 7.81 - 7.67 (4H, m, H8, H3'', H4'', H5''), 7.68 (1H, d, *J* = 7.7 Hz, H7), 7.60 - 7.53 (2H, m, H2'', H6''), 4.89 - 4.79 (2H, m, CH_2-1'), 3.26 (2H, t, *J* = 6.7 Hz, CH_2-6'), 2.01 (2H, s, br, CH_2-2'), 1.58 - 1.49 (2H, m, CH_2-3'), 1.42 - 1.23 (4H, m, CH_2-4', CH_2-5'). ^{13}C NMR (101 MHz, 0.75 mL $CDCl_3$ + 0.05 mL CF_3CO_2D) δ 163.82 (C), 138.43 (CH), 135.27 (C), 133.35 (C), 133.21 (CH), 133.09 (CH), 132.37 (CH), 131.21 (CH), 130.71 (CH), 130.05 (CH), 127.62 (CH), 126.38 (C), 125.10 (C), 124.83 (CH), 122.75 (CH), 119.35 (CH), 54.47 (CH_2), 51.02 (CH_2), 29.75 (CH_2), 28.06 (CH_2), 25.84 (CH_2), 25.62 (CH_2). ν_{Max}(ATR)cm^{-1} (as TFA salt): 2928 (C-H), 2856 (C-H), 1779 (TFA), 1738 (TFA), 1622 (C=N), 1588 (C_{Ar}=C_{Ar}), 1538(C_{Ar}=C_{Ar}). MS (NSI$^+$): 381 [M^+ (phenanthridinium cation), 38%], 256 (M^+ – C_6H_{12}, 100). HRMS: 381.2073. $C_{25}H_{25}N_4^+$ requires 381.2074.

3-Bromo-5-(hex-1'-yl)-6-phenyl-8-aminophenanthridinium chloride **373**

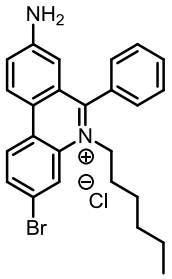

373

Nitrophenanthridinium **300** (250 mg, 0.50 mmol, 1.00 eq.) was dissolved in a 1:1 mixture of AcOH and EtOH (15.0 mL) then iron powder (346 mg, 6.20 mmol, 10.7 eq.) added and the mixture heated stirring to 40 ˚C for 90 min. The mixture was then poured into 1 M $HCl_{(aq)}$, and extracted with DCM (x 2). The combined organics were then washed with 1 M $HCl_{(aq)}$ and $NaHCO_{3(aq)}$ (x 2) sequentially, before drying ($MgSO_4$), filtering and removing the solvent under reduced pressure. The amine **373** was isolated as a red powder (200 mg, 85%). ^{1}H NMR (500 MHz, $CDCl_3$) δ 8.57 (1H, d, *J* = 8.9 Hz, H1), 8.48 (1H, d, *J* = 8.6 Hz, H10), 8.24 (1H, s, H4), 7.98 (1H, d, *J* = 8.7 Hz, H2), 7.83 - 7.68 (4H, m, H9, H3'', H4'', H5''), 7.49 (2H, d, *J* = 6.8 Hz, H2'', H6''), 6.52 (1H, s, H7), 4.95 (2H, s, br, NH_2), 4.63 (2H, t, *J* = 8.4 Hz, CH_2-1'), 1.95 - 1.83 (2H, m, CH_2-2'), 1.36 - 1.11 (6H, m, CH_2-3', CH_2-4', CH_2-5'), 0.84 (3H, t, *J* = 7.2 Hz, CH_2-6'). ^{13}C NMR (126 MHz, $CDCl_3$) δ 162.20 (C), 151.19 (C), 133.51 (CH), 132.28 (C), 131.91 (CH), 131.01 (C), 130.11 (CH), 129.92 (CH), 128.22 (CH), 127.55 (C), 126.08 (C), 125.78 (C), 125.45 (CH), 123.85 (C), 123.55 (CH), 122.14 (CH), 111.20 (CH), 54.75 (CH_2), 30.74 (CH_2), 29.67 (CH_2), 26.26 (CH_2), 22.34 (CH_2), 13.91 (CH_3). ν_{Max}(ATR)cm^{-1}: 3277 (N-H), 3133 (N-H), 2952 (C-H), 2929 (C-H), 2859 (C-H), 1609 (C=N), 1579 (C_{Ar}=C_{Ar}). MS (ESI$^+$): 435 [^{81}BrM$^+$ (phenanthridinium cation), 100%], 433 [^{79}BrM$^+$ (phenanthridinium cation], 100). HRMS: 435.1242, 433.1255. $C_{25}H_{26}{}^{81}BrN_2$ requires 435.1253, $C_{25}H_{26}{}^{79}BrN_2$ requires 433.1274. MP: 153 - 157 ˚C.

3,8-Diamino-5-(hex-1'-yl)-6-methyl-5,6-dihydrophenanthridine **375**

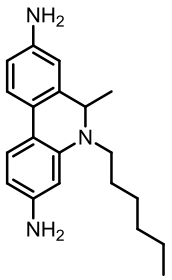

375

Enamine **369** (100 mg, 0.27 mmol, 1.00 eq.) was dissolved in a 1:1 mixture of AcOH and EtOH (4.0 mL) then iron powder (151 mg, 2.71 mmol, 10.0 eq.) added and the mixture heated stirring to 60 ˚C for 1 h. The mixture was then poured into 1 M $HCl_{(aq)}$, then the acidity reduced with $NaHCO_{3(aq)}$. Excess $NaBH_4$ was added and the aqueous extracted with $CHCl_3$ which was then dried ($MgSO_4$) and filtered, then the solvent removed under reduced pressure. The phenanthridine **375** was isolated as a solid (15 mg, 18%). ^{1}H NMR (500 MHz, $CDCl_3$) δ 7.41 (1H, d, *J* = 8.2 Hz, H10), 7.40 (1H, d, *J* = 8.1 Hz, H1), 6.62 (1H, dd, *J* = 8.3, 2.4 Hz, H9), 6.39 (1H, d, *J* = 2.4 Hz, H7), 6.15 (1H, dd, *J* = 8.1, 2.2 Hz, H2), 6.03 (1H, d, *J* = 2.1 Hz, H4), 4.26 (1H, q, *J* = 6.5 Hz, H6), 3.60 (4H, s, br, NH_2), 3.37 (1H, dt, *J* = 13.9, 7.0 Hz, CH_2-1'$_A$), 3.04 (1H, dt, *J* = 13.8, 7.7 Hz, CH_2-1'$_B$), 1.71 - 1.59 (2H, m, CH_2-2'), 1.41

- 1.19 (6H, m, CH_2-3', CH_2-4', CH_2-5'), 1.10 (3H, d, *J* = 6.5 Hz, C-6CH_3), 0.88 (3H, t, *J* = 7.0 Hz, CH_2-6'). ^{13}C NMR (101 MHz, $CDCl_3$) δ 146.27 (C), 144.38 (C), 144.16 (C), 137.87 (C), 123.44 (CH), 122.89 (CH), 122.60 (C), 114.93 (C), 114.74 (CH), 111.81 (CH), 104.81 (CH), 100.11 (CH), 58.31 (CH), 49.59 (CH_2), 31.86 (CH_2), 28.00 (CH_2), 27.13 (CH_2), 22.80 (CH_2), 18.57 (CH_3), 14.21 (CH_3). ν_{Max}(ATR)cm^{-1} (oxidised form): 3453 (N-H), 3351 (N-H), 3215 (N-H), 2956 (C-H), 2922 (C-H), 2855 (C-H), 1610 (C=N), 1495 (C_{Ar}=C_{Ar}). MS (ESI$^+$): 308 [M$^+$ (phenanthridinium cation), 100%, 294 [(M+H)$^+$ – CH_4, 28]. HRMS: 308.2110. $C_{20}H_{26}N_3$ requires 308.2121.

3,8-Diamino(2,2-dimethylpropyl)-6-phenylphenanthridine **405**

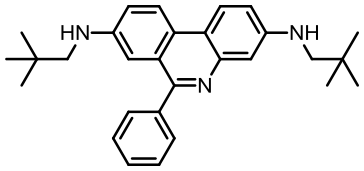

405

3,8-Diamino-6-phenylphenanthridine **133** (650 mg, 2.28 mmol, 1.00 eq.) and $NaBH(OAc)_3$ (1.45 g, 6.83 mmol, 3.00 eq.) were mixed in TFA (0.81 mL, 11 mmol, 4.7 eq.). The mixture was cooled to −15 ˚C under argon with an IPA/$CO_{2(s)}$ bath. DCM (6.5 mL) was added and the mixture stirred. 2,2-dimethylpropanal (0.54 mL, 5.0 mmol, 2.2 eq.) was then added by syringe and the mixture allowed to stir for 2 h, then the mixture was partitioned between DCM and H_2O, then the aqueous extracted with DCM. The combined organic layers were washed with brine, then extracted with DCM and the organics combined and solvent removed under reduced pressure. The material was dissolved in Et_2O and precipitated with excess ethereal HCl (2 M), then allowed to settle overnight. The solid was filtered, washed with Et_2O and dissolved in DCM then washed with $NaHCO_{3(aq)}$. The aqueous was re-extracted with DCM, then the combined organics dried ($MgSO_4$), filtered and the solvent removed under reduced pressure to give phenanthridine **405** as a foam (1.08 g, 99%). ^{1}H NMR ($CDCl_3$, 500 MHz): 8.28 (1H, d, *J* = 9.0 Hz, H10), 8.19 (1H, d, *J* = 8.9 Hz, H1), 7.68 – 7.63 (2H, m, H2'', H6''), 7.53 – 7.43 (3H, m, H3'', H4'', H5''), 7.26 (1H, d, *J* = 2.3 Hz, H4), 7.16 (1H, dd, *J* = 8.9, 2.5 Hz, H9), 7.02 – 6.97 (2H, m, H7, H2), 3.91 (2H, s, br, 3-NHR, 8-NHR), 3.02 (2H, s, 8-NHC**H$_2$**), 2.87 (2H, s, 3-NHC**H$_2$**), 1.00 [9H, s, 8-$NHCH_2C(CH_3)_3$)], 0.96 [9H, s, 3-$NHCH_2C(CH_3)_3$)]. ^{13}C NMR (126 MHz, $CDCl_3$) δ 159.91 (C), 148.65 (C), 146.73 (C), 143.19 (C), 139.57 (C), 129.51 (CH), 128.56 (CH), 128.25 (CH), 126.56 (C), 125.12 (C), 122.36 (CH), 121.94 (CH), 120.51 (CH), 117.04 (CH), 116.17 (C), 107.43 (CH), 107.33 (CH), 55.88 (CH_2), 55.84 (CH_2), 32.04 (C), 31.97 (C), 27.58 (CH_3), 27.56 (CH_3). IR (ATR cm^{-1}): 3424 (N-H), 3285 (N-H), 2953 (C-H), 2864 (C-H), 1620 (C=N), 1568 (C_{Ar}=C_{Ar}), 1512 (C_{Ar}=C_{Ar}). MS (EI$^+$): 425 (M$^{+\cdot}$, 72%), 368 [M$^{+\cdot}$ –$^{\cdot}$C$(CH_3)_3$, 100]. HRMS: 425.2837. $C_{29}H_{35}N_3$ requires 425.2831.

3,8-Diamino(2,2-dimethylpropyl)-5-*N*-ethyl-6-phenylphenanthridinium methanesulfonate **406**

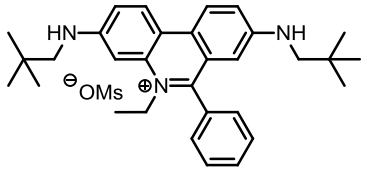

406

Phenanthridine **405** (100 mg, 0.23 mmol, 1.00 eq.) dissolved in Et_2O (1.0 mL), then stirred under argon at RT. Ethyl triflate (34 µL, 0.26 mmol, 1.1 eq.) was added by syringe followed by a further 0.2 mL Et_2O. After 20 h stirring at RT the reaction was quenched into H_2O, extracted with DCM (x 2) then the organic layers dried ($MgSO_4$), filtered and the solvent removed under reduced pressure. Column chromatography [SiO_2, gradient from DCM/MeOH/NEt_3 (200:2:1) to (100:2:1)] was followed by ion exchange to mesylate and salt **406** was isolated as purple foam (65 mg, 50%). ^{1}H NMR ($CDCl_3$, 400 MHz): 8.24 (1H, d, *J* = 9.3 Hz, H1), 8.05 (1H, d, *J* = 9.3 Hz, H10), 7.89 (1H, s, H4), 7.78 - 7.64 (3H, m, H3'', H4'', H5''), 7.48 (1H, dd, *J* = 9.2, 2.5 Hz, H9), 7.40 - 7.31 (3H, m, H2'', H6'', H2), 7.13 (1H, t, *J* = 6.0 Hz, NH), 5.97 (1H, d, *J* = 2.4 Hz, H7), 4.87-4.75 (3H, m, NC**H**$_2$$CH_3$, NH), 3.12 (2H, d, *J* = 6.1 Hz NHC**H**$_2$), 2.81 (3H, s, C**H**$_3$$SO_3^-$,) 2.65 (2H, d, *J* = 6.1 Hz, NHC**H**$_2$), 1.52 (3H, t, *J* = 7.1 Hz, NCH_2C**H**$_3$), 1.09 [9H, s, $C(CH_3)_3$], 0.86 [9H, s, $C(CH_3)_3$]. ^{13}C (101 MHz, $CDCl_3$) δ 157.40 (C), 152.30 (C), 147.64 (C), 134.79 (C), 132.08 (C), 131.07 (CH), 129.70 (CH), 128.99 (C), 128.15 (CH), 128.03 (CH), 124.73 (C), 124.17 (CH), 122.06 (CH), 117.78 (CH), 117.43 (C), 105.05 (CH), 98.30 (CH), 55.15 (CH_2), 54.96 (CH_2), 49.49 (CH_2), 32.65 (C), 32.39 (C), 27.63 (CH_3), 27.55 (CH_3), 14.48 (CH_3). IR (ATR cm^{-1}): 3350 (N-H), 2957 (C-H), 2864 (C-H), 1622 (C=N), 1535 (C_{Ar}=C_{Ar}). MS (as $CF_3SO_3^-$ salt, NSI^+): 454 (M^+, 100%). HRMS: 454.3211. $C_{31}H_{40}N_3$ requires 454.3217. MS (as $CF_3SO_3^-$ salt, NSI^-): 148 ($CF_3SO_3^-$, 100%). HRMS: 148.9530. CF_3SO_3 requires 148.9526. MP: Decomp > 180 ˚C.

1-Bromohexyltrifluoromethanesulfonate **408**

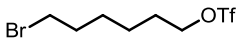

408

1-Bromohexan-6-ol **407** (1.00 g, 5.52 mmol, 1.00 eq.) was added to a 0 ˚C stirring solution of dry DCM (5.0 mL), dry pyridine (0.4 mL, 6.1 mmol, 1.1 eq.) and triflic anhydride (1.02 mL, 6.08 mmol, 1.10 eq.) under argon. After 90 min the mixture was quenched into DCM/H_2O, then the organic washed (x 2) with H_2O and dried ($MgSO_4$) then filtered and the solvent removed under reduced pressure. The triflate **408** was isolated as a brown oil (1.318 g, 76%). δ_H ($CDCl_3$, 400 MHz): 4.55 (2H, t, *J* = 6.4 Hz, CH_2OTf), 3.41 (2H, t, *J* = 6.6 Hz, CH_2Br), 1.93 - 1.81 (4H, m, C**H**$_2$$CH_2OTf$, C**H**$_2$$CH_2Br$), 1.57 - 1.42 (4H, m, CH_2C**H**$_2$C**H**$_2$$CH_2$). δ_c ($CDCl_3$, 100 MHz): 119.02 (q, *J* = 319.7 Hz, CF_3), 77.29 (CH_2), 33.66 (CH_2), 32.69 (CH_2), 29.47 (CH_2), 27.76 (CH_2), 24.71 (CH_2).

3,8-Diaminoneopentyl-5(6'-bromohexyl)-6-phenylphenanthridinium triflate **409**

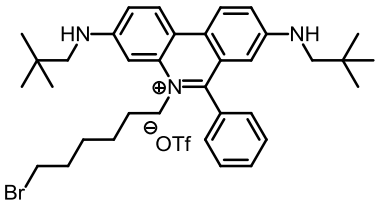

409

Triflate **408** (413 mg, 1.32 mmol, 1.02 eq) was dissolved in dry Et_2O (6.6 mL) stirring under argon and cooled to −30 ˚C, then phenanthridine **405** (549 mg, 1.29 mmol, 1.00 eq.) was added and the mixture allowed to warm to RT then stirred for 17 h. The mixture was quenched into H_2O and extracted into DCM, then dried ($MgSO_4$), filtered and the solvent removed under reduced pressure. Column chromatography [SiO_2, loaded in DCM, DCM/MeCN/NEt_3, gradient from (100:7.5:1) to (100:15:2)]. The fractions were dried ($MgSO_4$), filtered and the solvent was removed under reduced pressure. A mixture containing mostly the desired product **409** was obtained (450 mg, 50%) and used directly without further purification.

3,8-Diaminoneopentyl-5(6'-triphenylphosphoniohexyl)-6-phenylphenanthridinium mesylate **403**

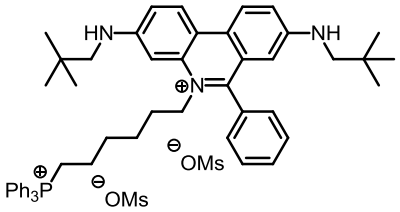

403

Bromophenanthridinium **409** (300 mg, 0.41 mmol, 1.00 eq.) was transferred to a flask in DCM which was then removed under reduced pressure. Triphenylphosphine was dried by azeotrope with PhMe, then added (1.07 g, 4.08 mmol, 10.0 eq.), followed by dry PhMe (6.0 mL). The reaction was heated to reflux for 15 h under argon stirring. The mixture was cooled to 70 ˚C then poured into PhMe. The residue was dissolved in $CHCl_3$, then the solvent removed under reduced pressure. The material was converted to chloride with an anion exchange resin [loaded in MeOH, eluted with MeOH/H_2O (1:1)]. Following column chromatography (SiO_2, loaded with $CHCl_3$, $CHCl_3$/MeOH/$NH_{3(aq)}$ gradient from (100:15:1) to (100:25:2)] product fractions were combined, then the solvent removed under reduced pressure. The material was dissolved in $CHCl_3$ and precipitated with Et_2O and Pet. ether. The resulting mixture was purified using HPLC in 20 mg/10 ml aliquots (9:1 H_2O/MeCN).

Column: C18 synergi Max-RP 10 µm 250 x 21.2 mm RT: 48.5 min

Time: (min)	0.1% $TFA_{(aq)}$: (%)	MeCN: (%)	Flow: (ml/min)
0	90	10	15
5	90	10	15
60	20	80	15
70	90	10	15

The clean fractions from the aliquots were combined and the solvent removed under reduced pressure. The counter ion was then exchanged (IRA 401 resin in mesylate form, loaded and eluted in 1:1 MeOH/H_2O) to the mesylate form. The double salt **403** was isolated as a purple glass (38 mg, 9%). δ_H ($CDCl_3$, 500 MHz): 8.34 (1H, d, *J* = 9.6 Hz, H1), 8.21 (1H, d, *J* = 9.2 Hz, H10), 7.97 (1H, apparent s, H4), 7.80 - 7.62 (19H, m, H9, P**Ph**$_3$, H2'', H4'', H6''), 7.34 - 7.30 (2H, m, H3'', H5''), 7.29 (1H, *J* = 9.4 Hz, 1.7 Hz, H2), 7.11 (1H, t, *J* = 6.1 Hz, C3-N**H**), 5.96 (1H, d, *J* = 2.4 Hz, H7), 5.18 (1H, t, *J* = 6.2 Hz, C8-N**H**), 4.68 (2H, apparent s, broad, CH_2-1'), 3.60 - 3.48 (2H, m, CH_2-6'), 3.08 (2H, d, *J* = 6.1 Hz, 3-NHC**H**$_2$), 2.70 (6H, s, C**H**$_3SO_3^-$), 2.63 (2H, d, *J* = 6.1 Hz, 8-NHC**H**$_2$), 1.83 (2H, apparent s, broad, CH_2-3'), 1.65 - 1.44 (6H, m, CH_2-3', CH_2-4', CH_2-5'), 1.01 [9H, s, 3-CH_2C(C**H**$_3$)], 0.83 [9H, s, 8-CH_2C(C**H**$_3$)]. δ_c ($CDCl_3$, 125 MHz): 157.52 (C), 152.91 (C), 148.40 (C), 135.29 (d, *J* = 2.7 Hz, CH), 135.18 (C), 133.90 (d, *J* = 10.0 Hz, CH), 132.49 (C), 131.31 (CH), 130.78 (d, *J* = 12.6 Hz, CH), 129.97 (CH), 129.32 (CH), 129.14 (C), 128.28 (CH), 124.92 (C), 124.53 (CH), 122.14 (CH), 118.74 (d, *J* = 86.1 Hz, C), 117.43 (C), 116.32 (CH), 104.70 (CH), 100.06 (CH), 55.46 (CH_2), 55.12 (CH_2), 53.65 (CH_2), 39.95 (CH_3), 33.10 (C), 32.87 (C), 29.44 (CH_2), 29.30 (CH_2), 28.01 (CH_3), 27.95 (CH_3), 25.04 (CH_2), 22.09 (d, *J* = 4.2 Hz, CH_2) 21.53 (d, *J* = 50.9 Hz, CH_2). ν_{Max}(ATR)cm^{-1}: 3298 (NH), 3059 (C_{Ar}-H), 2949 (C-H), 2936 (C-H), 2904 (CH), 2866 (C-H), 1618 (C=N), 1587 (C_{Ar}=C_{Ar}), 1541 (C_{Ar}=C_{Ar}), 1520 (C_{Ar}=C_{Ar}). MS (ESI^+): 386 (M^{++}, 100%). HRMS: 385.7332. $C_{53}H_{62}N_3P^{2+}$ requires 385.7335.

1,4-Bis(benzyloxy)benzene **420**

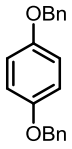

420

1,4-hydroquinone **414** (40.0 g, 363 mmol, 1.00 eq.) and benzyl chloride (101 mL, 878 mmol, 2.42 eq.) were suspended in ethanol (268 mL). Ethanolic KOH (250 mL, 2.85 M) was added and the mixture stirred mechanically for 3 h under argon then allowed to stand for 3 days. The mixture was quenched in H_2O and the off-white precipitate was filtered and crystallised in eight portions (14 g/500 mL) from boiling EtOH. The combined crystallisation leftovers were combined, then concentrated to give another crop of crystals. The combined solid was dried under vacuum to give ether **420** as needles (71.8 g, 68%). δ_H (400 MHz, $CDCl_3$): 7.45 - 7.28 (10H, m, OCH_2**Ph**), 6.90 [4H, s, **Ph**(Obn)$_2$], 5.01 (4H, s, OC**H**$_2$Ph). ^{13}C NMR (101 MHz, $CDCl_3$) δ 153.26 (C), 137.37 (C), 128.68 (CH), 128.02 (CH), 127.60 (CH), 115.90 (CH), 70.74 (CH_2). Consistent with literature data. [431,396]

1,4-Bis(benzyloxy)-2-nitrobenzene **421**

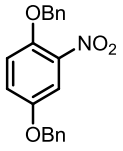

421

Protected quinol **420** (65.0 g, 224 mmol, 1.00 eq.) was suspended in glacial acetic acid (240 mL) and a solution of nitric acid in glacial acetic acid ($HNO_{3(aq)}$ 70% aqueous solution, 17 mL, 270 mmol, 1.2 eq. Made up to 75 mL with glacial acetic acid) was added to the mixture and

mechanically stirred for 2 h, then additional AcOH (300 mL) added and the reaction stirred at 50 ˚C for 18 h. The material was cooled to 0 - 5 ˚C for 4 h, then filtered. The filtrate was diluted (H_2O) and further precipitate collected, then the remaining solution concentrated under reduced pressure and the process repeated. Remaining H_2O and AcOH were removed by azeotrope with PhMe, which was then removed under reduced pressure. Nitro compound **421** was isolated as a yellow solid (73.2 g, 97%). δ_H (400 MHz, $CDCl_3$): 7.49 (1H, d, *J* = 3.0, H3), 7.46 - 7.30 (10H, m, OCH_2**Ph**), 7.12 (1H, dd, *J* = 9.2, 3.1 Hz, H5), 7.05 (1H, d, *J* = 9.2 Hz, H6), 5.18 (2H, s, C**H**$_2$), 5.05 (2H, s, C**H**$_2$). ^{13}C NMR (101 MHz, $CDCl_3$) δ 152.30 (C), 146.39 (C), 135.97 (C), 135.88 (C), 128.75 (CH), 128.70 (CH), 128.37 (CH), 128.22 (CH), 127.59 (CH), 127.15 (CH), 121.54 (CH), 117.24 (CH), 111.18 (CH), 72.10 (CH_2), 70.94 (CH_2). IR (ATR cm^{-1}): 1520 (NO_2), 1497 (C_{Ar}=C_{Ar}), 1341 (NO_2). MS (ESI^+): 358 [$(M+Na)^+$, 100]. HRMS: 358.1034. $C_{20}H_{17}NNaO_4$ requires 358.1050. Compound known but not previously fully characterised.[396]

4-Benzyloxy-2-nitrophenol **422**

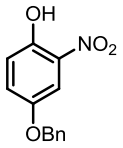

422

Nitroaryl **421** (4.50 g, 13.4 mmol, 1.00 eq.) was dissolved in $CHCl_3$ (65 mL) and stirred at 0 ˚C under argon. To the mixture a suspension of $AlCl_3$ (2.07 g, 15.5 mmol, 1.16 eq.) in $CHCl_3$ (10 mL) was added portionwise with additional $CHCl_3$ (20 mL). The reaction was monitored by TLC and was complete after 15 min. The mixture was quenched into $HCl_{(aq)}$ (1 M) and extracted with DCM (x 3). The combined organics were dried ($MgSO_4$), filtered and the solvent removed under reduced pressure. The residue was crystallised from boiling MeOH, then recrystallised from boiling MeOH with 5% H_2O added. The resulting crystals were washed (H_2O), then partitioned between H_2O and DCM. The organic layer was separated and the solvent removed under reduced pressure, giving nitrophenol **422** as a solid (1.88 g, 57%). δ_H (400 MHz, $CDCl_3$): 10.36 (1H, s, ArO**H**), 7.61 (1H, d, *J* = 3.1 Hz, H3), 7.46 - 7.33 (5H, m, OCH_2**Ph**), 7.29 (1H, dd, *J* = 9.2, 3.1 Hz, H5), 7.10 (1H, d, *J* = 9.2 Hz, H6). ^{13}C NMR (101 MHz, $CDCl_3$) δ 151.64 (C), 150.20 (C), 135.86 (C), 132.97 (C), 128.76 (CH), 128.42 (CH), 127.88 (CH), 127.65 (CH), 120.93 (CH), 107.19 (CH), 70.92 (CH_2). IR (ATR cm^{-1}): 3231 (O-H), 3123 (C_{Ar}-H), 3106 (C_{Ar}-H), 1584 (C_{Ar}=C_{Ar}), 1530 (NO_2), 1501 (C_{Ar}=C_{Ar}), 1485 (C_{Ar}=C_{Ar}), 1316 (NO_2). MS (EI^+): 245 (M^+, 18%), 91 ($C_7H_7^{+\cdot}$, 100). HRMS: 245.0696. $C_{13}H_{11}O_4N$ requires 245.0688. Compound known but not previously fully characterised.[396]

1-(2-bromoethoxy)-2-nitrobenzene **415**

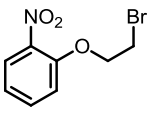

415

Following the method of Tsein and coworkers,[396] 2-nitrophenol **423** (3.99 g, 28.7 mmol, 1.00 eq.), 1,2-dibromoethane (7.5 mL, 87 mmol, 3.0 eq.) and K_2CO_3 (4.36 g, 31.6 mmol, 1.10 eq.) were combined in DMF (6.0 mL) and stirred at 120 °C for 3 h under argon. The precipitate was filtered off and washed with DCM and H_2O. The filtrate layers were separated and the organics were

washed with 0.5 M $NaOH_{(aq)}$ and saturated brine solution. The organics were dried ($MgSO_4$) and filtered, then the solvent was removed under reduced pressure to give the bromide **415** (4.53 g, 65%) as a solid. δ_H (400 MHz, $CDCl_3$): 7.85 (1H, dd, *J* = 8.3, 1.7 Hz, H6), 7.55 (1H, ddd, *J* = 8.4, 7.5, 1.7 Hz, H4), 7.12 - 7.06 (2H, m, H3, H5), 4.42 (2H, t, *J* = 6.5 Hz, OC**H**$_2$$CH_2$Br), 3.68 (2H, t, *J* = 6.5 Hz, OCH_2C**H**$_2$Br). This material is commercially available and ^{1}H NMR is consistent with literature data.[432]

2-Nitro-1-[2'-(4''-benzyloxy-2''-nitrophenoxy)ethoxy]benzene **416**

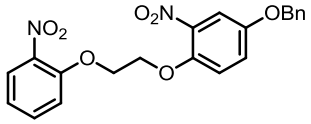

416

Following the method of Tsein and coworkers[396] 1-(2-bromoethoxy)-2-nitrobenzene **415** (10.9 g, 44.3 mmol, 1.47 eq.), nitrophenol **422** (7.0 g, 30 mmol, 1.0 eq.) and K_2CO_3 (3.0 g, 22 mmol, 0.7 eq.) were combined in dry DMF (17.0 mL) and stirred at 140 °C for 2 h under argon, then allowed to stir at RT for 12 h. The material was heated to 50 °C, and the precipitate was dissolved with dropwise addition of water. After 24 h stirring precipitate had formed and was collected by filtration. The material was then washed out in a mixture of acetone and hexane. The solvent was removed under reduced pressure and the compound dissolved in DCM then washed with water (x 3) and 5% $LiCl_{(aq)}$ solution, then the solvent removed from the combined organics to give the ether **416** in quantitative yield (12.4 g, quant.). δ_H (400 MHz, $CDCl_3$): 7.84 (1H, dd, *J* = 8.1, 1.7 Hz, H3), 7.57 (1H, ddd, *J* = 8.5, 7.4, 1.7 Hz, H5), 7.47 - 7.32 (6H, m, OCH_2**Ph**, H3''), 7.23 - 7.19 (3H, m, H6, H5'', H6''), 7.12 - 7.05 (1H, m, H4), 5.07 (2H, s, OC**H**$_2$Ph), 4.52 - 4.46 (4H, m, OC**H**$_2$C**H**$_2$O). δ_C ($CDCl_3$, 100 MHz): 152.95 (C), 151.956 (C), 146.37 (C), 140.63 (C), 140.20 (C), 135.90 (C), 134.34 (CH), 128.76 (CH), 128.38 (CH), 127.59 (CH), 125.68 (CH), 121.73 (CH), 121.24 (CH), 118.75 (CH), 115.61 (CH), 111.04 (CH), 70.96 (CH_2), 69.99 (CH_2), 68.77 (CH_2). IR (ATR cm^{-1}): 3094 (CH), 2960 (CH), 2929 (CH), 2871 (CH), 1606 (C_{Ar}=C_{Ar}), 1518 (NO_2), 1497 (C_{Ar}=C_{Ar}), 1487 (NO_2), 1451 (C_{Ar}=C_{Ar}). MS (EI$^+$): (410 $M^{+\cdot}$, 45%), 166 ($O_2NC_6H_4OCH_2CH_2^+$, 38), 122 ($C_4H_4NO_2^+$, 44), 91 ($PhCH_2^+$, 100). HRMS: 410.1114. $C_{21}H_{18}N_2O_7$ requires $M^{+\cdot}$ 410.1114. MP: 110 -111 °C.

1-Nitro-2-[2'-(2''-nitrophenoxy)ethoxy]benzene **426**

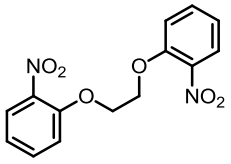

426

Dimer **426** (321 mg, 4%) was isolated as a side product of an earlier synthesis of ether **416**, and separated from ether **416** by column chromatography [SiO_2, Pet. ether/EtOAc (5:2)]. δ_H (400 MHz, d_6-DMSO): 7.86 (2H, dd, *J* = 8.0, 1.7 Hz, H6, H3''), 7.66 (2H, ddd, *J* = 8.4, 7.5, 1.7 Hz, H4, H5''), 7.44 (2H, *J* = 8.5, 1.0 Hz, H3, H6''), 7.15 (2H, m, H5, H4''), 4.54 (4H, s, OC**H**$_2$). δ_c (100 MHz, d_6-DMSO): 150.89 (C), 139.75 (C), 134.30 (CH), 124.83 (CH), 120.98 (CH), 115.55 (CH), 68.02 (CH_2). IR (ATR cm^{-1}): 2931 (C-H), 2878 (C-H), 1605 (C_{Ar}=C_{Ar}), 1512 (NO_2), 1358 (NO_2). MS (EI$^+$): 304 (M^+ 28%), 166

($C_8H_8NO_3^+$, 63%), 122 ($C_6H_4NO_2^+$, 100%). HRMS: 304.0698 requires 304.0695 $C_{14}H_{12}O_6N_2$. MP: 161 - 164 °C. Consistent with literature data.[433]

2-[2'-(2''-Aminophenoxy)ethoxy]-5-(benzyloxy)aniline **427**

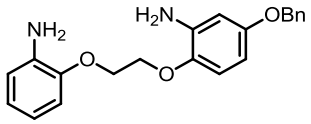

427

Dinitro compound **416** (100 mg, 0.24 mmol, 1.00 eq.) was dissolved in acetone (4.0 mL) and added to a stirring solution of NH_4HCO_2 (123 mg, 1.95 mmol, 8.13 eq.) in deionised water (1.0 mL). Iron filings (141 mg, 2.52 mmol, 10.5 eq.) were added and the reaction mixture was then stirred at 70 ˚C under argon for 17 h. The mixture was filtered through celite with acetone, then the solvent removed under reduced pressure. The residue was dissolved in DCM, then washed with brine and dried ($MgSO_4$), filtered and the solvent removed under reduced pressure, giving diamine **427** as a solid (52 mg, 61%). δ_H (400 MHz, $CDCl_3$): 7.44 - 7.34 (4H, m, H2''', H3''', H5''', H6''') 7.33 - 7.27 (1H, m, H4'''), 6.86 - 6.79 (2H, m, H4'', H6''), 6.77 (1H, d, *J* = 8.7 Hz, H6), 6.74 - 6.68 (2H, m, H3'', H5''), 6.39, (1H, d, *J* = 2.9 Hz, H3), 6.30 (1H, dd, *J* = 8.7, 2.9 Hz, H5), 4.98 (2H, s, OC**H$_2$**Ph), 4.35 - 4.27 (4H, m, OC**H$_2$**C**H$_2$**O), 3.83 (4H, s, N**H$_2$**). δ_C (100 MHz, $CDCl_3$): 154.37 (C), 146.26 (C), 140.85 (C), 138.24 (C), 137.47 (C), 136.89 (C), 128.52 (CH), 127.81 (CH), 127.43 (CH), 121.94 (CH), 118.38 (CH), 115.36 (CH), 114.31 (CH), 112.66 (CH), 103.46 (CH), 103.10 (CH), 70.43 (CH_2), 68.64 (CH_2), 67.64 (CH_2). IR (ATR cm^{-1}): 3454 (NH), 3433 (NH), 3367 (NH), 3350 (NH), 3063 (C_{Ar}-H), 3038 (C_{Ar}-H), 2959 (C-H), 2939 (C-H), 2886 (C-H), 1611 (C_{Ar}=C_{Ar}), 1601 (C_{Ar}=C_{Ar}), 1595 (C_{Ar}=C_{Ar}), 1207 (C-O). MS (EI^+): 350 ($M^{+\cdot}$, 70%), 241 (M^+ – $C_6H_4NH_2O$, 9), 215 ($C_{13}H_{13}NO_2^+$, 42), 214 ($C_{13}H_{14}NO_2^{+\cdot}$, 11), 136 ($C_8H_9NO^+$, 41), 91 ($C_7H_7^+$, 100). HRMS: 350.1629 requires 350.1630. MP: 146 ˚C.

Ethyl-2-N-(2''-{2'''-[4''''-(benzyloxy)-2''''-N,N-(2'''''-ethoxy-2'''''-oxoethyl)amino]phenoxy]ethoxy}phenyl)-N-(2'-ethoxy-2'-oxoethyl)amino]acetate **428**

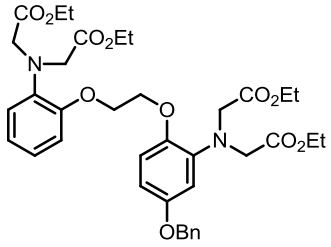

428

Aniline **427** (1.80 g, 5.14 mmol, 1.00 eq.) was dried by azeotrope twice in PhMe then combined under argon with NaI (2.12 g, 14.1 mmol, 2.75 eq., dried under vacuum at 100 ˚C for 6 h) and proton sponge (also dried by azeotrope in PhMe, 7.50 g, 35.0 mmol, 6.81 eq.) dry MeCN (10.0 mL) and ethyl bromoacetate (5.00 mL, 46.3 mmol, 9.01 eq.) were added to the stirring mixture which was then heated under reflux for 24 h. The solvent was then removed under reduced pressure and the residue was dissolved in PhMe and filtered. The filtrate was washed 5 times with dilute $HCl_{(aq)}$, then the organics were then combined and the solvent removed under vacuum. Crystallisation (Pet. ether/EtOAc) gave the diammine tetraester **428** (4.00 g, quant.) as needles. δ_H

(400 MHz, $CDCl_3$): 7.45 - 7.34 (4H, m, H2’’’’’, H3’’’’’, H5’’’’’, H6’’’’’) 7.33 - 7.28 (1H, m, H4’’’’’), 6.93 - 6.78 (4H, m, H3’’, H4’’, H5’’ H6’’), 6.76 (1H, d, *J* = 9.5 Hz, H6’’’’), 6.50 - 6.44 (2H, m, H3’’’’, H5’’’’), 4.97 (2H, s, OC**H$_2$**Ph), 4.23 (4H, s, OC**H$_2$**C**H$_2$**O), 4.16 (4H, s, NC**H$_2$**), 4.14 (4H, s, NC**H$_2$**), 4.055 (4H, q, *J* = 7.2 Hz, CO_2C**H**$_2$), 4.053 (4H, q, *J* = 7.2 Hz, CO_2C**H**$_2$), 1.16 (6H, t, *J* = 7.1 Hz, CH_2C**H**$_3$), 1.15 (6H, t, *J* = 7.1 Hz, CH_2C**H**$_3$). δ_C (100 MHz, $CDCl_3$): 171.60 (C), 171.42 (C), 153.61 (C), 150.32 (C), 144.73 (C), 140.58 (C), 139.36 (C), 137.22 (C), 128.53 (CH), 127.89 (CH), 127.53 (CH), 122.13 (CH), 121.40 (CH), 118.96 (CH), 114.43 (CH), 113.09 (CH), 107.22 (CH), 106.37 (CH), 70.45 (CH_2), 67.81 (CH_2), 67.11 (CH_2), 60.80 (CH_2), 60.75 (CH_2), 53.49 (CH_2), 53.44 (CH_2), 14.06 (CH_3), 14.03 (CH_3). IR (ATR cm^{-1}): 2986 (C-H), 2932 (C-H), 1736 (C=O), 1598 (C_{Ar}=C_{Ar}), 1512 (C_{Ar}=C_{Ar}). MS (NSI): 717 [(M+Na^+), 52%], 695 [(M+H)$^+$, 100],. HRMS: 695.3173. $C_{37}H_{47}O_{11}N_2$ requires 695.3180. MP: 96 - 97 °C.

Ethyl-2-[(2’’-{2’’’-[4’’’’-(benzyloxy)-2’’’’-[bis(2’’’’’-ethoxy-2’’’’’-oxoethyl)amino]5-formylphenoxy]ethoxy}phenyl)(2’-ethoxy-2’-oxoethyl)amino]acetate **429**

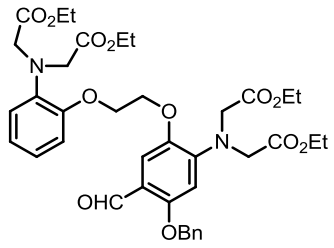

429

Tetraester **428** (1.02 g, 1.28 mmol, 1.00 eq.) was dried by azeotrope twice in PhMe then dissolved in dry DMF (62 mL) and stirred under argon at 0 ˚C. Dry pyridine (1.56 mL, 19.0 mmol, 14.8 eq.) was added followed by slow addition of $POCl_3$ (1.56 mL, 16.7 mmol, 13.4 eq.). After 30 min the reaction mixture was allowed to warm to RT, and the reaction was followed by TLC. After 1 h 10 min the mixture was quenched into cold 1 M $NaOH_{(aq)}$. After vacuum filtration the filtrate was extracted with PhMe (x 3), which was then removed under reduced pressure. The sample was dissolved in DCM and precipitated with hexane, the solid collected and the process repeated, giving aldehyde **429** (700 mg, 77%) as an amorphous solid. δ_H (400 MHz, $CDCl_3$): 10.31 (1H, s, CHO) 7.42 - 7.31 (5H, m, Ph), 7.29 (1H, s, H6’’’’), 6.93 - 6.79 (4H, m, H3’’, H4’’, H5’’ H6’’), 6.30 (1H, s, H3’’’’), 5.10 (2H, s, OC**H$_2$**Ph), 4.27 - 4.20 (4H, m, OC**H$_2$**C**H$_2$**O), 4.18 (4H, s, NC**H$_2$**), 4.14 (4H, s, NC**H$_2$**), 4.06 (4H, q, *J* = 7.1 Hz, CO_2C**H**$_2$), 4.03 (4H, q, *J* = 7.1 Hz, CO_2C**H**$_2$), 1.16 (6H, t, *J* = 7.2 Hz, CH_2C**H**$_3$), 1.14 (6H, t, *J* = 7.1 Hz, CH_2C**H**$_3$). δ_C (100 MHz, $CDCl_3$): 187.49 (CH), 171.51 (C), 170.7051 (C), 157.34 (C), 150.19 (C), 146.44 (C), 143.96 (C), 139.48 (C), 136.32 (C), 128.71 (CH), 128.24 (CH), 127.29 (CH), 122.10 (CH), 121.66 (CH), 119.10 (CH), 117.98 (C), 113.32 (CH), 110.62 (CH), 102.67 (CH), 71.10 (CH_2), 67.61 (CH_2), 66.90 (CH_2), 61.22 (CH_2), 60.76 (CH_2), 53.86 (CH_2), 53.50 (CH_2), 14.07 (CH_3), 14.02 (CH_3). IR (ATR cm^{-1}): 2975 (C-H), 2938 (C-H), 2928 (C-H), 2873 (C-H), 1745 (C=O), 1718 (C=O), 1662, 1598 (C_{Ar}=C_{Ar}), 1517 (C_{Ar}=C_{Ar}), 1508 (C_{Ar}=C_{Ar}). MS (NSI): 1462 [(2M+NH_4^+), 6%], 761 [(M+K^+), 3], 745 [(M+Na^+), 60], 740 [(M+NH_4^+), 45], 723 [(M+H^+), 100]. HRMS: 723.3121 requires 723.3129, $C_{38}H_{47}O_{12}N_2$. MP: 135 - 136 °C.

Ethyl-2-{[2''-(2'''-{2''''-[bis(2'''''-ethoxy-2'''''-oxoethyl)amino]-5''''-formyl-4''''-hydroxyphenoxy}ethoxy)phenyl](2'-ethoxy-2'-oxoethyl)amino}acetate **430**

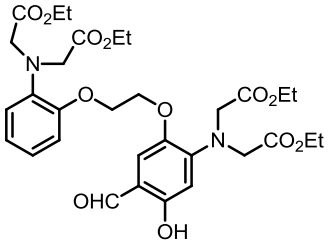

430

Aldehyde **429** (500 mg, 0.62 mmol, 1.00 eq.) was combined in acetic acid (6.0 mL) with palladium on carbon (10% loading by weight, 160 mg, 0.15 mmol, 0.24 eq.). After an initial 10 min flush with argon, the solution was frozen in $N_{2(l)}$ and the gas removed under vacuum. The mixture was then melted under $H_{2(g)}$, which was bubbled through the solution for 5 min. This procedure was repeated twice, then the mixture allowed to stir under $H_{2(g)}$ for 2 h 20 min. The mixture was then filtered through celite eluting with DCM then dried over ($MgSO_4$) filtered and the solvent removed under reduced pressure. Azeotrope with PhMe then removal of the solvent under reduced pressure was used to remove AcOH. This gave the desired phenol **430** (387 mg, 87%) as a solid. δ_H (400 MHz, $CDCl_3$): 11.21 (1H, s, PhO**H**), 9.61 (1H, s, CHO), 6.92 (1H, s, H6''''), 6.94 - 6.82 (4H, m, H3'', H4'', H5'' H6''), 6.15 (1H, s, H3''''), 4.23 (4H, s, O**CH_2CH_2**O), 4.22 (4H, s, N**CH_2**), 4.15 (4H, s, N**CH_2**), 4.08 (4H, q, *J* = 7.1 Hz, CO_2**CH_2**), 4.08 (4H, q, *J* = 7.1 Hz, CO_2**CH_2**), 1.19 (6H, t, *J* = 7.2 Hz, CH_2**CH_3**), 1.16 (6H, t, *J* = 7.2 Hz, CH_2**CH_3**). δ_C (100 MHz, $CDCl_3$): 193.22 (CH), 171.49 (C), 170.37 (C), 158.82 (C), 150.17 (C), 148.32 (C), 142.72 (C), 139.48 (C), 122.25 (CH), 121.78 (CH), 119.23 (CH), 115.90 (CH), 113.38 (CH), 113.06 (C), 104.22 (CH), 68.23 (CH_2), 66.92 (CH_2), 61.34 (CH_2), 60.78 (CH_2), 53.85 (CH_2), 53.48 (CH_2), 14.09 (CH_3), 13.97 (CH_3). IR (ATR cm^{-1}): 2977 (C_{Ar}-H), 2960 (C_{Ar}-H), 2937 (C_{Ar}-H), 2908 (C_{Ar}-H), 2877 (C_{Ar}-H), 1739 (CO), 1630 (CO), 1507 (C_{Ar}=C_{Ar}). MS (NSI): 671 [(M+K^+), 5%], 655 [(M+Na^+), 62], 650 [(M+NH_4^+), 22], 633 [(M+H^+), 100]. HRMS: 633.2652. $(M+H)^+$ $C_{31}H_{41}O_{12}N_2$ requires 633.2659. MP: 78 - 80 °C.

Ethyl-2-{[2''-(2'''-{2''''-[bis(2'''''-ethoxy-2'''''-oxoethyl)amino]-5''''-formyl-4''''-(prop-2''''''-en-1''''''-yloxy)phenoxy}ethoxy)phenyl](2'-ethoxy-2'-oxoethyl)amino}acetate **445**

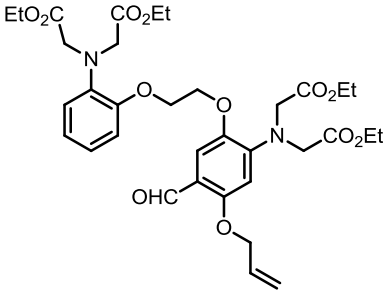

445

Phenol **430** (49 mg, 0.07 mmol, 1.0 eq.) was dried by azeotrope in PhMe and diluted in dry DMF(1.5 mL). This mixture was syringed into a dry vial containing a stirrer bar, K_2CO_3 (37 mg, 0.3 mmol, 3.7 eq.) and tetrabutylammonium bromide (2 mg, 6 µmol, 0.09 eq.), all of which had previously been dried by azeotrope in PhMe. The mixture was cooled with stirring to 0 ˚C under argon in the dark. Allyl bromide (10 µL, 0.11 mmol, 1.5 eq.) was added and the mixture warmed

to RT and allowed to stir for 48 h. The mixture was then filtered eluting with DCM and the filtrate was washed with water, saturated brine solution and then $NaHCO_{3(aq)}$ (saturated), and dried ($MgSO_4$). The mixture was filtered and the solvent removed under reduced pressure, to give phenol **445** impure (54 mg, estimate 44% purity from NMR). Data derived from the spectrum of the mixture. δ_H (400 MHz, $CDCl_3$): 10.30 (1H, s, C**H**O) 6.93 - 6.78 (5H, m, H3'', H4'', H5'', H6'', H6''''), 6.26 (1H, s, H3''''), 6.03 (1H, ddt, *J* = 17.3, 10.5, 5.2 Hz, $OCH_2C\mathbf{H}CH_2$), 5.41 [1H, dq, *J* = 17.3, 1.4 Hz, $CH_2CHCH_{(cis)}\mathbf{H}_{(trans)}$], 5.31 [1H, dq, *J* = 10.5, 1.4 Hz, $CH_2CHC\mathbf{H}_{(cis)}H_{(trans)}$], 4.56 (2H, dt, *J* = 5.2, 1.5 Hz), 4.23 - 4.19 (8H, m, $OC\mathbf{H}_2C\mathbf{H}_2O$, $NC\mathbf{H}_2$), 4.14 (4H, m, $NC\mathbf{H}_2$), 4.07 (4H, q, *J* = 7.2 Hz, $CO_2C\mathbf{H}_2CH_3$), 4.04 (4H, q, *J* = 7.2 Hz), 1.16 (6H, t, *J* = 7.2 Hz, $CH_2C\mathbf{H}_3$), 1.14(6H, t, *J* = 7.2 Hz, $CH_2C\mathbf{H}_3$). MS (NSI): 711 ([M+Na^+], 73%), 673 ([M+H^+], 100). HRMS: 673.2964 requires 673.2972, $C_{33}H_{45}O_{12}N_2$.

1,7-Diazoheptane **437**

437

1,7-dibromoheptane **436** (4.0 mL, 30 mmol, 1.0 eq.) and NaN_3 (11.4 g, 176 mmol, 5.87 eq.) were combined in deionised water (130 mL) and stirred at reflux under argon for 13 h 40 min. The desired product was then extracted into DCM. This solution was dried ($MgSO_4$), filtered, then the solvent removed under reduced pressure to give diazide **437** as an oil (4.5 g, 88%). δ_H (400 MHz, $CDCl_3$): 3.27 (4H, t, *J* = 6.9 Hz, $N_3C\mathbf{H}_2CH_2$), 1.65 - 1.56 (4H, m, $N_3CH_2C\mathbf{H}_2$), 1.45 - 1.31 (6H, m, $N_3CH_2CH_2C\mathbf{H}_2C\mathbf{H}_2C\mathbf{H}_2$). δ_C (400 MHz, $CDCl_3$): 51.41 (CH_2), 28.75 (CH_2), 28.70 (CH_2), 26.59 (CH_2). IR (ATR cm^{-1}): 2935 (C-H), 2876 (C-H), 2860 (C-H), 2091 (N_3), 1464, 1456. MS (APCI$^+$): 183 [(M+H)$^+$, 16%), 155 [(M – HN_2)$^+$, 100). HRMS: 183.1348. $C_7H_{15}N_6$ requires 183.1353. Consistent with literature data.[434]

7-Azidohept-1-amine **438**

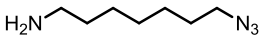

438

1,7-diazoheptane **437** (4.5 g, 20 mmol, 1.0 eq.) was dissolved in Et_2O (180 mL). Dilute $HCl_{(aq)}$ (1M, 135 mL) was added, followed by triphenylphosphine (6.0 g, 23 mmol, 1.1 eq.). The reaction mixture was then allowed to stir for 36 h at RT under argon, then the aqueous layer extracted with Et2O (100 mL, x 4) and DCM (100 mL, x 3), with $NaOH_{(aq)}$ (7 M) used to basify the aqueous between extractions. The organic layers were combined and dried ($MgSO_4$), then filtered and the solvent removed under reduced pressure to give amine **438** as an oil (2.98 g, 75%). δ_H (400 MHz, $CDCl_3$): 3.26 (2H, t, *J* = 6.9 Hz, $N_3C\mathbf{H}_2CH_2$), 2.69 (2H, t, *J* = 6.9 Hz, $H_2NC\mathbf{H}_2CH_2$), 1.66 - 1.54 (2H, m, $N_3CH_2C\mathbf{H}_2$), 1.50 - 1.26 (8H, m, 4 x $C\mathbf{H}_2$). δ_C (400 MHz, $CDCl_3$): 51.60 (CH_2), 42.35 (CH_2), 33.89 (CH_2), 28.93 (CH_2), 26.89 (CH_2), 26.84 (CH_2). IR (ATR cm^{-1}): 2928 (C-H), 2855 (C-H), 2093 (N_3), 1575, 1464, 1456. MS (APCI$^+$): 157 [(M+H)$^+$, 100%). HRMS: 157.1444. $C_7H_{17}N_4$ requires 157.1448.

1-Azido-7-isothiocyanatoheptane **439**

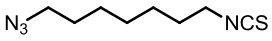

439

Azido compound **438** (2.8 g, 14 mmol, 1.0 eq.) and Ca_2CO_3 (2.9 g, 29 mmol, 2.1 eq.) were combined stirring under argon in DCM (62.2 mL) and deionised water (62.2 mL). Thiophosgene (1.6 mL, 22 mmol, 1.5 eq.) was then added slowly to the stirring mixture. After 1 h 30 min the reaction mixture was quenched into water, then extracted with DCM (100 mL, x 3), dried ($MgSO_4$), then filtered and the solvent removed under reduced pressure to give product **439** (88%). δ_H (400 MHz, $CDCl_3$): 3.52 (2H, t, *J* = 6.6 Hz, SCNC**H$_2$**CH_2), 3.27 (2H, t, *J* = 6.9 Hz, N_3C**H$_2$**CH_2), 1.76 - 1.66 (2H, m, $SCNCH_2$C**H$_2$**), 1.66 - 1.56 (2H, m, N_3CH_2C**H$_2$**), 1.50 - 1.31 (3 x C**H$_2$**, 6H). δ_C (400 MHz, $CDCl_3$): 204.39 (C), 51.38 (CH_2), 45.01 (CH_2), 29.85 (CH_2), 28.73 (CH_2), 28.38 (CH_2), 26.53 (CH_2), 26.46 (CH_2).

Methyl-2-{[(7-azidoheptyl)carbamothioyl]amino}acetate **440**

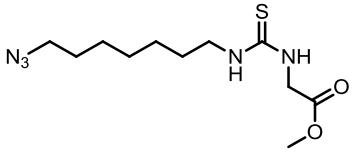

440

Isothiocyanate **439** (3.12 g, 15.8 mmol, 1.00 eq.) was combined in EtOAc (90 mL) with NEt3 (2.50 mL, 17.7, 1.12 eq.) and glycine methyl ester hydrochloride (2.22 g, 17.7 mmol, 1.12 eq.) and heated stirring under reflux and argon. The reaction mixture was partitioned between DCM and water and the organic layer washed with water and brine solution then dried ($MgSO_4$), filtered and the solvent removed under reduced pressure to give the product **440** (3.83 g, 85%), which was used without purification.

1-(7-Azidoheptyl)thiohydantoin **419**

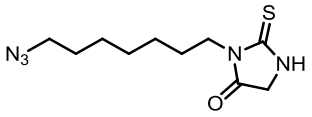

419

Carbamothioyl **440** (3.83 g, 14.7 mmol, 1.00 eq.) was refluxed stirring in a mixture of ethanol (190 mL) and 0.5 M $HCl_{(aq)}$ (25.9 mL) heated under argon. The solvent was then removed under reduced pressure and the mixture partitioned between DCM and water, then extracted with DCM (3 x 100 mL). The combined organics were dried ($MgSO_4$), then filtered and the solvent removed under reduced pressure. The material was then crystallised (Pet. ether/EtOAc) to give thiohydantoin **419** (2.58 g, 76%) as yellow needles. δ_H (400 MHz, $CDCl_3$): 4.06 (2H, d, *J* = 1.12 Hz, R(CO)NC**H$_2$**CO), 3.81 (2H, t, *J* = 7.54 Hz, (CS)RNC**H$_2$**), 3.26 (2H, t, *J* = 6.93 Hz, N_3C**H$_2$**CH_2), 1.75 - 1.54 (4H, m, N_3CH_2C**H$_2$**, $HNCH_2$C**H$_2$**), 1.44 - 1.28 (6H, m, other CH_2). δ_C (100 MHz, $CDCl_3$): 185.23 (C), 171.38 (C), 51.41 (CH_2), 48.30 (CH_2), 41.32 (CH_2), 28.73 (CH_2), 28.64 (CH_2), 27.40 (CH_2), 26.54 (CH_2). IR (ATR cm^{-1}): 1740 (CO), 3177 (NH), 2933 (C-H), 2854 (C-H), 2090 (N_3), 1538 (HNC), 1467, 1445 (CH_2), 1353 (HCN), 1273 (N_3). MS (Cl^+): 256 [$(M+H)^+$, 100%]. HRMS: 256.1236 requires 256.1232, $C_{10}H_{18}ON_5S$.MP: 66˚C

References

1. Nelson, D. L.; Cox, M. M. *Lehninger Principles of Biochemistry*; 6th ed.; W. H. Freeman and Company: New York, 2013; p. 505-510.

2. Harold, F. M. *The vital force: the study of bioenergetics*, 1st ed., New York, W. H. Freeman and Company, **1986**, Chapters 1 and 2.

3. Haynie, D. T. *Biological Thermodynamics*, 1st ed., Cambridge, Cambridge University Press. **2001**, p. 304-323.

4. Lodish, H.; Berk, A.; Kaiser, C.; Krieger, M.; Bretscher, A.; Ploeghe, H.; Amon, A.; Scott, M. P. *Molecular Cell Biology*; 7th ed.; W. H. Freeman and Company: New York, **2013**; p. 44.

5. Nelson, D. L.; Cox, M. M. *Lehninger Principles of Biochemistry*; 6th ed.; W. H. Freeman and Company: New York, **2013**; p. 21.

6. Nicholls, D. G., Ferguson, S. J., *Bioenergetics 3*, 3rd ed., Academic Press, **2002**, P. 31-55.

7. Demirel, Y.; Sandler, S. I. *Biophys. Chem.* **2002**, *97*, 87-111.

8. Schneider, E. D.; Kay, J. J. *Math. Comput. Model.,* **1994**, *19*, 25-48.

9. Eigen, M. *Die Naturwissenschaften* **1971**, *58*, 465–522.

10. Lodish, H.; Berk, A.; Kaiser, C.; Krieger, M.; Bretscher, A.; Ploeghe, H.; Amon, A.; Scott, M. P. *Molecular Cell Biology*; 7th ed.; W. H. Freeman and Company: New York, **2013**; p. 52.

11. Babloyantz, A. *Molecules, dynamics and life*, John Wiley and Sons, **1986**

12. Berg, J. M., Tymoczko, J. L., Stryer, L., *Biochemistry*, 7th edition, W. H. Freeman and Company, New York, **2013**

13. Cropped, ©Pearson Education limited, published as Prentice Hall

14. Accessed 14/4/2010, Slight variation on http://www.cartage.org.lb/en/themes/sciences/zoology/AnimalPhysiology/Anatomy/AnimalCellStructure/Mitochondria/mitochondria.jpg

15. Lane, N.; Martin, W. *Nature* **2010**, *467*, 929-934.

16. Alberts, B.; Bray, D.; Hopkin, K.; Johnson, A.; Lewis, J.; Raff, M.; Roberts, K.; Walter, P. *Essential Cell Biology*; 3rd.; Garland Science: New York and London, **2010**; p. 731.

17. Nelson, D. L.; Cox, M. M. *Lehninger Principles of Biochemistry*; 4th.; W. H. Freeman and Company: New York, **2005**; p. 1119.

18. Harvey, R. A.; Champe, P. C.; Ferrier, D. R. *Lippencott's Illustrated Reviews Biochemistry*; 3rd edition.; Lippincott Williams & Wilkins, **2005**; p. 534.

19. Wallace, D. C.; Fan, W.; Procaccio, V. *Annu. Rev. Pathol. Mech. Dis.,* **2010**, *5*, 297–348.

20. Alberts, B.; Johnson, A.; Lewis, J.; Raff, M.; Roberts, K.; Walter, P. *Molecular Biology of the cell*; 4th ed.; Garland Science: New York, **2002**.

21. Nelson, D. L.; Cox, M. M. *Lehninger Principles of Biochemistry*; 6th ed.; W. H. Freeman and Company: New York, **2013**; p. 544-558.

22. Murray, R. K.; Granner, D. K.; Mayes, P. A.; Rodwell, V. W. *Harper's Biochemistry*; 25th.; McGraw-Hill, **2000**; p. 927.

23. Accessed 2/09/2013, http://www.uic.edu/classes/bios/bios100/summer2003/resp-review.jpg

24. Devlin, T. M. *Textbook of Biochemistry with clinical corrolations*; 7th.; John Wiley & Sons, Inc, **2010**; p. 1240.

25. Reproduced with minor modifications with permission from: Moncada, S.; Erusalimsky, J. D. *Nat. Rev. Mol. Cell Bio.,* **2002**, *3*, 214–20.

26. Leys, D.; Scrutton, N. S. *Curr. Opin. Struct. Biol.,* **2004**, *14*, 642-647.

27. Akhmedov, D.; Braun, M.; Mataki, C.; Park, K.-S.; Pozzan, T.; Schoonjans, K.; Rorsman, P.; Wollheim, C. B.; Wiederkehr, A. *FASEB J.,* **2010**, *24*, 4613–26.

28. Boyer, P. D. *Annu. Rev. Biochem.* **1997**, *66*, 717-749.

29. Yoshida, M.; Muneyuki, E.; Hisabori, T. *Cell* **2001**, *2*, 669-677.

30. Walraven, H. S. V., Strotmann, H., Schwarz O., Rumberg, B., *FEBS Lett.*, **1996**, *379*, 309-313

31. Reprinted with minor modifications from *FEBS Lett.*, 587, Watanabe, R.; Noji, H, Chemomechanical coupling mechanism of *F*1-ATPase: Catalysis and torque generation, 1030-1035 Copyright **2013**, with permission from Elsevier

32. Wallace, D. C. *Nat. Rev. Cancer*, **2012**, *12*, 685-698.

33. Sivitz, W. I.; Yorek, M. A. *Antioxid. Redox. Sign.* **2010**, *12*, 537-577.

34. DiMauro S., Hirano M. MERRF. In: *GeneReviews* [Internet]. Pagon RA, Adam MP, Bird TD, et al., (editors), Seattle (WA): University of Washington, Seattle; **1993**-**2013**.

35. Halliwell, B.; Gutteridge, J. M. C. *Free Radicals in Biology and Medicine*; 3rd ed.; **1999**; p. 17.

36. Van Remmen, H.; Richardson, A, *Exp. Gerontol.,* **2001**, *36*, 957-68.

37. Sugamura, K.; Keaney, J. F. *Free Radical Bio. Med.,* **2011**, *51*, 978–92.

38. Imlay, J. *Annu. Rev. Microbiol.,* **2003**, *57*, 395-418.

39. Harman, D. *Ann. NY. Acad. Sci.*, **2006**, *1067*, 10-21.

40. Andrews, Z. B.; Diano, S.; Horvath, T. L. *Nature Rev. Neurosci*. **2005**, *6*, 829-40.

41. Rousset, S.; Alves-Guerra, M.; Mozo, J.; Miroux, B.; Cassard-Doulcier, A.; Bouillaud, F.; Ricquier, D. *Diabetes*. **2004**, *53*, S130-5.

42. Stout, A. K.; Raphael, H. M.; Kanterewicz, B. I.; Klann, E.; Reynolds, I. J. *Nat. Neurosci.* **1998**, *1*, 366-373.

43. Korshunov, S. S.; Skulachev, V. P.; Starkov, A. A. *FEBS Lett*. **1997**, *416*, 15-18.

44. Andrews, Z. B.; Horvath, B.; Barnstable, C. J.; Elsworth, J.; Elseworth, J.; Yang, L.; Beal, M. F.; Roth, R. H.; Matthews, R. T.; Horvath, T. L. *J. Neurosci*. **2005**, *25*, 184-91.

45. Tewari, B. B.; Mohan, D.; Kamaluddin *Colloid. Surface*. **1998**, *131*, 89-93.

46. Llopis, J.; McCaffery, J. M.; Miyawaki,A.; Farquhar, M. G.; Tsien, R. Y. *Proc. Natl. Acad. Sci*. **1998**, *95*, 6803-8.

47. Jeuken, L.; Bushby, R.; Evans, S. *Electrochem. Commun*. **2007**, *9*, 610-614.

48. Park, K.; Jo, I.; Pak, K.; Bae, S.; Rhim, H.; Suh, S.; Park, J.; Zhu, H.; So, I.; Kim, K. W.*: Eur. J. Physiol*. **2002**, *443*, 344-52.

49. Based on pictures from http://www.bmb.leeds.ac.uk/illingworth/oxphos/poisons.htm, accessed 27/4/10.

50. Lou, P.; Hansen, B. S.; Olsen, P. H.; Tullin, S.; Murphy, M. P.; Brand, M. D. *Biochem. J.*, **2007**, *407*, 129-40.

51. Parascandola, J. *Mol. Cell. Biochem*. **1974**, *5*, 69-77.

52. Berson, A.; Cazanave, S.; Tinel, M.; Grodet, A.; Wolf, C.; Pessayre, D. *Pharmacology* **2006**, *318*, 444–454.

53. Murphy, M. P., Smith, R. A. J., **2006**. *Annu. Rev. Pharmacol. Toxicol. 2007.*, *47*, 629-656.

54. Ross, M. F.; Kelso, G. F.; Blaikie, F. H.; James, a M.; Cochemé, H. M.; Filipovska, A; Da Ros, T.; Hurd, T. R.; Smith, R. A. J.; Murphy, M. P. *Biochemistry. Biokhimiia* **2005**, *70*, 222–30.
55. Flewelling, R. F. and Hubbell, W. L., *Biophys. J.,* 49(2), **1986**, 531-540.
56. Smith, R. A. J.; Hartley, R. C.; Murphy, M. P. *Antioxid. Redox. Sign.* **2011**, *15*, 3021-3038.
57. Adams, S. R.; Tsien, R. Y. *Annu. Rev. Physiol.* **1993**, *55*, 755–84.
58. Träger, J.; Härtner, S.; Heinzer, J.; Kim, H.; Hampp, N., *Chem. Phys. Lett*. **2008**, *455*, 307-310.
59. Li, Y.; Shi, J.; Cai, R.; Chen, X.; Guo, Q.; Liu, L. *Tetrahedron. Lett.* **2010**, *51*, 1609-1612.
60. Hartner, S., Kim, H. C..; Hampp, N., J. *Photochem. Photobiol*. *A*, **2007**, *187*, 242-246.
61. Modified from: Bley, F.; Schaper, K.; Görner, H., *Photochem. Photobiol*. **2008**, *84*, 162-71.
62. Mccray, J. A.; Trentham, D. R. *Annu. Rev. Biophys. Biophys. Chem*. **1989**, *18*, 239-270.
63. Kaplan, J. H.; Forbush, B.; Hoffman, J. F. *Biochemistry-US*. **1978**, *17*, 1929-35.
64. Du, L.; Zhang, S.; Wang, Y. *Tetrahedron*. *Lett.* **2005**, *46*, 3399-3402.
65. Conrad, P. G.; Givens, R. S.; Hellrung, B.; Rajesh, C. S.; Ramseier, M.; Wirz, J. *J. Am. Chem. Soc.* **2000**, *122*, 9346-9347.
66. Orth, R.; Sieber, S. A. *J. Org. Chem*. **2009**, *74*, 8476-9.
67. Givens, R. S.; Conrad, Peter G., I.; Yousef, A. L.; Lee, J.-I. In *CRC Handbook of Organic Photohemistry and Photobiology*; Horspool; W. M., L. F., Ed.; CRC Press, **2003**; Vol. 35, pp. 1-42.
68. Quin, C. PhD Thesis, University of Glasgow, **2009**
69. Asin-Cayuela, J.; Manas, A.-R. B.; James, A. M.; Smith, R. A. J.; Murphy, M. P. *FEBS lett.* **2004**, *571*, 9-16.
70. Betarbet, R.; Sherer, T. B.; Mackenzie, G.; Garcia-osuna, M.; Panov, A. V.; Greenamyre, J. T. *Nat. Neurosci.* **2000**, *3*, 1301-1306.
71. Chalmers, S.; Caldwell, S. T.; Quin, C.; Prime, T. A.; James, A. M.; Cairns, A. G.; Murphy, M. P.; Mccarron, J. G.; Hartley, R. C. *J. Am. Chem. Soc.* **2012**, *134*, 758-761.
72. Scaduto, R. C.; Grotyohann, L. W. *Biophys. J.* **1999**, *76*, 469-477.
73. Veal, E. A.; Day, A. M.; Morgan, B. A. *Mol. Cell.* **2007**, *26*, 1–14.
74. Yang, Y.; Zhao, Q.; Feng, W.; Li, F. *Chem. Rev.* **2013**, *113*, 192–270.
75. Workman, P.; Collins, I. *Chem. Biol.* **2010**, *17*, 561–577.
76. Bunnage, M. E.; Chekler, E. L. P.; Jones, L. H. *Nat. Chem. Biol.* **2013**, *9*, 195–199.
77. Zhang, J.; Campbell, R. E.; Ting, A. Y.; Tsien, R. Y. *Nat. Rev. Mol. Cell. Bio.* **2002**, *3*, 906–18.
78. Chan, J.; Dodani, S. C.; Chang, C. J. *Nature Chemistry* **2012**, *4*, 973–984.
79. Lin, W.; Buccella, D.; Lippard, S. J. *J. Am. Chem. Soc.* **2013**, 135, 13512-13520
80. Lichtman, J. W.; Conchello, J. *Nat. Methods* **2005**, *12*, 910–919.
81. Zhang, X.; Xiao, Y.; Qian, X. *Angew. Chem. Int. Ed.* **2008**, *47*, 8025-9.
82. Ju, J.; Ruan, C.; Fuller, C. W.; Glazer, A. N.; Mathies, R. A. *Proc. Natl. Acad. Sci.* **1995**, *92*, 4347-4351.
83. Sapsford, K. E.; Berti, L.; Medintz, I. L. *Angew. Chem. Int. Ed.* **2006**, *45*, 4562–4588.
84. Thomas, D.; Tovey, S. C.; Collins, T. J.; Bootman, M. D.; Berridge, M. J.; Lipp, P. *Cell Calcium* **2000**, *28*, 213–223.
85. Paredes, R. M.; Etzler, J. C.; Watts, L. T.; Zheng, W.; Lechleiter, J. D. *Methods* **2008**, *46*, 143–151.

86. Llinas, R.; Sugimori, M.; Silver, R. B. *Science* **1992**, *256*, 677–679.
87. Griffin, B. A.; Adams, S. R.; Tsien, R. Y. *Science* **1998**, *281*, 269–272.
88. Tour, O.; Adams, S. R.; Kerr, R. A.; Meijer, R. M.; Sejnowski, T. J.; Tsien, R. W.; Tsien, R. Y. *Nat. Chem. Biol.* **2007**, *3*, 423–431.
89. Levy, L. A.; Murphy, E.; Raju, B.; London, R. E. *Biochemistry* **1988**, *27*, 4041–4048.
90. Ko, S.-K.; Yang, Y.-K.; Tae, J.; Shin, I. *J. Am. Chem. Soc.* **2006**, *128*, 14150–5.
91. Guo, Z.; Zhu, W.; Zhu, M.; Wu, X.; Tian, H. *Chem. Eur. J.* **2010**, *16*, 14424–14432.
92. Sawaki, Y.; Foote, C. S. *J. Am. Chem. Soc.* **1979**, *101*, 6292–6296.
93. Abo, M.; Urano, Y.; Hanaoka, K.; Terai, T.; Komatsu, T.; Nagano, T. *J. Am. Chem. Soc.* **2011**, *133*, 10629–10637.
94. de Silva, A. P.; Gunaratne, H. Q. N.; Gunnlaugsson, T.; Huxley, A. J. M.; McCoy, C. P.; Rademacher, J. T.; Rice, T. E. *Chem. Rev.* **1997**, *97*, 1515–1566.
95. Cochemé, H. M.; Quin, C.; McQuaker, S. J.; Cabreiro, F.; Logan, A.; Prime, T. a; Abakumova, I.; Patel, J. V; Fearnley, I. M.; James, A. M.; Porteous, C. M.; Smith, R. a J.; Saeed, S.; Carré, J. E.; Singer, M.; Gems, D.; Hartley, R. C.; Partridge, L.; Murphy, M. P. *Cell metab.* **2011**, *13*, 340–50.
96. Dickinson, B. C.; Chang, C. J. *J. Am. Chem. Soc.* **2008**, *130*, 9638–9639.
97. Wardman, P. *Free Radical Biol. Med.* **2007**, *43*, 995-1022.
98. Murphy, M. P.; Holmgren, A.; Larsson, N.-G.; Halliwell, B.; Chang, C. J.; Kalyanaraman, B.; Rhee, S. G.; Thornalley, P. J.; Partridge, L.; Gems, D.; Nyström, T.; Belousov, V.; Schumacker, P. T.; Winterbourn, C. C. *Cell metabolism* **2011**, *13*, 361-6.
99. Stone, J. R.; Yang, S. *Antioxid. Redox. Sign.* **2006**, *8*, 243-270.
100. Valko, M.; Rhodes, C. J.; Moncol, J.; Izakovic, M.; Mazur, M. *Chem. Biol. Interact.* **2006**, *160*, 1–40.
101. Murphy, M. P. *Biochem. J.* **2009**, *417*, 1-13.
102. Balaban, R. S.; Nemoto, S.; Finkel, T. *Cell* **2005**, *120*, 483–95.
103. Reprinted with modifications from Free Radical Biology and Medicine, 52, Cardoso, A. R.; Chausse, B.; Fernanda, M.; Lue, L. A.; Marazzi, T. B. M.; Pessoa, P. S.; Queliconi, B. B.; Kowaltowski, A., Mitochondrial compartmentalisation of redox processes, 2201-2208, **2012**, with permission from Elsevier
104. Lagouge, M.; Larsson, N. *J. Intern. Med.* **2013**, *273*, 529–543.
105. Sies, H. *Eur. J. Biochem.* **1993**, *215*, 213–9.
106. Gutowski, M.; Kowalczyk, S. *Acta Biochim. Pol.* **2013**, *60*, 1–16.
107. Miller, D. M.; Buettner, G. R.; Aust, S. D. *Free Rad. Biol. Med.* **1990**, *8*, 95–108.
108. Cardoso, A. R.; Chausse, B.; Fernanda, M.; Lue, L. A.; Marazzi, T. B. M.; Pessoa, P. S.; Queliconi, B. B.; Kowaltowski, A. J. *Free Rad. Biol. Med.* **2012**, *52*, 2201–2208.
109. Brand, M. D. *Exp. Gerontol.* **2010**, *45*, 466–472.
110. Figueira, T. R.; Barros, M. H.; Camargo, A. a; Castilho, R. F.; Ferreira, J. C. B.; Kowaltowski, A. J.; Sluse, F. E.; Souza-Pinto, N. C.; Vercesi, A. E. *Antioxid. Redox. Sign.* **2013**, *18*, 2029–74.
111. Reproduced from Experimental gerontology, 45, Brand, M. D., 466–472, **2010** with permission from Elsevier
112. Hirst, J. *Annu. Rev. Biochem.* **2012**, *82*, 551–575.

113. Pryde, K. R.; Hirst, J. *J. Biol. Chem.* **2011**, *286*, 18056–18065.
114. Sena, L. A; Chandel, N. S. *Mol. Cell* **2012**, *48*, 158–67.
115. Bolisetty, S.; Jaimes, E. A *Int. J. Mol. Sci.,* **2013**, *14*, 6306–44.
116. Szabó, C.; Ischiropoulos, H.; Radi, R. *Nat. Rev. Drug. Discov.* **2007**, *6*, 662–80.
117. Giorgio, M.; Migliaccio, E.; Orsini, F.; Paolucci, D.; Moroni, M.; Contursi, C.; Pelliccia, G.; Luzi, L.; Minucci, S.; Marcaccio, M.; Pinton, P.; Rizzuto, R.; Bernardi, P.; Paolucci, F.; Pelicci, P. G. *Cell* **2005**, *122*, 221–33.
118. Rhee, S.; Yang, K.; Kang, S. W. *Antioxid. Redox. Sign.* **2005**, *7*, 619–626.
119. Cantu, D.; Schaack, J.; Patel, M. *PloS one* **2009**, *4*, e7095.
120. Tarpey, M. M.; Fridovich, I. *Circ. Res.* **2001**, *89*, 224–236.
121. Li, X.; Gao, X.; Shi, W.; Ma, H. *Chem. Rev.* **2013**. (in press)
122. Kundu, K.; Knight, S. F.; Willett, N.; Lee, S.; Taylor, W. R.; Murthy, N. *Angew. Chem. Int. Ed.* **2009**, *48*, 299–303.
123. Sekiya, M.; Umezawa, K.; Sato, A.; Citterio, D.; Suzuki, K. *Chem. Commun.,* **2009**, 3047–9.
124. Teranishi, K.; Hisamatsu, M.; Yamada, T. *Luminescence* **1999**, *14*, 297–302.
125. Macgregor, J. T.; Johnson, I. J. *Mutat. Res.* **1977**, *48*, 103–108.
126. Bucana, C.; Saiki, I.; Nayar, R. *J. Histochem. Cytochem.* **1986**, *34*, 1109–1115.
127. Rothe, G.; Valet, G. *J. Leukocyte Biol.* **1990**, *47*, 440–448.
128. Zhao, H.; Kalivendi, S.; Zhang, H.; Joseph, J.; Nithipatikom, K.; Vásquez-Vivar, J.; Kalyanaraman, B. *Free Radical Bio. Med.* **2003**, *34*, 1359–1368.
129. Zhao, H.; Joseph, J.; Fales, H. M.; Sokoloski, E. A.; Levine, R. L.; Vasquez-vivar, J.; Kalyanaraman, B. *Proc. Natl Acad. Sci. USA* **2005**, *102*, 5727-5732.
130. Zielonka, J.; Zhao, H.; Xu, Y.; Kalyanaraman, B. *Free Radical Bio. Med.* **2005**, *39*, 853–63.
131. Zielonka, J.; Sarna, T.; Roberts, J. E.; Wishart, J. F.; Kalyanaraman, B. *Arch. Biochem. Biophys.* **2006**, *456*, 39–47.
132. Zielonka, J.; Kalyanaraman, B. *Free Radical Bio. Med.* **2010**, *48*, 983–1001.
133. Kalyanaraman, B. *Biochem. Soc. T.* **2011**, *39*, 1221–1225.
134. Kalyanaraman, B.; Dranka, B. P.; Hardy, M.; Michalski, R.; Zielonka, J. *Biochim. Biophys. Acta.* **2013** (in press).
135. Meany, D. L.; Thompson, L.; Arriaga, E. A *Anal. Chem.* **2007**, *79*, 4588–94.
136. Robinson, K. M.; Janes, M. S.; Pehar, M.; Monette, J. S.; Ross, M. F.; Hagen, T. M.; Murphy, M. P.; Beckman, J. S. *Proc. Natl. Acad. Sci. USA* **2006**, *103*, 15038–15043.
137. Robinson, K. M.; Janes, M. S.; Beckman, J. S. *Nat. Protoc.* **2008**, *3*, 941–7.
138. Watkins, T. I. *J. Chem. Soc.* **1958**, 1443–1450.
139. Huber, R.; Amann, N.; Wagenknecht, H.-A. *J. Org. Chem.* **2004**, *69*, 744–51.
140. Tjarks, W.; Ghaneolhosseini, H.; Henssen, C. L. A.; Malmquist, J.; Sjberg, S. *Tetrahedron Lett.* **1996**, *37*, 6905–6908.
141. Ross, S. A.; Pitié, M.; Meunier, B. *J. Chem. Soc., Perkin Trans. 1* **2000**, 571–574.
142. Lee, M.-R.; Shin, I. *Angew. Chem. Int. Ed.* **2005**, *44*, 2881–4.
143. Lion, C.; Boukou-Poba, J. P.; Charvy, C. *Bull. Soc. Chim. Belg.* **1990**, *99*, 171–181.
144. Tobisu, M.; Koh, K.; Furukawa, T.; Chatani, N. *Angew. Chem. Int. Ed.* **2012**, *51*, 11363–11366.

145. Gilman, H.; Nelson, R. D. *J. Am. Chem. Soc.* **1948**, *70*, 3316–3318.
146. Tobisu, M.; Hyodo, I.; Chatani, N. *J. Am. Chem. Soc.* **2009**, *131*, 12070–12071.
147. Diaba, F.; Lewis, I.; Grignon-Dubois, M.; Navarre, S. *J. Org. Chem.* **1996**, *61*, 4830–4832.
148. Parenty, A. D. C.; Smith, L. V; Pickering, A. L.; Long, D.; Cronin, L. *J. Org. Chem.* **2004**, 69, 5934–5946.
149. Heald, R. A.; Stevens, M. F. G. *Org. Biomol. Chem.* **2003**, *1*, 3377–89.
150. Liang, Z.; Ju, L.; Xie, Y.; Huang, L.; Zhang, Y. *Chem. Eur. J.* **2012**, *18*, 15816–15821.
151. Liu, Y.; Song, R.; Wu, C.; Gong, L.; Hu, M. *Adv. Synth. Catal.* **2012**, 347–353.
152. Intrieri, D.; Mariani, M.; Caselli, A.; Ragaini, F.; Gallo, E. *Chem. Eur. J.* **2012**, *18*, 10487–10490.
153. Blanchot, M.; Candito, D. A.; Larnaud, F.; Lautens, M. *Org. Lett.* **2011**, *13*, 1486–1489.
154. Mcburney, R. T.; Walton, J. C. *J. Am. Chem. Soc.* **2013**, *135*, 7349–7354.
155. Krane, B. D.; Fagbule, M. O. .; Shamma, M. *J. Nat. Prod.* **1984**, *47*, 1–43.
156. Suchomelová, J.; Bochoráková, H.; Paulová, H.; Musil, P.; Táborská, E. *J. Pharmaceut. Biomed.* **2007**, *44*, 283–7.
157. Tane, P.; Wabo, H. K.; Connolly, J. D. *Fitoterapia* **2005**, *76*, 656–60.
158. Gillespie, J. P.; Amoros, L. G.; Stermitz, F. R. *J. Org. Chem.* **1974**, *39*, 3239-3241.
159. Prado, S.; Michel, S.; Tillequin, F.; Koch, M.; Pfeiffer, B.; Pierré, A.; Léonce, S.; Colson, P.; Baldeyrou, B.; Lansiaux, A.; Bailly, C. *Bioorg. Med. Chem.* **2004**, *12*, 3943-53.
160. Stermitz, F. R.; Gillespie, J. P.; Amoros, L. G.; Romero, R.; Stermitz, T. A.; Larson, K. A.; Earl, S.; Ogg, J. E. *J. Med. Chem.* **1975**, *18*, 708–713.
161. Kessar, S. V.; Gupta, Y. P.; Balakrishnan, P.; Sawal, K. K.; Mohammad, T.; Dutt, M. *J. Org. Chem.* **1988**, *53*, 1708–1713.
162. Kessar, S. V. *Proc. Indian Acad. Sci.* **1988**, *100*, 217–222.
163. Kessar, S. V.; Gopal, R.; Singh, M. *Tetrahedron* **1973**, *29*, 167–175.
164. Nakanishi, T.; Suzuki, M.; Mashiba, A.; Ishikawa, K. *J. Org. Chem.* **1998**, *63*, 4235–4239.
165. Peng, J.; Chen, T.; Chen, C.; Li, B. *J. Org. Chem.* **2011**, *76*, 9507–9513.
166. Takeda, D.; Hirano, K.; Satoh, T.; Miura, M. *Heterocycles* **2012**, *86*, 487–496.
167. Nakanishi, T.; Masuda, A.; Suwa, M.; Akiyama, Y.; Hoshino-abe, N. *Bioorg. Med. Chem. Lett.* **2000**, *10*, 2321–2323.
168. Kitson, P. J.; Parenty, A. D. C.; Richmond, C. J.; Long, D.; Cronin, L. *Chem. Comm.* **2009**, 4067–4069.
169. Evan's pKa table, http://evans.harvard.edu/pdf/evans_pka_table.pdf, accessed 19/09/2013
170. Chen, J.; Li, K.; Yang, D. *Org. Lett.* **2011**, *13*, 1658-1661.
171. Kallikat, J.; Bombrun, A.; Alagarsamy, P.; Jothi, A. *Tetrahedron Lett.* **2012**, *53*, 6280–6287.
172. Barluenga, J.; Fananas-mastral, M.; Aznar, F.; Valdes, C. *Angew. Chem. Int. Ed.* **2008**, *47*, 6594–6597.
173. Susan MacIntyre, Undergraduate Thesis, University of Glasgow, **2011**
174. Duan, X.-F.; Zeng, J.; Zhang, Z.-B.; Zi, G.-F. *J. Org. Chem.* **2007**, *72*, 10283-10286.
175. Wipf, P.; Maciejewski, J. P. *Organic Lett.* **2008**, *10*, 4383-6.
176. Amann, N.; Huber, R.; Wagenknecht, H.-A. *Angew. Chem. Int. Ed.* **2004**, *43*, 1845-1847.
177. Salomon, M. F.; Salomon, R. G. *J. Am. Chem. Soc.* **1979**, *101*, 4290-4299.
178. Smith, R. A. J., personal communication, **2011**.

179. Watanabe, M.; Soai, K. *J. Chem. Soc. Perk. T1* **1994**, 837.
180. Luedtke, N. W.; Liu, Q.; Tor, Y. *Chem. Eur. J.* **2005**, *11*, 495-508.
181. Seyden-Penne, J. *Reductions by the Alumino and Borohydrides in Organic Synthesis*; 2nd ed.; Wiley-VCH Verlag GmbH & Co. KGaA, **1997**; p. 18.
182. Carey, F. A.; Sundberg, R. J. *Advanced Organic Chemistry: Part B: Reaction and Synthesis*; 5th ed.; Springer Science, **2007**; p. 399.
183. Renslo, A. R.; Gao, H.; Jaishankar, P.; Venkatachalam, R.; Gordeev, M. F. *Org. Lett.* **2005**, *7*, 2627-2630.
184. Sotomayor, N.; Domínguez, E.; Lete, E. *J. Org. Chem.* **1996**, *61*, 4062-4072.
185. Tsang, W. C. P.; Munday, R. H.; Brasche, G.; Zheng, N.; Buchwald, S. L. *J. Org. Chem.* **2008**, *73*, 7603-10.
186. Iranpoor, N.; Firouzabadi, H.; Nowrouzi, N.; Khalili, D. *Tetrahedron* **2009**, *65*, 3893-3899.
187. Ayyangar, N. R.; Choudhary, A R.; Kalkote, U. R.; Natu, A. A. *Synthetic commun.* **1988**, *18*, 2011-2016.
188. Kazemi, F.; Kiasat, A. R.; Mombiani, B. *Synthetic commun.* **2007**, *37*, 3219-3223.
189. Brown, H. C.; Stocky, T. P. *J. Am. Chem. Soc.* **1977**, *99*, 8218-8226.
190. http://www.ch.imperial.ac.uk/rzepa/blog/?p=2902; Henry Rzepa, Anatomy of an arrow pushing tutorial: reducing a carboxylic acid; accessed 10/8/2013
191. Paquette, L. A. *Encyclopedia of Organic Reagents*; John Wiley & Sons, Inc, **1995**; p. 641.
192. Orelli, L. R.; Salerno, A.; Hedrera, M. E.; Perillo, I. A. *Synthetic commun.* **1998**, *28*, 1625-1639.
193. Youn, S. W.; Bihn, J. H. *Tetrahedron Lett.* **2009**, *50*, 4598-4601.
194. Mitchell, E. A.; Baird, M. C. *Organometallics* **2007**, *26*, 5230-5238.
195. Senn, H. M.; Ziegler, T. *Organometallics* **2004**, *23*, 2980-2988.
196. Ariafard, A.; Lin, Z. *Organometallics* **2006**, *25*, 4030-4033.
197. Alvarez, R.; Faza, O. N.; Lopez, C. S.; de Lera, A. R. *Org. Lett.* **2006**, *8*, 35-38.
198. Aliprantis, A. O.; Canary, J. W. *J. Am. Chem. Soc.* **1994**, *116*, 6985-6986.
199. Adamo, C.; Amatore, C.; Ciofini, I.; Jutand, A.; Lakmini, H. *J. Am. Chem. Soc.* **2006**, *128*, 6829-6836.
200. Xue, L.; Lin, Z. *Chemical Soc. Rev.* **2010**, *39*, 1692-1705.
201. Amatore, C.; Duc, G. L. L.; Jutand, A. *Chem. Eur. J.* **2013** *19*, 10082-10093.
202. Amatore, C.; Jutand, A.; Duc, L. **2011**, *17*, 2492-2503.
203. Amatore, C.; Jutand, A.; Duc, L. *Chem. Eur. J.* **2012**, *18*, 6616-6625.
204. Carrow, B. P.; Hartwig, J. F. *J. Am. Chem. Soc.* **2011**, *133*, 2116-2119.
205. Braga, A. A. C.; Morgon, N. H.; Ujaque, G. *J. Organomet. Chem.* **2006**, *691*, 4459-4466.
206. Amatore, C.; Jutand, A. *Acc. Chem. Res.* **2000**, *33*, 314–21.
207. Giovannini, R.; Knochel, P. *J. Am. Chem. Soc.* **1998**, *120*, 11186-11187.
208. Shekhar, S.; Hartwig, J. F. *J. Am. Chem. Soc. Society* **2004**, *126*, 13016-13027.
209. Hartwig, J. F. *Inorg. Chem.* **2007**, *46*, 1936-1947.
210. Yin, J.; Rainka, M. P.; Zhang, X.-xiang; Buchwald, S. L. *J. Am. Chem. Soc.* **2002**, *124*, 1162-1163.
211. Christmann, U.; Vilar, R. *Angew. Chem. Int. Ed.* **2005**, *44*, 366 -374.
212. Barrios-Landeros, F.; Carrow, B. P.; Hartwig, J. F. *J. Am. Chem. Soc.* **2009**, *131*, 8141-8154.

213. Molander, G. A.; Canturk, B. *Angew. Chem. Int. Ed.* **2009**, *48*, 9240-9261.
214. Martin, R.; Buchwald, S. L. *Accounts Chem. Res.* **2008**, *41*, 1461-73.
215. Barrios-landeros, F.; Hartwig, J. F. *J. Am. Chem. Soc. Society* **2005**, *127*, 6944-6945.
216. Ahlquist, M.; Fristrup, P.; Tanner, D.; Norrby, P.-O. *Organometallics* **2006**, *25*, 2066-2073.
217. Galardon, E.; Ramdeehul, S.; Brown, J. M.; Cowley, A.; Hii, K. K. M..; Jutand, A. *Angew. Chem. Int. Ed.* **2002**, *41*, 1760-1763.
218. Farina, V. *Adv.Synth. Catal.* **2004**, *346*, 1553-1582.
219. Barder, T. E.; Buchwald, S. L. *J. Am. Chem. Soc.* **2007**, *129*, 12003-12010.
220. Perez-Rodrıguez, M.; Braga, A. A. C.; Garcia-Melchor, M.; Perez-Temprano, M. H.; Casares, J. A.; Ujaque, G.; de Lera, A. R.; Lvarez, R. A.; Maseras, F.; Espinet, P. *J. Am. Chem. Soc.* **2009**, *131*, 3650-3657.
221. Ananikov, V. P.; Musaev, D. G.; Morokuma, K. *Eur. J. Inorg. Chem.* **2007**, *2007*, 5390-5399.
222. Kantchev, E. A. B.; O'Brien, C. J.; Organ, M. G. *Angew. Chem. Int. Ed.* **2007**, *46*, 2768-2813.
223. Boehme, C.; Frenking, G. *J. Am. Chem. Soc.* **1996**, *118*, 2039-2046.
224. Heinemann, C.; Mu, T.; Apeloig, Y. *J. Am. Chem. Soc.* **1996**, *118*, 2023-2038.
225. Bourissou, D.; Guerret, O.; Gabbaı, P.; Bertrand, G. *Chem. Rev.* **2000**, *100*, 39-92.
226. Reprinted from Coordination Chemistry Reviews, 253, Jacobsen, H.; Correa, A.; Poater, A.; Costabile, C.; Cavallo, L.; Understanding the M(NHC) (NHC=N-heterocyclic carbene) bond, 687-703, Copyright **2009**, with permission from Elsevier.
227. Jacobsen, H.; Correa, A.; Poater, A.; Costabile, C.; Cavallo, L. *Coord. Chem. Rev* **2009**, *253*, 687–703.
228. Nasielski, J.; Hadei, N.; Achonduh, G.; Kantchev, A. B.; Brien, C. J. O.; Lough, A.; Organ, M. G. *Chem. Eur. J.* **2010**, *16*, 10844-10853.
229. Organ, M. G.; Chass, G. A.; Fang, D.-C.; Hopkinson, A. C.; Valentea, C. *Synthesis* **2008**, *17*, 2776-2797.
230. Birkholz, M.-N.; Feirxa, Z.; Leeuwen, P. W. N. M. van *Chem. Soc. Rev.* **2009**, *38*, 1099-1118.
231. Fortman, G. C.; Nolan, S. P. *Chem. Soc. Rev.* **2011**, *40*, 5151-5169.
232. Billingsley, K. L.; Barder, T. E.; Buchwald, S. L. *Angew. Chem. Int. Ed.* **2007**, *46*, 5359-5363.
233. Molander, G. A.; Trice, S. L. J.; Kennedy, S. M.; Dreher, S. D.; Tudge, M. T. *J. Am. Chem. Soc.* **2012**, *134*, 11667–11673.
234. Applequist, D. E.; O'Brien, D. F. *J. Am. Chem. Soc.* **1963**, *85*, 743-748.
235. Bailey, W. F.; Patricia, J. J. *Journal of Organometallic Chemistry* **1988**, *352*, 1-46.
236. Ott, H.; Daschlein, C.; Leusser, D.; Schildbach, D.; Seibel, T.; Stalke, D.; Strohmann, C. *J. Am. Chem. Soc.* **2008**, *130*, 11901-11911.
237. Gessner, V. H.; Däschlein, C.; Strohmann, C. *Chem. Eur. J.* **2009**, *15*, 3320-3334.
238. Kottke, T.; Stalke, D. *Angew. Chem. Int. Ed.* **1992**, *32*, 580-582.
239. Jones, A. C.; Sanders, A. W.; Bevan, M. J.; Reich, H. J. *J. Am. Chem. Soc.* **2007**, *129*, 3492-3493.
240. Fisher, H. *J. Phys. Chem.-US* **1969**, *73*, 3834.
241. Ward, H. R. *J. Am. Chem. Soc.* **1967**, *89*, 5517-5518.
242. Bryce-Smith, D. *Journal of the Chemical Society* **1956**, 1603-1610.
243. Ashby, E. C.; Pham, T. N. *J. Org. Chem.* **1987**, 1291-1300.

244. Farnham, W. B.; Calabrese, J. C. *J. Am. Chem. Soc.* **1986**, *108*, 2451-2453.
245. Winkler, H. J. S.; Winkler, H. *J. Am. Chem. Soc.* **1966**, *88*, 964-969.
246. Winkler, H. J. S.; Winkler, H. *J. Am. Chem. Soc.* **1966**, *88*, 969-974.
247. Reich, H. J.; Phillips, N. H.; Reich, I. L. *J. Am. Chem. Soc.* **1985**, *107*, 4101-4103.
248. Bailey, W. F.; Carson, M. W. *J. Org. Chem.* **1998**, *63*, 9960-9967.
249. Lamrani, M.; Hamasaki, R.; Yamamoto, Y. *Tetrahedron Lett.* **2000**, *41*, 2499-2501.
250. Smith, M. B.; March, J. *March's Advanced Organic Chemistry*; 6th ed.; Wiley, **2007**; pp. 354-366.
251. Schulze, V.; Brönstrup, M.; Böhm, V. P. W.; Schwerdtfeger, P.; Schimeczek, M.; Hoffmann, R. W. *Angew. Chem. Int. Ed.* **1998**, *37*, 824-826.
252. Muller, M.; Bronstrup, M.; Knopff, O.; Schulze, V.; Hoffmann, R. W. *Organometallics* **2003**, *22*, 2931-2937.
253. Hoffmann, R. W.; Bronstrup, M.; Muller, M. *Org. Lett.* **2003**, *5*, 313-316.
254. Krasovskiy, A.; Straub, B. F.; Knochel, P. *Angew. Chem. Int. Ed.* **2006**, *45*, 159-162.
255. Sapountzis, I.; Dube, H.; Lewis, R.; Gommermann, N.; Knochel, P. *J. Org. Chem.* **2005**, *70*, 2445-54.
256. Petro, A. J.; Snyth, C. P.; Brooker, L. G. S. *J. Am. Chem. Soc.* **1956**, *78*, 3043-3048.
257. Zhao, B.; Lu, X. *Org. Lett.* **2006**, *8*, 5987-5990.
258. Zhang, X.; Han, J.-B; Li, P.-F; Ji, X. *Synthetic commun.* **2009**, *39*, 3804-3815.
259. Liu, T.-P; Liao, Y.-xi; Xing, C.-hui; Hu, Q.-S. *Org. Lett.* **2011**, *13*, 2452–2455.
260. Engle, K. M.; Wang, D.-hui; Yu, J.-quan *J. Am. Chem. Soc.* **2010**, *132*, 14137-14151.
261. Ackermann, L.; Vicente, R.; Kapdi, A. R. *Angew. Chem. Int. Ed.* **2009**, *48*, 9792-9826.
262. Campeau, L.-C.; Parisien, M.; Jean, A.; Fagnou, K. *J. Am. Chem. Soc.* **2006**, *128*, 581-90.
263. Packard, G. K.; Hu, Y.; Vescovi, A.; Rychnovsky, S. D. *Angew. Chem. Int. Ed.* **2004**, *43*, 2822-6.
264. M.; Hermansson, M.; Dong, H.; Ramström, O. *Eur. J. Org. Chem.* 2006, 4323-4326.
265. Rychnovsky, S. D.; Vaidyanathan, R. *J. Org. Chem.* **1999**, *64*, 310-312.
266. Jiang, N.; Ragauskas, A. J. *Org. Lett.* **2005**, *7*, 3689-3692.
267. Anelli, P. L.; Biffi, C.; Montanari, F.; Quici, S. *J. Org. Chem.* **1987**, *52*, 2559-2562.
268. Vogler, T..; Studer, A. *Synthesis* **2008**, *13*, 1979-1993.
269. Wolf, C.; Liu, S.; Reinhardt, B. C. *Chem. Comm.,* **2006**, 4242-4.
270. Wegner, H.; Reisch, H.; Rauch, K.; Demeter, A.; Zachariasse, K.; Meijere, A. D.; Scott, L. T. *J. Org. Chem.* **2006**, *71*, 9080-7.
271. Di Fabio, R.; Micheli, F.; Baraldi, D.; Bertani, B.; Conti, N.; Forno, G. D.; Feriani, A.; Donati, D.; Marchioro, C.; Messeri, T.; Missio, A.; Pasquarello, A.; Pentassuglia, G.; Pizzi, D. A.; Provera, S.; Quaglia, A. M.; Sabbatini, F. M. *Il Farmaco* **2003**, *58*, 723-738.
272. Mclaughlin, M.; Palucki, M.; Davies, I. W. *Org. Lett.* **2006**, *8*, 3307–3310.
273. Abdel-Magid, A. F.; Carson, K. G.; Harris, B. D.; Maryanoff, C. A; Shah, R. D. *J. Org. Chem.* **1996**, *61*, 3849-3862.
274. Varchi, G.; Kofink, C.; Lindsay, D. M.; Ricci, A.; Knochel, P. *Chem. Comm.* **2003**, *3*, 396-397.
275. Molander, G. A.; Trice, S. L. J.; Dreher, S. D. *J. Am. Chem. Soc.* **2010**, *132*, 17701-17703.

276. Hall, D. G. *Structure, Properties, and Preparation of Boronic Acid Derivatives. Overview of Their Reactions and Applications, in Boronic Acids: Preparation and Applications in Organic Synthesis and Medicine*; Hall, D. G., Ed.; Wiley-VCH Verlag GmbH & Co. KGaA: Weinheim, **2006**.
277. Hassan, J.; Se, M.; Gozzi, C.; Schulz, E.; Lemaire, M. *Chem. Rev.* **2002**, *102*, 1359-1470.
278. Rodriguez, J. M.; Hamilton, A. D. *Angew. Chem. Int. Ed.* **2007**, *46*, 8614-8617.
279. Calum McLeod, PhD Thesis, University of Glasgow **2003**, 96-99.
280. Sheikh, N. S.; Leonori, D.; Barker, G.; Firth, J. D.; Campos, K. R.; Meijer, A. J. H. M.; Brien, P. O.; Coldham, I. *J. Am. Chem. Soc.* **2012**, *134*, 5300-5308.
281. *The Chemistry of Organolithium Compounds*; Rappoport, Z.; Marek, I., Eds.; John Wiley & Sons, Inc, **2004**; p. 511.
282. Das, S.; Addis, D.; Zhou, S.; Junge, K.; Beller, M. *J. Am. Chem. Soc.* **2010**, *132*, 1770-1771.
283. Ishiyama, T.; Murata, M.; Miyaura, N. *J. Org. Chem.* **1995**, *60*, 7508-7510.
284. Nicolaou, K. C.; Hwang, C.-K.; Marron, B. E.; DeFrees, S. A.; Couladouros, E. A.; Abe, Y.; Carroll, P. J.; Snyder, J. P. *J. Am. Chem. Soc.* **1990**, *112*, 3040-3054.
285. Huang, Y.; Strobel, E. D.; Ho, C. Y.; Reynolds, C. H.; Conway, K. A.; Piesvaux, J. A.; Brenneman, D. E.; Yohrling, G. J.; Arnold, H. M.; Rosenthal, D.; Alexander, R. S.; Tounge, B. A.; Mercken, M.; Vandermeeren, M.; Parker, M. H.; Reitz, A. B.; Baxter, E. W. *Bioorg. Med. Chem. Lett.* **2010**, *20*, 3158-3160.
286. H. Amii, K. Uneyama, *Chem. Rev.* **2009**, *109*, 2119-2183.
287. Goulaouic-dubois, C.; Adams, D. R.; Chiaroni, A.; Riche, C.; Fowler, F. W.; Grierson, D. S. *Heterocycles* **1994**, *39*, 509-512.
288. Hansch, C.; Leo, A.; Taft, R. W. *Chem. Rev.* **1991**, *91*, 165-195.
289. http://www.chem.wisc.edu/areas/reich/handouts/nmr-c13/cdata.htm, accessed 13/06/13.
290. Anbarasan, P.; Neumann, H.; Beller, M. *Angew. Chem. Int Ed,* **2010**, *49,* 2219-2222.
291. Hirose, Y.; Wahl, G. H.; Zollinger, H. *Helv. Chim. Acta.* **1976**, *59*, 1427-1437.
292. Milner, D. J. *Synthetic commun.* **1992**, *22*, 73-82.
293. Furuya, T, Klein, J. E. M. N.; Ritter, T. *Synthesis* **2010**, 1804-1821.
294. Pazo-llorente, R.; Gonzalez-romero, E.; Bravo-diaz, C. *Int. J. Chem. Kinet.* **1999**, 210-220.
295. Fig. adapted from: Pazo-llorente, R.; Gonzalez-romero, E.; Bravo-diaz, C. *Int. J. Chem. Kinet.* **1999**, 210-220.
296. Swain, C. G.; Sheats, J. E.; Harbison, K. G. *J. Am. Chem. Soc.* **1975**, *74*, 783-790.
297. Canning, P. S. J.; Mccrudden, K.; Maskill, H.; Sexton, B. *Chem. Commun.* **1998**, 1971-1972.
298. Swain, C. G.; Rogers, R. J. *J. Am. Chem. Soc.* **1975**, 799-800.
299. Bunnett, J. F.; Yijima, C. *J. Org. Chem.* **1977**, *42*, 639-643.
300. Rossi, R. A.; Pierini, A. B.; Pen, A. B. *Chem. Rev.* **2003**, *103*, 71-167.
301. Bolton, B. R.; Williams, G. H. *Chem. Soc. Rev.* **1986**, *15*, 261-289.
302. Fernandez-Alonso, A.; Bravo-diaz, C. *Helv. Chim. Acta.* **2010**, *93*, 877-887.
303. L. G. Makarov, M. K. Matveeva, E. A. Gribchenko. *Bull. Acad. Sci. USSR, Div Chem. Sci.* **1958**, 1399-1406.
304. Detar, F. D.; Kazimi, A. A. *J. Am. Chem. Soc.* **1955**, *77*, 3842-3844.

305. Kovalchuk, E. P.; Reshetnyak, O. V.; Kozlovska, Ye, Z.; Błazejowski, J.; Gladyshevskyj, Ye, R.; Obushak, M. D. *Thermochim. Acta* **2006**, *444*, 1-5.

306. Butters, M.; Harvey, J. N.; Jover, J.; Lennox, A. J. J.; Lloyd-Jones, G. C.; Murray, P. M. *Angew. Chem. Int. Ed.* **2010**, *49*, 5156-5160.

307. PEPPSI: Instructions for Use, *Sigma Aldrich* 1-3.

308. Lu, C. C.; Peters, J. C. *J. Am. Chem. Soc.* **2004**, *126*, 15818-15832.

309. Lyga, J. W.; Henrie, R. N.; Meier, G. A.; Creekmore, R. W.; Patera, R. M. *Magn. Reson. Chem.* **1993**, *31*, 323-328.

310. T. Kubar, M. Hanus, F. Ryjacek, P. Hobza, *Chem. Eur. J.* **2006**, *12*, 280-290.

311. Wainwright, M. *Biotech. Histochem.* **2009**, *85*, 341-354.

312. Y. Bourne, H. C. Kolb, Z. Radic, K. B. Sharpless, P. Taylor, P. Marchot, *Proc. Natl. Acad. Sci. USA* **2004**, *101*, 1449-1454;

313. Nakanishi, T.; Suzuki, M.; Saimoto, A.; Kabasawa, T. *J. Nat. Prod.* **1999**, *62*, 864-867.

314. Clark, R. L.; Deane, F. M.; Anthony, N. G.; Johnston, B. F.; Mccarthy, F. O.; Mackay, S. P. *Bioorg. Med. Chem*. **2007**, *15*, 4741-4752.

315. Wang, L.-K; Johnson, R. K.; Hecht, S. M. *Chem. Res. Toxicol.* **1993**, *6*, 813-818.

316. Parhi, A.; Kelley, C.; Kaul, M.; Pilch, D. S.; Lavoie, E. J. *Bioorg. Med. Chem. Lett.* **2012**, *22*, 7080-7083.

317. Beuria, T. K.; Santra, M. K.; Panda, D. *Biochemistry* **2005**, *44*, 16584-16593.

318. Marivingt-Mounir, C., Norez, C., Dérand, R., Bulteau-Pignoux, L., Nguyen-Huy, D., Viossat, B.; Morgant, G.; Becq, F.; Vierfond, J.-M.; Mettey, Y. *J. Med. Chem.* **2004**, *47*, 962-972.

319. Marivingt-Mounir, C., Sarrouilhe, D., Mettey, Y., Vierfond, J.-M. *Pharm. Pharmacol. Commun.* **1998**, *4*, 23-25.

320. H. M. Wolff, K. Hartke, *Arch. Pharm.* **1980**, *313*, 266-279.

321. Collibee, S. E.; Yu, J. *Tetrahedron Lett.* **2005**, *46*, 4453-4455.

322. Slagt, V. F.; Vries, H. M. D.; Vries, J. G. D.; Kellogg, R. M. *Org. Process Res. Dev.* **2010**, *14*, 30-47.

323. Kappe, C. O.; Pieber, B.; Dallinger, D. *Angew. Chem. Int. Ed.* **2013**, *52*, 1088-1094.

324. Collot, Â.; Bovy, R.; Bouillon, A.; Lancelot, J.-charles *Tetrahedron* **2002**, *58*, 3323-3328.

325. Esteves, P. M.; Carneiro, W. D. M.; Cardoso, S. P.; Barbosa, G. H.; Laali, K. K.; Rasul, G.; Prakash, G. K. S.; Olah, G. A. *J. Am. Chem. Soc.* **2003**, *125*, 4836-4849.

326. Rosokha, S. V.; Kochi, J. K. *J. Org. Chem.* **2002**, *67*, 1727-1736.

327. Queiroz, J. F. D.; Carneiro, W. D. M.; Sabino, A.; Sparrapan, R.; Eberlin, M. N.; Esteves, P. M. *J. Org. Chem.* **2006**, *71*, 6192-6203.

328. Fievez, T.; Pinter, B.; Geerlings, P.; Bickelhaupt, F. M.; Proft, F. D. *European J. Org. Chem.* **2011**, 2958-2968.

329. Olah, A. *Acc. Chem. Res.* **1971**, *4*, 240-248.

330. Newmark, R. A.; Hill, J. R.; Paul, S. *Org. Magn. Resonance* **1977**, *9*, 589-592.

331. Hoggett, J. G.; Moodie, R. B.; Penton, J. R.; Schofield, K. *Nitration and Aromatic Reactivity*; 1st ed.; Cambridge University Press, **1971**; p. 86.

332. Schofield, K. *Aromatic Nitration*; Cambridge University Press, **1980**; p. 54.

333. Osby, J. O., Martin, M. G., Ganem, B., *Tetrahedron. Lett.*, **1984**, 25, 20, 2093-2096.
334. Cozzi, P. G.; Solaria, E.;Floriani, C.; Chiesi-villab, A.; Rizzolib, C. *Chem. Ber.* **1996**, *129*, 1361-1368.
335. Carlson, R.; Larsson, U.; Hansson, L. *Acta Chem. Scand.* **1992**, *46*, 1211-1214.
336. Holley, W. K.; Ryschkewitsch, G. E. *Phosphorus Sulfur* **1990**, *53*, 271-284.
337. Kleeberg, C.; Dang, L.; Lin, Z.; Marder, T. B. *Angew. Chem. Int. Ed.* **2009**, *48*, 5350-5354.
338. Acevedo, O.; Jorgensen, W. L. *Org. Lett.* **2004**, *6*, 2881–2884.
339. Otsuka, M.; Endo, K.; Shibata, T. *Chem. Commun.* **2010**, *46*, 336–8.
340. Sun, H.; DiMagno, S. G. *Angew. Chem. Int. Ed* **2006**, *45*, 2720–2725.
341. Ormazabal-Toledo, R.; Contreras, R.; Tapia, R. A.; Campodonico, P. R. *Org. Biomol. Chem.* **2013**, *11*, 2302–2309.
342. Destro, R.; Gramamacioli, G. M.; Simmoneta, M. *Nature* **1967**, *215*, 389-390
343. Schlosser, M.; Ruzziconi, R. *Synthesis* **2010**, *13*, 2111–2123.
344. Cheron, N.; El Kaim, L.; Grimaud, L.; Fleurat-lessard, P. *Chem. Eur. J.* **2011**, *17*, 14929–14934.
345. Ormazabal-toledo, R.; Santos, J. G.; Paulina, R.; Castro, E. A.; Campodo, P. R.; Contreras, R. *J. Phys. Chem. B* **2013**, *117*, 5908–5915.
346. Isanbor, C.; Babatunde, A. I. *J. Phys. Org. Chem.* **2009**, *22*, 1078–1085.
347. Jose, K. B.; Cyriac, J.; Moolayil, J. T.; Sebastian, V. S.; George, M. *J. Phys. Org. Chem.* **2011**, *24*, 714–719.
348. Ormazabal-toledo, R.; Contreras, R.; Campodonico, P. R. *J. Org. Chem.* **2013**, *78*, 1091–1097.
349. Fern, I.; Frenking, G.; Uggerud, E. *J. Org. Chem.* **2010**, *75*, 2971–2980.
350. Tanaka, K.; Deguchi, M.; Iwata, S. *J. Chem. Res.* **1999**, 528–529.
351. Goryunov, L. I.; Grobe, J.; Van, D. Le; Shteingarts, V. D.; Mews, R.; Lork, E.; Würthwein, E. *Eur. J. Org. Chem.* **2010**, 1111–1123.
352. Liljenberg, M.; Brinck, T.; Rein, T.; Tomasi, S.; Svensson, M. *J. Org. Chem.* **2012**, *77*, 3262–3269.
353. Glukhovtsev, M. N.; Bach, R. D.; Laiter, S.; Carolina, N. *J. Org. Chem.* **1997**, *62*, 4036–4046.
354. Ishihara, Y.; Azuma, S.; Choshi, T.; Kohno, K.; Ono, K.; Tsutsumi, H.; Ishizu, T.; Hibino, S. *Tetrahedron* **2011**, *67*, 1320–1333.
355. Based on data and diagrams provided by Dr Hans Senn
356. Allen, F. H.; Kennard, O.; Watson, D. G.; Brammer, L.; Orpen, A. G. *J. Chem. Soc. Perkin. Trans. 2* **1987**, 1-19.
357. Exner, O.; Krygowski, T. M. *Chem. Soc. Rev.* **1996**, *25*, 71-75.
358. Produced by Dr Senn for current draft of manuscript based on the outlined work.
359. Tanaka, K.; Deguchi, M.; Iwata, S. *J. Chem. Res. Synop.* **1999**, 528-529.
360. Chen, J.; Rogers, S. C.; Kavdia, M. *Ann. Biomed. Eng.* **2013**, *41*, 327–37.
361. Byun, E.; Hong, B.; De Castro, K. A; Lim, M.; Rhee, H. *J. Org. Chem.* **2007**, *72*, 9815-7.
362. Clayden, Jonathan, Greeves, Nick, Warren, S. *Organic Chemistry*; 2nd ed.; OUP Oxford, **2012**; p. 538.
363. Dickinson, B. C.; Srikun, D.; Chang, C. J. *Curr. Opin. Chem. Biol.* **2010**, *14*, 50-56.
364. Kreishman, G. P.; Chant, S. I. *J. Mol. Biol.* **1971**, *61*, 45-58.

365. http://www.chem.wisc.edu/areas/reich/Handouts/nmr-h/hdata.htm
366. Whitaker, M.; Larman, M. G. *Semin. Cell. Dev. Biol.* **2001**, *12*, 53-58.
367. Berridge, M. J.; Bootman, M. D.; Roderick, H. L. *Nat. Rev. Mol. Cell. biol.* **2003**, *4*, 517-29
368. Szabadkai, G.; Duchen, M. R. *Physiology*. **2008**, *23*, 84-94.
369. Bianchi, K.; Rimessi, A.; Prandini, A.; Szabadkai, G.; Rizzuto, R. **2004**, Biochim. Biophys. Acta. *1742*, 119-131
370. Pinton, P.; Pozzan, T.; Rizzuto, R. *EMBO*. **1998**, *J. 17*, 5298-5308.
371. Nicholls, D. G. *Cell Calcium*. **2005**, *38*, 311-317
372. Crompton, M.; Heid, I. *Eur. J. Biochem.* **1978**, *91*, 599-608.
373. Puskin, J. S.; Gunter, T. E.; Gunter, K. K.; Russell, P. R. *Biochemistry.* **1976**, *15*, 3834-3842.
374. Nicholls, D. G. *Eur. J. Biochem.* **1974**, 305-315
375. McCormack, J. G.; Halestrap, A. P.; Denton, R. M. *Physiol Rev*. **1990**, *70*, 391-425
376. Chalmers, S.; Nicholls, D. G. *J. Biol. Chem.* **2003**, *278*, 19062-19070
377. Pivovarova, N. B.; Nguyen, H. V.; Winters, C. A.; Brantner, C. A.; Smith, C. L.; Andrews, S. B. *J. Neurosci.* **2004**, *24*, 5611-5622.
378. Sattler, R.; Xiong, Z.; Lu, W. Y.; Hafner, M.; Macdonald, J. F.; Tymianski, M. *Science*. **1999**, *284*, 1845-1848
379. Esfandiarei, M.; Fameli, N.; Choi, Y. Y. H.; Tehrani, A. Y.; Hoskins, J. G.; Van, C. *PloS one* **2013**, *8*.
380. Stokes, D. L.; Wagenknecht, T. *Eur. J. Biochem.* **2000**, *267*, 5274–5279.
381. Toyoshima, C., Nakasako, M., Nomura, H., Ogawa, H. *Nature*, **2000**, *405*, 647-55
382. Dumollard, R., Marangos, P., Fitzharris, G., Swann, K., Duchen, M., Carroll, J., et al. **2004**, *Development, 131*, 3057-67.
383. Szabadkai, G.; Bianchi, K.; Várnai, P.; De Stefani, D.; Wieckowski, M. R.; Cavagna, D.; Nagy, A. I.; Balla, T.; Rizzuto, R. *J. Cell Biol.,* **2006**, *175*, 901-11
384. Yi, M.; Weaver, D.; Hajnóczky, G. *J. Cell Biol.,* **2004**, *167*, 661-72
385. Dai, J.; Kuo, K. H.; Leo, J. M.; Breemen, C. V.; Lee, C. H. *Cell Calcium*. **2005**, *37*, 333-340.
386. Wray, S.; Burdyga, T. *Physiol. Rev.* **2010**, *90*, 113-178.
387. Meissner, G. *Annu. Rev. Physiol*. **1994**, *56*, 485-508.
388. Ji, G.; Feldman, M. E.; Greene, K. S.; Sorrentino, V.; Xin, H.; Kotlikoff, M. I. *J. Gen. Physiol.* **2004**, *123*, 377-86.
389. Luo, D.; Nakazawa, M.; Yoshida, Y.; Cai, J.; Imai, S. *Gen. Pharma*. **2000**, *34*, 211-220.
390. Jaggar, J. H.; Porter, V. a; Lederer, W. J.; Nelson, M. T. *Am. J. Physiol.-Cell Ph.* **2000**, *278*, C235–56.
391. Berridge, M. J. *J. Physiol.* **2008**, *586*, 5047–5061.
392. Breemen, C. V.; Fameli, N.; Evans, A. M. *J. Physiol.* **2013**, *591*, 2043–2054.
393. Dabertrand, F.; Nelson, M. T.; Brayden, J. E. *Microcirculation* **2012**, *20*, 307–316.
394. Venturi, E.; Sitsapesan, R.; Yamazaki, D. *Eur J Physiol* **2013**, *465*, 187–195.
395. McCarron, J. G.; Chalmers, S.; Bradley, K. N.; MacMillan, D.; Muir, T. C. *Cell Calcium*. **2006**, *40*, 461-93.
396. Grynkiewicz, G.; Poenie, M.; Tsein, R. Y. *J. Biol. Chem.* **1985**, *260*, 3440-3450.
397. *Molecular Probes: The Handbook - A Guide to Fluorescent Probes and Labeling Technologies*; Invitrogen, Ed.; 11th ed.; **2013**; Section 19.2.
398. Spiteri, C.; Moses, J. E. *Angew. Chem. Int. Ed* **2010**, *49*, 31–33.
399. Kurebayashi, N.; Harkins, A. B.; Baylor, S. M. *Biophys. J.* **1993**, *64*, 1934–1960.

400. Gaillard, S.; Yakovlev, A.; Luccardini, C.; Oheim, M.; Feltz, A.; Mallet, J. *Org. Lett*. **2007**, *9*, 2629-32.
401. Ji, X.; Cheng, B.; Song, J.; Liu, C.; Wang, Y. *Synthetic Commun.* **2009**, *39*, 2053-2057
402. Pham, H. T.; Hanson, R. N.; Olmsted, S. L.; Kozhushnyan, A.; Visentin, A.; Weglinsky, P. J.; Massero, C.; Bailey, K. *Tetrahedron Lett.* **2011**, *52*, 1053-1056.
403. Macleod, C.; Mckiernan, G. J.; Guthrie, E. J.; Farrugia, L. J.; Hamprecht, D. W.; Macritchie, J.; Hartley, R. C. *Synthesis*, **2003**, 387-401.
404. Xiao, Z.-P.; Wang, Y.-C.; Du, G.-Y.; Wu, J.; Luo, T.; Yi, S.-F. *Synthetic Commun*. **2010**, *40*, 661-665.
405. Marson, C. M. *Tetrahedron* **1992**, *48*, 3659–3726.
406. Nicolaou, K. C.; Sasmal, P. K.; Xu, H.; Namoto, K.; Ritzén, A. *Angew. Chem. Int. Ed.* **2003**, 42, 4225-9.
407. Etter, E. F.; Kuhn, M. A; Fay, F. S. *J. Biol. Chem.* **1994**, 269, 10141-9.
408. Lee, J. W.; Jun, S. I.; Kim, K. *Tetrahedron Lett.* **2001**, 42, 2709-2711.
409. Tian, W. Q.; Wang, Y. A. *J. Org. Chem.* **2004**, *69*,4299-4308.
410. Bebbington, M. W. P.; Bourissou, D. *Coord. Chem. Rev.* **2009**, *253*, 1248-1261.
411. Bazureau, J. P. *Tetrahedron Lett*. **2002**, *43*, 8745-8749.
412. Ansar, M.; Al Akoum Ebrik, S.; Mouhoubl, R.; Berthelotl, P.; Vaccher, C.; Vaccher, M.; Flouquetl, N.; Caignard, D. H.; Renard, P.; Pirard, B.; Rettori, M. C.; Evrard, G. Durant, F., Debaert, M., Eur. *J. Med. Chem.* **1996**, 449-460.
413. Drake, M. D.; Bright, F. V.; Detty, M. R. *J. Am. Chem. Soc.* **2003**, *125*, 12558-66.
414. Caroline Quin, PhD thesis, University of Glasgow, **2009**.
415. *FT-NMR* **1** (2), 1671:B / *RegBook* **1** (2), 2275:F / *Structure Index* **1**, 356:B:3;
Beil. **16**, IV, 983
416. Stephen McQuaker, PhD Thesis, University of Glasgow, **2013**.
417. Rangarajan, S.; Friedman, S. H. *Bioorg. Med. Chem. Lett.* **2007**, *17*, 2267-73.
418. Shimojo, M.; Matsumoto, K.; Hatanaka, M. *Tetrahedron* **2000**, *56*, 9281-9288.
419. Chu, Q., Brahmi, M. M., Solovyev, A., Ueng, S. H., Curran, D. P., Malacria, M., Fensterbank, L., Lacote, E. *Chem. Eur. J.* **2009**, *15*, 12937-12940.
420. Korthals, K. A; Wulff, W. D. *J. Am. Chem. Soc.* **2008**, *130*, 2898-9.
421. Gwaltney II, S. L.; Sakata, S. T.; Shea, K. J. *J. Org. Chem.* **1996**, *61*, 7438-7451.
422. Clasby, M. C.; Craig, D.; Slawin, A. M. Z.; White, A. J. P.; Williams, D. J. *Tetrahedron* **1995**, *51*, 1509–1532.
423. Narayan, R. S.; Borhan, B. *J. Org. Chem.* **2006**, *71*, 1416-29.
424. Nacsa, E. D.; Lambert, T. H. *Org. Lett.* **2013**, *15*, 38–41.
425. Welzel, P.; Dietz, C.; Eckhardt, G.; Welzel, P.; Dietz, C. *Chem. Ber.* **1975**, *108*, 3550-3565.
426. Lermer, L.; Neeland, E. G.; Ounsworth, J. P.; Sims, R. J.; Tischler S. A.; Weiler, L. *Can. J. Chemistry* **1992**, *70*, 1427–1445.
427. Wilson, D. A.; Wilson, C. J.; Moldoveanu, C.; Resmerita, A.-maria; Corcoran, P.; Hoang, L. M.; Rosen, B. M.; Percec, V. *J. Am. Chem. Soc.* **2010**, *132*, 1800-1801.
428. Ngai, M. H.; Yang, P.-yu; Liu, K.; Shen, Y.; Wenk, M. R.; Yao, Q.; Lear, M. J. *Chem. Commun.* **2010**, *46*, 8335-8337.
429. Kuykendall, D. W.; Anderson, C. A.; Zimmerman, S. C. *Org. Lett.* **2009**, *11*, 61–64.
430. Müller, T. E.; Pleier, A. *J. Chem. Soc. Dalton Trans.* **1999**, 583–587.
431. Edelson-averbukh, M.; Etinger, A.; Mandelbaum, A. *J. Chem. Soc. Perkin Trans. 2,* **1999**, 1095-1105.
432. Dong, X.; Yang, Y.; Sun, J.; Liu, Z.; Liu, B. *Chem. Comm.,* **2009**, 3883-3885
433. Naguib, Y. M. A. *Molecules* **2009**, 3600-3609.
434. Nagao, Y. U.; Takasu, A. *J. Polym. Sci. A1* **2010**, *48*, 4207-4218.